CONF-961208--

BNL - 52525
Formal Report

NSF-ITP-96-155I

BEAM STABILITY & NONLINEAR DYNAMICS

December 3 - 5, 1996

Edited / Compiled

by

Zohreh Parsa

INSTITUTE FOR THEORETICAL PHYSICS
UC, SANTA BARBARA, CALIFORNIA,
93106-4030 USA

&

BROOKHAVEN NATIONAL LABORATORY
UPTON, NY 11973 - 5000 USA

DISCLAIMER

BNL-52525
NSF-ITP-96-155i

BEAM STABILITY & NONLINEAR DYNAMICS

December 3 - 5, 1996

Edited/ Compiled

by

Zohreh Parsa

INSTITUTE FOR THEORETICAL PHYSICS
UC, SANTA BARBARA, CALIFORNIA,
93106-4030 USA

Support for this symposium was provided by
NSF-PHY-94-07194, and also
under the auspices of the Department of Energy,
Under Contract No. DE-AC02-76CH00016 (USA)

DISCLAIMER

Portions of this document may be illegible in electronic image products. Images are produced from the best available original document.

FORWARD

This Report includes copies of transparencies and notes from the presentations made at the Symposium on Beam Stability and Nonlinear Dynamics, December 3 - 5, 1996 at the Institute for Theoretical Physics, University of California, Santa Barbara California, that was made available by the authors. Editing, reduction and changes to the authors contributions were made only to fulfill the printing and publication requirements.

We would like to take this opportunity to thank the speakers for their informative presentations and for providing copies of their transparencies and notes for inclusion in this Report.

We also would like to thank the ITP staff for their assistance, with our special thanks to Ms. Deborah Storm for her continuous efforts and help with the meeting, announcements and processing of this Report.

Zohreh Parsa
Symposium Chairperson
Institute for Theoretical Physics
UC, Santa Barbara California, USA.

INSTITUTE FOR THEORETICAL PHYSICS

UNIVERSITY OF CALIFORNIA
SANTA BARBARA, CALIFORNIA 93106-4030
http://www.itp.ucsb.edu

CONFERENCES/VISAS: (805) 893-3178
OFFICE FAX: (805) 893-2431
CREDIT CARD FAX: (805) 893-3486

ITP Conference on

Particle Beam Stability and Nonlinear Dynamics

December 3-5, 1996

Coordinator, Zohreh Parsa

SCHEDULE

Tuesday, December 3, 1996:

Time:	Speaker:	Title:
Convener:	**Z. Parsa**	
8:00 am	Registration	ITP Front Lobby
8:40	Welcome	J. Hartle, ITP Director
	Intro. & Welcome	Z. Parsa, BNL
9:00	J. Meiss, U Colorado	Single-Particle Hamiltonian Dynamics
9:45	Refreshment Break	ITP Center Patio
Convener:	**G. Guignard**	
10:15	J. Marsden, Cal Tech	Symplectic Geometry, Maps, Integrators
11:00	M. Berz, Michigan State	From Taylor Series to Taylor Models & Remainder Differential Algebra with Interval Arithmetic
11:45	A. Dragt, UM	Factorization of Taylor Maps
12:25 pm	Lunch Break	ITP Center Patio
Convener:	**J. Hagel**	
2:00	J. Irwin, SLAC	One-Turn Map Generators Aberration Sources, Consequences, and Corrective Actions
2:40	E. Todesco, INFN	Long-Term Orbit Stability Predictions (Lypunov estimates, Normal Forms)
3:25	Refreshment Break	ITP Center Patio
Convener:	**W. Lysenko**	
4:00	J. Laskar, BDL	Frequency Map Analysis - Theory & Experiments
4:45	R. Warnock, SLAC	The Effect of Resonances on Long-Term Stability & Symplectic Full Turn Maps
5:30	Wine & Cheese	ITP Center Patio
6:15	Conference Dinner	ITP Center Patio

Wednesday, December 4, 1996

Time:	Speaker:	Title:
Convener:	**D. Robin**	
8:30 am	V. Balandin, DESY	Nonlinear Spin Dynamics
9:10	F. Schmidt, CERN	Dynamic Aperture - Simulation and Experiment
9:55	Refreshment Break	ITP Center Patio
Convener:	**J. Ellison**	
10:25	F. Ruggiero, CERN	Longitudinal Beam Echoes & Diffusion Rates
11:05	R. Siemann, SLAC	Sawtooth Instability & Over-Shoot Phenomena
11:45	H. Yoshida, NAO	Instability of Periodic Orbit and Non-Integrability of Hamiltonian System
12:25pm	Lunch Break	ITP Center Patio
Convener:	**J. Krommes**	
1:40	P. Zenkevitch, ITEP	Neutralized Beams: Landau Damping in Systems with Strong Nonlinearity
2:20	G. Guignard, CERN	Stability of Beams in a High Frequency Linac with Strong Wakefields
3:05	Refreshment Break	ITP Center Patio
Convener:	**E. Lessner**	
3:35	M. Zeitlin, IPME	Wavelet Analysis of Hamiltonian System and its Perturbations
4:20	S. Andrianov, St. Petersburg	Nonlinear Aberration Correction
4:55	S. Heifets, SLAC	Search of the Mechanism of the Saw-Tooth Instability
5:30	Reception	ITP Center Patio

Thursday, December 5, 1996

Time:	Speaker:	Title:
Convener:	**A. Chao**	
8:30	F. Ruggiero, CERN	Collective Effects in LHC
9:05	J. Hagel, Univ Maderia	Galaxy Dynamics: Resonance Analysis in Celestial Mechanics
9:50	Refreshment Break	ITP Center Patio
Convener:	**M. Berz**	
10:20	A. Pankin, INR	Nonlinear Structure Near Boundary of Marginal Stability
10:40	G. Stupakov	Nonlinear Dynamics of Single Bunch Instability in Accelerators
11:10	V. Zadorozhny, IC	The Dynamic 2-D Electron Beams of the Plasma Lense
11:30	TBA	Map Measurements
11:45	G. Guinard	Statistical Analysis of Emittance Growth
12:20 pm	Lunch Break	ITP Center Patio
Convener:	**R. Siemann**	
1:50	Round Table Discussions on Outstanding Issues in Beam Instabilities and Nonlinear Accelerator Dynamics	Z. Parsa, A. Dragt, G. Guignard, J. Laskar, J. Meiss, E. Todesco, & other speakers and participants
3:00	Z. Parsa, BNL	Summary and Closing Talk

Conference Ends

TBA = To be announced
* = late contributions
BNL = Brookhaven National Laboratory
FNAL = Fermi National Laboratory
LANL = Los Alamos National Laboratory
SLAC = Stanford Linear Accelerator Center
DOE = Department of Energy
NSF = National Science Foundation
UCLA = Univ. California Los Angeles
UCSB = Univ. California Santa Barbara

BEAM STABILITY & NONLINEAR DYNAMICS

INTRODUCTION

Z. Parsa, BNL/ITP

"Beam Stability & Nonlinear Dynamics Symposium"

December 3 - 5, 1996"

Zohreh Parsa,
Brookhaven National Lab/ITP

This is the 3rd Symposium we are holding at the ITP as part of our 5 month program on bf "NEW IDEAS FOR PARTICLE ACCELERATORS" (sponsored by ITP).

To put this symposium in context; this program started in July 22, 1996 and has hosted 12 - 15 residence Physicists who study variety of problems related to particle accelerator physics.

In addition to this symposium, we hosted a week long symposium on New Modes of Particle Accelerations - Techniques and Sources August 19 - 23, 1996. Some of the highlights of that meeting included Novel modes of laser, plasma, wake field acceleration techniques and sources.

Our second symposium on "Future High Energy Colliders" was held October 21-25, 1996.

The purpose of the symposium was to discuss the future direction of high energy physics by bringing together leaders from the theoretical, experimental and accelerator physics communities. Their talks provided personal perspectives on the physics objectives and the technology demands of future high energy colliders. Collectively, they formed a vision for where the field should be heading and how it might best reach its objectives.

A unique feature of the symposium was the bringing together of many physicists who will have a major impact on the future direction of the field. Especially important was the set of presentations made by the Department of Energy Director of Energy Research M. Krebs, by B. Kayser of the National Science Foundation, and by the directors of the three U.S. High Energy Physics laboratories, J. Peoples (Fermilab), B. Richter (Stanford Linear Accelerator Center) and N. Samios (Brookhaven National Laboratory). Their perspectives combined with presentations by internationally distinguished high energy and accelerator physicists provided a comprehensive picture of the issues involved in formulating appropriate goals for the future. The difficult aspects and the far reaching consequences of the decisions that must be made were further clarified during a unique panel discussion designed to initiate the process of

reaching accord in the high energy community as to what the future physics and accelerator priorities should be. Although there is not unanimity of opinion in all matters, there is a consensus that an NLC should be built somewhere in the world and vigorous R & D should be pursued in promising new areas such as the muon collider concept and new modes of particle acceleration.

The perspectives that were presented at the symposium on the state and future of high energy physics are vital ingredients in the continuing discussion of how the U.S. High Energy Physics community should best marshal its national scientific resources while continuing a high level of international collaboration. They should provide valuable input for ongoing discussions and in making decisions regarding the future direction of the field.

In this symposium we will be focusing on Nonlinear Dynamics and Beam Stability: Which would deal with some of the fundamental theoretical problems associated with accelerator physics [e.g see program]

I would like to take this opportunity to thank ITP and its supporting agency National Science Foundation (NSF) for hosting our program and providing such a nice setting for the Symposium

```
From ZOHREH@bnlajc.bnl.gov Tue Jul 23 19:47:04 1996
To: PARSA@itp.ucsb.edu
CC: ZOHREH@bnlarm.bnl.gov
Content-Length: 970
X-Lines: 32
```

[Parsa@bnl.gov
after Dec 20, 96
Tel 516-344-2085]

I. Nonlinear Dynamics

A. Single particle orbit theory

1. Symplectic geometry. 2. Hamiltonian systems.

3. Bifurcation theory 4. Long-term orbit prediction.

5. Symplectic integrators. 6. Long-term stability of orbits.

7 Long-term stability estimates 8. Symbolic methods.

9. Truncated power series and truncated Poisson series algebra.

10 Lie methods. 11. Transformation methods. 12. Normal forms.

13. Computation, manipulation, and analysis of maps. 14. Iteration of maps.

B. Many particle effects

1. Galaxy formation and galactic dynamics 2. Globular clusters.

3. Laser cooled Penning traps. 4. Crystal beams.

4. Generation and transport of intense space-charge dominated beams.

6. Beam-beam effects. 7. Wake-field effects.

etc, ...

INSTITUTE FOR THEORETICAL PHYSICS

UNIVERSITY OF CALIFORNIA
SANTA BARBARA, CALIFORNIA 93106-4030
http://www.itp.ucsb.edu

CONFERENCES/VISAS: (805) 893-3170
OFFICE FAX: (805) 893-2431
CREDIT CARD FAX: (805) 893-3486

ITP Conference on

Particle Beam Stability and Nonlinear Dynamics

December 3-5, 1996

Coordinator, Zohreh Parsa

SCHEDULE

Tuesday, December 3, 1996:

Time:	Speaker:	Title:
Convener:	Z. Parsa	
8:00 am	Registration	ITP Front Lobby
8:40	Welcome	J. Hartle, ITP Director
	Intro. & Welcome	Z. Parsa, BNL
9:00	J. Meiss, U Colorado	Single-Particle Hamiltonian Dynamics
9:45	Refreshment Break	ITP Center Patio
Convener:	G. Guignard	
10:15	J. Marsden, Cal Tech	Symplectic Geometry, Maps, Integrators
11:00	M. Berz, Michigan State	From Taylor Series to Taylor Models & Remainder Differential Algebra with Interval Arithmetic
11:45	A. Dragt, UM	Factorization of Taylor Maps
12:25 pm	Lunch Break	ITP Center Patio
Convener:	J. Hagel	
2:00	J. Irwin, SLAC	One-Turn Map Generators Aberration Sources, Consequences, and Corrective Actions
2:40	E. Todesco, INFN	Long-Term Orbit Stability Predictions (Lypunov estimates, Normal Forms)
3:25	Refreshment Break	ITP Center Patio
Convener:	W. Lysenko	
4:00	J. Laskar, BDL	Frequency Map Analysis - Theory & Experiments
4:45	R. Warnock, SLAC	The Effect of Resonances on Long-Term Stability & Symplectic Full Turn Maps
5:30	Wine & Cheese	ITP Center Patio
6:15	Conference Dinner	ITP Center Patio

Wednesday, December 4, 1996

Time:	Speaker:	Title:
Convener:	D. Robin	
8:30 am	V. Balandin, DESY	Nonlinear Spin Dynamics
9:10	F. Schmidt, CERN	Dynamic Aperture - Simulation and Experiment
9:55	Refreshment Break	ITP Center Patio
Convener:	J. Ellison	
10:25	F. Ruggiero, CERN	Longitudinal Beam Echoes & Diffusion Rates
11:05	R. Siemann, SLAC	Sawtooth Instability & Over-Shoot Phenomena
11:45	H. Yoshida, NAO	Instability of Periodic Orbit and Non-Integrability of Hamiltonian System
12:25pm	Lunch Break	ITP Center Patio
Convener:	J. Krommes	
1:40	P. Zenkevitch, ITEP	Neutralized Beams: Landau Damping in Systems with Strong Nonlinearity
2:20	G. Guignard, CERN	Stability of Beams in a High Frequency Linac with Strong Wakefields
3:05	Refreshment Break	ITP Center Patio
Convener:	E. Lessner	
3:35	M. Zeitlin, IPMB	Wavelet Analysis of Hamiltonian System and its Perturbations
4:20	S. Andrianov, St. Petersburg	Nonlinear Aberration Correction
4:55	S. Heifets, SLAC	Search of the Mechanism of the Saw-Tooth Instability
5:30	Reception	ITP Center Patio

Thursday, December 5, 1996

Time:	Speaker:	Title:
Convener:	A. Chao	
8:30	F. Ruggiero, CERN	Collective Effects in LHC
9:05	J. Hagel, Univ Maderia	Galaxy Dynamics: Resonance Analysis in Celestial Mechanics
9:50	Refreshment Break	ITP Center Patio
Convener:	M. Berz	
10:20	A. Pankin, INR	Nonlinear Structure Near Boundary of Marginal Stability
10:40	G. Stupakov	Nonlinear Dynamics of Single Bunch Instability in Accelerators
11:10	V. Zadorozhny, IC	The Dynamic 2-D Electron Beams of the Plasma Lense
11:30	TBA	Map Measurements
11:45	G. Guinard	Statistical Analysis of Emittance Growth
12:20 pm	Lunch Break	ITP Center Patio
Convener:	R. Siemann	
1:50	Round Table Discussions on Outstanding Issues in Beam Instabilities and Nonlinear Accelerator Dynamics	Z. Parsa, A. Dragt, G. Guignard, J. Laskar, J. Meiss, E. Todesco, & other speakers and participants
3:00	Z. Parsa, BNL	Summary and Closing Talk

Conference Ends

TBA = To be announced
* = late contributions
BNL = Brookhaven National Laboratory
FNAL = Fermi National Laboratory
LANL = Los Alamos National Laboratory
SLAC = Stanford Linear Accelerator Center
DOE = Department of Energy
NSF = National Science Foundation
UCLA = Univ. California Los Angeles
UCSB = Univ. California Santa Barbara

Welcome

Particle Beam Stability and
Nonlinear Dynamics
Conference Participants

&

The conference coordinator
hosts an

Opening Buffet Dinner

Tuesday Evening, December 3rd

All conference registrants are welcome.
Guest tickets are available from
your conference assistant for $35 each.
Children under 12 are free.

5:30 pm - Wine and Cheese
6:15 pm - Buffet Dinner
all events in ITP center patio, weather permitting

This gourmet dinner will be presented by the UCSB Special Events Catering. There will be vegetarian dishes available.

Join us for an hors d'oeuvres reception

for the ITP conference on
Particle Beam Stability
and Nonlinear Dynamics

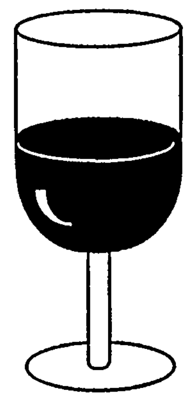

Wednesday Evening,
December 4th
5:30 pm

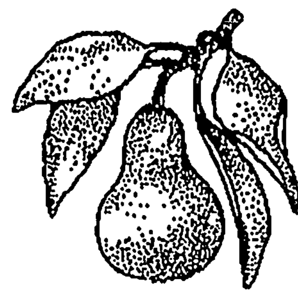

All conference registrants are welcome.
Guests are $25 (children under 12 free)
See the conference staff for tickets.

INSTITUTE FOR THEORETICAL PHYSICS

UNIVERSITY OF CALIFORNIA
SANTA BARBARA, CALIFORNIA 93106-4030
http://www.itp.ucsb.edu

CONFERENCES/VISAS: (805) 893-3178
OFFICE FAX: (805) 893-2431
CREDIT CARD FAX: (805) 893-3436

December 3, 1996

PARTICIPANTS in the Conference on *Particle Beam Stability and Nonlinear Dynamics:*

Welcome to the ITP! The following arrangements have been made for your visit:

Building Security: The ITP uses an extensive security system. Between the hours of 8:00am and 5:00pm the building is open to all with access through the front door. Before 8:00am and after 4:30pm the building is locked with exit/entrance to the building through the front door only and *entrance* by security card. **All exterior doors are locked and alarms will sound if exit is attempted at any exterior door other than the front door.** Please be aware of these security precautions and notify your conference assistant should you inadvertently cause any alarm to sound.

Computer Terminal: A terminal has been set up for you to access your home e-mail in Room 1001 directly outside the ITP Main Seminar Room. There are other terminals available in the Computer Room on the second floor, Room 2202 (Please note that this room has the same security restrictions as above.) The *Username* is GUEST. Refer to the instructions directly above the terminals for the *password*. The terminals are not enabled for receiving mail. If you have any questions regarding this, please contact your conference assistant.

Telephone: A guest telephone is available in Room 1001. Please reverse long distance charges.

Copying Machines: Ask your conference assistant for help should you have any copying needs.

Messages: A message board will be near the conference desk which is located in the lobby of Kohn Hall. Messages will be posted there before the breaks and before lunch.

Questions: Dorene Iverson, Monica Curry and Dan Mason are your conference assistants. They are able to answer most of your questions and provide you with supplies. One will be stationed at the conference desk most of the time.

SINGLE-PARTICLE HAMILTONIAN DYNAMICS

J. Meiss, U Colorado

Symplectic Maps

See Review paper

Meiss, Rev. Mod. Phys. <u>64</u>, 795 (92)

Why study?

① Poincaré Maps of Hamiltonian flows are symplectic

② Maps model impulsive forces well

③ Many mysteries remain to be solved

2D, Area preserving maps fairly well understood, but 4D & higher still <u>hard</u>.

Symplectic Maps

$$\underset{\sim}{x}' = f(\underset{\sim}{x}) \qquad \underset{\sim}{x} = \begin{pmatrix} \underset{\sim}{q} \\ \underset{\sim}{p} \end{pmatrix}$$

— preserve loop actions

$$\oint_L p \cdot dq = \oint_{f(L)} p \cdot dq$$

L – loop in phase space

(may <u>not</u> be contractable – "exact")

locally this is a condition on the derivative (Jacobian)

$$\delta x' = Df(x)\,\delta x \qquad Df(x) = \left.\frac{\partial f}{\partial x}\right|_{\underset{\sim}{x}}$$

then

$$Df^T \omega\, Df = \omega \qquad \omega = \begin{pmatrix} 0 & -I \\ I & 0 \end{pmatrix}$$

— Volume preserving & orientation preserving

$$\det(Df) = +1$$

— Eigenvalues

reflexivity: $\det(Df - \lambda I) = 0 \Rightarrow \lambda^{-1}$ also eigenvalue

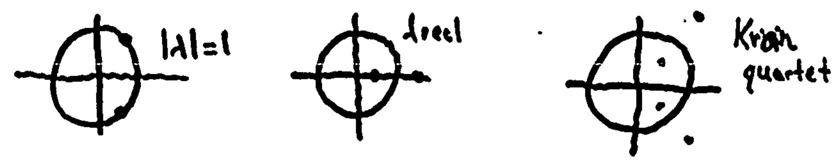

Lagrangian Variational Formulation – Symplectic Maps

Discrete		Continuous
x_i	Coordinates	$x(t)$
$x_{i+1} - x_i$		$\dot{x}(t)$
$F(x_i, x_{i+1})$	Lagrangian	$L(x, \dot{x})$
$W = \sum_i F(x_i, x_{i+1})$	Action	$W = \int dt\, L$

$\delta W = 0 \Rightarrow$ orbits

$0 = F_1(x_i, x_{i+1}) + F_2(x_{i-1}, x_i)$	$0 = -\frac{d}{dt}\frac{\partial L}{\partial \dot{x}} + \frac{\partial L}{\partial x}$

Example:

$$F(x, x') = \frac{1}{2}(x' - x)^2 + \frac{k}{4\pi^2}\cos(2\pi x)$$

$$\delta W = 0 \Rightarrow \quad x_{i+1} - 2x_i + x_{i-1} = -\frac{k}{2\pi}\sin(2\pi x_i)$$

(Standard Map)

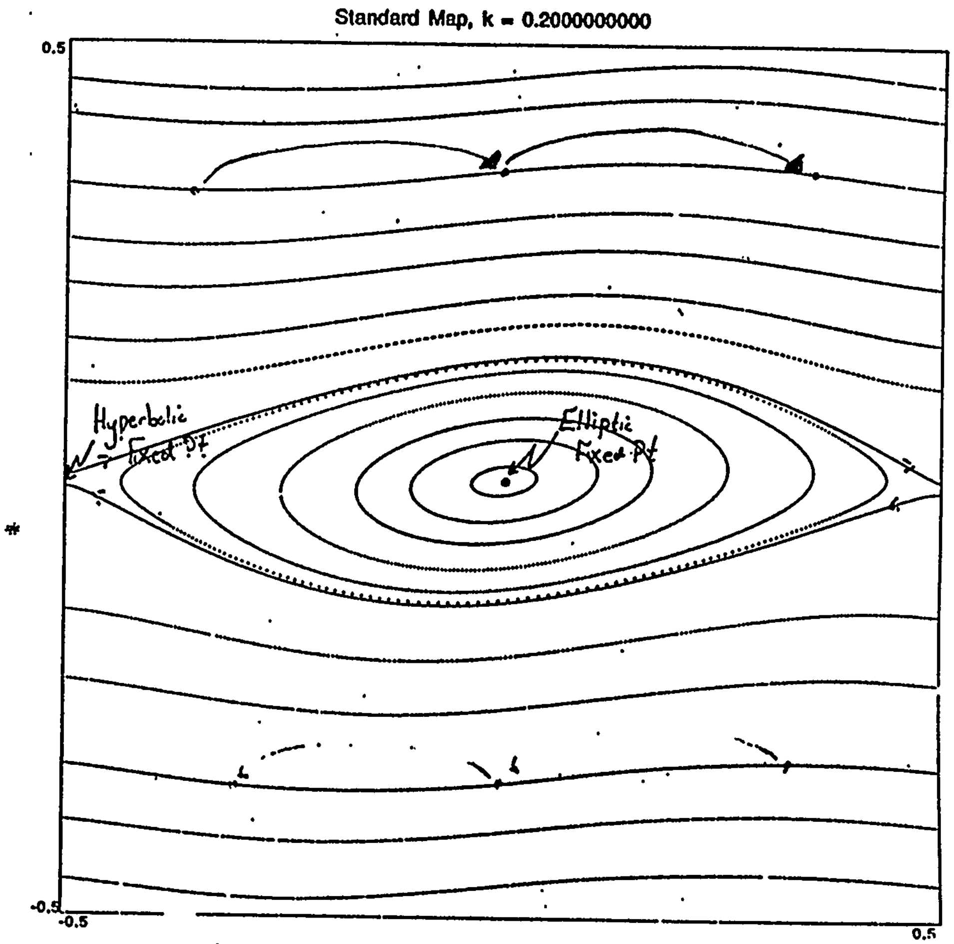

$$y' = y - \frac{k}{2\pi}\sin(2\pi x)$$
$$x' = x + y'$$

Standard Map, k = 0.9000000000

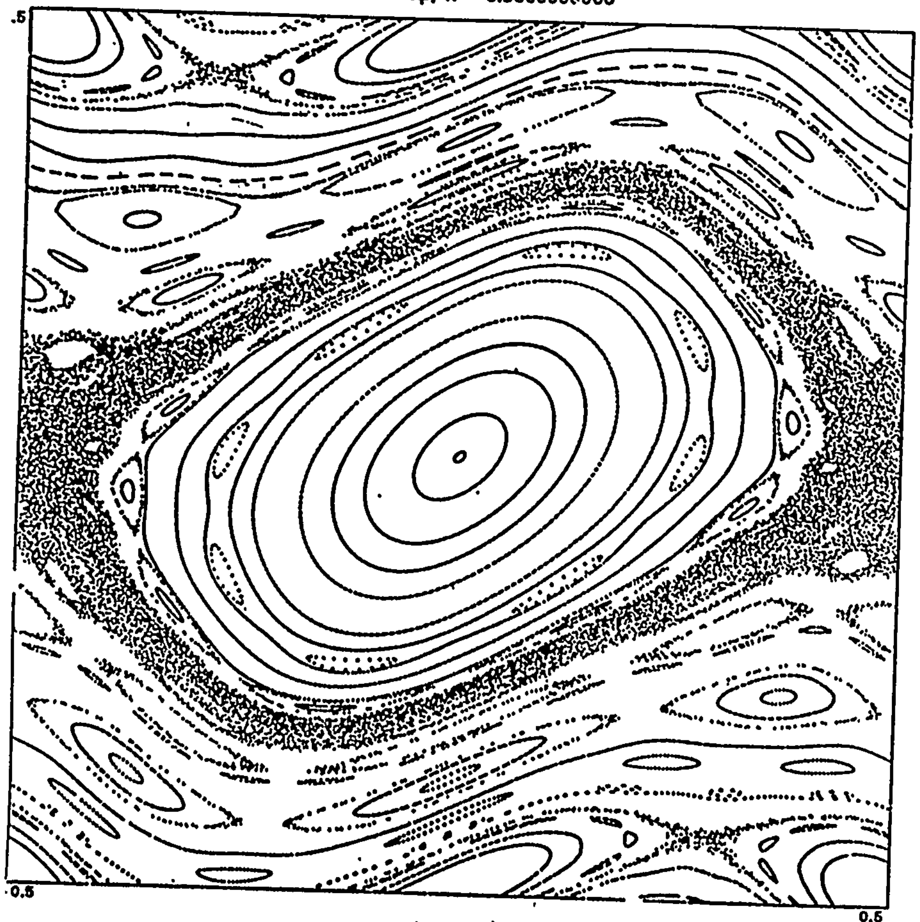

Islands around Islands

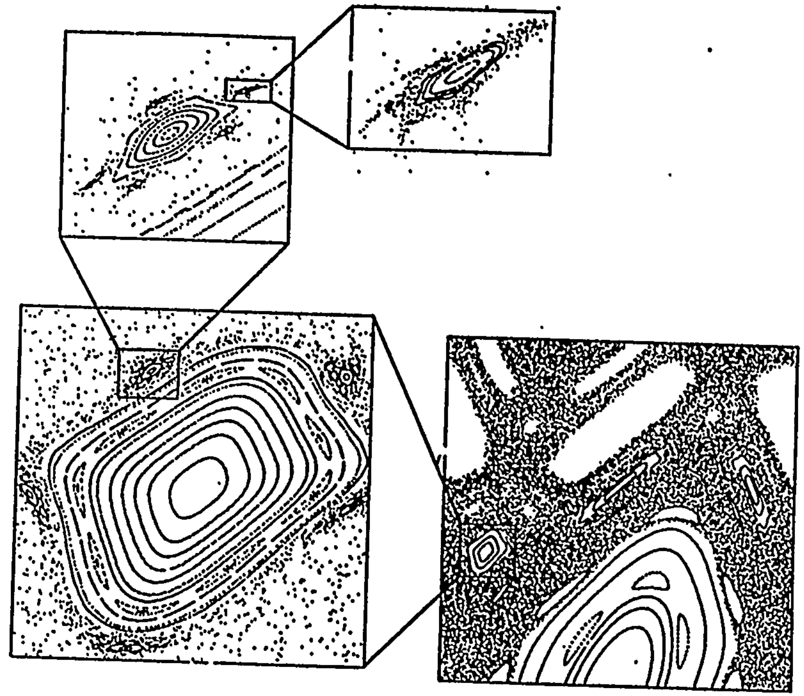

Std. Map $k = 1.20141333$ - period 5 fixed point

See Meiss Phys. Rev. **34A** 2375 (86)

Twist Mappings

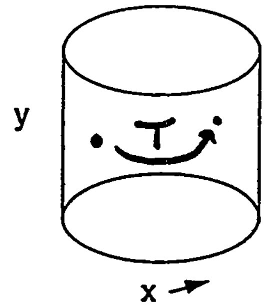

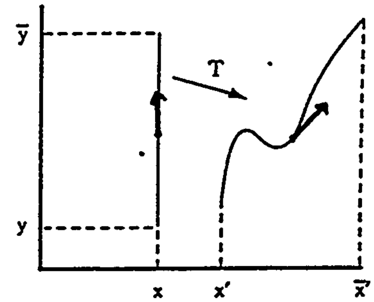

Consider a cylindrical phase space
With a symplectic Map T: (x,y) →(x′,y′)

" increasing momentum means increasing velocity "

T is a twist mapping if $\left.\dfrac{dx'}{dy}\right|_x \geq K > 0$

$$\begin{pmatrix} \delta x' \\ \delta y' \end{pmatrix} = \begin{bmatrix} \dfrac{\partial x'}{\partial x} & \dfrac{\partial x'}{\partial y} \\ \dfrac{\partial y'}{\partial x} & \dfrac{\partial y'}{\partial y} \end{bmatrix} \begin{pmatrix} \delta x \\ \delta y \end{pmatrix} = M \begin{pmatrix} \delta x \\ \delta y \end{pmatrix}$$

$$\det(M) = 1 \Rightarrow \left.\frac{\partial x}{\partial y'}\right|_{x'} = -\left.\frac{\partial x'}{\partial y}\right|_x \leq -K$$

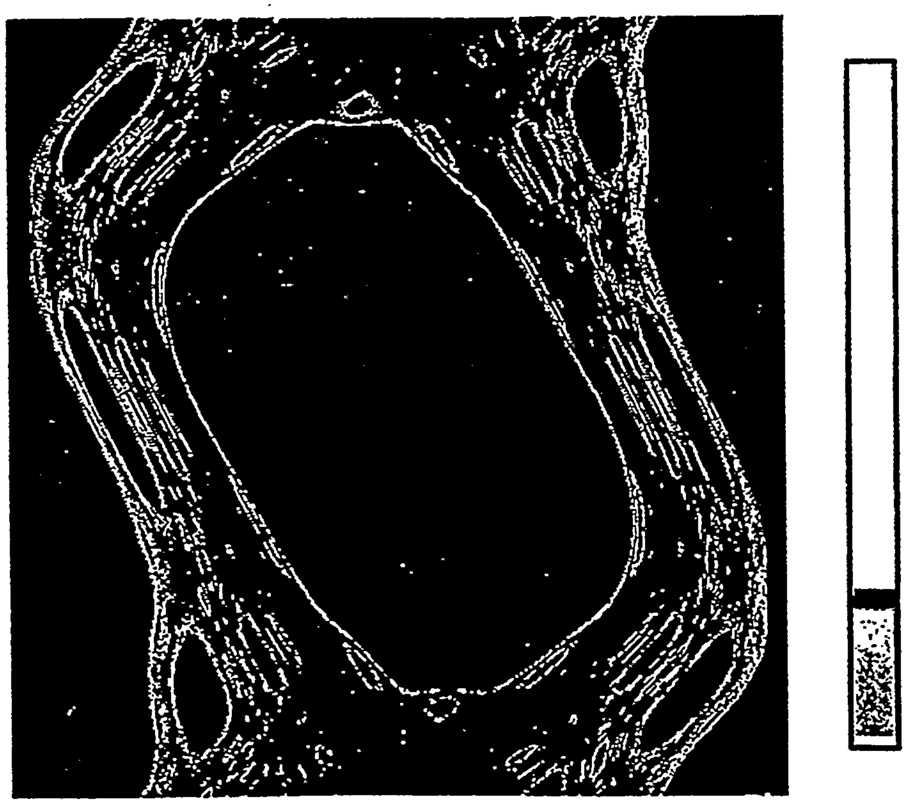

k = 0.971635, 500x500 cells, t = 6(10)^9

colors, i=1,200

See Meiss Physica D 74, 254 (94)

Aubry - Mather Theorem

Proves existence of minimizing orbits

1) There exists a sequence $\{\dots x_{-1}, x_0, x_1 \dots\}$ s.t.

$$W[x] \equiv \sum_i F(x_i, x_{i+1})$$

is minimized — all variations with compact support have larger action

$$W[x+\Delta x] - W[x] > 0$$

2) Moreover every such minimizing orbit is ordered and thus has a definite frequency

$$\omega = \lim_{t\to\infty} \frac{x_t}{t}$$

3) If ω is irrational then the orbit is either dense on a Lipschitz graph of a circle or a cantor set:

Kolmogorov - Arnold - Moser Theorem

For k sufficiently small, and ω sufficiently irrational $\exists$ an orbit with frequency ω which densely covers an invariant circle

$$|\omega - p/q| > q^{-\tau} \quad \forall\, p, q$$
& some $\tau \geq 2$

Herman: $\exists$ at least one rotational invariant circle for $k < 1/34$

Mather: There are no rotational invariant circles when $k > 4/3$

Cantori

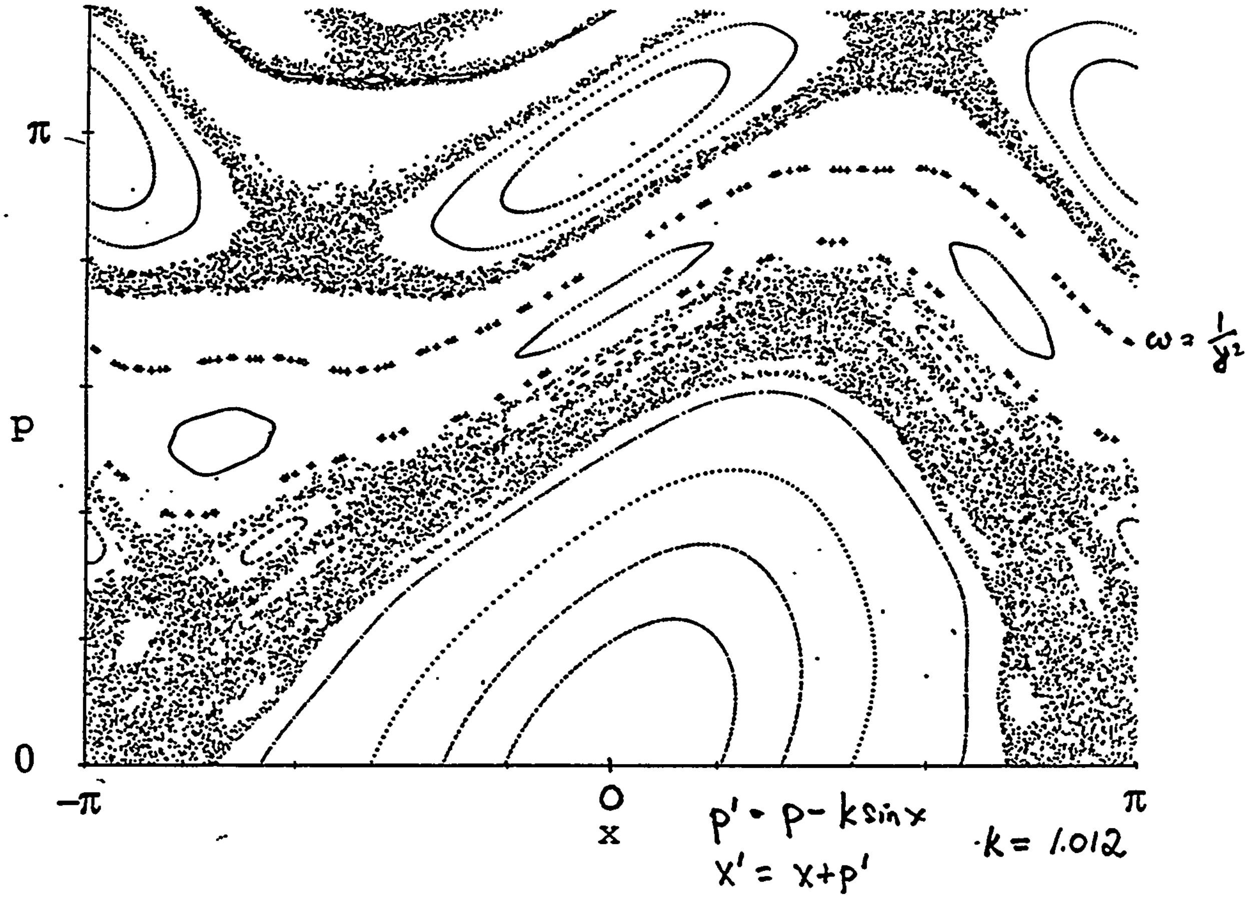

π
p
0
−π
0
x
π
ω = 1/γ²
p' = p − k sin x
x' = x + p'
k = 1.012

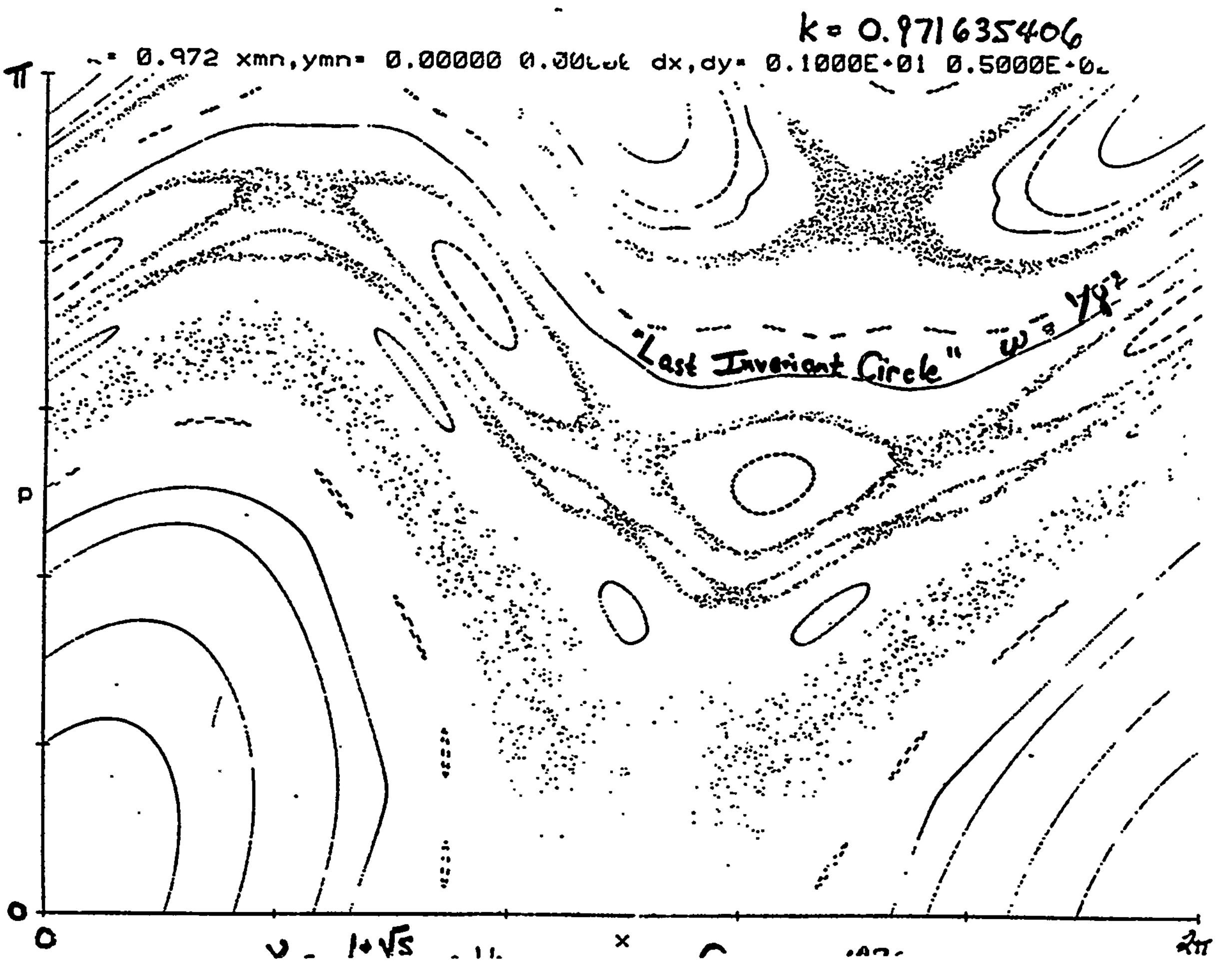

k = 0.971635406
0.972 xmn,ymn= 0.00000
dx,dy= 0.1000E+01
π
p
0
0
x
2π
"Last Invariant Circle"
ω = 1/γ²

III The Cantorus (or Aubry-Mather Set)

Percival, Aubry, Mather, Katok

Consider rotational invariant circle with irrational ν

Invariant set with gaps

1 gap

$\Downarrow$

2 gaps

$\Downarrow$

3 gaps

$\Downarrow$

$\vdots$

1) Because ν is irrational there are an ∞ of gaps

2) Total length of gaps finite – most very small

3) Cantorus is unstable orbit (not proved)

The Turnstile

Mackay, Meiss, Percival
Physica D '84

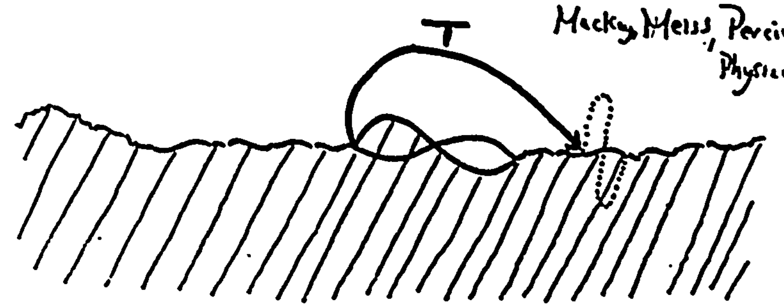

Define: "Below" cantorus } Relative to Partial Barrier
"Above" cantorus

In one iteration the area of one lobe, ΔW, crosses from "below" to "above"

$$\text{FLUX} = \Delta W$$

The partial barrier is an "almost" invariant curve ... in fact it is the <u>closest</u> one can get to an invariant <u>curve</u>!

Resonances, Std Map

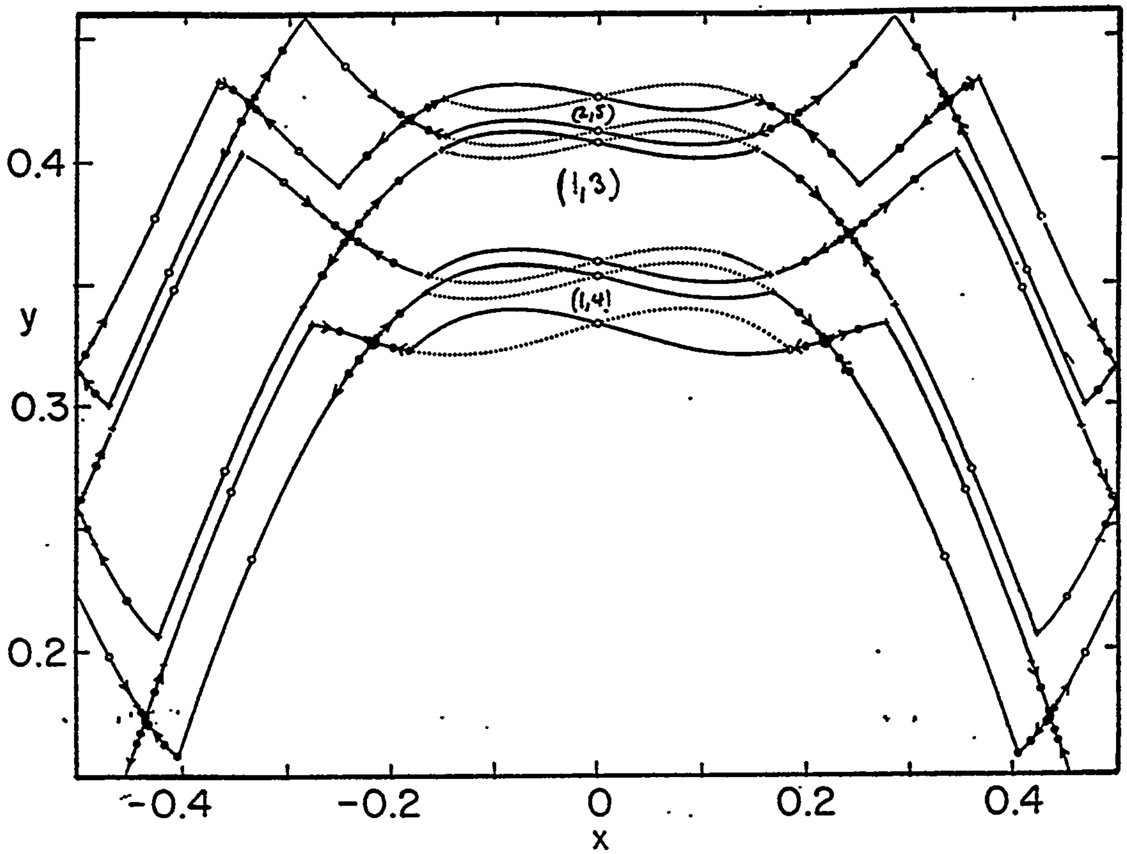

Period 5 Resonance

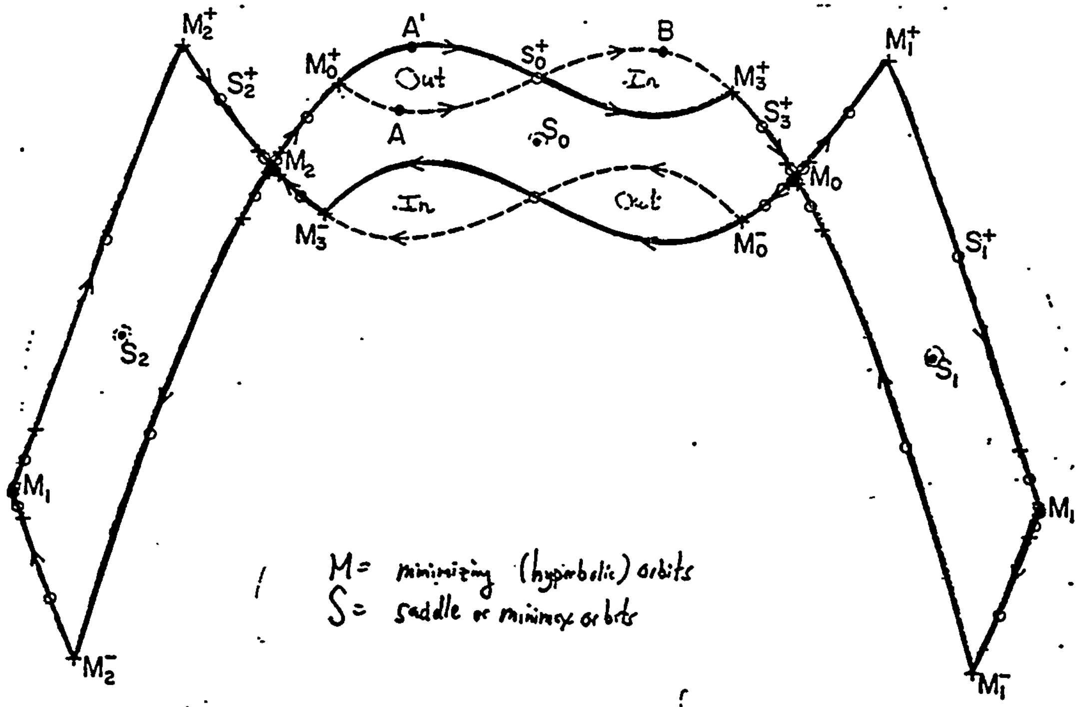

M = minimizing (hyperbolic) orbits
S = saddle or minimax orbits

from
MacKay, Meiss, & Percival

Fig 2.1

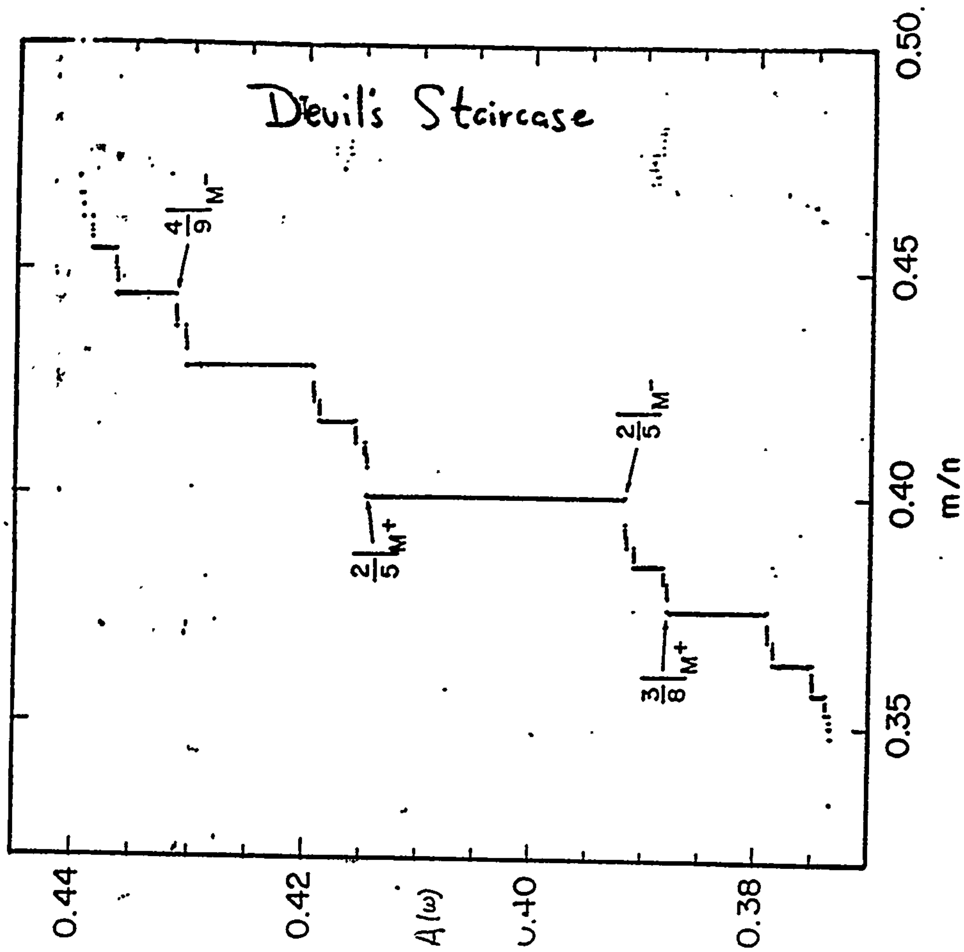

Fig 4.3

Area Und. Partial Separatrices

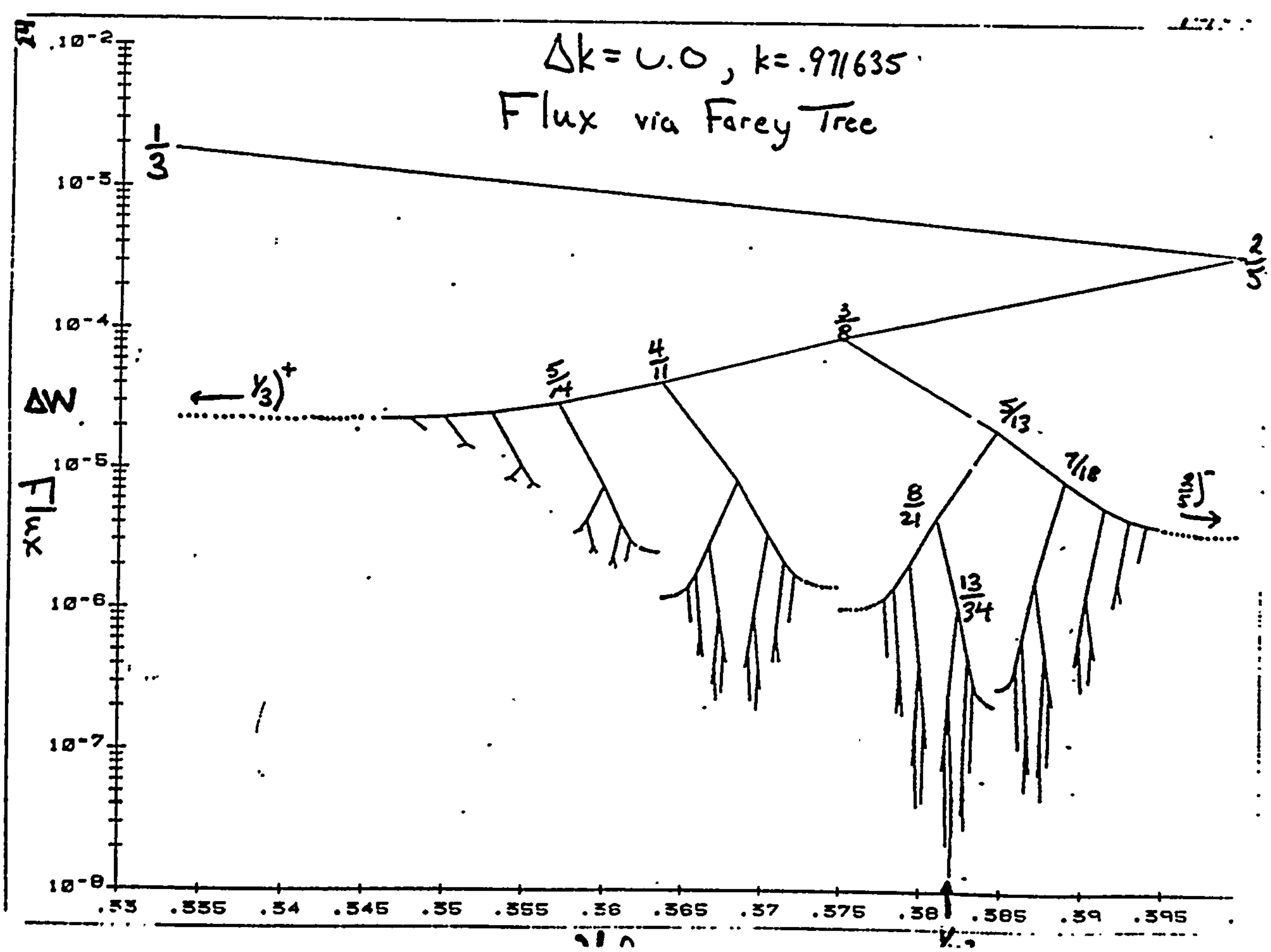

Anti-Integrable Limit & Cantori

MacKay & Meiss Nonlinearity 5, 14

Let $F(x,x')$ $x \in \mathbb{R}^d$ generate a map

$$T : (x,y) \to (x',y')$$

$$y = -\frac{\partial}{\partial x} F(x,x')$$ to solve for x' [illegible] requires a non-degeneracy condition, e.g. det $F_{12} \neq 0$

$$y' = \frac{\partial}{\partial x'} F(x,x')$$

we say F is an "Action Generating Function" & T is a symplectic (canonical) map

In fact orbits $\{x_t, y_t\}$ are determined by stationary points of the action W:

$$W[x_0, x_1, \dots x_n] = \sum_{t=0}^{n-1} F(x_t, x_{t+1})$$

$\delta W = 0$ for given x_0, x_n gives

$$\underbrace{F_2(x_{t-1}, x_t)}_{y_t} + \underbrace{F_1(x_t, x_{t+1})}_{-y_t} = 0$$

Ex: Std Map

$$F(x,x') = \underbrace{\tfrac{1}{2}(x'-x)^2}_{\text{Kinetic}} - \underbrace{V(x)}_{\text{potential}}, \quad V(x) = \frac{k}{4\pi^2}\cos(2\pi x)$$

Generally suppose

$$F(x,x') = \varepsilon T(x,x') - V(x)$$

KAM theory deals with the case of small $V(x)$ perturbations to Kinetic Term

The <u>anti-integrable limit</u> is $\varepsilon = 0$

$$F(x,x') \to -V(x)$$

<u>No</u> map is <u>generated</u>, however, we still have stationary configurations of W

$$W_0[x] = -\sum_{t=0}^{n-1} V(x_t)$$

$$\delta W = 0 \implies \frac{\partial V}{\partial x}(x_t) = 0$$

$\{x_t\}$ are critical pts of V;

Orbit in the A-I limit

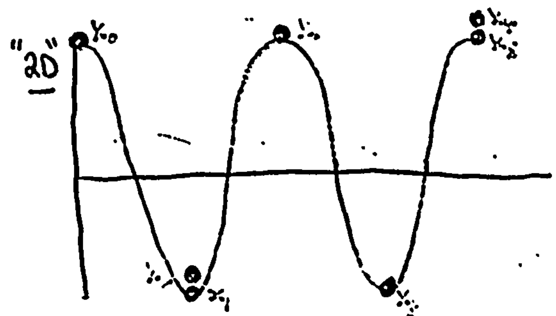

$\{x_0, x_1, x_2 \dots\}$
sequence of critical pts

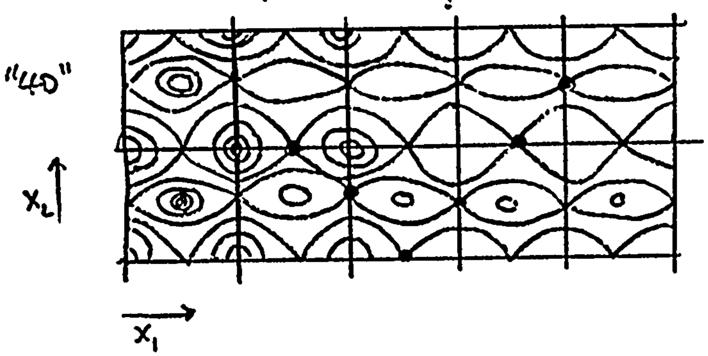

So any sequence of critical pts is an "orbit" at $\varepsilon = 0$

Query: Which sequences persist for $\varepsilon \neq 0$?

Theorem (Mackay-Meiss) Persistence of A-I orbits

Let $\{\dots x_t, x_{t+1}, x_{t+2} \dots\}$ be a sequence of nondegenerate critical points of $V(x)$ such that the acceleration

$$b\{x\} = \sup_t | x_{t+1} - 2x_t + x_{t-1} | \leq B$$

is finite. Then $\exists$ $\varepsilon_c(B)$ such that for $\varepsilon < \varepsilon_0$ there is an orbit of

$$F(x, x') = \varepsilon T(x, x') - V(x)$$

near $\sigma_\emptyset$ and it remains nondegenerate.

Choose sequence corresponding to a frequency ω

$$x_t = [t\omega] + x_0$$

$[t\omega]$: integer pt. x_0: a critical pt

Continuation of these gives Cantor Sets (cantori)

see Mackay & Meiss, Nonlinearity 5, 149 (92)

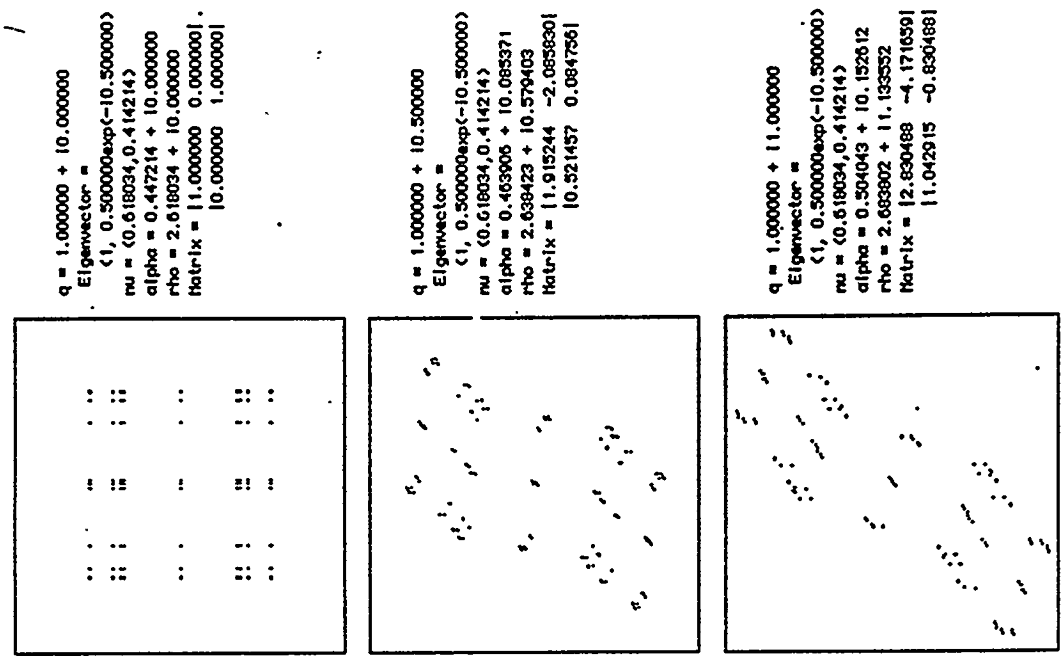

Example I

$\lambda q = (0.02, 0.03)$

B = rotation by 0.5

$\omega = [(3-\sqrt{5})/2, \sqrt{2}-1]$

Golden mean   silver mean

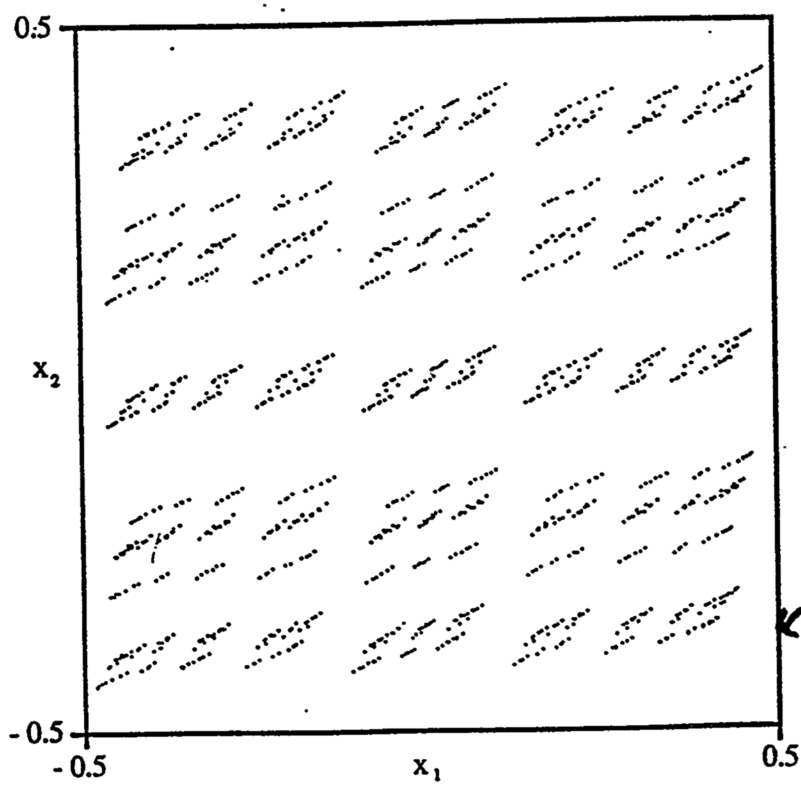

discontinuity surface

Transport

- Given a dynamics (flow, map)
- Given regions of interest, A & B (inside, the wall)

→ Find time to get to B from A

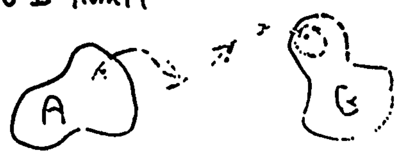

Examples

Particle Accelerators - keep particles trapped for 10^{10} revolutions

Plasma Confinement .. keep plasma confined for seconds

Fluid Mixing - find efficient, time independent mixers

Chemistry - compute reaction rates for simple reactions, $A+B \rightleftarrows AB$

Exit Times & Transit Times

Let f be a homeomorphism $f: M \circlearrowleft$

→ preserves a measure μ.

→ choose a set A

exit time for a point $a \in A$

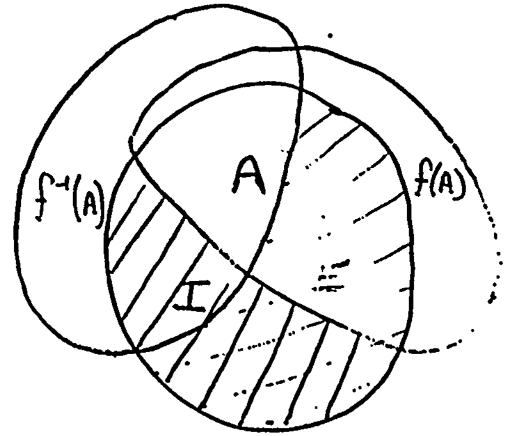

$$t^+(a) = \min_{n>0} \left(n : f^n(a) \notin A\right)$$

backwards exit time

$$t^-(a) = \min_{n>0} \left(n : f^{-n}(a) \notin A\right)$$

transit time

$$t_{transit}(a) = t^+(a) + t^-(a) - 1$$

= # of iterates orbit (a) remains in A.
(note: orbit invariant)

Exit Set for A

$E = \{a : t^+(a) = 1\} = A \setminus f^{-1}(A)$

Entry Set for A

$$I = \{a : t^-(a) = 1\} = A \setminus f(A)$$

Hénon Map

k=0.5

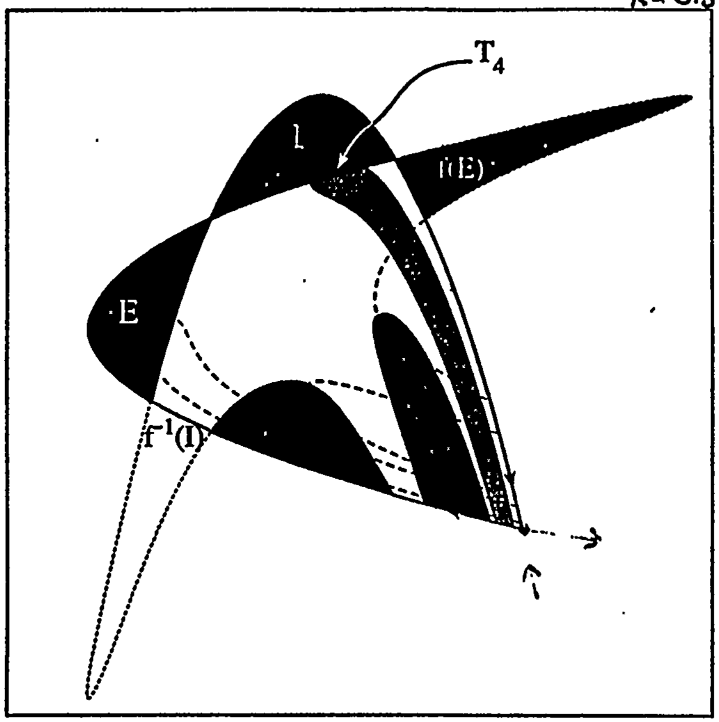

$$H : \begin{Bmatrix} x \to y - k + x^2 \\ y \to -x \end{Bmatrix}$$

$$x_f = -y_f = 1 + \sqrt{1+k}\ , \quad k > -1$$

Resonance + Lobe Areas
Hénon Map

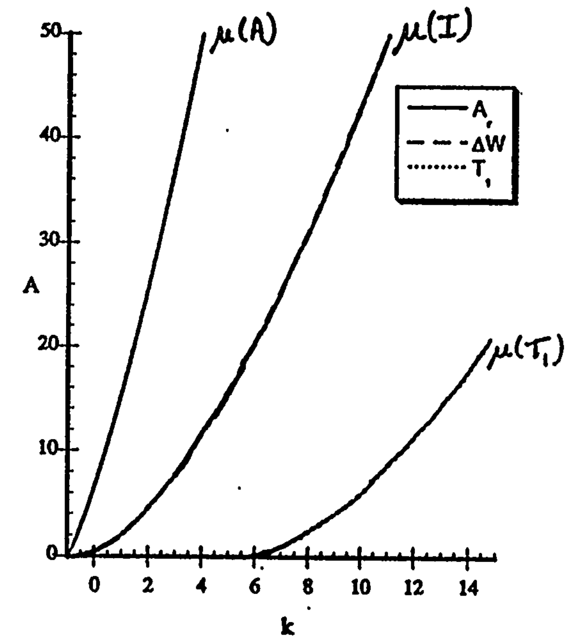

Compute these using MacKay-Meiss-Percival Action Formula

Area = Action(Homoclinic Orbit) − Action(Fixed Pt)

$$\text{Action} = W[x_t] = \sum_t F(x_t, x_{t+1})$$

$$F_\mu(x, x') = -xx' - kx + \tfrac{1}{3}x^3$$

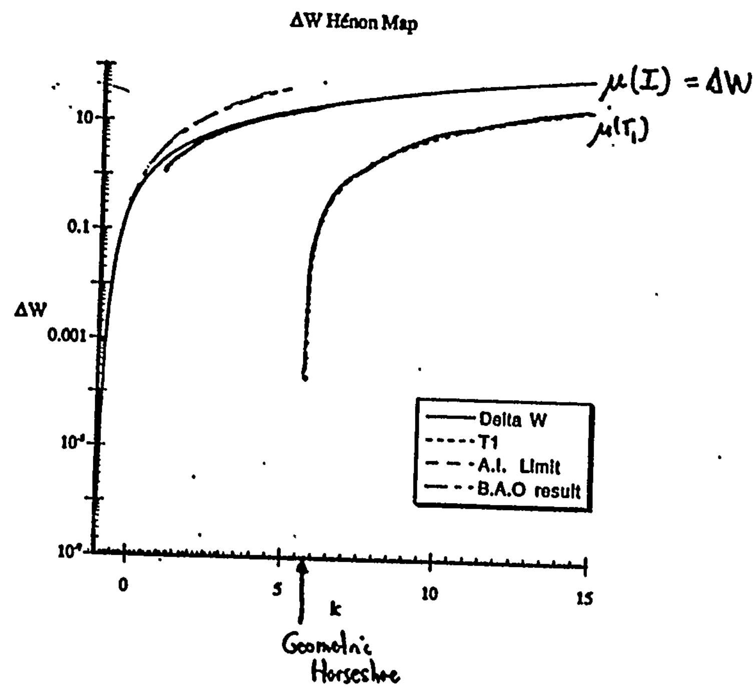

[illegible] Result (Transit [illegible])

$\Delta W =$ [illegible]

$\lambda =$ fixed pt multiplier

Anti-Integrable Limit (MacKay + Meiss)

$$\Delta W = \frac{4}{3}k^{3/2} + 4k + O(k^{?})$$

Transit Time Decomposition

Let T_j be the portion of I with transit time j (same as exit time)

$$T_j = I \cap f^{-j+1}(E)$$

① Note: the sets T_j are disjoint

② Measure preservation implies that almost every point that enters A must eventually exit, so

$$\mu(E) = \mu(I) = \sum_{j=1}^{\infty} \mu(T_j)$$

The transit time probability distribution is

$$P_t = \frac{\mu(T_t)}{\mu(I)}$$

so P_t = Prob of exit in t steps for points in I

The Survival probability is

$$P_{survival}(t) = \sum_{j=t+1}^{\infty} P_t .$$

Note $P_{surv.}(0) = 1$.

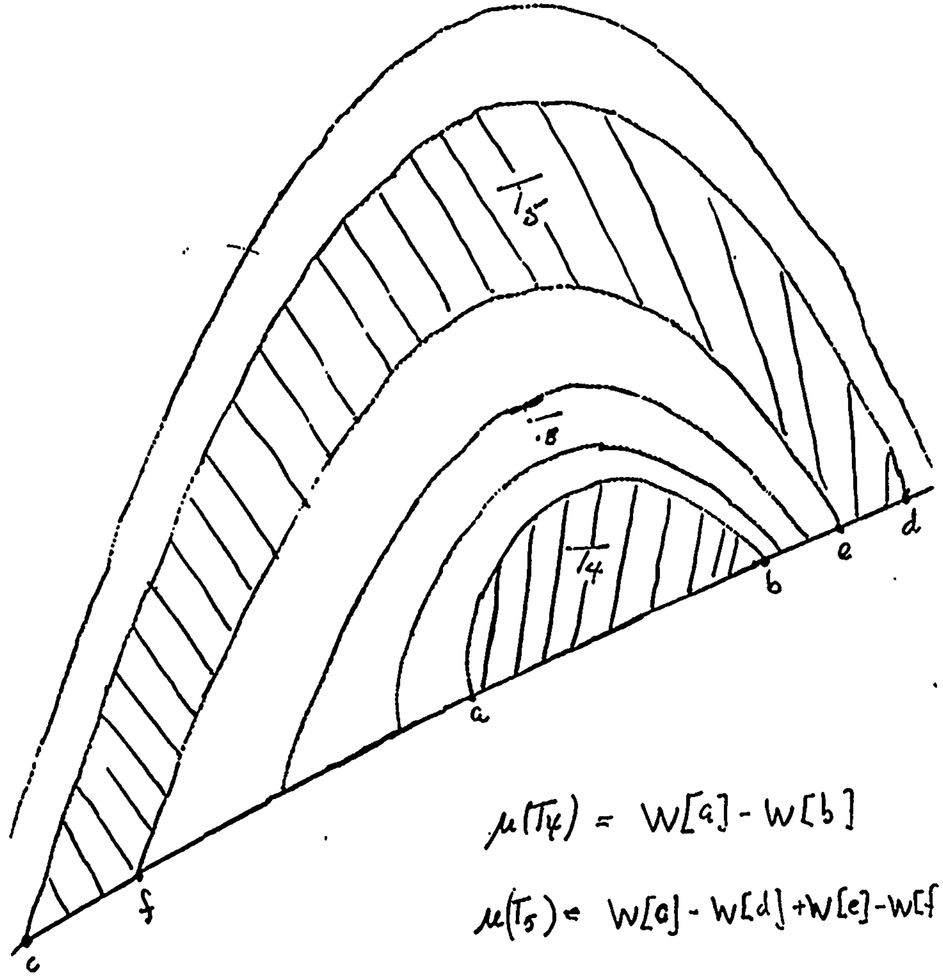

$\mu(T_4) = W[a] - W[b]$

$\mu(T_5) = W[c] - W[d] + W[e] - W[f]$

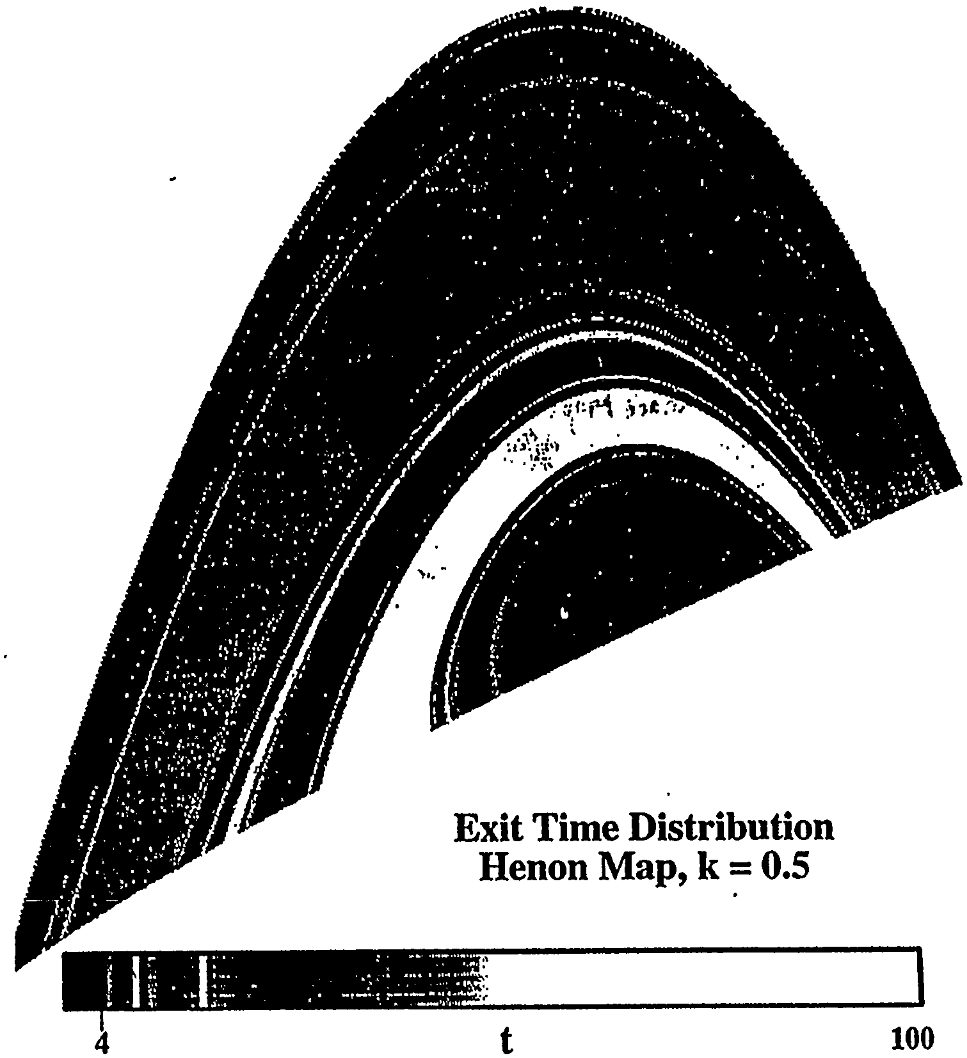

$$W[z] = \sum_{t=-\infty}^{\infty} \left[F(z_t, z_{t+1}) - F(x_f, x_f) \right]$$

$$F(x,x') = -x x' - k x + \tfrac{1}{3} x^3$$

Choice of region A is unimportant asymptotically:

Theorem (Easton '92) Any two isolating neighborhoods of a given invariant set have asymptotically similar survival sequences.

N is an isolating neighborhood if for some $i > 0$

$$f^{i}(N) \cap f^{-i}(N) \cap N \subset \text{interior}(N)$$

[illegible]

[illegible]

Ex: $R_{\text{exponential}}(p) = \sup_{z \geq 0} \{ z : P_t < e^{-zt} \text{ for } t \text{ large} \}$

$R_{\text{algebraic}}(p) = \sup_{z \geq 0} \{ z : P_t < \frac{1}{t^z} \text{ for } t \text{ large} \}$

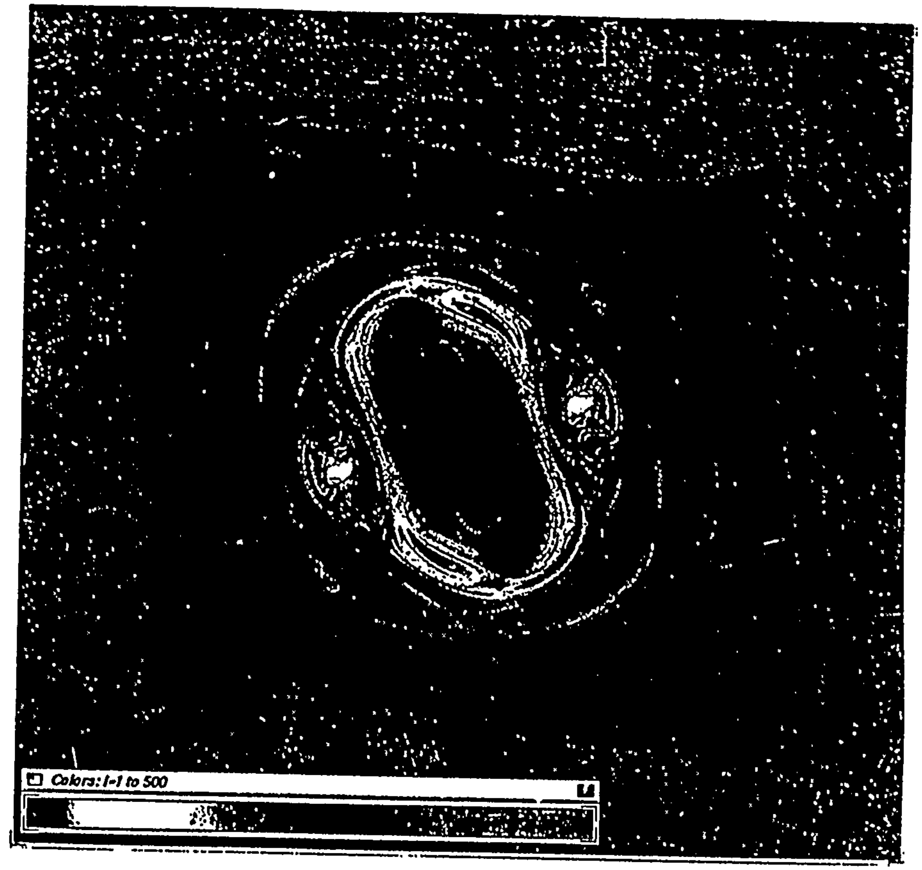

x_1-y_2 plane $x_2 = 0$

Froeschlé's Map $(a,b,c) = (3,1,0,0)$

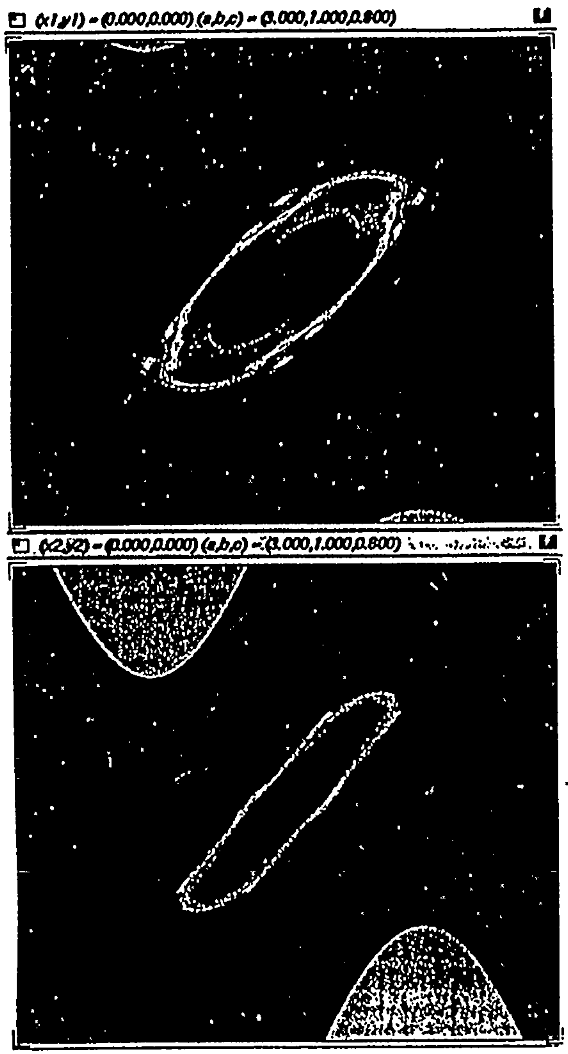

Froeschlé Map 500 iterates
Min. Escape time

Average Exit Time

Define $\langle t^+ \rangle_I = \frac{1}{\mu(I)} \int_I t^+( )$

Lemma: The average exit time for entering orbits is

$$\langle t^+ \rangle_I = \frac{\mu(A_{acc})}{\mu(I)}$$

where A_{acc} is the accessible subset of A (reached from outside)

$$A_{acc} = \{ x \in A : t^-(x) < \infty \}$$

Proof: Is elementary – Since $T_j \subset I$ are disjoint sets with exit time j we have

$$\langle t^+ \rangle_I = \frac{1}{\mu(I)} \sum_{j=1}^{\infty} j \mu(T_j)$$

one the otherhand $f^i(T_j) \quad i = 0, 1, \dots j-1$ are disjoint subsets of A and make-up the entire accessible part of A so

$$\mu(A_{acc}) = \mu\left(\bigcup_{j=1}^{\infty} \bigcup_{i=0}^{j-1} f^i(T_j) \right) = \sum_{j=1}^{\infty} \sum_{i=0}^{j-1} \mu(f^i(T_j))$$

by measure preservation

$$\mu(A_{acc}) = \sum_{j=1}^{\infty} j \mu(T_j)$$

Q.E.D.

Consequences

① Since $\mu(A_{acc}) = \sum_{j=1}^{\infty} j\,\mu(T_j) < \infty$

we must have $\mu(T_j) < O(j^{-2})$

so transit time distribution $\underline{P_t \sim t^{-z} \quad z > 2}$

② Kac's Theorem (see eg. Cornfeld, Fomin + Sinai)

Suppose $\mu(M) = 1$, then the average first return time to A is

$$\langle t_{return} \rangle_A = \frac{\mu(M_{acc})}{\mu(A)}$$

where M_{acc} is the portion of M accessible to orbits beginning in A

③ Suppose we average over A_{acc} instead of I, then

$$\langle t_{transit} \rangle_{A_{acc}} = \frac{1}{\mu(A_{acc})} \sum_{j=1}^{\infty} j^2 \mu(T_j)$$

$\underline{\underline{\text{if}}}$ the sum exists (but it need not ...)

Similarly

$$\langle t^{+} \rangle_{A_{acc}} = \frac{1}{2}\left(1 + \langle t_{transit} \rangle_{A_{acc}}\right)$$

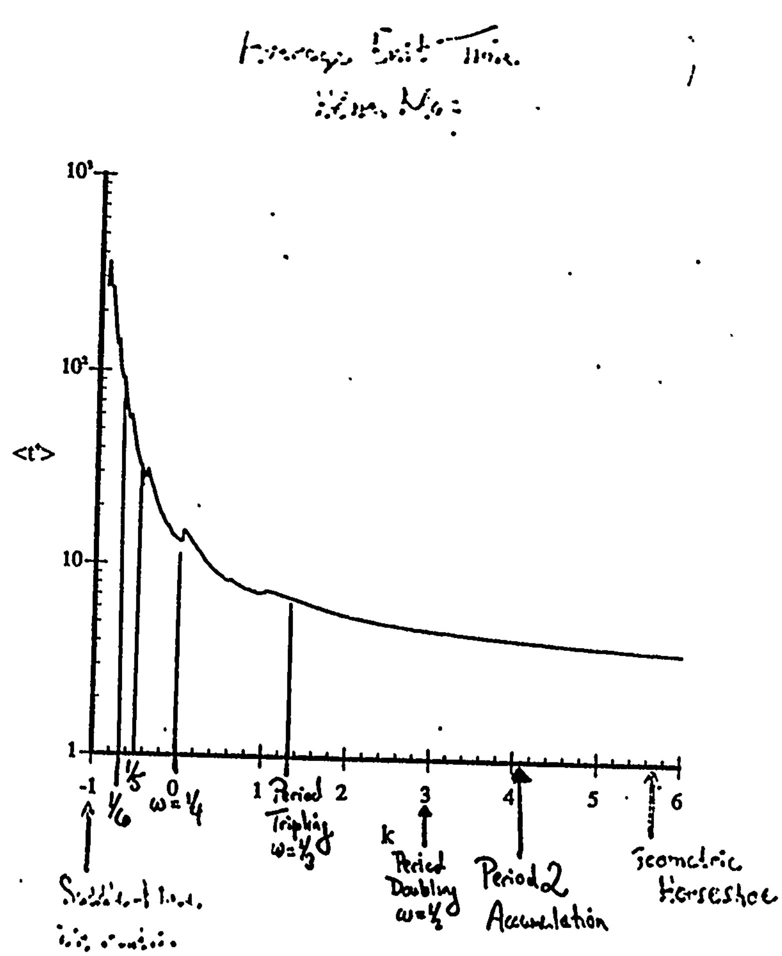

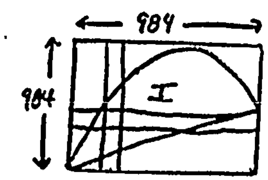

984×984 pixels
(window + title bar fits neatly on SGI screen)

Accessible Area, Hénon Map

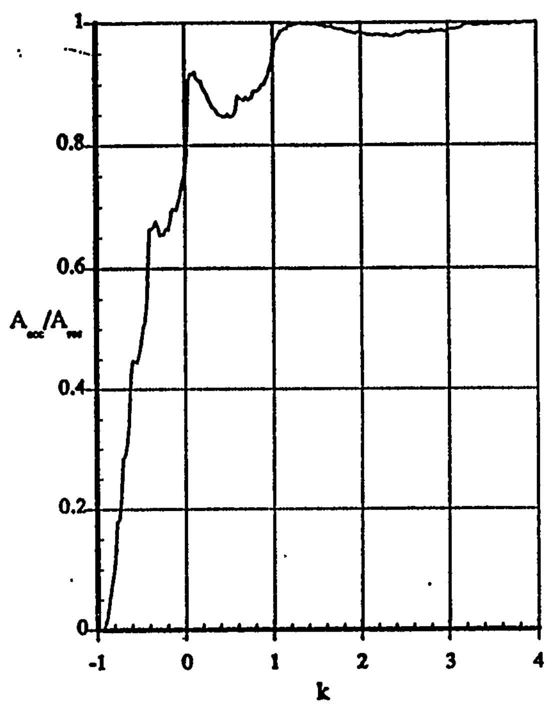

Inaccessible Area

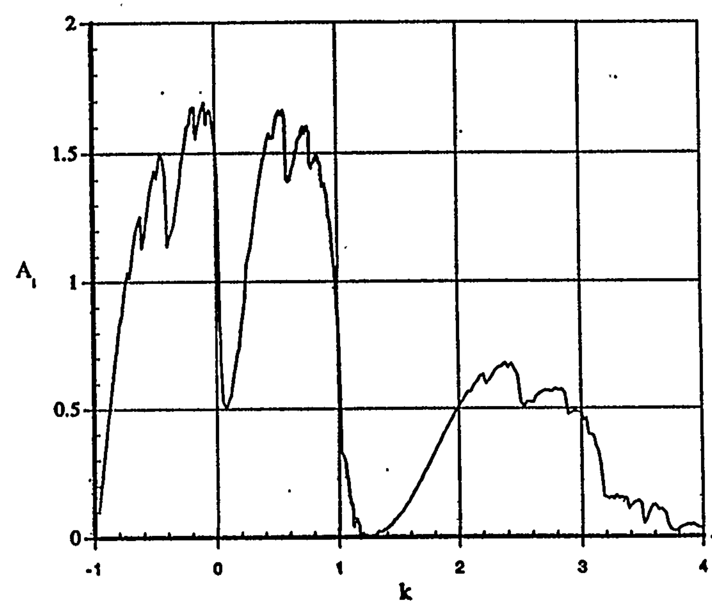

Inaccessible Fraction

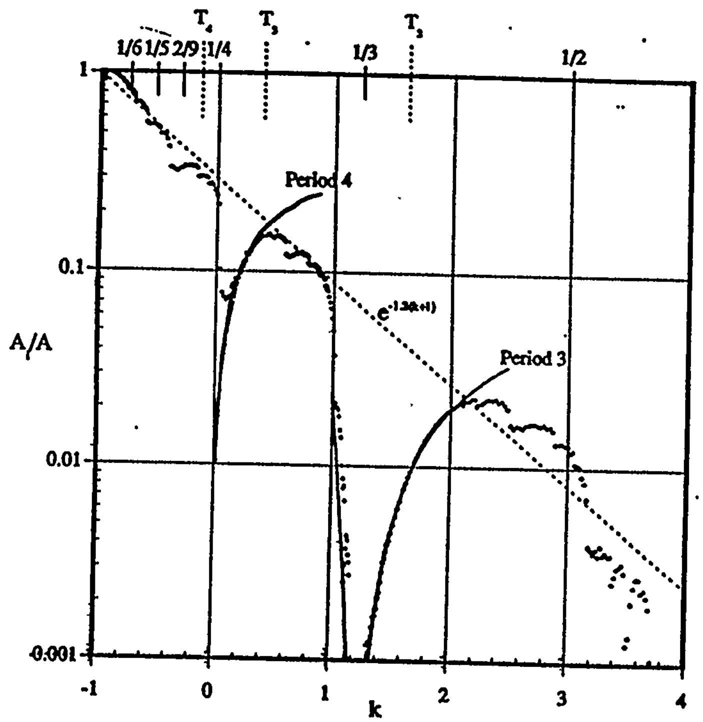

SYMPLECTIC GEOMETRY, MAPS, INTEGRATORS

J. Marsden, Cal Tech

Variational Principles and Symplectic-Momentum Integrators

Jerry Marsden and Jeff Wendlandt

Control and Dynamical Systems 116-81
California Institute of Technology
Pasadena, CA 91125

marsden@cds.caltech.edu

http://cds.caltech.edu/marsden/

&

Mechanical Engineering and EECS
University of California at Berkeley
Berkeley, CA 94720

wents@eecs.berkeley.edu

http://robotics.eecs.berkeley.edu/wents/

SOME MAIN POINTS

- Topics: variational principles for mechanical systems with symmetry with applications to integration algorithms.
- We construct in a systematic way, a class of integration algorithms based *directly* on variational principles using a discretization of Hamilton's principle (built on ideas of Veselov).
- General idea: directly discretize Hamilton's principle rather than the equations of motion in a way that preserves the original systems invariants, notably the symplectic form and, via a discrete version of Noether's theorem, the momentum map.
- The resulting mechanical integrators are second-order accurate, implicit, symplectic-momentum algorithms.
- The resulting integrators are applied to the **rigid body** and the **double spherical pendulum** to show that the techniques are competitive with existing integrators.
- The techniques here are systematic and theoretically attractive; constraints are handled efficiently.
- The relation with, eg, Verlet and Shake/Rattle is discussed.

Mechanical Integrators.

- Numerical integration methods that preserve energy, momentum, or the symplectic form, are called **mechanical integrators**.
- Mechnaical integrators often have good behavior for long time simulations.
- Literature is already huge (some given below). Some of this (eg, work of Ruth) was concerned with accelerator physics.
- A result of Ge and Marsden [1988] states, roughly speaking, that if the energy and momentum map include all the integrals of motion, then one cannot create integrators that are symplectic, energy preserving, *and* momentum preserving unless they coincidentally integrate the equations exactly up to a time parametrization
- Accordingly, the class of mechanical integrators divides into *symplectic-momentum* and *energy-momentum* integrators.
- By exploiting the structure of mechanical systems, one can hope to create mechanical integrators that are not only theoretically attractive, but are more computationally efficient and have good long term simulation properties.

Variational Integrators.

- We present a method to construct symplectic-momentum integrators for Lagrangian systems defined on a linear space with holonomic constraints.
- The constraint manifold, Q, is assumed to be embedded in a linear space V.
- A discrete version of the Lagrangian is formed and a discrete variational principle is applied to the discrete Lagrangian.
- The resulting discrete equations define a generally implicit numerical integration algorithm on $Q \times Q$ that approximates the flow of the continuous Euler-Lagrange equations on TQ.

- The algorithm equations are called the *discrete Euler-Lagrange (DEL)* equations or a *variational integrator (VI)*.
- The method need not preserve energy, but the numerical examples suggest that the energy oscillates about a constant value in many cases. The energy variations decrease and the constant value approaches the continuous energy as the step size decreases.
- Dissipation is often treated using time splitting (product formulas).

Brief Comments on the Literature.

- Our approach to the discrete variational principle is based on a long line of papers, such as Maeda [1981], Veselov [1988], Veselov [1991] and Moser and Veselov [1991], MacKay [1992] and Lewis and Kostelec [1996]. It is shown that the DEL equations preserve a symplectic form.
- Some authors discretize the principle of least action instead of Hamilton's principle: Itoh and Abe [1988] and Shibberu [1994]. The resulting equations explicitly enforce energy, and the equations preserve quadratic invariants.
- Energy-momentum integrators have been developed by Simo and his co-workers; for example, Simo and Tarnow [1992]. Energy-momentum integrators were derived based on discrete directional derivatives and discrete versions of Hamiltonian mechanics in Gonzalez [1996a]. Symplectic, momentum and energy conserving schemes for the rigid body are presented in Lewis and Simo [1995].
- The literature on symplectic schemes for Hamiltonian systems is vast: see Channell and Scovel [1990], Sanz-Serna [1991] and McLachlan and Scovel [1996] for background and references. References related to our work are Reich [1993], Reich [1994], McLachlan and Scovel [1995], and Jay [1996]. Reich [1993] gives an integration method for Hamiltonian systems that enforces position and velocity constraints in a way making the method symplectic.

It is shown in McLachlan and Scovel [1995] and in Reich [1994] that the algorithm also conserves momentum corresponding to a linear symmetry group when the constraint manifold is embedded in a linear space. See also Barth and Leimkuhler [1996a]. Leimkuhler and Patrick [1996] develop an intrinsic treatement of symplectic-momentum integrators on Riemannian manifolds using generating functions.

- The Verlet [1967] algorithm (and variants of it) is common in molecular dynamics simulations; see, for example, Leimkuhler and Skeel [1994]. An extension to handle holonomic constraints is the SHAKE algorithm (Ryckaert, Ciccotti and Berendsen [1977]). SHAKE was extended to handle velocity constraints with RATTLE in Anderson [1983]. For a presentation of the symplectic nature of the *Verlet*, SHAKE, and RATTLE algorithms, see Leimkuhler and Skeel [1994].
- Special choices of our construction reporduces the SHAKE algorithm.
- One may recover the *variational Verlet* algorithm from our construction if the Lagrangian system has no constraints (Gillilan and Wilson [1992]).

Accuracy and Energy as a Monitor.

- Our construction method produces 2-step methods that have a second order local truncation error. The position error in the numerical examples show second order convergence.
- One should be able to use the methods in Yoshida [1990] to increase the order of accuracy.
- In the simulations, we use energy as a monitor to catch any obvious problems, as in Channell and Scovel [1990] and Simo and Gonzalez [1993].
- It is still unknown if this is a generally reliable indicator of accuracy, but based on the Ge-Marsden result, it may well be. Another indication is the analysis with energy oscillation and nearby

Hamiltonian systems in Sanz-Serna [1991, p.277–278], Sanz-Serna and Calvo [1994, p. 139–140] and Sanz-Serna [1996].

- Energy conservation alone does not imply good performance as is shown in Ortiz [1986].

1 Variational Principles and Symmetry

- Hamilton's principle: one obtains the Euler-Lagrange equations from extremizing the integral of the Lagrangian subject to fixed endpoint conditions:

$$\delta \int_a^b L(q,\dot{q})\,dt = 0.$$

- One may obtain the conservation laws of Noether directly from Hamilton's principle
- Consider a Lie group G (with Lie algebra denoted $\mathcal{G}$) acting on a configuration manifold Q and lift this action to the tangent bundle TQ using the tangent operation.
- Given a G-invariant Lagrangian $L : TQ \to \mathbb{R}$, the corresponding momentum map is the mapping $\mathbf{J} : TQ \to \mathcal{G}^*$ defined by

$$\langle \mathbf{J}(v_q), \xi \rangle = \langle \mathcal{F}L(v_q), \xi_Q(q) \rangle \tag{1.1}$$

where $\mathcal{F}L : TQ \to T^*Q$ is the fiber derivative, and ξ_Q denotes the infinitesimal generator associated with a Lie algebra element $\xi \in \mathcal{G}$. *If you are not familiar with the notation, think of the momentum map* $\mathbf{J}$ *as a generalization of angular momentum.*

Theorem 1.1 (Classical Noether Theorem) *Along a solution of the Euler-Lagrange equations,* $\mathbf{J}$ *is a constant in time.*

The Rigid Body and Reduced Variational Principles.

- We regard an element $R \in \mathrm{SO}(3)$ giving the configuration of the body as a map of a *reference configuration* $\mathcal{B} \subset \mathbf{R}^3$ to the current configuration $R(\mathcal{B})$ taking a reference or label point $X \in \mathcal{B}$ to a current point $x = R(X) \in R(\mathcal{B})$.
- For a rigid body in motion, the matrix R is time dependent and the velocity of a point of the body is $\dot{x} = \dot{R}X = \dot{R}R^{-1}x$. Since R is an orthogonal matrix, $R^{-1}\dot{R}$ and $\dot{R}R^{-1}$ are skew matrices, and so we can write
$$\dot{x} = \dot{R}R^{-1}x = \omega \times x, \tag{1.2}$$
which defines the *spatial angular velocity* vector ω. The corresponding *body angular velocity* is defined by
$$\Omega = R^{-1}\omega, \quad i.e., \quad R^{-1}\dot{R}v = \Omega \times v \tag{1.3}$$
so that Ω is the angular velocity relative to a body fixed frame.
- The kinetic energy is
$$K = \frac{1}{2}\int_{\mathcal{B}} \rho(X)\|\dot{R}X\|^2 d^3X, \tag{1.4}$$
where ρ is a given mass density. Since
$$\|\dot{R}X\| = \|\omega \times x\| = \|R^{-1}(\omega \times x)\| = \|\Omega \times X\|,$$
K is a quadratic function of Ω. Writing $K = \Omega^T \mathcal{I}\Omega/2$ defines the *moment of inertia tensor* $\mathcal{I}$. This quadratic form, can be diagonalized, and this defines the *principal axes and moments of inertia*. In this basis, we write $\mathcal{I} = \mathrm{diag}(I_1, I_2, I_3)$.

The well known relation between the motion in R space and in Ω space is as follows:

Theorem 1.2 *The curve $R(t) \in \mathrm{SO}(3)$ satisfies Hamilton's principle, i.e., the Euler-Lagrange equations for*
$$L(R, \dot{R}) = \frac{1}{2}\int_{\mathcal{B}} \rho(X)\|\dot{R}X\|^2 d^3X \tag{1.5}$$
if and only if $\Omega(t)$ defined by $R^{-1}\dot{R}v = \Omega \times v$ for all $v \in \mathbf{R}^3$ satisfies Euler's equations: $\mathcal{I}\dot{\Omega} = \mathcal{I}\Omega \times \Omega$.

Theorem 1.3 *Hamilton's principle $\delta \int_a^b L\,dt = 0$ on $\mathrm{SO}(3)$ is equivalent to the reduced variational principle $\delta \int_a^b l\,dt = 0$ on $\mathbf{R}^3$ where the variations $\delta\Omega$ are of the form $\delta\Omega = \dot{\Sigma} + \Omega \times \Sigma$ with $\Sigma(a) = \Sigma(b) = 0$.*

The Euler-Poincaré Equations and Variational Principles. There is a generalization of the rigid body equations to general Lie groups using the Euler-Lagrange equations and the variational principle as a starting point.

Theorem 1.4 *Let G be a Lie group and $L : TG \to \mathbf{R}$ a left invariant Lagrangian. Let $l : \mathcal{G} \to \mathbf{R}$ be its restriction to the identity. For a curve $g(t) \in G$, let $\xi(t) = g(t)^{-1} \cdot \dot{g}(t)$; i.e., $\xi(t) = T_{g(t)}L_{g(t)^{-1}}\dot{g}(t)$. Then the following are equivalent*

- *$g(t)$ satisfies the Euler-Lagrange equations for L on G*
- *Hamilton's principle holds, for variations with fixed endpoints*
- *the* Euler-Poincaré equations *hold:*
$$\frac{d}{dt}\frac{\delta l}{\delta \xi} = \mathrm{ad}^*_\xi \frac{\delta l}{\delta \xi} \tag{1.6}$$
- *the variational principle*
$$\delta \int l(\xi(t))dt = 0$$
holds on $\mathcal{G}$, using variations of the form $\delta\xi = \dot{\eta} + [\xi, \eta]$ where η vanishes at the endpoints.

In coordinates on the Lie algebra, the Euler-Poincaré equations read as follows
$$\frac{d}{dt}\frac{\partial l}{\partial \xi^d} = C^b_{ad}\frac{\partial l}{\partial \xi^b}\xi^a, \tag{1.7}$$
where C^b_{ad} are the structure constants of the Lie algebra.

This discussion was generalized to arbitrary configuration spaces and symmetry groups by Marsden and Scheurle [1993b] who developed the general *Reduced Euler-Lagrange Equations.*

2 Generalities on Integration Algorithms

General Integrators.

- An algorithm on a phase space P is a collection of maps $F_\tau : P \to P$ depending on a small real parameter τ and $z \in P$). Sometimes we write $z^{k+1} = F_\tau(z^k)$ for the algorithm and we write Δt or h for the *step size* τ.
- An algorithm is **consistent** or is **first order accurate** with a vector field X on P if

$$\frac{d}{d\tau}F_\tau(z)\bigg|_{\tau=0} = X(z). \tag{2.1}$$

(Higher order accuracy is defined similarly using Taylor series).

- We say the algorithm is **convergent** when

$$\lim_{n\to\infty}(F_{t/n})^n(z) = \varphi_t(z) \tag{2.2}$$

where φ_t is the flow of X. Of course one is also interested in the error estimates.

- Some general theorems guarantee convergence, with an important hypothesis being **stability**; *i.e.,* $(F_{t/n})^n(z)$ must remain close to z for small t and all $n = 1, 2, \ldots$. (See Chorin, Hughes, Marsden and McCracken [1978] and Abraham, Marsden and Ratiu [1988] for details.) For example, one has the Lie-Trotter formula

$$e^{t(A+B)} = \lim_{n\to\infty}(e^{tA/n}e^{tB/n})^n \tag{2.3}$$

for the time-splitting of linear problems and their nonlinear generalizations.

Mechanical Integrators.

- For a Hamiltonian system on a symplectic manifold which has symmetry, an algorithm F_τ is a **symplectic-integrator** if each F_τ is symplectic, an **energy-integrator** if $H \circ F_\tau = H$ (where $X = X_H$), a **momentum-integrator** if $\mathbf{J} \circ F_\tau = \mathbf{J}$. (If an integrator has one of these three properties, then so does any iterate of it.)

Example 1. A first order explicit symplectic scheme in the plane is $(q_0, p_0) \mapsto (q, p)$ defined by

$$\begin{aligned} q &= q_0 + (\Delta t)p_0 \\ p &= p_0 - (\Delta t)V'(q_0 + (\Delta t)p_0). \end{aligned} \tag{2.4}$$

This map is consistent with the flow of Hamilton's equations for the Hamiltonian $H = (p^2/2) + V(q)$.

Example 2. An implicit second order symplectic scheme in the plane for the same Hamiltonian as in Example 1 is

$$\begin{aligned} q &= q_0 + (\Delta t)(p + p_0)/2 \\ p &= p_0 - (\Delta t)V'((q + q_0)/2). \end{aligned} \tag{2.5}$$

The second order accurate mid-point rule is symplectic (Feng [1987]).

Example 3. In a symplectic vector space the *mid point rule* is symplectic:

$$\frac{z^{k+1} - z^k}{\Delta t} = X_H\left(\frac{z^k + z^{k+1}}{2}\right). \tag{2.6}$$

Symplecticity is shown using the *Cayley transform.*

Example 4. An implicit energy preserving algorithm (from Chorin, Hughes, Marsden and McCracken [1978].) Consider a Hamiltonian system for $\mathbf{q} \in \mathbb{R}^n$ and $\mathbf{p} \in \mathbb{R}^n$:

$$\dot{\mathbf{q}} = \frac{\partial H}{\partial \mathbf{p}}, \quad \dot{\mathbf{p}} = -\frac{\partial H}{\partial \mathbf{q}}. \tag{2.7}$$

Define the following implicit scheme

$$\mathbf{q}_{n+1} = \mathbf{q}_n + \Delta t\frac{H(\mathbf{q}_{n+1}, \mathbf{p}_{n+1}) - H(\mathbf{q}_{n+1}, \mathbf{p}_n)}{\lambda^T(\mathbf{p}_{n+1} - \mathbf{p}_n)}\lambda, \tag{2.8}$$

$$\mathbf{p}_{n+1} = \mathbf{p}_n - \Delta t\frac{H(\mathbf{q}_{n+1}, \mathbf{p}_n) - H(\mathbf{q}_n, \mathbf{p}_n)}{\mu^T(\mathbf{q}_{n+1} - \mathbf{q}_n)}\mu, \tag{2.9}$$

where

$$\lambda = \frac{\partial H}{\partial \mathbf{p}}(\alpha\mathbf{q}_{n+1} + (1-\alpha)\mathbf{q}_n, \beta\mathbf{p}_{n+1} + (1-\beta)\mathbf{p}_n), \tag{2.10}$$

$$\mu = \frac{\partial H}{\partial \mathrm{q}}(\gamma \mathrm{q}_{n+1} + (1-\gamma)\mathrm{q}_n, \delta \mathrm{p}_{n+1} + (1-\delta)\mathrm{p}_n), \tag{2.11}$$

and where $\alpha, \beta, \gamma, \delta$ are arbitrarily chosen constants in $[0,1]$.

This algorithm is consistent and energy preserving, but is not symplectic.

Example 5. Simple pendulum:

$$\frac{d}{dt}\begin{pmatrix} \varphi \\ p \end{pmatrix} = \begin{pmatrix} p \\ 0 \end{pmatrix} + \begin{pmatrix} 0 \\ -\sin\varphi \end{pmatrix}.$$

Each vector field in the sum can be integrated explicitly to give maps $G_\tau(\varphi, p) = (\varphi + \tau p, p)$ and $H_\tau(\varphi, p) = (\varphi, p - \tau \sin\varphi)$, each of which is symplectic. Thus, the composition $F_\tau = G_\tau \circ H_\tau$, namely,

$$F_\tau(q,p) = (\varphi + \tau p - \tau^2 \sin\varphi, p - \tau\sin\varphi)$$

is a first order symplectic scheme, closely related to the *standard map*. The orbits of F_τ need not preserve energy and they may be chaotic, whereas the trajectories of the simple pendulum are of course not chaotic.

There are many more examples of this type, including symplectic Runge-Kutta schemes. All the implicit members of the Newmark family, perhaps the most widely used time-stepping algorithms in nonlinear structural dynamics, *are not designed to conserve energy and also fail to conserve momentum.* Among the explicit members, only the central difference method preserves momentum (see Simo, Tarnow and Wong [1991]).

An algorithm is **group equivariant** if each F_h commutes with the action of the given symmetry group. To derive momentum-conservative algorithms, one should look for algorithms to be group equivariant. There are general theorems to this effect, and in our context of discrete versions of Hamilton's principle, this is exactly what happens.

3 The Discrete Variational Principle

The Discrete Variational Principle.

- **A discrete Lagrangian** on a configuration manifold Q is a map $\mathcal{L} : Q \times Q \to \mathbf{R}$. Fixing a positive integer N, **the action sum** is the map $\mathcal{S} : Q^{N+1} \to \mathbf{R}$ defined by

$$\mathcal{S} = \sum_{k=0}^{N-1} \mathcal{L}(q_{k+1}, q_k), \tag{3.1}$$

where $q_k \in Q$ and $k \in \mathbf{z}$ is the discrete time.

- **The discrete variational principle** states that the evolution equations extremize the action sum given fixed end points, q_0 and q_N.

- Extremizing $\mathcal{S}$ over $q_1, \cdots, q_{N-1}$ leads to the DEL equations:

$$D_2\mathcal{L}(q_{k+1}, q_k) + D_1\mathcal{L}(q_k, q_{k-1}) = 0 \tag{3.2}$$

for all $k = 1, \cdots, N-1$, *i.e.*,

$$D_2\mathcal{L} \circ \Phi + D_1\mathcal{L} = 0, \tag{3.3}$$

where $\Phi : Q \times Q \to Q \times Q$ is defined implicitly by $\Phi(q_k, q_{k-1}) = (q_{k+1}, q_k)$.

- If $D_2\mathcal{L}$ is invertible, then Equation (3.3) defines the discrete map, Φ, which flows the system forward in discrete time.

Conservation of the Symplectic Structure.

- **The discrete fiber derivative** is defined by

$$\mathcal{FL} : Q \times Q \to T^*Q; \qquad (q_1, q_0) \mapsto (q_0, D_2\mathcal{L}(q_1, q_0)) \tag{3.4}$$

- define a 2-form ω on $Q \times Q$ by pulling back the canonical 2-form Ω_{CAN} on T^*Q:

$$\omega = \mathcal{FL}^*(\Omega_{\mathrm{CAN}}) = \mathcal{FL}^*(-\mathrm{d}\Theta_{\mathrm{CAN}}) = -\mathrm{d}(\mathcal{FL}^*(\Theta_{\mathrm{CAN}})), \tag{3.5}$$

where $\mathbf{d}$ is the exterior derivative. Choose coordinates, q^i, on Q and choose the canonical coordinates, (q^i, p_i), on T^*Q. In these coordinates, $\Omega_{\mathrm{CAN}} = dq^i \wedge dp_i$ and $\Theta_{\mathrm{CAN}} = p_i dq^i$.

- The DEL equations are

$$-\frac{\partial \mathcal{L}}{\partial q_k^i} \circ \Phi\left(q_{k+1}, q_k\right) + \frac{\partial \mathcal{L}}{\partial q_{k+1}^i}\left(q_{k+1}, q_k\right) = 0 \tag{3.6}$$

i.e.,

$$\frac{\partial \mathcal{L}}{\partial q_{k+1}^i}\left(q_{k+2}, q_{k+1}\right) + \frac{\partial \mathcal{L}}{\partial q_{k+1}^i}\left(q_{k+1}, q_k\right) = 0. \tag{3.7}$$

The symplectic form is

$$\omega = \frac{\partial^2 \mathcal{L}}{\partial q_k^i \partial q_{k+1}^j}\left(q_{k+1}, q_k\right) dq_k^i \wedge dq_{k+1}^j. \tag{3.8}$$

Theorem 3.1 *The map Φ preserves the symplectic form ω, i.e. $\Phi^*\omega = \omega$ where $\Phi^*\omega$ denotes the pullback of ω by the map Φ.*

This means that when the algorithm is transferred to the cotangent bundle via the discrete fiber derivative, one gets a symplectic integrator for the standard symplectic structure. The proof of the theorem is a rather simple verification in this set up.

The Discrete Noether Theorem.

- Assume $\mathcal{L}$ is invariant under G and let $\xi \in \mathcal{G}$.
- Invariance of $\mathcal{L}$ and the DEL equations gives

$$D_2\mathcal{L}(q_{k+2}, q_{k+1}) \cdot \xi_Q(q_{k+1}) - D_2\mathcal{L}(q_{k+1}, q_k) \cdot \xi_Q(q_k) = 0. \tag{3.9}$$

- If we define the momentum map, $\mathcal{J} : Q \times Q \to \mathcal{G}^*$, by

$$\langle \mathcal{J}(q_{k+1}, q_k), \xi \rangle \triangleq \langle D_2\mathcal{L}(q_{k+1}, q_k), \xi_Q(q_k) \rangle, \tag{3.10}$$

then (3.9) shows that the momentum map is preserved by $\Phi : Q \times Q \to Q \times Q$:

Theorem 3.2 *Assume that the discrete Lagrangian $\mathcal{L}$ is invariant under the diagonal action of a Lie group G and let the discrete momentum map be defined by (3.10). Then $\mathcal{J} \circ \Phi = \mathcal{J}$.*

4 Construction of Mechanical Integrators

Constrained Formulation.

- Consider a mechanical system on a vector space V with constraints $Q \subset V$, and and unconstrained Lagrangian $L : TQ \to \mathbb{R}$; the *constrained Lagrangian* is its restriction $L^c : TQ \to \mathbb{R}$.
- Given: a vector valued constraint function, $g : V \to \mathbb{R}^k$, such that $g^{-1}(0) = Q \subset V$, with 0 a regular value of g.
- **The discrete, unconstrained Lagrangian,** $\mathcal{L} : V \times V \to \mathbb{R}$ is

$$\mathcal{L}(y, x) = L\left(\frac{y+x}{2}, \frac{y-x}{h}\right), \tag{4.1}$$

where $h \in \mathbb{R}_+$ is the time step.

- **The discrete unconstrained action sum** is defined by

$$\mathcal{S} = \sum_{k=0}^{N-1} \mathcal{L}\left(v_{k+1}, v_k\right). \tag{4.2}$$

- Extremize $\mathcal{S} : V^{N+1} \to \mathbb{R}$ subject to the constraint $v_k \in Q$. Lagrange multipliers gives

$$D_2\mathcal{L}\left(v_{k+1}, v_k\right) + D_1\mathcal{L}\left(v_k, v_{k-1}\right) + \lambda_k^T Dg\left(v_k\right) = 0 \tag{4.3}$$

(no sum over k), with constraints $g\left(v_k\right) = 0$, for all $k+1, \cdots, N-1$.

- Algorithm: For $v_k, v_{k-1} \in Q \subset V$, solve (4.3) along with the constraints $g\left(v_{k+1}\right) = 0$ for v_{k+1} and λ_k.

Example: if the continuous Lagrangian system is of the form

$$L(q, \dot{q}) = \frac{1}{2}\dot{q}^T M \dot{q} - V(q) \tag{4.4}$$

with constraints $g(q) = 0$, where M is a constant mass matrix, and V is the potential energy, then the DEL equations are

$$M\left(\frac{v_{k+1} - 2v_k + v_{k-1}}{h^2}\right) + \frac{1}{2}\left(\frac{\partial V}{\partial q}\left(\frac{v_{k+1} + v_k}{2}\right) + \frac{\partial V}{\partial q}\left(\frac{v_k + v_{k-1}}{2}\right)\right)$$
$$-D^T g\left(v_k\right)\lambda_k = 0.$$

Intrinsic (generalized coordinate) Formulation.

- Summary: Form the discrete Lagrangian and the action sum restricted to $Q \subset V$, and then perform the extremization on Q.
- The constrained, discrete Lagrangian is the map $\mathcal{L}^c : Q \times Q \to \mathbf{R}$, defined by $\mathcal{L}^c = \mathcal{L}|_{Q\times Q}$.
- The constrained action sum is

$$\mathcal{S}^c = \sum_{k=0}^{N-1} \mathcal{L}^c(q_{k+1}, q_k). \tag{4.5}$$

- Extremizing $\mathcal{S}^c : Q^{N+1} \to \mathbf{R}$ gives the intrinsic discrete Euler-Lagrange (DEL) equations:

$$D_2\mathcal{L}^c(q_{k+1}, q_k) + D_1\mathcal{L}^c(q_k, q_{k-1}) = 0. \tag{4.6}$$

- We solve for q_{k+1} given q_k and q_{k-1} to advance the flow one time step.

Equivalence of the Formulations. *The constrained and generalized coordinate formulations are in fact equivalent!*

Strategy.

- Solve the DEL equations using Newton-Raphson equation solvers.
- These solvers require the construction of a Jacobian. For many applications, the resulting Jacobian is *nearly symmetric and sparse*; this and scaling tricks can be exploited to increase the simulation efficiency.
- For tree structured multibody systems, the linear equations involving the Jacobian can be solved in linear time. Sparse matrix techniques and symplectic integration are also used for multibody systems in Barth and Leimkuhler [1996a].

Local Truncation Error and Solvability.

- The local truncation error of the method is *second order*. The coefficient of the h^2 term is a lengthy expression involving second, third, and fourth partial derivatives of $L : TV \to \mathbf{R}$.
- If one uses the discrete Lagrangian:

$$\mathcal{L}(y, x) = L\left(y, \frac{y-x}{h}\right),$$

then the resulting DEL equations will only be first order accurate for a general Lagrangian. However, in some cases, the resulting DEL equations may be explicit while the DEL equations earlier are implicit.

Summary of the Theory. *If one constructs integrators using a discretization of Hamilton's principle then one gets, in a natural way, second order accurate integrators that* exactly *preserve the symplectic structure and the momentum map associated to any symmetry group.*

5 Numerical Examples

The Rigid Body.

- Why use quaterniions (Related to Cayley-Klein parameters)? Avoids coordinate patching (essential for chaotic tumbling if the system is perturbed) and the constraints are few.
- The algorithm updates quaternion variables.
- The configuration manifold is $Q = S^3 \subset V$ where $V = \mathbf{R}^4$. The three sphere is isomorphic to $SU(2)$ which is a double cover of $SO(3)$.
- Literature: Rigid body integrators that preserve certain mechanical properties have been created by several researchers as we noted in the introduction. An energy-momentum integrator is presented in Simo and Wong [1991]. A symplectic integrator which preserves

the momentum and energy is presented in Lewis and Simo [1995]. A symplectic-momentum integrator is presented in McLachlan and Scovel [1995]. A rigid body integrator based on a discrete variational principle and in terms of 3×3 matrices with constraints is presented in Moser and Veselov [1991].

Example Simulation The DEL equations for the rigid body and relevant Jacobian are created in Mathematica and exported to C-code for simulation. The initial conditions and rigid body parameters are

$$q_0 = \begin{bmatrix} 1 \\ 0 \\ 0 \\ 0 \end{bmatrix}; \quad \omega_b = \begin{bmatrix} 0 \\ 3 \\ 4 \end{bmatrix}; \quad \mathcal{I} = \begin{bmatrix} 1 & 0 & 0 \\ 0 & 2 & 0 \\ 0 & 0 & 3 \end{bmatrix}. \qquad (5.1)$$

The error versus time step is shown in Figure 5.1. The plot shows a second order relationship between error and time step, consistent with the theory.

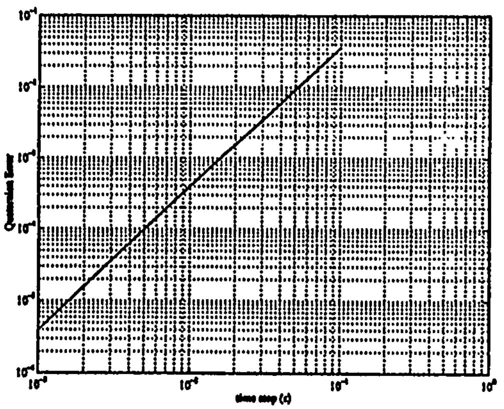

Figure 5.1: Quaternion Error Versus Time Step

Figure 5.2 compares the plot of the quaternion, q_y, versus time for the simulations at $h = 10^{-4}$s and $h = 10^{-1}$s. The trajectory for the large time step exhibits the same qualitative behavior as the small time step, but the deviations increase for longer simulation times.

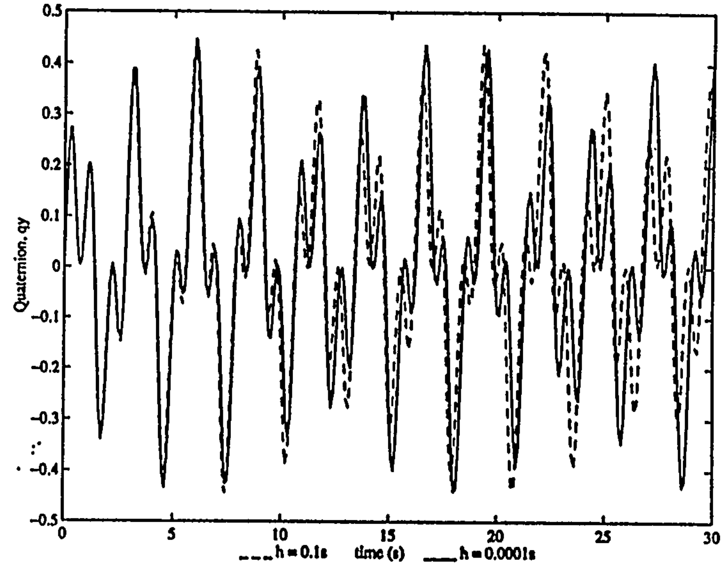

Figure 5.2: Quaternion Coordinate Versus Time

The energy error versus time step reveals a second order relationship between energy error and time step. The energy for the $h = 10^{-4}$s simulation deviates between 32.999999359J and 32.999999349J. The energy for the simulation at $h = 10^{-3}$s deviates between 32.999937236J and 32.999937235J. There is no deviation in energy for the $h = 10^{-2}$s and $h = 10^{-1}$s simulations.

The Double Spherical Pendulum. The simulation in this section is motivated by our work on pattern evocation for the double spherical pendulum given in Marsden and Scheurle [1995] and Marsden, Scheurle and Wendlandt [1996].

- The double spherical pendulum consists of two constrained point masses.
- The configuration space is $Q = S^2 \times S^2$ and the linear space is $V = \mathbf{R}^3 \times \mathbf{R}^3$.
- The position of the first mass is $q_1 = (x_1, y_1, z_1)$, and the position of the second mass is $q_2 = (x_2, y_2, z_2)$.
- The constraint are given by the pendulum length constraints.
- The DVP algorithm for the DSP is identical to the SHAKE algorithm:

$$\frac{1}{h} M \left[q^{n+1} - 2q^n + q^{n-1}\right] + hu - hD^T g\left(q^n\right) \lambda = 0$$

with the constraint $g\left(q^{n+1}\right) = 0$, where u is the column vector with components $(0, 0, m_1 g, 0, 0, m_2 g)$, m_1 and m_2 are the masses, and

$$M = \begin{bmatrix} m_1 I & 0 \\ 0 & m_2 I \end{bmatrix}, \qquad q = \begin{bmatrix} q_1 \\ q_2 \end{bmatrix}. \tag{5.2}$$

- Here one can compare the simulation from the discrete variational principle (DVP) construction to an energy-momentum (EM) formulation based on Gonzalez [1996a], and applied to the DSP in Wendlandt [1995].

Example Simulation.

- Parameters: $m_1 = 2.0\text{Kg}$, $m_2 = 3.5\text{Kg}$, $l_1 = 4.0\text{m}$, $l_2 = 3.0\text{m}$, and $g = 9.81\text{m/s}^2$.
- Initial conditions: $x_1 = 2.820\text{m}$, $y_1 = 0.025\text{m}$, $x_2 = 5.085\text{m}$, $y_2 = 0.105\text{m}$, $\dot{x}_1 = 3.381\text{m/s}$, $\dot{y}_1 = 2.506\text{m/s}$, $\dot{x}_2 = 2.497\text{m/s}$, and $\dot{y}_2 = 10.495\text{m/s}$. The position and velocity of the z-coordinate is

determined from the constraints, and the z-coordinate for both masses is taken to be negative.

- The output of the EM simulation at a time step of 0.0001s is used as the standard and initializes the second step in the DVP simulations. The DVP simulations are slightly faster for each time step and both CPU times drop off nearly linearly with increasing time step.

The position error for the EM and DVP simulations is shown in Figure 5.3. Both simulations show a second order relationship between position error and time step. The error for the EM simulation is slightly greater than the error for the DVP simulation for $h \geq 10^{-3}$s.

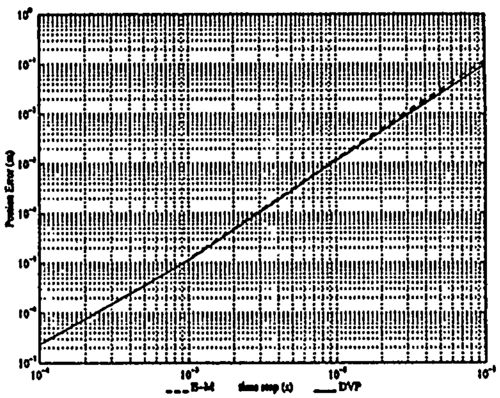

Figure 5.3: Position Error Versus Time Step for the DSP Simulation

The y position of the second mass is shown in Figure 5.4 for the EM and DVP simulations for $h = 0.0001$s and $h = 0.1$s. Both the EM and DVP simulations at $h = 0.0001$s overlap and cannot be distinguished when plotted on the same graph. For both the EM and DVP simulations, reasonably accurate and fast trajectories are produced at large time steps, $h = 0.1$s.

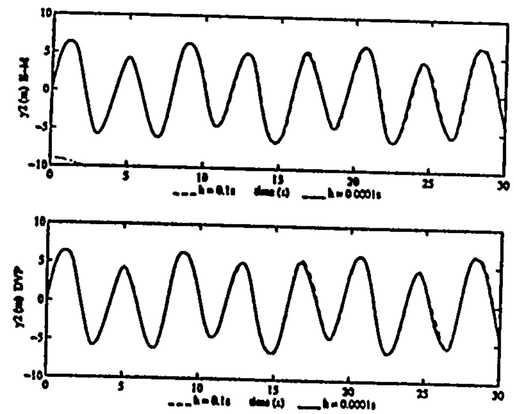

Figure 5.4: Position Coordinate Versus Time for the DSP Simulation

The DVP energy error drops off as the square of the time step, at least for the large time steps. The energy error is zero for all time steps for the EM simulation. The energy for the DVP simulation at $h = 0.0001s$ deviates between 24.9444951109J and 24.9444999828J and deviates between 20.910805793J and 25.583335766J for $h = 0.1s$.

Figure 5.5 shows the energy for the DVP simulations versus time for $h = 0.1s$ and $0.01s$ in the lower graph. The upper graph shows energy versus time for $h = 0.001s$ and $0.0001s$. The energy oscillates about a constant value, and the constant value approaches the true energy. The amplitude of the oscillations decrease as the step size decreases. The fluctuations in energy appear to be related to the constraint forces. The middle graph is a plot of the multipliers versus time, and the fluctuations in the multipliers is correlated to the fluctuations in energy (see Barth and Leimkuhler [1996a], who use variable step size to decrease the energy oscillation.)

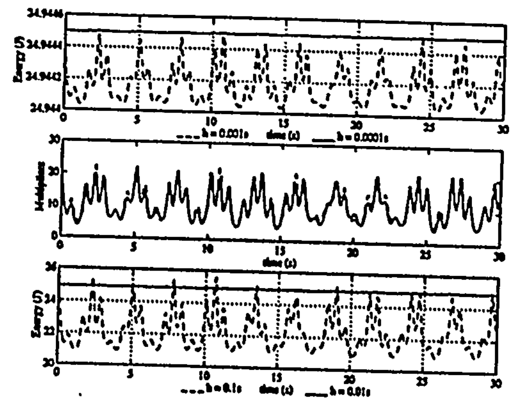

Figure 5.5: Energy and Multipliers Versus Time for the DSP Simulation

Where do we go from here?

Spacetime Integrators. Use multisymplectic geometry rather than symplectic geometry for field (continuum) theories.

Additional Examples. Eg, dynamics of an underwater vehicle studied by Leonard [1995a,b] and Leonard and Marsden [1996].

Discrete Lagrangian Reduction. What are the *discrete reduced Euler-Lagrange equations?*

Nonholonomic Systems. For nonholonomic systems, the standard symplectic form is not preserved, and there are momentum equations and not conservation laws. What happens if you form the discrete Lagrange d'Alembert principle?

Multistep Methods and Time Step Control. It seems possible to modify the method to construct multistep mechanical integrators to increase the accuracy of the method. One would also like to modify the method to allow variable time steps to improve efficiency.

External Forces. Add external and control forces for controlled mechanical systems such as biped robots.

References

Abraham, R. and J.E. Marsden [1978] *Foundations of Mechanics*. Second Edition, Addison-Wesley.

Abraham, R., J.E. Marsden, and T.S. Ratiu [1988] *Manifolds, Tensor Analysis, and Applications*. Second Edition, Applied Mathematical Sciences 75, Springer-Verlag.

Anderson, H. [1983]. Rattle: A velocity version of the shake algorithm for molecular dynamics calculations. *J. Comp. Phys.*, 52, 24–34.

Armero, F. and J.C. Simo [1996] Long-Term Dissipativity of Time-Stepping Algorithms for an Abstract Evolution Equation with Applications to the Incompressible MHD and Navier-Stokes Equations. *Comp. Meth. Appl. Mech. Eng.* 131, 41–90.

Arnold, V.I. [1989] *Mathematical Methods of Classical Mechanics*. Second Edition, Graduate Texts in Mathematics 60, Springer-Verlag.

Austin, M. and P.S. Krishnaprasad [1993] Almost Poisson Integration of Rigid Body Systems, *J. Comp. Phys.* 106

Baez, J. C. and J. W. Gilliam [1995]. An algebraic approach to discrete mechanics. Preprint, http://math.ucr.edu/home/baez/ca.tex.

Barth, E. and B. Leimkuhler [1996a]. A semi-explicit, variable-stepsize integrator for constrained dynamics. Mathematics department preprint series, University of Kansas.

Barth, E. and B. Leimkuhler [1996b]. Symplectic methods for conservative multibody systems. *Fields Institute Communications*, 10, 25–43.

Bloch, A.M., P.S. Krishnaprasad, J.E. Marsden, and T.S. Ratiu [1994] Dissipation Induced Instabilities, *Ann. Inst. H. Poincaré, Analyse Nonlineare* 11, 37–90.

Bloch, A.M., P.S. Krishnaprasad, J.E. Marsden, and T.S. Ratiu [1996] The Euler-Poincaré equations and double bracket dissipation. *Comm. Math. Phys.* 175, 1–42.

Bloch, A.M., P.S. Krishnaprasad, J.E. Marsden, and R. Murray [1996] Nonholonomic mechanical systems with symmetry. *Arch. Rat. Mech. An.* (to appear).

Bretherton, F.P. [1970] A note on Hamilton's principle for perfect fluids. *J. Fluid Mech.* 44, 19-31.

Channell, P. and C. Scovel [1990] Symplectic integration of Hamiltonian systems, *Nonlinearity* 3, 231–259.

Chorin, A.J, T.J.R. Hughes, J.E. Marsden, and M. McCracken [1978] Product Formulas and Numerical Algorithms, *Comm. Pure Appl. Math.* 31, 205–256.

Feng, K. [1986] Difference schemes for Hamiltonian formalism and symplectic geometry. *J. Comp. Math.* 4, 279–289.

Feng, K. and Z. Ge [1988] On approximations of Hamiltonian systems, *J. Comp. Math.* 6, 88–97.

Feng, K. and M.Z. Qin [1987] The symplectic methods for the computation of Hamiltonian equations, *Springer Lecture Notes in Math.* 1297, 1–37.

Ge, Z. [1990] Generating functions, Hamilton-Jacobi equation and symplectic groupoids over Poisson manifolds, *Indiana Univ. Math. J.* 39, 859–876.

Ge, Z. [1991a] Equivariant symplectic difference schemes and generating functions, *Physica D* 49, 376–386.

Ge, Z. [1991b] A constrained variational problem and the space of horizontal paths, *Pacific J. Math.* 149, 61–94.

Ge, Z. [1994] Generating functions, Hamilton-Jacobi equations and symplectic groupoids on poisson manifolds. *Indiana U. Math. J.* 39, 850–875.

Ge, Z. and J.E. Marsden [1988] Lie-Poisson integrators and Lie-Poisson Hamilton-Jacobi theory, *Phys. Lett. A* 133, 134–139.

Gillilan, R. and K. Wilson [1992]. Shadowing, rare events, and rubber bands: A variational Verlet algorithm for molecular dynamics. *J. Chem. Phys.*, 97, 1757–1772.

Gonzalez, O. [1996a] *Design and Analysis of Conserving Integrators for Nonlinear Hamiltonian Systems with Symmetry*, Thesis, Stanford University, Mechanical Engineering.

Gonzalez, O. [1996b]. Time integration and discrete Hamiltonian systems. *Journal of Nonlinear Science, to appear.*

Itoh, T. and K. Abe [1988]. Hamiltonian-conserving discrete canonical equations based on variational difference quotients. *Journal of Computational Physics*, 77, 85–102.

Jay, L. [1996]. Symplectic partitioned runge-kutta methods for constrained Hamiltonian systems. *SIAM Journal on Numerical Analysis*, 33, 368–387.

Koon, W.S. and J.E. Marsden [1996] Optimal control for holonomic and nonholonomic mechanical systems with symmetry and Lagrangian reduction. *SIAM J. Control and Optim (to appear).*

Labudde, R. A. and D. Greenspan [1974]. Discrete mechanics-a general treatment. *Journal of Computational Physics*, 15, 134–167.

Labudde, R. A. and D. Greenspan [1976a]. Energy and momentum conserving methods of arbitrary order for the numerical integration of equations of motion-I. Motion of a single particle. *Numer. Math.*, 25, 323–346.

Labudde, R. A. and D. Greenspan [1976b]. Energy and momentum conserving methods of arbitrary order for the numerical integration of equations of motion-II. Motion of a system of particles. *Numer. Math.*, 26, 1–16.

Leimkuhler, B. and G. Patrick [1996]. Symplectic integration on Riemannian manifolds. *J. of Nonl. Sci.* 6, 367–384.

Leimkuhler, B. and R. Skeel [1994]. Symplectic numerical integrators in constrained Hamiltonian systems. *Journal of Computational Physics*, 112, 117–125.

Leonard, N.E. [1995a] Control synthesis and adaptation for an underactuated autonomous underwater vehicle, *IEEE J. of Oceanic Eng.* 20, 211–220.

Leonard, N.E. [1995b] Stability of a bottom-heavy underwater vehicle, *Mechanical and Aerospace Engineering, Princeton University Technical Report 2048*, to appear in *Automatica* 33, March 1997.

Leonard, N.E. and J.E. Marsden [1996] Stability and Drift at Nongeneric Momenta and Underwater Vehicle Dynamics, *Mechanical and Aerospace Engineering, Princeton University Technical Report 2075*, Lewis, D. and J.C. Simo [1995] Conserving algorithms for the dynamics of Hamiltonian systems on Lie groups. *J. Nonlinear Sci.* **4**, 253–299.

Lewis, H. and Kostelec, P. [1996]. The use of Hamilton's principle to derive time-advance algorithms for ordinary differential equations. *Comp. Phys. Commun., to appear.*

MacKay, R. [1992]. Some aspects of the dynamics of Hamiltonian systems. In Broomhead, D. S. and Iserles, A., eds, *The Dynamics of numerics and the numerics of dynamics*, 137–193. Clarendon Press, Oxford.

Maeda, S. (1981). Lagrangian formulation of discrete systems and concept of difference space. *Math. Japonica*, **27**, 345–356.

Marsden, J.E. [1992], *Lectures on Mechanics* London Mathematical Society Lecture note series, **174**, Cambridge University Press.

Marsden, J. E., G. W. Patrick, and W. F. Shadwick [1996] *Integration Algorithms and Classical Mechanics.* Fields Inst. Commun., **10**, Am. Math. Society.

Marsden, J.E. and T.S. Ratiu [1994] *Symmetry and Mechanics.* Texts in Applied Mathematics, **17**, Springer-Verlag.

Marsden, J.E. and J. Scheurle [1993a] Lagrangian reduction and the double spherical pendulum, *ZAMP* **44**, 17–43.

Marsden, J.E. and J. Scheurle [1993b] The reduced Euler-Lagrange equations, *Fields Inst. Comm.* **1**, 139–164.

Marsden, J.E. and J. Scheurle [1995] Pattern evocation and geometric phases in mechanical systems with symmetry, *Dyn. and Stab. of Systems.* **10**, 315–338.

Marsden, J.E., J. Scheurle and J. Wendlandt [1996] Visualization of orbits and pattern evocation for the double spherical pendulum, *ICIAM 95: Mathematical Research, Academie Verlag, Ed. by K. Kirchgässner, O. Mahrenholtz and R. Mennicken* **87**, 213–232.

McLaughlin, R.I. and C. Scovel [1995] Equivariant constrained symplectic integration. *J. of Nonl. Sci.* **5**, 233–256.

McLachlan, R. I. and C. Scovel [1996]. A survey of open problems in symplectic integration. *Fields Inst. Comm.*, **10**, 151–180.

Montgomery, R., J.E. Marsden, and T.S. Ratiu [1984] Gauged Lie-Poisson structures, *Cont. Math. AMS* **28**, 101–114.

Moser, J. and A.P. Veselov [1991] Discrete versions of some classical integrable systems and factorization of matrix polynomials. *Comm. Math. Phys.* **139**, 217–243.

Murray, R., Z. Li, and S. Sastry [1994]. *A Mathematical Introduction to Robotic Manipulation.* CRC Press, Boca Raton, Fl.

Ortiz, M. (1986). A note on energy conservation and stability of nonlinear time-stepping algorithms. *Computers and Structures*, **24**, 167–168.

Reich, S. [1993]. Symplectic integration of constrained Hamiltonian systems by Runge-Kutta methods. Technical Report 93-13, University of British Columbia.

Reich, S. [1994] *Symplectic integrators for systmes of rigid bodies.* (preprint, Inst. Angw. Anal. Stch.)

Reich, S. (1994). Momentum preserving symplectic integrators. *Physica D*, **76**(4):375–383.

Ryckaert, J., G. Ciccotti, and H. Berendsen [1977]. Numerical integration of the cartesian equations of motion of a system with constraints: molecular dynamics of n-alkanes. *J. of Comp. Phys.*, **23**, 327–341.

Sanz-Serna, J. M. [1988] Runge-Kutta schemes for Hamiltonian systems, *BIT* **28**, 877–883.

Sanz-Serna, J. M. [1991] Symplectic integrators for Hamiltonian problems: an overview. *Acta Num.*, **1**, 243–286.

Sanz-Serna, J. M. [1996] Backward error analysis of symplectic integrators. *Fields Inst. Comm.*, **10**, 193–205.

Sanz-Serna, J. M. and M. Calvo [1994] *Numerical Hamiltonian Problems.* Chapman and Hall, London.

Seliger, R.L. and G.B. Whitham [1968] Variational principles in continuum mechanics, *Proc. Roy. Soc. Lond.* **305**, 1–25.

Shibberu, Y. [1994]. Time-discretization of Hamiltonian systems. *Computers Math. Applic.*, **28**, 123–145.

Simo, J.C. and F. Armero [1994] Unconditional Stability and Long-Term Behavior of Transient Algorithms for the Incompressible Navier-Stokes and Euler Equations. *Comp. Meth. Appl. Mech. Eng.* **111**, 111–154.

Simo, J.C. and M. Doblare [1991], Nonlinear Dynamics of Three-Dimensional Rods: Momentum and Energy Conserving Algorithms, *Intern. J. Num. Methods in Eng.*

Simo, J.C.and O. Gonzalez. [1993], Assessment of Energy-Momentum and Symplectic Schemes for Stiff Dynamical Systems. *Proc. ASME Winter Annual Meeting, New Orleans*, Dec. 1993.

Simo, J.C., D.R. Lewis, and J.E. Marsden [1991] Stability of relative equilibria I: The reduced energy momentum method, *Arch. Rat. Mech. Anal.* **115**, 15-59.

Simo, J.C. and J.E. Marsden [1984] On the rotated stress tensor and a material version of the Doyle Ericksen formula, *Arch. Rat. Mech. Anal.* **86**, 213–231.

Simo, J.C., J.E. Marsden, and P.S. Krishnaprasad [1988] The Hamiltonian structure of nonlinear elasticity: The material, spatial, and convective representations of solids, rods, and plates, *Arch. Rat. Mech. Anal.* **104**, 125–183.

Simo, J.C., T.A. Posbergh, and J.E. Marsden [1990] Stability of coupled rigid body and geometrically exact rods: block diagonalization and the energy-momentum method, *Physics Reports* **193**, 280–360.

Simo, J.C., T.A. Posbergh, and J.E. Marsden [1991] Stability of relative equilibria II: Three dimensional elasticity, *Arch. Rat. Mech. Anal.* **115**, 61–100.

Simo, J.C. and N. Tarnow [1992] The discrete energy momentum method. Conserving algorithms for nonlinear elastodynamics, *ZAMP* **43**, 757–792.

Simo, J.C. and N. Tarnow [1994] A New Energy Momentum Method for the Dynamics of Nonlinear Shells, *Int. J. Num. Meth. Eng.*, **37**, 2527–2549.

Simo, J.C. and N. Tarnow and M. Doblare [1993] Nonlinear Dynamics of Three-Dimensional Rods: Exact Energy and Momentum Conserving Algorithms. *Comp. Meth. Appl. Mech. Eng.*

Simo, J.C., N. Tarnow, and K.K. Wong [1992] Exact energy-momentum conserving algorithms and symplectic schemes for nonlinear dynamics *Comp. Meth. Appl. Mech. Eng.* 100, 63–116.

Simo, J.C. and K.K. Wong [1989] Unconditionally stable algorithms for the orthogonal group that exactly preserve energy and momentum, *Int. J. Num. Meth. Eng.* 31, 19–52, addendum, 33, 1321-1323, 1992.

Verlet, L. [1967]. Computer experiments on classical fluids. *Phys. Rev*, 159, 98–103.

Veselov, A.P. [1988] Integrable discrete-time systems and difference operators. *Funct. An. and Appl.* 22, 83–94.

Veselov, A.P. [1991] Integrable Lagrangian correspondences and the factorization of matrix polynomials. *Funct. An. and Appl.* 25, 112–123.

Wendlandt, J. [1995]. Pattern evocation and energy-momentum integration of the double spherical pendulum. MA thesis, University of California at Berkeley. Department of Mathematics, CPAM-656.

Wendlandt, J.M. and J.E. Marsden [1996] Mechanical integrators derived from a discrete variational principle, *Caltech CDS Technical Report 96-013.*

Wendlandt, J. and Sastry, S. [1996]. Recursive workspace control of multibody systems: A planar biped example, *IEEE CDC*, Kobe, Japan, Dec., 1996.

Wisdom, J., and M. Holman [1992] Symplectic maps for the N body problem, *Astron. J.*, 102, 1528–1538.

Wisdom, J., and M. Holman and J. Touma [1996] *Symplectic correctors. Fields Inst. Comm.*, 10, 217–244.

Yoshida, H. [1990]. Construction of higher order symplectic integrators. *Phys. Lett. A*, 150, 262–268.

FROM TAYLOR SERIES TO TAYLOR MODEL & REMAINDER DIFFERENTIAL ALGEBRWITH INTERVAL ARITHMETIC

M. Berz, Michigan State

Description and Analysis of Optical Systems

Easiest way to study optical system: trace rays through system. Light Optics: Snell's Law. Particle Optics: numerical integration through electromagnetic fields.

Very easy to do, But: does not provide much insight. Hard to see what to change if a system has problems.

Better to look at the Map of the system:

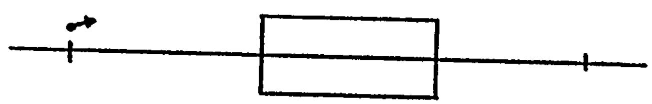

$$\begin{pmatrix} x_i \\ a = p_{xi}/p_0 \\ y_i \\ b = p_{yi}/p_0 \\ \Delta E/E \\ \Delta m/m \\ \vec{s} \end{pmatrix} \xrightarrow{\mathcal{M}} \begin{pmatrix} x_f \\ a_f \\ y_f \\ b_f \\ \Delta E/E \\ \Delta m/m \\ \vec{s} \end{pmatrix}$$

The Map

A section of an accelerator can be described by a map:

$$\vec{z}_f = \mathcal{M}(\vec{z}_i, \vec{\delta})$$

$\vec{z}$: collection of phase space coordinates,

$\vec{\delta}$: system parameters.

Tracking a particle (with certain values for the system parameters) means evaluating the map.

We want to describe the map as a whole. We could:

- Interpolate the map
- Expand map in Taylor series around origin
- Expand map around several reference points and interpolate
- Expand map in other complete set of functions

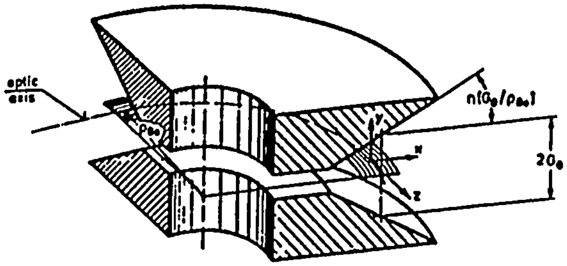

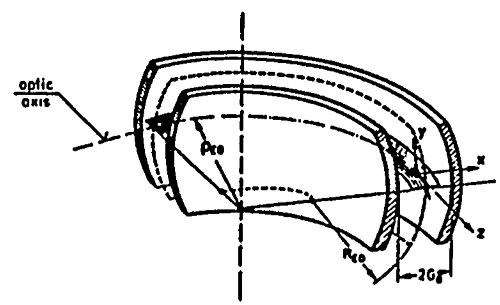

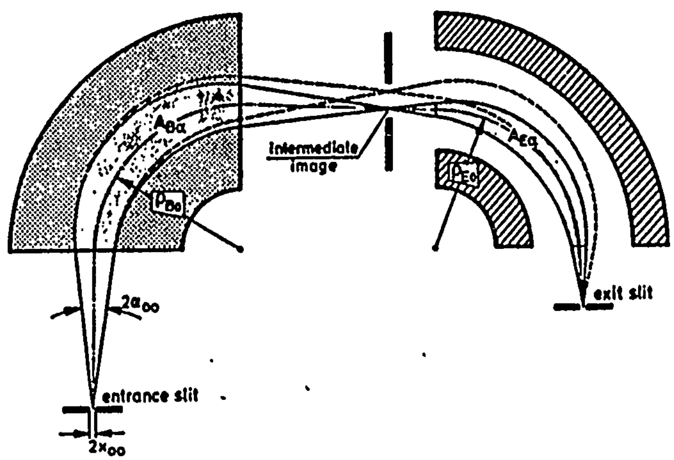

An angle- and energy-focusing mass spectrometer $[(x|a) = (x|\delta_K) = 0, (x|\delta_m) \neq 0]$. Note that ions of one mass-charge ratio but two energy-charge ratios are focused to different positions in the middle and one at the end of the mass spectrometer.

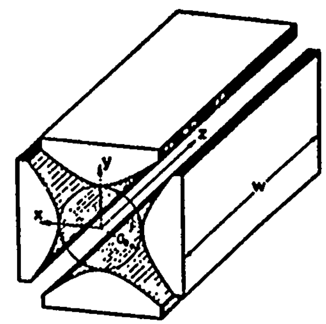

(a)

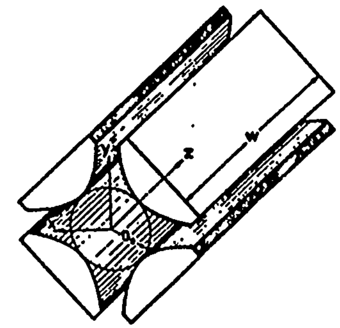

(b)

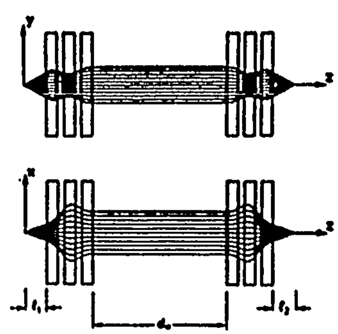

The determination of terms of order higher than fourth is very laborious in all but the simplest cases. For this reason, algebraic calculations are usually restricted to the domain of the Seidel theory, supplemented where necessary by ray tracing.

Principles of Optics,
Sixth Edition,
Born-Wolf, Pergamon 1989

:
: 26,840 lines further...
:

```
      L(433,7) = (+0.375D+00*(-TT1715-TT6913)+0.1875D+00*TT6912
     * +0.75D+00*TT1716+0.1953125D+00*TT345-0.9765625D-01*TT346
     * -0.392578125D+00*TT1717+0.1962890625D+00*TT6914+0.15625D+00*TT
     * 1718+0.53125D+00*TT1719-0.3046875D+00*TT6915+0.859375D-01*(+TT
     * 1693+TT1721)-0.4296875D-01*TT1694+0.52734375D-01*(-TT1695-TT
     * 6916)+0.263671875D-01*TT6872+0.3125D-01*(+TT6873+TT6874-TT6920)
     * -0.234375D-01*TT6875-0.171875D+00*TT1720+0.10546875D+00*TT1722
     * +0.625D-01*(-TT6917-TT6918)+0.46875D-01*TT6919+0.15625D-01*TT
     * 6921+0.78125D-02*TT6922-0.390625D-02*TT6923)
      L(448,7) = (-0.48828125D-01*TT59+0.244140625D-01*TT347
     * +0.28564453125D+00*TT1723-0.14282226563D+00*TT6924-0.390625D-01
     * *TT348-0.5078125D+00*TT1724+0.263671875D+00*TT6925
     * -0.232421875D+00*TT8+0.1162109375D+00*TT9+0.53466796875D+00*TT
     * 60-0.26733398438D+00*TT351-0.1484375D+00*TT10-0.8046875D+00*TT
     * 61+0.439453125D+00*TT352+0.18359375D+00*TT349-0.91796875D-01*TT
     * 350-0.2490234375D+00*TT1725+0.12451171875D+00*TT6926
     * +0.109375D+00*(+TT1726+TT1728)+0.296875D+00*TT1727
     * -0.17578125D+00*TT6927-0.546875D-01*TT1729-0.5859375D-01*TT
     * 1730+0.29296875D-01*TT6928+0.3125D-01*(+TT6929+TT6930)
     * -0.234375D-01*TT6931+0.78125D-02*(+TT6892+TT6933)+0.390625D-02*(
     * -TT6893+TT6934)+0.1953125D-02*(-TT6894-TT6935)+0.9765625D-03*TT
     * 6895-0.15625D-01*TT6932)
      L(457,7) = (+0.1953125D-01*TT8-0.29296875D-01*TT9+0.322265625D+00
     * *TT60-0.4638671875D+00*TT351+0.23071289063D+00*TT1731
     * -0.38452148438D-01*TT6936+0.1171875D+00*TT10-0.859375D+00*TT61
     * +0.111328125D+01*TT352-0.52734375D+00*TT1732+0.8544921875D-01*TT
     * 6937)
      L(264,7) = (+0.41015625D-01*(+TT53-TT54)+0.87890625D-02*(+TT325-TT
     * 327)+0.1025390625D-01*(-TT1678+TT1680)+0.56396484375D-01*(+TT
     * 6850-TT6852)+0.234375D-01*(-TT326+TT1679+TT328-TT1681+TT1687+TT
     * 6856-TT6859)+0.123046875D+00*(-TT6851+TT6853)-0.8203125D-01*TT
     * 329-0.17578125D-01*TT330+0.205078125D-01*TT1682
     * +0.7470703125D-01*TT6854+0.46875D-01*(+TT1683-TT1684)
     * -0.12890625D+00*TT6855-0.9375D-01*TT1685+0.3125D-01*(-TT1686+TT
     * 6857-TT6858)+0.78125D-02*(-TT6860-TT6865)+0.390625D-02*(-TT
     * 6861+TT6866)+0.1953125D-02*(+TT6862+TT6867)+0.9765625D-03*TT
     * 6863-0.15625D-01*TT6864)
      L(299,7) = (+0.1875D+00*TT6868-0.375D+00*TT6869-0.3515625D+00*TT
     * 333-0.9765625D-01*TT334+0.87890625D-01*TT1690+0.1962890625D+00
     * *TT6870+0.15625D+00*(+TT1691-TT1692)-0.3046875D+00*TT6871
     * -0.1171875D+00*TT1693-0.4296875D-01*TT1694+0.29296875D-01*TT
     * 1695+0.263671875D-01*TT6872+0.3125D-01*(+TT6873-TT6874-TT6880)
     * -0.234375D-01*TT6875-0.234375D+00*TT1696-0.859375D-01*TT1697
     * +0.5859375D-01*TT1698+0.52734375D-01*TT6876+0.625D-01*(+TT6877
     * -TT6878)-0.46875D-01*TT6879-0.15625D-01*TT6881+0.78125D-02*TT
     * 6882+0.390625D-02*TT6883)
      L(369,7) = (-0.87890625D-01*TT56-0.244140625D-01*TT335
     * +0.2197265625D-01*TT1699+0.14282226563D+00*TT6884+0.390625D-01*(
     * +TT336-TT1700)-0.263671875D+00*TT6885-0.380859375D+00*TT8
     * -0.1162109375D+00*TT9+0.9521484375D-01*TT60+0.26733398438D+00*TT
     * 351+0.1484375D+00*(+TT10-TT61)-0.439453125D+00*TT352
     * -0.29296875D+00*TT337-0.91796875D-01*TT338+0.732421875D-01*TT
     * 1701+0.12451171875D+00*TT6886+0.109375D+00*(+TT1702-TT1703)
     * -0.17578125D+00*TT6887-0.140625D+00*TT1704-0.546875D-01*TT1705
     * +0.3515625D-01*TT1706+0.29296875D-01*TT6888+0.3125D-01*(+TT
     * 6889-TT6890)-0.234375D-01*TT6891+0.78125D-02*(-TT6892-TT6897)
     * +0.390625D-02*(-TT6893+TT6898)+0.1953125D-02*(+TT6894+TT6899)
     * +0.9765625D-03*TT6895-0.15625D-01*TT6896)
      L(424,7) = (+0.41015625D-01*(-TT57+TT54)+0.87890625D-02*(-TT339+TT
     * 327)+0.1025390625D-01*(+TT1707-TT1680)+0.56396484375D-01*(-TT
     * 6900+TT6852)+0.234375D-01*(+TT340-TT1708-TT328+TT1681+TT1714+TT
     * 6904-TT6907)+0.123046875D+00*(+TT6901-TT6853)-0.8203125D-01*TT
     * 341-0.17578125D-01*TT342+0.205078125D-01*TT1709
     * +0.7470703125D-01*TT6902+0.46875D-01*(+TT1710-TT1711)
     * -0.12890625D+00*TT6903-0.9375D-01*TT1712+0.3125D-01*(-TT1713+TT
     * 6905-TT6906)+0.78125D-02*(-TT6860+TT6909)+0.390625D-02*(-TT
     * 6861-TT6910)+0.1953125D-02*(+TT6862-TT6911)+0.9765625D-03*TT
     * 6863+0.15625D-01*TT6908)
      L(434,7) = (-0.1875D+00*TT6912+0.375D+00*TT6913+0.3515625D+00*TT
     * 345+0.9765625D-01*TT346-0.87890625D-01*TT1717-0.1962890625D+00
     * *TT6914+0.15625D+00*(-TT1718+TT1719)+0.3046875D+00*TT6915
     * +0.1171875D+00*TT1693+0.4296875D-01*TT1694-0.29296875D-01*TT
     * 1695-0.263671875D-01*TT6872+0.3125D-01*(-TT6873+TT6874-TT6920)
     * +0.234375D-01*TT6875-0.234375D+00*TT1720-0.859375D-01*TT1721
     * +0.5859375D-01*TT1722+0.52734375D-01*TT6916+0.625D-01*(+TT6917
     * -TT6918)-0.46875D-01*TT6919-0.15625D-01*TT6921+0.78125D-02*TT
     * 6922+0.390625D-02*TT6923)
      L(449,7) = (-0.87890625D-01*TT59-0.244140625D-01*TT347
     * +0.2197265625D-01*TT1723+0.14282226563D+00*TT6924+0.390625D-01*(
     * +TT348-TT1724)-0.263671875D+00*TT6925-0.380859375D+00*TT8
     * -0.1162109375D+00*TT9+0.9521484375D-01*TT60+0.26733398438D+00*TT
     * 351+0.1484375D+00*(+TT10-TT61)-0.439453125D+00*TT352
     * +0.29296875D+00*TT349+0.91796875D-01*TT350-0.732421875D-01*TT
     * 1725-0.12451171875D+00*TT6926+0.109375D+00*(-TT1726+TT1727)
     * +0.17578125D+00*TT6927+0.140625D+00*TT1728+0.546875D-01*TT1729
     * -0.3515625D-01*TT1730-0.29296875D-01*TT6928+0.3125D-01*(-TT
     * 6929+TT6930)+0.234375D-01*TT6931+0.78125D-02*(+TT6892-TT6933)
     * +0.390625D-02*(+TT6893+TT6934)+0.1953125D-02*(-TT6894+TT6935)
     * -0.9765625D-03*TT6895-0.15625D-01*TT6932)
      L(458,7) = (+0.234375D-01*TT8-0.390625D-02*TT9-0.8203125D-01*TT
     * 60+0.380859375D+00*TT351-0.32470703125D+00*TT1731
     * +0.76904296875D-01*TT6936+0.15625D-01*TT10+0.21875D+00*TT61
     * -0.9140625D+00*TT352+0.7421875D+00*TT1732-0.1708984375D+00*TT
     * 6937)
      L(459,7) = (+0.390625D-01*TT8+0.390625D-02*TT9-0.1171875D-01*TT
     * 60-0.68359375D-01*TT351+0.18798828125D+00*TT1731
     * -0.76904296875D-01*TT6936-0.15625D-01*TT10+0.3125D-01*TT61
     * +0.1640625D+00*TT352-0.4296875D+00*TT1732+0.1708984375D+00*TT
     * 6937)
      L(460,7) = (+0.13671875D+00*TT8+0.29296875D-01*TT9+0.5859375D-02
     * *TT60-0.48828125D-02*TT351-0.25634765625D-01*TT1731
     * +0.38452148438D-01*TT6936-0.1171875D+00*TT10-0.15625D-01*TT61
     * +0.1171875D-01*TT352+0.5859375D-01*TT1732-0.8544921875D-01*TT
     * 6937)
*
  500 IF(NORDER.EQ.5) GOTO 1000
*
 1000 CONTINUE
*
      RETURN
      END
```

```
      SUBROUTINE elmm(L,Z,K01,K02,K03,K04,K05,K27,K32,NORDER,NG,ND)
*     ***************************************************************
*
*
      IMPLICIT DOUBLE PRECISION (A - Z)
*
      INTEGER NORDER, NG, ND
*
      DOUBLE PRECISION L(0:461,7)
*
*     K01    : QUADRUPOLE STRENGTH
*     K02    : HEXAPOLE STRENGTH
*     K03    : OCTUPOLE STRENGTH
*     K04    : DECAPOLE STRENGTH
*     K05    : DODECAPOLE STRENGTH
*     K27    : 1./(MAGNETIC RIGIDITY)
*     K32    : ENERGY/(M*C**2)
*
      K30    = 1./(1+K32)
      K31    = 1./(1+K32/2.)
*
      FX2 = -K01*K27
*
      FY2 = +K01*K27
*
      IF(FX2.LT.-1.D-8) THEN
         AFX = SQRT(-FX2)
         CX  = COS(AFX*Z)
         SX  = SIN(AFX*Z)/AFX
      ELSEIF(FX2.GT.1.D-8) THEN
         AFX = SQRT(FX2)
         EX  = EXP(AFX*Z)
         EEX = 1.D0/EX
         CX  = (EX + FEX)/2.D0
         SX  = (EX - EEX)/2.D0/AFX
      ELSE
         CX  = 1.D0
         SX  = Z
         FX2 = 1.D-8
      FNDIF
*
      IF(FY2.LT.-1.D-8) THEN
         AFY = SQRT(-FY2)
         CY  = COS(AFY*Z)
         SY  = SIN(AFY*Z)/AFY
      ELSEIF(FY2.GT.1.D-8) THEN
         AFY = SQRT(FY2)
         EY  = EXP(AFY*Z)
         EEY = 1.D0/EY
         CY  = (EY + EEY)/2.D0
         SY  = (EY - EEY)/2.D0/AFY
      ELSE
         CY  = 1.D0
         SY  = Z
         FY2 = 1.D-8
      ENDIF
*
*
      CS2 = CX
      CS3 = SX
      CS4 = CY
      CS5 = SY
      CS6 = Z
      KK2 = K31*K32
      KK3 = K30*K32
      FF2 = FX2
      TT2 = CS2
      TT3 = CS3
      TT4 = CS3*FF2
      TT5 = CS4
      TT6 = CS5
      TT7 = CS5*FF2
      TT8 = CS6
      TT9 = CS6*KK2
      TT10 = CS6*KK3
      L(1,1) = (+TT2)
      L(2,1) = (+TT3)
      L(1,2) = (+TT4)
      L(2,2) = (+TT2)
      L(3,3) = (+TT5)
      L(4,3) = (+TT6)
      L(3,4) = (-TT7)
      L(4,4) = (+TT5)
*
      IF(ND.EQ.0.AND.NG.EQ.0) GOTO 100
*
      L(6,6) = (+1)
      L(6,7) = (-0.5D+00*TT8-0.25D+00*TT9+TT10)
*
      IF(NG.EQ.0) GOTO 100
*
      L(5,5) = (+1)
      L(5,7) = (+0.5D+00*TT8+0.25D+00*TT9-TT10)
*
  100 IF(NORDER.EQ.1) GOTO 1000
*
      CS7 = CS3*CX
      CS8 = CS3*SX
      CS9 = CS4*CX
      CS10 = CS4*SX
      CS11 = CS5*CX
      CS12 = CS5*SX
      CS13 = CS5*CY
      CS14 = CS5*SY
      CS15 = CS6*CX
      CS16 = CS6*SX
      CS17 = CS6*CY
      CS18 = CS6*SY
      KK4 = KK2*K31*K32
      KK5 = KK3*K31*K32
      KK6 = K02*K27
      FF3 = 1/FX2/FX2
      FF4 = FF3*FX2
      TT11 = KK6*FF4
      TT12 = CS2*KK6*FF4
      TT13 = CS8*KK6
      TT14 = CS3*KK6*FF4
      TT15 = CS7*KK6*FF4
      TT16 = KK6*FF3
      TT17 = CS2*KK6*FF3
      TT18 = CS8*KK6*FF4
      TT19 = CS14*KK6
      TT20 = CS13*KK6*FF4
      TT21 = CS14*KK6*FF4
      TT22 = CS16*FF2
      TT23 = CS16*KK2*FF2
      TT24 = CS3*KK2
      TT25 = CS15
```

Number Fields and Floating Point Numbers

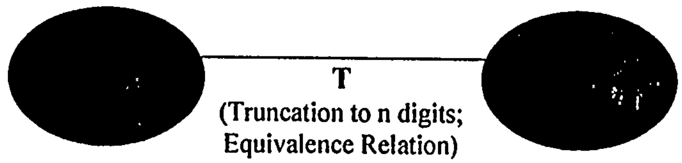

T
(Truncation to n digits; Equivalence Relation)

Real Numbers | Floating Point "Numbers"

$c = a + b$

$$\begin{tikzcd} \cdot \arrow[r, "T"] \arrow[d, "+"'] & \cdot \arrow[d, "\oplus"] \\ \cdot \arrow[r, "T"] & \cdot \end{tikzcd}$$

$c_T = a_T \oplus b_T$

$c = a \cdot b$

$$\begin{tikzcd} \cdot \arrow[r, "T"] \arrow[d, "\cdot"'] & \cdot \arrow[d, "\odot"] \\ \cdot \arrow[r, "T"] & \cdot \end{tikzcd}$$

$c_T = a_T \odot b_T$

Field
(Also want "exp", "sin" etc: Banach Field)

Diagrams commute "approximately"

Field
("approximately")

T: Extracts Information considered relevant

Function Algebras

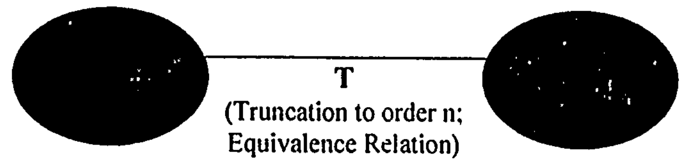

T
(Truncation to order n; Equivalence Relation)

Space of C^∞ Functions | Taylor Polynomials

$h = f + g$

$$\begin{tikzcd} \cdot \arrow[r, "T"] \arrow[d, "+"'] & \cdot \arrow[d, "\oplus"] \\ \cdot \arrow[r, "T"] & \cdot \end{tikzcd}$$

$h_T = f_T \oplus g_T$

$h = f \cdot g$

$$\begin{tikzcd} \cdot \arrow[r, "T"] \arrow[d, "\cdot"'] & \cdot \arrow[d, "\odot"] \\ \cdot \arrow[r, "T"] & \cdot \end{tikzcd}$$

$h_T = f_T \odot g_T$

$h = \partial f$

$$\begin{tikzcd} \cdot \arrow[r, "T"] \arrow[d, "\partial"'] & \cdot \arrow[d] \\ \cdot \arrow[r, "T"] & \cdot \end{tikzcd}$$

$h_T = \oslash g$

Algebra | TPSA

Differential Algebra | DA

Differential Algrebra
(also want "exp", "sin" etc: Banach DA)

Diagrams commute exactly

Differential Algebra
(even Banach DA)

T: Extracts Information considered relevant

-0.8492502	-0.7343950	0.0000000E+00	0.0000000E+00	1	1	0	0	0	0
0.3244383E-03	-1.177229	-0.0000000E+00	0.0000000E+00	1	0	1	0	0	0
0.0000000E+00	0.0000000E+00	1.415443	1.469144	1	0	0	1	0	0
0.0000000E+00	0.0000000E+00	-0.9056520	-0.2335189	1	0	0	0	1	0
4.551361	0.6207835E-01	0.0000000E+00	0.0000000E+00	1	0	0	0	0	1
-2.104380	0.2825658	0.0000000E+00	0.0000000E+00	2	2	0	0	0	0
-6.215887	0.4587265	0.0000000E+00	0.0000000E+00	2	1	1	0	0	0
-4.991802	-0.8558133E-02	0.0000000E+00	0.0000000E+00	2	0	2	0	0	0
0.0000000E+00	0.0000000E+00	14.51399	2.615398	2	1	0	1	0	0
0.0000000E+00	0.0000000E+00	22.16059	3.463827	2	0	1	1	0	0
-11.74554	0.2175125	0.0000000E+00	0.0000000E+00	2	0	0	2	0	0
0.0000000E+00	0.0000000E+00	-0.7310245	-0.3767736E-01	2	1	0	0	1	0
0.0000000E+00	0.0000000E+00	-1.435207	-0.4989981E-01	2	0	1	0	1	0
1.731014	0.2950818	0.0000000E+00	0.0000000E+00	2	0	0	1	1	0
3.086312	-0.8911827	0.0000000E+00	0.0000000E+00	2	1	0	0	0	1
3.410136	-1.328959	0.0000000E+00	0.0000000E+00	2	0	1	0	0	1
0.0000000E+00	0.0000000E+00	-2.967764	-1.406842	2	0	0	1	0	1
-0.1231448	-0.2607501E-01	0.0000000E+00	0.0000000E+00	2	0	0	0	2	0
0.0000000E+00	0.0000000E+00	-0.9598581	-0.5857453	2	0	0	0	1	1
-2.597101	-0.3682995	0.0000000E+00	0.0000000E+00	2	0	0	0	0	2
-5.305332	1.452180	0.0000000E+00	0.0000000E+00	3	3	0	0	0	0
-20.80242	5.934979	0.0000000E+00	0.0000000E+00	3	2	1	0	0	0
-27.93722	8.039299	0.0000000E+00	0.0000000E+00	3	1	2	0	0	0
-13.13509	3.388476	0.0000000E+00	0.0000000E+00	3	0	3	0	0	0
0.0000000E+00	0.0000000E+00	9.495018	2.090857	3	2	0	1	0	0
0.0000000E+00	0.0000000E+00	33.51742	5.662971	3	1	1	1	0	0
0.0000000E+00	0.0000000E+00	28.29020	3.884218	3	0	2	1	0	0
-24.20185	-1.249737	0.0000000E+00	0.0000000E+00	3	1	0	2	0	0
-28.61959	-0.2489199	0.0000000E+00	0.0000000E+00	3	0	1	2	0	0
0.0000000E+00	0.0000000E+00	5.362778	4.140607	3	0	0	3	0	0
0.0000000E+00	0.0000000E+00	1.010153	0.3127397	3	2	0	0	1	0
0.0000000E+00	0.0000000E+00	2.158411	0.8073099	3	1	1	0	1	0
0.0000000E+00	0.0000000E+00	1.499370	1.007342	3	0	2	0	1	0
3.082702	0.8966252	0.0000000E+00	0.0000000E+00	3	1	0	1	1	0
4.440578	1.135125	0.0000000E+00	0.0000000E+00	3	0	1	1	1	0
0.0000000E+00	0.0000000E+00	0.3698255	0.5194395	3	0	0	2	1	0
0.2331147	-0.1484277	0.0000000E+00	0.0000000E+00	3	2	0	0	0	1
0.1686105E-01	-1.170449	0.0000000E+00	0.0000000E+00	3	1	1	0	0	1
0.3591492	-1.027763	0.0000000E+00	0.0000000E+00	3	0	2	0	0	1
0.0000000E+00	0.0000000E+00	0.4672848	-1.492605	3	1	0	1	0	1
0.0000000E+00	0.0000000E+00	-8.171200	-2.940918	3	0	1	1	0	1
24.83422	4.136724	0.0000000E+00	0.0000000E+00	3	0	0	2	0	1
0.2896029	0.1648165E-01	0.0000000E+00	0.0000000E+00	3	1	0	0	2	0
-0.6968171	-0.2218572	0.0000000E+00	0.0000000E+00	3	0	1	0	2	0
0.0000000E+00	0.0000000E+00	0.7921144	0.8022800E-01	3	0	0	1	2	0
0.0000000E+00	0.0000000E+00	-6.645480	-0.9852435	3	1	0	0	1	1
0.0000000E+00	0.0000000E+00	-9.595127	-1.282002	3	0	1	0	1	1
6.034936	-0.6671751	0.0000000E+00	0.0000000E+00	3	0	0	1	1	1
-4.637374	-0.3177884	0.0000000E+00	-0.0000000E+00	3	1	0	0	0	2
-5.708369	0.2412283	0.0000000E+00	-0.0000000E+00	3	0	1	0	0	2
0.0000000E+00	0.0000000E+00	0.7545583	1.065663	3	0	0	1	0	2
0.0000000E+00	0.0000000E+00	0.4460511	0.4935677	3	0	0	0	3	0
-0.5806638	-0.1069925	0.0000000E+00	0.0000000E+00	3	0	0	0	2	1
0.0000000E+00	0.0000000E+00	1.742148	-0.9767705	3	0	0	0	1	2
3.077817	0.5564029	0.0000000E+00	-0.0000000E+00	3	0	0	0	0	3
4.383797	1.177032	0.0000000E+00	0.0000000E+00	4	4	0	0	0	0
27.84163	7.486818	0.0000000E+00	0.0000000E+00	4	3	1	0	0	0
63.09656	17.28630	0.0000000E+00	0.0000000E+00	4	2	2	0	0	0
59.76168	17.52259	0.0000000E+00	0.0000000E+00	4	1	3	0	0	0
19.39444	6.547632	0.0000000E+00	0.0000000E+00	4	0	4	0	0	0
0.0000000E+00	0.0000000E+00	-12.19187	1.259706	4	3	0	1	0	0
0.0000000E+00	0.0000000E+00	-38.56813	5.092074	4	2	1	1	0	0
0.0000000E+00	0.0000000E+00	-35.83799	6.983817	4	1	2	1	0	0

0.0000000E+00	0.0000000E+00	-3.076604	4.109645	4	0	3	1	0	0
-52.30585	-4.788655	0.0000000E+00	0.0000000E+00	4	2	0	2	0	0
-134.6480	-11.46749	0.0000000E+00	0.0000000E+00	4	1	1	2	0	0
-87.72529	-7.269435	0.0000000E+00	0.0000000E+00	4	0	2	2	0	0
0.0000000E+00	0.0000000E+00	22.05171	5.053127	4	1	0	3	0	0
0.0000000E+00	0.0000000E+00	37.52868	6.850985	4	0	1	3	0	0
-52.38496	-8.923650	0.0000000E+00	0.0000000E+00	4	0	0	4	0	0
0.0000000E+00	0.0000000E+00	5.154693	0.3654179	4	3	0	0	1	0
0.0000000E+00	0.0000000E+00	20.81942	1.456122	4	2	1	0	1	0
0.0000000E+00	0.0000000E+00	32.67062	2.799320	4	1	2	0	1	0
0.0000000E+00	0.0000000E+00	19.43224	1.989246	4	0	3	0	1	0
2.949888	0.7242497	0.0000000E+00	0.0000000E+00	4	2	0	1	1	0
10.62403	2.288043	0.0000000E+00	0.0000000E+00	4	1	1	1	1	0
1.447042	1.952150	0.0000000E+00	0.0000000E+00	4	0	2	1	1	0
0.0000000E+00	0.0000000E+00	-12.68742	0.2780089	4	1	0	2	1	0
0.0000000E+00	0.0000000E+00	-16.76695	0.2928249	4	0	1	2	1	0
0.2911365	1.453493	0.0000000E+00	0.0000000E+00	4	0	0	3	1	0
13.33638	0.8078899	0.0000000E+00	0.0000000E+00	4	3	0	0	0	1
52.68270	1.116530	0.0000000E+00	0.0000000E+00	4	2	1	0	0	1
69.23424	-1.432753	0.0000000E+00	0.0000000E+00	4	1	2	0	0	1
31.58815	-2.032779	0.0000000E+00	0.0000000E+00	4	0	3	0	0	1
0.0000000E+00	0.0000000E+00	10.81177	-3.340195	4	2	0	1	0	1
0.0000000E+00	0.0000000E+00	18.47221	-10.10203	4	1	1	1	0	1
0.0000000E+00	0.0000000E+00	2.317954	-7.621907	4	0	2	1	0	1
75.10638	9.845267	0.0000000E+00	0.0000000E+00	4	1	0	2	0	1
100.0823	10.14189	0.0000000E+00	0.0000000E+00	4	0	1	2	0	1
0.0000000E+00	0.0000000E+00	-16.62974	-7.335777	4	0	0	3	0	1
0.3504618	0.1051327	0.0000000E+00	0.0000000E+00	4	2	0	0	2	0
-0.4690411	0.4892541	0.0000000E+00	0.0000000E+00	4	1	1	0	2	0
-0.9034674	0.4617898	0.0000000E+00	0.0000000E+00	4	0	2	0	2	0
0.0000000E+00	0.0000000E+00	2.334044	0.4440320E-01	4	1	0	1	2	0
0.0000000E+00	0.0000000E+00	8.304848	0.9277731	4	0	1	1	2	0
-0.9762085	-0.5165069E-01	0.0000000E+00	0.0000000E+00	4	0	0	2	2	0
0.0000000E+00	0.0000000E+00	-5.899160	-1.432191	4	2	0	0	1	1
0.0000000E+00	0.0000000E+00	-19.79540	-4.047618	4	1	1	0	1	1
0.0000000E+00	0.0000000E+00	-17.63018	-4.060433	4	0	2	0	1	1
15.07953	0.4717990	0.0000000E+00	0.0000000E+00	4	1	0	1	1	1
16.35545	-0.5359251	0.0000000E+00	0.0000000E+00	4	0	1	1	1	1
0.0000000E+00	0.0000000E+00	-1.002845	-5.689218	4	0	0	2	1	1
-5.959664	-0.9582827	0.0000000E+00	0.0000000E+00	4	2	0	0	0	2
-13.86366	-1.466755	0.0000000E+00	0.0000000E+00	4	1	1	0	0	2
-9.276368	-0.5963471	0.0000000E+00	0.0000000E+00	4	0	2	0	0	2
0.0000000E+00	0.0000000E+00	-8.176414	1.145855	4	1	0	1	0	2
0.0000000E+00	0.0000000E+00	-3.371150	2.782659	4	0	1	1	0	2
-47.68696	-8.804511	0.0000000E+00	0.0000000E+00	4	0	0	2	0	2
0.0000000E+00	0.0000000E+00	4.884030	0.8767356	4	1	0	0	3	0
0.0000000E+00	0.0000000E+00	7.197690	1.148644	4	0	1	0	3	0
-7.688784	0.1707115	0.0000000E+00	0.0000000E+00	4	0	0	1	3	0
-0.8029029	-0.3275044	0.0000000E+00	0.0000000E+00	4	1	0	0	2	1
0.3126405	-0.3637355	0.0000000E+00	0.0000000E+00	4	0	1	0	2	1
0.0000000E+00	0.0000000E+00	-1.319613	-0.4722055	4	0	0	1	2	1
0.0000000E+00	0.0000000E+00	4.812526	1.330852	4	1	0	0	1	2
0.0000000E+00	0.0000000E+00	10.65257	2.098605	4	0	1	0	1	2
-20.83225	-2.281103	0.0000000E+00	0.0000000E+00	4	0	0	1	1	2
7.760417	1.208879	0.0000000E+00	0.0000000E+00	4	1	0	0	0	3
9.187532	0.6067143	0.0000000E+00	0.0000000E+00	4	0	1	0	0	3
0.0000000E+00	0.0000000E+00	0.3012560	-0.8669586	4	0	0	1	0	3
0.5769994	0.9880361E-01	0.0000000E+00	0.0000000E+00	4	0	0	0	4	0
0.0000000E+00	0.0000000E+00	-1.997857	-1.243515	4	0	0	0	3	1
-0.2429743	0.2892302	0.0000000E+00	0.0000000E+00	4	0	0	0	2	2
-0.0000000E+00	0.0000000E+00	-1.630331	-1.181740	4	0	0	0	1	3
4.577576	-0.9066385	0.0000000E+00	0.0000000E+00	4	0	0	0	0	4
14.26097	1.720045	0.0000000E+00	0.0000000E+00	5	5	0	0	0	0
82.99886	10.85139	0.0000000E+00	0.0000000E+00	5	4	1	0	0	0

0.0000000E+00	0.0000000E+00	272.6448	-29.32036	7	0	3	1	2	1
56.17611	2.494439	0.0000000E+00	0.0000000E+00	7	2	0	2	2	1
302.7076	20.35415	0.0000000E+00	0.0000000E+00	7	1	1	2	2	1
375.5345	29.37260	0.0000000E+00	0.0000000E+00	7	0	2	2	2	1
0.0000000E+00	0.0000000E+00	78.33996	-7.585433	7	1	0	3	2	1
0.0000000E+00	0.0000000E+00	46.68450	-16.04720	7	0	1	3	2	1
105.3312	8.190675	0.0000000E+00	0.0000000E+00	7	0	0	4	2	1
0.0000000E+00	0.0000000E+00	-32.13896	12.92030	7	4	0	0	1	2
0.0000000E+00	0.0000000E+00	-178.5809	73.69698	7	3	1	0	1	2
0.0000000E+00	0.0000000E+00	-369.4682	162.1071	7	2	2	0	1	2
0.0000000E+00	0.0000000E+00	-317.0106	167.3906	7	1	3	0	1	2
0.0000000E+00	0.0000000E+00	-76.22867	72.13765	7	0	4	0	1	2
-417.4287	-50.44886	0.0000000E+00	0.0000000E+00	7	3	0	1	1	2
-1762.407	-188.9214	0.0000000E+00	0.0000000E+00	7	2	1	1	1	2
-2709.950	-268.2342	0.0000000E+00	0.0000000E+00	7	1	2	1	1	2
-1487.805	-132.9680	0.0000000E+00	0.0000000E+00	7	0	3	1	1	2
0.0000000E+00	0.0000000E+00	354.0549	84.88082	7	2	0	2	1	2
0.0000000E+00	0.0000000E+00	1062.422	239.6767	7	1	1	2	1	2
0.0000000E+00	0.0000000E+00	855.3967	197.7827	7	0	2	2	1	2
-1052.714	-190.5045	0.0000000E+00	0.0000000E+00	7	1	0	3	1	2
-1336.863	-211.4685	0.0000000E+00	0.0000000E+00	7	0	1	3	1	2
0.0000000E+00	0.0000000E+00	277.7161	115.4744	7	0	0	4	1	2
103.9723	25.18422	0.0000000E+00	0.0000000E+00	7	4	0	0	0	3
470.2270	106.8326	0.0000000E+00	0.0000000E+00	7	3	1	0	0	3
761.9900	153.8209	0.0000000E+00	0.0000000E+00	7	2	2	0	0	3
515.7608	78.06458	0.0000000E+00	0.0000000E+00	7	1	3	0	0	3
118.8647	3.647564	0.0000000E+00	0.0000000E+00	7	0	4	0	0	3
0.0000000E+00	0.0000000E+00	169.5593	-0.3770634	7	3	0	1	0	3
0.0000000E+00	0.0000000E+00	797.5193	-7.586529	7	2	1	1	0	3
0.0000000E+00	0.0000000E+00	1232.615	-20.11668	7	1	2	1	0	3
0.0000000E+00	0.0000000E+00	626.2421	-18.11362	7	0	3	1	0	3
1016.493	173.7559	0.0000000E+00	0.0000000E+00	7	2	0	2	0	3
2611.824	402.7570	0.0000000E+00	0.0000000E+00	7	1	1	2	0	3
1805.227	258.5918	0.0000000E+00	0.0000000E+00	7	0	2	2	0	3
0.0000000E+00	0.0000000E+00	-358.7314	-12.76016	7	1	0	3	0	3
0.0000000E+00	0.0000000E+00	-638.0853	-26.74049	7	0	1	3	0	3
1620.142	297.4638	0.0000000E+00	0.0000000E+00	7	0	0	4	0	3
-3.925356	0.4077369	0.0000000E+00	0.0000000E+00	7	3	0	0	4	0
-16.89333	2.962293	0.0000000E+00	0.0000000E+00	7	2	1	0	4	0
-28.78358	6.463100	0.0000000E+00	0.0000000E+00	7	1	2	0	4	0
-16.79480	4.370139	0.0000000E+00	0.0000000E+00	7	0	3	0	4	0
0.0000000E+00	0.0000000E+00	-19.08557	3.404158	7	2	0	1	4	0
0.0000000E+00	0.0000000E+00	-50.37190	10.05068	7	1	1	1	4	0
0.0000000E+00	0.0000000E+00	-26.23580	10.91245	7	0	2	1	4	0
9.096949	1.879187	0.0000000E+00	0.0000000E+00	7	1	0	2	4	0
4.388093	2.251736	0.0000000E+00	0.0000000E+00	7	0	1	2	4	0
0.0000000E+00	0.0000000E+00	-15.59496	5.813275	7	0	0	3	4	0
0.0000000E+00	0.0000000E+00	22.52218	-1.778761	7	3	0	0	3	1
0.0000000E+00	0.0000000E+00	73.28570	-9.628226	7	2	1	0	3	1
0.0000000E+00	0.0000000E+00	48.74783	-20.61273	7	1	2	0	3	1
0.0000000E+00	0.0000000E+00	-33.18682	-17.53103	7	0	3	0	3	1
182.5158	17.97944	0.0000000E+00	0.0000000E+00	7	2	0	1	3	1
525.1490	16.50805	0.0000000E+00	0.0000000E+00	7	1	1	1	3	1
436.3882	34.67298	0.0000000E+00	0.0000000E+00	7	0	2	1	3	1
0.0000000E+00	0.0000000E+00	-134.5124	-18.20940	7	1	0	2	3	1
0.0000000E+00	0.0000000E+00	-218.0256	-28.83783	7	0	1	2	3	1
400.0532	69.24387	0.0000000E+00	0.0000000E+00	7	0	0	3	3	1
-46.72803	-2.242560	0.0000000E+00	0.0000000E+00	7	3	0	0	2	2
-251.0516	-11.10414	0.0000000E+00	0.0000000E+00	7	2	1	0	2	2
-451.2677	-16.72836	0.0000000E+00	0.0000000E+00	7	1	2	0	2	2
-272.3934	-6.761505	0.0000000E+00	0.0000000E+00	7	0	3	0	2	2
0.0000000E+00	0.0000000E+00	-18.25131	[illegible].27749	7	2	0	1	2	2
0.0000000E+00	0.0000000E+00	-88.40754	[illegible]24976	7	1	1	1	2	2
0.0000000E+00	0.0000000E+00	-68.49352	71.15384	7	0	2	1	2	2

-109.6657	-20.58854	0.0000000E+00	0.0000000E+00	7	1	0	2	2	2
-246.0886	-36.06984	0.0000000E+00	0.0000000E+00	7	0	1	2	2	2
0.0000000E+00	0.0000000E+00	-0.1833213	45.71732	7	0	0	3	2	2
0.0000000E+00	0.0000000E+00	48.71169	-3.505475	7	3	0	0	1	3
0.0000000E+00	0.0000000E+00	190.9520	-18.01386	7	2	1	0	1	3
0.0000000E+00	0.0000000E+00	237.5891	-34.00185	7	1	2	0	1	3
0.0000000E+00	0.0000000E+00	72.10666	-25.10724	7	0	3	0	1	3
435.9339	63.76096	0.0000000E+00	0.0000000E+00	7	2	0	1	1	3
1219.109	157.7391	0.0000000E+00	0.0000000E+00	7	1	1	1	1	3
1035.465	129.6821	0.0000000E+00	0.0000000E+00	7	0	2	1	1	3
0.0000000E+00	0.0000000E+00	-196.6065	-28.00481	7	1	0	2	1	3
0.0000000E+00	0.0000000E+00	-369.0779	-45.47282	7	0	1	2	1	3
1026.274	204.6144	0.0000000E+00	0.0000000E+00	7	0	0	3	1	3
-166.9558	-36.86505	0.0000000E+00	0.0000000E+00	7	3	0	0	0	4
-701.3548	-146.3982	0.0000000E+00	0.0000000E+00	7	2	1	0	0	4
-1020.017	-200.1861	0.0000000E+00	0.0000000E+00	7	1	2	0	0	4
-515.8607	-93.00321	0.0000000E+00	0.0000000E+00	7	0	3	0	0	4
0.0000000E+00	0.0000000E+00	-35.06134	4.877494	7	2	0	1	0	4
0.0000000E+00	0.0000000E+00	-126.0184	20.96209	7	1	1	1	0	4
0.0000000E+00	0.0000000E+00	-102.1119	20.41700	7	0	2	1	0	4
-797.5440	-144.2564	0.0000000E+00	0.0000000E+00	7	1	0	2	0	4
-948.3623	-145.5734	0.0000000E+00	0.0000000E+00	7	0	1	2	0	4
0.0000000E+00	0.0000000E+00	160.1856	13.32972	7	0	0	3	0	4
0.0000000E+00	0.0000000E+00	3.179614	0.7675013	7	2	0	0	5	0
0.0000000E+00	0.0000000E+00	13.67970	2.697057	7	1	1	0	5	0
0.0000000E+00	0.0000000E+00	14.96166	3.302116	7	0	2	0	5	0
-16.90704	-0.7627503	0.0000000E+00	0.0000000E+00	7	1	0	1	5	0
-25.07770	-0.3238824	0.0000000E+00	0.0000000E+00	7	0	1	1	5	0
0.0000000E+00	0.0000000E+00	8.349618	3.908544	7	0	0	2	5	0
13.68413	0.9944160	0.0000000E+00	0.0000000E+00	7	2	0	0	4	1
33.49082	1.055084	0.0000000E+00	0.0000000E+00	7	1	1	0	4	1
34.35350	-0.5239913	0.0000000E+00	0.0000000E+00	7	0	2	0	4	1
0.0000000E+00	0.0000000E+00	23.53642	-4.579323	7	1	0	1	4	1
0.0000000E+00	0.0000000E+00	22.32465	-8.083286	7	0	1	1	4	1
67.36324	8.148308	0.0000000E+00	0.0000000E+00	7	0	0	2	4	1
0.0000000E+00	0.0000000E+00	-8.429376	6.578245	7	2	0	0	3	2
0.0000000E+00	0.0000000E+00	-3.715601	23.09357	7	1	1	0	3	2
0.0000000E+00	0.0000000E+00	26.11489	26.25361	7	0	2	0	3	2
-228.4248	-27.90990	0.0000000E+00	0.0000000E+00	7	1	0	1	3	2
-326.5470	-29.55670	0.0000000E+00	0.0000000E+00	7	0	1	1	3	2
0.0000000E+00	0.0000000E+00	83.27780	36.57706	7	0	0	2	3	2
41.55391	4.839621	0.0000000E+00	0.0000000E+00	7	2	0	0	2	3
126.9867	12.87402	0.0000000E+00	0.0000000E+00	7	1	1	0	2	3
120.5161	10.11373	0.0000000E+00	0.0000000E+00	7	0	2	0	2	3
0.0000000E+00	0.0000000E+00	21.98186	-8.602154	7	1	0	1	2	3
0.0000000E+00	0.0000000E+00	24.14422	-16.12410	7	0	1	1	2	3
199.2143	35.29463	0.0000000E+00	0.0000000E+00	7	0	0	2	2	3
0.0000000E+00	0.0000000E+00	-14.30908	6.236932	7	2	0	0	1	4
0.0000000E+00	0.0000000E+00	-33.80752	21.44846	7	1	1	0	1	4
0.0000000E+00	0.0000000E+00	-12.30968	21.70526	7	0	2	0	1	4
-350.8958	-59.55836	0.0000000E+00	0.0000000E+00	7	1	0	1	1	4
-461.9033	-63.26451	0.0000000E+00	0.0000000E+00	7	0	1	1	1	4
0.0000000E+00	0.0000000E+00	100.4002	32.81258	7	0	0	2	1	4
80.18404	16.68081	0.0000000E+00	0.0000000E+00	7	2	0	0	0	5
173.4974	33.08663	0.0000000E+00	0.0000000E+00	7	1	1	0	0	5
106.0285	18.87622	0.0000000E+00	0.0000000E+00	7	0	2	0	0	5
0.0000000E+00	0.0000000E+00	17.74187	0.6487541	7	1	0	1	0	5
0.0000000E+00	0.0000000E+00	33.61333	-0.7991250	7	0	1	1	0	5
363.5322	70.16022	0.0000000E+00	0.0000000E+00	7	0	0	2	0	5
-1.857805	0.1052536	0.0000000E+00	0.0000000E+00	7	1	0	0	6	0
-1.864441	0.2444205	0.0000000E+00	0.0000000E+00	7	0	1	0	6	0
0.0000000E+00	0.0000000E+00	1.805629	1.736612	7	0	0	1	6	0
0.0000000E+00	0.0000000E+00	-7.195567	-2.053119	7	1	0	0	5	1
0.0000000E+00	0.0000000E+00	-20.42802	-4.204549	7	0	1	0	5	1

COSY INFINITY

MICHIGAN STATE UNIVERSITY

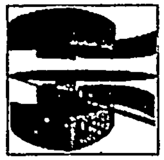

Beam Theory and Dynamical Systems Group

Welcome to the official COSY INFINITY site on the world wide web! There is information about the code, its users, and its uses. One can also register as a user and download the code for various platforms.

Directory of Services

Visitors

News
What is COSY
Download Manual

Registered Users

Uses of COSY
COSY References
Acknowledgments
Help

New Users

User Registration
User's Agreement
Download Code

Visitors

News

- There will be a COSY User's Meeting, and a summary talk about its features, at CAP96 in Williamsburg, Virginia. Time and place of the User's meeting will be announced at the conference.
- In the spring term 1997 beginning in January, we will offer an online web course on Introductory Beam Physics. Participation only requires access to www and/or standard video conferencing equipment.
- Version 7 of COSY INFINITY can now be downloaded by registered users.

What is COSY

COSY INFINITY is an arbitrary order beam dynamics simulation and analysis code. It allows the study of accelerator lattices, spectrographs, beamlines, electron microscopes, and many other devices. It can determine high-order maps of combinations of particle optical elements of arbitrary field configurations. The

Uses of COSY

Some of the various projects COSY has been used for over time are listed here. Also listed are names of local contact persons connected to each of the activities.

KFA Juelich	Simulation of COSY Juelich Ring	Phil Meads
	Resonance Extraction	Sig Martin
TRIUMF	General Beam Dynamics Simulation	Roger Servranckx
	Resonance Correction	Paul Tupper
	Simulation of Electrostatic Elements	Richard Baartman
SSC	Maps for Tracking	Martin Berz
	LEB Ring Design Questions	Xiaoyu Wu
	Resonance Correction	Roger Servranckx
DESY	HERA Fringe Field Studies	Georg Hoffstaetter
	Random Errors	Desmond Barber
	Spin Dynamics	Nina Golubeva
NSCL	High-Precision Fringe Field Treatment	Brad Sherrill
	Measured Field Data	Kyoko Makino
	Achromat Design	Weishi Wan
	Reconstructive Correction of Aberrations	Martin Berz
CEBAF	Reconstructive Correction of Spectrographs	Mohammad Khayat
	Spin Dynamics	Rolf Ent
ANL	Spectrometer Design and Correction	David Potterveld
	Simulation of RFQ Dynamics	Jerry Nolen

	Resonance Correction	Roger Servranckx
DESY	HERA Fringe Field Studies	Georg Hoffstaetter
	Random Errors	Desmond Barber
	Spin Dynamics	Nina Golubeva
NSCL	High-Precision Fringe Field Treatment	Brad Sherrill
	Measured Field Data	Kyoko Makino
	Achromat Design	Weishi Wan
	Reconstructive Correction of Aberrations	Martin Berz
CEBAF	Reconstructive Correction of Spectrographs	Mohammad Khayat
	Spin Dynamics	Rolf Ent
ANL	Spectrometer Design and Correction	David Potterveld
	Simulation of RFQ Dynamics	Jerry Nolen

COSY References

Below follows a partial list of papers describing some of the features of COSY INFINITY that can be used as references.

M. Berz, COSY INFINITY Version 7 Reference Manual, NSCL Technical Report MSUCL-977, Michigan State University, 1995

K. Makino and M. Berz, New Features in COSY INFINITY, in: Proceedings 1996 Computational Accelerator Physics Conference, to appear

M. Berz, G. Hoffstaetter, W. Wan, K. Shamseddine and K. Makino, COSY INFINITY and its Applications in Nonlinear Dynamics, in: Computational Differentiation: Techniques, Applications, and Tools, SIAM 1996

M. Berz, New Features in COSY INFINITY, in: Proceedings, Third Computational Accelerator Physics Conference, AIP Conference Proceedings 297, 1993, p. 267

M. Berz, COSY INFINITY Version 6, in "Nonlinear Effects in Accelerators", M. Berz, S. Martin and K. Ziegler (Eds.), IOP Publishing, 1992, p. 125

M. Berz, COSY INFINITY, in: Proceedings 1991 Particle Accelerator Conference, San Francisco

M. Berz, Computational Aspects of Design and Simulation: COSY INFINITY, Nuclear Instruments and Methods A298 (1990) 473

COSY Polynomial Operations

Storage

- One Double Precision Taylor polynomial coefficient
- One Short Integer exponent identifier
- Full exploitation of sparsity

Multiplication

```
      DO 100 IB = NBNO(NOIB),NENO(NOIB)
         NCIB = NC(IB)
         ICC = IA2(I2IA+IE2(NCIB)) + IA1(I1IA+IE1(NCIB))
         CDA(ICC) = CDA(ICC) + CCIA*CC(IB)
 100  CONTINUE
```

- Dominated by Double Precision multiplication
- Indexing: 3 Short Integer additions, 4 array look ups
- **Indexing takes only 30% of floating point effort** (VAX/VMS)
- Full exploitation of sparsity of DA vectors
- By far **dominates overall computational expense**

Addition

- Merging/Adding of sorted lists of DA vectors
- Full exploitation of sparsity of DA vectors
- Addition only when both coefficients nonzero
- Typical contribution to overall computational expense <10%

Derivation

```
      DO 100 IA=NBEG(INA),NEND(INA),ITA
         NCIA = NC(IA)
         IC = IC + 1
         CC(IC) = CC(IA)* IJJ(IDIF,NCIA)
         NC(IC) = IA1(IE1(NCIA)-ID1) + IA2(IE2(NCIA)-ID2)
 100  Continue
```

- Single pass through vector
- Indexing: 5 array look ups, 3 Short Integer additions
- Typical contribution to overall computational expense <5%

A Fifth Order Achromat

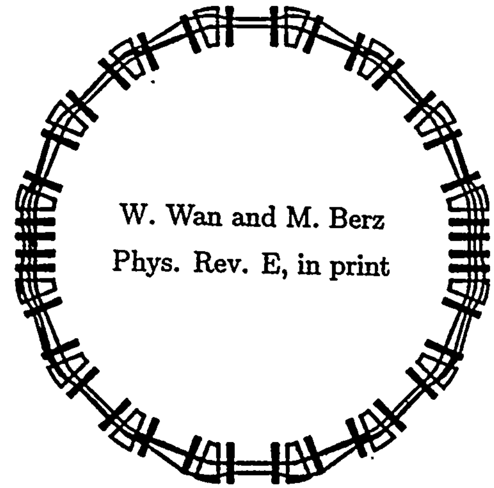

- Circumference: 266.64 m
- Number of elements per cell (half of the ring)

Dipoles:		8
Quadrupoles	(long multipoles):	18
Sextupoles	(not shown here):	4
Octupoles	(not shown here):	15
Decapoles	(not shown here):	15
Duodecapoles	(not shown here):	39

- Emittance: 30π mm mrad
- Dispersion: 0.3%

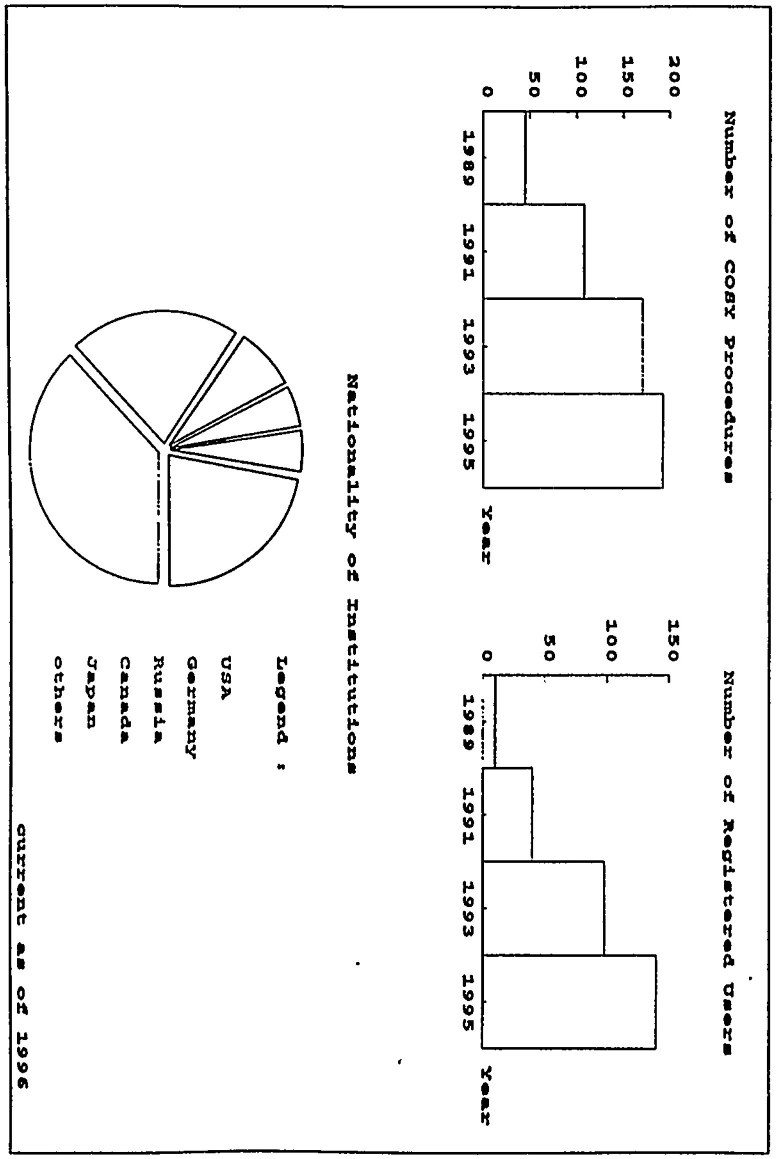

DA Computation of Spin Motion

Instead of motion in nine variables, it is sufficient to use six dimensional DA to determine Taylor expansion of $\hat{A}(\vec{z})$:

Autonomous Case (Main Fields): Utilize existence of two invariant subspaces of mixed symplectic-orthogonal propagator $\exp(sL_{\vec{F}})$ with directional derivative

$$L_{\vec{F}} = \vec{f}^t \cdot \vec{\nabla}_{\vec{z}} + (\hat{W} \cdot \vec{s})^t \cdot \vec{\nabla}_{\vec{s}}$$

and exploit

$$\vec{M}(\vec{z}_i, \vec{s}_i, s) = \exp(sL_{\vec{F}})\ \vec{I}.$$

Non-Autonomous Case (Fringe Fields, Wigglers, Measured Fields etc.): Integrate equations of motion for orbit and spin matrix in DA.

Composition of Maps: Let $(\vec{M}_{1,2}, \hat{A}_{1,2})$ and $(\vec{M}_{2,3}, \hat{A}_{2,3})$ be given. Then we get

$$\vec{M}_{1,3} = \vec{M}_{2,3} \circ \vec{M}_{1,2}$$
$$\hat{A}_{1,3}(\vec{z}) = \hat{A}_{2,3}(\vec{M}_{1,2}) \cdot \hat{A}_{1,2}(\vec{z})$$

Motion Of Spin Matrix

Nine dimensional motion of particle with spin, neglecting spin-orbit coupling

$$\begin{pmatrix} \vec{z} \\ \vec{s} \end{pmatrix}' = \vec{F}(\vec{z}, \vec{s}, s) = \begin{pmatrix} \vec{f}(\vec{z}, s) \\ \hat{W}(\vec{z}, s) \cdot \vec{s} \end{pmatrix}$$

$$\begin{pmatrix} \vec{z}_f \\ \vec{s}_f \end{pmatrix} = \vec{M}(\vec{z}_i, \vec{s}_i, s) = \begin{pmatrix} \mathcal{M}(\vec{z}_i, s) \\ \hat{A}(\vec{z}_i, s) \cdot \vec{s} \end{pmatrix}$$

To *reduce dimensionality* and *utilize linearity*, it is advantageous to set up EOM for $\hat{A}$. Insertion yields EOM for 3×3 spin matrix depending on only the 6 orbital variables:

$$\hat{A}'(\vec{z}, s) = \hat{W}(\vec{z}, s) \cdot \hat{A}(\vec{z}, s)$$

What areDerivatives?

Differential Quotients?
- Idea of Newton, Leibniz
- Very intuitive
- Liked by many Physicists
- Would be nice for Numerics!

Rigorous Mathematics:
- Epsilon-Delta Arguments
- Necessary for Rigor
- Not very intuitive
- Scares many Physicists
- Not so easy for Numerics

Try to do Both!
- Be fully rigorous
- Satisfy intuition
- Understand Delta Functions
- Provide Numerical Tool

Structures with Infinitesimals

Schmieden, Laugwitz
- Numbers are sequences
- A statement is true if it's true for almost all elements
- not totally ordered, no field
- Calculus rather easy
- Derivatives are Diff. Quotients
- Not directly useful for Numerics

Nonstandard Analysis
- Generalization of S+L
- Based on Formal Logic
- Strikingly general: everything about R continues to hold
- Derivatives are Diff. Quotients
- Not directly useful for Numerics

Others:
- Surreal Numbers
- ...

Levi-Civita Numbers
- Found 100 years ago
- Totally ordered field
- Connected to Hahn Theorem
- What calculus can be done?

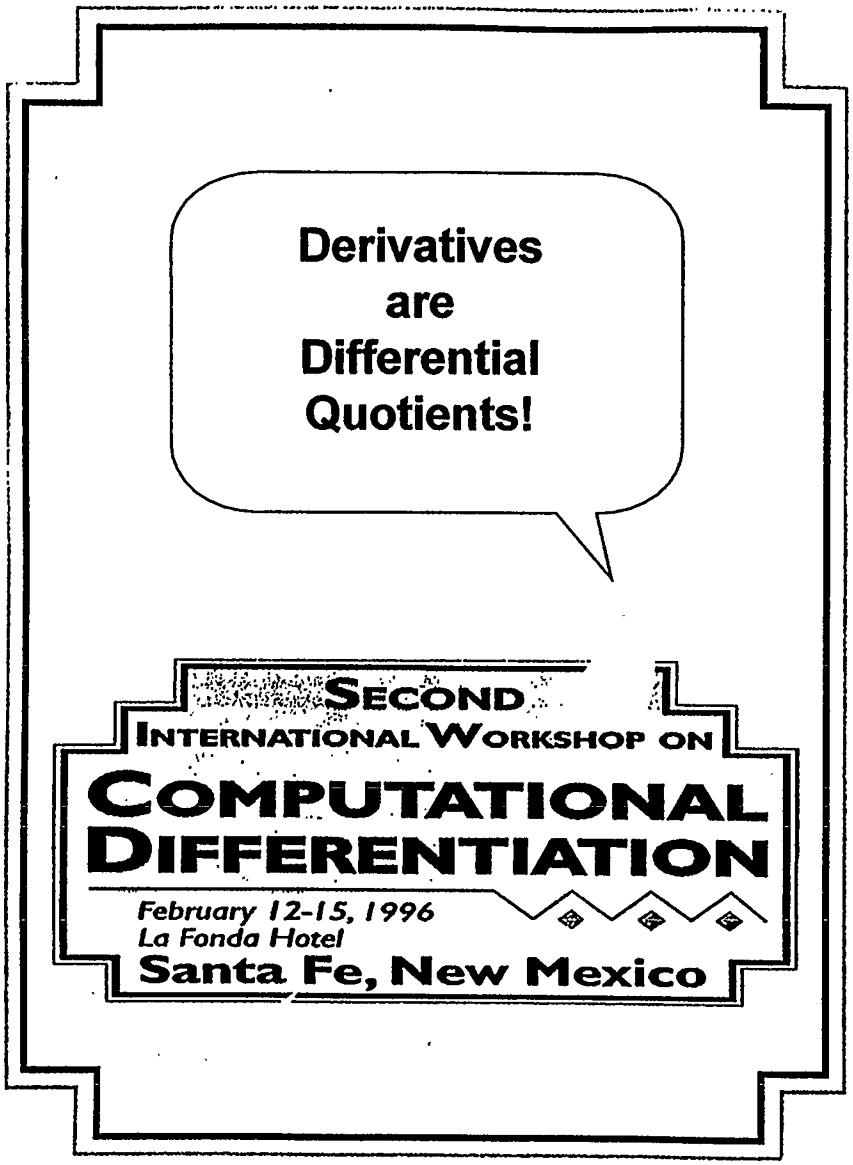

The set L

Let L be the set of all functions $x : Q \to R, q \to x[q]$ whose support is finite below every bound:

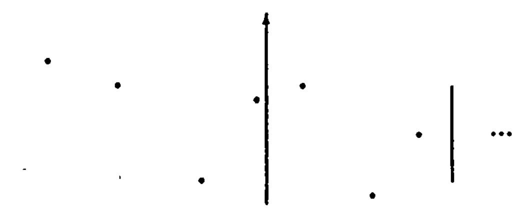

Define addition componentwise. Define a multiplication as follows:

$$(x \cdot y)[q] = \sum_{q_x + q_y = q} x[q_x] \cdot y[q_y]$$

For each q, the sum in the product has at most finitely many terms. Furthermore, $(x \cdot y)$ is nonzero for only finitely many q below every bound. Thus L is closed under addition and multiplication.

Delta Functions

Can directly use intuitive concept of a delta function:

$$\delta(x) = \begin{cases} 0 & \text{if } |x| \gg 1 \\ \pi^{-\frac{1}{2}} d^{-1} \cdot \exp(-x^2/d^2) & \text{else} \end{cases}$$

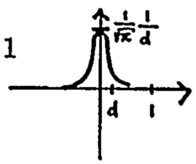

Nonzero only for infinitely small x. Infinitely large value $(1/d)$ at origin.

Can do calculus with delta functions. In particular, for a large class of functions f one can show that

$$\int_{-1}^{1} f(x)\, \delta(x)\, dx = f(0)$$

up to an infinitely small error.

Contents

The DA Normal Form Algorithm

Assume linear part of map has been diagonalized by a linear change of basis:

$$\mathcal{M} = \mathcal{R} + \mathcal{S}$$

where $\mathcal{R}$ has on its diagonal the values $r_j \cdot e^{\pm i\nu_j}$ (pair structure).

Now attempt to simplify the map by a nonlinear transformation. Choose transformation

$$\mathcal{A}_m = \mathcal{E} + \mathcal{T}_m$$

Up to order m, the inverse is $\mathcal{A}_m^{-1} =_m \mathcal{E} - \mathcal{T}_m$, and we obtain

$$\begin{aligned}
& \mathcal{A} \circ \mathcal{M} \circ \mathcal{A}^{-1} \\
=_m & \ (\mathcal{E} + \mathcal{T}_m) \circ (\mathcal{R} + \mathcal{S}_{m-1}) \circ (\mathcal{E} - \mathcal{T}_m) \\
=_m & \ (\mathcal{E} + \mathcal{T}_m) \circ (\mathcal{R} + \mathcal{S}_{m-1}) \circ (\mathcal{E} - \mathcal{T}_m) \\
=_m & \ \mathcal{R} + \mathcal{S}_{m-1} + (\mathcal{T}_m \circ \mathcal{R} - \mathcal{R} \circ \mathcal{T}_m)
\end{aligned}$$

Removing Terms in the Normal Form Step

We can use the commutator $\mathcal{C}$ of $\mathcal{T}_m$ and $\mathcal{R}$ to remove terms from $\mathcal{S}_{m-1}$. We write

$$\mathcal{T}_{mj}^{\pm} = \sum \left(\mathcal{T}_{mj}^{\pm} | k_1^+, k_1^-, ..., k_n^+, k_n^-\right) \cdot (v_1^+)^{k_1^+} (v_1^-)^{k_1^-} \cdot ... \cdot (v_n^+)^{k_n^+} (v_n^-)^{k_n^-}$$

$$\mathcal{C}_{mj}^{\pm} = \sum \left(\mathcal{C}_{mj}^{\pm} | k_1^+, k_1^-, ..., k_n^+, k_n^-\right) \cdot (v_1^+)^{k_1^+} (v_1^-)^{k_1^-} \cdot ... \cdot (v_n^+)^{k_n^+} (v_n^-)^{k_n^-}$$

Because of the simple form of $\mathcal{R}$, we obtain

$$\begin{aligned}
& (\mathcal{C}_j^{\pm} | k_1, k_1^-, ..., k_n^+, k_n^-) \\
= & \ -\mathcal{C}_j^{\pm}(\vec{k}^+, \vec{k}^-) \cdot (\mathcal{T}_j^{\pm} | k_1^+, k_1^-, ..., k_n^+, k_n^-)
\end{aligned}$$

where

$$\mathcal{C}_j^{\pm}(\vec{k}^+, \vec{k}^-) = r_j \cdot e^{\pm i\nu_j} - \left(\prod_{j=1}^{n} (r_j)^{k_j^+ + k_j^-} \right) \cdot e^{i\vec{\nu}\cdot(\vec{k}^+ - \vec{k}^-)}$$

So we can remove every term for which $\mathcal{C}_j^{\pm}(\vec{k}^+, \vec{k}^-)$ is nonzero!

Removable Terms in the Symplectic Case

In the symplectic case, all r_j are one (no damping). Then everything is removable except if

$$\vec{\nu} \cdot (\vec{k}^+ - \vec{k}^-) = l \cdot 2\pi \pm \nu_j \;\; \forall l$$

This can occur in the following cases:

1. $\vec{n} \cdot \vec{\nu} = l \cdot 2\pi$ has nontrivial solutions (we are on a resonance; physics case)
2. $k_l^+ = k_l^- \;\; \forall\, l \neq j$, and $k_j^+ = k_j^- \pm 1$ (unavoidable; mathematics case)

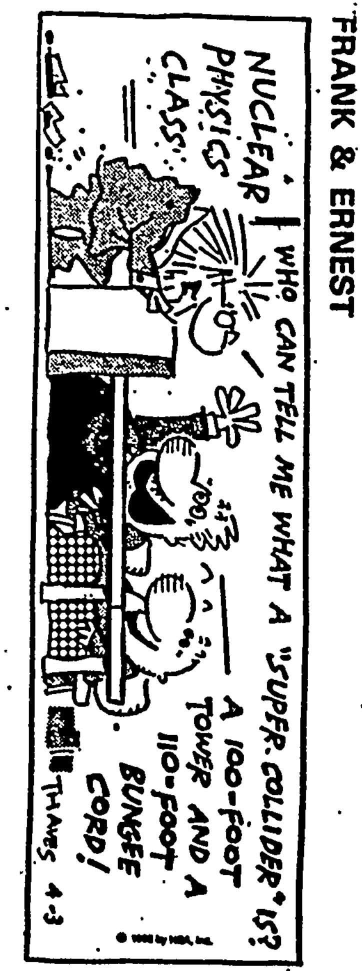

Dead man's bungee cord was 70 feet too long

Associated Press

ARVADA, Colo. — Police are considering homicide charges against a company that gave a man a free bungee jump that killed him because the cord was 70 feet too long.

Bungee America ignored safety standards that would have prevented William Brotherton's death Sunday when he lept from a tethered hot-air balloon over a field, said a report by Carl Finocchiaro, safety committee chairman of the North American Bungee Association.

Brotherton, 20, was taking a free jump in exchange for testing equipment. Finocchiaro's report was turned over to police. He concluded:

■ The balloon was hovering at 190 feet. For Brotherton not to have hit the ground, it needed to be 260 feet up.

■ Communication between the ground crew and balloon pilot was inadequate. The ground crew tried to warn the pilot, by shouting, that the balloon was too low.

Bungee America wasn't insured or licensed by the state. A recording on the company's telephone said the line had been disconnected.

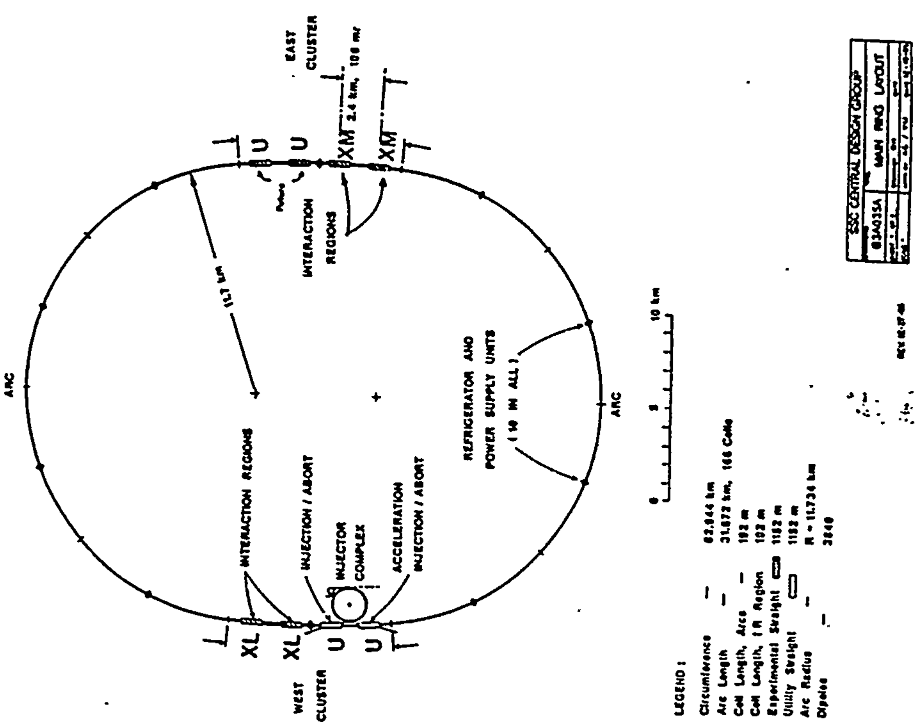

SSC LEB

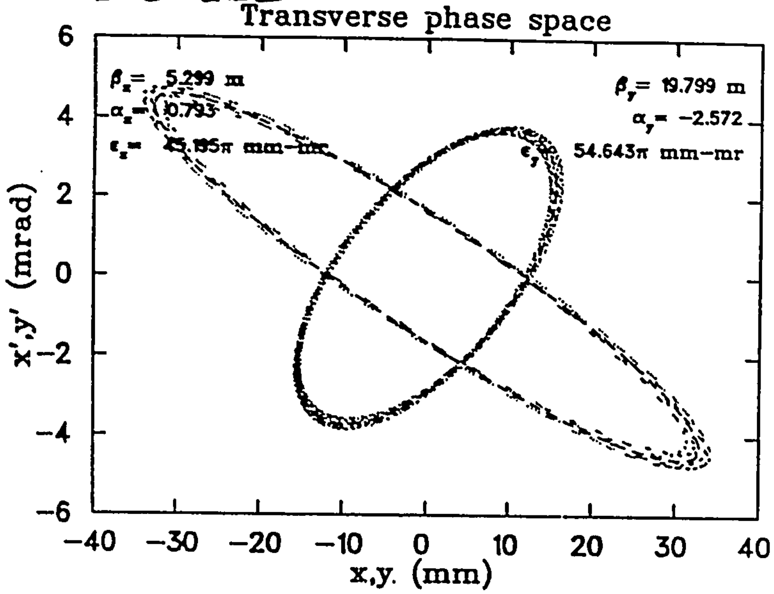

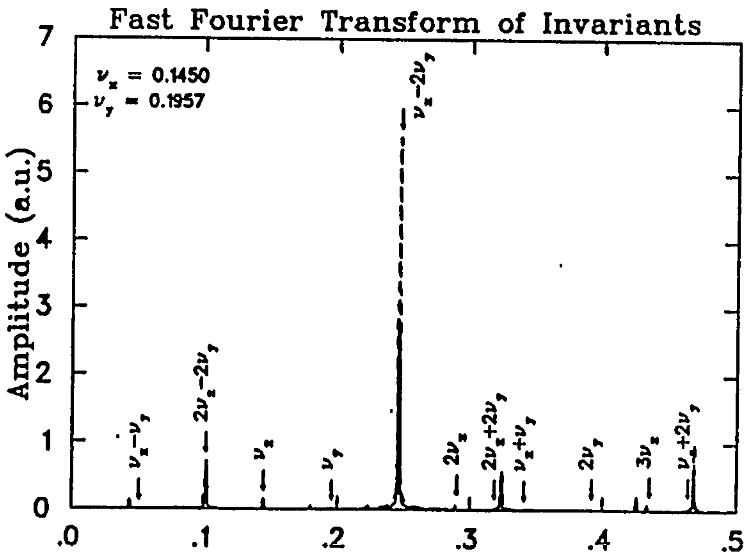

Courtesy R. Servranckx

SSC LEB

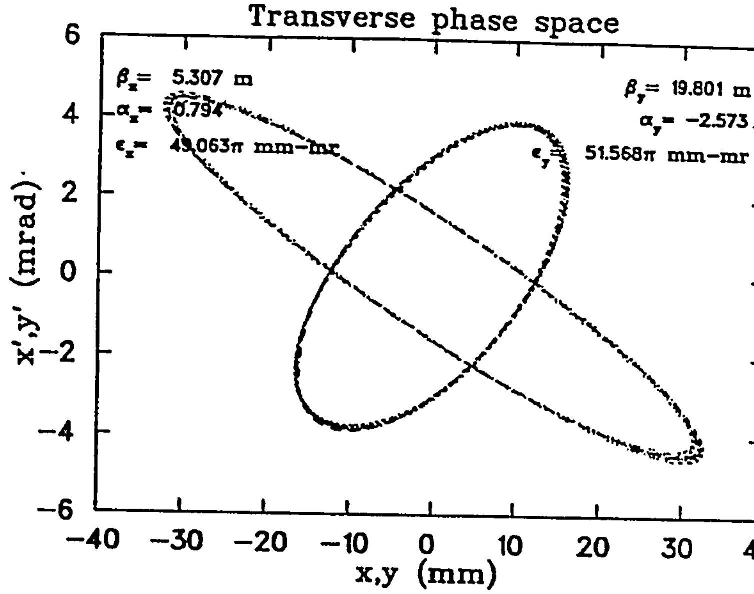

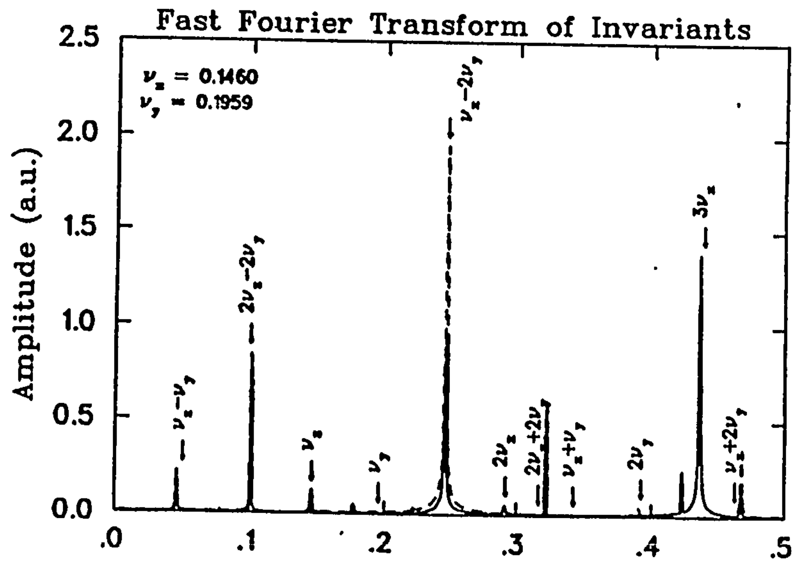

Courtesy R. Servranckx

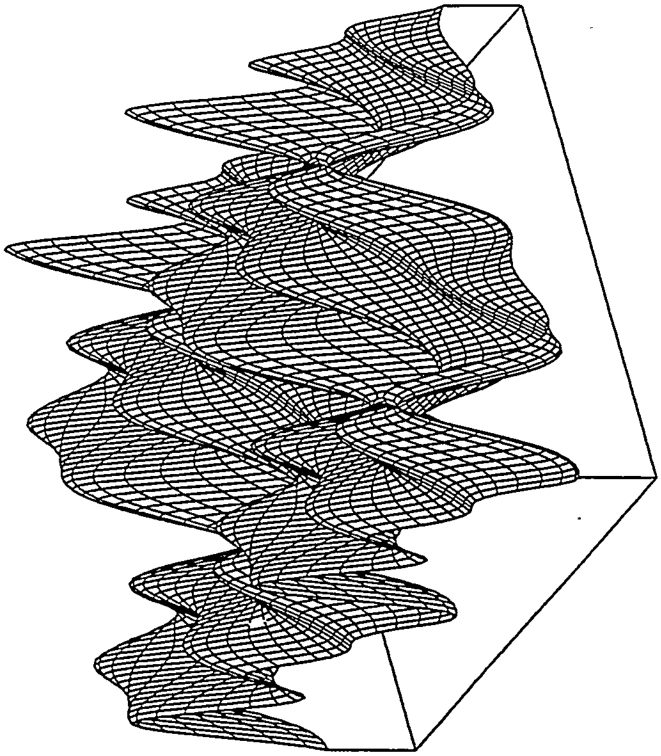

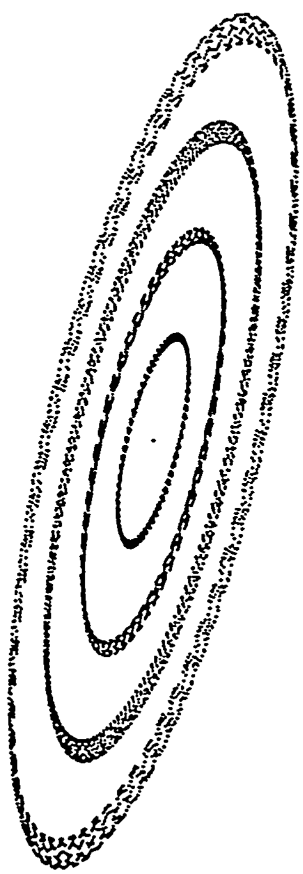

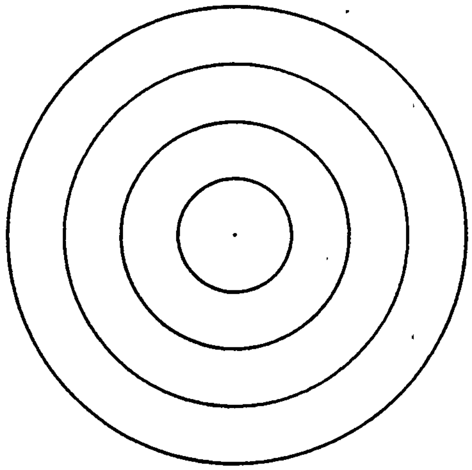

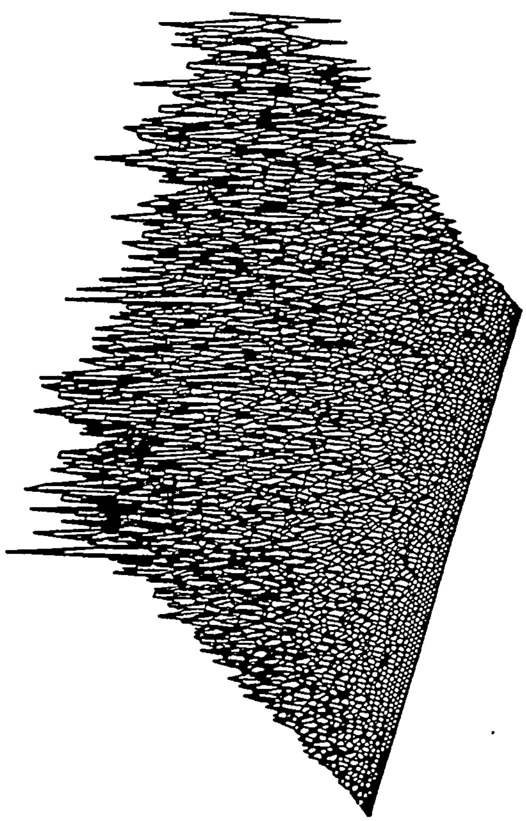

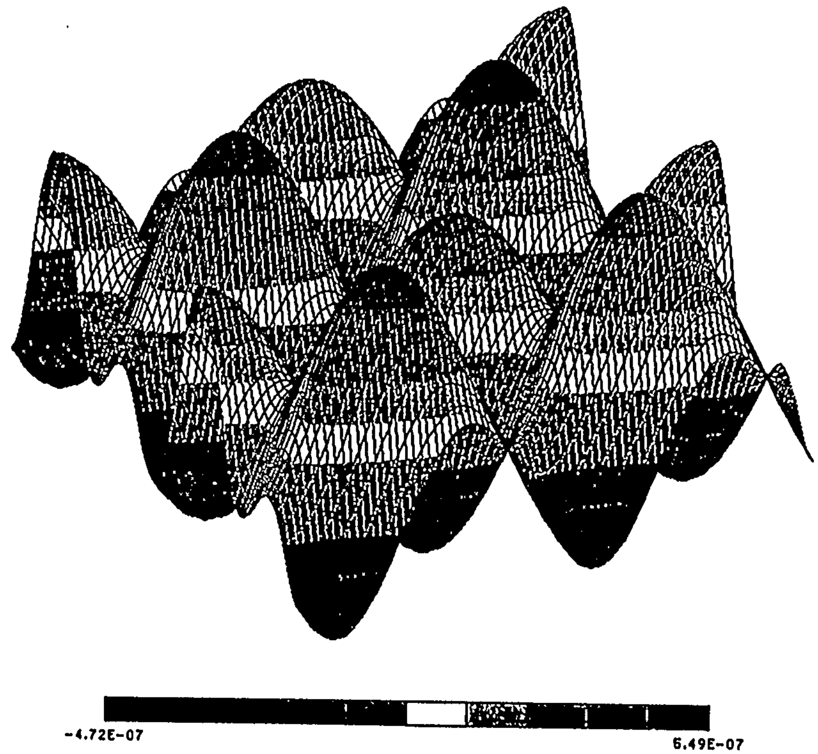
-4.72E-07
6.49E-07

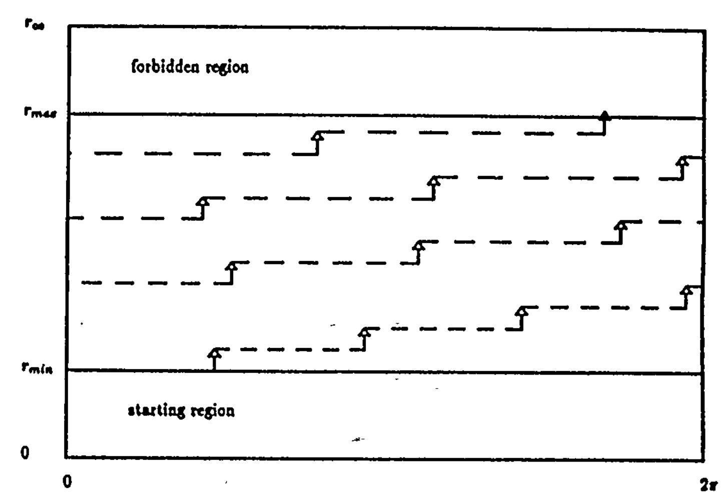
r_∞
r_{max}
r_{min}
0
forbidden region
starting region
0
2π

Number Field Inclusions (Intervals)

Real Numbers — I (Interval Inclusion: Equivalence Relation) — **Floating Point Intervals**

$c = a + b$

$$\begin{tikzcd} \cdot \arrow[r, "I"] \arrow[d, "+"'] & \cdot \arrow[d, "\oplus"] \\ \cdot \arrow[r, "I"'] & \cdot \end{tikzcd}$$

$c_I = a_I \oplus b_I$

$c = a \cdot b$

$$\begin{tikzcd} \cdot \arrow[r, "I"] \arrow[d, "\cdot"'] & \cdot \arrow[d, "\odot"] \\ \cdot \arrow[r, "I"'] & \cdot \end{tikzcd}$$

$c_I = a_I \odot b_I$

Field
(Also want "exp", "sin" etc: Banach Field)

Diagrams commute exactly!

Little algebraic structure

I: Extracts Information considered relevant

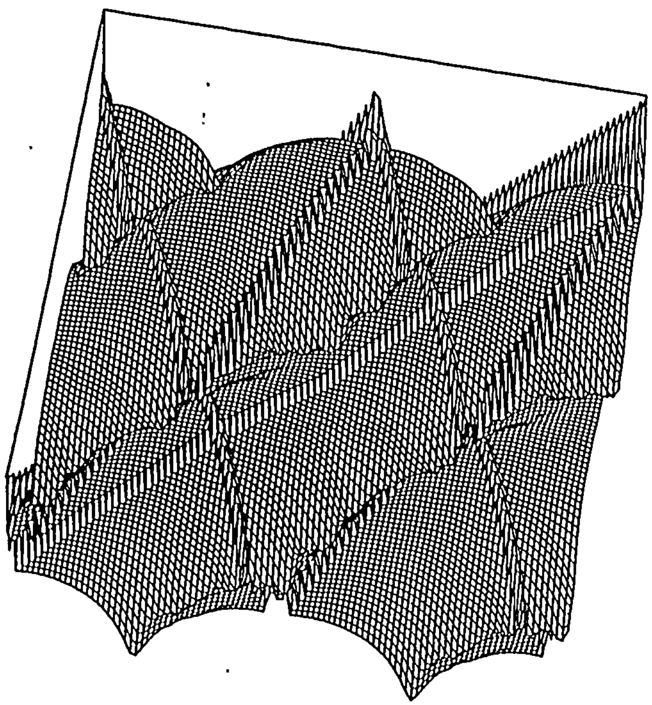

Interval Arithmetic

A method to perform exact calculations on computer by presenting all numbers by intervals.

$$[a,b]+[c,d]=[a+c,b+d]$$
$$[a,b]-[c,d]=[a-d,b-c]$$
$$[a,b]\cdot[c,d]=[\min(ac,ad,bc,bd),\max(ac,ad,bc,bd)]$$
$$[a,b]/[c,d]=[\min(a/c,a/d,b/c,b/d),\max(a/c,a/d,b/c,b/d)]$$

Not a group because $[a,b]-[c,d]\neq[0,0]$ unless $a=b, c=d$. In particular,

$$[a,b]-[a,b]=[a-b,b-a]$$
$$[a,b]/[a,b]=[\min(1,a/b,b/a),\max(1,a/b,b/a)]$$

Thus, operations lead to blow up, which can become large with time.

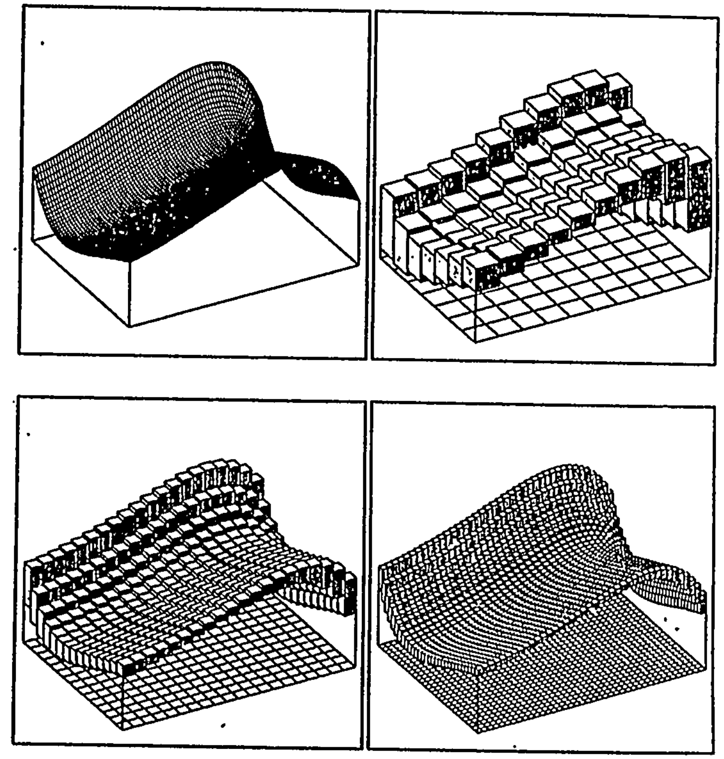

Figure 4.1: Top left: The function of which an upper bound should be found. Others: Covering the region of interest with smaller intervals reduces the overestimation of the maximum.

COSY Graphics

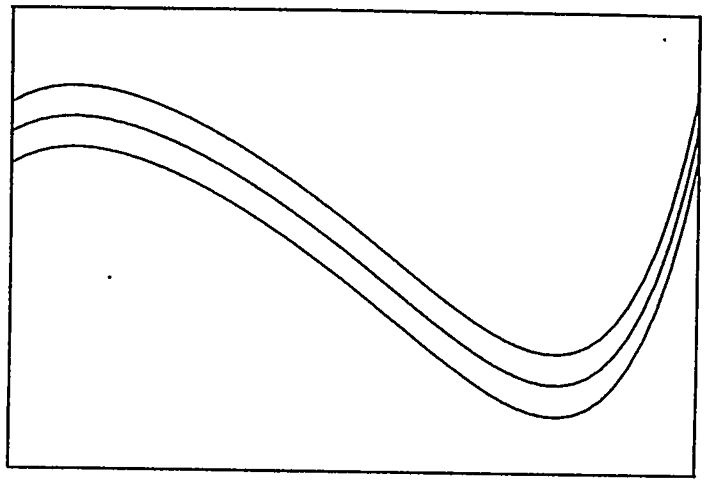

COSY Graphics

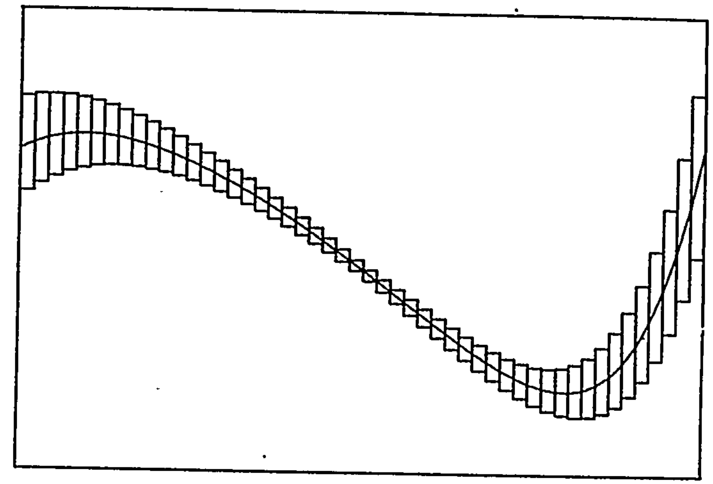

Example of Missing Information

$$f(x) = \begin{cases} \exp(-1/x^2) & \text{if } x \neq 0 \\ 0 & \text{if } x = 0 \end{cases}$$

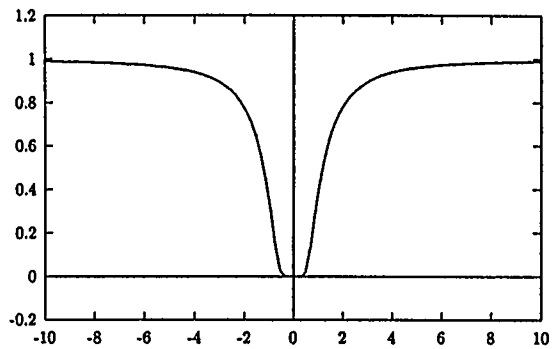

$f(0) = 0,\ f^{(k)}(0) = 0,\ k = 1, 2, \cdots$

So, Taylor polynomial around $x = 0$ to any order is $P(x) = 0$.

Function Algebra Inclusions

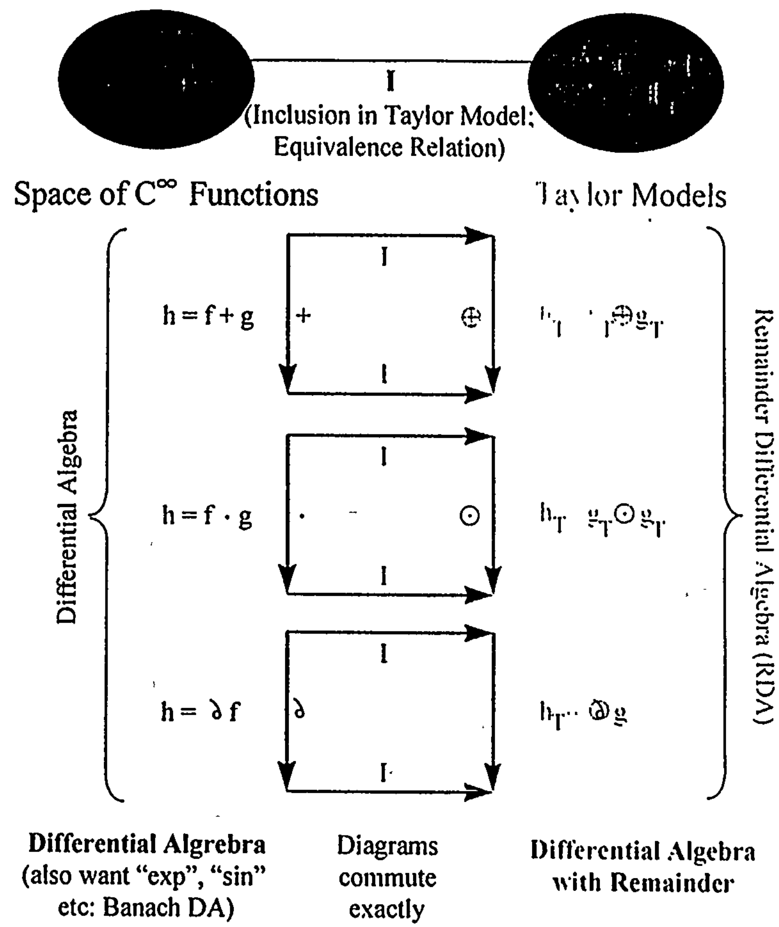

I: Extracts Information considered relevant

Taylor Models

Let f be C^∞ on $D_f \subset R^v$, and $\vec{B} = [a_1, b_1] \times ... \times [a_v, b_v] \subset D_f$ be an interval box containing the origin. Let $P_{n,f}$ be the Taylor polynomial of f around the origin. Call the interval $I_{n,f}$ a remainder of f to order n if

$$f(\vec{x}) - P_{n,f}(\vec{x}) \in I_{n,f} \text{ for all } \vec{x} \in \vec{B}$$

We call the pair $(P_{n,f}, I_{n,f})$ an nth order Taylor model of f.

Simple observations:

- For any f, there is always at least one finite such $I_{n,f}$.
- Polynomials p of order less than n have $(p, [0,0])$ as a Taylor model.
- Because of Taylor's theorem, $I_{n,f}$ can be chosen "of order $\vec{B}^{n+1}$" and hence if $\vec{B}$ is "fine", $I_{n,f}$ is "much finer".

Addition of Taylor Models

Let $f(\vec{x}) \in P_{n,f}(\vec{x}) + I_{n,f}$ for all $\vec{x} \in \vec{B}$, $g(\vec{x}) \in P_{n,g}(\vec{x}) + I_{n,g}$ for all $\vec{x} \in \vec{B}$. Then obviously,

$$(f+g)(\vec{x}) \in (P_{n,f} + P_{n,g})(\vec{x}) + (I_{n,f} + I_{n,g}) \text{ for all } \vec{x} \in \vec{B}$$

and so $(P_{n,f} + P_{n,g}, I_{n,f} + I_{n,g})$ is a Taylor model for $(f+g)$ on $\vec{B}$.

Note that if $I_{n,f}$, $I_{n,g}$ are "fine of order $\vec{B}^{n+1}$", so is $I_{n,f+g} = (I_{n,f} + I_{n,g})$.

Multiplication of Taylor Models

Let $f(\vec{x}) \in P_{n,f}(\vec{x}) + I_{n,f}$ for all $\vec{x} \in \vec{B}$, $g(\vec{x}) \in P_{n,g}(\vec{x}) + I_{n,g}$ for all $\vec{x} \in \vec{B}$.Let $P_{n,h}^{(k)}$ denote the k-th order part of the Taylor polynomial of h. Then for all $\vec{x} \in \vec{B}$,

$$\begin{aligned}
(f \cdot g)(\vec{x}) &\in (P_{n,f}(\vec{x}) + I_{n,f}) \cdot (P_{n,g}(\vec{x}) + I_{n,g}) \Rightarrow \\
(f \cdot g)(\vec{x}) &\in P_{n,f\cdot g}(\vec{x}) + \textstyle\sum_{m=0}^{n} \sum_{j=n-m+1}^{n} P_{n,f}^{(m)}(\vec{x}) \cdot P_{n,g}^{(j)}(\vec{x}) + \\
&\qquad P_{n,f}(\vec{x}) \cdot I_{n,g} + P_{n,g}(\vec{x}) \cdot I_{n,f} + I_{n,f} \cdot I_{n,g} \Rightarrow \\
(f \cdot g)(\vec{x}) &\in P_{n,f\cdot g}(\vec{x}) + I_{n,f\cdot g}, \qquad \text{where}
\end{aligned}$$

$$\begin{aligned}
I_{n,f\cdot g} = \textstyle\sum_{m=0}^{n} \sum_{j=n-m+1}^{n} & P_{n,f}^{(m)}(\vec{B}) \cdot P_{n,g}^{(j)}(\vec{B}) + \\
& P_{n,f}(\vec{B}) \cdot I_{n,g} \ + \ P_{n,g}(\vec{B}) \cdot I_{n,f} \ + \ I_{n,f} \cdot I_{n,g}
\end{aligned}$$

is a remainder interval for $f \cdot g$. Note that if $I_{n,f}$, $I_{n,g}$ are "fine of order $\vec{B}^{n+1}$", so is $I_{n,f\cdot g}$.

Intrinsic Functions of Taylor Models

Let $f(\vec{x}) \in P_{n,f}(\vec{x}) + I_{n,f}$ for all $\vec{x} \in \vec{B}$, and let g be an intrinsic function. Want to find Taylor model for $g \circ f$. Strategy depends somewhat on g, but usually it consists of using

1)An addition theorem for g; 2) The Taylor formula with remainder for g; and 3) The treatment of constant and non-constant parts of f separately.

Example: $g(x) = \exp(x)$. Taylor formula around origin: $g(x) = P_{n,\exp}(x) + \exp(\xi)x^{n+1}/(n+1)!$, where ξ is between 0 and x. Let c be the constant part of $P_{n,f}$, and let $\bar{P}_{n,f} = P_{n,f} - c$. Then

$$\begin{aligned}
&\exp(P_{n,f}(\vec{x}) + I_{n,f}) = \exp(c) \exp(\bar{P}_{n,f}(\vec{x}) + I_{n,f}) \subset \exp(c) \cdot \\
&P_{n,\exp}(\bar{P}_{n,f}(\vec{x}) + I_{n,f}) + \exp(\bar{P}_{n,f}(\vec{B}) + I_{n,f}) \cdot \tfrac{(\bar{P}_{n,f}(\vec{B}) + I_{n,f})^{n+1}}{(n+1)!}
\end{aligned}$$

The evaluation of $P_{n,\exp}(\bar{P}_{n,f}(\vec{x}) + I_{n,f})$ requires only additions and multiplications of Taylor models. The second term contributes only to the remainder, which is again "fine of order $\vec{B}^{n+1}$".

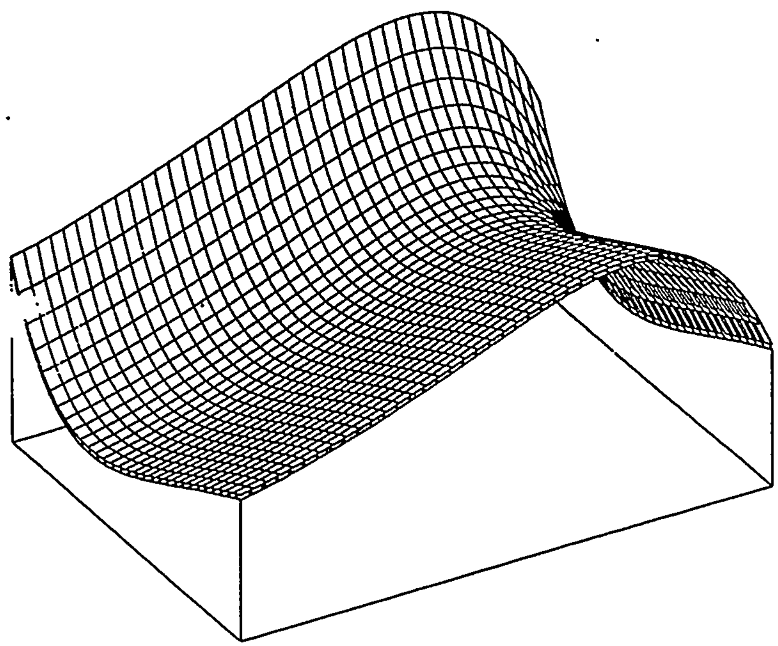

Interval Evaluation of Functions Prone to Blow Up

Often important: evaluate f with interval arguments (for example, interval optimization).

If f consist of large numbers of arithmetic operations, often there is substantial blow up for reasonable interval sizes.

Interval blow up can be reduced by

1. Determining Taylor model of f, where blow up only influences the naturally small remainder, and
2. Evaluating the Taylor polynomial, which can be done with no or little blow up.

Order of Invariant	Interval Bounding (guaranteed)	Interval Chains (guaranteed)	Conventional Rastering (optimistic)
3	11,252	743,667	849,195
4	11,252	743,667	849,195
5	11,306	876,059,284	982,129,435
6	11,306	876,059,284	982,129,435
7	11,306	432,158,877,713	636,501,641,854
8	11,306	432,158,877,713	636,501,641,854

Table 1.5: Predictions of the number of stable turns as a function of the order of the polynomials describing the normal form transformation for the physical pendulum with a maximum elongation of 1/10 rad. Because of energy conservation, the map is known to be permanently stable.

Order	Pendulum	Henon Map	Coupled Pendulums
2	434	6	43
3	434	41	915
4	1,039,578	1,109	85,907
5	1,039,578	7,149	2,577,221
6	455,537,706	27,556	61,418,923
7	455,537,706	176,827	1,535,527,685
8	92,114,163,553	1,474,124	29,750,319,370
9	92,114,163,553	9,133,037	357,584,630,384
Order	**IUCF**	**PSR II**	**Demo**
2	9	806	6
3	321	831	129
4	1,288	252,893	1,220
5	19,995	235,650	25,657
6	370,294	6,977,545	84,087
7	3,265,268	8,255,710	1,320,751
8	11,277,884	65,472,668	4,554,994
9	65,734,218	76,092,850	55,548,695

Table 1.3: Minimum number of turns required to move from the initial region to the forbidden region. The initial emittance was chosen to be half the acceptance. The maps were evaluated in order eight, whereas the pseudo invariants were computed to the indicated order. Scanning was performed with 20^k points for k relevant dimensions.

Lower bound for	Pendulum	Henon map
Simplest application	92,114,163,553	9,133,037
Length and Strength uncertainty 1%	23,556,300,993	8,167,533
Divided phase space	452,868,876,965	44,999,781
Multi-turn maps	388,804,862,856	1,456,171,297
Both	1,895,348,117,634	4,779,711,057
Lower bound for	PSR II	Demo
Simplest application	76,092,850	55,548,695
Quad field uncertainty 0.01%	47,166,060	51,963,620
Divided phase space	373,642,327	284,008,517
Multi-turn maps	21,172,838,624	1,042,575,616
Both	18,731,455,785	5,121,716,506
Coup. Pendulum	predicted turns	stable emittance
Simplest application	357,584,630,384	$5 \times 5\pi$m mrad
Length uncertainty 1%	144,173,434,143	$3.4 \times 3.4\pi$m mrad
Divided phase space	1,765,031,547,898	$11.3 \times 11.3\pi$m mrad
Multi-turn maps	1,029,815,934,687	$6 \times 6\pi$m mrad
Both	5,087,629,041,331	$14.5 \times 14.5\pi$m mrad
IUCF ring	predicted turns	stable emittance
Simplest application	65,734,218	$3.3 \times 2.0\pi$mm mrad
Quad field uncertainty 0.01%	18,535,102	$2.9 \times 1.7\pi$mm mrad
Divided phase space	335,420,083	$4.8 \times 2.9\pi$mm mrad
Multi-turn maps	5,804,832,818	$8.1 \times 4.8\pi$mm mrad
Both	27,745,480,680	$13 \times 7.7\pi$mm mrad

Table 1.4: Lower bounds on the turns of particles for initial emittance of one half the acceptance and lower bounds on the stable emittances for 10^8 turns obtained by various variations of the PIE method.

Introduction to Beam Physics

PHY861 - Spring 1997

Organized by Martin Berz

MICHIGAN STATE UNIVERSITY

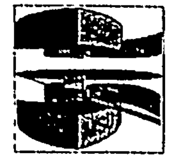

Beam Theory and Dynamical Systems Group

PHY861, Introduction to Beam Physics, will be presented again in the spring term of 1997. This time, the course will be open not only to participants at MSU, but also to individuals at other universities and laboratories all over the world via video teleconferencing. We will support both conventional teleconferencing equipment as well as the new mechanisms offered by the world wide web. Course material will be posted on the web, and homework problems can be submitted in a variety of ways.

Prerequisites

- Undergraduate Degree in Physics or equivalent (like german "Vordiplom")
- Graduate Level Mechanics, equivalent to MSU PHY820; Graduate Level Electrodynamics, equivalent to MSU PHY841

Registration and Credit

It is possible to participate and obtain credit for this course in a variety of ways, depending on the specific needs of the individual. There is no fee for participation or attendance, except for the normal MSU course fees for individuals registering at MSU. Participation is open to any individual interested, but MSU requirements demand that anyone participating in any activity beyond reading this introductory page has to register his name and address. The detailed ways of participation are as follows.

Mode	Target Audience	Requirements
Regular MSU Credit	individuals requiring formal credit for transfer	MSU Registration for Course
	MSU Ph.D. and M.Sc. students in Beam Physics	Homework
	MSU PA students using PHY861 as elective course	Final Exam
		Physical Attendance (for MSU students)
Certificate of Passing	Individuals desiring official acknowledgment of proficiency in material	Homework
	European students requiring official University Certificate of Proficiency, like german Uebungsschein	Final Exam
Certificate of Participation	Individuals interested in certain parts of the course only	Selected Lectures
		Selected Homework
Registered Attendance	Individuals participating in any course activity	None
	Individuals wishing to access any detailed course material	

For individuals outside MSU who want to formally register for the course, special arrangements have been made to treat all remote participants as in-state, resulting in a substantially reduced fee of $209.75 per credit hour. Due to additional special arrangements, participants from the Big Ten Universities as well as the University of Chicago can formally register for the course without any charge; for details, please contact us.

In order to receive mailings about the course or attend any of the activities, please send an email to berz@pa.msu.edu. An automated registration form will be available from here soon.

Lectures

The lectures will take place Tuesday and Thursday at 10:20 to 11:40 Eastern Time. They can be attended in the following ways.

- MSU Lecture Room (HEP Conference Room)
- PictureTel Videoconferencing Systems at Major Laboratory Sites
- Telecasting over Internet with Standard Hardware and Software

FACTORIZATION OF TAYLOR MAPS

A. Dragt, Univ. Maryland

Cremona Symplectification of Taylor Maps

Alex J. Dragt and Dan T. Abell

Physics Department
University of Maryland
College Park, Maryland 20742

Outline

I. Introduction

- A. Concept of a Map
- B. Symplectic Map
- C. Lie Representation
- D. Jets

II. Symplectic Completion of Jets

- A. Necessity
- B. Cremona Maps
- C. Optimal Jolt Decomposition
- D. Construction of Cremona Map
- E. Sample Construction of Optimal Cremona Map

Taylor Series Expansion

write

$$z_a^{fin} = K_a + \sum_b R_{ab} z_b^{in}$$
$$+ \sum_{b,c} T_{abc} z_b^{in} z_c^{in}$$
$$+ \sum_{b,c,d} U_{abcd} z_b^{in} z_c^{in} z_d^{in}$$
$$+ \cdots .$$

a) Entries of $R, T, U, \cdots,$ inter-related by symplectic condition. Coefficients far from being independent.

---

b) Expansion generally not symplectic if truncated.

2. Elementary Lie Algebraic Methods

a) Lie Operators

Let $f(z)$ be any function.
Define the associated (differential) Lie Operator $:f:$ by

$$\boxed{:f: \stackrel{\text{def}}{=} \sum_i \frac{\partial f}{\partial q_i}\frac{\partial}{\partial p_i} - \frac{\partial f}{\partial p_i}\frac{\partial}{\partial q_i}} .$$

Let $h(z)$ be any other function.

Then,

$$\boxed{:f:h = \sum_i \frac{\partial f}{\partial q_i}\frac{\partial h}{\partial p_i} - \frac{\partial f}{\partial p_i}\frac{\partial h}{\partial q_i} = [f,h]} ,$$

or $\boxed{:f:h = [f,h]}$. Poisson Bracket

b) Lie Transformations

Define powers of $:f:$ by

$$:f:^0 h = h$$

$$:f: h = [f, h]$$

$$:f:^2 h = [f, [f, h]], \text{ etc.}$$

Define the operator $\exp(:f:)$ by

$$\boxed{\exp(:f:) \overset{\text{def}}{=} \sum_{n=0}^{\infty} :f:^n / n!}$$

Lie Transformation.

Explicitly, this gives

$$\exp(:f:)\, h = h + [f, h] + [f, [f, h]]/2! + \cdots.$$

<u>Notation:</u> Sometimes write

$$\exp(:f:) = e^{:f:}.$$

c) Factorization Theorem

Suppose $\mathcal{M}$ is an arbitrary symplectic map expanded in a Taylor series. Then, one can write

$$\boxed{\mathcal{M} = e^{:f_1:}\, e^{:f_2:}\, e^{:f_3:}\, e^{:f_4:} \cdots}$$

where each f_n is a <u>homogeneous polynomial</u> in the z's of degree n.

<u>Correspondence to Taylor Series</u>

$$\begin{tikzcd}
\mathcal{M} = e^{:f_1:} \arrow[d, leftrightarrow] & e^{:f_2:} \arrow[d, leftrightarrow] & e^{:f_3:} \arrow[d, leftrightarrow] \arrow[dr, leftrightarrow] & e^{:f_4:} \arrow[d, leftrightarrow] & \cdots \\
K & R & T & U &
\end{tikzcd}$$

errors

linear behavior

nonlinear behavior
Aberrations
Particle loss

E. Jets (Truncated Taylor Maps)

Write

$$\mathcal{M} = \underset{\substack{\uparrow \\ \mathcal{D} \\ \text{displacement}}}{e^{:f_1:}} \; \underset{\substack{\uparrow \\ \mathcal{L} \\ \text{linear}}}{e^{:f_2:}} \; \underbrace{e^{:f_3:} \cdots e^{:f_{n+1}:}}_{\mathcal{N}} \Big\} \cdots$$

Worry about treatment of $\mathcal{N}$.

Consider

$$z^f = \mathcal{N} z^i .$$

Then,

$$z_a^f = z_a^i + \sum_{m=2}^{\infty} \underbrace{t_a(m, z^i)}_{\substack{\text{homogeneous} \\ \text{polynomials} \\ \text{of degree } m.}}$$

<u>Define</u> an n-jet by writing

$$\tilde{z}_a^f = z_a^i + \sum_{m=2}^{n} t_a(m, z^i) , \quad \text{or}$$

$$\longleftrightarrow \quad \tilde{z}^f = \mathcal{T}_n z^i .$$

Def: $\mathcal{T}_n$ is a <u>symplectic</u> n-jet

iff

$$[\mathcal{T}_n z_a^i, \mathcal{T}_n z_b^i] = J_{ab} + \underbrace{r_{ab}(\geq n, z^i)}_{\substack{\text{remainder} \\ \text{of degree} \\ \geq n.}}$$

II. Symplectic Completion of Symplectic Jets

A. Necessity

Jets generally violate the symplectic condition, and this violation builds up with repeated application. Therefore not suitable for long-term tracking.

Simple 2-dimensional example:

$$\mathcal{M} = \mathcal{R}(\phi)\,\mathcal{N}, \quad \mathcal{R} = \text{rotation}\left(\begin{smallmatrix}\text{phase}\\ \text{advance}\end{smallmatrix}\right)$$

$\mathcal{N}$ defined by

$$q^f = \mathcal{N} q^i = q^i (1-p_i)^2$$

$$p^f = \mathcal{N} p^i = p^i \sum_0^\infty (p_i)^n$$

$$= p^i/(1-p^i)$$

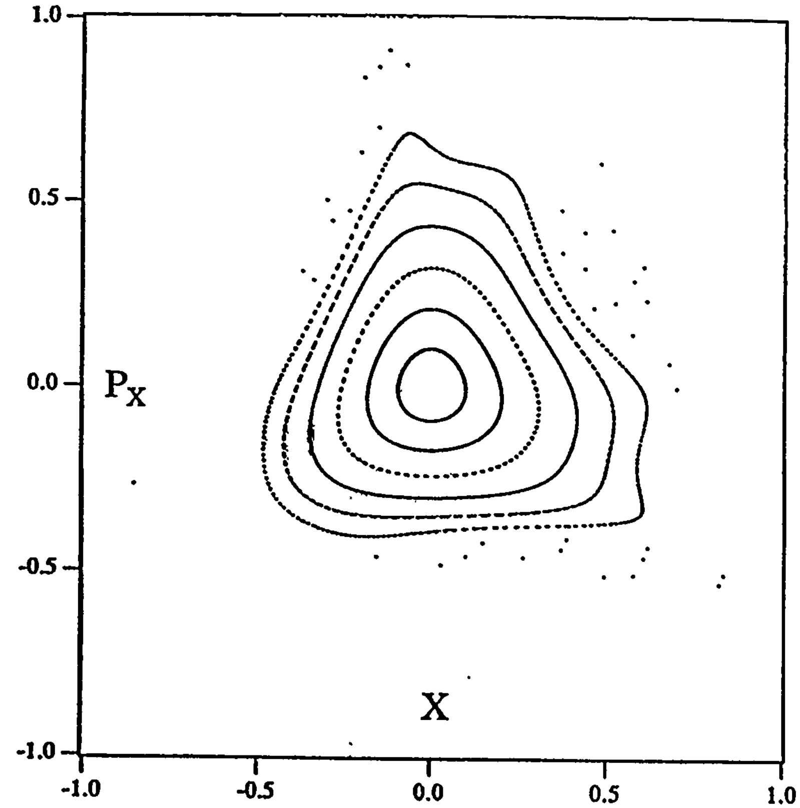

Exact Map

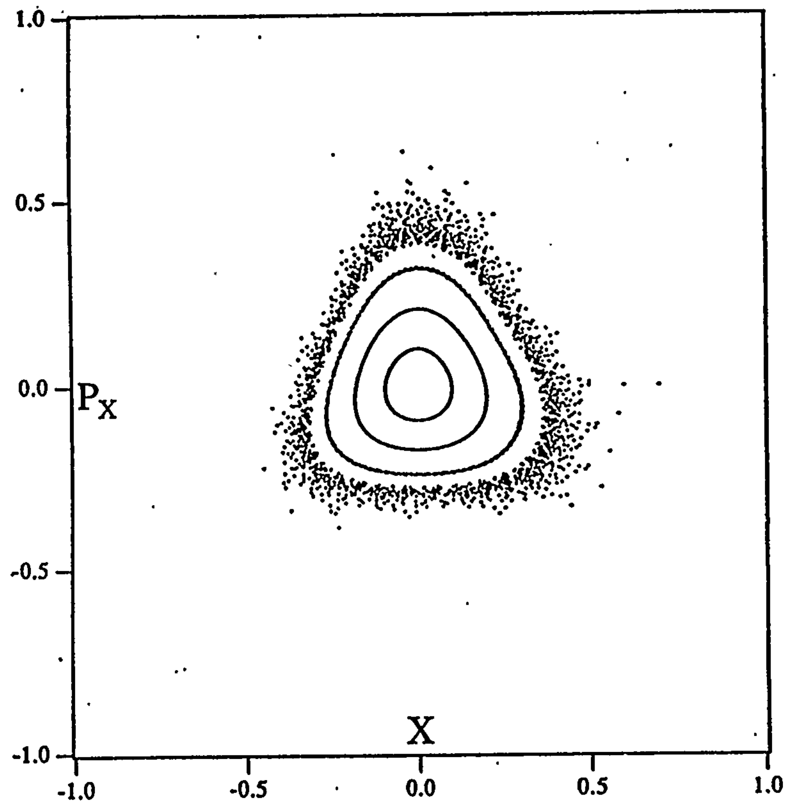

Truncated Taylor Approximation

F. Cremona Map

<u>Definition</u>: A Cremona map is a map whose Taylor series terminates (map is polynomial) and is yet exactly symplectic.

<u>Strategy</u>: Given a symplectic $\mathcal{M}$, get T_n that approximates $\mathcal{M}$, find a Cremona map whose Taylor expansion agrees with T_n through terms of degree n. Call this map $\mathcal{C}$. Then use

$$\mathcal{M}_a = \mathcal{C}.$$

Note: Cremona maps form a group.

Construction of Cremona Maps

Let $M(m,d) = M_{md}$ = number of monomials of degree m in a d-dimensional space. Combinatorics $\Rightarrow$

$$M(m,d) = (m+d-1)!/[m!\,(d-1)!].$$

Let Q_k^m with $k = 1, 2, \cdots M(m,3)$ denote the monomials of degree m in the variables q_1, q_2, q_3.

Def.: Let $\mathcal{L}$ denote any "linear" symplectic map, a map of the form $\mathcal{L} = \exp(:f_2:)$. Then, a Lie operator of the form

$$\mathcal{L} : \sum_k b_k^m Q_k^m : \mathcal{L}^{-1}$$

$$= : \sum_k b_k^m \mathcal{L} Q_k^m :$$

is called a Jolt.

Thrm.:

$$\mathcal{C} = \exp(: \sum_k b_k^m \mathcal{L} Q_k^m :)$$

is a Cremona map.

Challenge: Given $h_3, h_4, \cdots h_n$

(homogeneous polynomials in q_1, q_2, q_3

and p_1, p_2, p_3), find $N(n)$, $\mathcal{L}_\ell$, and

$a^m_{\ell k}$ such that

$$h_m = (N M_{m3})^{-1} \sum_{\ell=1}^{N} \sum_{k=1}^{M_{m3}} a^m_{\ell k} \mathcal{L}_\ell Q^m_k$$

with $m = 3, 4, \cdots n$.

<u>Irwin</u> <u>Decomposition</u>

Select the $\mathcal{L}_\ell$ and the $a^m_{\ell k}$ in such a way that the $a^m_{\ell k}$ are minimized. Called an

<u>Optimal</u> <u>Jolt</u> <u>Decomposition</u>

<u>Application</u>: Given

$$\mathcal{N} = \exp(:f_3:)\exp(:f_4:)\cdots\exp(:f_n:),$$

make a Jolt decomposition of

$$h_3 = f_3, \quad h_4 = \tilde{f}_4, \quad h_5 = \tilde{\tilde{f}}_5, \cdots \Rightarrow$$

Cremona map approximation $\mathcal{C}_{345\cdots n}$ to $\mathcal{N}$ of the form

$$\mathcal{C}_{345\cdots n} = \prod_{\ell=1}^{N} \mathcal{L}_\ell$$

$$\exp\Big[\frac{1}{N}(:\frac{1}{M_{33}}\sum_{k_3=1}^{M_{33}} a^3_{\ell k_3} Q^3_{k_3}$$

$$+\frac{1}{M_{43}}\sum_{k_4=1}^{M_{43}} a^4_{\ell k_4} Q^4_{k_4} + \cdots + \frac{1}{M_{n3}}\sum_{k_n=1}^{M_{n3}} a^n_{\ell k_n} Q^n_{k_n}:)\Big]\mathcal{L}^{-1}_\ell$$

Conclusion: Solution to Jolt Decomposition (Irwin) problem $\Rightarrow$ Cremona approximation to $\mathcal{N}$.

Construction of

Optimal Jolt Factorization

Want the $a^m_{\ell k}$ to be small in order to minimize higher-order terms produced by the factorization process.

Thrm: $Sp(2n)$ has a $U(n)$ subgroup. Given any set of $\mathcal{L}_\ell$ drawn from $Sp(2n)$, there is a related set $\mathcal{L}'_\ell$ drawn from $U(n)$ that will do the same job.

Modified Iwasawa Factorization

$$M = \begin{pmatrix} F & 0 \\ G & F^{-1} \end{pmatrix} M(\bar{u})$$

$M(\bar{u})$ in $U(n)$

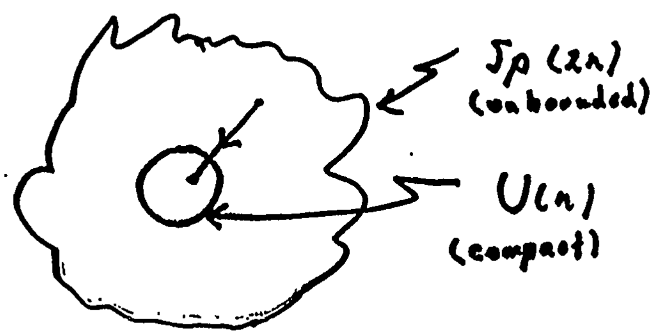

So, look only in $U(2)$ or $U(3)$.

Definition of inner product.

Let

$$G_r^m(q,p) = \frac{q_1^{\mu_1} q_2^{\mu_2} q_3^{\mu_3} p_1^{\nu_1} p_2^{\nu_2} p_3^{\nu_3}}{[\mu_1!\mu_2!\mu_3!\nu_1!\nu_2!\nu_3!]^{1/2}}$$

$$Q_k^m(q) = \frac{q_1^{\mu_1} q_2^{\mu_2} q_3^{\mu_3}}{[\mu_1!\mu_2!\mu_3!]^{1/2}}$$

Here $\mu_1+\mu_2+\mu_3+\nu_1+\nu_2+\nu_3 = m.$

$$r = \{\mu_1 \mu_2 \mu_3 \nu_1 \nu_2 \nu_3\}$$

Define an inner product $\langle , \rangle$ by the rule

$$\langle G_{r'}^{m'}, G_r^m \rangle = \delta_{m'm}\, \delta_{r'r}.$$

Invariant under $U(3) \subset Sp(6)$ and $USp(6)$.

For each m define sensitivity vectors σ^r by the rule

$$\underbrace{\sigma^{r}_{\ell k}}_{\text{components}}{}^{\swarrow \text{label}} = \langle G_r^m, \mathcal{L}_\ell Q_k^m \rangle$$

Next define a Gram matrix Γ by the rule

$$\Gamma_{rs} = \{\sigma^r, \sigma^s\}$$

$$= \frac{1}{N(\ell)} \frac{1}{M(m,3)} \sum_{\ell k} \sigma^r_{\ell k} \sigma^s_{\ell k}$$

Thm: Selecting the $\mathcal{L}_\ell$ to maximize the minimum eigenvalue of $\Gamma \Rightarrow$ Optimal Jolt Factorization

Optimal Spectrum of Γ:

= Spectrum in continuum limit.

We have the result Γ_{rs} =

$$\{\sigma^r, \sigma^s\} = \frac{1}{N}\sum_{\ell=1}^{N} \frac{1}{M_{m3}} \sum_{k=1}^{M_{m3}} \sigma^r_{k\ell}\, \sigma^s_{k\ell}$$

$$= \frac{1}{N}\sum_{\ell=1}^{N} \frac{1}{M_{m3}} \sum_{k=1}^{M_{m3}} \langle G^m_r, \mathcal{L}_\ell Q^m_k \rangle \langle \mathcal{L}_\ell Q^m_k, G^m_s \rangle.$$

Use Dirac dyad notation to write

$$\Gamma = \frac{1}{N}\sum_{\ell=1}^{N} \frac{1}{M_{m3}} \sum_{k=1}^{M_{m3}} |\mathcal{L}_\ell Q^m_k \rangle \langle \mathcal{L}_\ell Q^m_k |$$

In $\begin{matrix} 4 \text{ dim} \\ 6 \text{ dim} \end{matrix}$ replace $\mathcal{L}_\ell$ by $\mathcal{L}(u)$

with $u \in \begin{matrix} SU(2) \\ SU(3) \end{matrix}$ and replace

$$\frac{1}{N}\sum_{\ell} \quad \text{with} \quad \begin{matrix} \int_{SU(2)} du \\ \int_{SU(3)} du \end{matrix} \quad \Rightarrow$$

$$\boxed{\Gamma = \int_{SU(*)} du \; \frac{1}{M_{m*}} \sum_{k} |\mathcal{L}(u) Q^m_k \rangle \langle \mathcal{L}(u) Q^m_k |}$$

Use group theory to compute spectrum of Γ.

Achievement of Optimal Spectrum in Discrete Case using Quadrature (Cubature) Formulas:

Write

$$\Gamma = \int_{SU(n)} du \; \Gamma(u)$$

where $\Gamma(u)$

$$= \frac{1}{M_{n*}} \sum_{\lambda} |\mathcal{L}(u)\, \varphi_{\lambda}^{m}\rangle \langle \mathcal{L}(u)\, \varphi_{\lambda}^{m}| .$$

Write the coset decomposition

$$u = \underset{\substack{\uparrow \\ \text{coset}}}{c}\, h^{\swarrow \text{ subgroup element}}$$

with $h \in SO(n)$ for $u \in SU(n)$.

Theorem: $\Gamma(u) = \Gamma(c)$.

Also, $du = dc\, dh \Rightarrow$

$$\Gamma = \int_{SU(n)/SO(n)} dc \; \Gamma(c) \int_{SO(n)} dh$$

Find a cubature formula such that

$$\int_{SU(n)/SO(n)} dc \; \Gamma(c) = \sum_{\ell} w_{\ell}\, \Gamma(c_{\ell}) .$$

Then the set $\mathcal{L}_{\ell} = \mathcal{L}(c_{\ell})$ will work and yields the optimum (continuum) spectrum.

Condition for $\mathcal{C}$ to approximate $\mathcal{N}$: $\mathcal{N}$ must not be too large over region of phase space of interest.

Define $$n(z) = \frac{\| \mathcal{N} z - z \|}{\| z \|}$$

Expect method to work when $n(z)$ not too large over region of interest. Example: One sector map for Berkeley ALS. Make histogram of $n(z)$ over spheres in 4-d phase space. (First normalize $\mathcal{M}$ and hence $\mathcal{N}$ so that $\mathcal{M}$: perfect tori → perfect tori near origin.)

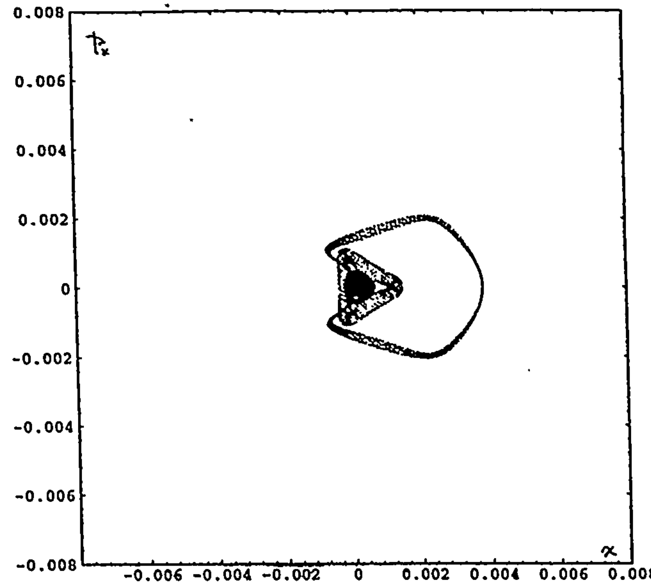

ALS... Exact

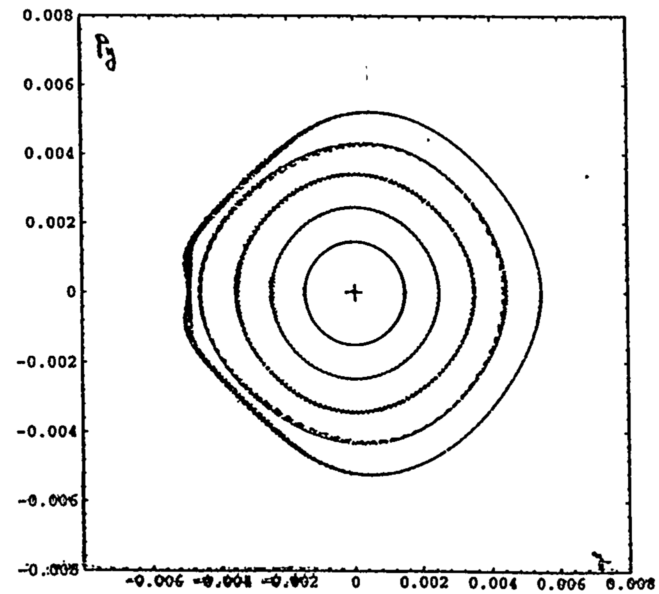

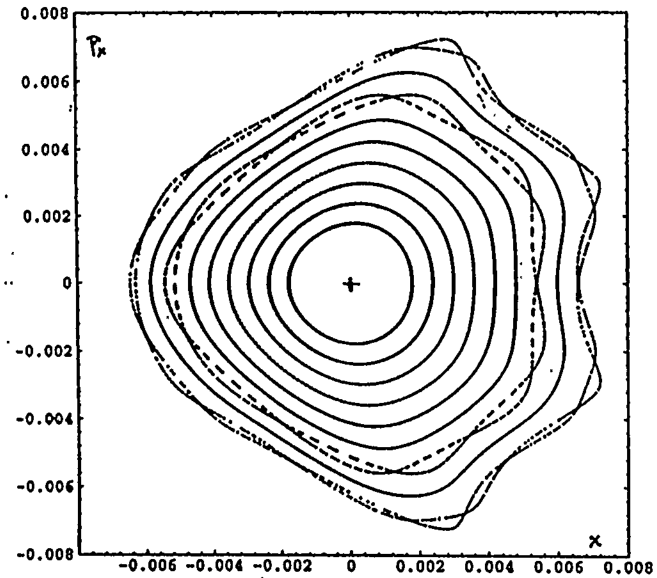

0.008
0.006
0.004
0.002
0
-0.002
-0.004
-0.006
-0.008
p_x
x
-0.006 -0.004 -0.002 0 0.002 0.004 0.006 0.008

ALS Exact

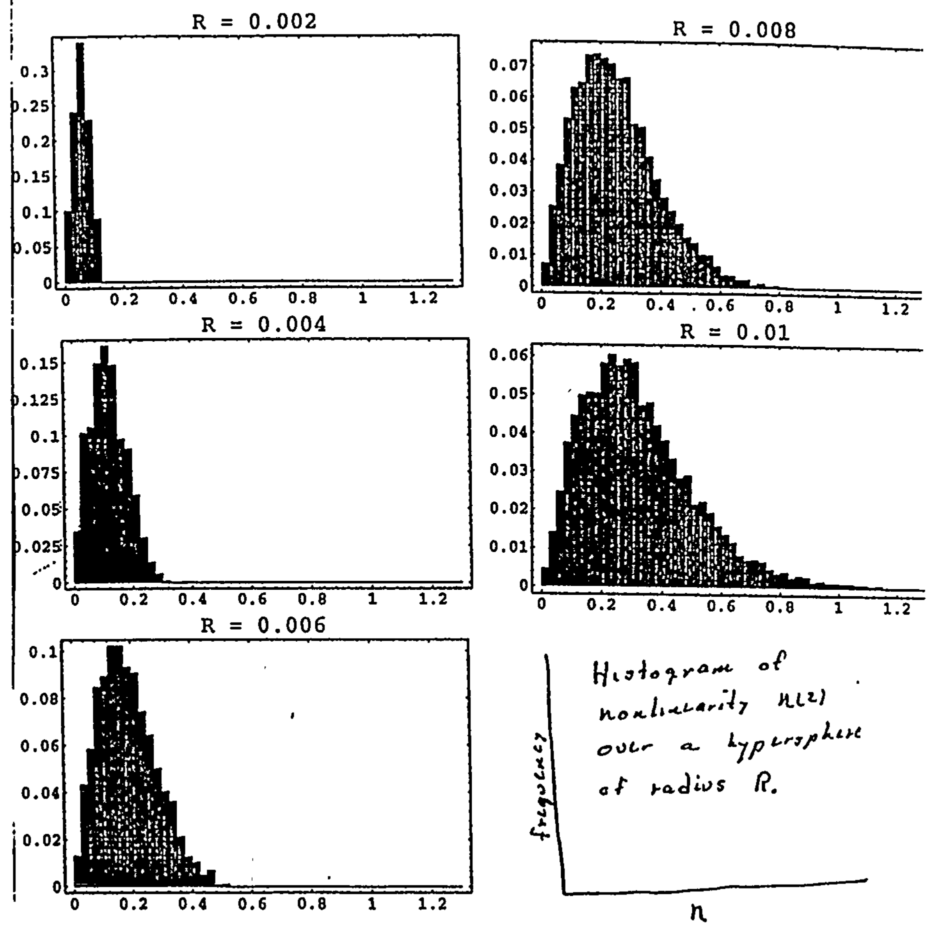

R = 0.002
R = 0.004
R = 0.006
R = 0.008
R = 0.01
0 0.2 0.4 0.6 0.8 1 1.2
Histogram of nonlinearity n(z) over a hypersphere of radius R.
frequency
n

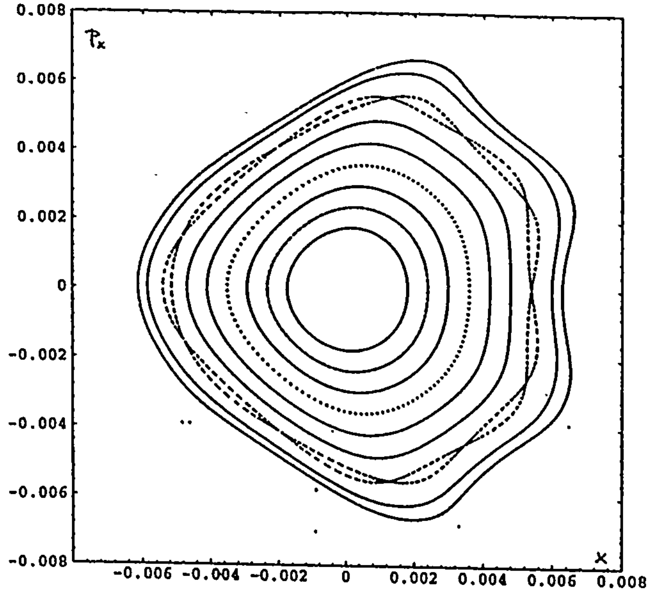

Cremona through f_7.

Requires 24 point
cubature formula on S^2.

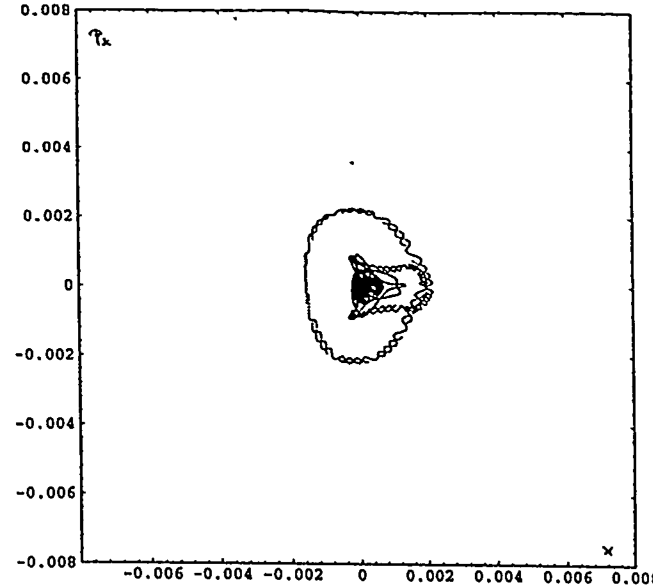

Cremona through f_7

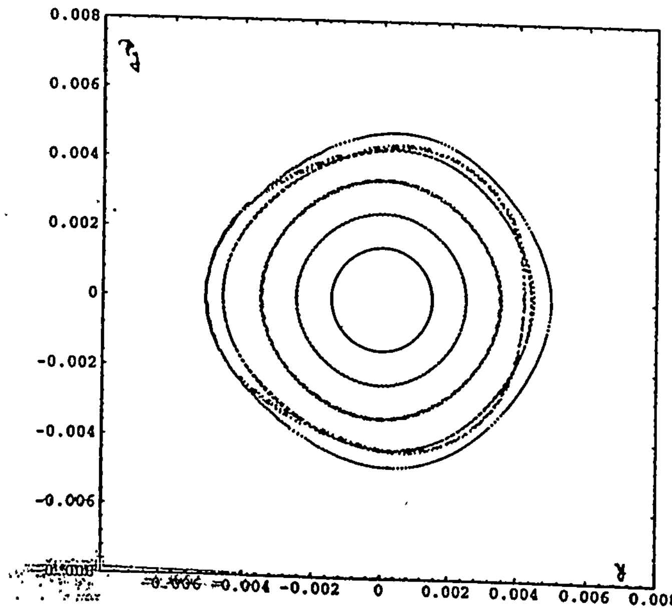

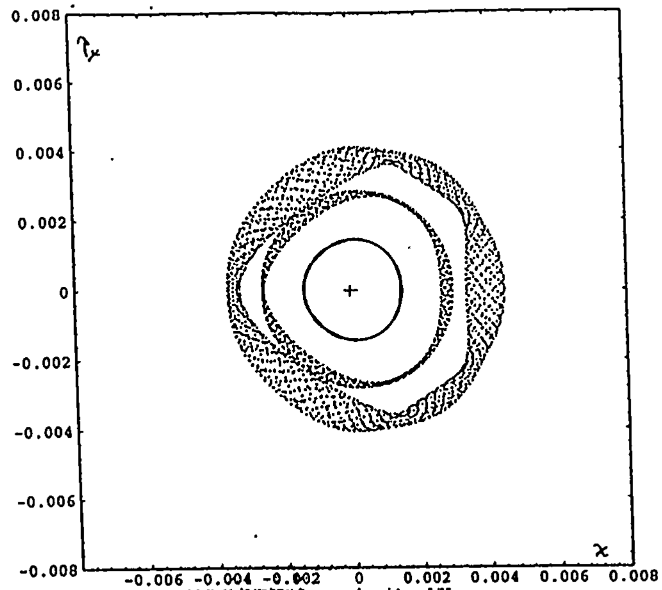

ALS: Exact

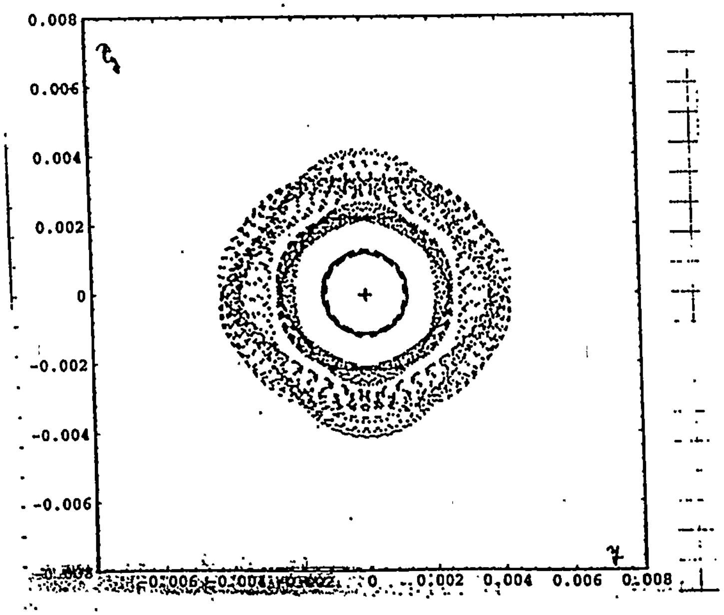

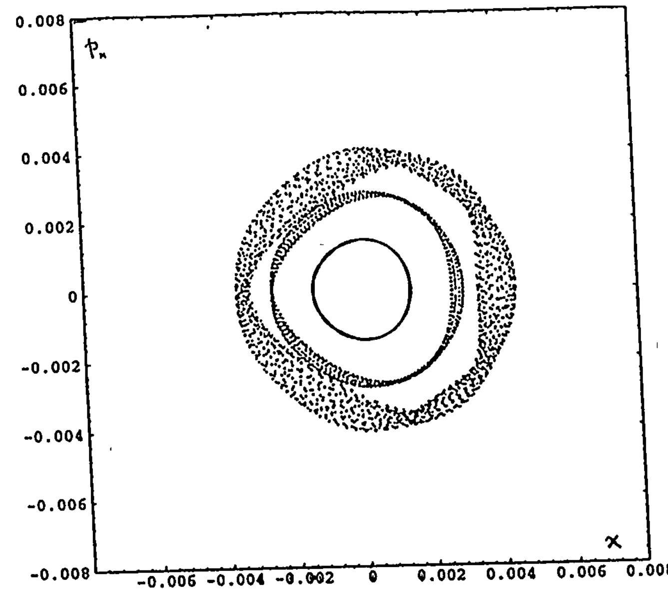

Cremona through f_7

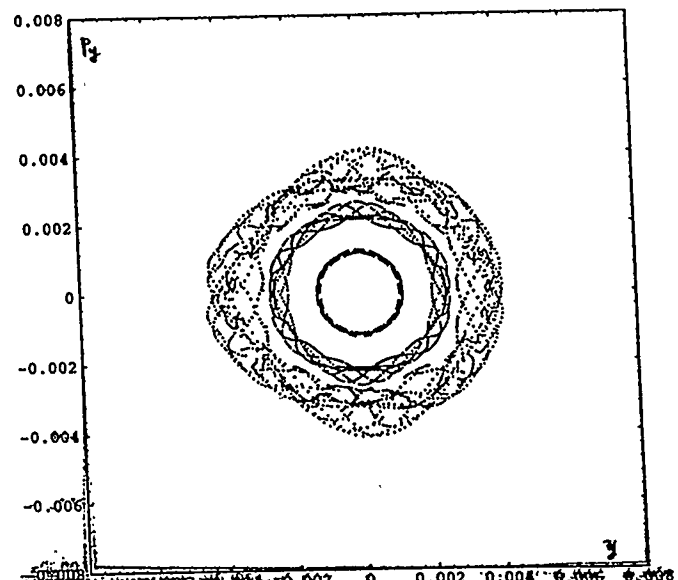

Cremona Symplectification of Taylor Maps

Alex J. Dragt and Dan T. Abell

Summary

In practical calculations the computation of transfer maps can generally be carried out only as Taylor series to some finite order. Truncated Taylor expansions generally violate the symplectic condition because of truncation, and are therefore not suitable for long-term stability studies.

A map that is both polynomial and exactly symplectic is called a Cremona map. Given any truncated Taylor expansion of a symplectic map (a symplectic jet), it is a remarkable result that it is possible to add to the map only a finite number of higher-order terms (terms of higher order than the truncation order) in such a way that the resulting map is exactly symplectic. (Recall that the symplectic condition itself is nonlinear.) Thus, any truncated Taylor expansion of a symplectic map can be approximated by a Cremona map in such a way that the truncated Taylor expansion of the Cremona map is identical to the truncated Taylor expansion of the original symplectic map. Moreover, it can be shown that there are many such Cremona approximations which, by construction, differ only in terms that are higher order than the truncation order.

Since Cremona map approximations are intended to be used to carry out long-term stability studies, what remains to be fully understood is how the added higher-order terms required for symplectification can be made small so that they alter as little as possible the underlying dynamics. Cremona approximations which minimize the added higher-order terms are called optimal Cremona approximations. It is shown that the construction of a class of optimal Cremona approximations is related to cubature formulas on the manifolds U(2)/SO(2) and SU(3)/SO(3) in the cases of 4- and 6-dimensional phase spaces, respectively. The algorithm for constructing such optimal Cremona factorizations is purly group-theoretical, and is universal in the sense that it is the same for any symplectic jet.

Some optimal Cremona factorizations have been constructed and applied to the transfer map for the Berkeley Advanced Light Source ring (which is known to be to be quite nonlinear) and have been used to study long-term stability with good success. Similar studies are being made for the transfer map of the CERN Large Hadron Collider.

LONG-TERM ORBIT STABILITY PREDICTIONS (LYPUNOV ESTIMATES, NORMAL FORMS)

E. Todesco, INFN

PREDICTION OF LONG-TERM STABILITY IN HADRON ACCELERATORS

M. Giovannozzi, W. Scandale, E. Todesco

University of Bologna, Italy, and CERN

Contents

Thanks to M. Böge, J. Laskar, F. Schmidt, G. Turchetti, and B. Warnock

The problem

We analyse *4D betatronic motion* in hadron colliders

Problem: *predict long-term dynamic aperture* for high number of turns (10^7 turns, i.e. 20 min in the LHC before energy ramping)

Open questions:

- Is there some indication that there exist *a core* of phase space *stable for infinite times* ?
- What is the *pattern* of long-term particle losses ?
- What is the relation between numerical simulations and the theory (i.e., *KAM and Nekhoroshev theorems*) ?
- Is it possible to *avoid* very-long-term tracking (Lyapunov, tune variation) ?

We use non-perturbative tools:

- Plain element-by-element *symplectic tracking*
- Evaluation of the *tunes* with high precision
- *Lyapunov* exponent

Main approaches to long-term prediction

- *Bounds on invariants*: choose an invariant (frequencies, actions evaluated through normal forms, actions evaluated through numerical tools) and extrapolate short term drift in the action space to long-term. Works by Warnock and Ruth, Dumas and Laskar, Berz and Hoffstätter ...

- *Early indicators*: choose an early indicator to select regular from chaotic orbits (Lyapunov exponents, variation of the frequencies). Works by Schmidt, Willeke and Zimmermann, by Laskar Celletti and Froeschlé, by Giovannozzi, Scandale and Todesco ...

- *Survival plots*: use tracking to extrapolate long-term behaviour. Works by Yan et al. (SSC), Schmidt and Galluccio (LHC) ...

Model

We analyse *transverse betatron motion* in hadron accelerators. Nonlinear transverse dynamics modelized by a sequence of symplectic maps:

$$\mathbf{x}' = \mathrm{M}_l \circ \mathrm{M}_{l-1} \circ \mathrm{M}_{l-2} \circ \ldots \mathrm{M}_1(\mathbf{x})$$

where $\mathbf{x} = (x, p_x, y, p_y)$ are the Courant-Snyder phase space coordinates

$\mathbf{x}'$: phase space position after one turn of the accelerator; we have finite difference equation.

Analysed models:

- A simplified model: 4D Hénon map (linear + sex)
- SPS lattice used for experiments (linear + 8 sexs)
- Realistic models of the LHC with nonlinear errors

Explicit form of the *4D Hénon map* (a linear lattice plus a sextupole in the one-kick approximation):

$$\begin{pmatrix} x' \\ p'_x \\ y' \\ p'_y \end{pmatrix} = \begin{pmatrix} \cos\omega_1 & \sin\omega_1 & 0 & 0 \\ -\sin\omega_1 & \cos\omega_1 & 0 & 0 \\ 0 & 0 & \cos\omega_2 & \sin\omega_2 \\ 0 & 0 & -\sin\omega_2 & \cos\omega_2 \end{pmatrix} \begin{pmatrix} x \\ p_x + x^2 - y^2 \\ y \\ p_y - 2xy \end{pmatrix}$$

the ratio of the beta functions in the sextupole is fixed to one.

Phenomenological analysis of long-term losses

Simulations using tracking and frequency analysis.

We choose initial conditions on the *plane* (x, y). The momenta p_x and p_y are set to zero. Either polar or rectangular grid.

Three numerical tools:

- *Long-term diagram* (plain tracking). Plot of stable initial conditions in the (x, y) plane. About 10^3 conditions, 10^7 turns.
- *Tune footprint* (à la Laskar). Plot of frequencies of stable initial conditions in the (Q_x, Q_y) plane. About 10^4 conditions, 1024 turns.
- *Network of resonances* (new). Plot of stable initial conditions (x, y) of the orbits whose nonlinear frequencies are resonant

$$\nu_x(x,y)q + \nu_y(x,y)p = l + \epsilon \qquad \epsilon \ll 1$$

we choose $\epsilon = 0.0002$ with 1024 iterations. About 10^5 conditions, 1024 turns.

Main results

Long-term particle loss occur in three cases:

- In *macroscopic bands of chaoticity*, where there is a set of scattered intial conditions locked on low-order resonances. Very relevant.
- At the *end of a resonant channel*, i.e., where the resonance mets dynamic aperture.
- On the *border of a resonant channel* (where hyperbolic structures are present), but close to the dynamic aperture.

The resonant channels are *stable* when sufficiently far from the dynamic aperture, even *though they are very wide*.

The mechanism of diffusion *along the network* of resonances (heteroclinic intersections) is *negligible*.

There is a *full domain* of stability: Arnold diffusion is totally negligible.

Long-term tracking and survival plots

Survival plots:

- usually one considers only a scan with *equal emittances* $x = y$. Amplitude versus number of turns.
- it is *difficult* to carry out an *inter/extrapolation* of the survival plots.

A definition of dynamic aperture

Dynamic aperture: radius where first particle loss occurs at N turns *averaged over the phase space* (Todesco and Giovannozzi, PRE 53 (1996) 4067-77)

$$D(N) = \left(\int_0^{\pi/2} [r(\alpha;N)]^4 \sin(2\alpha) d\alpha \right)^{1/4}$$

where $r(\alpha;N)$ is the amplitude along the $\alpha = \mathrm{atan} y/x$ direction where the first particle loss occurs at N turns

Inverse logarithm decaying of dynamic aperture

Using this definition we compute $D(N)$ as a function of N: the pattern is *smooth* and an interpolation is possible

Tracking data agree with the very simple formula (see Giovannozzi, Scandale and Todesco, LHC Project 45, and Part. Accel., in press)

$$D(N) = D_\infty \left(1 + \frac{b}{\log_{10} N}\right)$$

The formula depends only on *two parameters*:

- D_∞: is the dynamic aperture extrapolated for infinite number of turns
- b: gives the strength of the long-term phenomena.

Averaging over the ratio of emittances is crucial to obtain better interpolations

Theoretical considerations

Heuristic interpretation; if one assumes that phase space is divided into two parts:

- *Inner region* of KAM tori *stable forever* and a negligible set of unstable motion (Arnold diffusion)
- *Outer region* where almost all the KAM tori are destroyed, and the *rate of emptying* phase space *agrees* with the Nekhoroshev estimate.

Nekoroshev bound: initial conditions inside r are stable for at least N turns, where N depends on r:

$$N = N_0 \exp\left(\frac{R}{r}\right)^\eta$$

reversing the formula, one obtains

$$r(N) = \frac{R}{\log^{1/\eta}(N/N_0)}$$

where η and N_0 are suitable constants. For $N \to \infty$, one has $r(N) \to 0$: this is due to Arnold diffusion.

Indeed, KAM theorem states that for very weak perturbations (i.e. small r) *almost all* (neglecting Arnold diffusion) the phase space is *stable forever*. Let us call r_∞ this radius.

Adding the Nekhoroshev and the KAM theorems, one obtains the formula

$$r(N) = r_\infty + \frac{R}{\log^{1/\eta}(N/N_0)}$$

that for $\eta = N_0 = 1$ becomes our empirical law (this is NOT a theorem)

Open problems

- Validity limits of this regime
- Optimal value of the constants N_0 and η.

Maximal Lyapunov Exponent

We consider the initial conditions x and $\hat{\mathrm{x}} = \mathrm{x} + \delta$

$$\lambda_{max} = \lim_{n\to\infty} \lambda_{max}(n) = \lim_{n\to\infty} \lim_{\|\delta\|\to 0} \frac{1}{n} \log \frac{\|\mathrm{x}^{(n)} - \hat{\mathrm{x}}^{(n)}\|}{\|\delta\|}$$

- *Regular* orbits: $\|\mathrm{x}^{(n)} - \hat{\mathrm{x}}^{(n)}\| = An \qquad \Longrightarrow$ *stable*
- *Chaotic* orbits: $\|\mathrm{x}^{(n)} - \hat{\mathrm{x}}^{(n)}\| = Ae^{\lambda n} \qquad \Longrightarrow$ *unstable*

Automation and thresholds for Lyapunov

How to *automate* the decision stable / unstable ?

We define a *threshold* $\sigma_\lambda(n)$

If $\lambda_{max}(n) > \sigma_\lambda(n)$ $\rightarrow$ chaos

If $\lambda_{max}(n) < \sigma_\lambda(n)$ $\rightarrow$ regular

Since all the regular particles have $\lambda_{max}(n) = \frac{1}{n}\log(An)$ we define the threshold

$$\sigma_\lambda(n) = \frac{1}{n}\log(A_\lambda n)$$

One can prove that A_λ is *related to* the derivative of *detuning* w. r. t. phase space coordinates at maximum amplitude

$$A_\lambda = \max_{\mathbf{x}\in regular} \frac{1}{\|\delta\|}\sqrt{(x^2+p_x^2)(\Delta\Omega_1)^2 + (y^2+p_y^2)(\Delta\Omega_2)^2}$$

where $\Delta\Omega_1$ and $\Delta\Omega_2$ are the tune differences between $\mathbf{x}$ and $\hat{\mathbf{x}}$.

Very *weak dependence* on A_λ (thresholds appears to be independent of the model). We use $A_\lambda = 0.5$

1.2 Tune variation

Let $\nu_x(\mathbf{x}; n_1, n_2)$ and $\nu_y(\mathbf{x}; n_1, n_2)$ be the *nonlinear tunes* in the two phase planes *computed over the iterates* $n_1, n_1+1, n_1+2, ..., n_2$. Then,

$$\tau(n) = \sqrt{\sum_{i=x,y} [\nu_i(\mathbf{x}; 1, n) - \nu_i(\mathbf{x}; n+1, 2n)]^2}$$

is the *variation of the tune* from the iterates $1, .., n$ to the iterates $n+1, ..., 2n$ (proposed by J. Laskar)

Automation and thresholds for tune variation

- If $\tau(n) > \sigma_\tau(n) \rightarrow$ *wide* tune *variation* $\rightarrow$ we are not on an invariant torus $\rightarrow$ *chaotic motion*
- If $\tau(n) < \sigma_\tau(n) \rightarrow$ *small* tune *variation* $\rightarrow$ we are on an invariant torus $\rightarrow$ *regular motion*

Empirical threshold optimized over tracking at 10^7 turns

$$\sigma_\tau(N) = \frac{A_\tau}{N} \qquad A_\tau = 0.2$$

Results

Low number of turns: $N = 10^3 - 10^4$

- Lyapunov: agrees with tracking at 10^7 turns
- Tune variation: agrees with tracking at 10^7 turns

High number of turns: $N = 10^5 - 10^6$

- Lyapunov: agrees with extrapolation at infinity
- Tune variation: agrees with tracking at 10^7 turns
- Extrapolation: reliable

The *inverse logarithm conjecture* has been also tested for realistic LHC models using SIXTRACK by Böge and Schmidt

Conclusions

- We proposed a numerical tool to investigate the network of resonances
- Long-term particle loss takes place in *chaotic bands* where all the integrable structures are destroyed
- Diffusion along the network of resonances is *not relevant*
- *Inverse logarithm* decaying of the dynamic aperture with the number of turns close to the KAM region
- Numerical evidence for a *non-zero dynamic aperture* for infinite number of turns
- Agreement of Lyapunov prediction with extrapolation at infinite number of turns

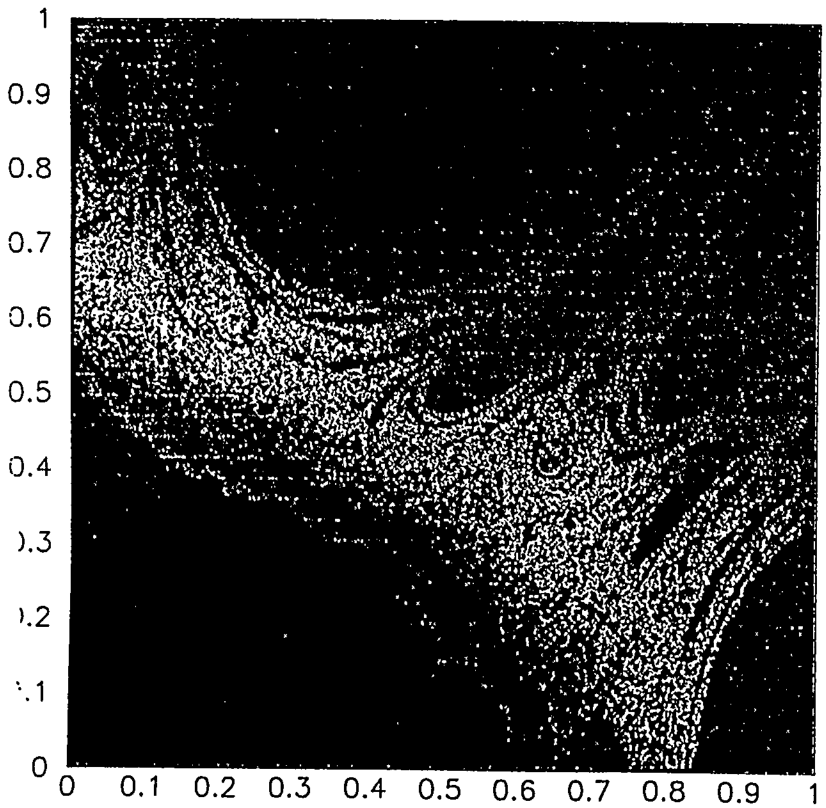
1
0.9
0.8
0.7
0.6
0.5
0.4
0.3
0.2
0.1
0
0 0.1 0.2 0.3 0.4 0.5 0.6 0.7 0.8 0.9 1

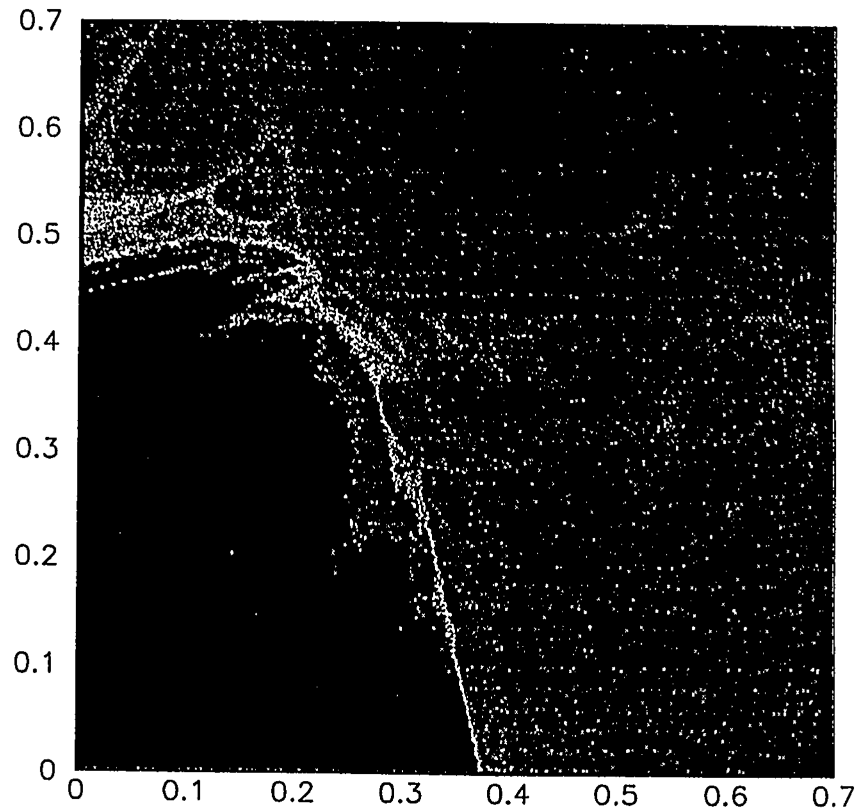
0.7
0.6
0.5
0.4
0.3
0.2
0.1
0
0 0.1 0.2 0.3 0.4 0.5 0.6 0.7

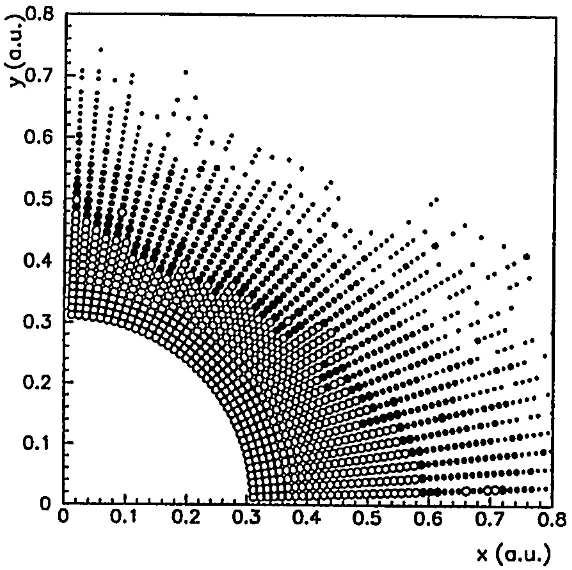

Figure 1: Stability diagram of the 4D Hénon map at $\nu_1 = 0.168$ $\nu_2 = 0.201$. Initial conditions stable for at least $2 \cdot 10^9$ iterates (empty circles), lost between $2 \cdot 10^9$ and 10^7 iterates (large circles), between 10^7 and 10^5 iterates (medium circles) and between 1000 and 10^5 iterates (small circles). Horizontal and vertical Courant-Snyder coordinates are in abscissa and ordinata respectively

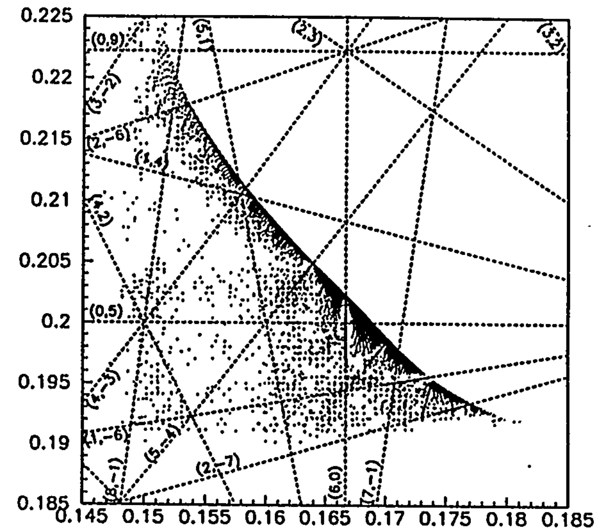

Figure 2: Tune footprint of the 4D Hénon map at $\nu_1 = 0.168$ $\nu_2 = 0.201$. Horizontal and vertical betatron frequencies are in abscissa and ordinata respectively

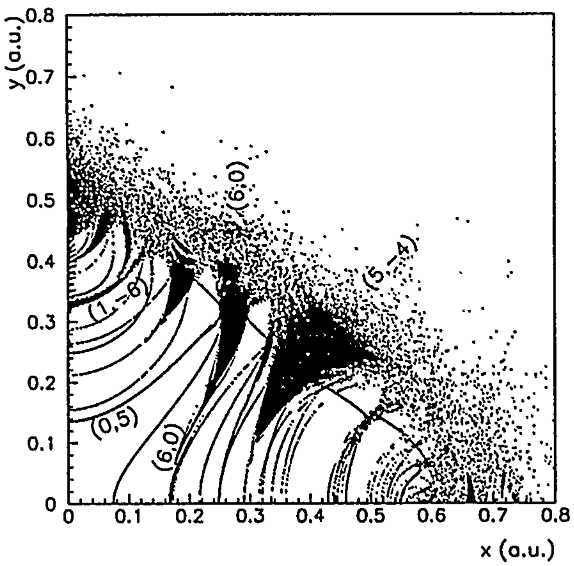

Figure 3: Network of resonances of the 4D Hénon map at $\nu_1 = 0.168$ $\nu_2 = 0.201$. Initial conditions locked on resonances up to order 15 are shown. Horizontal and vertical Courant-Snyder coordinates are in abscissa and ordinata respectively

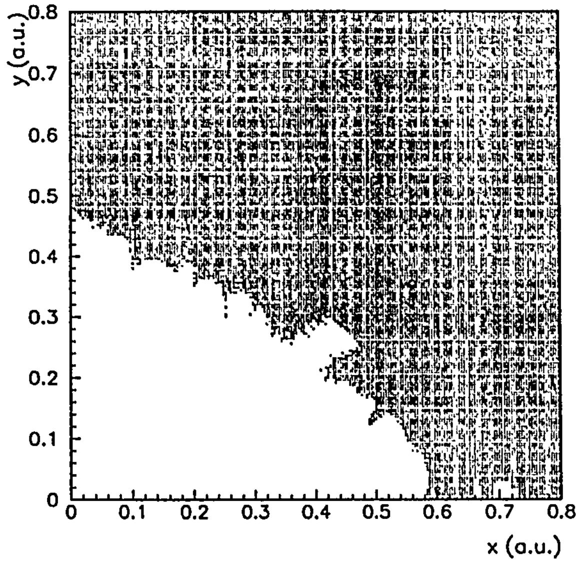

Figure 4:

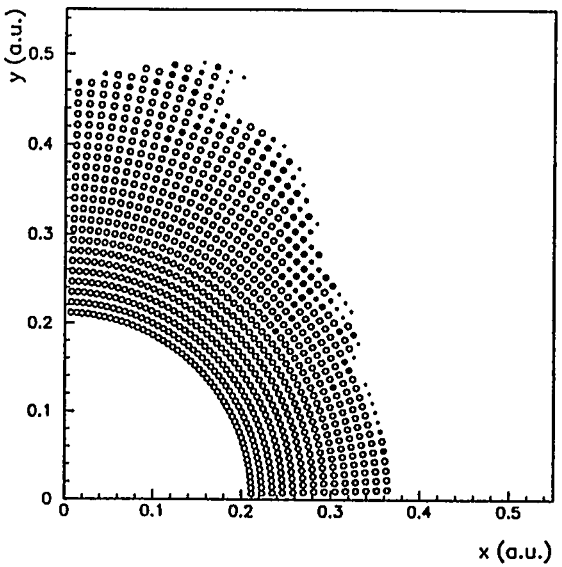

Figure 5: Stability diagram of the 4D Hénon map plus an octupolar term at $\nu_1 = 0.28$ $\nu_2 = 0.31$. Initial conditions stable for at least 10^7 iterates (empty circles), lost between 10^7 and 10^5 iterates (large circles), between 10^5 and 10^4 iterates (medium circles) and between 10^4 and 1000 iterates (small circles). Horizontal and vertical Courant-Snyder coordinates are in abscissa and ordinata respectively

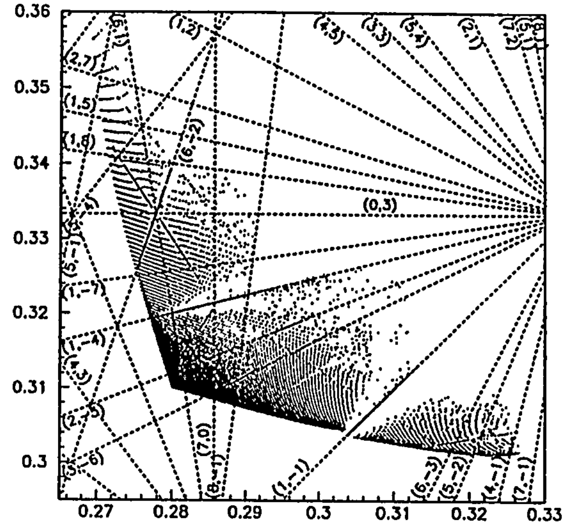

Figure 6: Tune footprint of the 4D Hénon map plus an octupolar term at $\nu_1 = 0.28$ $\nu_2 = 0.31$. Horizontal and vertical betatron frequencies are in abscissa and ordinata respectively

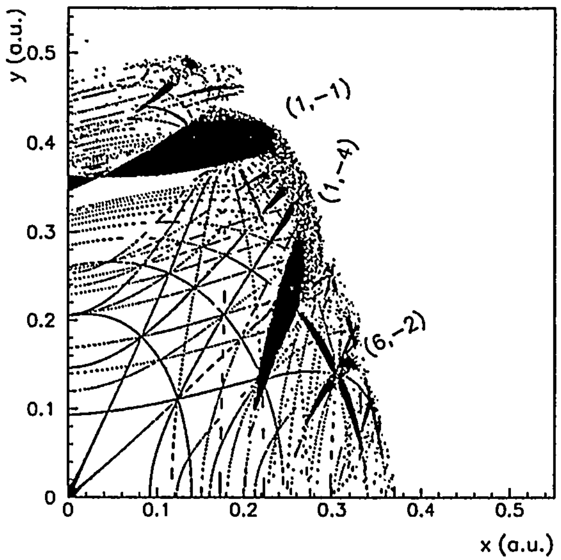

Figure 7: Network of resonances of the 4D Hénon map plus an octupolar term at $\nu_1 = 0.28$ $\nu_2 = 0.31$. Initial conditions locked on resonances up to order 15 are shown. Horizontal and vertical Courant-Snyder coordinates are in abscissa and ordinata respectively

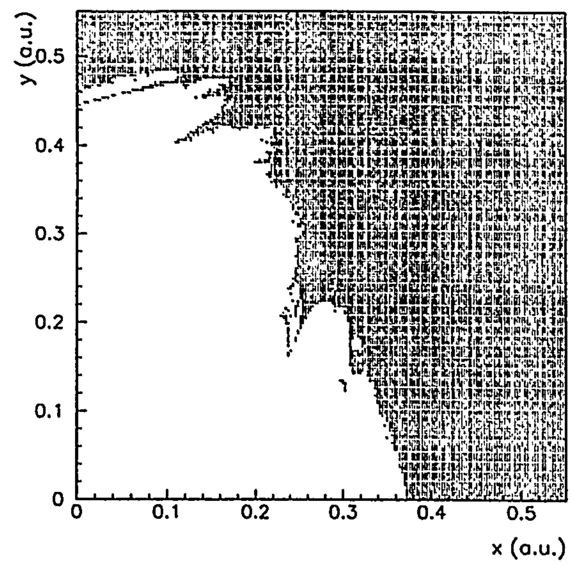

Figure 8:

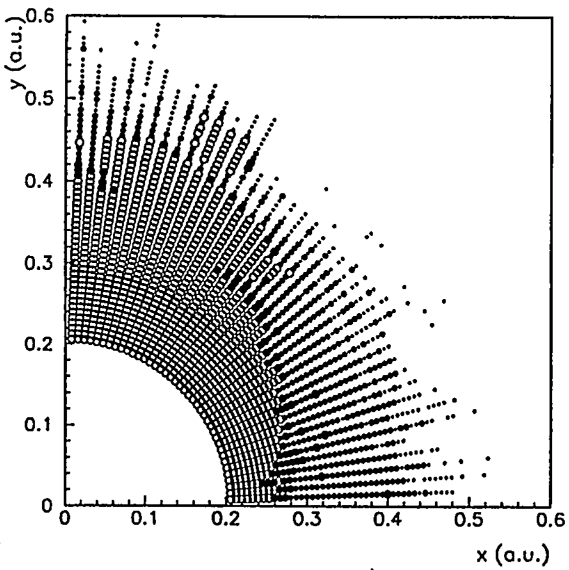

Figure 9: Stability diagram of the 4D Hénon map at $\nu_1 = 0.201$ $\nu_2 = 0.112$. Initial conditions stable for at least 10^7 iterates (empty circles), lost between 10^7 and 10^5 iterates (large circles), between 10^5 and 10^4 iterates (medium circles) and between 10^4 and 1000 iterates (small circles). Horizontal and vertical Courant-Snyder coordinates are in abscissa and ordinata respectively

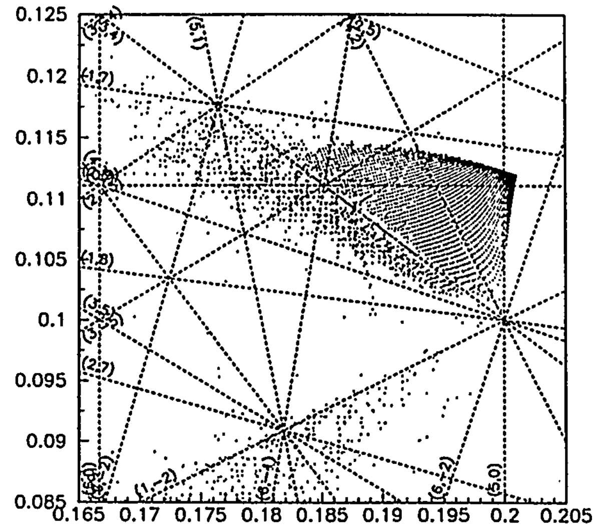

Figure 10: Tune footprint of the 4D Hénon map at $\nu_1 = 0.201$ $\nu_2 = 0.112$. Horizontal and vertical betatron frequencies are in abscissa and ordinata respectively

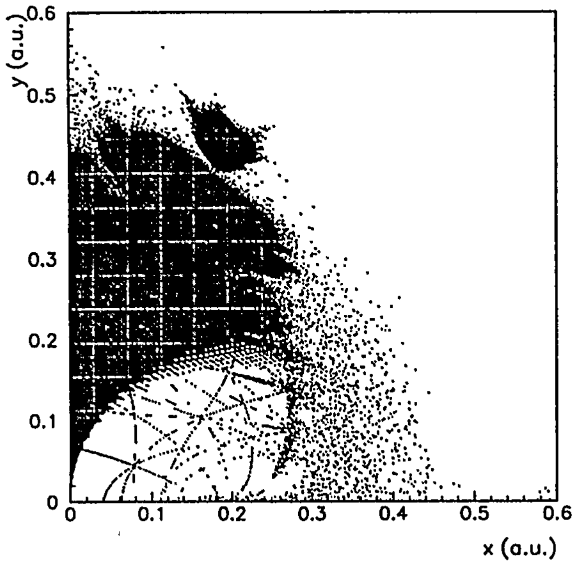

Figure 11: Network of resonances of the 4D Hénon map at $\nu_1 = 0.201$ $\nu_2 = 0.112$. Initial conditions locked on resonances up to order 15 are shown. Horizontal and vertical Courant-Snyder coordinates are in abscissa and ordinata respectively

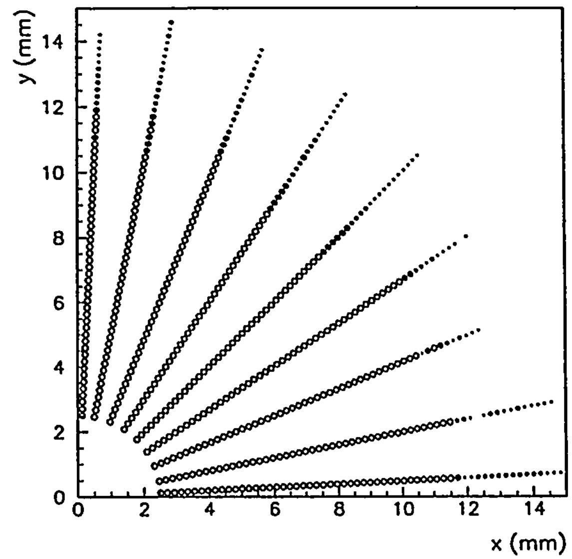

Figure 12: Stability diagram of a 4D LHC model. Initial conditions stable for at least 10^5 iterates (empty circles), lost between 10^5 and 10^4 iterates (large circles), between 10^4 and 10^3 iterates (medium circles) and between 10^3 and 100 iterates (small circles). Horizontal and vertical Courant-Snyder coordinates are in abscissa and ordinata respectively

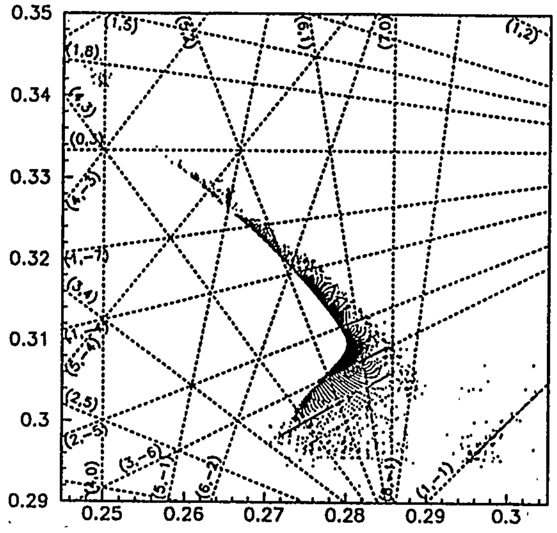

Figure 13: Tune footprint of a 4D LHC model. Horizontal and vertical betatron frequencies are in abscissa and ordinata respectively

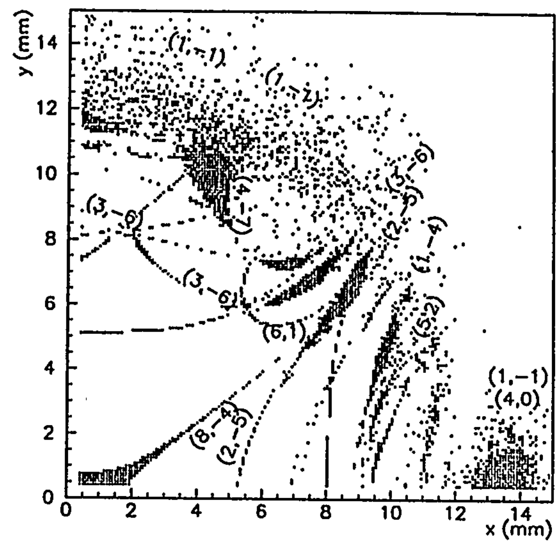

Figure 14: Network of resonances of a 4D LHC model. Initial conditions locked on resonances up to order 15 are shown. Horizontal and vertical Courant-Snyder coordinates are in abscissa and ordinata respectively

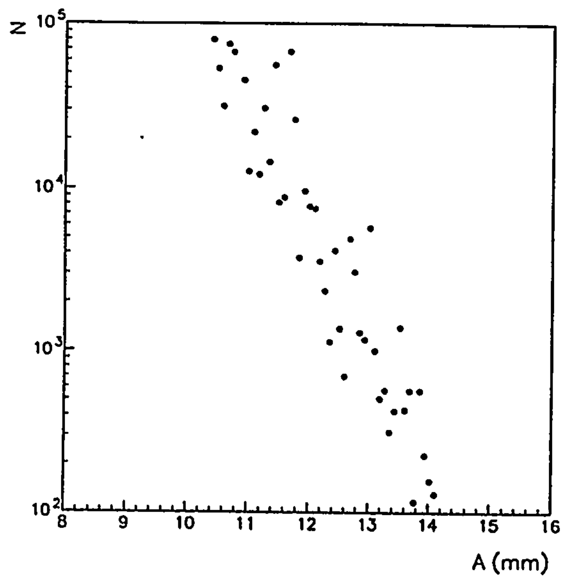

Figure 15: Survival plot for a 4D LHC model

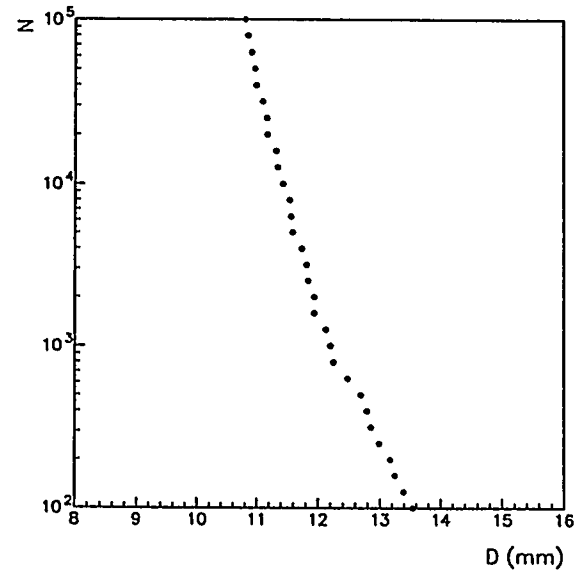

Figure 16: Dynamic aperture averaged over 9 angles as a function of the number of turns for a 4D LHC model

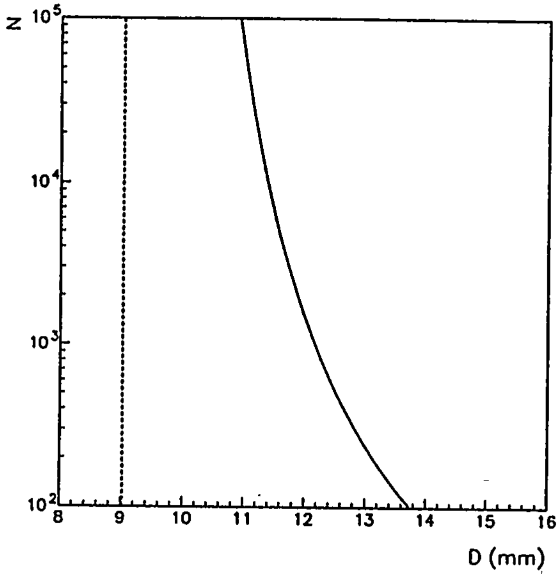

Figure 17: Interpolation of the dynamic aperture for a 4D LHC model

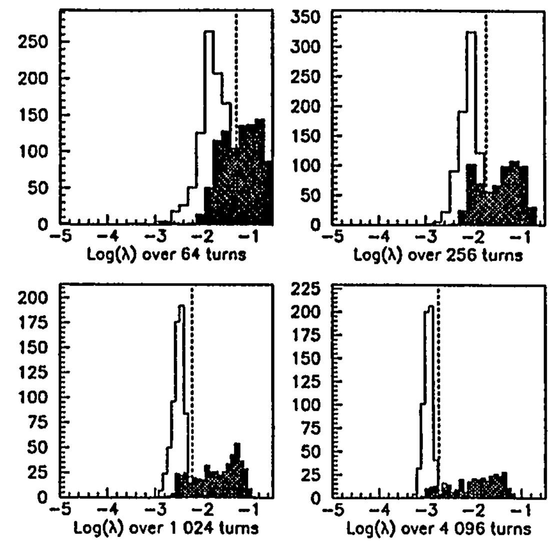

Figure 18: Distribution of the Lyapunov evaluated at four different number of turns for the Hénon map at $\omega_x/2\pi = 0.168$, $\omega_y/2\pi = 0.201$; particles lost before $2 \cdot 10^9$ turns are marked in black

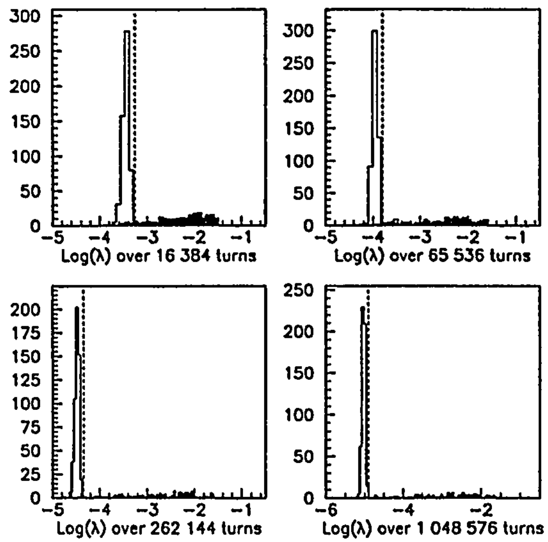

Figure 19: Distribution of the Lyapunov evaluated at four different number of turns for the Hénon map at $\omega_x/2\pi = 0.168$, $\omega_y/2\pi = 0.201$; particles lost before $2 \cdot 10^9$ turns are marked in black

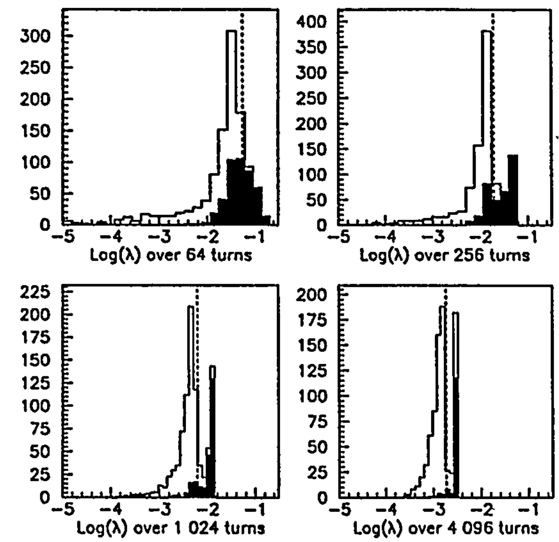

Figure 20: Distribution of the Lyapunov evaluated at four different number of turns for a 4D LHC model; particles lost before 10^5 turns are marked in black

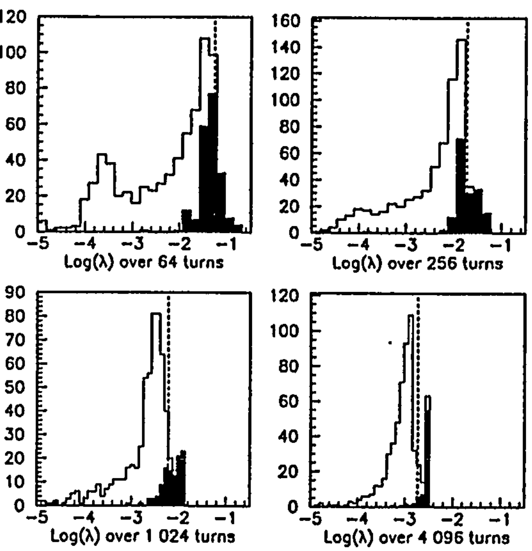

Figure 21: Distribution of the Lyapunov evaluated at four different number of turns for a 6D LHC model; particles lost before 10^5 turns are marked in black

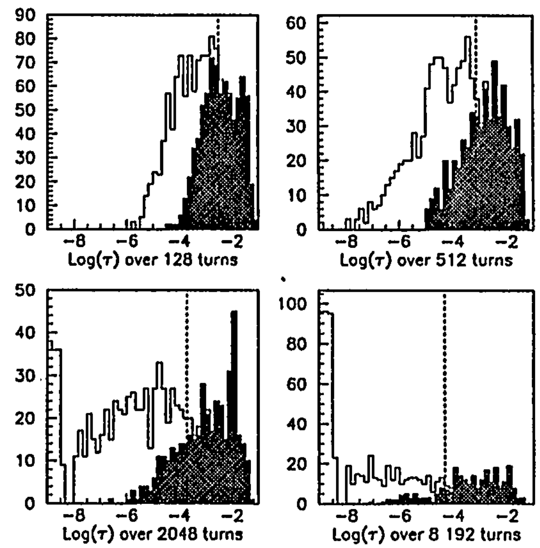

Figure 22: Distribution of the tune variation evaluated at four different number of turns for the Hénon map at $\omega_x/2\pi = 0.168$, $\omega_y/2\pi = 0.201$; particles lost before $2 \cdot 10^9$ turns are marked in black

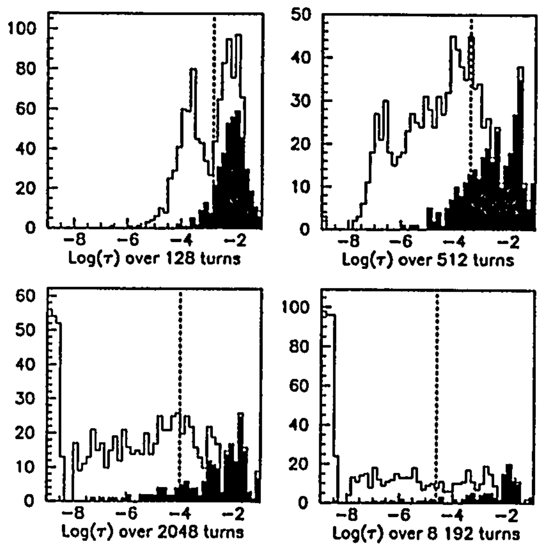

Figure 23: Distribution of the tune variation evaluated at four different number of turns for a 4D LHC model; particles lost before 10^5 turns are marked in black

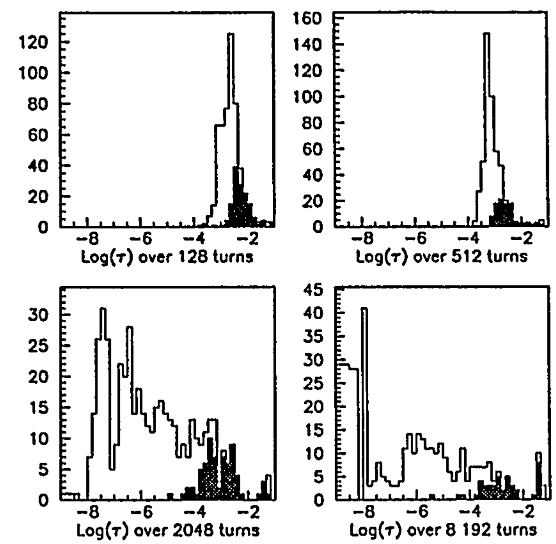

Figure 24: Distribution of the tune variation evaluated at four different number of turns for a 6D LHC model; particles lost before 10^5 turns are marked in black

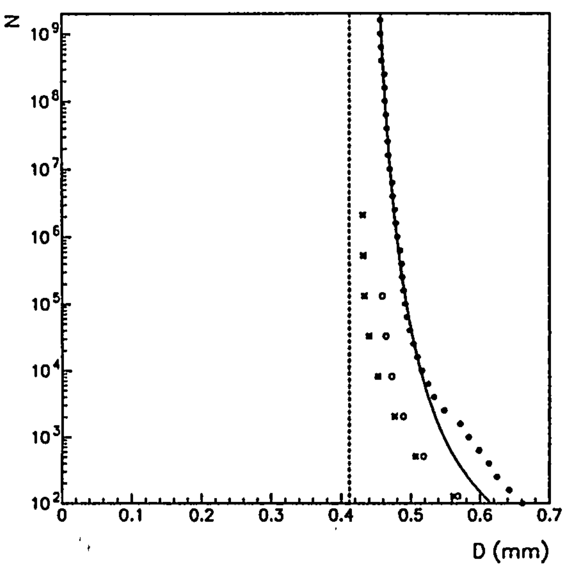

Figure 25: Dynamic aperture through tracking (dots), interpolation through the inverse logarithm (solid line), extrapolation at infinity (dotted line), and estimate through Lyapunov exponent (stars) and tune variation (circles) for the 4D Hénon map at $\nu_1 = 0.168$ $\nu_2 = 0.201$

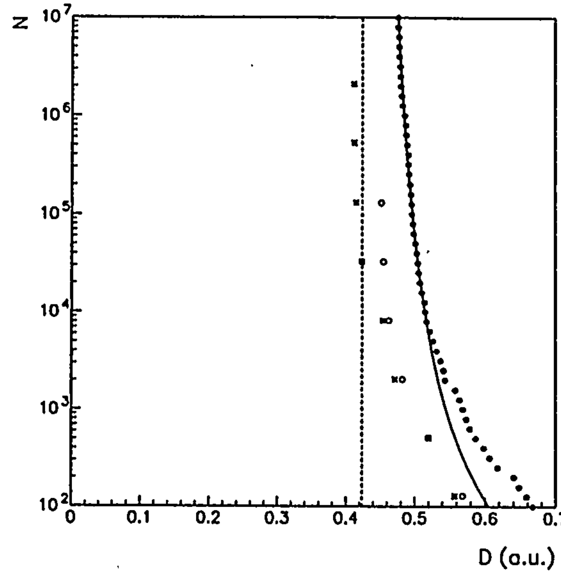

Figure 26: Dynamic aperture through tracking (dots), interpolation through the inverse logarithm (solid line), extrapolation at infinity (dotted line), and estimate through Lyapunov exponent (stars) and tune variation (circles) for the 4D Hénon map at $\nu_1 = 0.201$ $\nu_2 = 0.168$

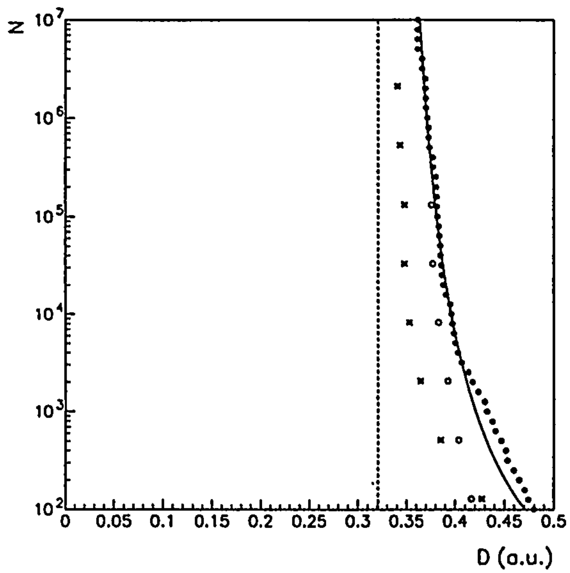

Figure 27: Dynamic aperture through tracking (dots), interpolation through the inverse logarithm (solid line), extrapolation at infinity (dotted line), and estimate through Lyapunov exponent (stars) and tune variation (circles) for the 4D Hénon map at $\nu_1 = 0.201$ $\nu_2 = 0.112$

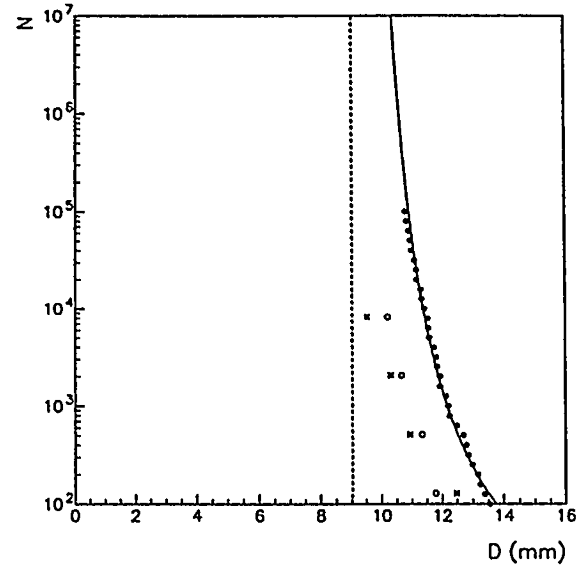

Figure 28: Dynamic aperture through tracking (dots), interpolation through the inverse logarithm (solid line), extrapolation at infinity (dotted line), and estimate through Lyapunov exponent (stars) and tune variation (circles) for a 4D LHC model

FREQUENCY MAP ANALYSIS - THEORY & EXPERIMENTS

J. Laskar, BDL
Paris, France

FREQUENCY MAP ANALYSIS

Solar System

Laskar, Icarus 88, 266 (1990)

2D Map (2 degrees of Freedom)

Laskar, Froeschlé, Celletti Physica D 56, 253 (199[illegible]

4D Map (3 degrees of Freedom)

Laskar Physica D 67, 257 (1993)

Dumas, Laskar Phys. Rev. Lett. 70, 2975 (199[illegible]

1 + n degrees of Freedom

Laskar, Robutel Nature 361, 608 (1993)

Laskar, Joutel, Robutel Nature 361, 615 (1993)

Atomic Dynamics

Vonmilczewski, Diercksen, Uzer PRL (1996)

[illegible]

Frequency Map Analysis:

Theory and Experiment

Jacques Laskar

CNRS, Bureau des Longitudes, Paris

and

David Robin

Lawrence Berkeley National Laboratory

Frequency map.

$$H(I,\theta) = H_0(I) + \varepsilon H_1(I,\theta) \qquad (I,\theta) \in B^n \times T^n$$

$\varepsilon = 0$

$$\dot{I}_j = 0 \qquad \dot{\theta}_j = \frac{\partial H_0(I)}{\partial I_j} = \nu_j(I)$$

$$z_j = I_j e^{i\theta_j} \longrightarrow z_j(t) = z_{0j} e^{i\nu_j t}$$

---

nondegenerate

$$\left|\frac{\partial \nu(I)}{\partial I}\right| = \left|\frac{\partial^2 H_0(I)}{\partial I^2}\right| \neq 0$$

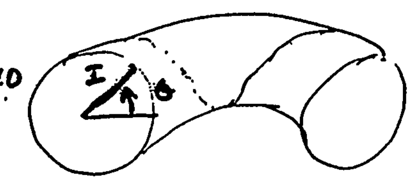

$$F : B^n \longrightarrow \mathbb{R}^n$$
$$(I) \longmapsto (\nu)$$

diffeomorphism on $F(B^n) = \Omega$.

$\varepsilon \neq 0$

KAM theorem

$\exists\ \Omega_\varepsilon$ Cantor set $\subset \Omega$

$(\nu) \in \Omega_\varepsilon \implies$ quasi periodic solutions.

$|\langle k,\nu\rangle| \geq \frac{\varepsilon_\varepsilon}{|k|^m} \quad m > n-1$

Pöschel (1982)

$$\Psi : \mathbb{T}^n \times \Omega \longrightarrow \mathbb{T}^n \times B^n$$
$$(\varphi, \nu) \longrightarrow (\theta, I)$$

Ψ Diffeo – analytical / φ – C^∞ / ν on $\mathbb{T}^n \times \Omega_\varepsilon$

$$\begin{cases} \dot{\nu}_j = 0 \\ \dot{\varphi}_j = \nu_j \end{cases}$$

Thus, if $\nu \in \Omega_\varepsilon$

$$z_j = I_j e^{i\theta_j} \qquad z_j(t) = z_{j0} e^{i\nu_j t} + \sum_{(m)} a^j_m(\nu) e^{i\langle m,\nu\rangle t}$$

Frequency Map $F^*_{\theta_0}$

$$\Psi : \mathbb{T}^n \times \Omega \longrightarrow \mathbb{T}^n \times B^n$$
$$(\varphi, \nu) \longmapsto (\theta, I)$$

$\theta = \theta_0$

$$\begin{array}{ccc} B^n & \longrightarrow & \mathbb{T}^n \times \Omega \\ (I) & \longleftrightarrow & \Psi^{-1}(\theta_0, I) \\ & \searrow^{F^*_{\theta_0}} & \downarrow P_2 \\ & & \Omega \\ & & (\nu) \end{array}$$

ε small.

$F^*_{\theta_0}$ diffeo on its image.

(I,θ), (I',θ') on the same KAM tori

$\hookrightarrow$ $F^*_{\theta}(I) = F^*_{\theta'}(I')$.

Frequency map $F^T_{\theta_0}$

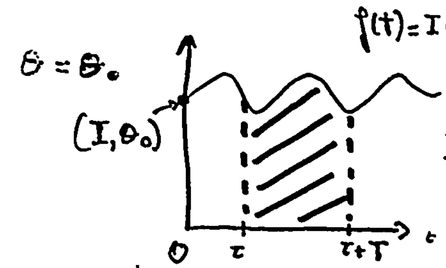

$\Longrightarrow$ $\tilde{\rho}(t) = \sum \alpha_k e^{i\omega_k t}$

$\Downarrow$

$\tilde{\rho}(t) = \sum \alpha_k e^{i\langle k,\nu\rangle t}$

$\Downarrow$

$(\nu_1, \nu_2, \dots \nu_n)$

$$F^T_{\theta_0} : \mathbb{R}^n \times \mathbb{R} \longrightarrow \mathbb{R}^n$$
$$I, \tau \longrightarrow (\nu_1, \nu_2, \dots \nu_n)$$

$\mathcal{A} : \{ I \, . \, (I, \theta_0) \in \text{KAM tori} \}$.

* on $\mathcal{A}$ $\displaystyle\lim_{T \to +\infty} F^T_{\theta_0} = F^*_{\theta_0}$ $\forall$

* on $\mathcal{A}$

I fixed • $F^T_{\theta_0}$ "constant" $/\tau$

τ fixed • $F^T_{\theta_0}$ "diffeo"

Transformée d'une fonction de poids (1

Transform of a weight function

$$\langle f, g \rangle_T^{\chi} = \frac{1}{2T} \int_{-T}^{T} f(t)\, \bar{g}(t)\, \chi(t/T)\, dt$$

weight function.

$\chi(t)$ fonction de poids.

- $\chi(t) \geq c$

Transformée de χ

$$\varphi_\chi(x) = \langle e^{ixt}, 1 \rangle_1^{\chi}$$

Lemme 1.

- $\varphi_\chi(0) = 1$
- $\varphi_\chi'(0) = 0$
- $\varphi_\chi''(0) < 0$

- $\forall n \in \mathbb{N} \quad |\varphi_\chi^{(n)}(x)| \leq 1$
- $\forall n \in \mathbb{N} \quad |x\, \varphi_\chi^{(n)}(x)| \leq M_n$.

FREQUENCY ANALYSIS :

$f(t)$ almost periodic function

$$f(t) = e^{i\omega_1 t} + \sum_k a_k e^{i\omega_k t}.$$

ω_1^T such that $\phi(\omega) = \left| \langle f(t), e^{i\omega t} \rangle_T^{\chi} \right|$

maximum in a vicinity of ω_1

Theorem (Laskar, 1996)

- χ weight function. φ_χ its transform
- $\varphi_\chi^{(p)}(x) = \dfrac{g_p(x)}{x^n} + o\left(\dfrac{1}{x^n}\right) \quad p = 0, 1, 2 \qquad |g_p(x)| < B_p$
- $\sum \left| \dfrac{a_k}{\Omega_k^p} \right|$ cv $\quad p = 0, 1, \dots n$

$\Omega_k = \omega_k - \omega_1$

Then when $T \to +\infty$

$$\omega_1 - \omega_1^T = \frac{-1}{\varphi''(0)\, T^{n+1}} \sum_k \frac{Re(a_k)}{\Omega_k^n} g_1(\Omega_k T) + o\left(\frac{1}{T^{n+1}}\right).$$

Exemples.

Lemme 5. $$\chi_p(t) = \frac{2^p (p!)^2}{(2p)!}(1+\cos\pi t)^p$$

- $\chi_0 = 1$
- $\chi_1 = 1 + \cos\pi t$ (Hanning).

$$\varphi_p(x) = \frac{1}{2}\int_{-1}^{1} e^{ixt}\chi_p(t)\,dt = \frac{(-1)^p \pi^{2p}(p!)^2 \sin x}{x(x^2-\pi^2)\cdots(x^2-p^2\pi^2)}$$

$$\varphi_p^{(n)}(x) = \frac{(-1)^p \pi^{2p}(p!)^2 \sin^{(n)} x}{x^{2p+1}} + o\left(\frac{1}{x^{2p+1}}\right)$$

$$\varphi_p(x) = 1 + \frac{\varphi_p''(0)}{2}x^2 + o(x^2).$$

$$\varphi_p''(0) = -\frac{2}{\pi}\left(\frac{\pi^2}{6} - \sum_{k=1}^{p}\frac{1}{k^2}\right)$$

$$\sum \left|\frac{a_k}{\Omega_k^n}\right| \quad \text{cv} \quad \text{pour} \quad n = 0, 1, \ldots 2p+1$$

$$\omega_1 - \omega_1^T = \frac{(-1)^{p+1}\pi^{2p}(p!)^2}{\varphi_p''(0)\,T^{2p+2}} \sum \frac{B(a_k)}{\Omega_k^{2p+1}}\cos\Omega_k T + o\left(\frac{1}{T^2}\right)$$

$\chi_0 = 1 \longrightarrow 1/T^2$

χ_1 (Hanning) $\longrightarrow 1/T^4$

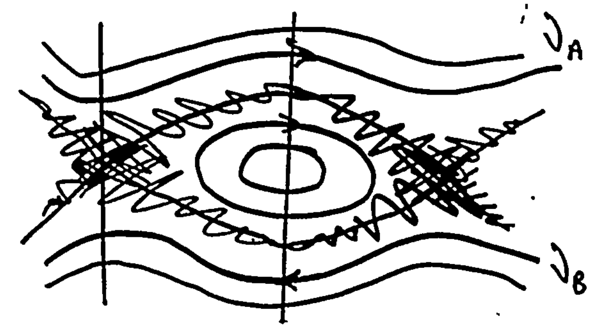

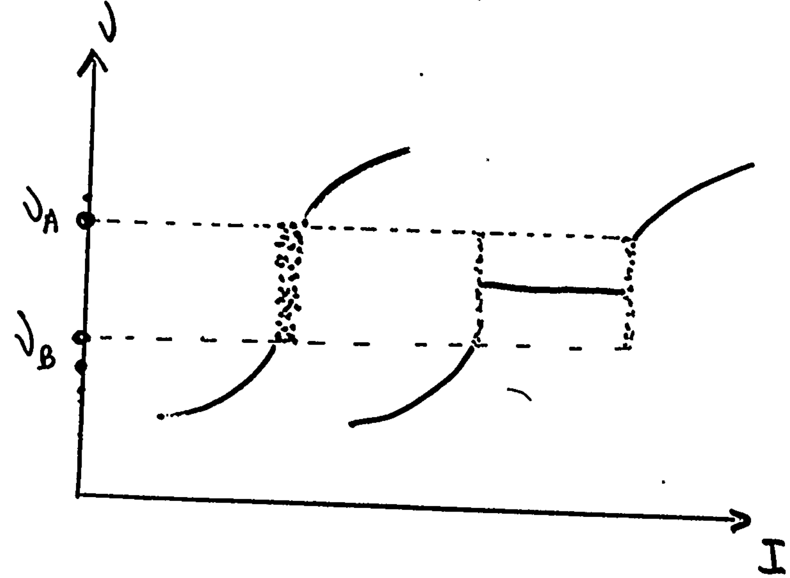

INTRODUCTION TO FREQUENCY MAP ANALYSIS

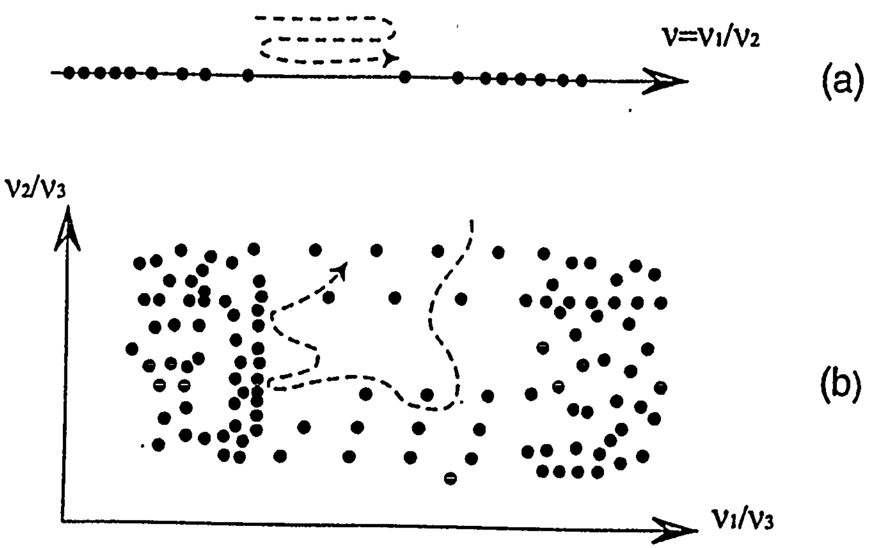

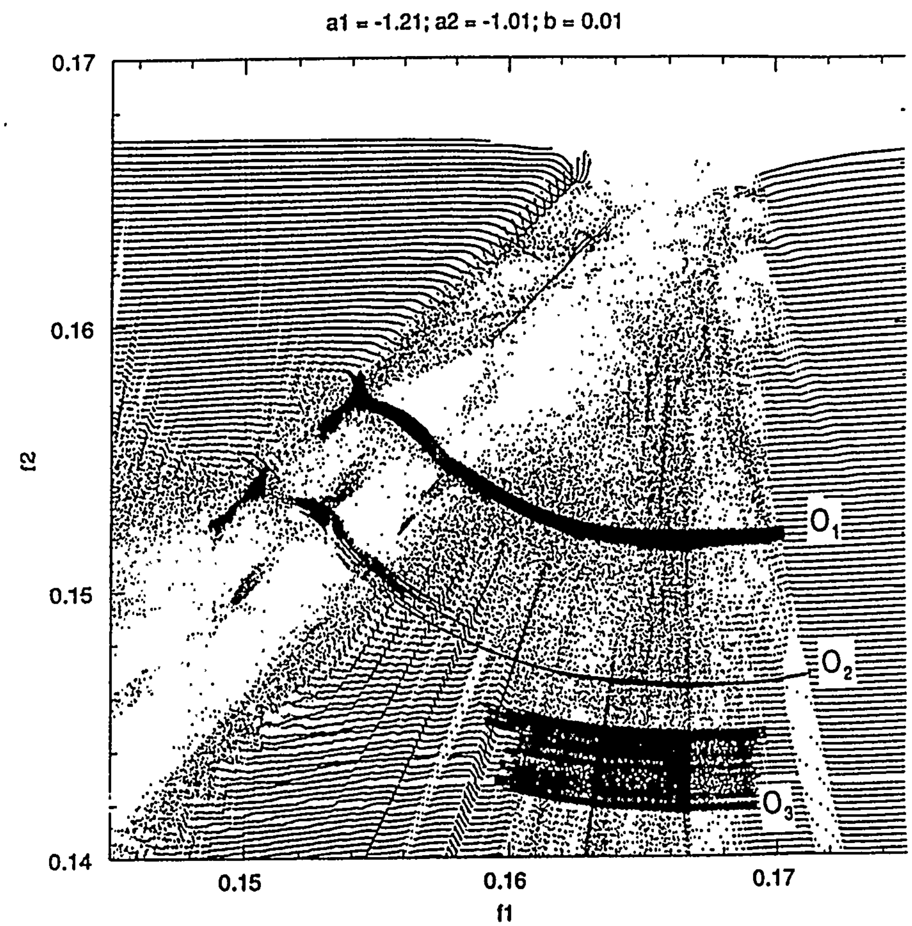

Laskar, 1993, Physica D

'Da

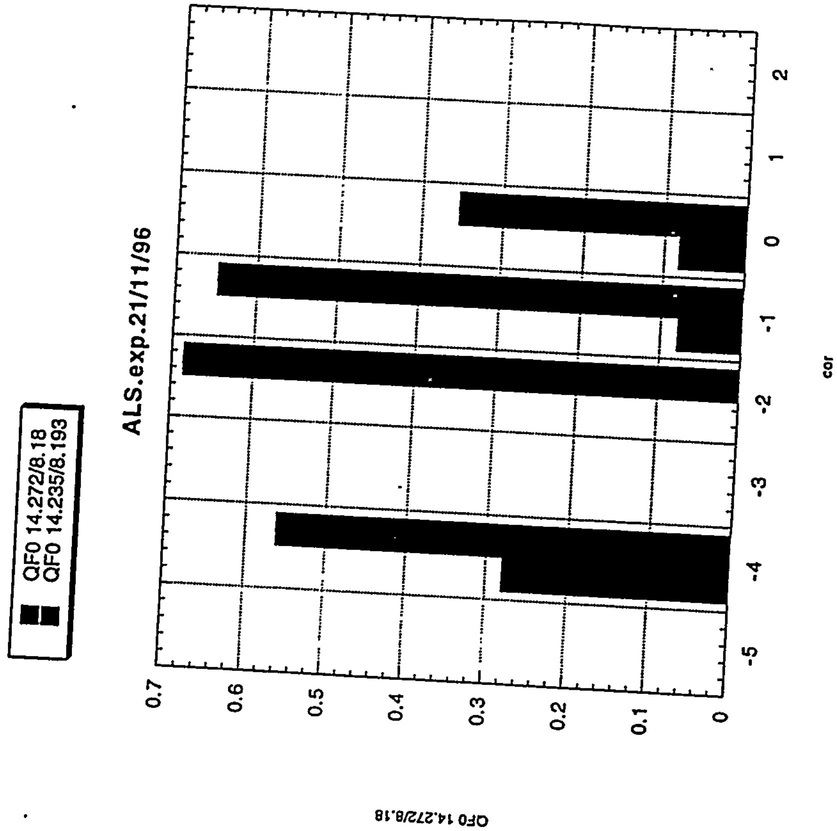

Changing the Working Point

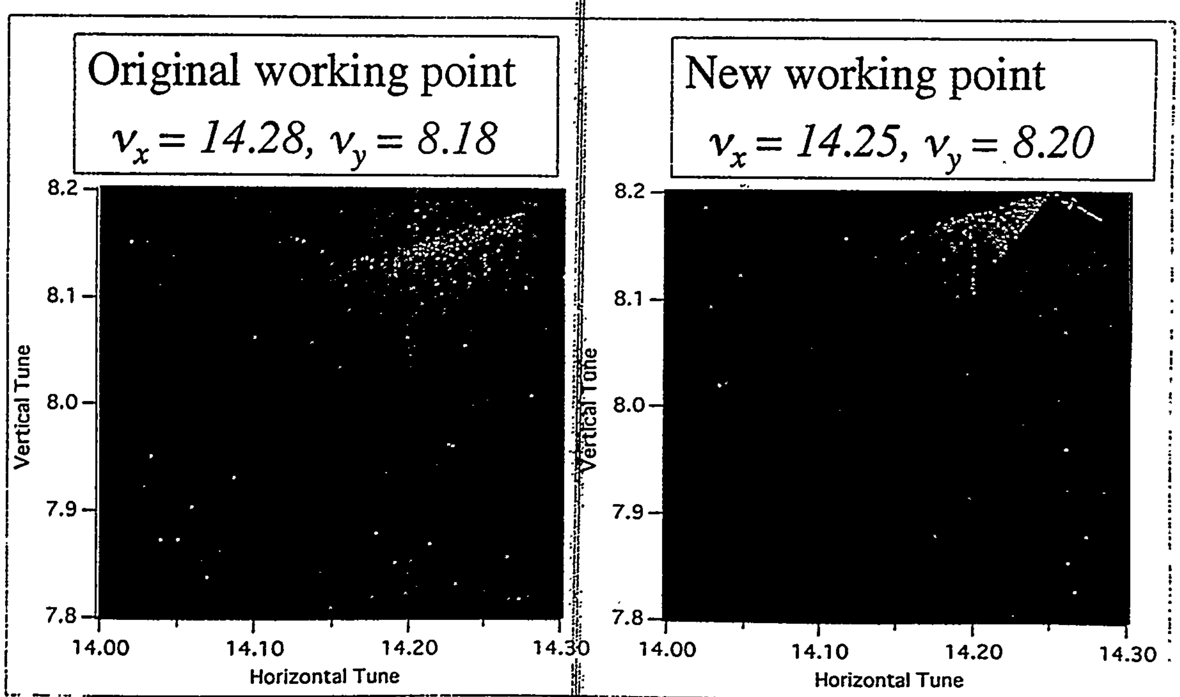

THE EFFECT OF RESONANCES ON LONG-TERM STABILITY & SYMPLECTIC FULL TURN MAPS

R. Warnock, SLAC

FAST SYMPLECTIC MAPPING AND LONG-TERM STABILITY [IN THE LHC]

R. Warnock (SLAC) and J. S. Berg (CERN)

Thanks to É. Forest, F. Schmidt, R. Ruth

TOPICS

- Construction and testing of symplectic full-turn maps
- Construction of quasi-invariants of maps
- Long-term bounds on motion
- Quasi-invariants near strong resonances
  - * Local pendulum motion in partially normalized coordinates
  - * Local description of motion by isolated-resonance Hamiltonian
- Simplified picture of 6-d motion
  - * Sinusoidal external modulation of momentum
  - * stroboscopic view: resonances and invariants on surface of section at synchrotron period
- Chaotic region near dynamic aperture; orbits that escape precipitously after millions of turns
- Convergence proof for Fourier-spline representation of map generator (with J. Ellison, U. of New Mexico
- Survey of computer codes

ALL EXAMPLES FOR LHC INJECTION LATTICE

THE <u>NECESSITY</u> OF MAPS IN STUDYING LONG-TERM MOTION

Basic Dynamical Model: Symplectic element-by-element tracking in a "realistic" lattice

Difficulty: Tracking over desired storage time of the beam is much too expensive

Responses to this difficulty:

a) Use highly simplified lattice (Ritson)

b) Look for "early indicators" of instability

Rapid divergence of initially close orbits (Schmidt et al.)

Behavior of pseudo-tunes from windowed time series; extrapolation of dyn. aperture in N (Scandale et al.; Lasker)

c) Full-turn map as approximation to full dynamics of tracking code.

With appropriate technique, maps closely describ. the basic dynamical model <u>and</u> allow study of long-term behavior.

Taylor series representation of map:

1) Not sufficiently symplectic (for long-term behavior of hadron machines at large amplitudes).

2) Expensive to compute at required high order.

Symplectic map representations;

Explicit: "jolt" factorization ([illegible])

Implicit: mixed variable generator

a) Cartesian coordinates, power series for generator ([illegible], Forest, Douglas; Yen, Channell, Syphers, SSCL 1994)

b) Polar coordinates, Fourier-spline representation of generator (Warnock, Berg, Forest, Ruth)

advantages of (b):

- robust generator construction*, even at large amplitudes. Avoids power series.
- approximation theory is almost elementary
- map construction and iteration are fast

disadvantage of (b):

- fails in regions where one action is large and the other small (coordinate singularity of polar system)

* However, analogous construction of generators can also be done in Cartesian coordinates.

CANONICAL GENERATOR OF SOURCE MAP T_0

Notation for $T_0(I, \Phi) = (I', \Phi')$ in action-angle coordinates:

$$I' = I + R(I, \Phi)$$
$$\Phi' = \Phi + \Theta(I, \Phi) \qquad (\dagger)$$

Canonical generator G of the same map:

$$I' = I + G_{\Phi'}(I, \Phi')$$
$$\Phi = \Phi' + G_I(I, \Phi')$$

To find G, solve the PDE's,

$$G_{\Phi'}(I, \Phi') = R(I, \Phi)$$
$$G_I(I, \Phi') = -\Theta(I, \Phi)$$

where $\Phi = \Phi(I, \Phi')$ is given as solution of $(\dagger)$

$$x_i = \sqrt{\beta_i I_i}\cos\Phi_i$$
$$p_i = \frac{dx_i}{ds} = -\sqrt{\frac{I_i}{\beta_i}}\sin\Phi_i \qquad i = 1, 2, \ldots, n$$

$$T_0: \ R_+^n \times T^n \longrightarrow R_+^n \times T^n$$

REPRESENTATION OF G AND SOLUTION OF PDE's

$$G(I,\Phi') = \sum_m g_m(I)\, e^{im\cdot\Phi'}$$

$$i m g_m(I) = \frac{1}{2\pi}\int_0^{2\pi} e^{-im\cdot\Phi'} G_{\Phi'}(I,\Phi')\, d\Phi'$$

$$= \frac{1}{2\pi}\int_0^{2\pi} e^{-im\cdot\Phi'} R(I,\Phi')\, d\Phi'$$

$$= \frac{1}{2\pi}\int_0^{2\pi} e^{-im\cdot(\Phi+\theta(I,\Phi))} R(I,\Phi) \overset{det}{\wedge} (1+\theta_\Phi(I,\Phi))\, d\Phi \qquad (1$$

Determines g_m for $m \neq 0$

For $m = 0$,

$$\frac{\partial g_0(I)}{\partial I} = \frac{1}{2\pi}\int_0^{2\pi} G_I(I,\Phi')\, d\Phi'$$

$$= -\frac{1}{2\pi}\int_0^{2\pi} \theta(I,\Phi)(1+\theta_\Phi(I,\Phi))\, d\Phi \qquad (2$$

For I-dependence,

$$g_m(I) = \sum_j \lambda_{mj}\, \beta_j(I)$$

$\{\beta_j(I)\}$ = Kronecker product B-spline basis

Discretize integrals (1), (2), compute them on mesh $\{I_i\}$ in I, solve linear equations for coefficients λ_{mj}.

-6-

Newsjournal of the Society for Industrial and Applied Mathematics

siam news

B-Splines and Geometric Design

By Paul Davis

The morphing of Arnold Schwarzenegger's adversary into the various forms he takes on in *Terminator 2* is really a bit of mathematical magic: It is B-splines that drive the sophisticated computer graphics. B-splines are also responsible for the slower but economically more important transformation that has brought geometric design from the era of clay models and hand measurements to megaflop computation and three-dimensional renderings on desktop computers. Whenever free-form curves and surfaces are represented mathematically, as they are in computer-aided design, analysis, and manufacturing, B-splines are the foundation of an efficient implementation.

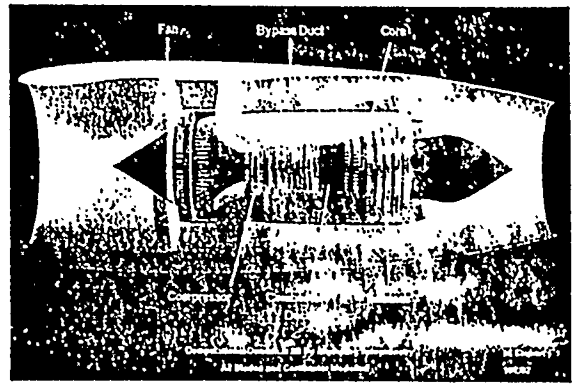

Cut-away of a jet engine modeled with NURBS—Non-Uniform Rational B-Splines: the spline geometry library DT_NURBS, developed at Boeing for the David Taylor Model Basin, was used in the modeling. (Model and picture courtesy of the NASA Lewis Research Center.)

B-splines are especially important in the aircraft and automotive industries, where shape is all important. Asking about the impact of B-splines in geometric design, says Ray Sarraga of General Motors Research, "is like asking 'What is the impact of the gasoline engine in the use of cars?'" Tom Grandine of The Boeing Company adds, "No plane leaves Boeing without many billions of B-spline evaluations behind it. Splines demonstrate some of the good things that happen when you get the math right!"

From the Designer's Vision To the Production Line

Until recently, designers in the automotive industry did their dreaming in clay. To transfer the shapes envisioned by the designers to the dies used to stamp body panels for a new car, full-sized clay models were painstakingly measured along hundreds of profiles.

The polygonal shapes outlined by measurements along individual profiles were too rough for production. Connecting the measured points with a long, flexible ruler—a drafting spline—smoothed the profiles sufficiently for use in the construction of stamping dies. This process of hand lofting was slow and expensive, especially for complex shapes like automobiles and aircraft. And it left undone the work of blending adjacent profiles into a smooth surface.

Today, B-splines make possible mathematical representations of surfaces that are far beyond the range of hand techniques. At Boeing, computations involving 30–50,000 data points are routine. Imagine measuring, plotting, and smoothing 50,000 data points by hand!

And spline-based computations in the

An Expanding Role for Level Sets

By Barry A. Cipra

SIAM members planning to attend this year's annual meeting in Kansas City may want to arrive on Saturday—not just to save on airfare, and not so much to take in the wild nightlife Kansas City has to offer, but to learn about some exciting new techniques in numerical ary, as in the problem of finding the shortest path for a robot navigating around obstacles under constraints. The goal of level set methods is to unify these seemingly disparate interface problems under a common language, and to devise general numerical approaches that quickly and accurately find their solution.

6

SIAM's First Stu

Carl de Boor, whose 1972 description of a simple, stable recursion formula for evaluating B-splines set in motion a revolution in geometric design, will give The John von Neumann Lecture at the 1996 SIAM Annual Meeting in Kansas City.

Convergence of Fourier-spline representation of G:

T_0 (tracking code) is polynomial (of very high order) in (x, p) $\Rightarrow$

$R(I, \varphi)$ is entire function of φ

$\theta(I, \varphi)$ is analytic in φ in a strip,

$$|\mathrm{Im}\,\varphi| < \sigma, \quad \text{for } I < I_0$$

Analysis of explicit formula for g_m shows that for $I < I_1 < I_0$,

$$|g_m(I, \varphi)| \le A e^{-a|m|}$$

Fourier series for $G(I, \varphi)$ converges uniformly, defines function analytic in strip $|\mathrm{Im}\,\varphi| < \eta <$

Also, $G(I, \varphi)$ is analytic in I at real φ except near $I = 0$, so that spline expansion for I dependence will converge

Can use splines of any order, get arbitrary smoothness,

- Long-term behavior of transverse coordinates is strongly influenced by energy oscillations, but the latter remain roughly harmonic. $\Longrightarrow$

  Reasonable approximation: modulate p_τ externally, neglect τ. $\left(p_\tau = \delta = -\frac{(p-p_0)}{p_0} \right.$

- Study LHC in injection mode, for which synchrotron period is 129.97 turns. Approximate as 130 turns.

  Change in p_τ localized at r.f. cavity. Just after cavity

  $$p_\tau = \delta \sin\left(\frac{2\pi n}{130}\right) \quad \text{at } n\text{-th turn.}$$

- Transverse motion at constant p_τ represented by 4-d generator $\quad G(I_1, \Phi_1, I_2, \Phi_2 ; p_\tau)$

  $I_1 = I_2 = 0$ at p_τ-dependent fixed point of 4-d map.

- Fourier coeff., constructed by method above, is

  $$g_m(I_1, I_2, p_\tau) = \sum_{ijk} g_{mijk} \underbrace{B_i^{(1)}(\sqrt{I_1})\, B_j^{(2)}(\sqrt{I_2})}_{\text{B-spline basis fcns.}} B_k^{(3)}(p_\tau)$$

Our guess concerning full 6-d map:

- Construction time about the same
- Iteration time about 20% greater

For fast evaluation of map,

1) Throw away negligible F. amplitudes g_m
   For $|m| \le M \approx 10$–20 <u>many</u> are very small.

2) Use cubic or quartic B-splines; (program allows arbitrary order)
   B-spline basis fcns. have "limited support" — only a few are non-zero at any point.

3) Compute and store

   $$\sum_k g_{mijk}\, B_k^{(3)}(p_\tau)$$

   for all 130 values of p_τ

4) Start Newton iteration to solve

   $$\Phi = \Phi' + G_I(I, \Phi')$$

   with a good guess from a rough <u>explicit</u> map,

   $$\Phi' = \Phi + \underbrace{\tilde{\theta}(I, \Phi)}_{\text{F. series with 2-3 terms.}}$$

EXAMPLE OF MAP CONSTRUCTION AND MAP ITERATION

- Start with symplectic tracking, defining source map T_0 (thanks to F. Schmidt and É. Forest)

  Requires 68 ms/turn (IBM RS6000 – 590)

- Determine short-term (2000 turn) dynamic aperture by tracking
- Construct generator for region somewhat below short-term aperture, with

$$|m_1|, |m_2| \leq 10 \implies 21 \text{ points in } \Phi_1 \text{ or } \Phi_2$$

$$\left.\begin{array}{l} 10 \text{ spline interpolation pts. in } I_1 \text{ or } I_2 \\ 6 \quad '' \quad '' \quad '' \quad '' \quad p_\tau \end{array}\right\} \text{cubic splines}$$

Covers relatively small rectangle in I_1, I_2 space

String together several such rectangles to cover a band running parallel to short-term aperture line.

- Construction time per rectangle:

$$21^2 \cdot 10^2 \cdot 6 = 264600 \text{ turns of tracking} \longrightarrow 5 \text{ hours}$$

Time for one iteration of map = 1.2 ms

Thus, 0.156 s for T_1^{130}

3.6 hrs for 10^7 turns

Speed-up by factor of 57 over straight tracking

Recall that 7×10^6 turns needed for injection in LHC

SHORT-TERM DYNAMIC APERTURE

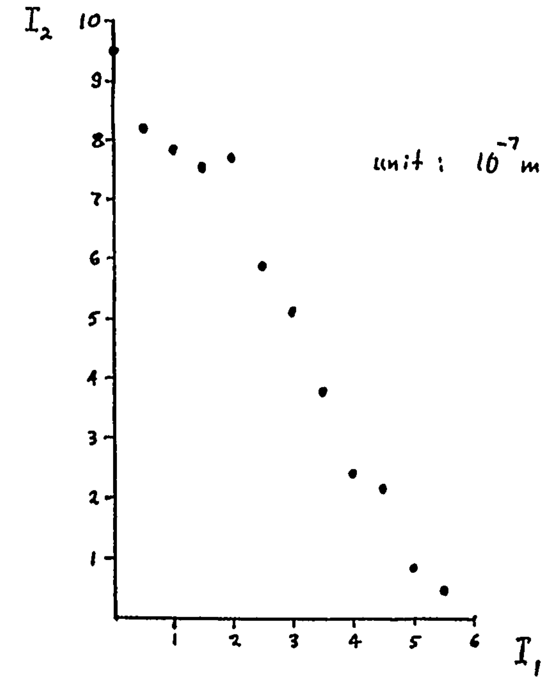

- $\longleftrightarrow$ orbit with this point as initial condition outside physical aperture at 2000 turns ($\Phi_1(0) = \Phi_2(0) = 0$)

Recall $I \sim x^2 = (\text{transverse displacement})^2$

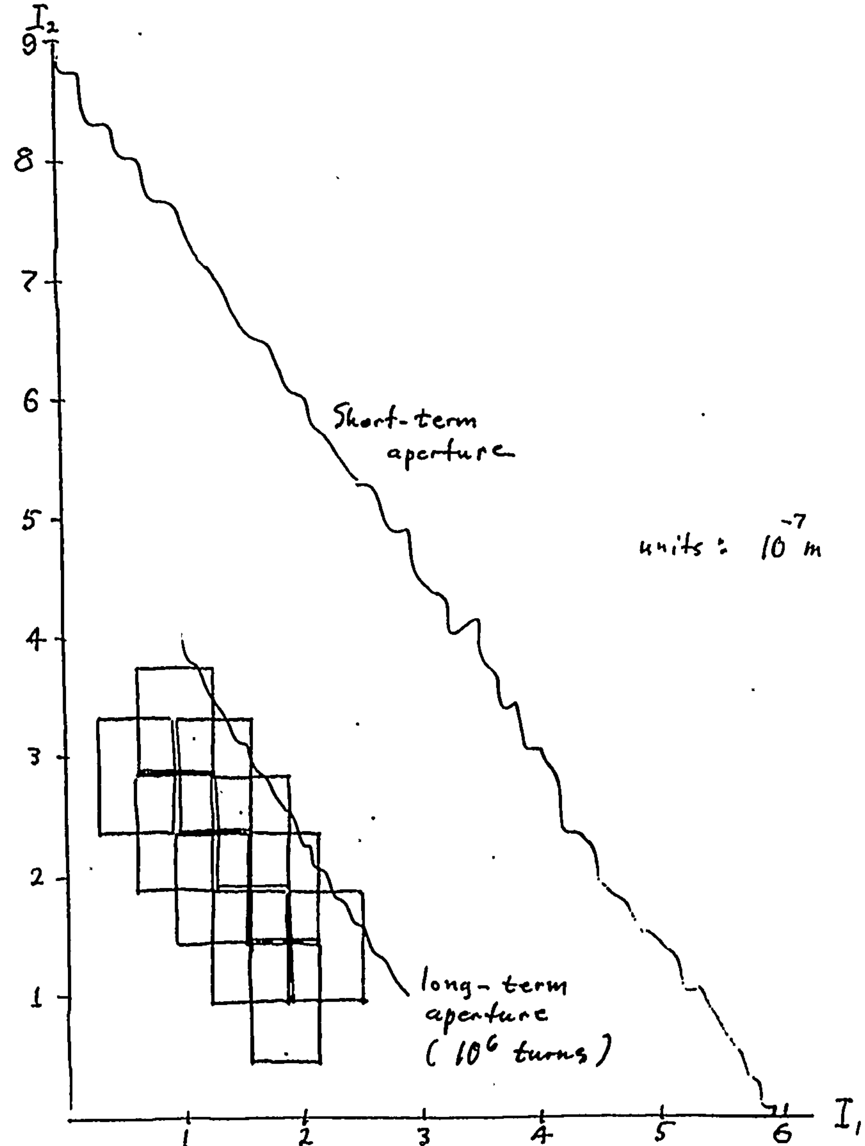

VALIDATION OF MAP AS A REPRESENTATION OF TRACKING

$T_1 \approx T_0$ in what sense?

1) Check quantitative agreement of map with tracking, for many initial conditions

But .... how much agreement is enough?

Can improve agreement essentially at will by expanding Fourier – spline basis; but it will be unnecessarily expensive to overdo it!

A more physical approach (but not effective in large-amplitude chaotic region):

2) Compare resonances of map with those of tracking (on surface Σ at synchrotron period)

Identify resonances by $\Phi_1 - \Phi_2$ plot.

3) Construct quasi-invariant surface of map, and check its invariance under tracking.

4) See whether map and tracking give the same dynamic aperture, on longest feasible runs. An expensive approach!

5) See whether borders of chaotic regions agree for map and tracking

RESULTS ON VALIDATION OF MAP WITH FOURIER - SPLINE BASIS AS DESCRIBED ABOVE (AMPLITUDE x BELOW SHORT-TERM APERTURE BY $1/\sqrt{3}$)

1) At 1 turn, map and tracking agree to about 2 parts in 10^4

2) Relatively broad, low-order resonances (presumably the most dangerous) evolve from same initial conditions in map and tracking (on several trials

A narrow, high-order resonance may occur at slightly different initial conditions in map and tracking. Example: 59th order

$$[I_1(0), I_2(0)] = \begin{cases} [1.1, 1.1] \cdot 10^{-7} & \text{tracking} \\ [1.09983, 1.1] \cdot 10^{-7} & \text{map} \end{cases}$$

3) Surface invariant under map to 1 part in 10^5 is invariant under tracking to 1 part in 10^4

Conclusion: Map of modest accuracy (see item (1)) seems to represent a physical system very similar to that of tracking

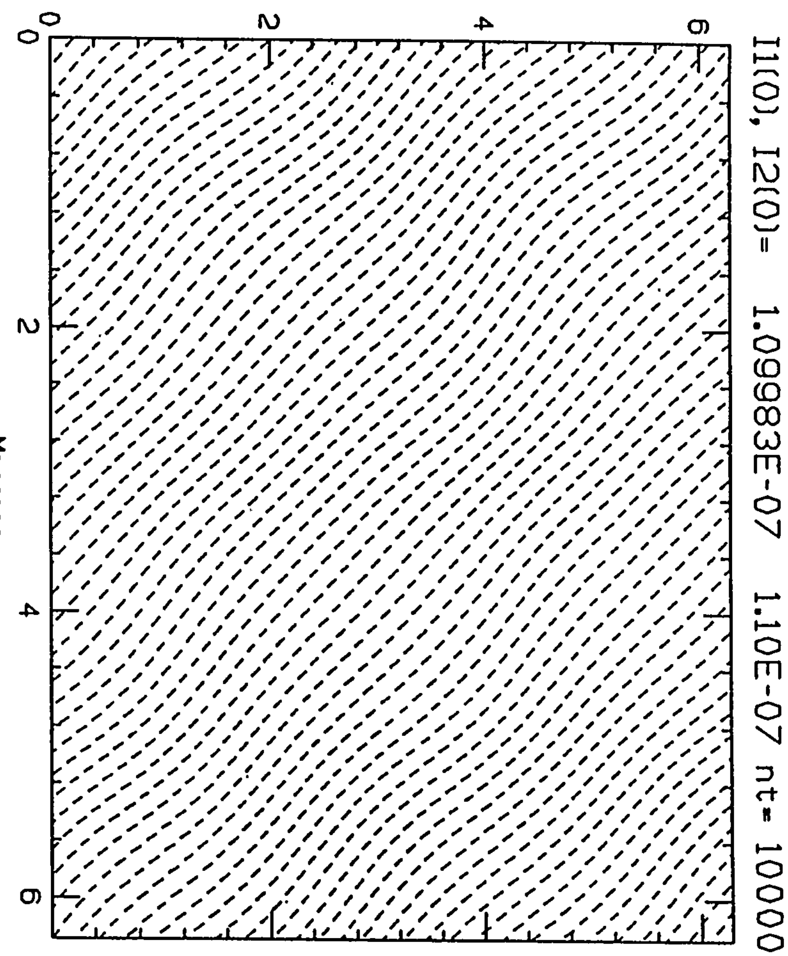

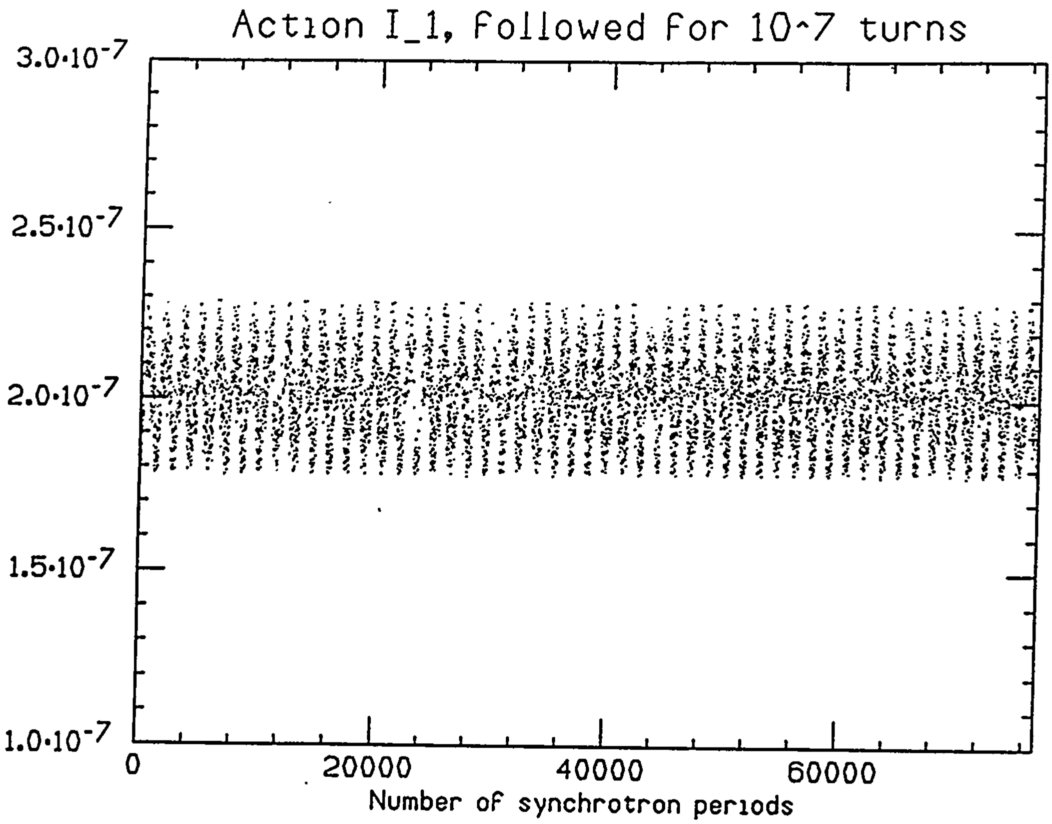
Action I_1, Followed for 10^7 turns
3.0·10^-7
2.5·10^-7
2.0·10^-7
1.5·10^-7
1.0·10^-7
0
20000
40000
60000
Number of synchrotron periods

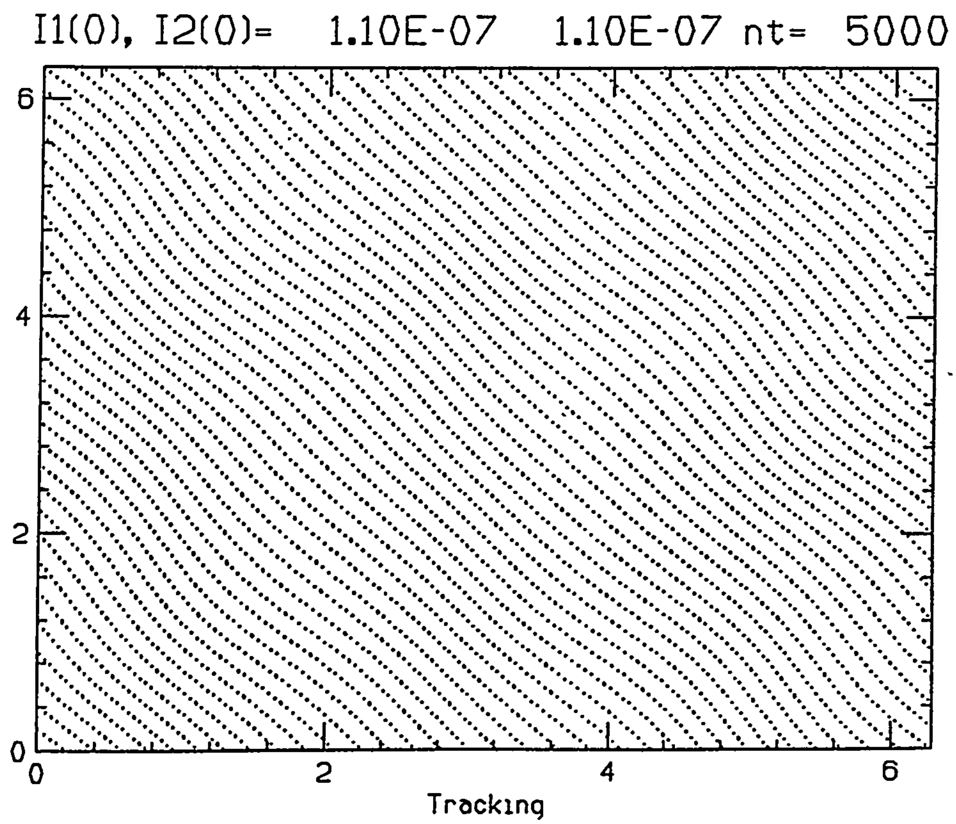
I1(0), I2(0)= 1.10E-07 1.10E-07 nt= 5000
0
2
4
6
Tracking

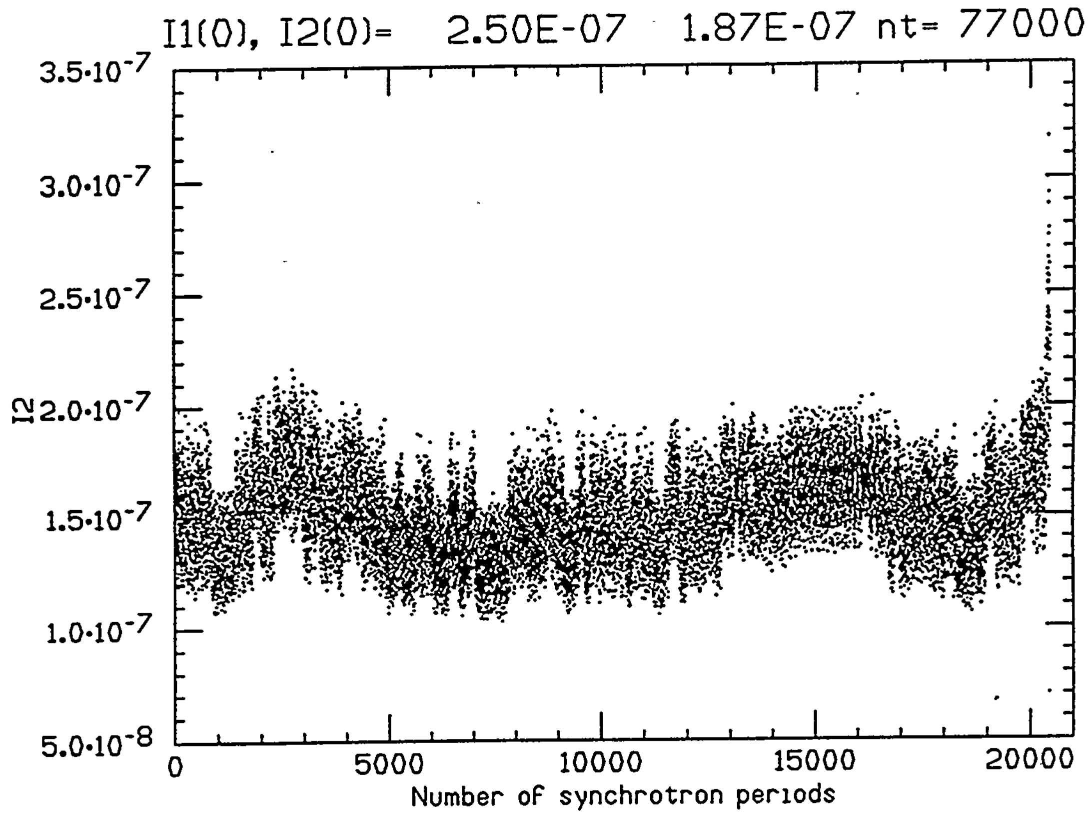
I1(0), I2(0)= 2.50E-07 1.87E-07 nt= 77000
I2
3.5·10^-7
3.0·10^-7
2.5·10^-7
2.0·10^-7
1.5·10^-7
1.0·10^-7
5.0·10^-8
0
5000
10000
15000
20000
Number of synchrotron periods

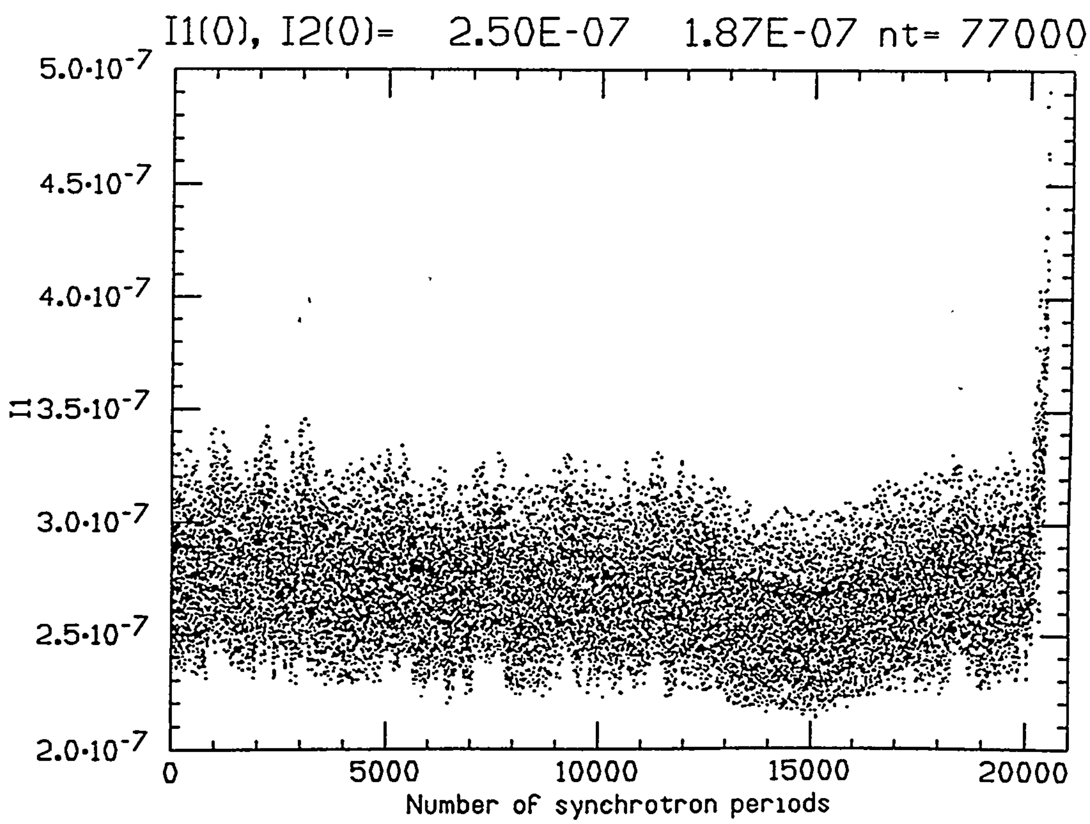
I1(0), I2(0)= 2.50E-07 1.87E-07 nt= 77000
I1
5.0·10^-7
4.5·10^-7
4.0·10^-7
3.5·10^-7
3.0·10^-7
2.5·10^-7
2.0·10^-7
0
5000
10000
15000
20000
Number of synchrotron periods

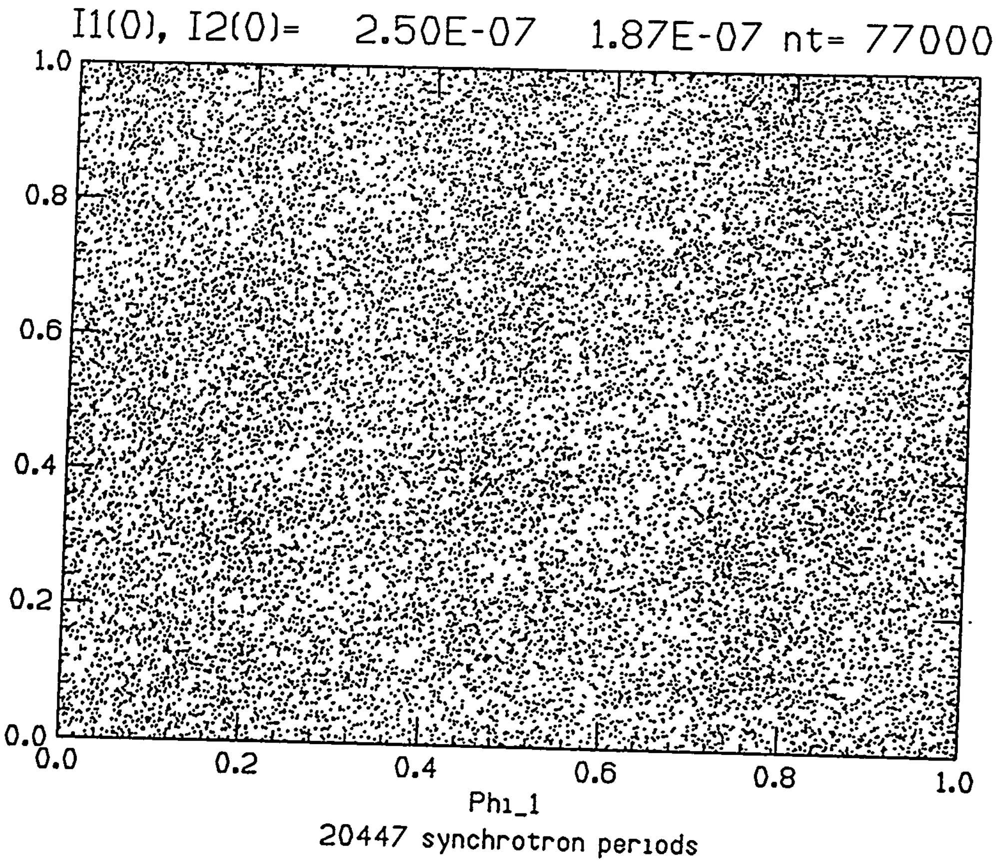
I1(0), I2(0)= 2.50E-07 1.87E-07 nt= 77000
1.0
0.8
0.6
0.4
0.2
0.0
Phi_2
0.0
0.2
0.4
0.6
0.8
1.0
Phi_1
20447 synchrotron periods

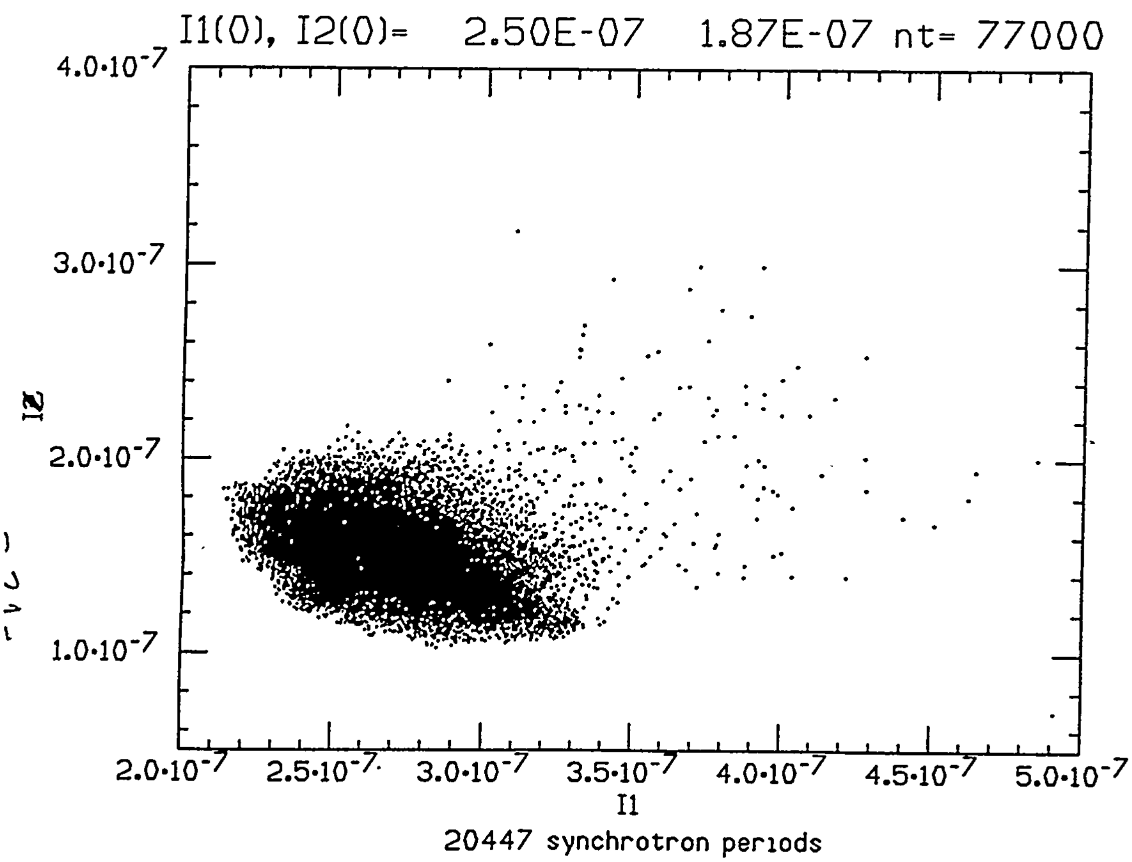
I1(0), I2(0)= 2.50E-07 1.87E-07 nt= 77000
4.0·10⁻⁷
3.0·10⁻⁷
2.0·10⁻⁷
1.0·10⁻⁷
I2
2.0·10⁻⁷
2.5·10⁻⁷
3.0·10⁻⁷
3.5·10⁻⁷
4.0·10⁻⁷
4.5·10⁻⁷
5.0·10⁻⁷
I1
20447 synchrotron periods

To simplify the description, make a canonical transformation

$$(I, \Phi) \longrightarrow (J, \Psi)$$

so that under $\vec{T}_0 : (J, \Psi) \longmapsto (J', \Psi')$

$$J' \approx J$$

$$\Psi' \approx \Psi + 2\pi\nu(J)$$

"Perfect" transformations, $\approx \longrightarrow =$, exist only on Cantor sets in J-space (KAM theory)

"Imperfect" transformations can be

- defined globally (on open sets Ω)
- smooth (C^1 or better)

Deviations of J from constancy become large in some regions of phase space, and indicate interesting behavior — for instance

- strong, but quasi-stable resonance
- large scale chaos, fast transport

GENERATOR OF CANONICAL TRANSFORMATION

$$S(J, \Phi) = J\cdot\Phi + G(J, \Phi)$$

Transformation $(I, \Phi) \longrightarrow (J, \Psi)$ defined by

$$I = J + G_{\Phi}(J, \Phi)$$

$$\Psi = \Phi + G_J(J, \Phi)$$

Periodic solution of Hamilton-Jacobi equation:

$$\mathcal{G}_{\Phi}(J, \Phi, s) = \mathcal{G}_{\Phi}(J, \Phi, s+c), \qquad J = \text{const.}$$

$$G_{\Phi}(J, \Phi) = \mathcal{G}_{\Phi}(J, \Phi, s = 0 \,(\text{mod } C))$$

Notice that

$$J = \frac{1}{(2\pi)^n} \int_{T^n} d\Phi \; I(J, \Phi)$$

If

$$G = \sum_{m \in \mathbb{Z}^n} g_m(J)\, e^{im\cdot\Phi}$$

$$G_{\Phi} = \sum_m im\, g_m(J)\, e^{im\cdot\Phi}$$

$$I = J + \sum_{m \neq 0} im\, g_m(J)\, e^{im\cdot\Phi}$$

NUMERICAL METHOD TO DETERMINE G

Orbit of map: $\{(I^{(i)}, \Phi^{(i)}),\ i = 1, 2, \ldots\}$

- On invariant torus (of nearly-integrable system), the $\Phi^{(i)}$ fill the torus

$$\|(I, \Phi) - (I^{(i)}, \Phi^{(i)})\| < \varepsilon \quad \text{for some } i$$

- Many orbits of our map give $\Phi^{(i)}$ that seem to fill the torus, and corresponding $I^{(i)}$ that seem to lie on a surface

For such orbits, determine F. coeffs. u_m so tl

$$I^{(i)} \approx \sum_{\|m\| \le M} u_m e^{i m \cdot \Phi^{(i)}}$$

Identify

$$J = u_0 \qquad i m g_m = u_m, \quad m \neq 0$$

Then

$$I = J + \sum_{m \neq 0}^{M} i m g_m(J) e^{i m \cdot \Phi}$$

- Other orbits have $\Phi^{(i)}$ that do not fill torus. Resonances!

FITTING FOURIER SERIES TO ORBIT DATA

$$\underline{I} = \sum_{\underline{m}} u_{\underline{m}} e^{i \underline{m} \cdot \underline{\Phi}}$$

Orbit:

$\underline{I}(\theta)$, $\underline{\Phi}(\theta)$ $\qquad \theta = 0, 2\pi, 4\pi, \ldots$

Problems:

- Values of $\underline{\Phi}$ scattered. Can't simply take FFT.
- Can't directly solve linear equations for $u_{\underline{m}}$, Matrix too large, all elements $O(1)$

Solution:

1) Take values of $\underline{I}(\underline{\Phi})$ on uniform $\underline{\Phi}$ mesh as unknowns.
2) Select data points $\underline{\Phi}(\theta)$ sufficiently close to mesh points, 1 for 1.

Then matrix is close to 1, can solve by iteration.

$$\underbrace{I(\Phi_j)}_{\text{data}} = \sum_{k=0}^{K-1} \underbrace{\frac{\sin \pi (x_j - k)}{K \sin \frac{\pi}{K}(x_j - k)}}_{\approx\, \delta_{jk}} \underbrace{I\left(\frac{2\pi k}{K}\right)}_{\text{unknowns}}$$

$$\Phi_j = \frac{2\pi x_j}{K}$$

Discrete form of Dirichlet Kernel

R.L.W., Phys. Rev. Lett. 66, 1803 (1991)

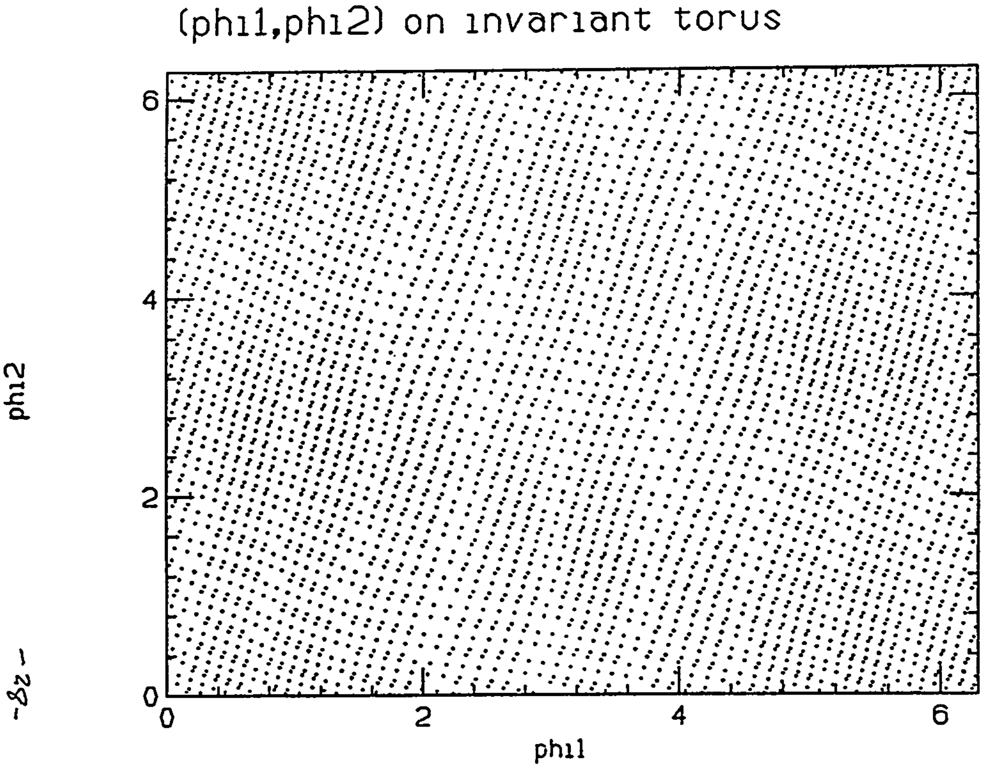

Figure 3

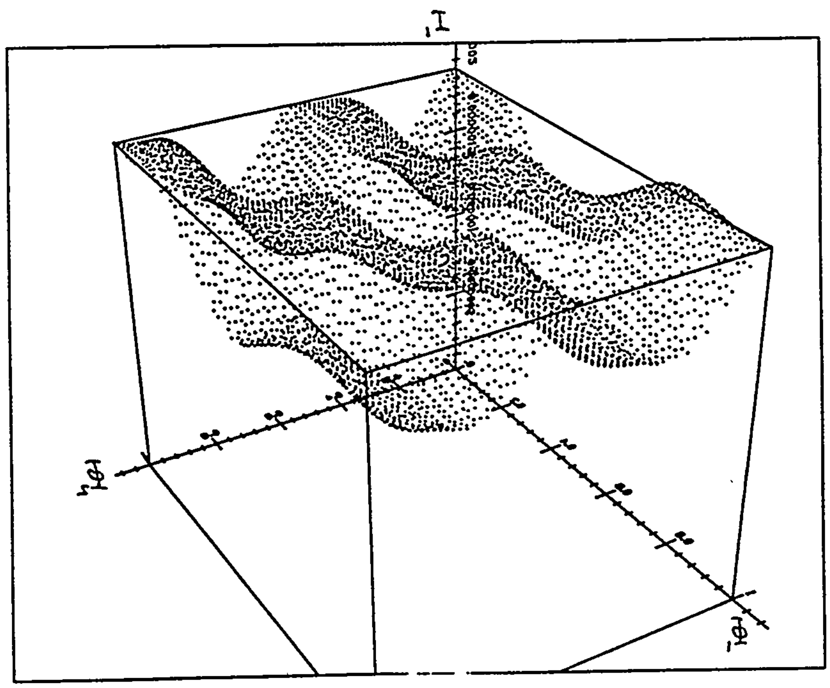

Figure 6

k1,k2= 6 3 f= 4.94E-01 I1,I2= 9.3750E+00 2.0625E+01

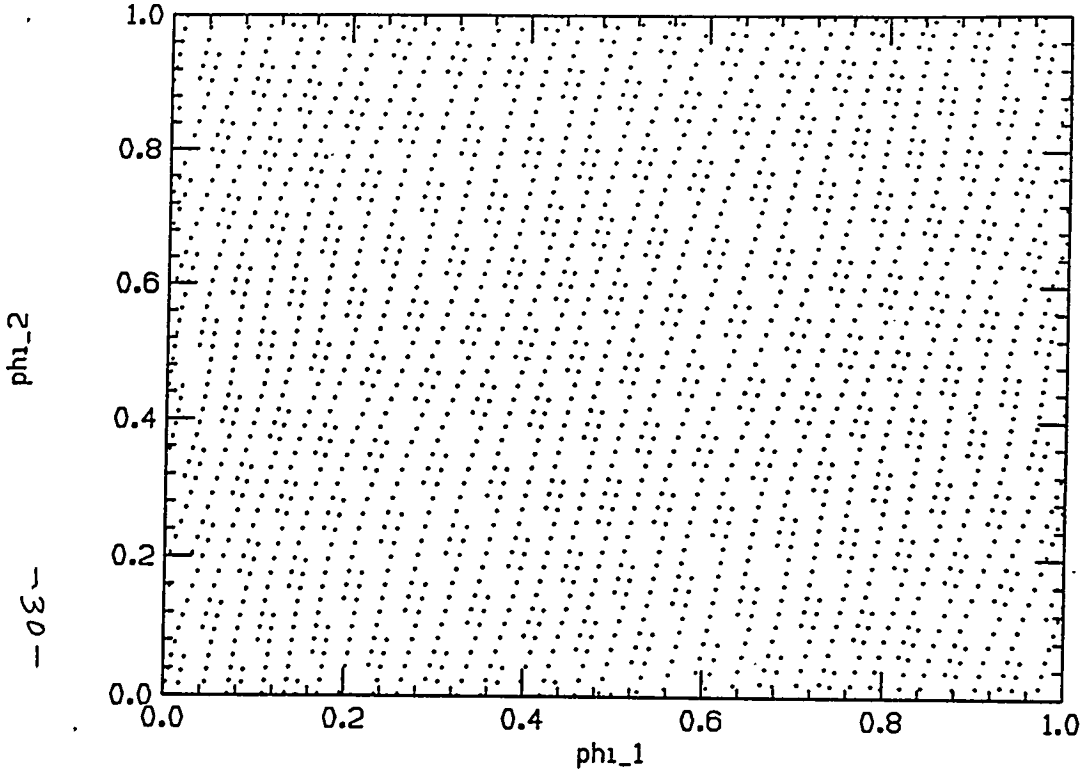

no. periods= 2000

k1,k2= 4 10 f= 4.90E-01 I1,I2= 8.1250E+00 2.7188E+01

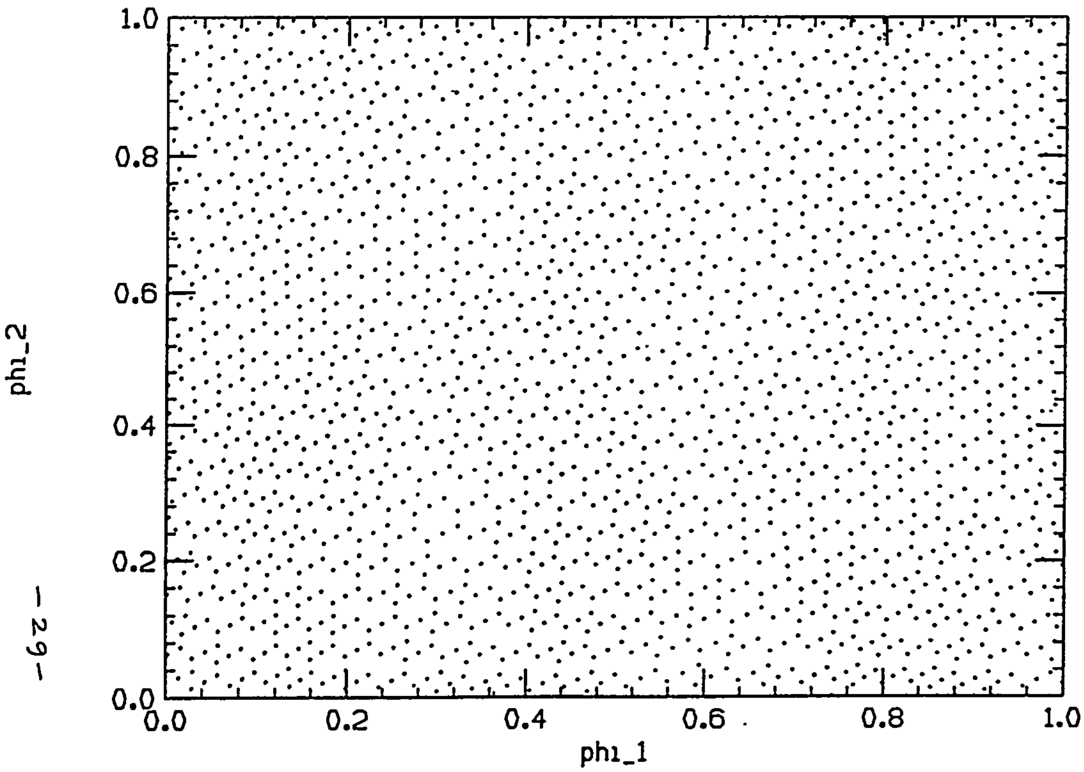

no. periods= 2000

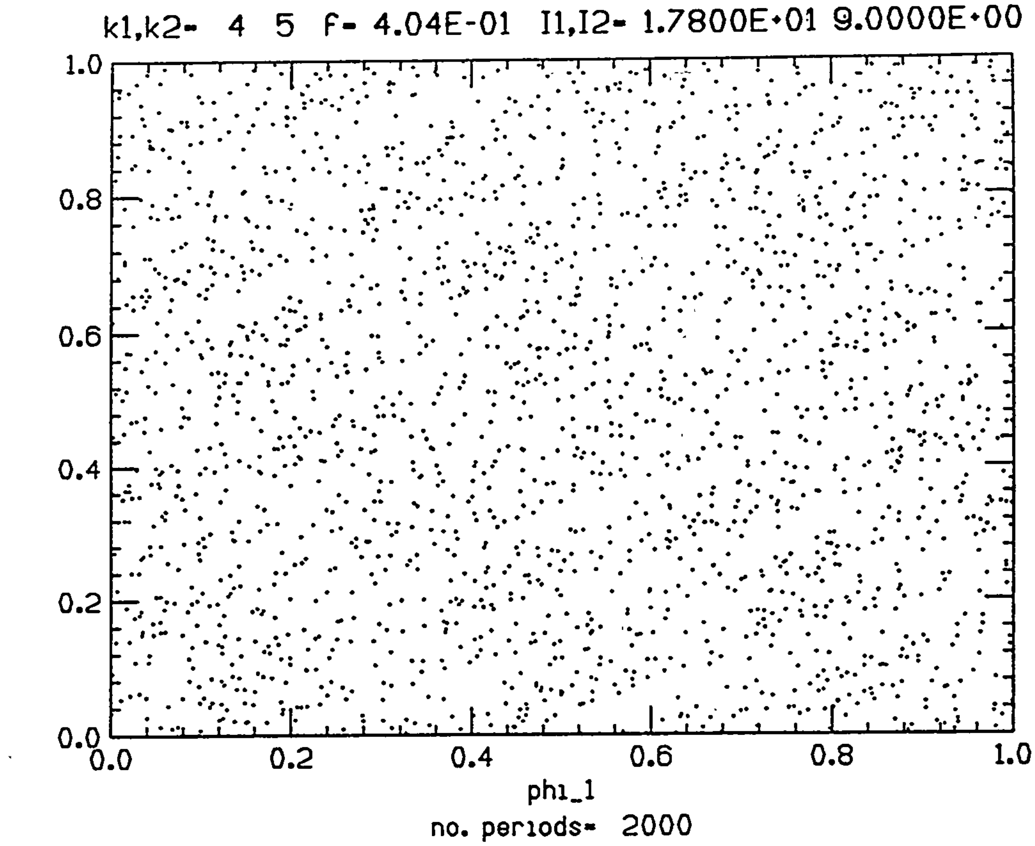
k1,k2= 4 5 f= 4.04E-01 I1,I2= 1.7800E+01 9.0000E+00
1.0
0.8
0.6
0.4
0.2
0.0
phi_2
0.0
0.2
0.4
0.6
0.8
1.0
phi_1
no. periods= 2000

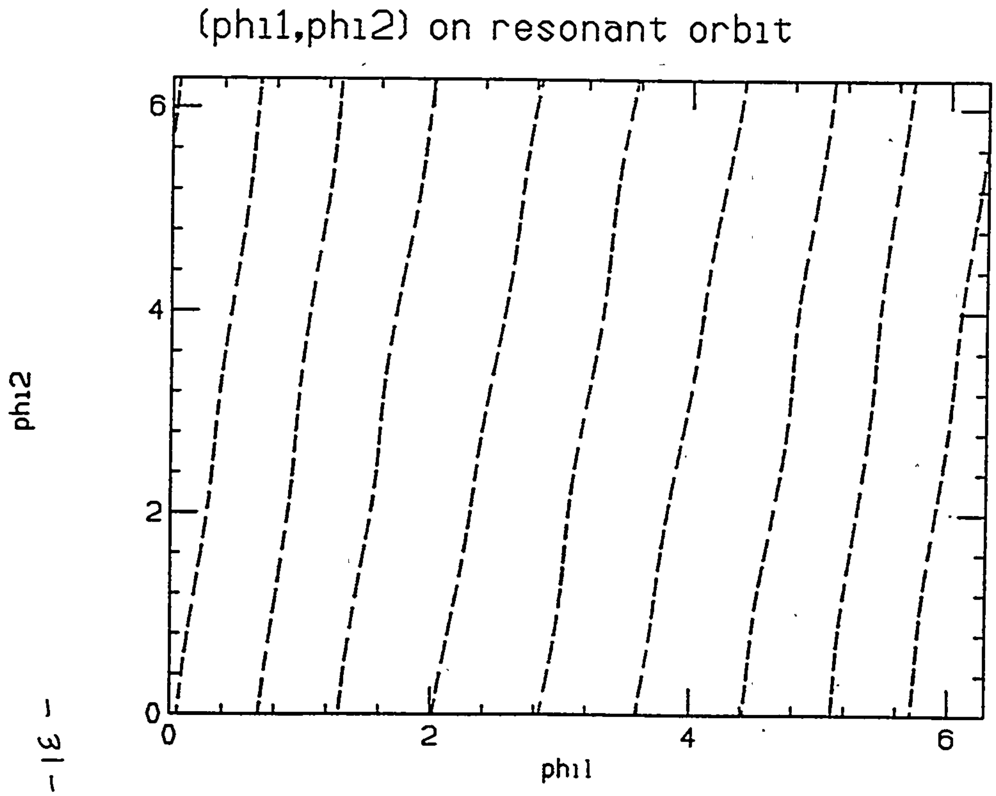
(phi1,phi2) on resonant orbit
6
4
2
0
phi2
0
2
4
6
phi1

Figure 4

INTERPOLATE IN J TO DEFINE G GLOBALLY

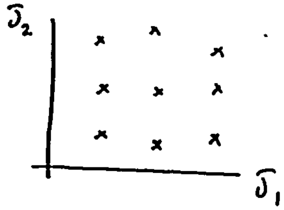

Typically, make C^2 interpolation with cubic splines

$$\text{Define} \begin{cases} g_{m_j}(J) = \dfrac{u_m}{i m_j}, & m_j = \\ g_0(J) = 0 \end{cases}$$

We then have global definition,

$$G(J, \Phi) \in C^2$$

Define frequencies (tunes) $\nu(J)$ on fitted tori by

$$2\pi\nu(J) = \Phi' + G_J(J, \Phi') - \Phi - G_J(J, \Phi)$$

$$(= \Psi' - \Psi)$$

Interpolate to define $\nu(J)$ globally

Use inverse function $J(\nu)$ to map resonance lines

$$m_1\nu_1 + m_2\nu_2 = n$$

into J-space.

In interesting large-amplitude regions, $J(\nu)$ is substantially nonlinear

EXTERNAL MODULATION OF MOMENTUM
POINCARÉ SECTION AT MULTIPLES OF SYNCHROTRON PERIOD

$H(I, \Phi, P_\tau(s), s)$ is now periodic in s with period $130\,C$, "$2\frac{1}{2}$ degrees of freedom"

$$G \longleftrightarrow T_1 = \text{1-turn map}$$

$T_1^{130} : \Sigma \to \Sigma$ is symplectic map on section

$$\Sigma = \{ (I, \Phi, s) \mid s = 0 \pmod{130\,C} \}$$

Study resonances and quasi-invariant tori of T_1^{130}: just as we usually study resonances and tori of T_1 in pure betatron motion ($P_\tau \equiv 0$)

- Can compute T_1^{130} quickly enough to make this possible
- In comparison to $T_1\,(P_\tau \equiv 0)$, we find many more low-order, ... resonances. Naturally!

  $N(m_1\nu_1 + m_2\nu_2) = P$ has more solutions than $m_1\nu_1 + m_2\nu_2$.
- For long-term bounds, can construct quasi-invariant tori of T_1^{130} by fitting Fourier series for I to its non-resonant orbits.

  Hard to get quasi-invariants of T_1^{130} by power series normal-form method of Forest, Irwin, + Berz; Turchetti et

Values of (nu1,nu2) on regular mesh in (J1,J2)

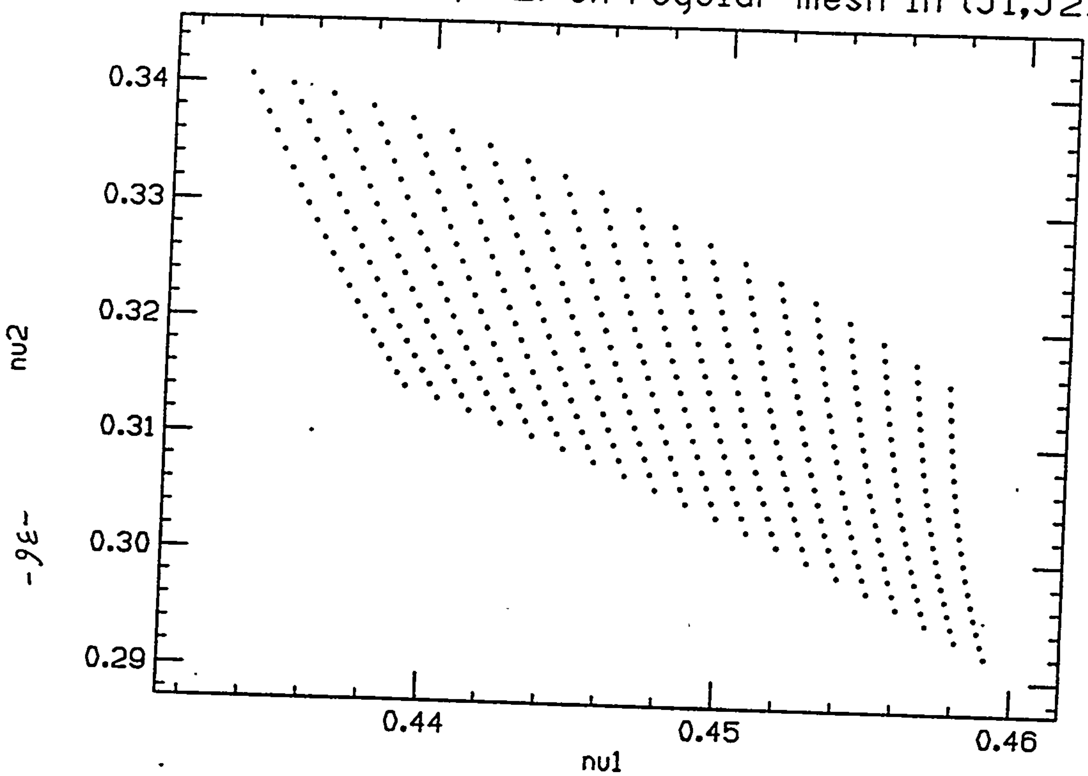

All resonances with abs(m1)+abs(m2) .le. 8

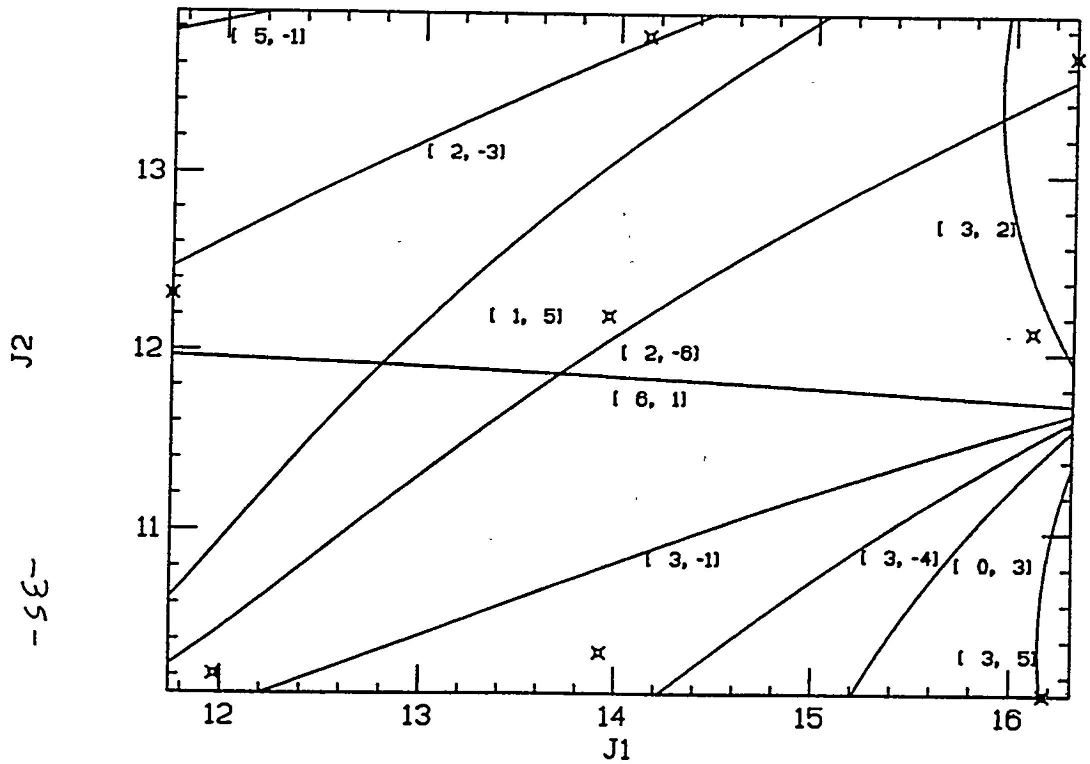

LONG-TERM BOUNDS - THE IDEA

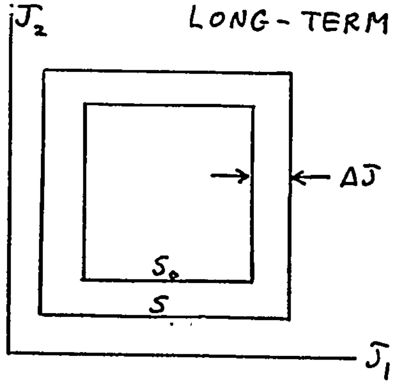

Maximum change in J_i during N_0 turns $< \delta J$
(for any orbit starting inside S)

Orbit starting inside square S_0 cannot reach square S in fewer than

$$N = p N_0 \quad \text{turns} \qquad (\dagger)$$

where

$$p\,\delta J = \Delta J$$

To be useful :

1) Must be able to compute δJ reliably
2) $p = \dfrac{\Delta J}{\delta J}$ = "amplification factor" must be large.

$\delta J << $ acceptable excursion ΔJ

IMPORTANT: If p is large, $N = p N_0$ seems to be a very conservative estimate for the number of turns to reach S.

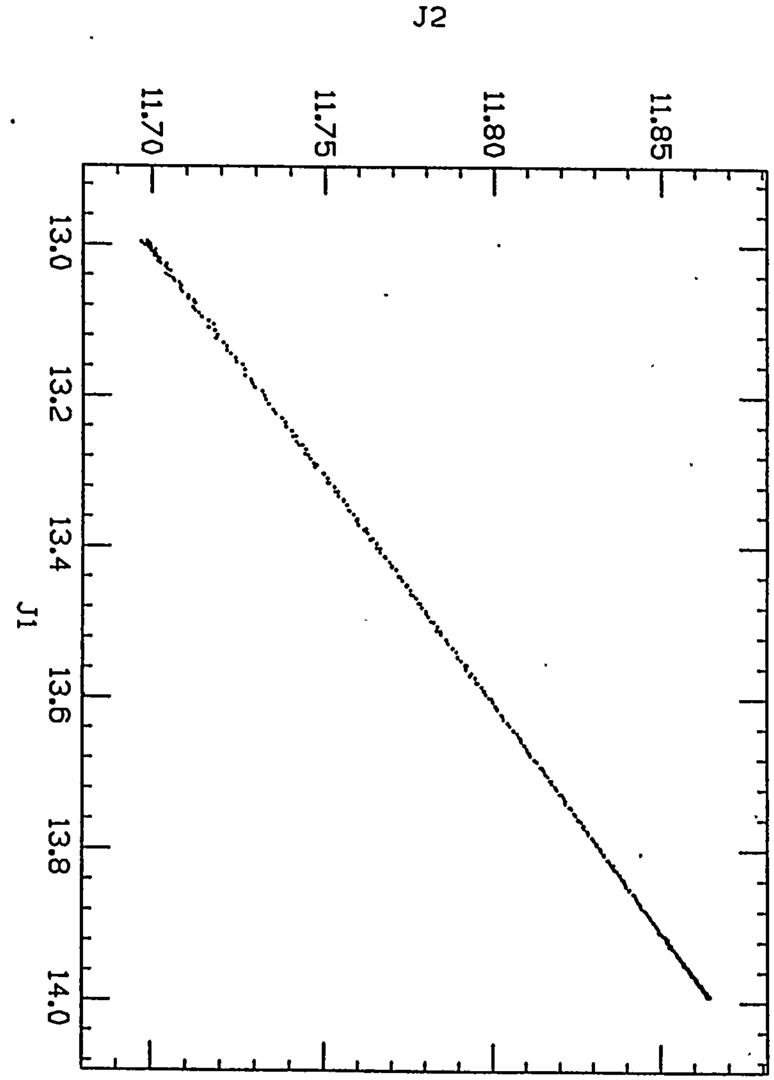

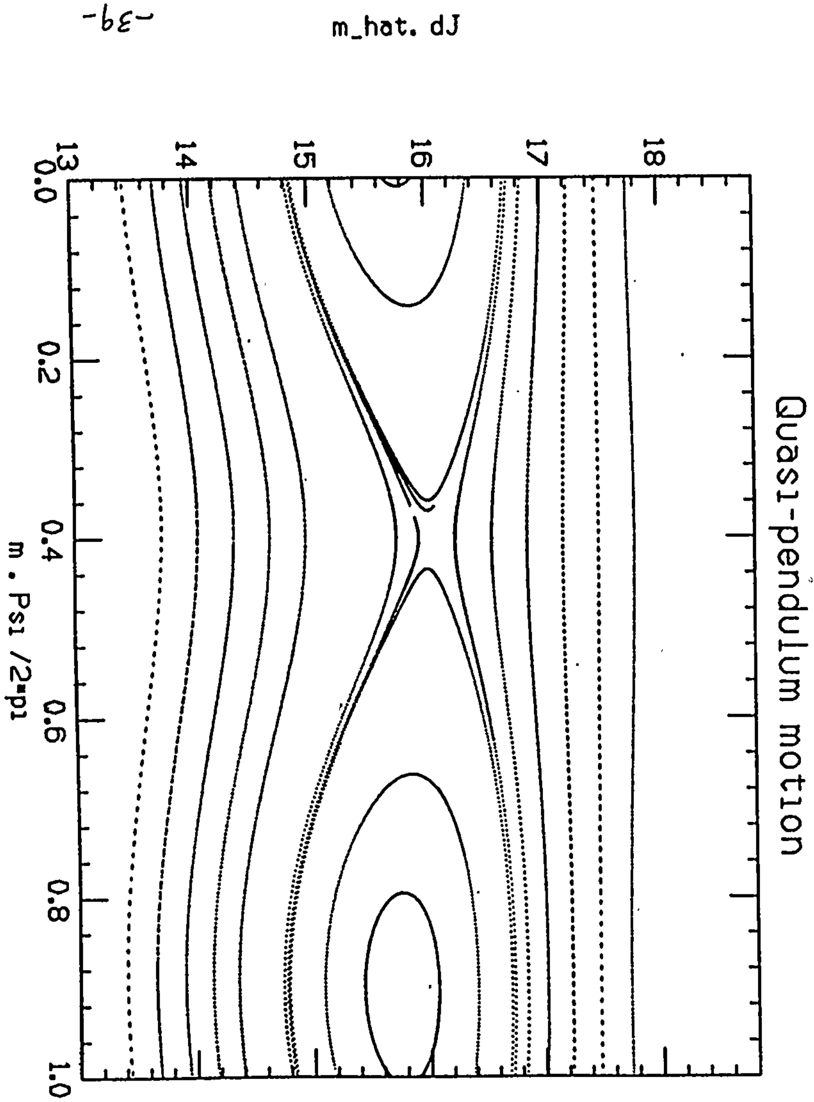

ISOLATED RESONANCE MODEL

$$H = \sum_n h_n(\underline{m}\cdot\underline{J},\ \underline{m}\times\underline{J})\, e^{in(\underline{m}\cdot\underline{\Psi})}$$

No dependence on $\underline{m}\times\underline{\Psi} \implies$

$$K = \underline{m}\times\underline{J} = \text{constant}$$

The simple pseudo-pendulum motion cannot be seen in the original variables I, Φ

Must remove the "principal smear" by the transformation

$$I, \Phi \longrightarrow J, \Psi$$

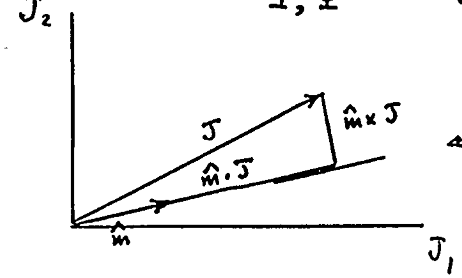

oscillation on red line in $\hat{m}\cdot J$

In departure from pure pendulum motion, there may be slow drift in $m\times J$, and in center of oscillation of $\hat{m}\cdot J$.

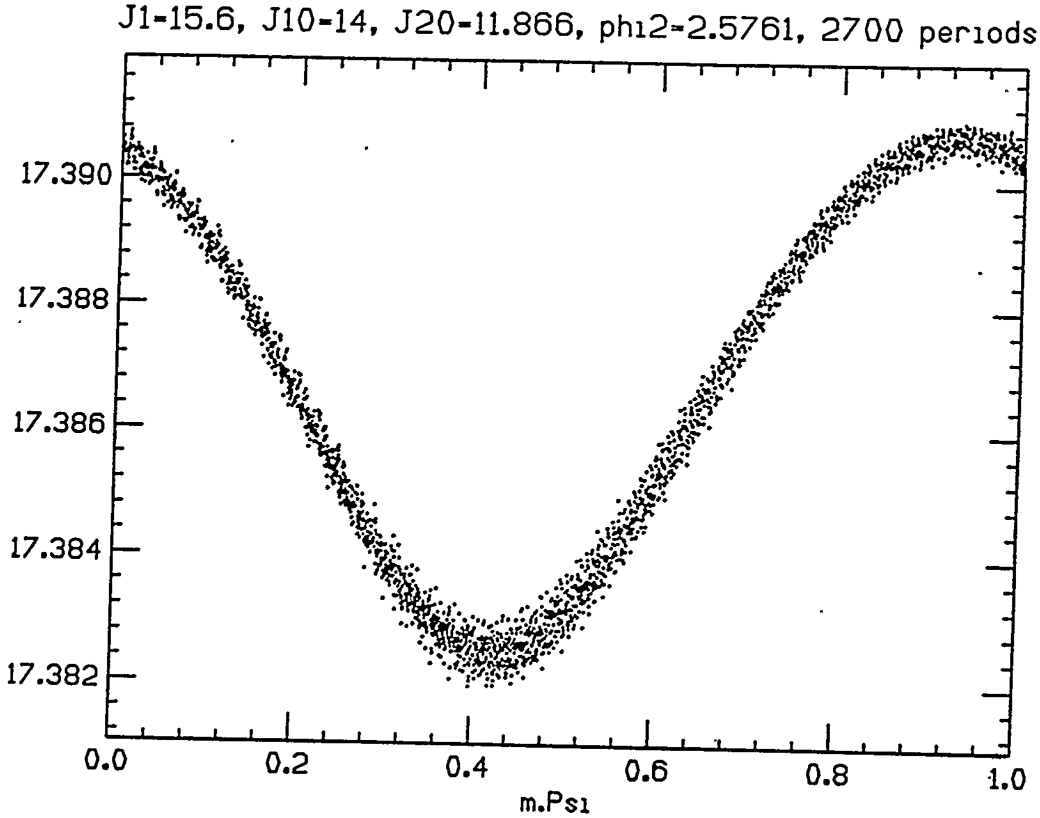
J1=15.6, J10=14, J20=11.866, phi2=2.5761, 2700 periods
m_hat.J
17.390
17.388
17.386
17.384
17.382
0.0
0.2
0.4
0.6
0.8
1.0
m.Psi

-42-

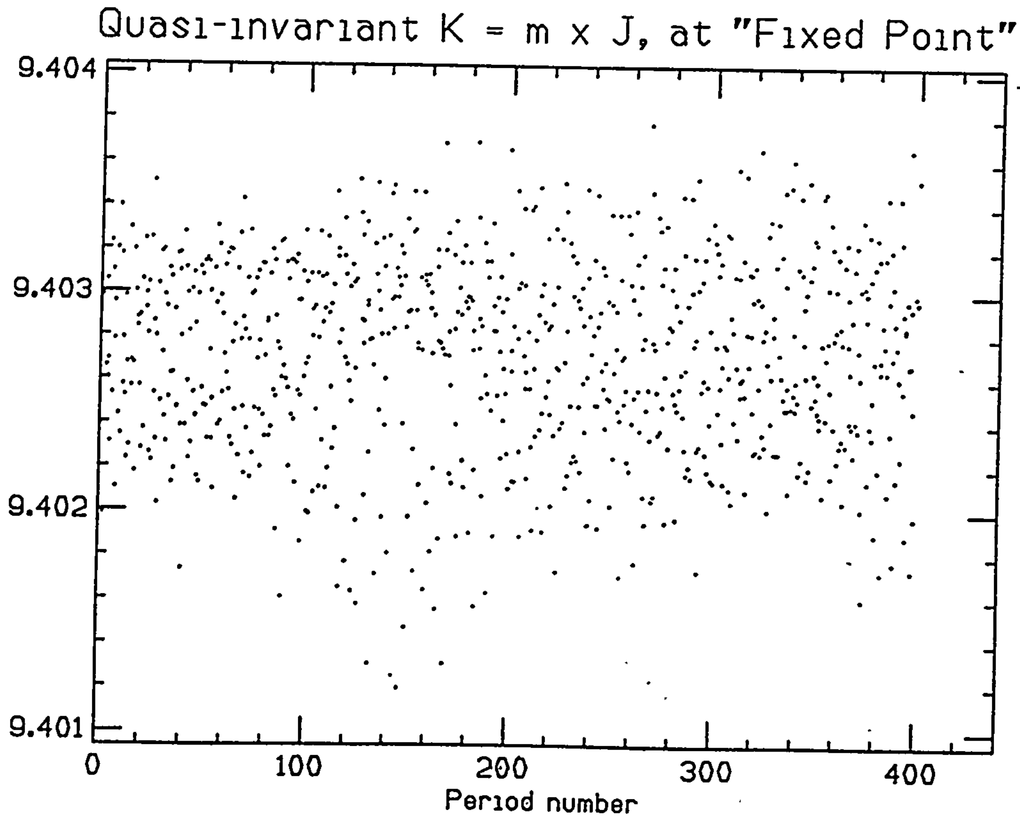
Quasi-invariant K = m x J, at "Fixed Point"
9.404
9.403
9.402
9.401
0
100
200
300
400
Period number

-41-

"Fixed Point" of pseudo-pendulum motion

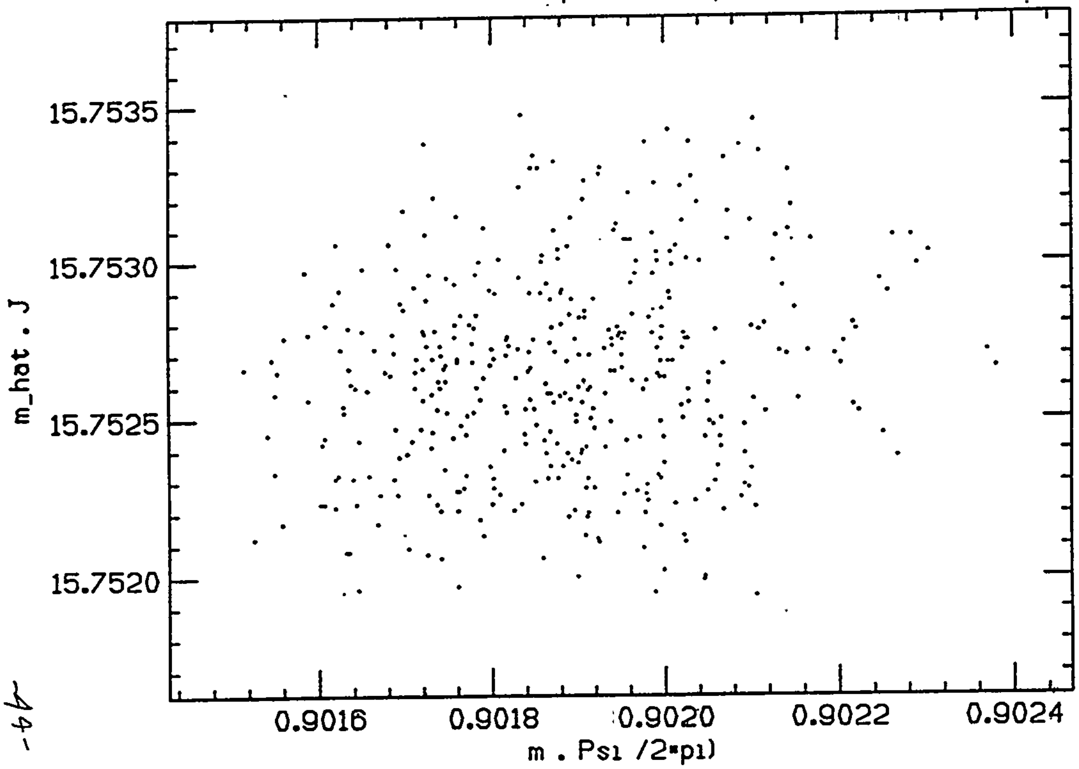

700 iterates of 1 turn map.

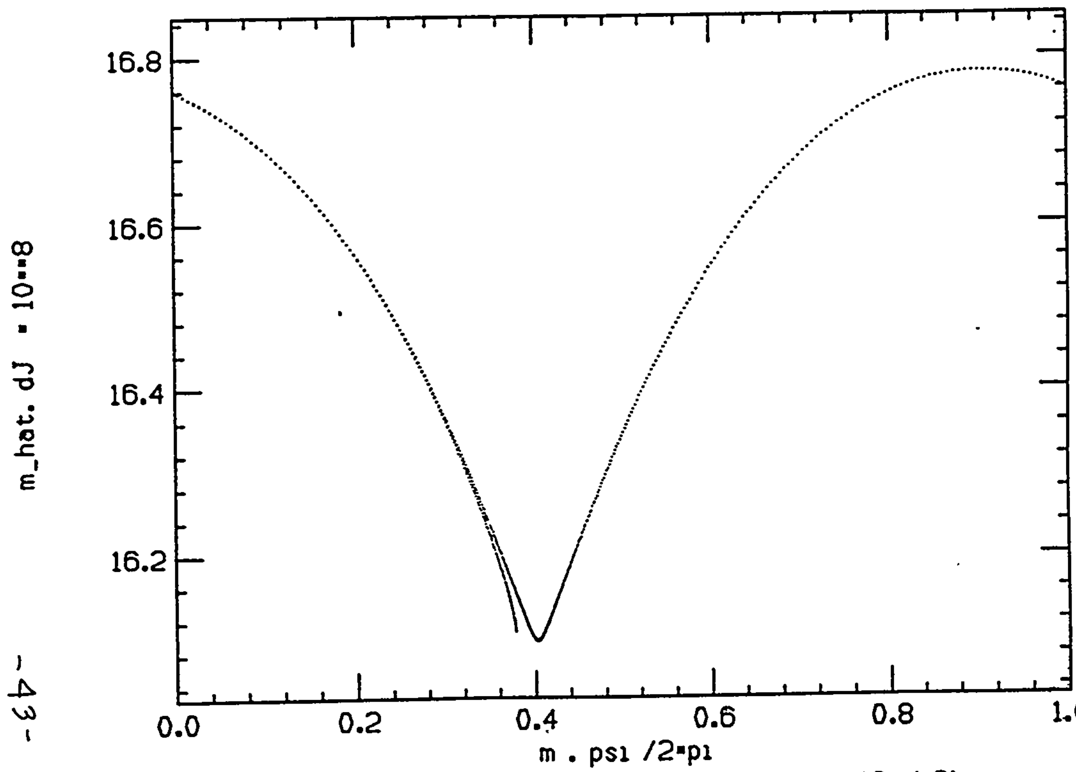

J10= 1.400000E+01 J20= 1.185000E+01 *10**(-8)m

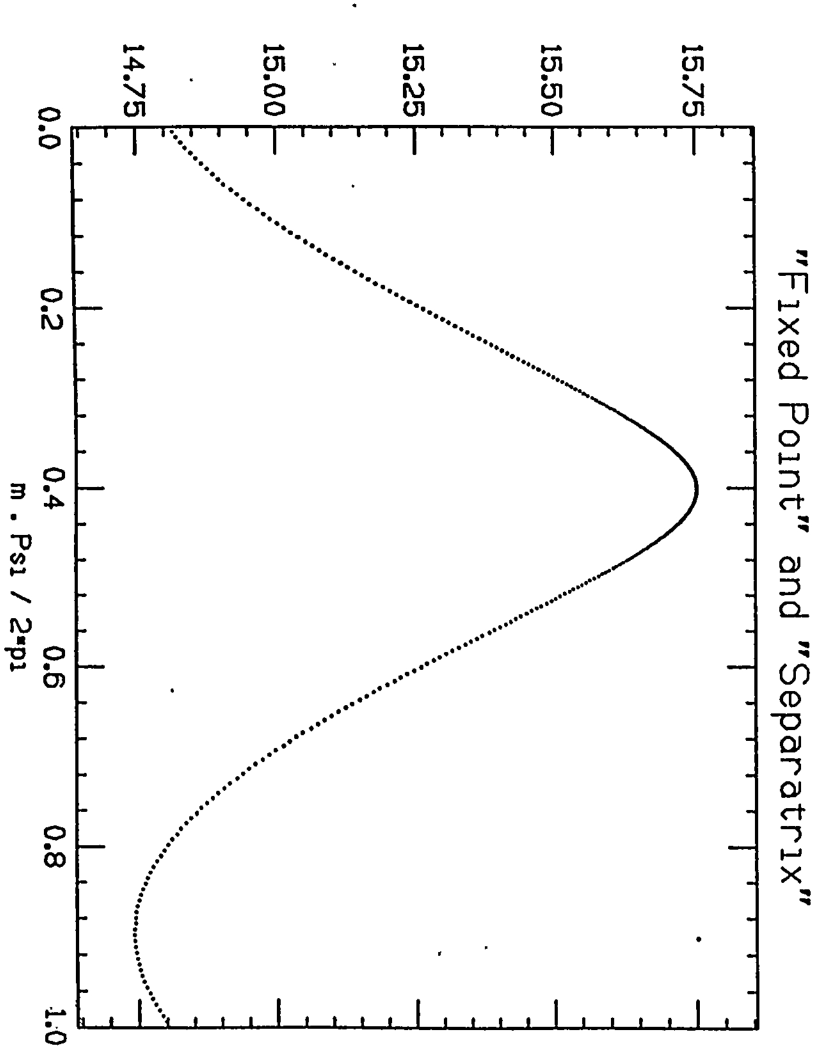

Quasi-invariants near strong resonances:

Define $K_1 = \hat{\underline{m}} \cdot \underline{J}$, $\chi_1 = \underline{m} \cdot \underline{\Psi}$

$K_2 = \hat{\underline{m}} \times \underline{J} \approx \text{const}$ $\chi_2 = \underline{m} \times \underline{\Psi}$

Rotation curves represented as

$$K_1 = \bar{K}_1 + \sum_{n \neq 0} a_n(\bar{K}_1, K_2) e^{in\chi_1} \quad (†)$$

$$\bar{K}_1 = \frac{1}{2\pi} \int_0^{2\pi} K_1 \, d\chi_1 = \text{action for rotational pendulum motion}$$

$\bar{K}_1, K_2$ are the new quasi-invariants

Think of residual change in $\bar{K}_1$ as a slow drift in the center of oscillation of K_1

Determine coefficients in (†) by fitting Fourier series to a few orbits corresponding to a mesh in $\bar{K}_1, K_2$, then interpolate in $\bar{K}_1, K_2$.

We are dealing with a second canonical transform:

$$(I_1, \Phi_1, I_2, \Phi_2) \longrightarrow (J_1, \Psi_1, J_2, \Psi_2) \rightarrow (\bar{K}_1, \bar{\chi}_1, K_2, \ldots$$

$\bar{\chi}_1$ = angle conjugate to $\bar{K}_1$

All resonances with abs(m1)+abs(m2) .le. 8

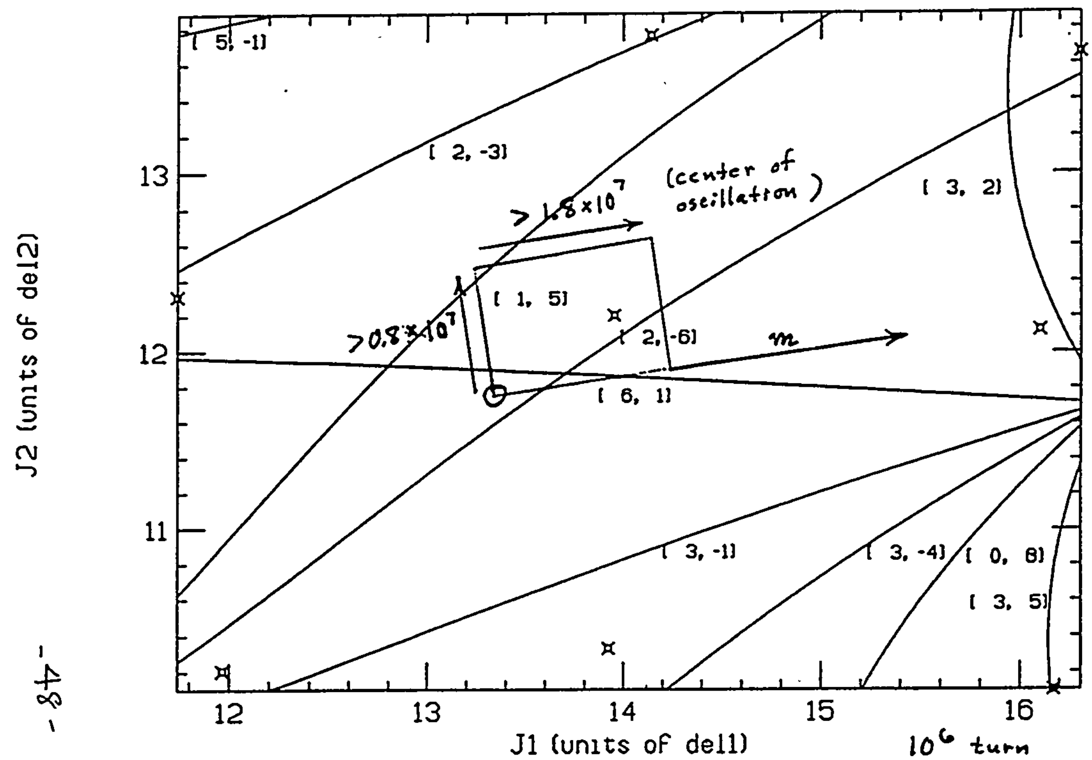

Amplitude x at ≈ 80% of long-term aperture

Four fitted curves, plus data

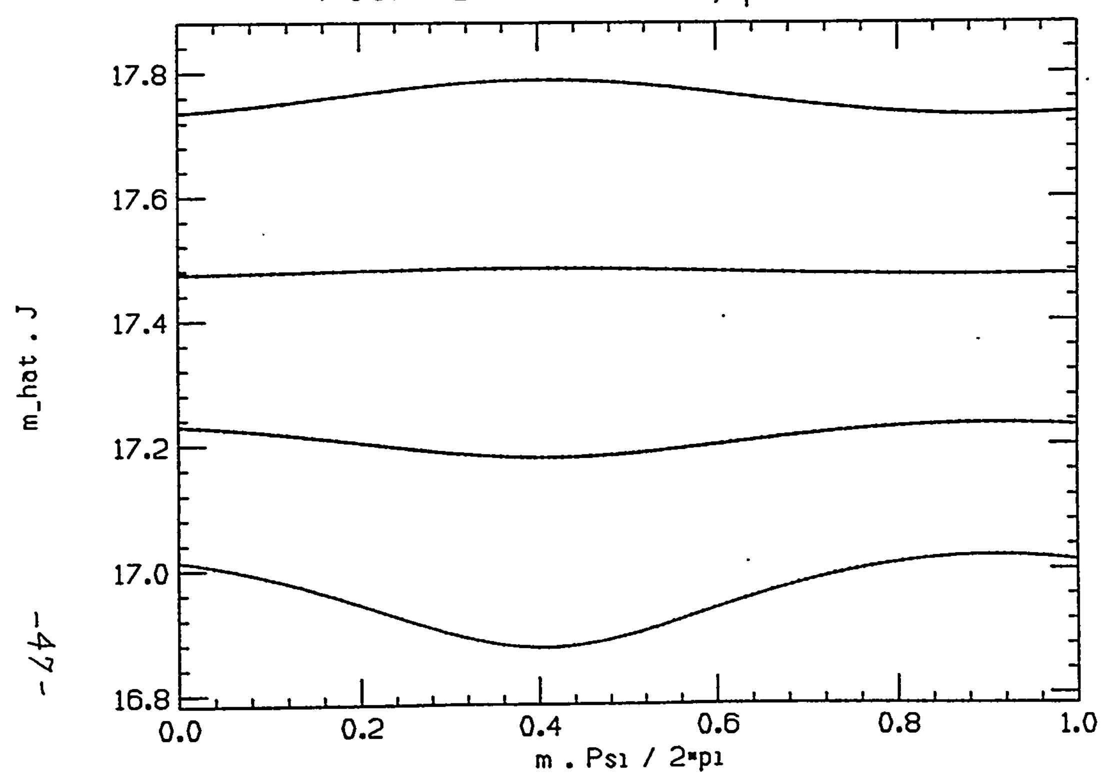

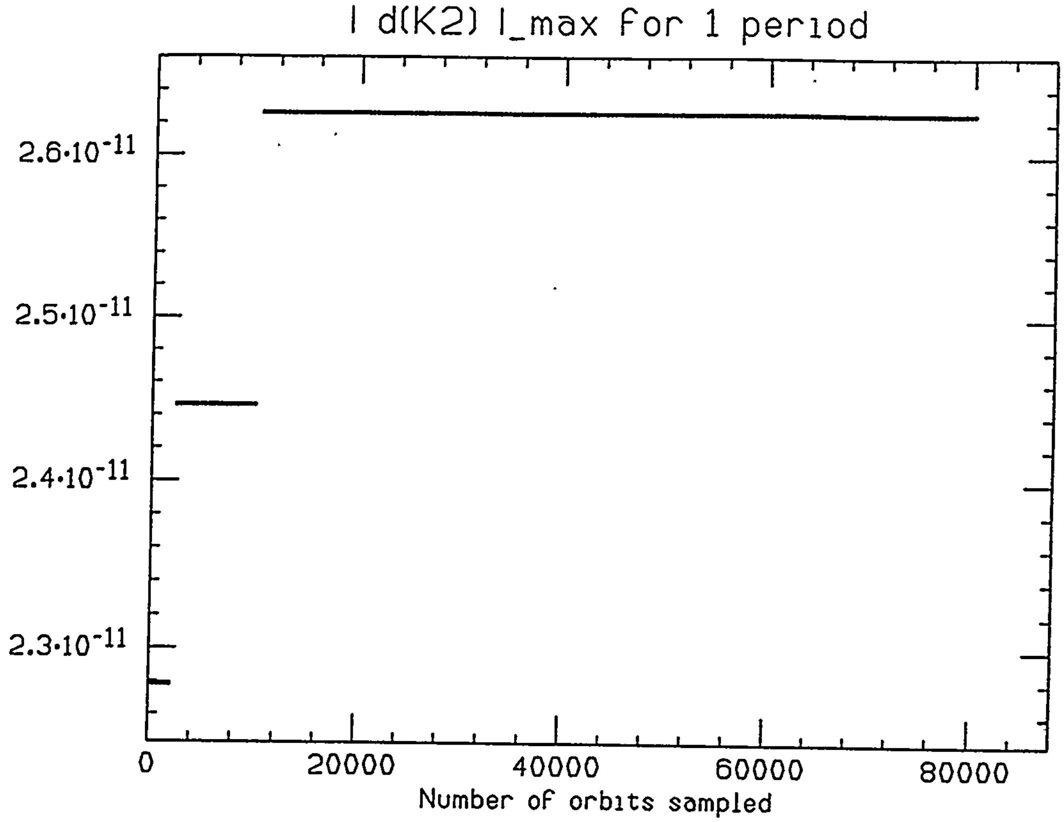

| d(K2) |_max for 1 period
2.6·10^-11
2.5·10^-11
2.4·10^-11
2.3·10^-11
0
20000
40000
60000
80000
Number of orbits sampled

-50-

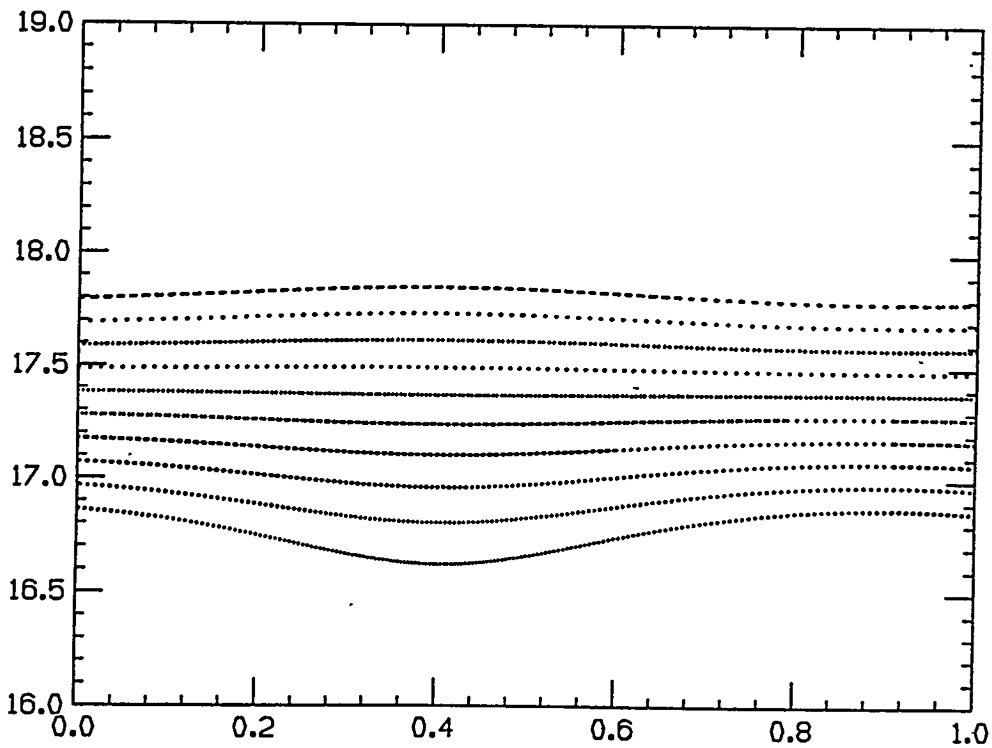

19.0
18.5
18.0
17.5
17.0
16.5
16.0
0.0
0.2
0.4
0.6
0.8
1.0

-49-

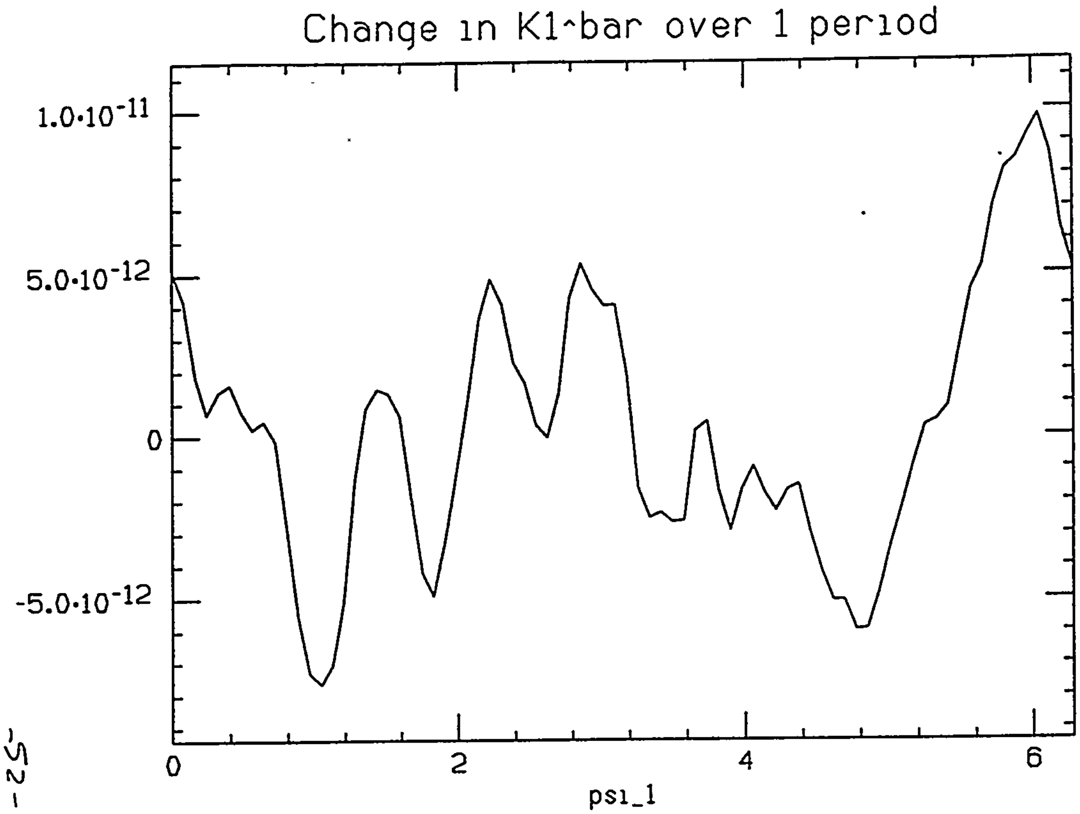
Change in K1^bar over 1 period
1.0·10^-11
5.0·10^-12
0
-5.0·10^-12
0
2
4
6
psi_1

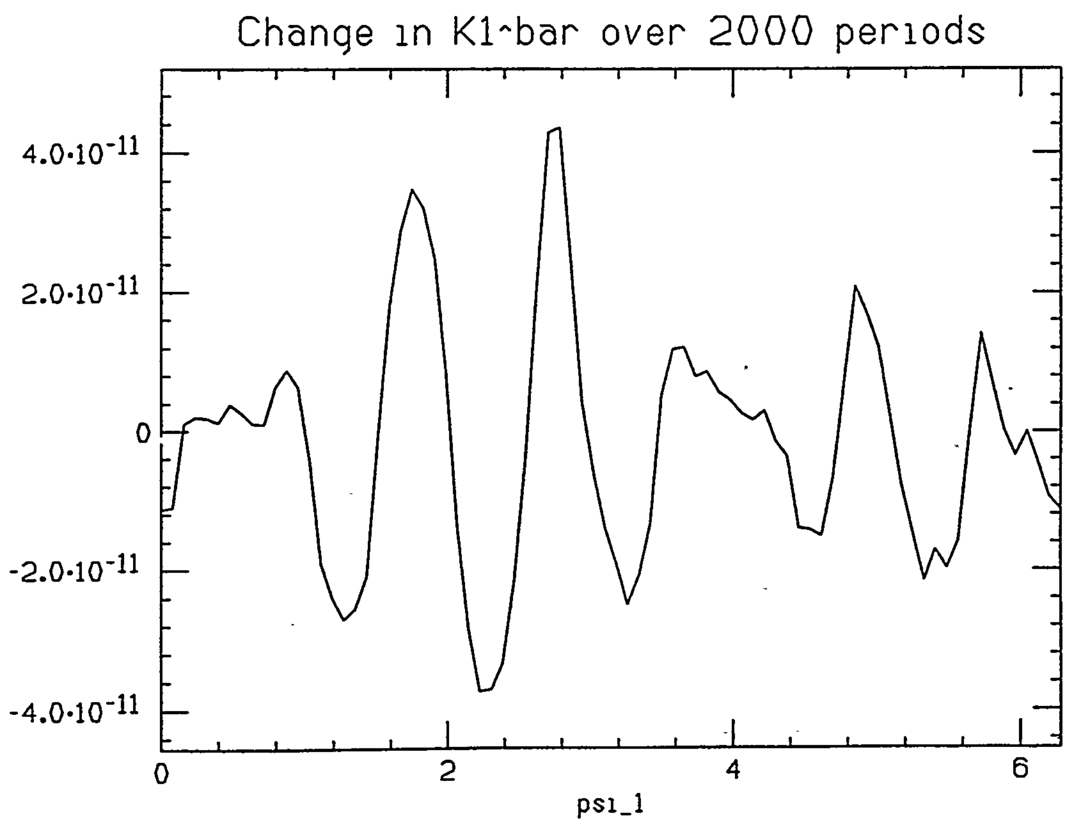
Change in K1^bar over 2000 periods
4.0·10^-11
2.0·10^-11
0
-2.0·10^-11
-4.0·10^-11
0
2
4
6
psi_1

Fit to isolated-resonance Hamiltonian :

$$H = H_0 + \sum_{n=1}^{N} \sum_{p=0}^{P} \left[c_{np} K_1^p \cos n\chi_1 + s_{np} K_1^p \sin n\chi_1 \right]$$

$$H_0 = \sum_{p=0}^{P} c_{0p} K_1^p$$

c_{np}, s_{np} are functions of K_2

Make least-squares fit of H to many orbits of K_1, χ_1 (at fixed K_2), including tune information.

$\left\langle \frac{\partial H_0}{\partial K_1} \right\rangle_{orbit}$ fitted to tunes on a few rotation curves

Typical fit :

48 orbits , 8 orbit tunes

$N = 2$, $P = 3$

Get good fit , but process is "badly conditioned". Does not improve with increasing $P > 3$, $N > 2$, and resulting coefficients c_{np}, s_{np} change with increasing P, N.

Perhaps : H is quite literally an (approximate) Hamiltonian of the complicated system (in a rotating frame), in a restricted region of phase space.

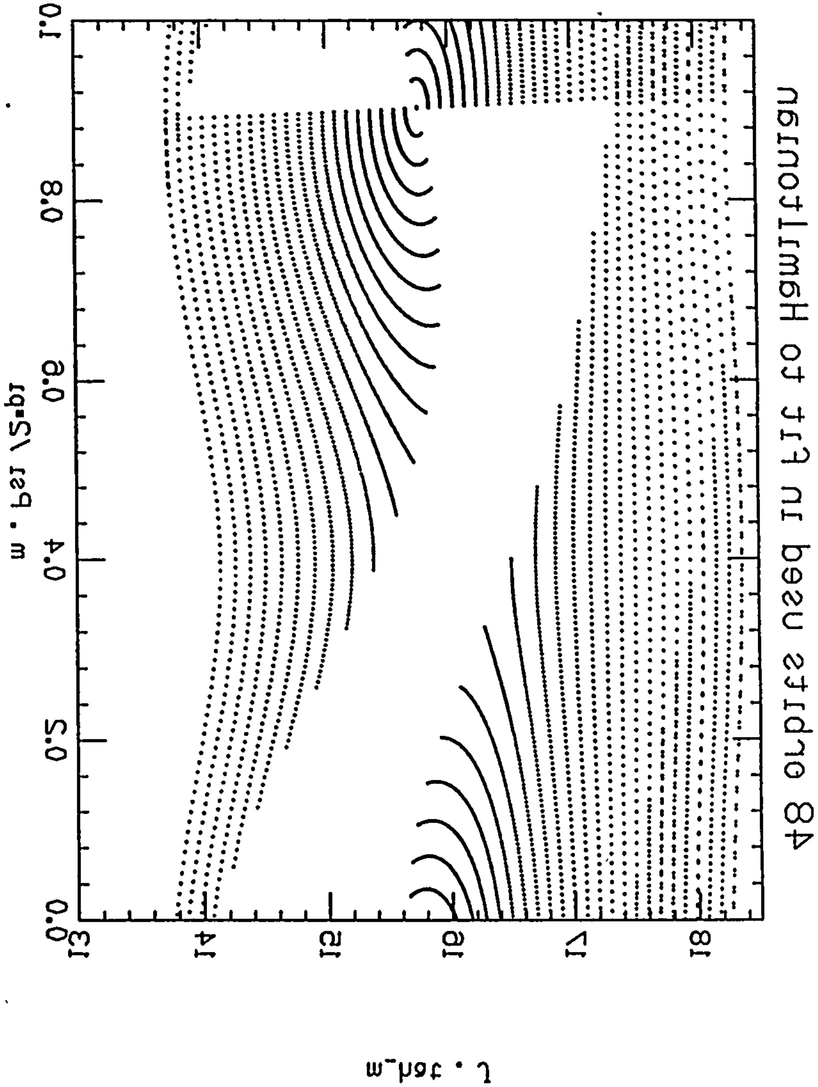

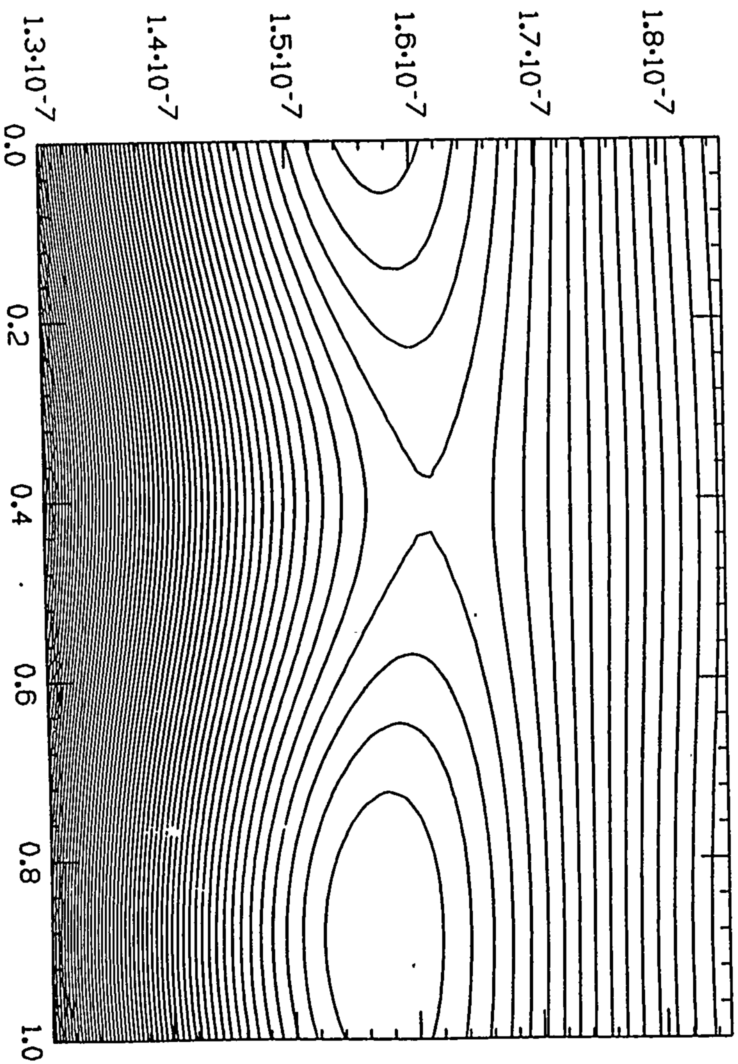

CONCLUSIONS

- Single-turn tracking from many-initial conditions
  → Symplectic full-turn map
- There is increasing evidence that fast maps of modest accuracy give a good representation of the physical system defined by tracking
- Fast maps on Poincaré surface at synchrotron period enable us to
  - i) follow orbits over times comparable to beam injection and storage times
  - ii) study resonances, quasi-invariant surfaces, and long-term bounds on the motion

OP-ED PAGE

Methods in the spirit of modern numerical analysis are

- convenient
- well-founded in theory
- extremely flexible → "free form modeling"
- efficient at any chosen accuracy

So why be restricted to power series, which constitute a very rigid framework ?

NONLINEAR SPIN DYNAMICS

V. Balandin, DESY

1

Vladimir Balandin

Polarized Proton Beams in Storage Rings and Circular Accelerators

I wish to thank NINA GOLUBEVA for her contributions to this study.

Spin-Orbit Motion Equations.

The quasi-classical description of the motion of relativistic non-radiating particles with spin in accelerators and storage rings includes the

equations of orbit motion

which we will take in the Hamiltonian form

$$\frac{d\vec{q}}{dt} = \frac{\partial H_{orbit}}{\partial \vec{p}}, \qquad \frac{d\vec{p}}{dt} = -\frac{\partial H_{orbit}}{\partial \vec{q}}$$

and the

Tomas-BMT equation for classical spin vector

$$\frac{d\vec{s}}{dt} = \vec{W} \times \vec{s}.$$

Here

$$H_{orbit} = c\sqrt{\vec{\pi}^2 + m_0^2c^2} + e\Phi,$$

$$\vec{W} = -\frac{e}{m_0\gamma c}\left((1+\gamma G)\,\vec{B} - \frac{G\left(\vec{\pi}\cdot\vec{B}\right)\vec{\pi}}{m_0^2c^2(1+\gamma)} - \frac{1}{m_0c}\left(G + \frac{1}{1+\gamma}\right)\left[\vec{\pi}\times\vec{E}\right]\right),$$

and t is the time, $\vec{q}$ and $\vec{p}$ are canonical position and momentum variables, and $\vec{s} = (s_1, s_2, s_3)$ is the classical spin vector of length $\hbar/2$ in a fixed Cartesian coordinate system, e and m_0 are the charge and the rest mass of the particle, c is the velocity of light, $G = (g-2)/2$ which quantifies the anomalous spin g factor, γ is the Lorentz factor, $\vec{\pi}$ is kinetic momentum vector, $\vec{E}$ and $\vec{B}$ are the electric and magnetic fields, and $\vec{A}$ and Φ are the vector and scalar potentials.

Lateron we will refer to this system as the triangular system (the equations of spin motion contain the orbital variables but the evolution of orbital variables does not depend on the spin degree of freedom).

Behaviour of Spin Vector on Chosen Tranjectory of Orbital Motion

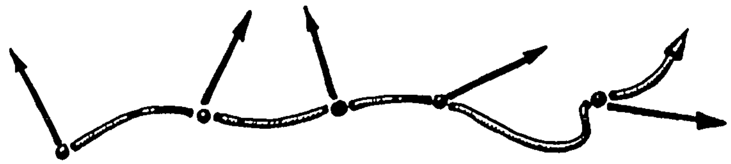

$$\frac{d\vec{s}}{dt} = \underset{\vec{W}(t,t_0,\vec{x}_0)}{\underset{\parallel \mathrm{def}}{\vec{W}(t,\vec{x}(t,t_0,\vec{x}_0))}} \times \vec{s} = \begin{pmatrix} 0 & -W_3 & W_2 \\ W_3 & 0 & -W_1 \\ -W_2 & W_1 & 0 \end{pmatrix} \stackrel{\mathrm{def}}{=} C(t)\cdot\vec{s} \qquad (*)$$

The matrix $C(t)$ in $(*)$ is real skewsymmetric: $C^T(t) = -C(t)$

The fundamental matrix solution $M(t,t_0)$ of $(*)$ is an orthogonal matrix and $\det M = 1$, i.e. $M \in SO(3)$

a) The norm of every solution is conserved: $|\vec{s}(t)| \equiv |\vec{s}(t_0)|$.
b) The angle between two every solutions is conserved.
c) If $\vec{s}_1(t)$ and $\vec{s}_2(t)$ are solutions of the system $(*)$, then $\vec{s}_3(t) = \vec{s}_1(t) \times \vec{s}_2(t)$ is the solution too.
d) The function $\vec{n}(t)\cdot\vec{s}$ is the constant of motion of the system $(*)$ if and only if $\vec{n}(t)$ is its solution.
e) If the vector $\vec{W}(t)$ in $(*)$ has period $\mathbf{T}$ in t, then the system $(*)$ has a $\mathbf{T}$-periodic solution.

Spin-Orbit Motion in a Constant Uniform Magnetic Field

The constant uniform magnetic field $\vec{B} = (0, B_0, 0)$ can be described by a vector potential

$$A_1 = 0, \quad A_2 = 0, \quad A_3 = -B_0 \cdot q_1 .$$

The corresponding orbital Hamiltonian is solvable and it leads to well-known formulas:

$$\begin{cases} q_1(t) = \left(q_1(0) + \frac{1}{k} p_3(0)\right)\cdot\cos(\omega t) + \frac{1}{k}\left(p_1(0)\cdot\sin(\omega t) - p_3(0)\right), \\ p_1(t) = p_1(0)\cdot\cos(\omega t) - k\left(q_1(0) + \frac{1}{k} p_3(0)\right)\cdot\sin(\omega t), \\ q_2(t) = q_2(0) + \alpha\cdot p_2(0)\cdot t, \quad p_2(t) = p_2(0), \\ q_3(t) = q_3(0) + \left(q_1(0) + \frac{1}{k} p_3(0)\right)\cdot\sin(\omega t) + \frac{1}{k} p_1(0)\cdot(1 - \cos(\omega t)), \\ p_3(t) = p_3(0) \end{cases}$$

where $k = \frac{eB_0}{c}$, $\alpha = \frac{1}{m_0\gamma}$, $\omega = k\cdot\alpha = \frac{eB_0}{m_0 c\gamma}$.

$$\boxed{\left[q_1(t) - \left(-\frac{1}{k} p_3(0)\right)\right]^2 + \left[q_3(t) - \left(q_3(0) + \frac{1}{k} p_1(0)\right)\right]^2 = \left[q_1(0) + \frac{1}{k} p_3(0)\right]^2 + \left[\frac{1}{k} p_1(0)\right]^2 \stackrel{\mathrm{def}}{=} R^2}$$

$$T=\frac{2\pi}{\omega}=2\pi\cdot\frac{m_0 c\gamma}{eB_0}$$

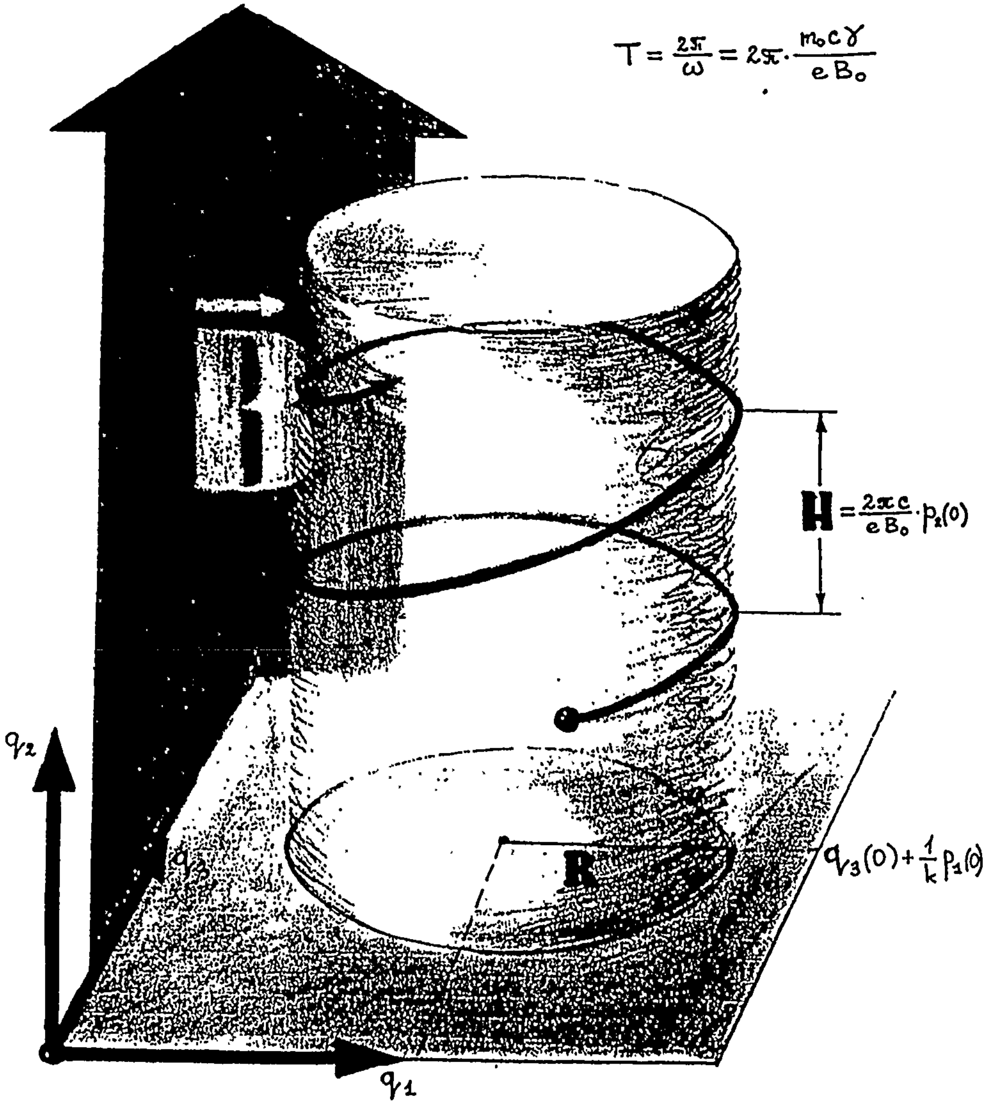

$$R^2=\left(q_1(0)+\frac{1}{k}p_3(0)\right)^2+\left(\frac{1}{k}p_1(0)\right)^2$$

Spin-Orbit Motion in a Constant Uniform Magnetic Field

$$\begin{cases} W_1 = \omega\dfrac{G}{m_0^2c^2(1+\gamma)}\,p_2(0)\cdot p_1(t), \\ W_2 = -\omega\left[(1+\gamma G)-\dfrac{G}{m_0^2c^2(1+\gamma)}\,p_2^2(0)\right], \\ W_3 = \omega\dfrac{G}{m_0^2c^2(1+\gamma)}\,p_2(0)\cdot\left(p_3(0)+kq_1(t)\right). \end{cases}$$

Here $\gamma=\dfrac{1}{m_0c}\sqrt{m_0^2c^2+p_2^2(0)+k^2R^2}=\text{const}.$

1. $p_2(0)=0$:

$W_1=0,\ W_2=-\omega(1+\gamma G),\ W_3=0.$

$$\Omega_{spin}=-\omega(1+\gamma G)=-\frac{e}{m_0c\gamma}(1+\gamma G)\cdot B_0.$$

2. $R=0$:

$W_1=0,\ W_2=-\omega(1+G),\ W_3=0.$

$$\Omega_{spin}=-\omega(1+G)=-\frac{e}{m_0c\gamma}(1+G)\cdot B_0.$$

3. General case:

$\vec{S}_*(t)=\left(-p_2(0)\cdot p_1(t),\ m_0^2c^2(1+\gamma)+k^2R^2,\ -p_2(0)\cdot(p_3(0)+kq_1(t))\right)$

In the precession frame connected with $\vec{n}(t)=\dfrac{1}{|\vec{S}_*(0)|}\cdot\vec{S}_*(t)$

$$\Omega_{spin}=-\sqrt{\omega^2\left[\left(\frac{GkR\,p_2(0)}{m_0^2c^2(1+\gamma)}\right)^2+\left[\gamma G-\frac{G\,p_2^2(0)}{m_0^2c^2(1+\gamma)}\right]^2\right]}$$

⑥

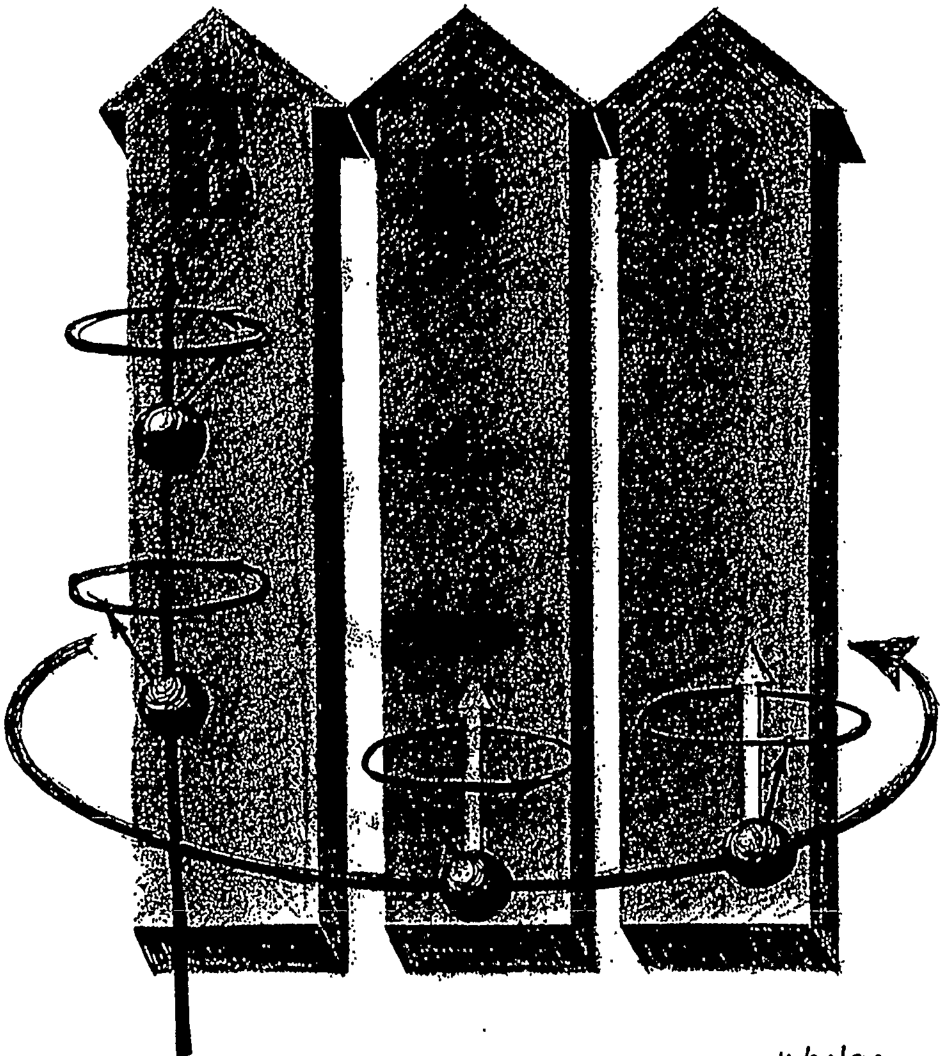

11/21/96

⑦

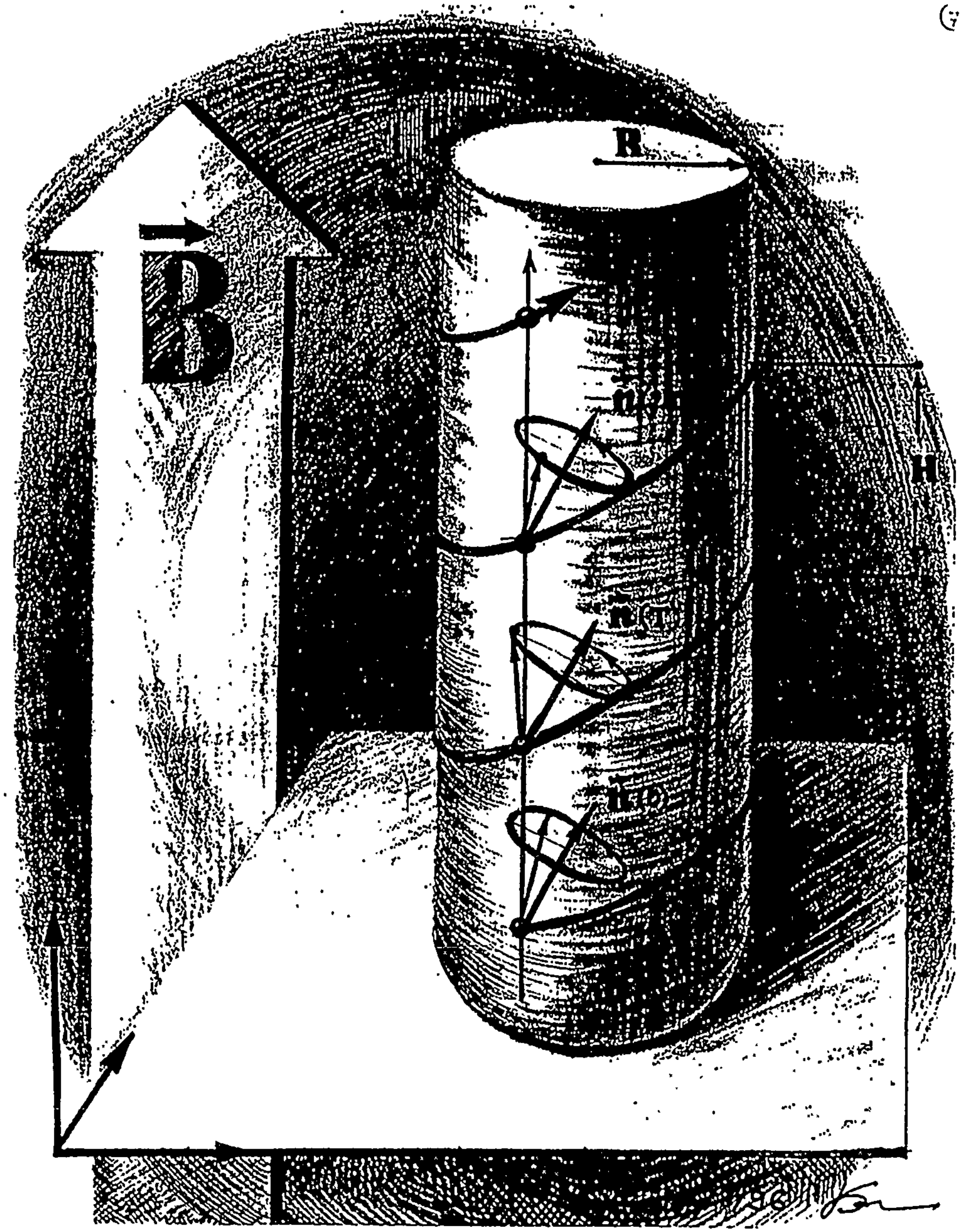

SPIN PRECESSION ON THE CLOSED ORBIT IN AN IDEAL CIRCULAR PARTICLE ACCELERATOR

① FLAT RINGS WITHOUT MISALIGNMENTS
(PARTICLE ON CLOSED ORBIT SEE ONLY VERTICAL FIELD)

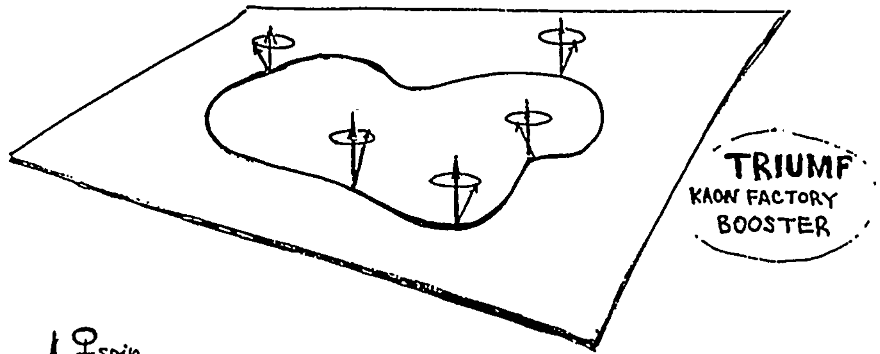

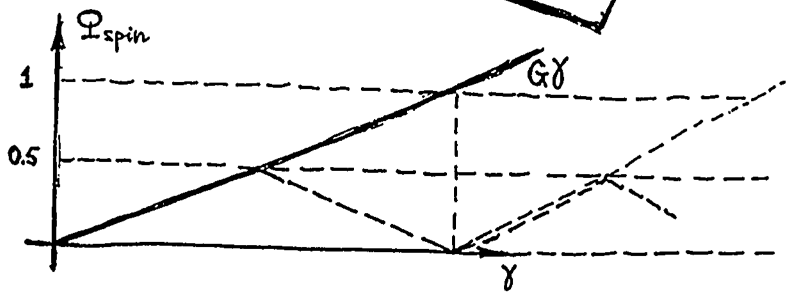

② ... Nonflat rings, rings with solenoids, ...

HERA-p
WITHOUT EAST

	IP - East	
a	HBEND	1.5128515970
b	VBEND	-0.0057438700
c	HBEND	0.0604149598
d	VBEND	0.0057433499
e	HBEND	0.0029594000
	IP - South	
e	HBEND	0.0029594000
d	VBEND	0.0057433499
c	HBEND	0.0604149598
b	VBEND	-0.0057438700
a	HBEND	1.5103747370
f	VBEND	0.0000014000
	IP - West	
a	HBEND	1.5103739970
b	VBEND	-0.0057438700
c	HBEND	0.0604149598
d	VBEND	0.0057433499
e	HBEND	0.0029594000
	IP - North	
e	HBEND	0.0029594000
d	VBEND	0.0057433499
c	HBEND	0.0604149598
b	VBEND	-0.0057438700
a	HBEND	1.5128515970

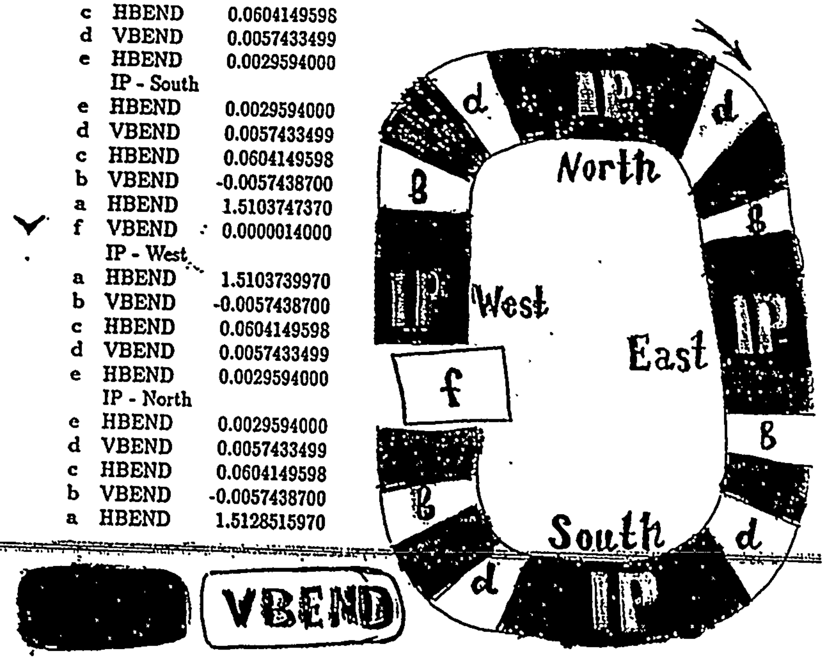

PERIODICITIES

MIRROR SYMMETRY

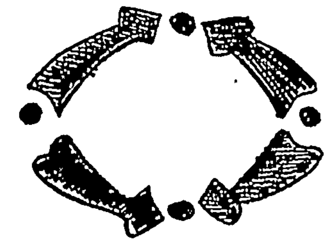

Figure 1: The magnet structure of the nonflat HERA-p along the design orbit (i.e. in zeroth approximation with respect to orbital motion). Groups of successive horizontal (vertical) bending magnets are represented as one element (i.e. lumped together).

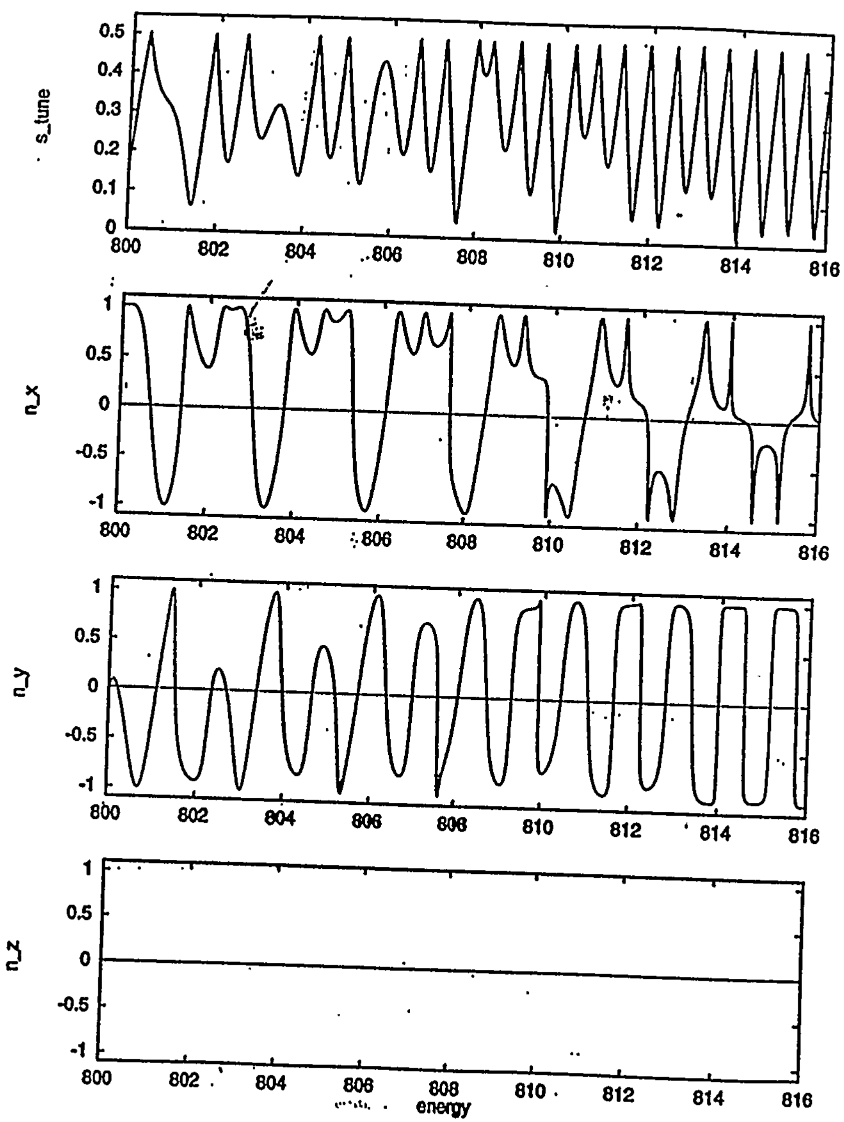

Figure 7: Behaviour of the spin tune and the vector $\vec{n}_0$ with beam energy (GeV) in the nonflat HERA-p. The view point is the East IP. Here the continuous branches of the spin tune and the vector $\vec{n}_0$ are chosen.

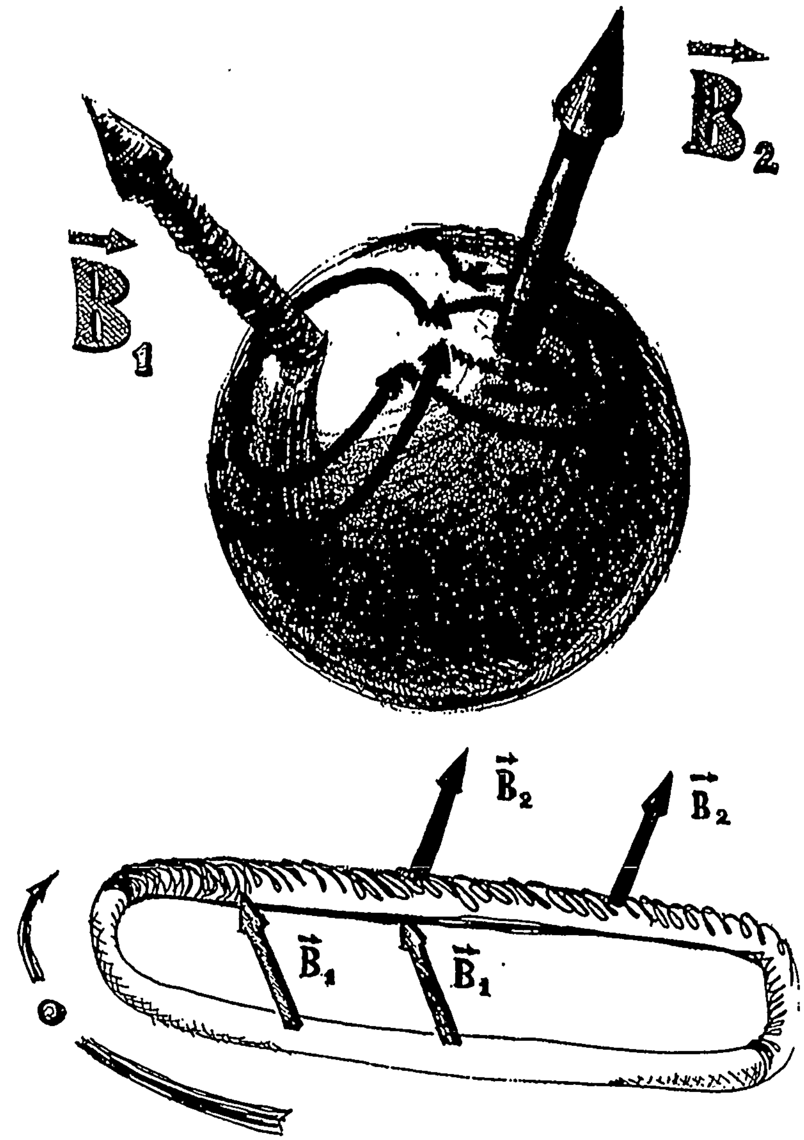

(12)

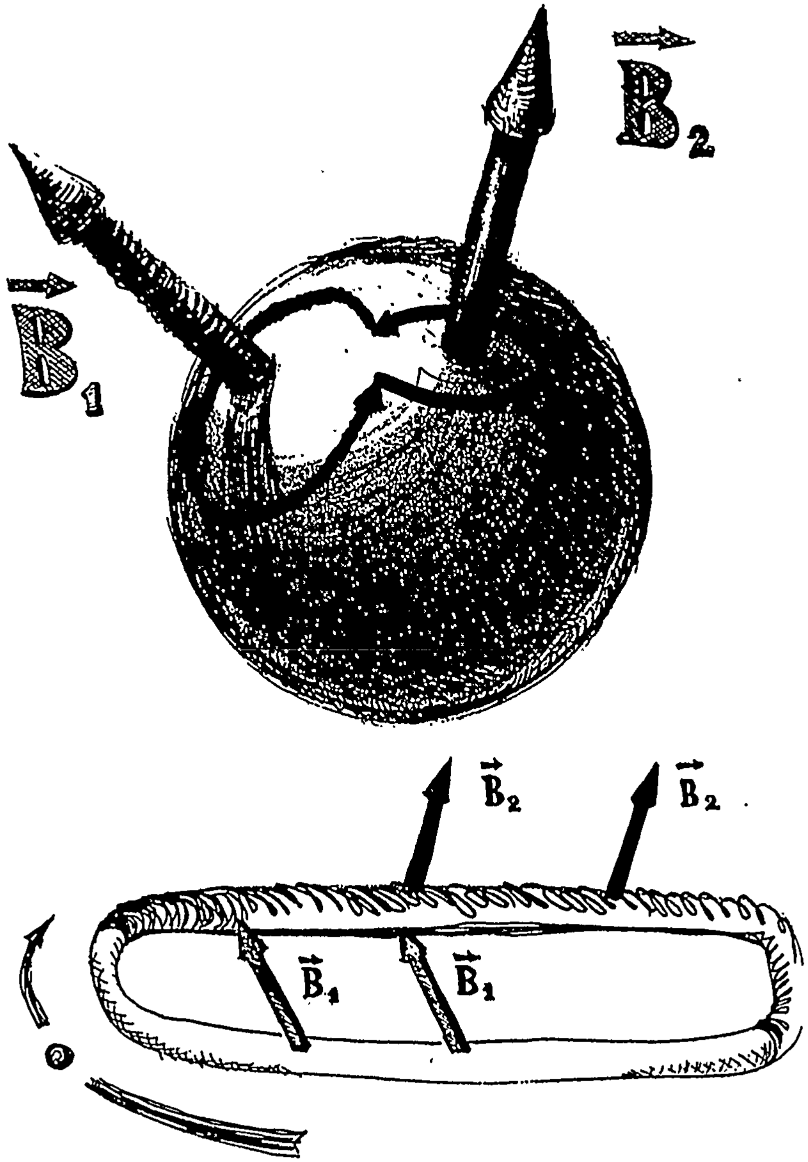

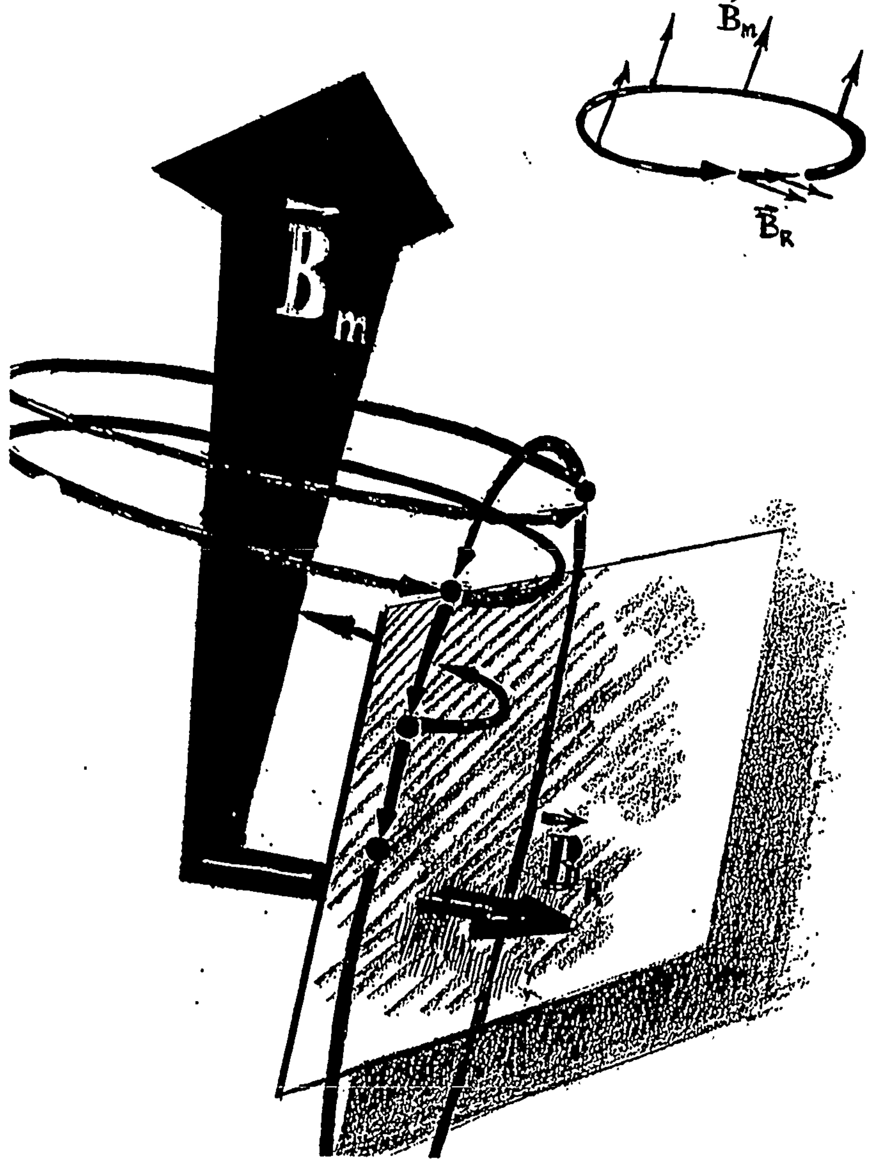

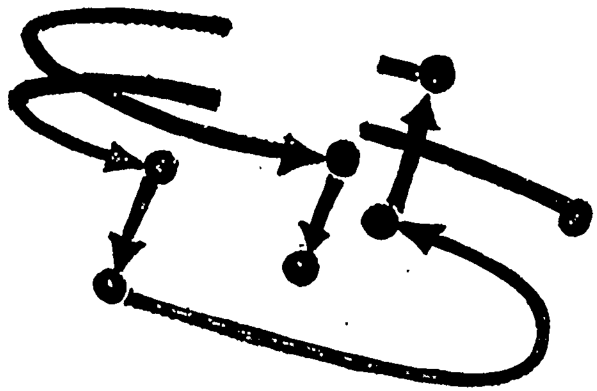

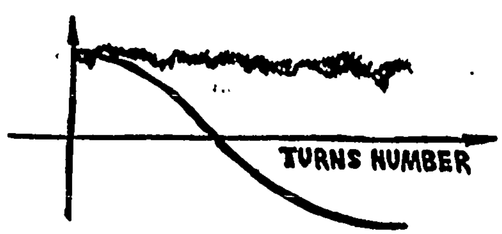

Spin-orbit resonance condition:

$$\boxed{\nu_s = \ell_1 Q_1 + \ell_2 Q_2 + \ell_3 Q_3 \quad (\mathrm{mod}\ 1)}$$

$Q_1; Q_2$ - tunes of transverse motion
Q_3 - longitudinal tune

The first order resonances for which $|\ell_1| = 1$ or $|\ell_2| = 1$ are often called the linear intrinsic resonances.

Strength of Linear Intrinsic Resonances;

$$\vec{w}(t) = \vec{w}_0(t) + \vec{w}_\varepsilon(t, \vec{u}(t, t_0, \vec{u}_0))$$

$\vec{u} = (x, p_x, y, p_y, z, p_z)$ – vector of orbital coordinates, and t is the length along the ring.

$$\vec{w}_0(t + L) \equiv \vec{w}_0(t).$$

Let $A(t, t_0)$ be the fundamental matrix solution of the spin motion on the periodic orbit, $\vec{u}(t, t_0, \vec{u}_0)$ be the solution of the linearized equations of the orbital oscillations and $\vec{n}_0(t_0)$ be the eigenvector of the one-turn revolution matrix: $A(t_0 + L, t_0)\vec{n}_0(t_0) = \vec{n}_0(t_0)$, $|\vec{n}(t_0)| = 1$.

$$\vec{w}_r(t_0, \vec{u}_0) = \lim_{T \to \infty} \frac{1}{T} \int_{t_0}^{t_0+T} A^{-1}(t, t_0) \cdot \vec{w}_\varepsilon(t, t_0, \vec{u}_0)\, dt$$

Divide $\vec{w}_r(t_0, \vec{u}_0)$ into two parts: $\parallel$ and $\perp$ to $\vec{n}_0(t_0)$:

$$\vec{w}_r(t_0, \vec{u}_0) = (\vec{w}_r(t_0, \vec{u}_0) \cdot \vec{n}_0(t_0)) \cdot \vec{n}_0(t_0) + \vec{v}_r(t_0, \vec{u}_0).$$

Resonance strength: $\varepsilon_r(\vec{u}_0) = \frac{L}{2\pi} |\vec{v}_r(t_0, \vec{u}_0)|$

Spin tune shift: $\partial_r(\vec{u}_0) = \frac{L}{2\pi} \vec{w}_r(t_0, \vec{u}_0) \cdot \vec{n}_0(t_0)$

TRIUMF booster.

Upper figure is for the special case of the racetrack lattice (straight section are transparent for spin)

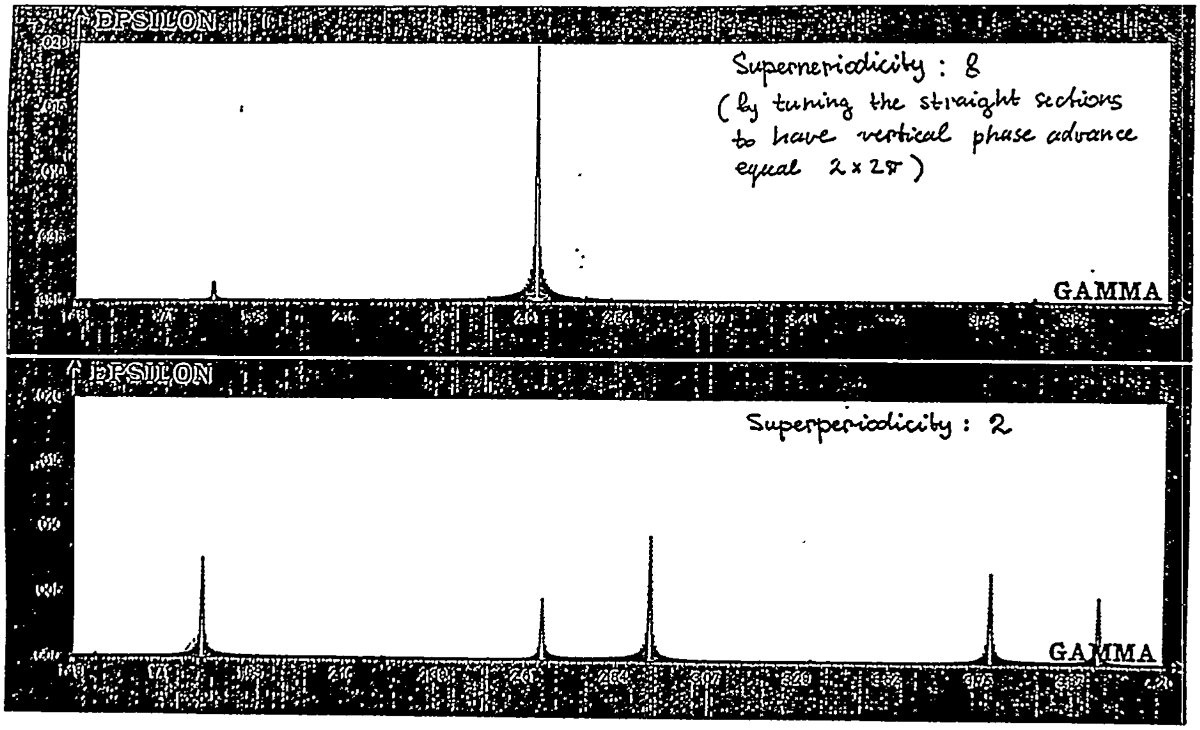

Figure 2

Remark 1: In general, the spin tune shift is nonzero even if we are not on resonance.

Remark 2: In the case when synchrotron frequency is very small compared to the other frequencies in the system it is not necessary to carry out the averaging along trajectories of the 6-D linearized equations of the orbital motion. Instead, it is sufficient to average along the trajectories of the 4-D linearized equations of the betatron motion at fixed z, p_z.

Frossart-Stora Formula:

$$S_{+\infty} = S_{-\infty}\left(2\exp\left(-\frac{\pi|\varepsilon_r|^2}{2\alpha}\right) - 1\right),$$

$S_{-\infty} = \pm 1$, α is the speed of the passage through the resonance.

Remark 3: In an ideal machine resonance condition can be written as

$$\nu_s = l_1 Q_1 + l_2 Q_2 + l_3 Q_3 \pmod{S},$$

where S is the superperiodicity of the ring.

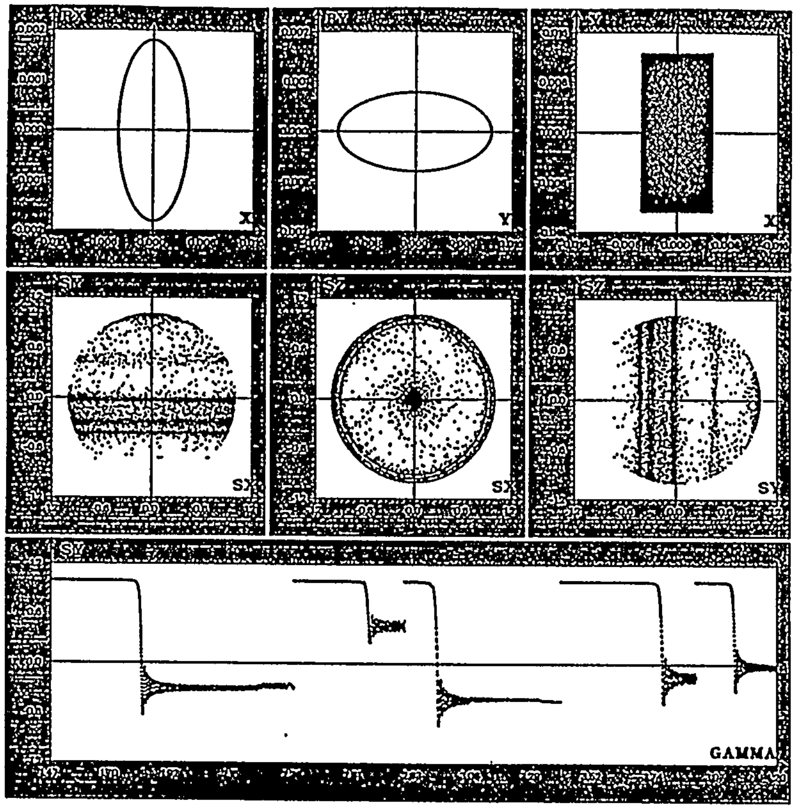

Figure 17a

1 Proton Spin Motion on the Closed Orbit

At a fixed point P on the ring, we can represent the one turn spin transformation (in zeroth approximation with respect to betatron and synchrotron oscillations) as the rotation

$$R(\vec{n}_0(P,\gamma_0),\varphi(\gamma_0))$$

around the unit vector $\vec{n}_0$ by an angle φ. Here the parameter γ_0 is the Lorentz factor and the ratio $\nu_s^0 = \varphi/2\pi$ is called the spin tune.

For the flat ring $\vec{n}_0$ is vertical and $\nu_s^0 = \gamma_0 G$, where $G = 1.793$ for protons.

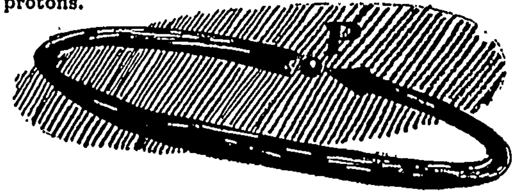

2 Full and Partial Siberian Snakes (A.M.Kondratenko and Ya.S.Derbenev)

2.1 Composition of two rotations

$$R\left(\vec{n}_0^{new},\varphi^{new}\right) = R\left(\vec{m},\alpha\right) \circ R\left(\vec{n}_0,\varphi\right).$$

$$\cos(\varphi^{new}) = -1 + 2\left[\cos\left(\frac{\alpha}{2}\right)\cos\left(\frac{\varphi}{2}\right) - \sin\left(\frac{\alpha}{2}\right)\sin\left(\frac{\varphi}{2}\right)(\vec{m}\cdot\vec{n}_0)\right]^2,$$

$$\vec{n}_0^{new} = \frac{1}{\sin\left(\frac{\varphi^{new}}{2}\right)}\left(\sin\left(\frac{\alpha}{2}\right)\cos\left(\frac{\varphi}{2}\right)\cdot\vec{m} + \cos\left(\frac{\alpha}{2}\right)\sin\left(\frac{\varphi}{2}\right)\cdot\vec{n}_0 - \right.$$

$$\left. - \sin\left(\frac{\alpha}{2}\right)\sin\left(\frac{\varphi}{2}\right)\cdot[\vec{m}\times\vec{n}_0]\right).$$

2.2 Symmetrical composition of three rotations

$$R\left(\vec{n}_0^{new}, \varphi^{new}\right) = R\left(\vec{n}_0, \frac{\varphi}{2}\right) \circ R(\vec{m}, \alpha) \circ R\left(\vec{n}_0, \frac{\varphi}{2}\right).$$

$$\cos(\varphi^{new}) = -1 + 2\left[\cos\left(\frac{\alpha}{2}\right)\cos\left(\frac{\varphi}{2}\right) - \sin\left(\frac{\alpha}{2}\right)\sin\left(\frac{\varphi}{2}\right)(\vec{m}\cdot\vec{n}_0)\right]^2,$$

$$\vec{n}_0^{new} = \frac{1}{\sin\left(\frac{\varphi^{new}}{2}\right)}\left(æ\cdot\vec{n}_0 + \sin\left(\frac{\alpha}{2}\right)\cdot\vec{m}\right),$$

where

$$æ = \cos\left(\frac{\alpha}{2}\right)\sin\left(\frac{\varphi}{2}\right) - \sin\left(\frac{\alpha}{2}\right)\left(1 - \cos\left(\frac{\varphi}{2}\right)\right)(\vec{m}\cdot\vec{n}_0).$$

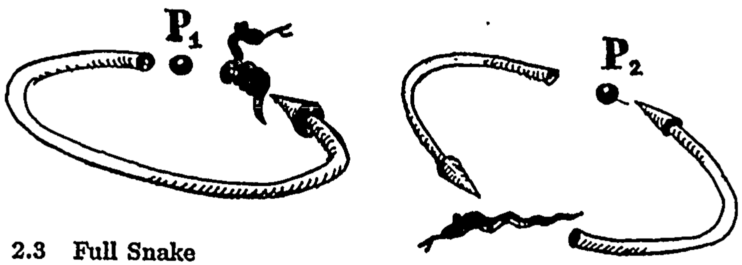

2.3 Full Snake

Let $\vec{m} \perp \vec{n}_0$ and $\alpha = \pi$. Then $\varphi^{new} = \pi$ and $\vec{n}_0^{new}(P_2) = \vec{m}$.

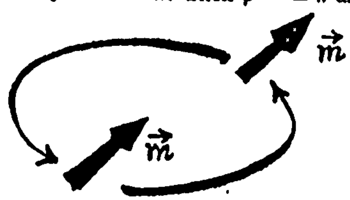

2.4 Partial Snake

Let $\vec{m} \perp \vec{n}_0$, but $\alpha \neq \pi$.

Then

$$\cos(\varphi^{new}) = -1 + 2\cos^2\left(\frac{\alpha}{2}\right)\cos^2\left(\frac{\varphi}{2}\right)$$

and for $\cos(\alpha) \neq 1$ $\qquad \varphi^{new}(\gamma_0) \neq 0 \pmod{2\pi}$.

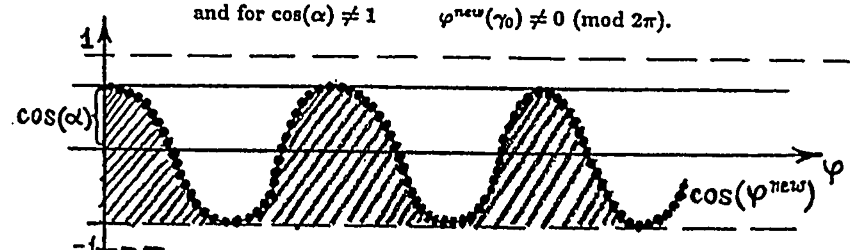

$$\vec{n}_0^{new}(P_3) = \frac{1}{\sin\left(\frac{\varphi^{new}}{2}\right)}\left(\cos\left(\frac{\alpha}{2}\right)\sin\left(\frac{\varphi}{2}\right)\cdot\vec{n}_0 + \sin\left(\frac{\alpha}{2}\right)\cdot\vec{m}\right).$$

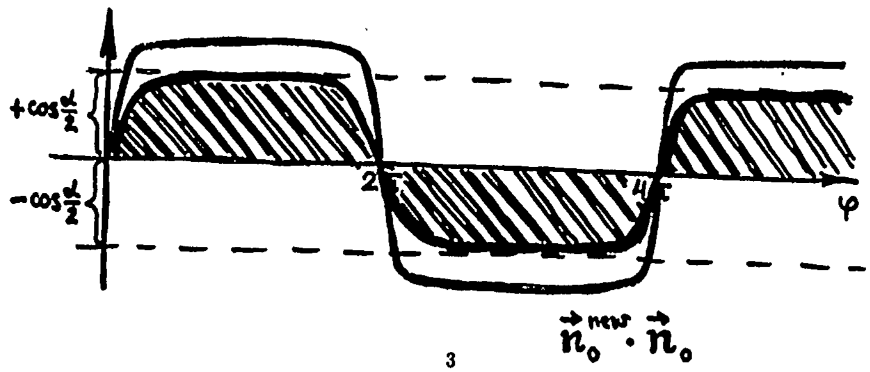

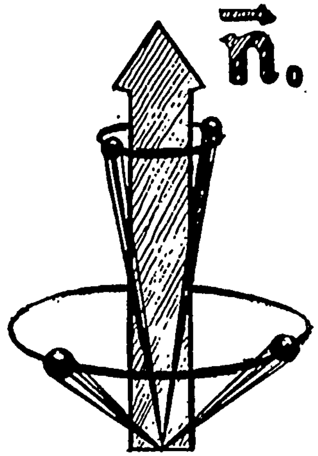

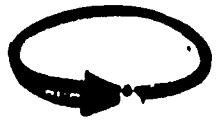

$$\begin{cases} \vec{x}_f = \vec{F}(\vec{x}_i) \\ \vec{S}_f = A(\vec{x}_i)\cdot\vec{S}_i \end{cases}$$

The function $V(\vec{x},\vec{s})$ is called an invariant function of this map if

$$V(\vec{x},\vec{s}) = V(\vec{F}(\vec{x}), A(\vec{x})\vec{s})$$

Taking V in the form

$$V = \vec{n}(\vec{x})\cdot\vec{S}$$

we have the equation for the vector $\vec{n}(\vec{x})$

$$\boxed{A(\vec{x})\cdot\vec{n}(\vec{x}) = \vec{n}(\vec{F}(\vec{x}))}$$

$$\vec{n}_0 = \vec{n}(\vec{0}).$$

$$V(\vec{x},\vec{s}) = \vec{n}(\vec{x})\cdot\vec{s}$$

$$\boxed{A(\vec{x})\cdot\vec{n}(\vec{x}) = \vec{n}(\vec{F}(\vec{x}))}$$

1. $|\vec{n}(\vec{x})|^2$ is an ivariant function of the map $\vec{x}_f = \vec{F}(\vec{x}_i)$.

2. If $f(\vec{x})$ is invariant for orbital map, then
$$V(\vec{x},\vec{s}) = f(\vec{x})\cdot\vec{n}(\vec{x})\cdot\vec{s}$$
is an inveriant function.

<u>Definition:</u> $V(\vec{x},\vec{s})$ – nondegenerate, if $|\vec{n}(\vec{0})| \neq 0$.

3. If $V_1 = \vec{n}_1\cdot\vec{s}$ and $V_2 = \vec{n}_2\cdot\vec{s}$ are invariant functions, then
$$V_3 = (\vec{n}_1 \times \vec{n}_2)\cdot\vec{s} \text{ is an}$$
invariant functions.

$$V = \frac{1}{|\vec{n}(x)|}\vec{n}(\vec{x})\cdot\vec{S} \overset{\text{def}}{=} \vec{n}_{new}(\vec{x})\cdot\vec{S} \quad \left(\text{if nondegenerate}\right)$$

$$|\vec{n}_{new}(x)| = 1$$

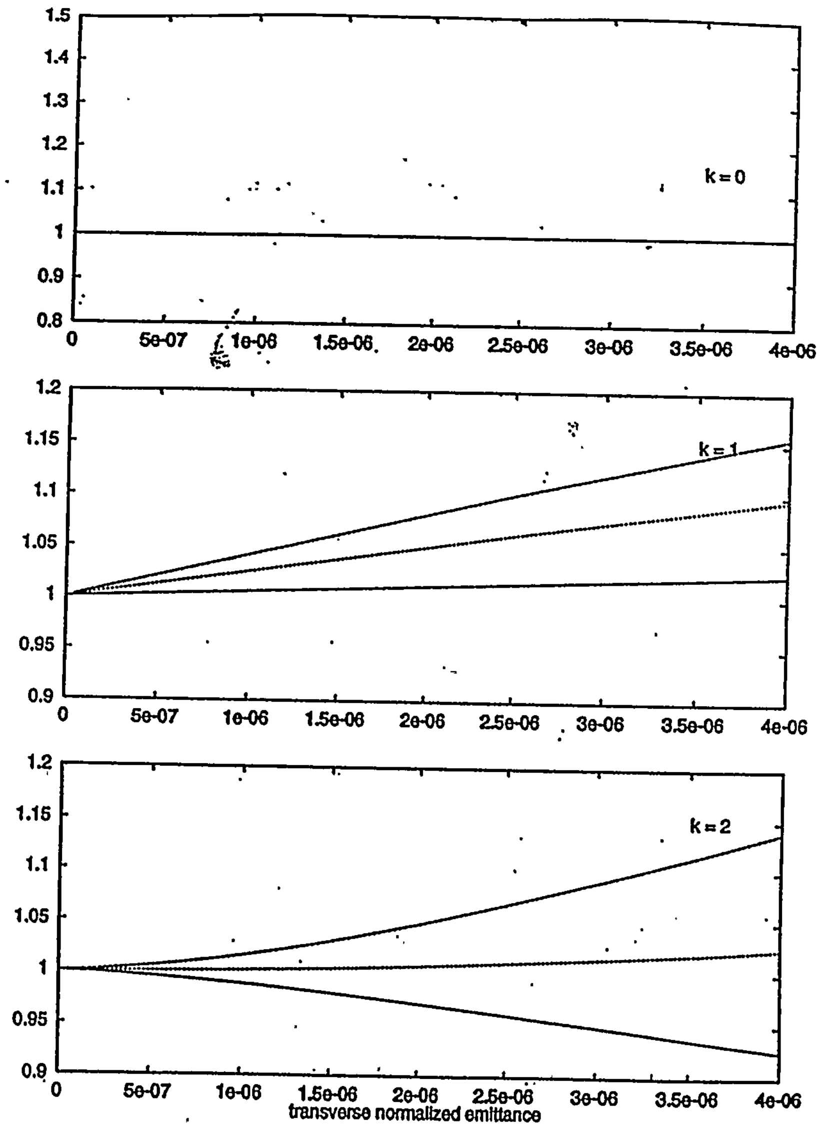

Figure 22: Flat HERA-p at E = 820 GeV. The view point is the East IP. The dependence of the maximum, the average value and the minimum of the vector norm $| \vec{n}_k |$ on the value of transverse emittance.

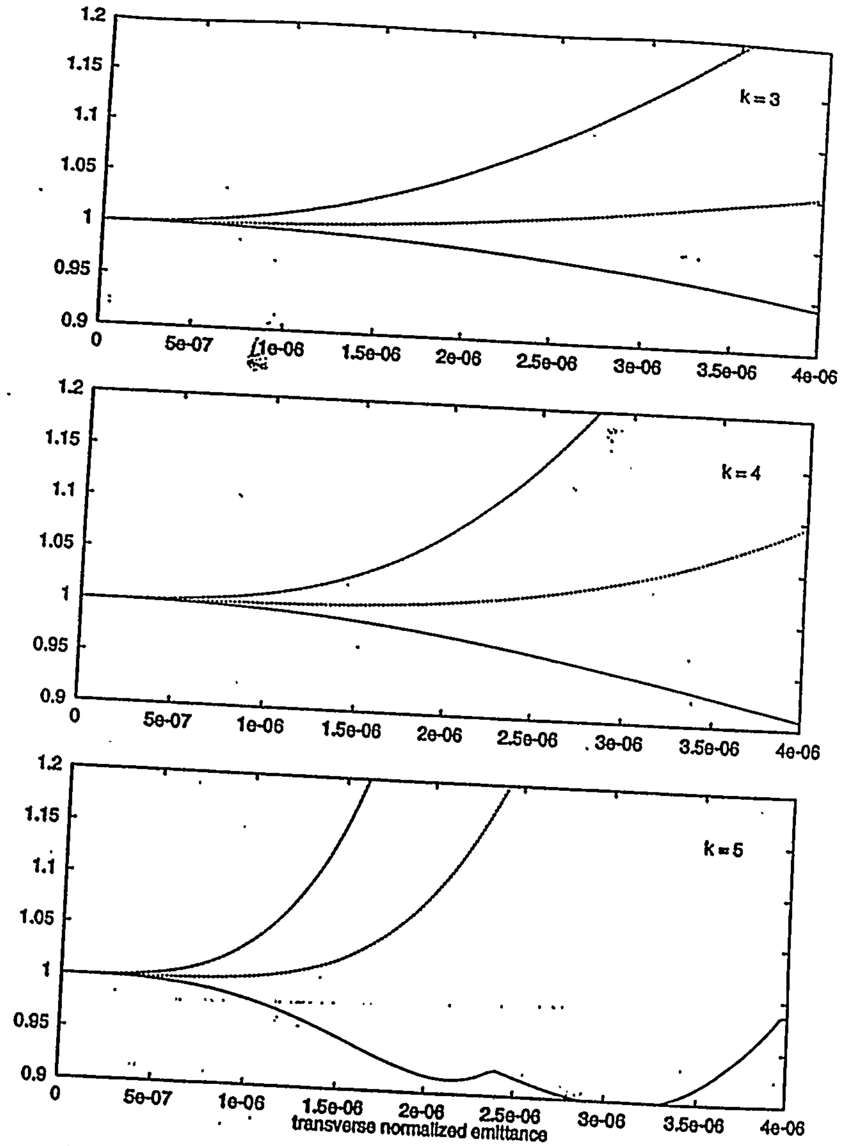

Figure 23: Flat HERA-p at E = 820 GeV. The view point is the East IP. The dependence of the maximum, the average value and the minimum of the vector norm $| \vec{n}_k |$ on the value of transverse emittance.

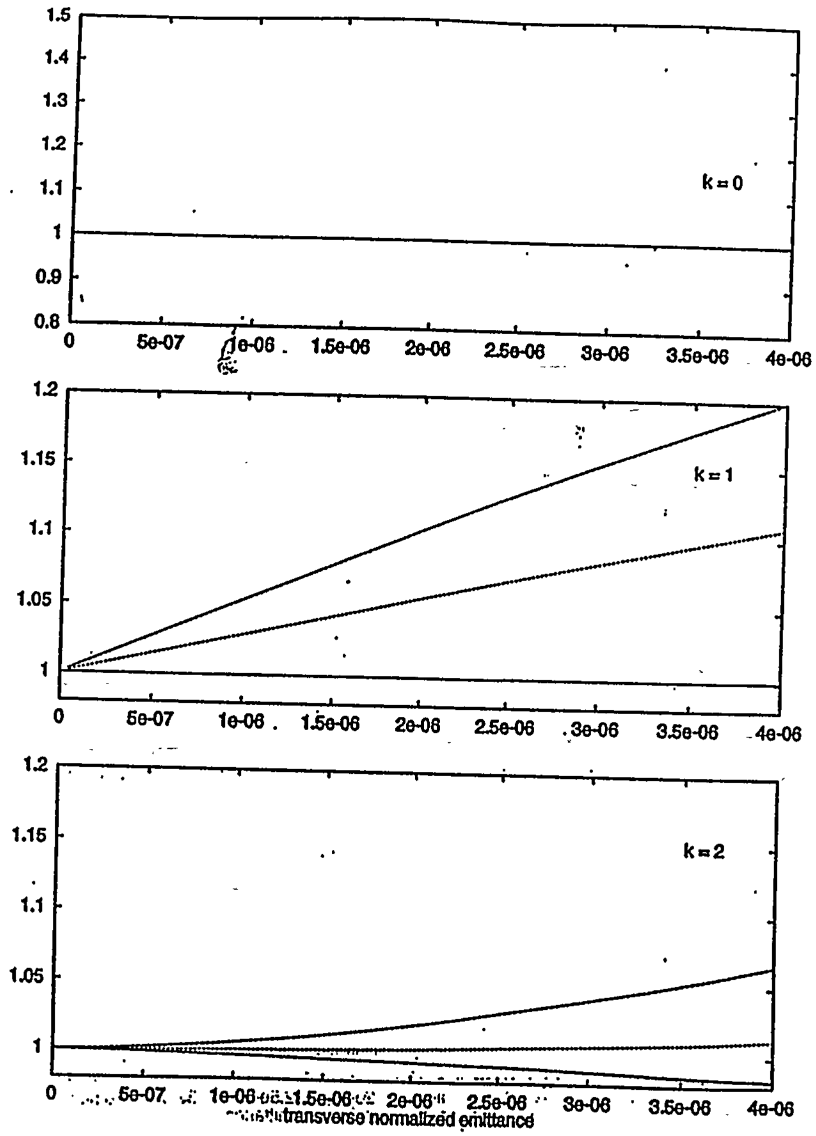

Figure 25: Flat HERA-p with two snakes at E = 820 GeV. The view point is the East IP. The dependence of the maximum, the average value and the minimum of the vector norm $|\vec{n}_k|$ on the value of transverse emittance.

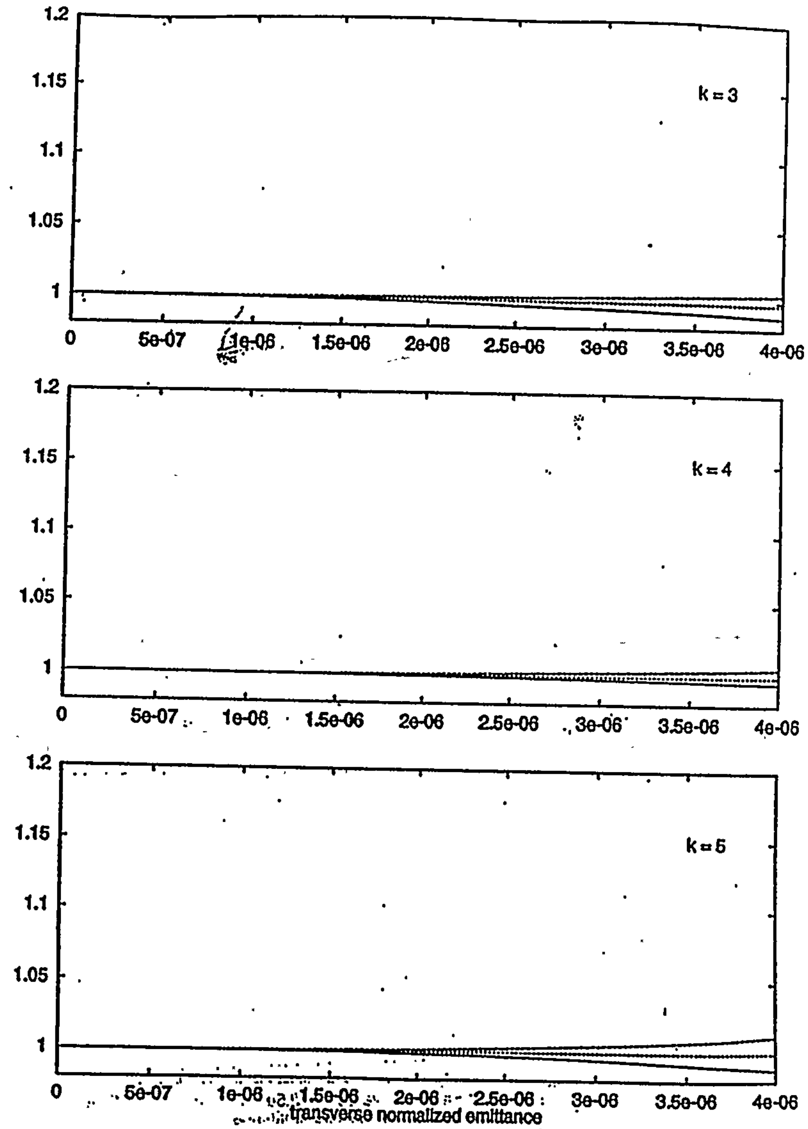

Figure 26: Flat HERA-p with two snakes at E = 820 GeV. The view point is the East IP. The dependence of the maximum, the average value and the minimum of the vector norm $|\vec{n}_k|$ on the value of transverse emittance.

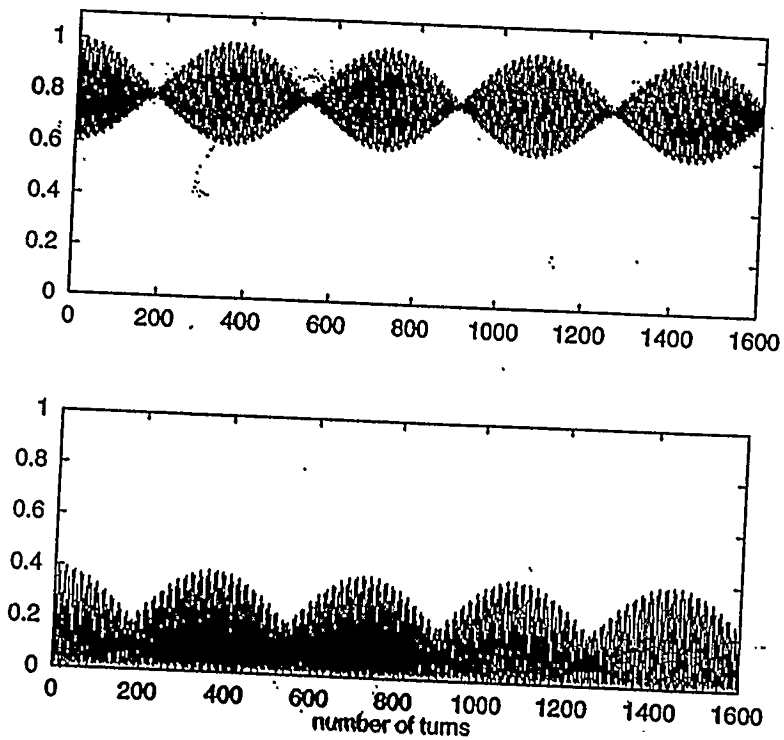

Figure 36: Flat HERA-p at E = 820 GeV with two snakes (longitudinal snake in the West and radial snake in the East). The view point is the East IP. Tracking of N = 64 particles for 1600 turns. Top: $< \vec{s} \cdot \vec{n}_0 >$. Bottom: $D\vec{s}$. Emittances: $\epsilon_x = 4.0 \cdot 10^{-6} \pi m \cdot rad$, $\epsilon_y = 4.0 \cdot 10^{-6} \pi m \cdot rad$, $\epsilon_z = 0.0$. There are no RF cavities.

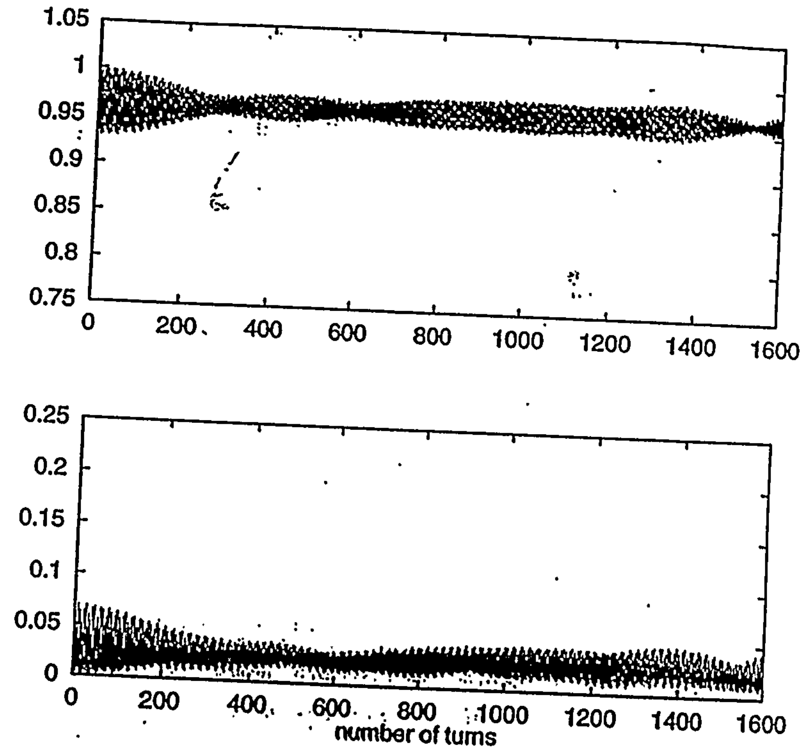

Figure 52: Nonflat HERA-p at E = 820 GeV with 4 snakes (one longitudinal snake in the West and one radial snake in the South, the North and the East respectively). The view point is the East IP. Tracking of N = 64 particles for 1600 turns. Top: $< \vec{s} \cdot \vec{n}_0 >$. Bottom: $D\vec{s}$. Emittances: $\epsilon_x = 4.0 \cdot 10^{-6} \pi m \cdot rad$, $\epsilon_y = 4.0 \cdot 10^{-6} \pi m \cdot rad$, $\epsilon_z = 1.5 \cdot 10^{-5} m \cdot rad$.

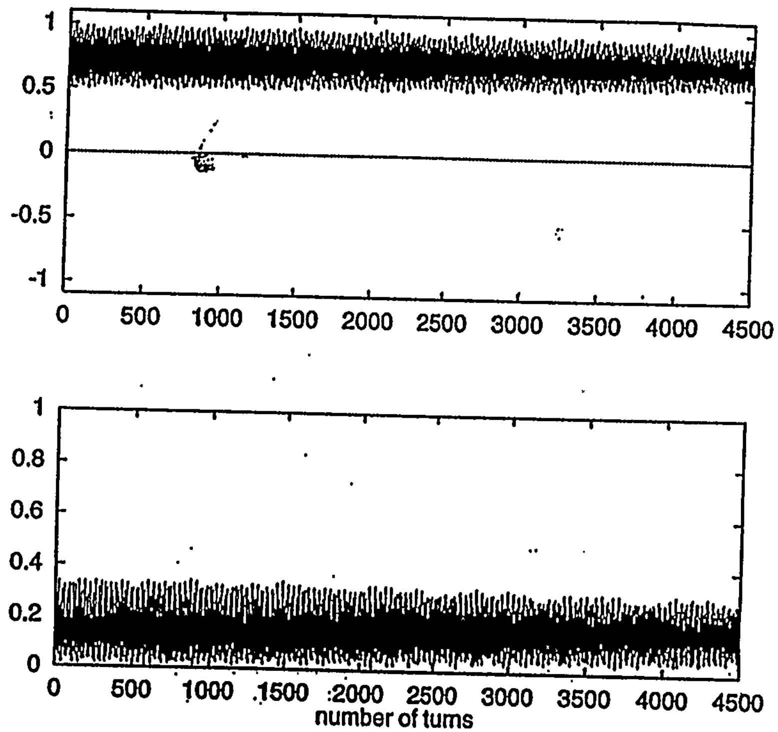

Figure 21: Nonflat HERA-p (without vertical bend in the East) at E = 820 GeV. The view point is the East IP. Tracking of N = 64 particles for 4500 turns. Top: $< \vec{s} \cdot \vec{n}_0 >$. Bottom: $D\vec{s}$. Emittances: $\epsilon_x = 4.0 \cdot 10^{-6} \pi m \cdot rad$, $\epsilon_y = 4.0 \cdot 10^{-6} \pi m \cdot rad$, $\epsilon_s = 0.0$. There are no RF cavities.

$$\begin{cases} \vec{x}_f = \vec{F}(\vec{x}_i) \\ \vec{S}_f = A(\vec{x}_i)\cdot\vec{S}_i \end{cases}, \quad \vec{F}(\vec{0}) = \vec{0}$$

$$A(\vec{x}) = \begin{bmatrix} \cos(\lambda(\vec{x})) & \sin(\lambda(\vec{x})) & 0 \\ -\sin(\lambda(\vec{x})) & \cos(\lambda(\vec{x})) & 0 \\ 0 & 0 & 1 \end{bmatrix}$$

$$V = \mathbb{S}_3 \Rightarrow \vec{n} = (0, 0, 1)$$

$$\boxed{SO(3) \Leftrightarrow SU(2)}$$

$$L = \begin{bmatrix} s_3 & s_1 + i s_2 \\ s_1 - i s_2 & -s_3 \end{bmatrix}$$

$$\begin{cases} \vec{x}_f = \vec{F}(\vec{x}_i) \\ L_f = U(\vec{x}_i)\cdot L_i\, U^*(\vec{x}_i) \end{cases}$$

Hamiltonian extension of the equations of classical spin-orbit motion

Introduce the Poisson bracket

$$\{f(\vec{z}), g(\vec{z})\} = f_{\vec{q}} \cdot g_{\vec{p}} - f_{\vec{p}} \cdot g_{\vec{q}} + [f_{\vec{s}} \times g_{\vec{s}}] \cdot \vec{s} \tag{1}$$

in 9-dimensional phase space $\vec{z} = (\vec{x}, \vec{s})$ of 6 orbital $\vec{x} = (\vec{q}, \vec{p})$ and 3 spin $\vec{s}$ variables and consider a Hamiltonian system of ordinary differential equations

$$\frac{d\vec{z}}{dt} = \{\vec{z}, H\} \tag{2}$$

with the Hamiltonian function

$$H = H_{orbt}(\vec{x}, t) + \vec{W}(\vec{x}, t) \cdot \vec{s}. \tag{3}$$

In variables $\vec{q}$, $\vec{p}$ and $\vec{s}$ the system (2) can be written as

$$\frac{d\vec{q}}{dt} = \frac{\partial H_{orbt}}{\partial \vec{p}} + \frac{\partial\left(\vec{W} \cdot \vec{s}\right)}{\partial \vec{p}}, \quad \frac{d\vec{p}}{dt} = -\frac{\partial H_{orbt}}{\partial \vec{q}} - \frac{\partial\left(\vec{W} \cdot \vec{s}\right)}{\partial \vec{q}} \tag{4}$$

$$\frac{d\vec{s}}{dt} = \left[\vec{W} \times \vec{s}\right] \tag{5}$$

and we will understand the equations (4)-(5) as the Hamiltonian extension of the equations of classical spin-orbit motion.

Not ascribing any physical sense to the spin dependent members in the right sides of equations (4), we wish to point out some ways for establishing the connections between properties and solutions of system (4)-(5) and initial triangular system (truncation procedures [1]).

[1]Note that some authors consider the spin depended members in the right sides of equations (4) as the possibility to treat the quasi-classical effect of the spin on the orbit motion, and in this case no truncations of results will be needed.

Connection between Triangular System and its Hamiltonian Extension

1. If $\vec{z}(t, t_0, \vec{z}_0) = (\vec{x}(t, t_0, \vec{x}_0, \vec{s}_0),\ \vec{s}(t, t_0, \vec{x}_0, \vec{s}_0))$ is the solution of Hamiltonian equations which passes through the point $\vec{z}_0 = (\vec{x}_0,\ \vec{s}_0)$ when $t = t_0$, then

$$\vec{z}_*(t, t_0, \vec{z}_0) = (\vec{x}_*(t, t_0, \vec{x}_0),\ \vec{s}_*(t, t_0, \vec{x}_0, \vec{s}_0)),$$

where

$$\vec{x}_*(t, t_0, \vec{x}_0) = \vec{x}(t, t_0, \vec{x}_0, \vec{0}) \quad \text{and} \quad \vec{s}_*(t, t_0, \vec{x}_0, \vec{s}_0)) = \left.\frac{\partial \vec{s}}{\partial \vec{s}_0}\right|_{\vec{s}_0 = \vec{0}} \cdot \vec{s}_0,$$

gives us the solution of initial triangular system.

2. If the Hamiltonian system admits an invariant function $V(\vec{z}, t)$ which can be represented in the form

$$V(\vec{z}, t) = V_m(\vec{z}, t) + V_{>m}(\vec{z}, t),$$

where V_m is a homogeneous polynomial of degree m in variables $\vec{s}$, and

$$\lim_{|\vec{s}| \to 0} \frac{V_{>m}}{|\vec{s}|^m} = 0,$$

then $V_m(\vec{z}, t)$ is a first integral of the triangular system.

3. If $\vec{x}(t, t_0, \vec{x}_0) \stackrel{\text{def}}{=} \vec{\phi}(t, t_0, \vec{x}_0)$ is the solution of orbital motion equations, then the triangular system can be written as a family of Hamiltonian systems depending on parameters $\vec{x}_0$, t_0 with Hamiltonian function

$$H = \vec{W}\left(\vec{\phi}(t, t_0, \vec{x}_0), t\right) \cdot \vec{s}$$

Hamiltonian Methods for Extended System

Degenerate Poisson Brackets for Global Variables, or Local Darboux Coordinates ?

The spin-orbit Poisson bracket is degenerate. It has the nontrivial **Casimir function** $|\vec{s}|^2$ and on the level surface $|\vec{s}|^2$ =const> 0 its rank is constant and is equal to 8. This means that we can decrease the dimensions of the system by introducing the atlas of local **Darboux coordinates** in which the structural matrix of the spin-orbit Poisson bracket will have the form

$$\begin{pmatrix} O_{44} & I_4 & O_{41} \\ -I_4 & O_{44} & O_{41} \\ O_{14} & O_{14} & O_{11} \end{pmatrix}.$$

Thus in local coordinates we obtain the classical **Hamiltonian system** with 4 degrees of freedom depending on one **parameter** $|\vec{s}|^2$. It is clear that the Darboux coordinates are not unique and may be introduced in different ways. We consider only one typical example.

Let $\vec{i}$, $\vec{j}$, $\vec{k}$ be an arbitrary orthogonal system of unit vectors in three dimensional space R^3 satisfying the condition $\vec{i}\cdot[\vec{j}\times\vec{k}] = 1$. We introduce three new spin variables I, J, ψ by the equations:

$$\vec{s}\cdot\vec{i} = J, \quad \vec{s}\cdot\vec{j} = \sqrt{I-J^2}\cos(\psi), \quad \vec{s}\cdot\vec{k} = \sqrt{I-J^2}\sin(\psi). \tag{1}$$

Here J is the projection of the spin vector on the $\vec{i}$-axis, ψ is the polar angle in the transverse plane and $I = |\vec{s}|^2$.

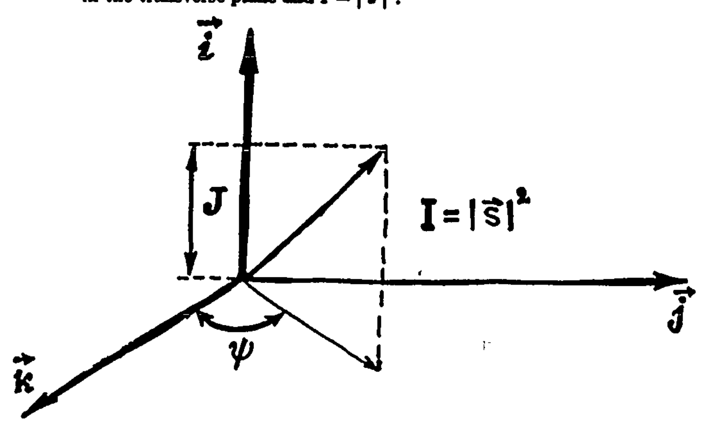

In the new variables the spin part of Hamiltonian equations becomes

$$\dot{\psi} = H_J, \qquad \dot{J} = -H_\psi, \qquad \dot{I} = 0, \tag{2}$$

where the initial Hamiltonian takes on the form

$$H = H_{orbt} + \left(\vec{W}\cdot\vec{i}\right)J + \sqrt{I-J^2}\left(\left(\vec{W}\cdot\vec{j}\right)\cos(\psi) + \left(\vec{W}\cdot\vec{k}\right)\sin(\psi)\right).$$

Unfortunately, when $\left(\vec{W}\cdot\vec{j}\right)^2 + \left(\vec{W}\cdot\vec{k}\right)^2 \neq 0$, this coordinate system cannot be extended onto the whole sphere I =const> 0, since it has a singularity for $I - J^2 = 0$. This means we need to have a whole atlas of local coordinates systems (at least two local coordinate systems defined by different vectors $\vec{i}_1$, $\vec{j}_1$, $\vec{k}_1$ and $\vec{i}_2$, $\vec{j}_2$, $\vec{k}_2$ in (1)) for a complete description of spin motion on the sphere in the electric and magnetic fields depending on time and position of the particle. We will have the same difficulties with any other Darboux coordinates because they are defined by the topological properties of the sphere. So the way pointed by the Darboux theorem does not look like the most natural or straightforward approach to the problem of investigation of polarized beam dynamics and we prefer to study the equations of spin-orbit motion using initial global variables $\vec{x}$, $\vec{s}$ and the degenerate Poisson bracket.

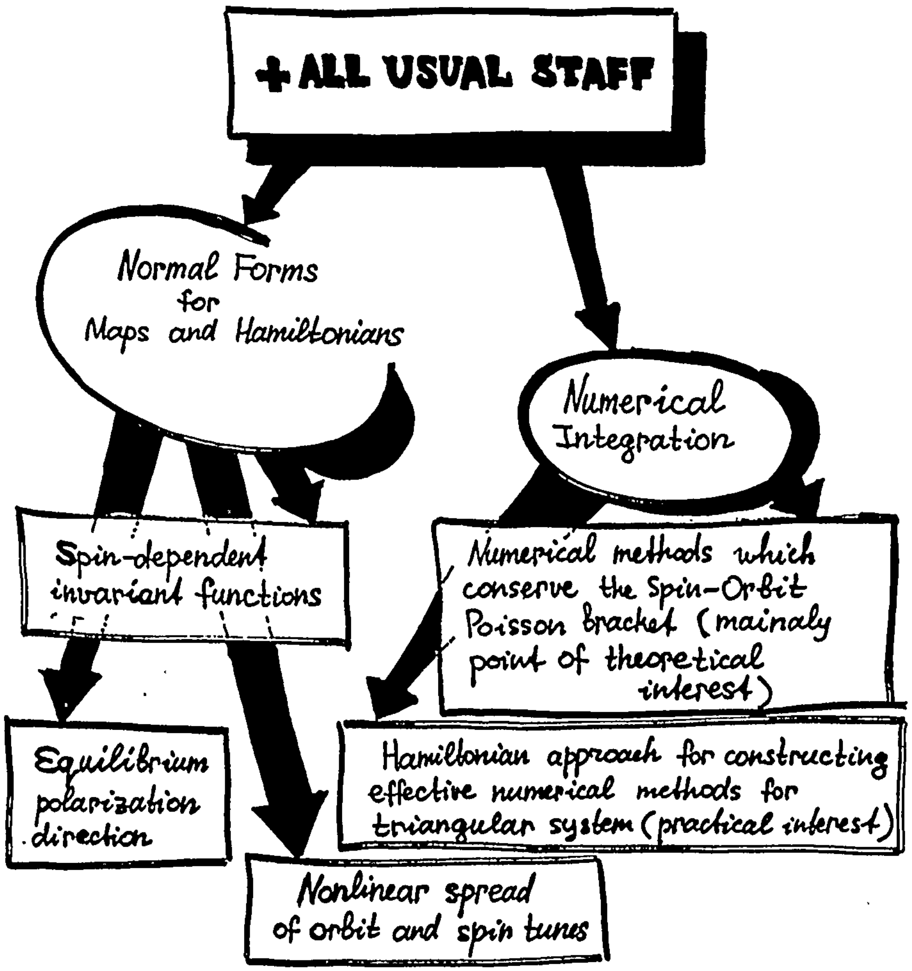

Canonical Transformations of Spin-Orbit Variables which Maps the Origin into Itself

We shall be working with a phase space consisting of $2n+3$ variables
$$\vec{z} = (\vec{x}, \vec{s}) = (q_1, \ldots, q_n, p_1, \ldots, p_n, s_1, s_2, s_3).$$
$$\vec{z}_f = \vec{M}(\vec{z}_i), \quad \vec{M}(\vec{0}) = \vec{0}. \qquad (*)$$

The map $(*)$ is canonical if $\det\left[\frac{\partial \vec{M}}{\partial \vec{z}}\right] \neq 0$ and
$$\hat{J}(\vec{M}(\vec{z})) = \left[\frac{\partial \vec{M}}{\partial \vec{z}}\right] \cdot \hat{J}(\vec{z}) \cdot \left[\frac{\partial \vec{M}}{\partial \vec{z}}\right]^T,$$
where
$$\hat{J}(\vec{z}) = (\{z_i, z_j\}) = \left(\begin{array}{cc|ccc} 0 & I & & & \\ -I & 0 & & 0 & \\ \hline & & 0 & s_3 & -s_2 \\ & 0 & -s_3 & 0 & s_1 \\ & & s_2 & -s_1 & 0 \end{array}\right)$$
is structural matrix of spin-orbit Poisson bracket.

Lemma 1: *The nonsingular real linear transformation*
$$\vec{z}_f = A\,\vec{z}_i$$
is canonical one if and only if the matrix A has the form
$$A = \mathrm{diag}(A_{orbt}, A_{spin}),$$
where $A_{orbt} \in Sp(2n)$, $A_{spin} \in SO(3)$.

In a more extended form the vector-function $\vec{M}(\vec{z})$ can be written as
$$\vec{M}(\vec{z}) = (\vec{X}(\vec{x}, \vec{s}), \vec{S}(\vec{x}, \vec{s})).$$

Lemma 2: *The linearization of the canonical map $(*)$ is linear canonical map if and only if* $\frac{\partial \vec{X}}{\partial \vec{s}}(\vec{0}, \vec{0}) = 0$.

Definition 1: A polynomial $P(\vec{z}) = P(\vec{x}, \vec{s})$ is quasi-homogeneous of degree m in its arguments $\vec{x}, \vec{s}$ if it satisfies the equation

$$P(t\vec{x},\ t^2\vec{s}) = t^m \cdot P(\vec{x}, \vec{s})$$

for every value of t.

The set of all quasi-homogeneous polynomials of degree m $(m = 0, 1, 2, \dots)$ will be denoted by $\mathcal{H}_s(m)$.

Definition 2: The quasi-linearization of the map $(*)$ is named a linear transformation $\vec{z}_f = A_s \vec{z}_i$, which acts invariantly on classes $\mathcal{H}_s(m)$ and minimizes the Euclidean norm of the difference

$$\frac{\partial \vec{M}}{\partial \vec{z}}(\vec{0}) - A_s.$$

Lemma 3: The quasi-linearization of the map $(*)$ exists, is unique and is canonical map and is defined by the matrix

$$A_s = \mathrm{diag}\left(\frac{\partial \vec{X}}{\partial \vec{x}}(\vec{0}, \vec{0}),\ \frac{\partial \vec{S}}{\partial \vec{s}}(\vec{0}, \vec{0})\right).$$

Definition 3: We will say that function $V(\vec{z}) \in \mathcal{O}_s(m)$ if

$$\exists \lim_{t \to 0} \frac{1}{t^m} V(t\vec{x}, t^2\vec{s}) \in \mathcal{H}_s(m).$$

Factorization Theorem: For every canonical map of the form $(*)$ and for every natural $m \geq 3$ the functions $G_k(\vec{z}) \in \mathcal{H}_s(k)$ $(3 \leq k \leq m)$ can be found, such that

$$\vec{M}(\vec{z}) =_m :A_s: \exp(:G_3:) \dots \exp(:G_m:) \vec{z}.$$

Here A_s is the matrix of the quasi-linearization of the map $(*)$ and the symbol $=_m$ means that the difference of right and left parts is the function out of the class $\mathcal{O}_s(m)$.

V. BALANDIN
&
N. GOLUBEVA

(1992)

The computer code **FORGET-ME-NOT** has been written for the study of polarized beam dynamics and includes the following options:

1. Calculation of strengths of imperfection spin resonances and first order intrinsic spin resonances with betatron oscillations with the help of an averaging method.
2. Calculation of one-turn Taylor maps for orbit and spin motion up to arbitrarily high order with respect to the amplitudes of the betatron and synchrotron oscillations and determination of:
   - 2.1. Invariant functions of the orbit motion.
   - 2.2. Equilibrium polarization direction.
   - 2.3. Dependence of orbit and spin tunes on invariants of orbit motion (spread of orbit and spin tunes).
3. Numerical tracking of particles with spin in accelerators and storage rings:
   - 3.1. Symplectic with respect to the 6-D orbit motion.
   - 3.2. Orthogonal with respect to the 3-D spin motion.

All options use the same physical model. The use of various approaches allows the computed results to understand from various points of view. **FORGET-ME-NOT** has been applied to the investigation of scheme for preserving polarization in the **TRIUMF KAON** Booster and to the investigation of spin motion at high energy in the **HERA** proton ring.

DYNAMIC APERTURE - SIMULSTION AND EXPERIMENT

F. Schmidt, CERN

Dynamic Aperture — Simulation & Experimen[t]

- LHC Tracking Results
  M. Böge, H. Grote, Q. Qing, F. Schmidt
  - Correlation ☺ E. Todesco, F. Schmidt
- The Inverse log Conjecture
  - Henon revisited ☺ E. Todesco, F. Schm[idt]
  - LHC M. Böge, F. Schmidt
- Nonperturbative Resonance Correction R. Bartolini ☺, F. Schmidt

(- Work in progress
  - Jolt Factorisation ☺ D. Abell
  - Map Analysis à la Yan & Irwin)

- Dynamic Aperture Experiments
  - SPS W. Fischer et al.
  - (Hera [illegible]

Studied Cases

- Errors

- Case I

<u>no</u> linear imperfections, i.e. b_1, a_1, b_2, a_2, misalignments

→ Systematics by arc:

Octupoles: $b_4 = a_4 = 2 \cdot 10^{-5}$ at $R_r = 10$ mm (European !)

- Case II

as I but: Correction of a_4, b_4 bias over 1. turn

new

- Case III

as I but: $b_4 = 0.7 \cdot 10^{-5}$, $a_4 = 1.0 \cdot 10^{-5}$

- Case IV

as III but all linear imperfections [illegible]

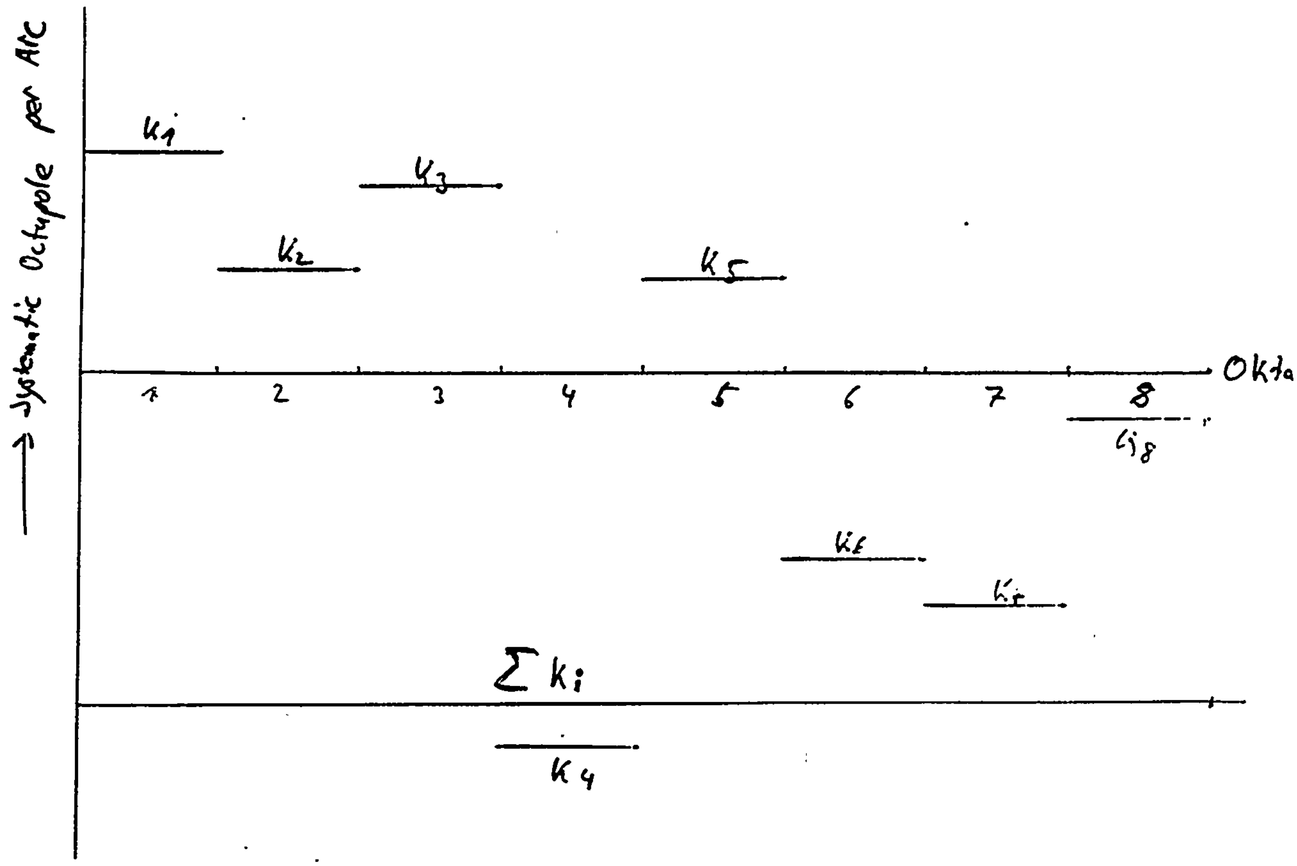

<u>Magnet Errors</u>: $B_y + iB_x = B_0 \sum_n (b_n + i a_n) \left(\frac{z}{R_r}\right)$

	persistent			geometric			ramp					
	Mean	Unce.	Rand.	Mean	Unce.	Rand.	Mean	Unce.	Random	$\Sigma_{p,g}M$	$\Sigma_{p,g}U$	$\sqrt{\Sigma_{p,g} R^2}$
b_1				0.	5.00000	10.00000	9.00000	0.	0.	0.	± 5.00000	10.00000
b_2	0.	0.	0.	0.	0.50000	0.40000	0.	0.	0.05600	0.	± 0.50000	0.40000
b_3	-3.60000	0.70000	0.07000	0.	0.30000	0.50000	0.45000	0.	0.	-3.60000	± 1.00000	0.50488
b_4	0.	0.	0.	0.	$\boxed{0.07000}$	0.10000	0.	0.	0.03400	0.	± 0.20000	0.10000
b_5	0.18000	0.	0.00400	0.	0.05000	0.08000	0.17000	0.	0.	0.18000	± 0.05000	0.08010
b_6	0.	0.	0.	0.	0.00400	0.02000	0.	0.	0.	0.	± 0.00400	0.02000
b_7	0.	0.	0.	-0.02600	0.	0.01000	0.	0.	0.	-0.02600	0.	0.01000
b_8	0.	0.	0.	0.	0.	0.00500	0.	0.	0.	0.	0.	0.00500
b_9	0.	0.	0.	0.00600	0.	0.00300	0.	0.	0.	0.00600	0.	0.00300
b_{10}	0.	0.	0.	0.	0.	0.00200	0.	0.	0.	0.	0.	0.00200
b_{11}	0.	0.	0.	0.00800	0.	0.00100	0.	0.	0.	0.00800	0.	0.00100
a_1	0.	0.	0.	0.	0.	0.	0.	0.	0.	0.	0.	0.
a_2	0.	0.	0.	0.	0.30000	1.00000	0.	0.	1.00000	0.	± 0.30000	1.00000
a_3	0.	0.	0.	0.	0.30000	0.15000	0.	0.	0.11000	0.	± 0.30000	0.15000
a_4	0.	0.	0.	J.	$\boxed{0.10000}$	0.10000	0.	0.	0.11000	0.	± 0.20000	0.10000
a_5	0.	0.	0.	0.	0.05000	0.04000	0.	0.	0.03400	0.	± 0.05000	0.04000
a_6	0.	0.	0.	0.	0.00400	0.01000	0.	0.	0.	0.	± 0.00400	0.01000
a_7	0.	0.	0.	0.	0.	0.01000	0.	0.	0.	0.	0.	0.01000
a_8	0.	0.	0.	0.	0.	0.00500	0.	0.	0.	0.	0.	0.00500
a_9	0.	0.	0.	0.	0.	0.00400	0.	0.	0.	0.	0.	0.00400
a_{10}	0.	0.	0.	0.	0.	0.00200	0.	0.	0.	0.	0.	0.00200
a_{11}	0.	0.	0.	0.	0.	0.00100	0.	0.	0.	0.	0.	0.00100

Table 1: Expected multipole performance for element (MB) at injection (in units of 10^{-4} relative field error at 10 mm) from [1]

b_n : "normal"
a_n : "skew"

ex: b_3 = sextupole
a_2 = skew quad

Tracking Parameters

- Tunes : 63.28
  63.31
- Chromaticity :
  Case I – III $Q' = 0.0$
  Case IV $Q' = 2.0$
- Amplitude Variation : 6D only!
  $x' = y' = \sigma = 0.0$, $\delta_0 = 7.5 \cdot 10^{-4}$
  (bucket $\delta = 1 \cdot 10^{-3}$)
  Varied x, y
  with $\frac{\varepsilon_{II}}{\varepsilon_{I}} = C \xRightarrow[\text{Space}]{\text{Amplitude}}$ Angle = atan($\sqrt{C}$)
  Case I, II, IV mostly $C = 1.0$
  Case III extensive study 9 Angles
  $\{1^\circ, \dots, 45^\circ, \dots, 89^\circ\}$ $45^\circ \triangleq C = 1.0$

→ - Dense 30 pairs per transverse beam sigma
- No Phase Variation :
  instead study of phase space distortions
  (smear, average–, max–, min–, amplitude)
- Ripple : started for Case III

Computers

1.) End of 1995

8 SP1 RS 6000/370
Power 62.5 MHz

2.) Beginning of 1996

8 SP2 RS 6000/390
Power 67 MHz

3.) Middle of 1996

10 DEC ALPHA Server 8400
350 MHz

	Speed	[Sixtrack] Time/Turn [ms]	Turns/Day [10^6]
1	1	7.5	92
2	1.5	5	138
3	3.75	2	432

Non Linear Behavior

- Detuning:
  - a.) transverse
    all seeds, 10σ, all $c = \frac{\varepsilon_{II}}{\varepsilon_{I}}$
    $|\Delta Q_{x,y}| \leq 6 \cdot 10^{-3}$
  - b.) momentum deviation δ
    all seeds $\delta = \pm 10^{-3}$
    $|\Delta Q_{x,y}| \leq 5 \cdot 10^{-3}$
- Smear:
  9% – 33%
- Averaged Amplitude
  ~ 6%
- Min – Max Amplitude
  ~ ± 10%
- Onset of Chaos
  DA (100,000 Turns) – (20-30)%

Tracking Engine (shell script driven)

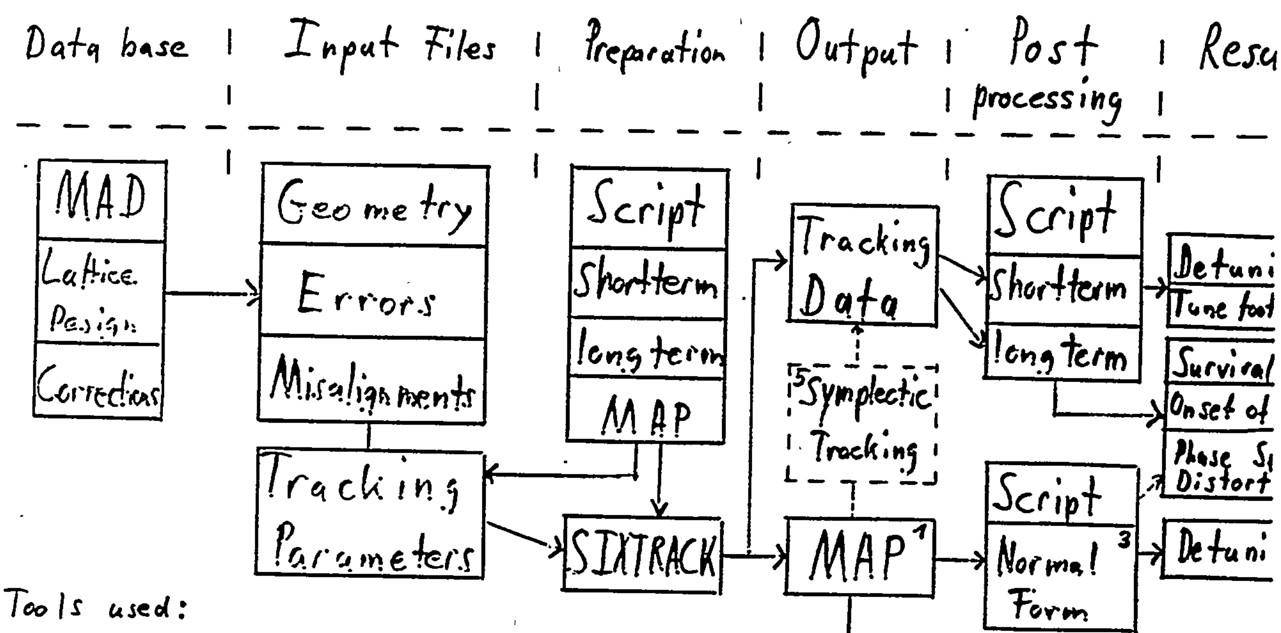

Tools used:

1) M. Berz, DA Package
) R. Bartolini, Sussix
) E. Forest, Lie lib
) E. Todesco, Nero
) D. Abel (E. Forest) Tolt Factorisation – future application)

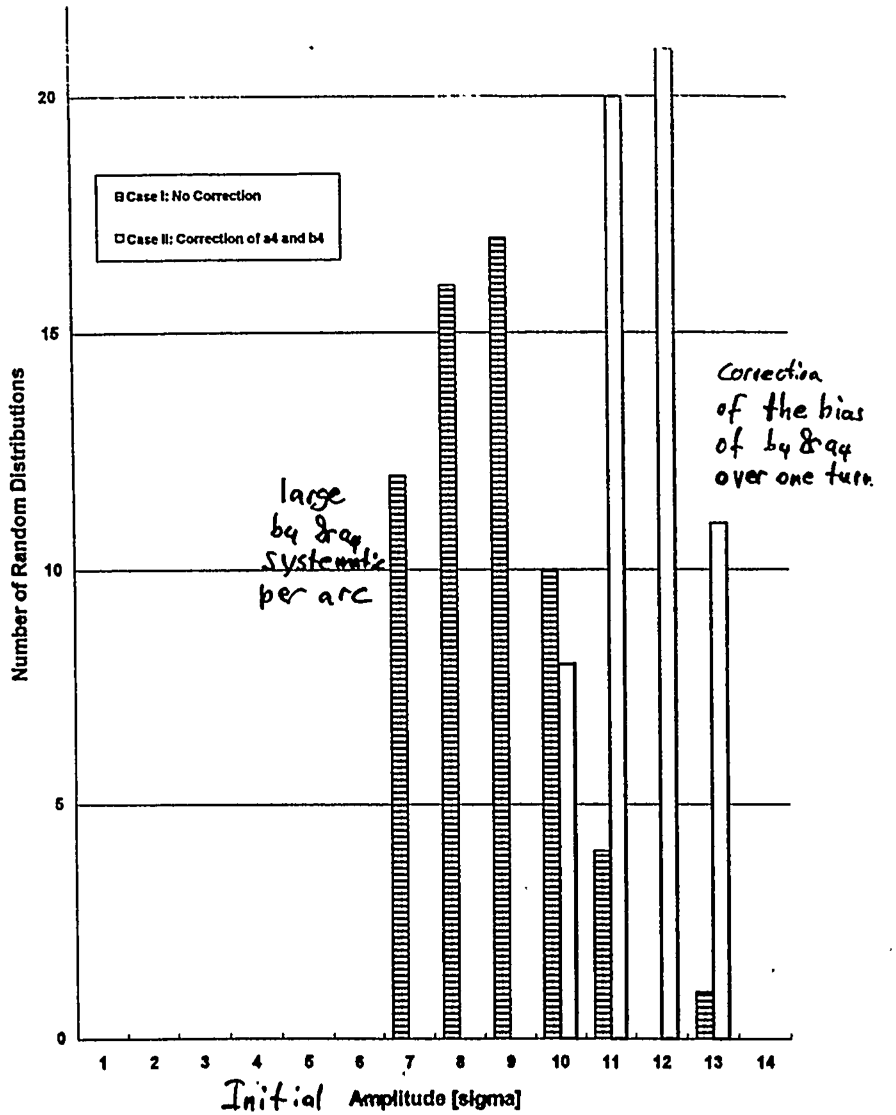

Case I: No Correction
Case II: Correction of a4 and b4
Number of Random Distributions
Initial Amplitude [sigma]
large
b4 & a4
systematic
per arc
Correction
of the bias
of b4 & a4
over one turn

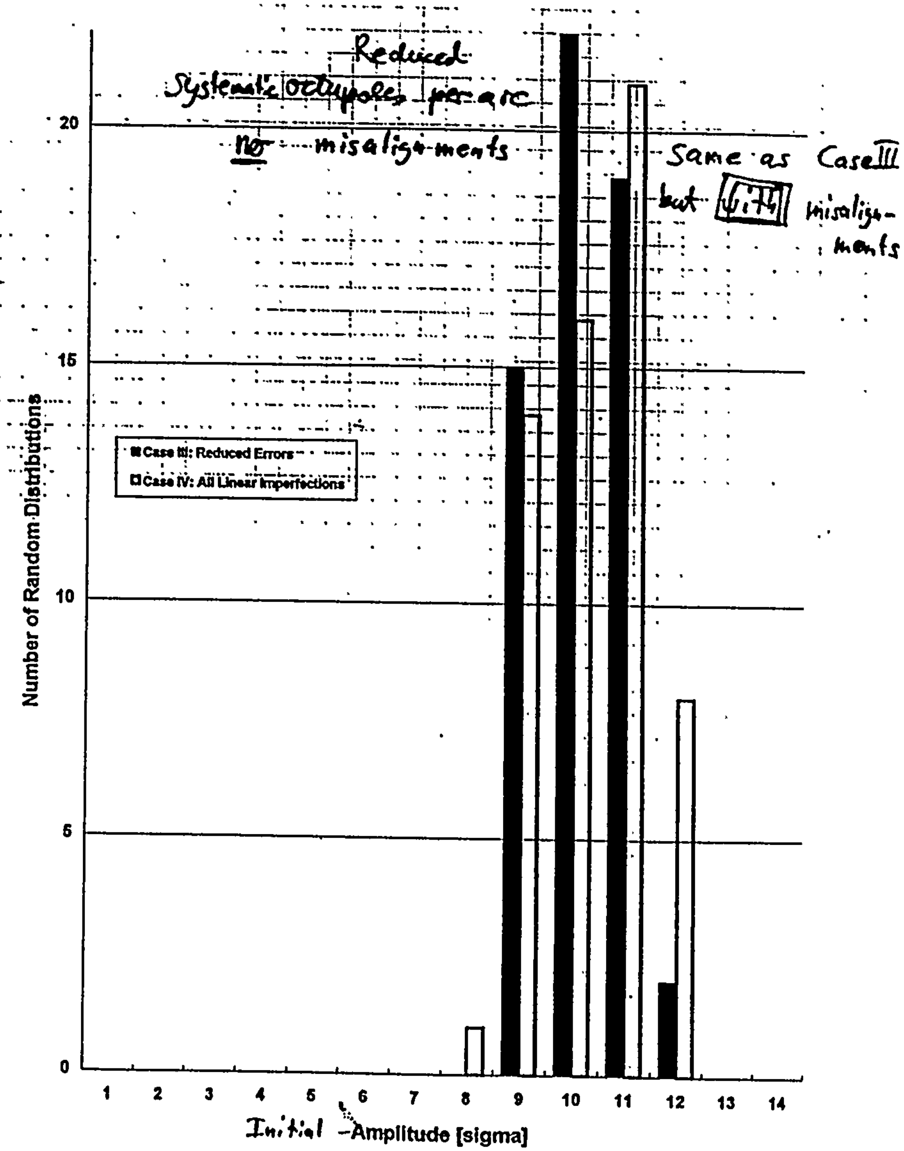

Case III: Reduced Errors
Case IV: All Linear Imperfections
Number of Random Distributions
Initial Amplitude [sigma]
Reduced
Systematic octupoles per arc
no misalignments
Same as Case III
but with misalignments

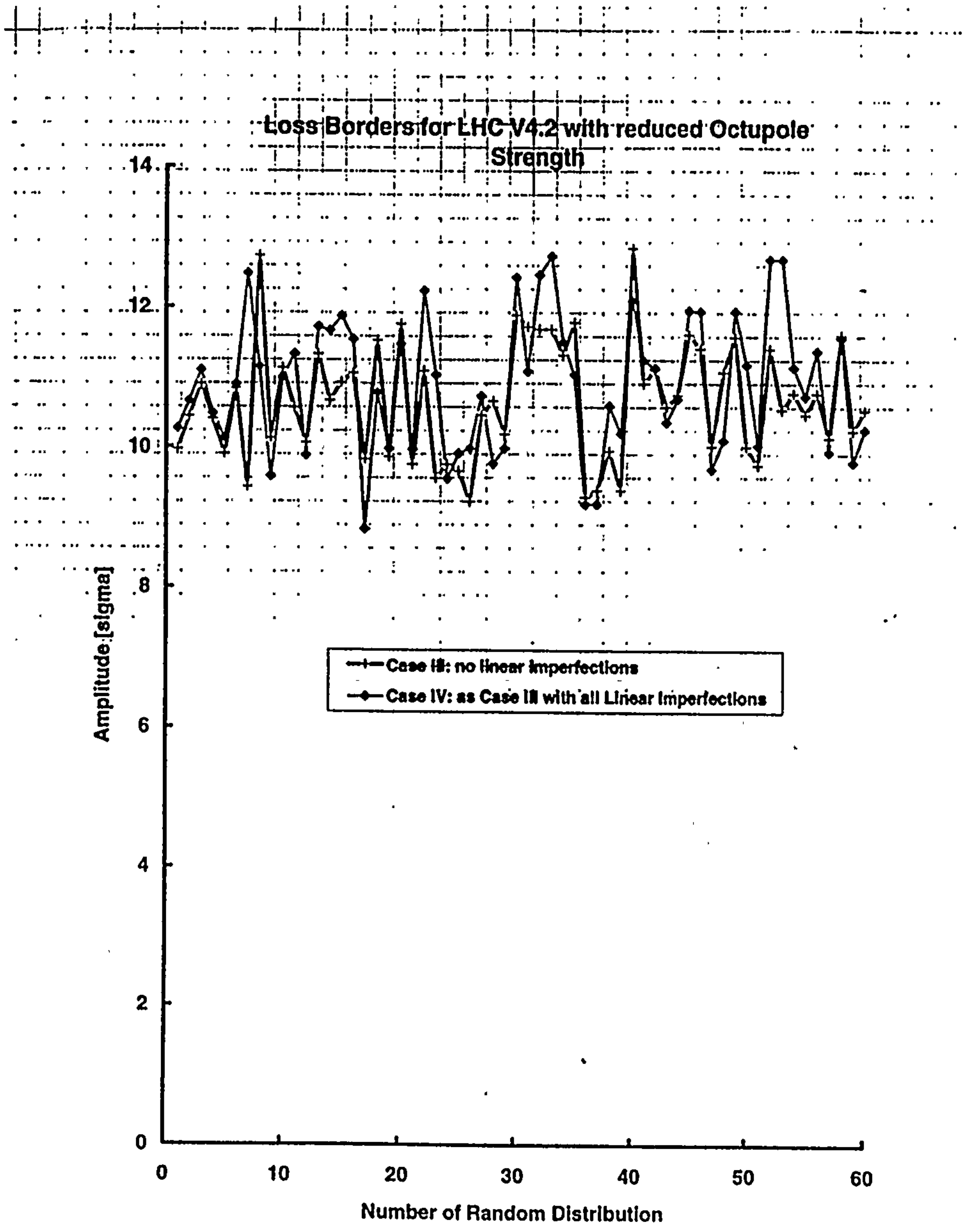
Loss Borders for LHC V4.2 with reduced Octupole Strength
Amplitude [sigma]
Number of Random Distribution
Case III: no linear imperfections
Case IV: as Case III with all Linear Imperfections
0
2
4
6
8
10
12
14
0
10
20
30
40
50
60

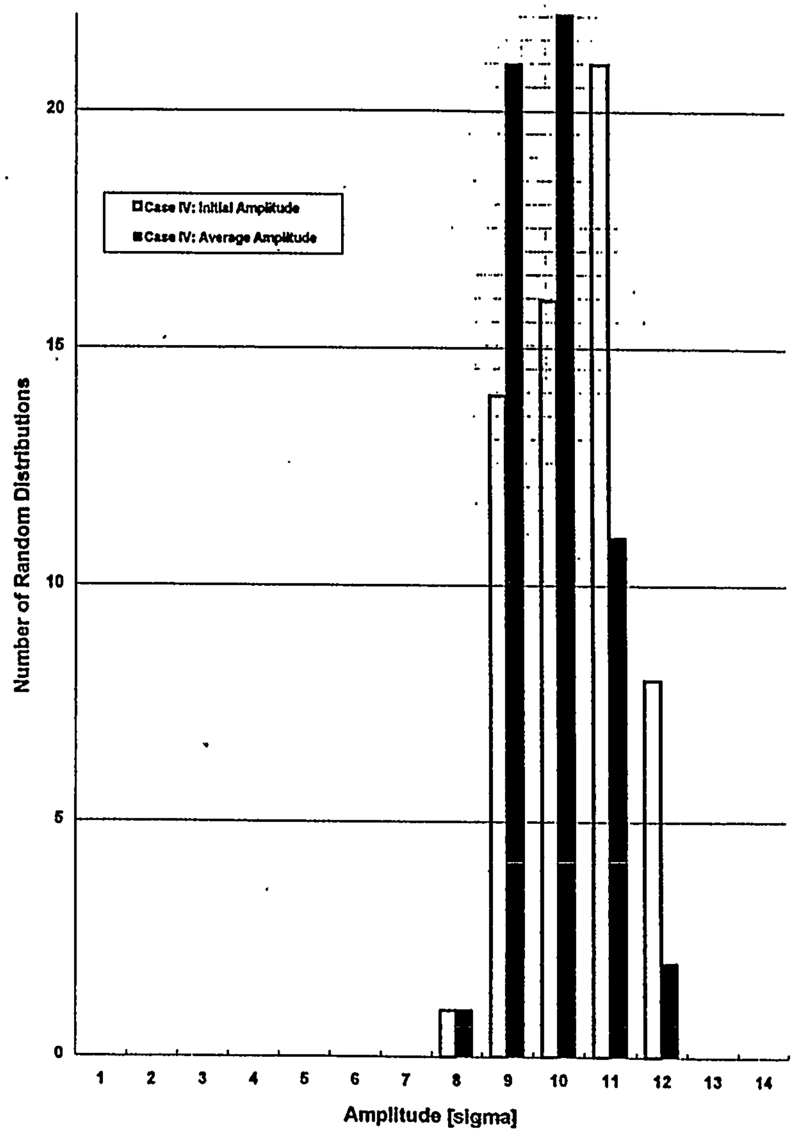
Case IV: Initial Amplitude
Case IV: Average Amplitude
Number of Random Distributions
Amplitude [sigma]
0
5
10
15
20
1
2
3
4
5
6
7
8
9
10
11
12
13
14

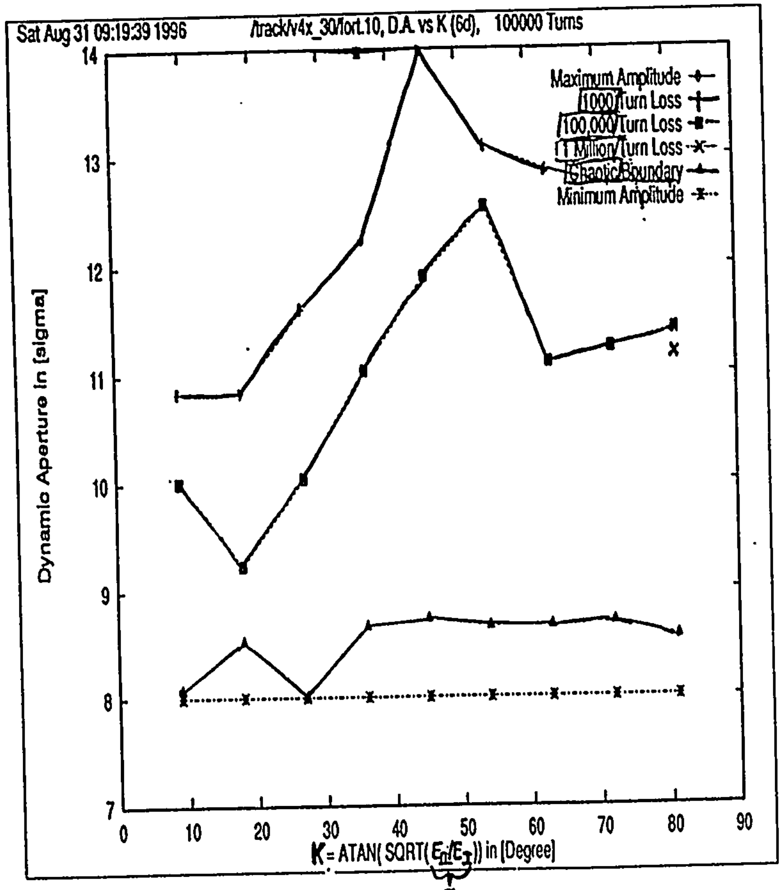
Sat Aug 31 09:19:39 1996
/track/v4x_30/fort.10, D.A. vs K (6d), 100000 Turns
Maximum Amplitude
1000 Turn Loss
100,000 Turn Loss
1 Million Turn Loss
Chaotic Boundary
Minimum Amplitude
Dynamic Aperture in [sigma]
K = ATAN(SQRT(E_II/E_⊥)) in [Degree]
C

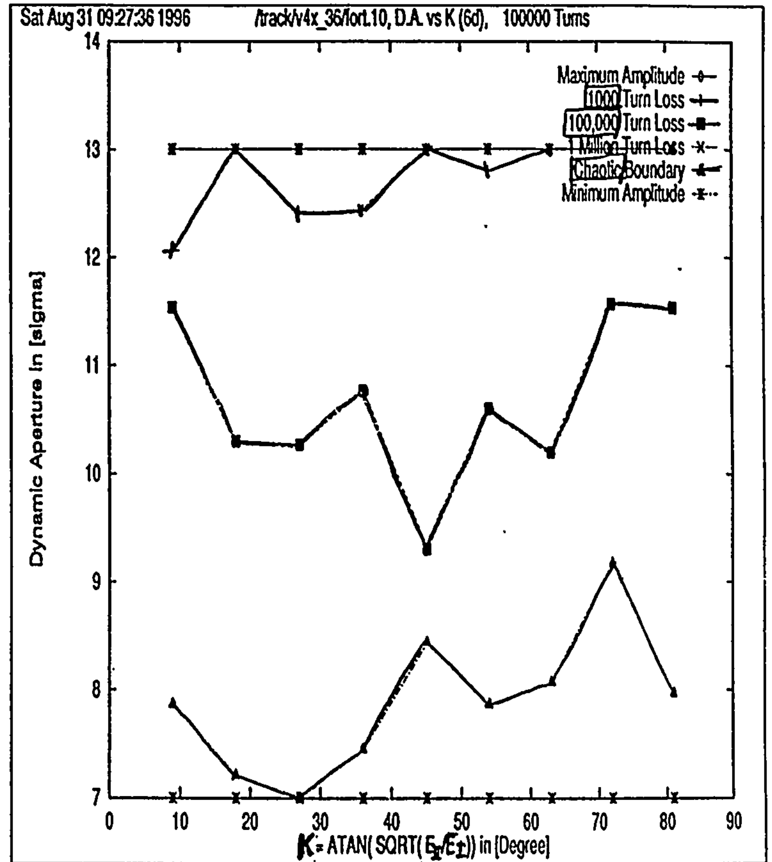
Sat Aug 31 09:27:36 1996
/track/v4x_36/fort.10, D.A. vs K (6d), 100000 Turns
Maximum Amplitude
1000 Turn Loss
100,000 Turn Loss
1 Million Turn Loss
Chaotic Boundary
Minimum Amplitude
Dynamic Aperture in [sigma]
K = ATAN(SQRT(E_II/E_⊥)) in [Degree]
C

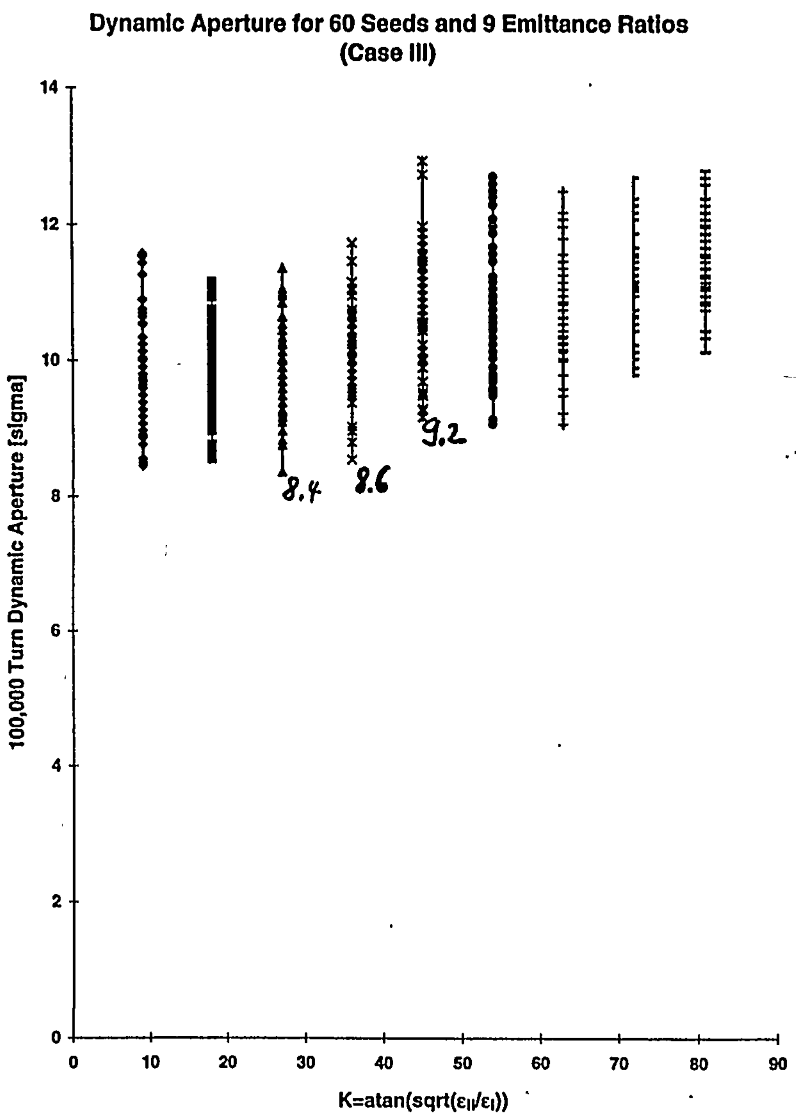

Status

- Fast Computers + automated Tracking Procedures
- Variation of Emittance ratio $C = \frac{\varepsilon_{II}}{\varepsilon_{I}}$ leads to a reduction of Dyn. Apr. 5–10% in Average and Minimum
- The reduction of the systematic octupole components per arc by 3 and 2 respectively
  $\Rightarrow$ 7.1 [sigma] $\longrightarrow$ 9.2 [sigma] Minimum Dyn. Aper.

  but still dominant
- Adding all linear imperfections
  $\Rightarrow$ Practically <u>no</u> effect $\boxed{8.9\ [\text{sigma}]}$
- Work in progress to "understand" dynamic aperture in terms of high order resonances
- Conjecture may bridge $10^5 - 10^7$ turns
  - stays within chaotic regime

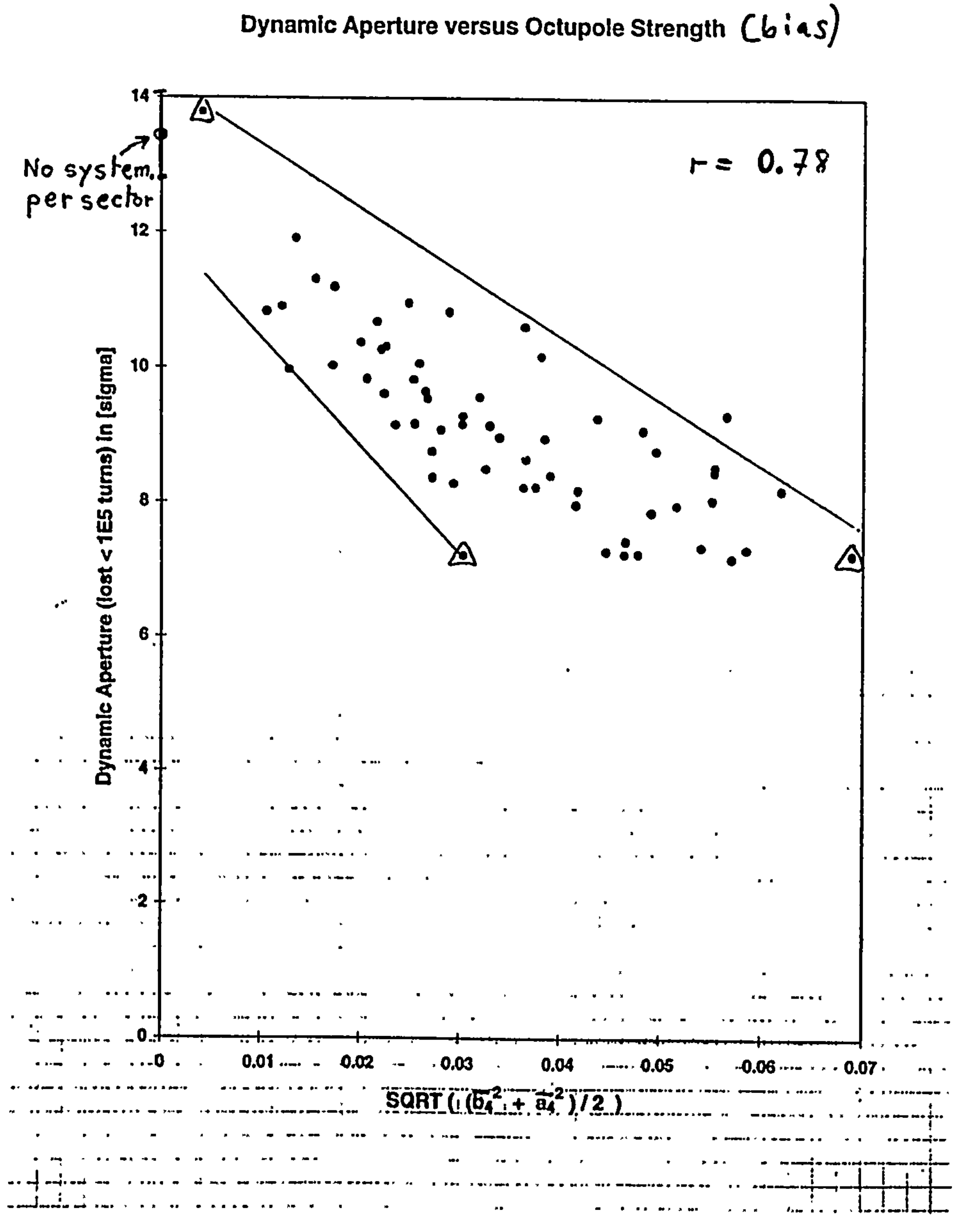

Dynamic Aperture versus Octupole Strength (bias)
r = 0.78
No system per sector
Dynamic Aperture (lost < 1E5 turns) in [sigma]
SQRT ((b_4^2 + a_4^2) / 2)

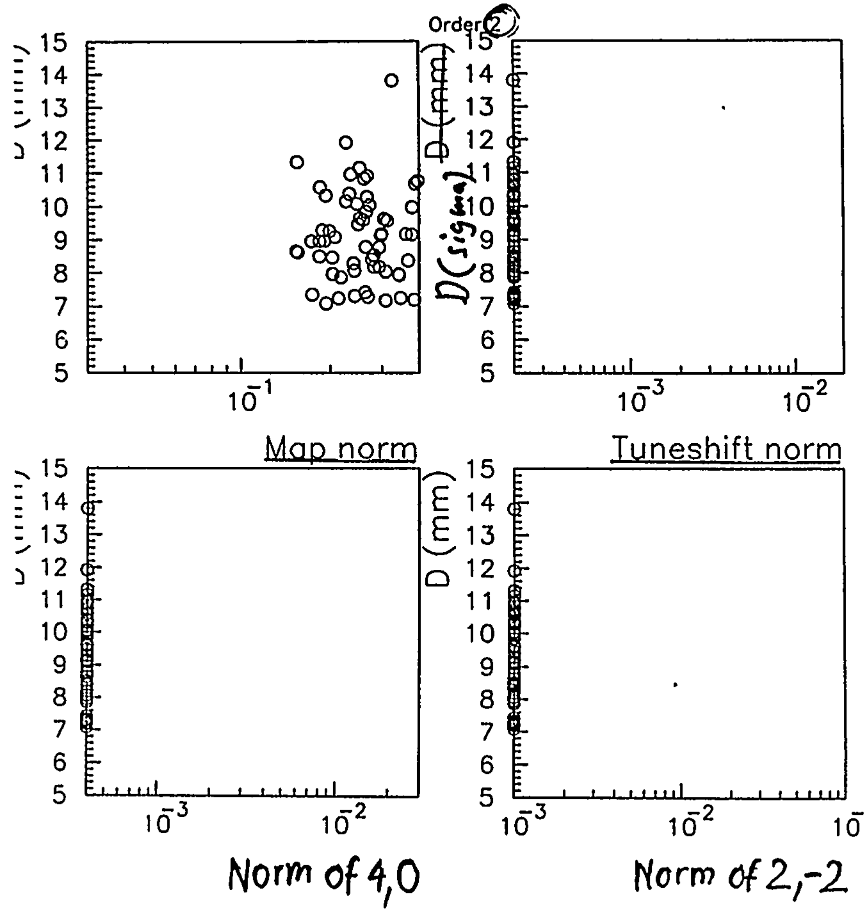

Order 2
D (mm)
D(sigma)
Map norm
Tuneshift norm
Norm of 4,0
Norm of 2,-2

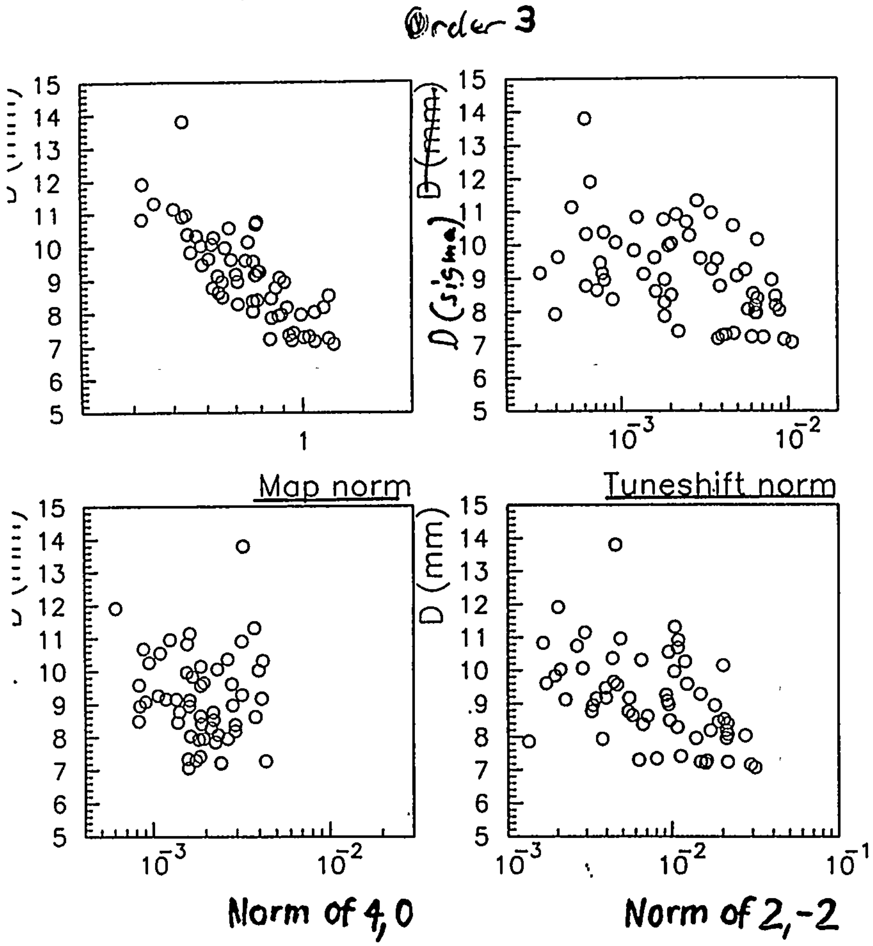
Order 3
D (mm)
D (sigma)
Map norm
Tuneshift norm
Norm of 4,0
Norm of 2,-2

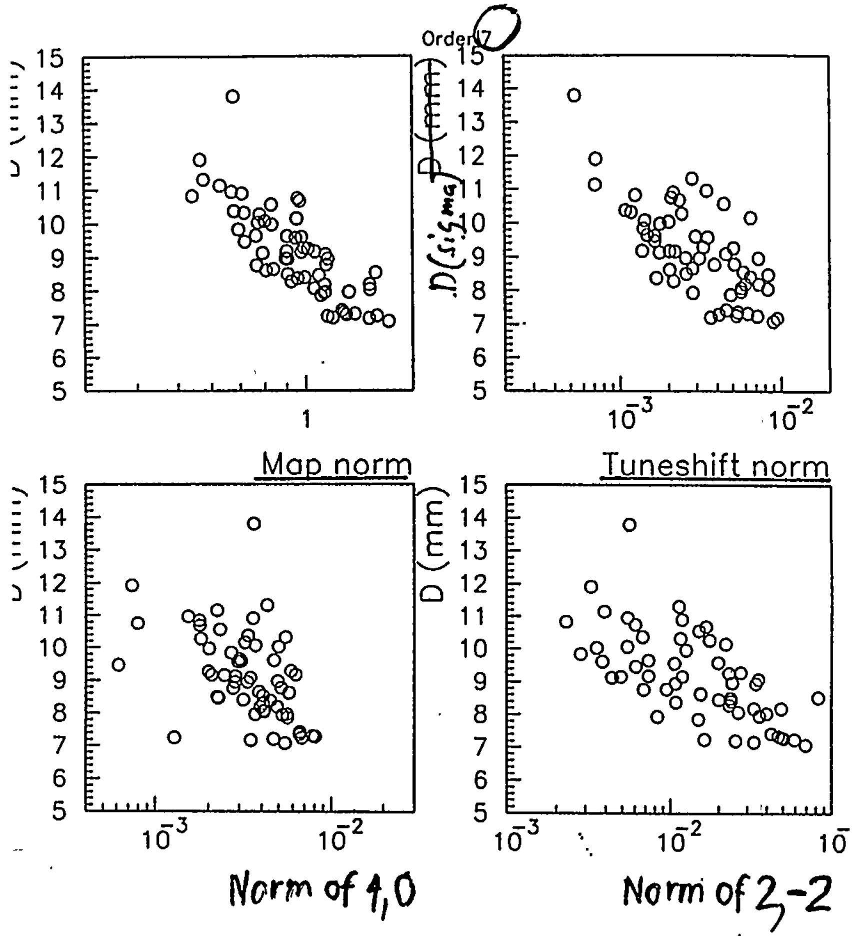
Order 7
D (mm)
D (sigma)
Map norm
Tuneshift norm
Norm of 4,0
Norm of 2,-2

LHC Version 4.2
Correction of bias of Octupoles

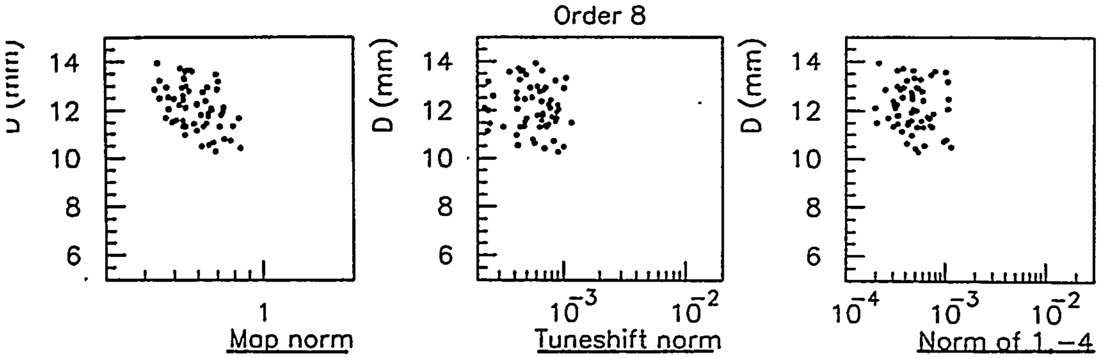

LHC Version 4.2 large bias due to systematic per Arc

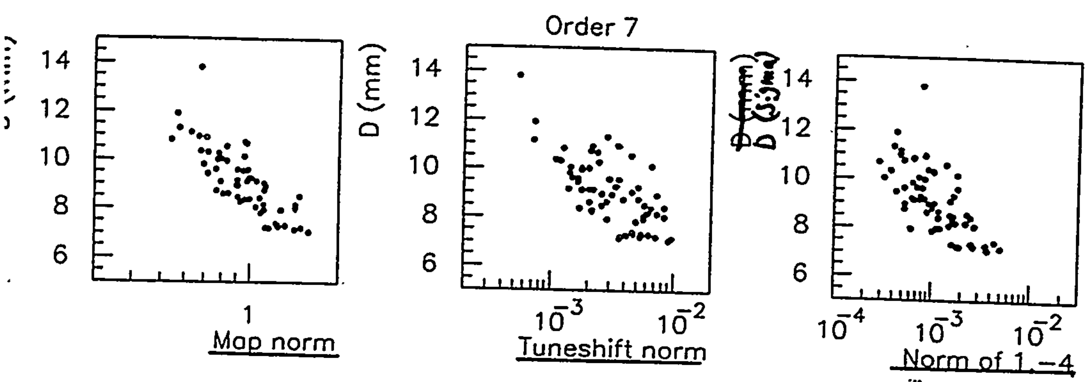

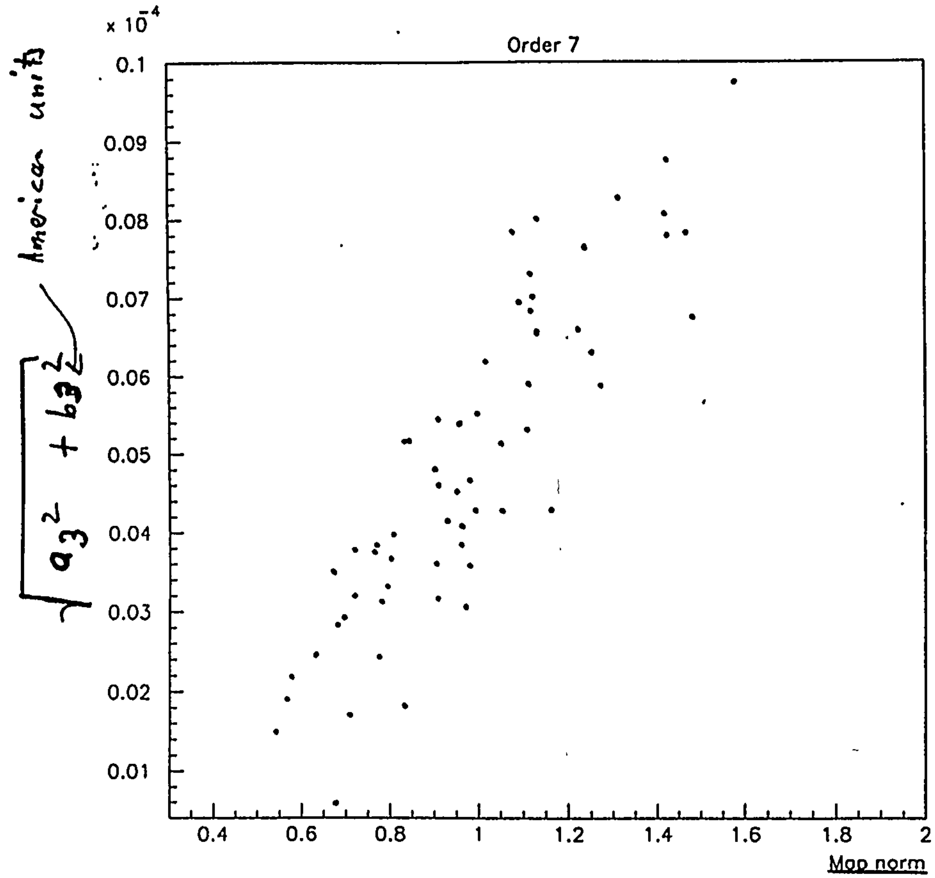

Visualization of the law:

Giovannozzi et al.
$\boxed{\text{LHC Proj. Rep. 45}}$
Part. Accel. in print

$$D(N) = D_\infty \left(1 + \frac{b}{\log N}\right)$$

$$\Rightarrow \quad \boxed{\log N \, D(N)} = \boxed{D_\infty} \log N + \boxed{D_\infty b}$$

Fit these values

" Survival Plot "

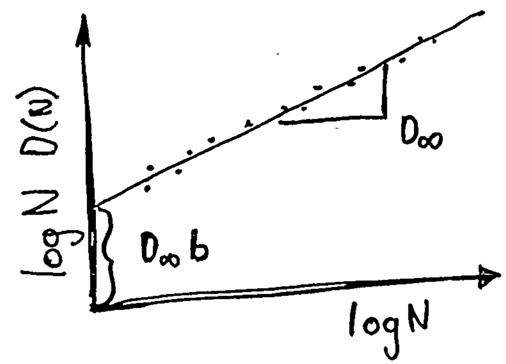

$\Rightarrow$ D_∞ with
b

$\Rightarrow$ $D(N)$ scaled with

Is this fulfilled ?

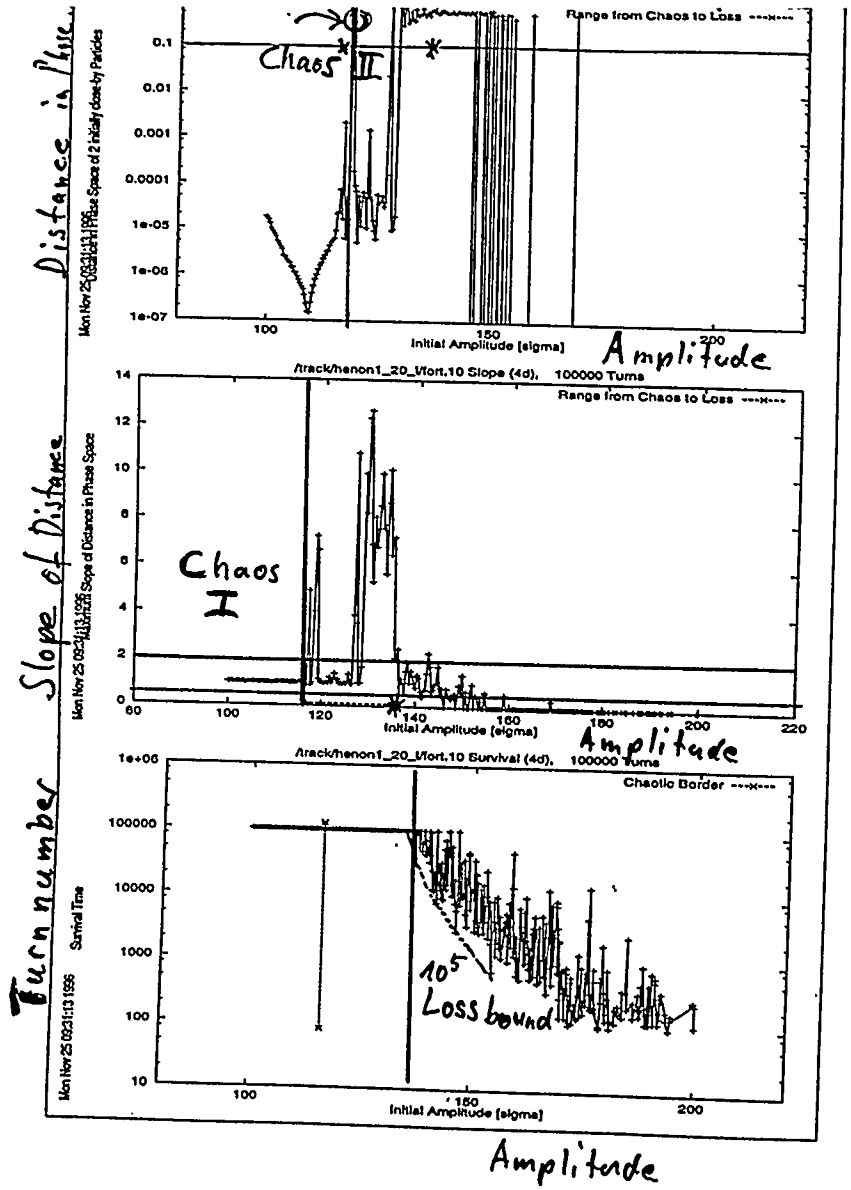
Distance in Phase
Chaos II
Range from Chaos to Loss
Initial Amplitude [sigma]
Amplitude
/track/henon1_20_Vfort.10 Slope (4d), 100000 Turns
Slope of Distance
Maximum Slope of Distance in Phase Space
Chaos I
Range from Chaos to Loss
Amplitude
/track/henon1_20_Vfort.10 Survival (4d), 100000 Turns
Turnnumber
Survival Time
Chaotic Border
10^5 Loss bound
Initial Amplitude [sigma]
Amplitude

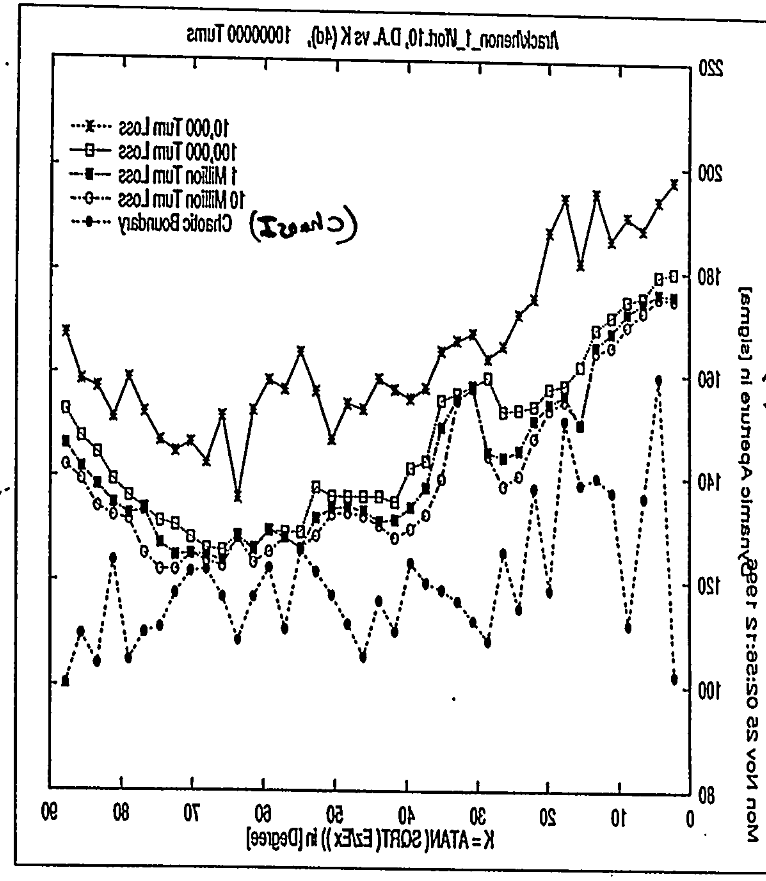
/track/henon_1_Vfort.10, D.A. vs K (4d), 10000000 Turns
10,000 Turn Loss
100,000 Turn Loss
1 Million Turn Loss
10 Million Turn Loss
Chaotic Boundary
(Chaos I)
Mon Nov 25 02:56:12 1996
Dynamic Aperture in [sigma]
D (N)
K = ATAN(SQRT(Ez/Ex)) in [Degree]

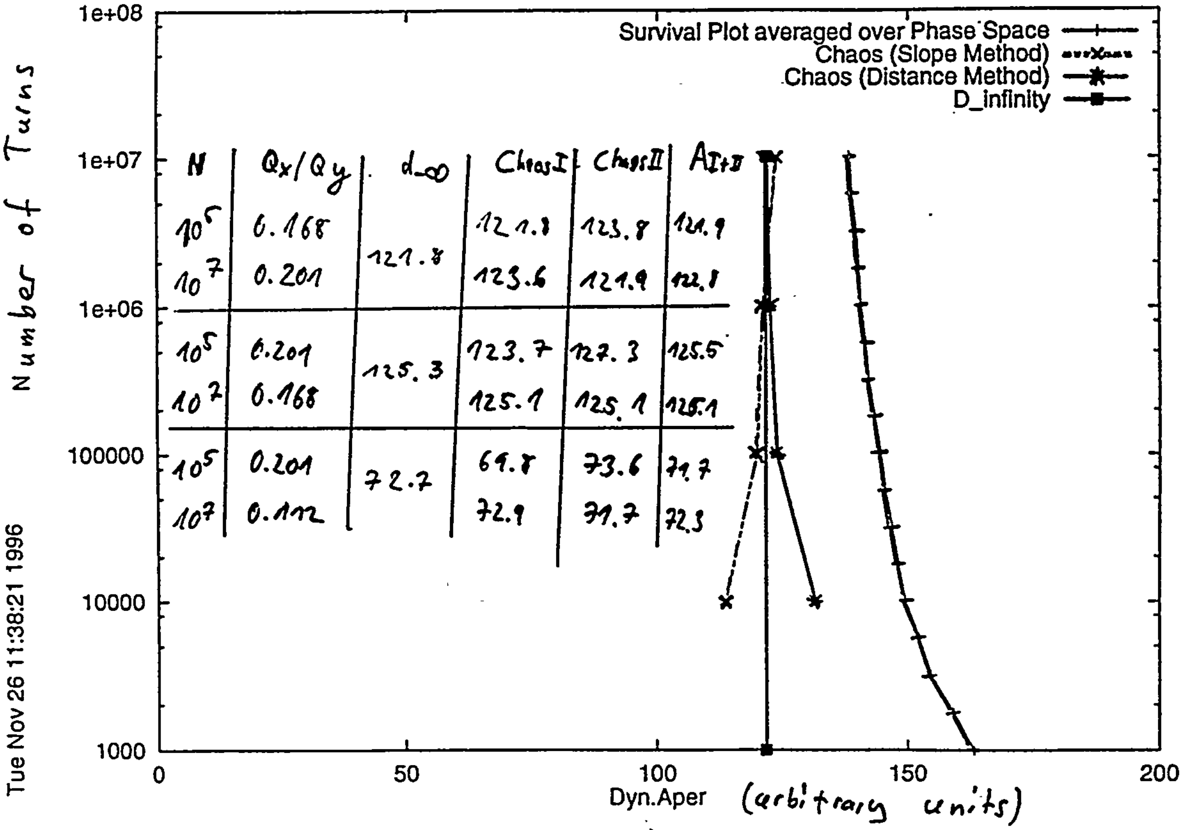

N	Q_x/Q_y	d_∞	Chaos I	Chaos II	A_{I+II}
10^5	0.168	121.8	121.8	123.8	121.9
10^7	0.201		123.6	121.9	122.8
10^5	0.201	125.3	123.7	127.3	125.5
10^7	0.168		125.1	125.1	125.1
10^5	0.201	72.7	69.8	73.6	71.7
10^7	0.112		72.9	71.7	72.3

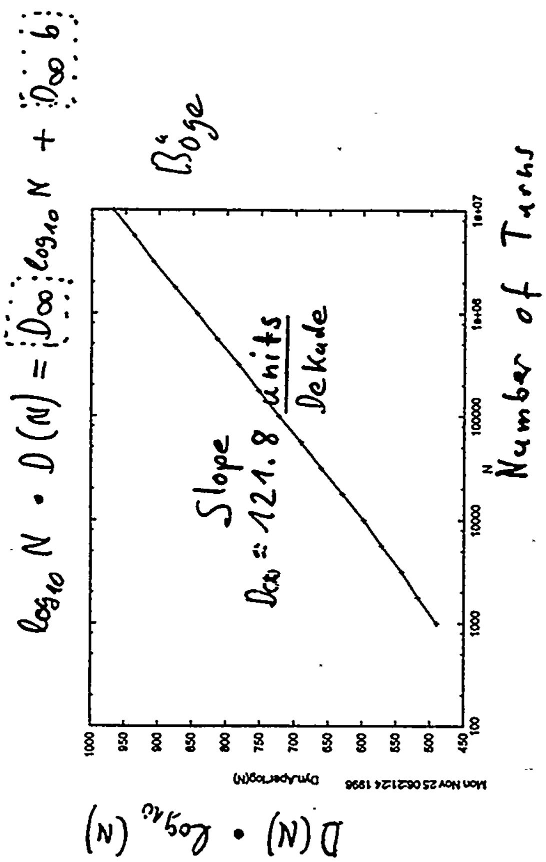

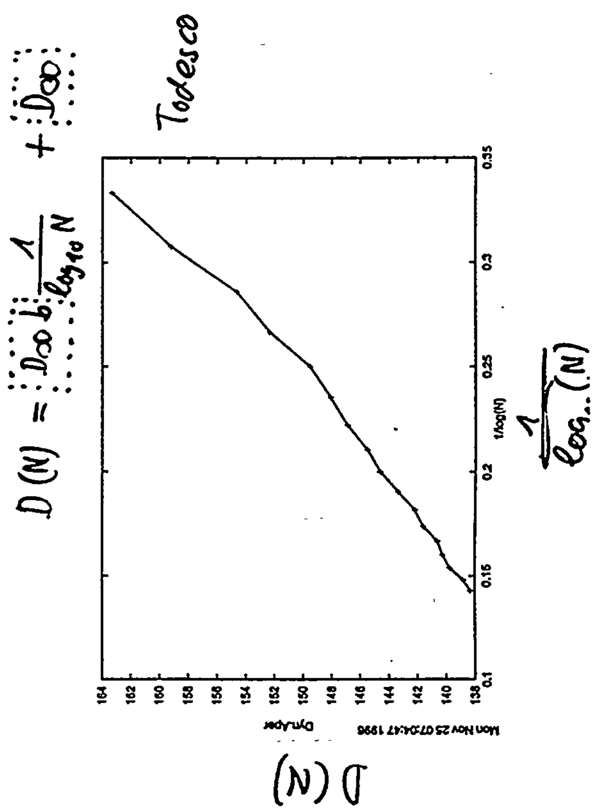

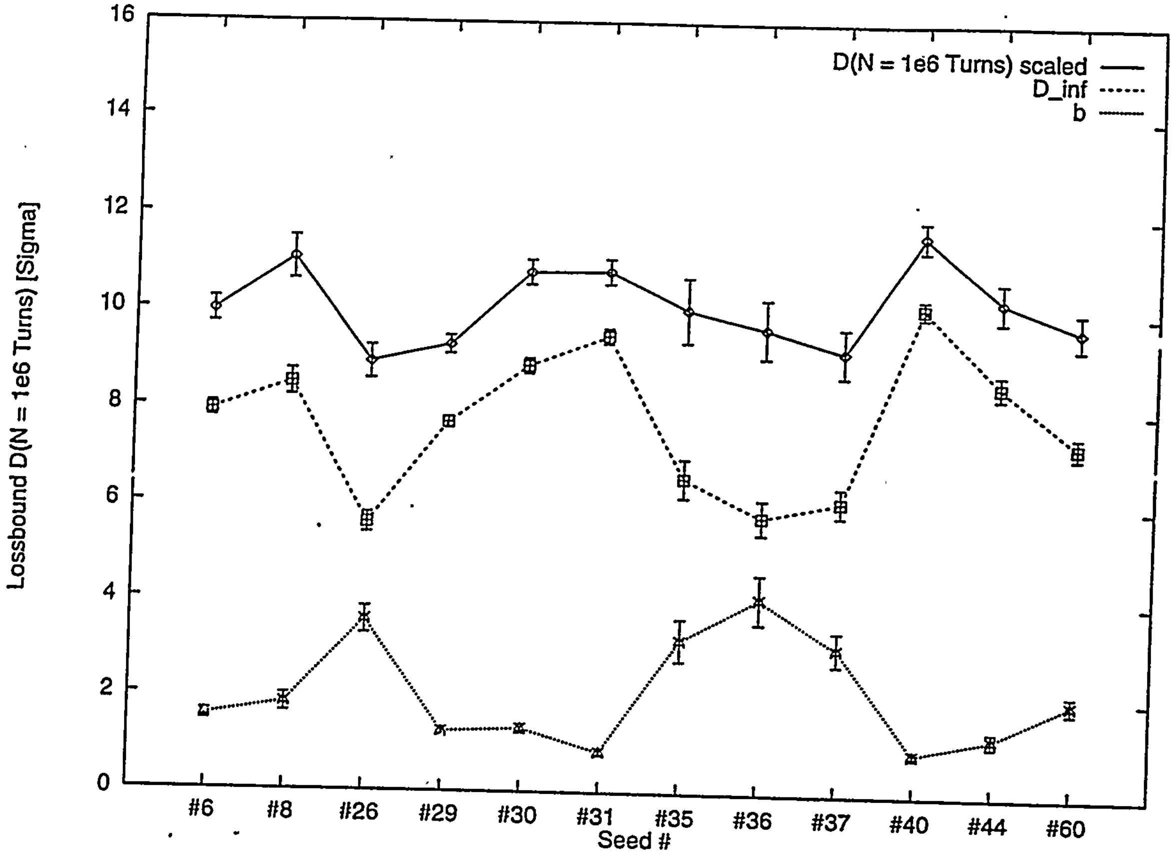

Dynamic Aperture plotted à la conjecture for 12 c

(→100,000 Turns)

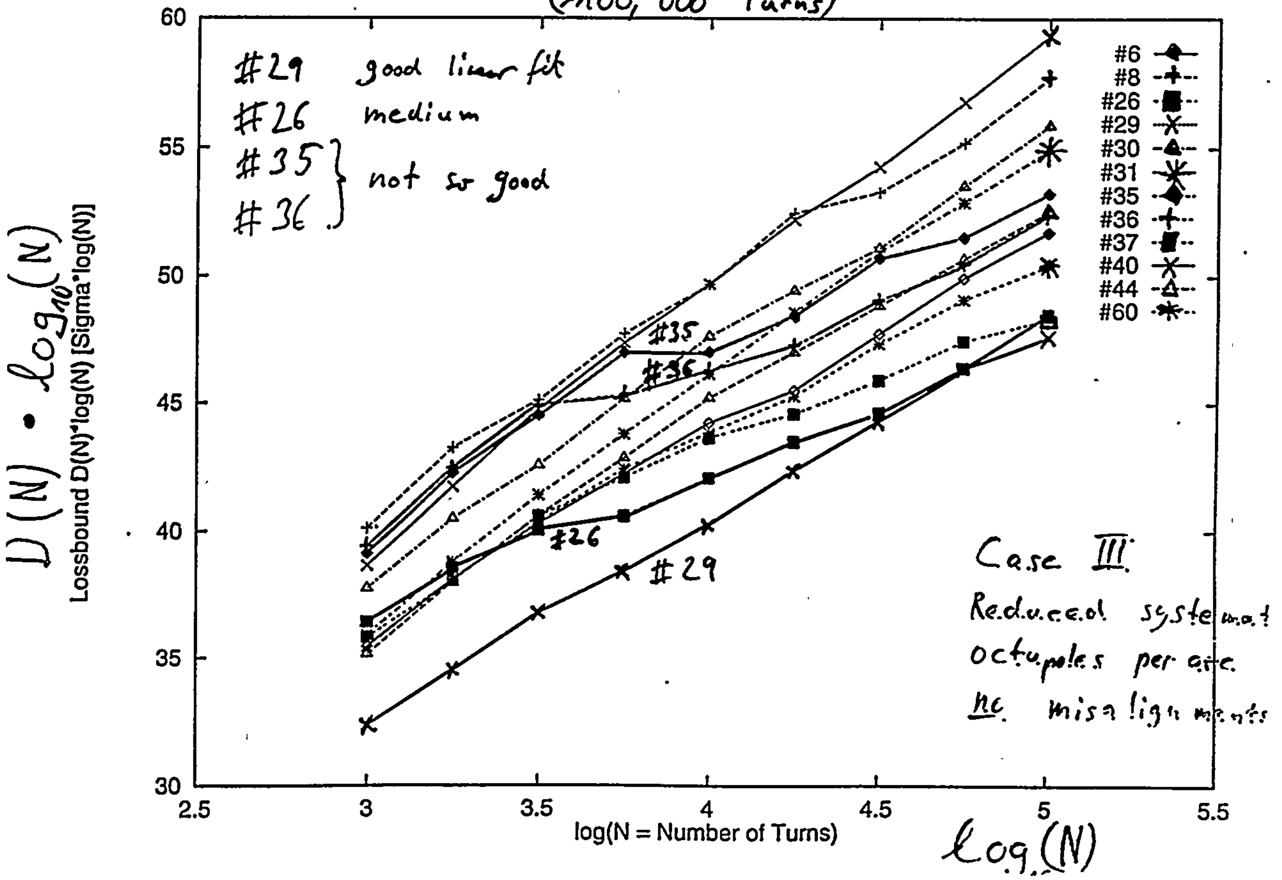

HIGH PRECISION TECHNIQUES FOR FREQUENCY ANALYSIS OF BETATRON MOTION

* J. LASKAR, C. FROESCHLE, A. CELLETTI
PHYSICA D 56, (1992), 253-269

* R. BARTOLINI, A. BAZZANI, M. GIOVANNOZZI, W. SCANDALE
E. TODESCO PART. ACC. 52, (1996), 147-177

- HIGH PRECISION ALGHORITMS FOR TUNE MEASUREMENT

$$z(n) = x(n) + i\,p_x(n) \qquad n = 1, \ldots, N$$

FFT $\quad \nu_j = \dfrac{j}{N} \qquad \varepsilon_{FFT} \propto \dfrac{1}{N}$

- INTERPOLATED FFT $\quad \nu \in [0,1] \qquad \varepsilon_{INT} \propto \dfrac{1}{N^2}$

\+ HANNING FILTER $\qquad \varepsilon_{HAN} \propto \dfrac{1}{N^4}$

- ITERATIVE SUBTRACTION PROCEDURE (LASKAR)

$$z(n) = \sum_k a_k\, e^{2\pi i \nu_k n} \qquad a_k \in \mathbb{C}$$

- IDENTIFICATION OF THE FREQUENCIES AS HARMONICS OF THE TUNES Q_x, Q_z

$$\nu_k = l\,Q_x + m\,Q_z + p$$

- LIMITS:

THE DECOMPOSITION WORKS FOR QUASI-PERIODIC SIGNALS (REGULAR MOTION) NOT IN CHAOTIC REGIONS

$\sqrt{\hat{X}^2 + \hat{P}_x^2}$

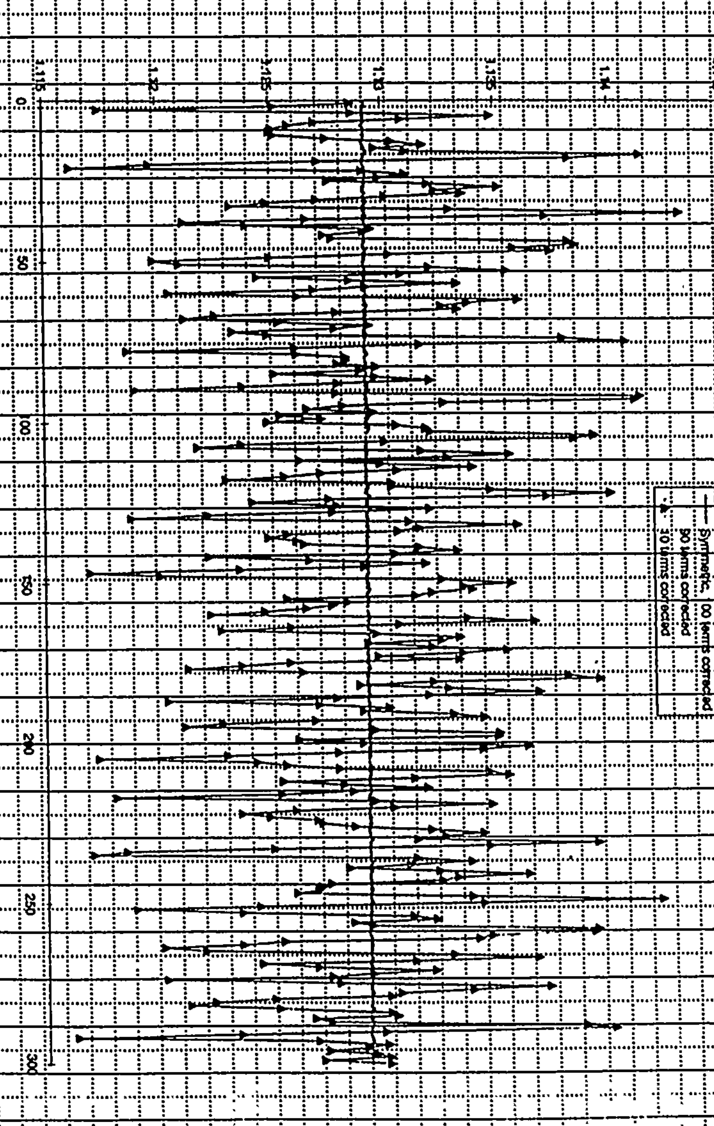

10 lines ⇒ 90% reduction

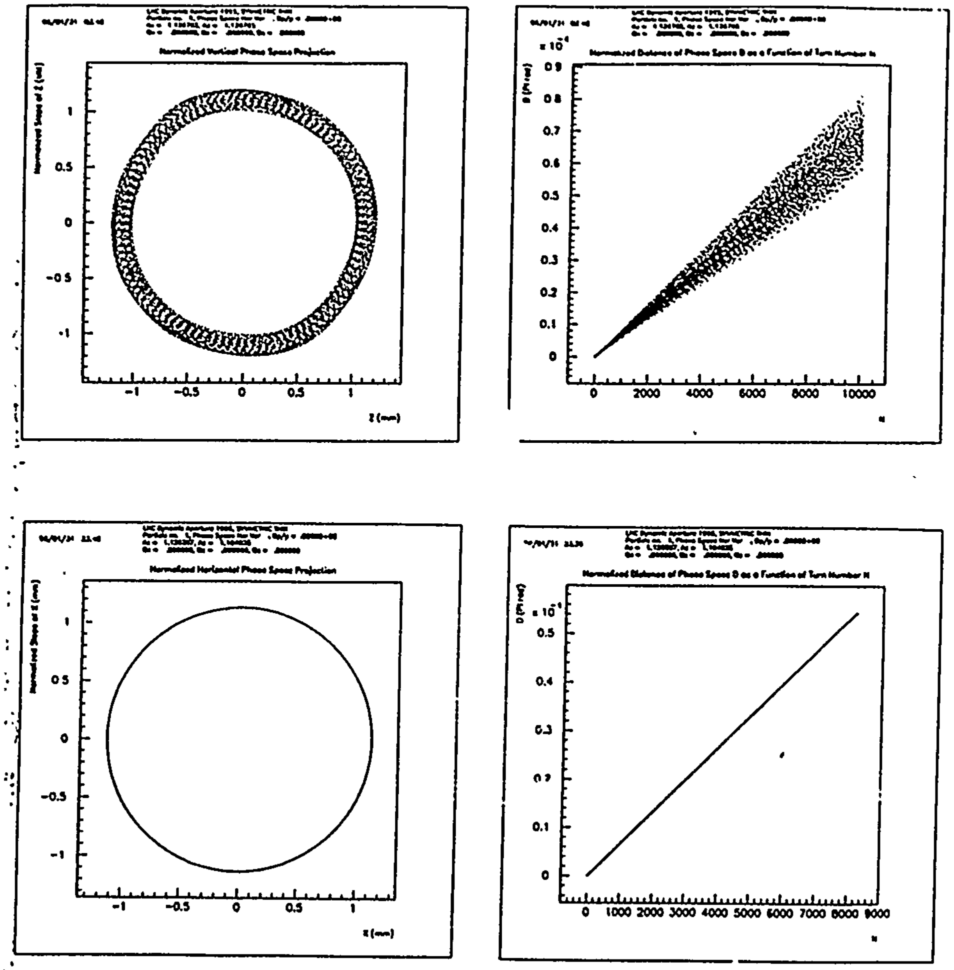

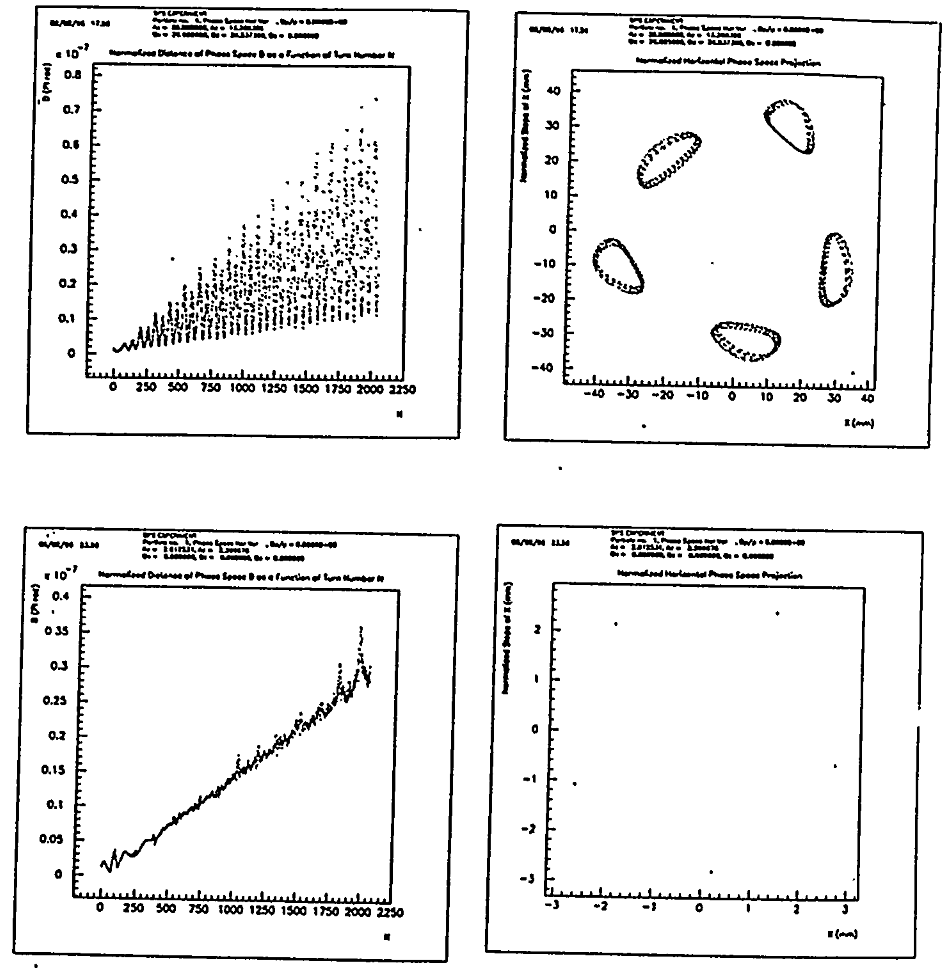

- SUBSEQUENT SUBTRACTION OF NEXT TO LEADING FREQUENCY TAKES OUT THE DISTORTION OF THE ORBIT IN PHACE SPACE AND IN THE DISTANCE IN PHASE SPACE

- HIGHER TERMS IN THE FREQUENCY DECOMPOSITION ARE .

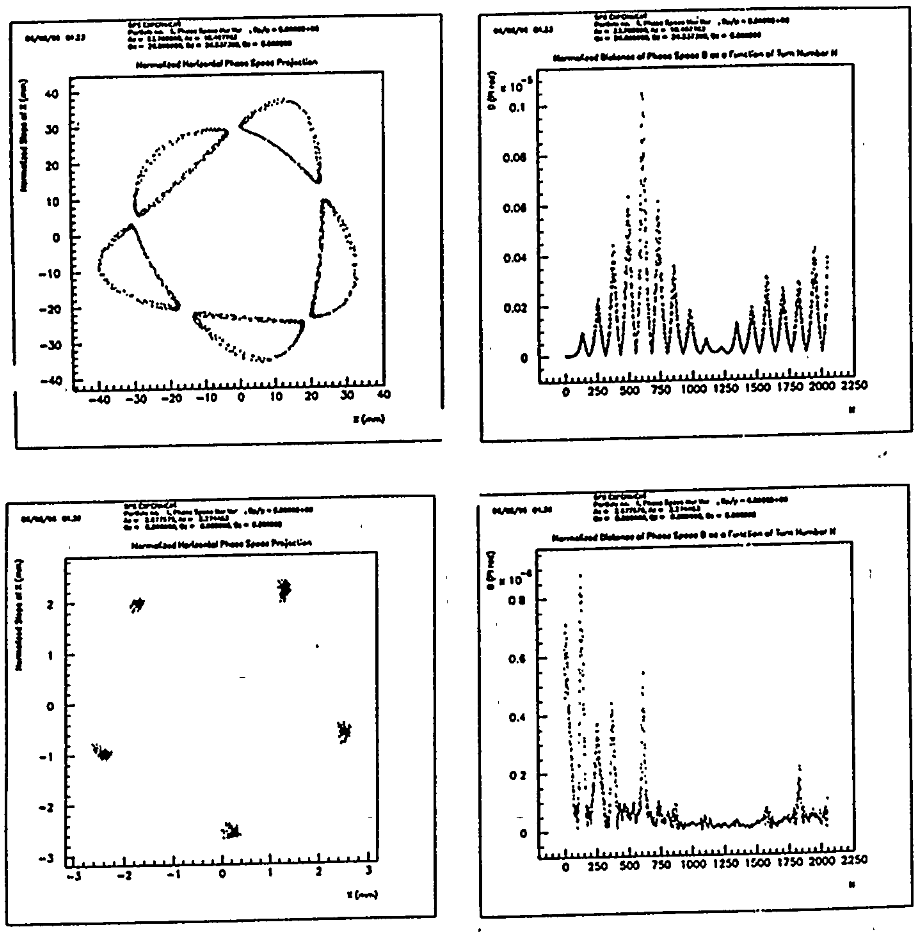
Normalized Horizontal Phase Space Projection
Normalized Distance of Phase Space D as a Function of Turn Number N

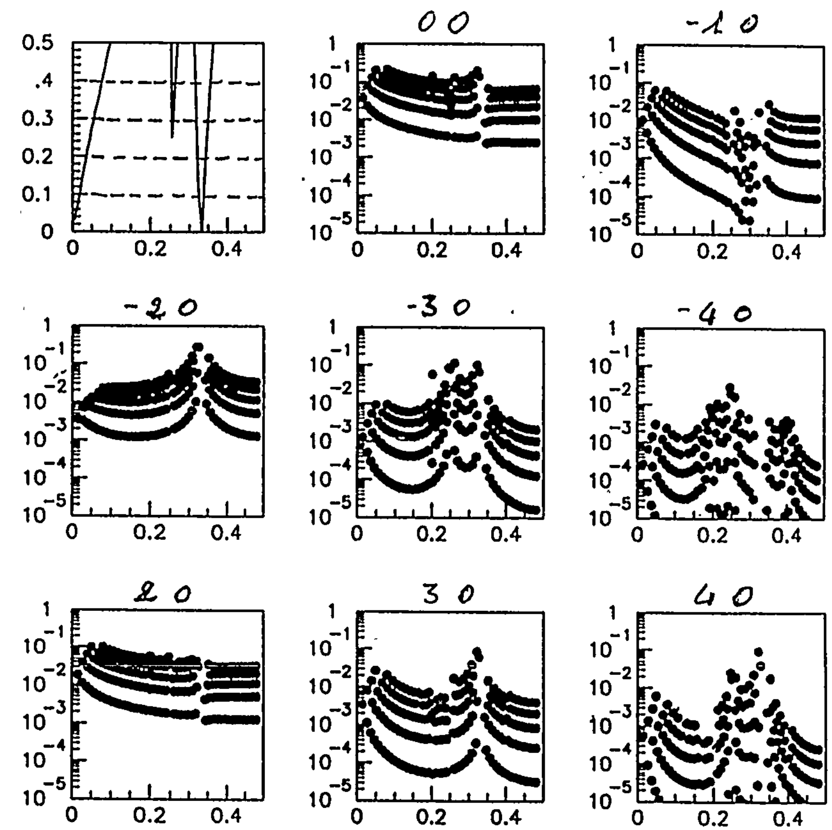
0 0
-1 0
-2 0
-3 0
-4 0
2 0
3 0
4 0

Position of Correctors for (3,0) Resonance

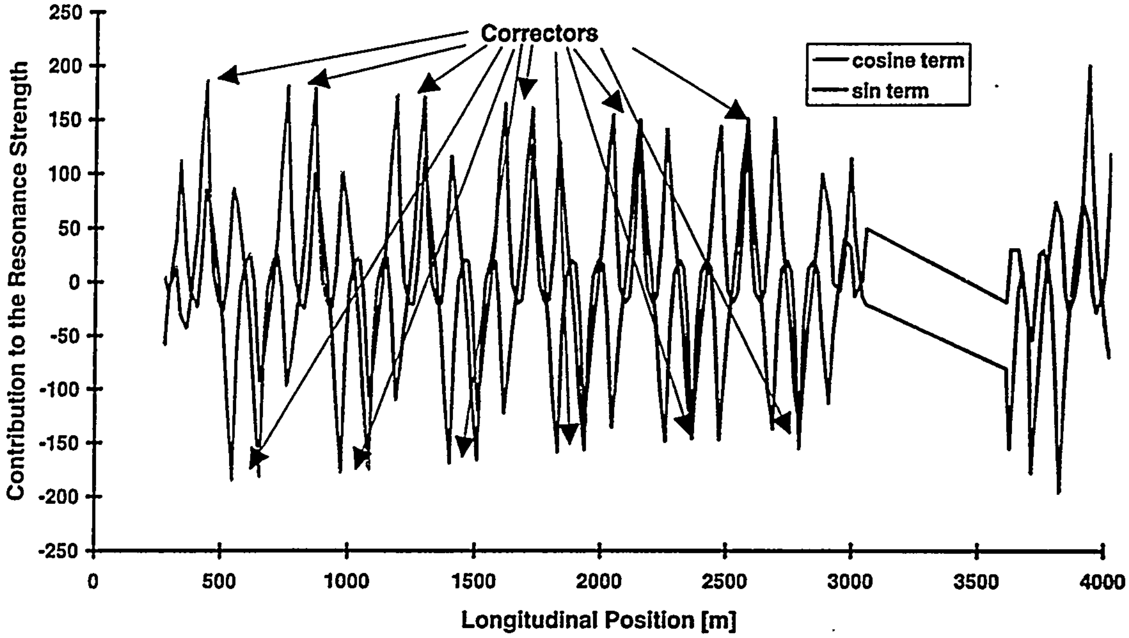

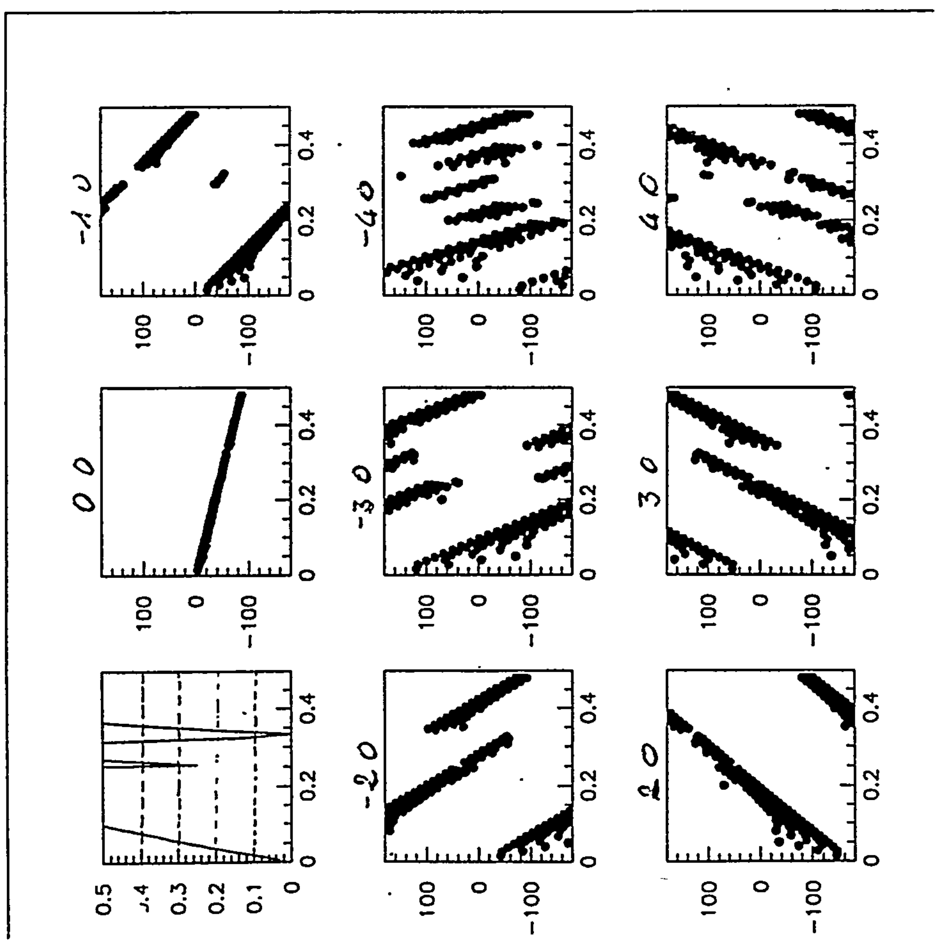

CORRECTION OF (3,0) AND (1,2) IN THE UNPERIODIC LHC

- NOT WITH THE LINES BUT REDUCING THE DRIVING TERM (1.st ORDER IN GRADIENT)
- 5 FAMILIES OF CORRECTORS TAKEN FROM A SINGLE FAMILY MEANT TO CORRECT THE b_3 COMPONENT OF THE DIPOLES

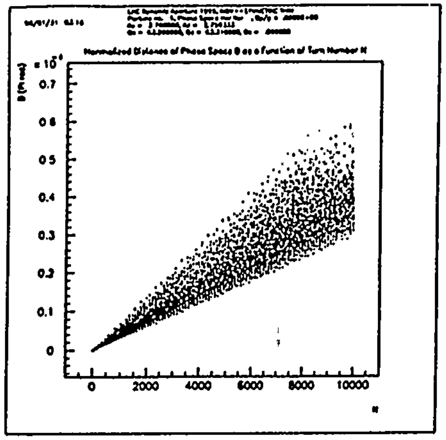

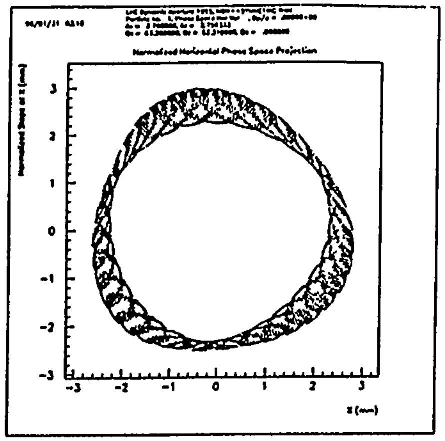

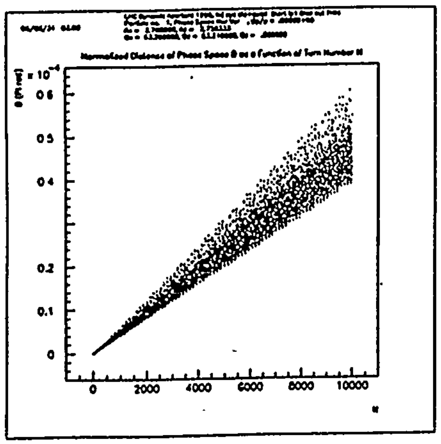

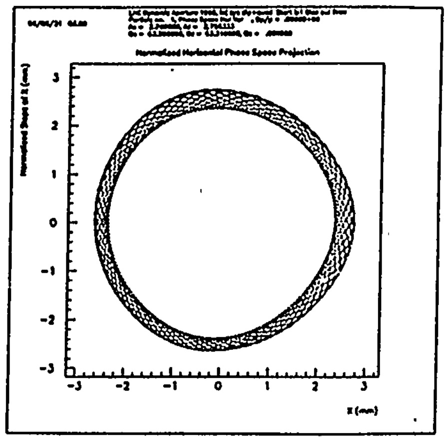

RESULTS	PERIODIC	NO CORR.	UNPERIODIC (3,0) CORR	(3,0) and (1,2)
REGULAR	18.0	15.6	16.1	16.9
CHAOS	18.25	16.0	16.4	17.1
LOST (1MT)	18.5	16.9	17.1	18.0

LONGITUDINAL BEAM ECHOES & DIFFUSION RATES

F. Ruggiero, CERN

MEASUREMENT OF LONGITUDINAL BEAM ECHOES IN THE CERN-SPS

O. BRÜNING, T. LINNECAR, F. RUGGIERO
W. SCANDALE, E. SHAPOSHNIKOVA, D. STELLFELD

- ILLUSTRATION & MOTIVATION
- ANALYTIC ESTIMATES
- EXPERIMENTAL DATA
  - COASTING BEAM : DIFFUSION RATES
  - BUNCHED BEAM : VERY RECENT

http://wwwslap.cern.ch/collective

Echo Phenomenon

1950: Spin Echoes (E. Hahn)

1968: Plasma Wave Echoes
(T. O'Neil & R. Gould)

1992: Echo Effect in Hadron Colliders
(G. Stupakov) (Theory)

1994: Longitudinal Beam Echoes
(P. Colestock & L. Spentzouris)
(Theory & Measurement)

1995: Beam Echoes in the SPS
(Theory & Measurement)

G. Stupakov & S. Kauffman SSCL-587, '92

'Echo Effect in Accelerators' (Transverse Plane)

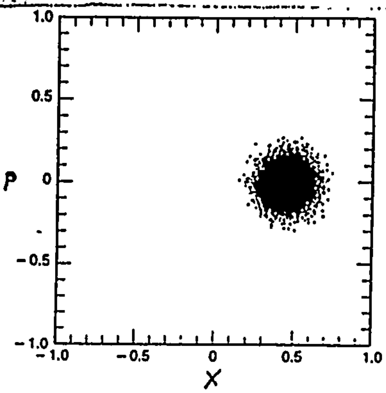

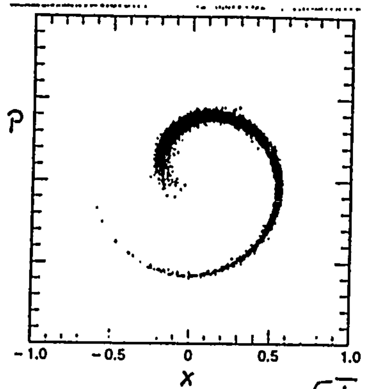

5 Turns

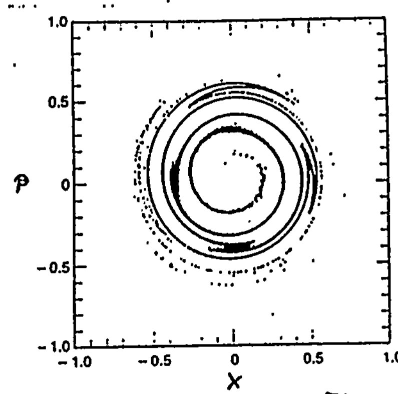

30 Turns

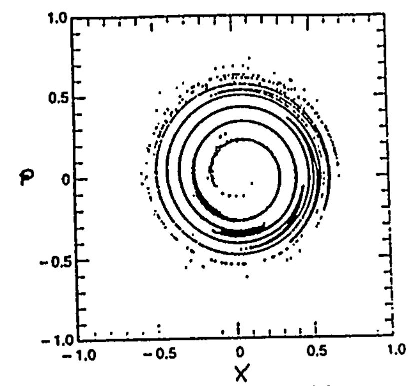

35 Turns

$Q_x = Q_x(A)$

<X> vs. Time

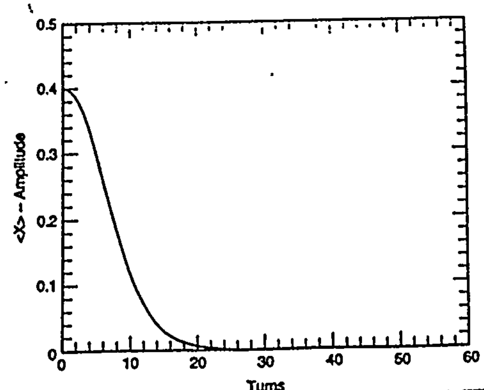

Quad Kick:

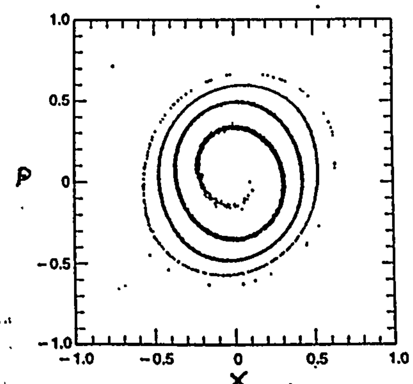

[illegible] Turns

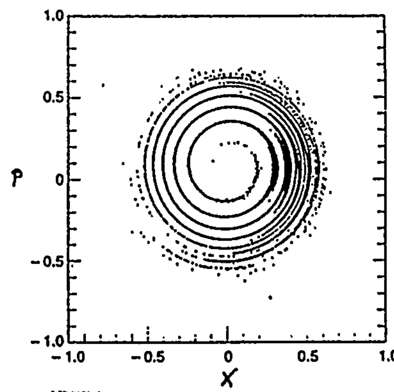

40 Turns

<X> vs. time

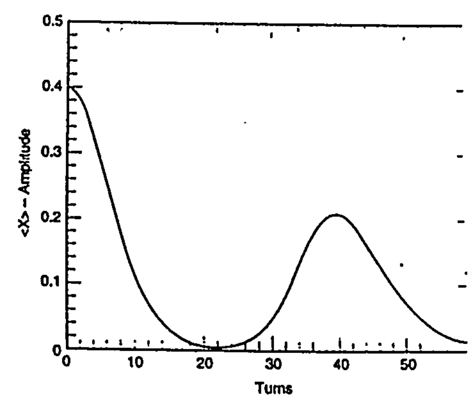

Longitudinal Echo Formation

$h = 1 \rightarrow \omega_{RF} = \omega_{Rev}$

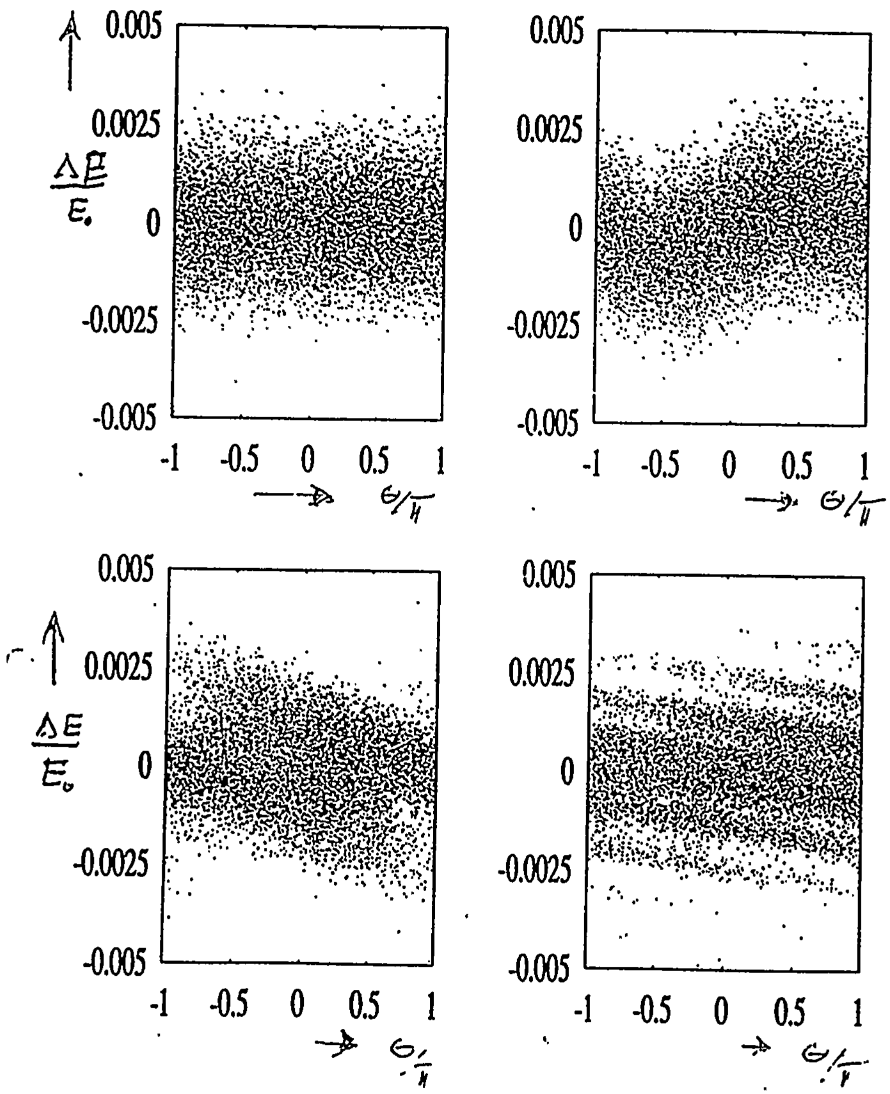

$h = 2 \rightarrow \omega_{RF} = 2 \cdot \omega_{Rev}$

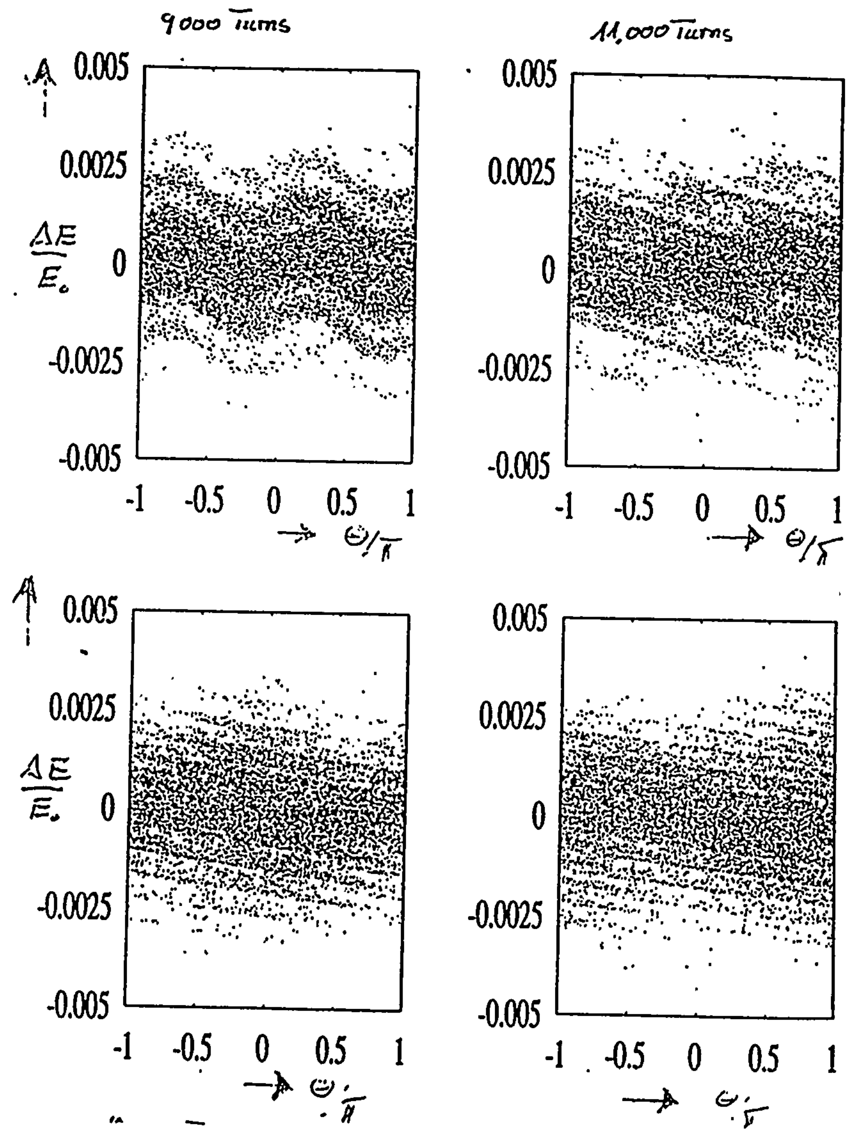

Echo Response in the beam current

$$I(t,\Theta) = e \cdot \omega_0 \cdot \int \rho\left(\frac{\Delta E}{E_0}, \Theta, t\right) d\frac{\Delta E}{E_0}$$

$$\rho\left(\frac{\Delta E}{E_0}, \Theta, t\right) = \sum_l \rho_l\left(\frac{\Delta E}{E_0}, t\right) \cdot e^{il\Theta}$$

$$\rightarrow \quad \underline{I(t,\Theta) = \sum_l I_l(t)\, e^{il\Theta}}$$

$l=1$ Mode

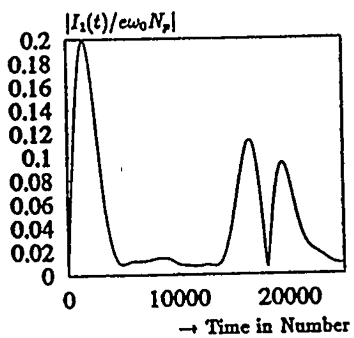

$l=2$ Mode

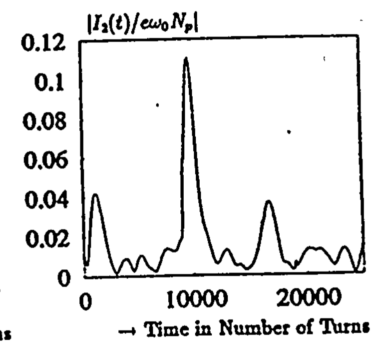

First Measurements in the Fermilab $\bar{p}$ Accumulato.

$f_{rev} = 687\,\mathrm{KHz}$, $N_p = 5\cdot10^{10} \leftrightarrow \underline{2\cdot10^{11}}$, $\eta = 0.023$

$E_0 = 8.696\,\mathrm{GeV}$, $\frac{\Delta P}{P_0} = 5\cdot10^{-4}$

$h_1 = 9$

$h_2 = 10$ Echo: $h = 1$

(Spentzouris, Ostiguy, Colestock '95)

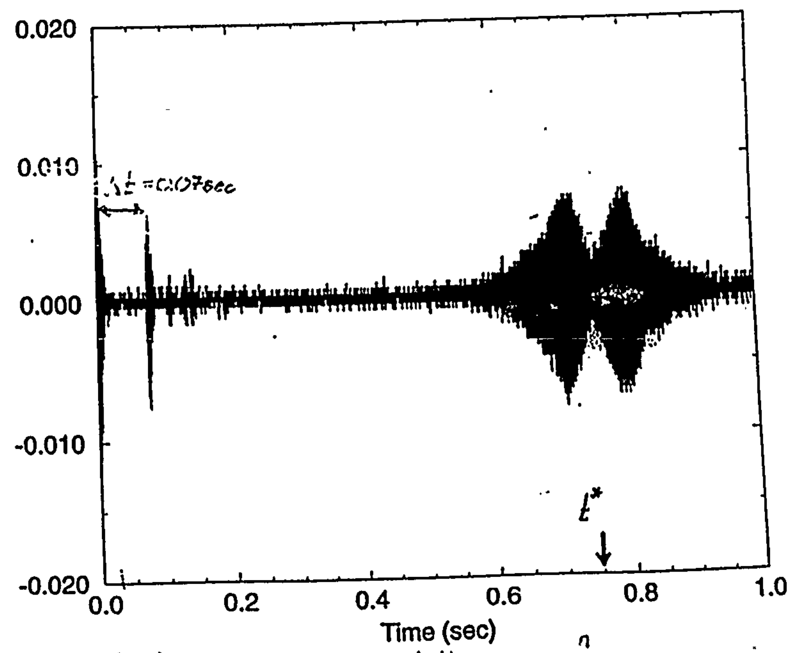

The Echo Signal relies on an accurate Reconstruction of the Phase Space Information

→ Measure for small disturbances

- Coulomb scattering
- Noise
- Diffusion

→ Instantaneous measurement of Diffusion or Cooling

→ Measurement of the Beamdistrib.

Echo Response

▶ Two Sin - RF Kicks with harmonic numbers h_1 and h_2 length T_1 and T_2 and a time separation Δt :

→ Echo at harmonic $h_2 - h_1$

→ $t^* = \frac{h_2}{h_2 - h_1} \cdot \Delta t \qquad h_2 > h_1$

$$I_{h_2-h_1}(t) = \underbrace{F_{env}}_{\text{Envelope}} \cdot \underbrace{F_{FF}}_{\text{Form Factor}} \cdot \underbrace{F_D}_{\text{Diffusion / Damping}}$$

Echo Envelope

$$\left| I_{h_2 - h_1}(\tau) \right| \propto e\,\omega_0 \left| J_1(\varepsilon_1 \tau) \cdot J_1(x + \varepsilon_2 \tau) \right|$$

with $\varepsilon_i = \dfrac{\omega_0 T_i}{2\pi} \cdot \dfrac{e V_i}{E_0}$

$$\tau = \frac{\omega_0 \eta}{\beta^2} \cdot (h_2 - h_1) \cdot (t - t^*)$$

$$x = h_1 \varepsilon_2 \cdot \frac{\omega_0 \eta}{\beta^2} \cdot \Delta t$$

$\Longrightarrow$ Function of RF-parameters only

$\Longrightarrow$ Max. Echo response around $x = 1.8$

$\Longrightarrow$ Asymmetry for $J_1'(x) \neq 0$

$\Longrightarrow$ Valid for <u>impulsive</u> RF-kicks to all orders in ε_i

SPS Parameter

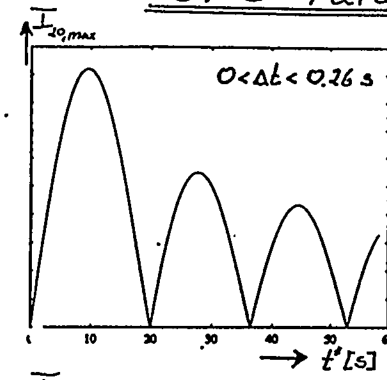

$f_{rev} = 43.3$ kHz

$\eta = 1.8 \cdot 10^{-3}$

$\frac{\Delta p}{p_0} = 10^{-3}$

$E_0 = 120$ GeV

$h_1 = 4600$

$h_2 = 4620$

$T_i = 4$ Turns

$V_i = 500$ kV

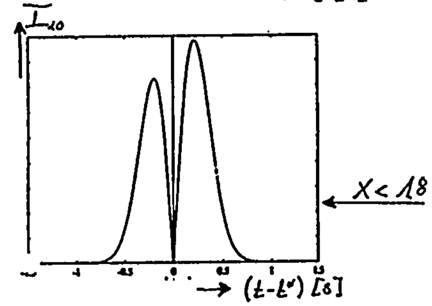

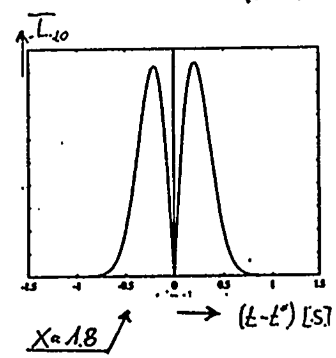

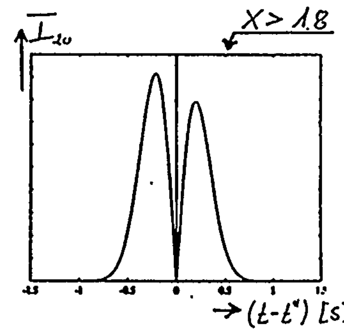

Form Factor

▶ Symmetric Distribution:

$$\rho(\delta) = \rho(-\delta) \qquad \delta = \frac{\Delta E}{E_0}$$

$$I(\tau) \propto \tau \cdot \underbrace{\int \rho(\delta) \cdot \cos(\delta\tau)\, d\delta}$$

$$\underline{\frac{1}{2}\left[\mathcal{F}[\rho(\delta)] + \mathcal{F}[\rho(-\delta)]\right] \cdot \tau}$$

→ The Beamdistribution can be recovered from the Echo Shape

Gaussian Distribution

$$\rho(\delta) = \frac{1}{\sqrt{2\pi}\,\sigma_\delta} \cdot e^{-\delta^2/2\sigma_\delta^2}$$

$$\rightarrow \tau \int \rho(\delta) \cdot \cos(\delta\tau)\, d\delta = \underline{\tau \cdot e^{-\tau^2\sigma_\delta^2/2}}$$

- Scaling with $(h_2 - h_1)$:
  $(\tau \propto h_2 - h_1)$
- Scaling with σ_δ :

$$\Delta\tau = 2/\sigma_\delta$$

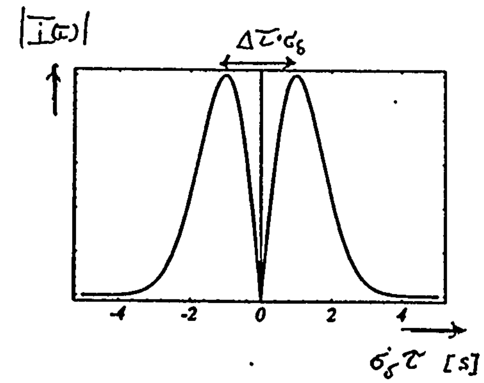

Parabolic Distribution

$$\rho(\delta) = a\cdot\left(1-\frac{\delta^2}{\delta_m^2}\right)\;;\quad \delta < \delta_m$$

$$\longrightarrow \tau\cdot\int \rho(\delta)\cdot\cos(\delta\tau)\,d\delta = 4\left[\frac{\sin(\tau\cdot\delta_m)}{\delta_m^2\cdot\tau^2} - \frac{\cos(\tau\cdot\delta_m)}{\delta_m\cdot\tau}\right]$$

- scaling with (h_2-h_1) and δ_m

$$\Delta\tau\cdot\delta_m = 4$$

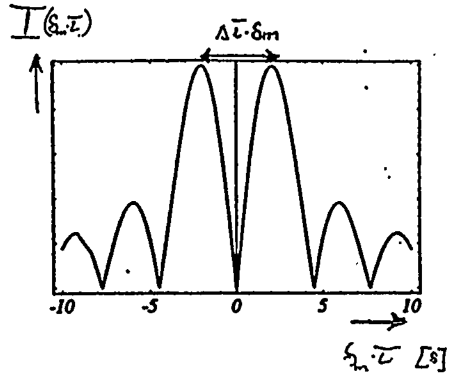

Diffusion

$$I(t) \propto \exp\cdot\left(-D\cdot k_0^2\cdot(h_2-h_1)^2\cdot t^3/3\right)\;;\quad k_0 = \frac{\omega_0\cdot 2}{\beta^2}$$

$$\Longrightarrow \quad D_{min} \approx 10^{-12}\,s^{-1} \quad \text{for} \quad t < 30\,\text{sec}$$

$$\Delta\sigma^2 = D\cdot t$$

$$\Delta\sigma = 10^{-3} \longrightarrow t = 11 \text{ days}$$

$\Longrightarrow$ Instantaneous measurement of Diffusion or Cooling for small Diffusion Coefficients

Experimental Setup

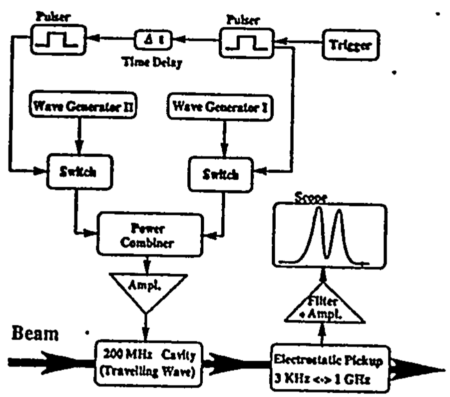

Figure 1: Schematic setup for the Echo measurements.

Parameters:

$h_1 = 4600$ $\quad h_2 = 4620$

$V_i = 500\,kV$

$T_i = 92.22\,\mu s$ $\quad$ 4 Turns

Δt : $5\,ms \longleftrightarrow 300\,ms$

t^* : $1\,s \longleftrightarrow 30\,s$

Echo Shape

- Gaussian Distribution:

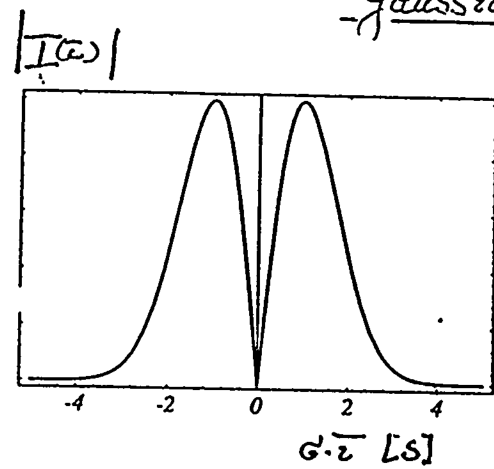

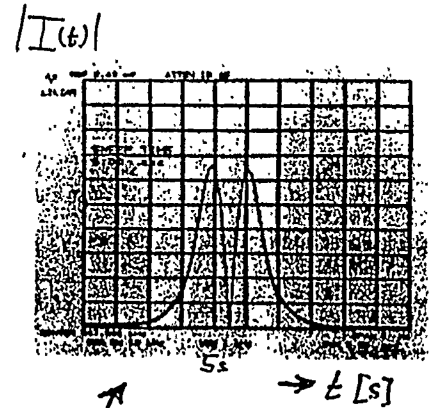

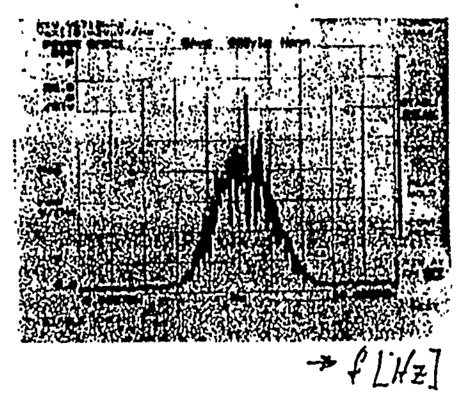

$\Rightarrow \quad \sigma_{Echo} = 4.1 \cdot 10^{-4} \qquad \sigma_{Sch} \approx 5 \cdot 10^{-4}$

$$f(\rho) = \left(1 - \frac{\rho^2}{\rho_m^2}\right)$$

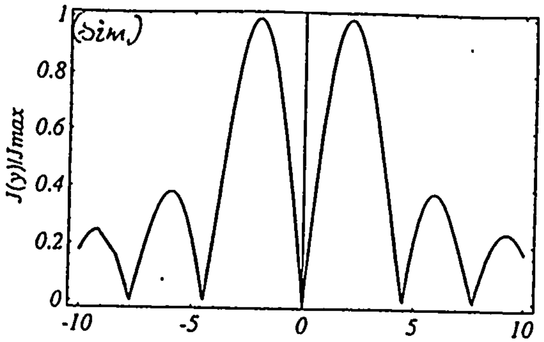

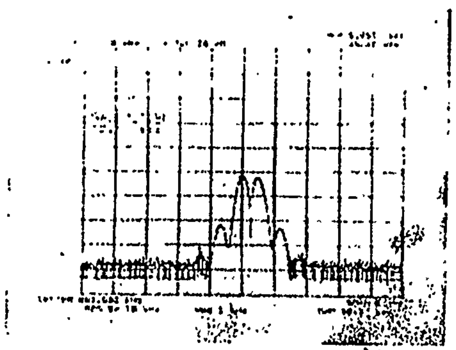

Meas.

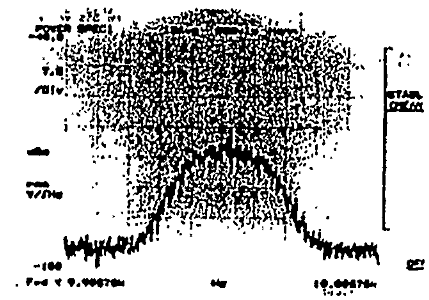

(Meas)

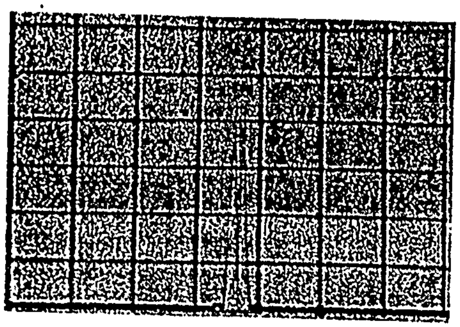

Meas

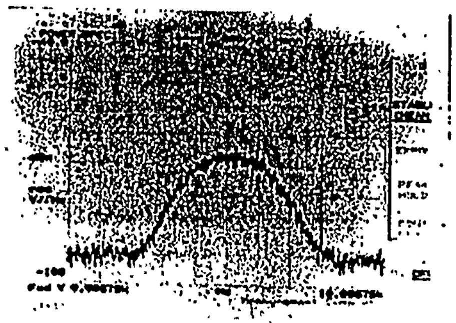

Meas

SPS: December 1995

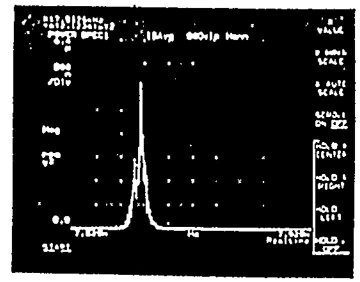

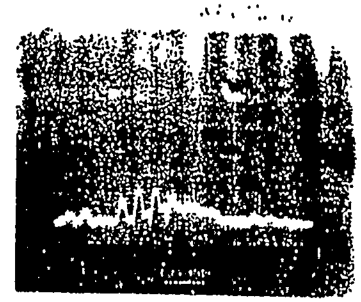

$\Delta t = 15$ msec

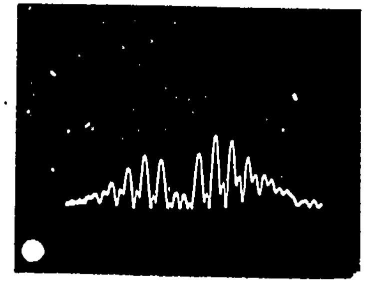

$\Delta t = 25$ msec

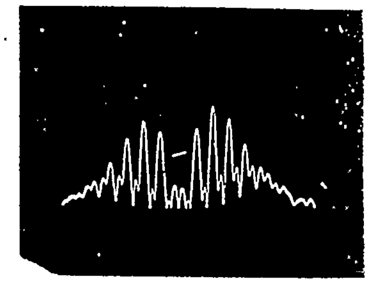

$\Delta t = 35$ msec

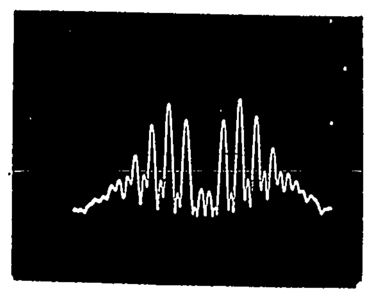

$\Delta t = 45$ msec

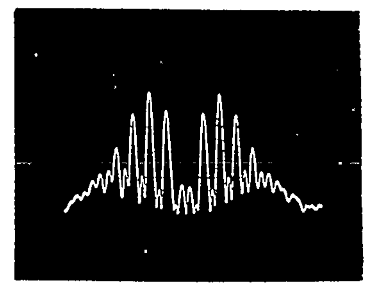

Diffusion:

$$\frac{d}{dt}\left(\frac{\Delta p}{p_0}\right) = \sqrt{2D} \cdot \xi(t)$$

$\xi(t)$ = White Noise

$[D] = 1/s$

$\longrightarrow \quad \underline{\Delta\sigma^2_{\Delta p/p_0} = D \cdot t}$

$\longrightarrow$ Calibration of the Noise Signal with the Schottky Signal

$\Delta t = 100\,s$; different Noise Amplitudes

$D \propto (\text{Noise Amplitude})^2$

$-31.6\,dB \longrightarrow D \approx 5 \cdot 10^{-8}\,s^{-1}$

$-42.5\,dB \longrightarrow D = 7 \cdot 10^{-9}\,s^{-1}$ $\Downarrow$

$-63\,dB \longrightarrow D = 7 \cdot 10^{-11}\,s^{-1}$

50sec

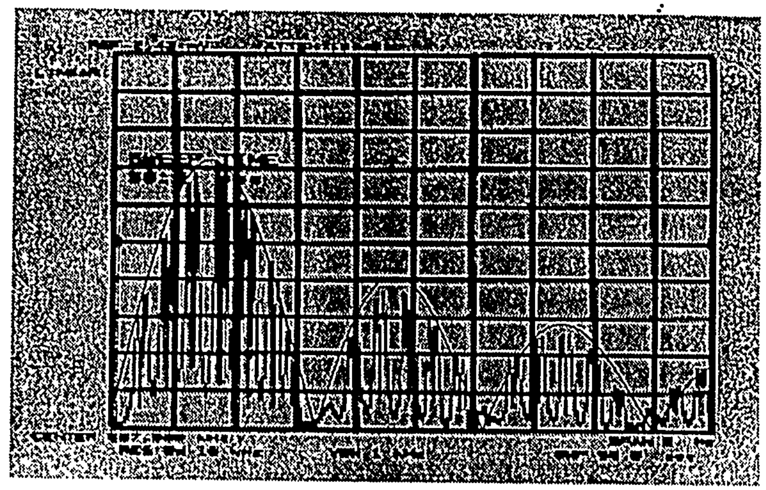

The super-imposition of 22 echo measurements with different time separation Δt between the two RF-kicks. The vertical axis shows the absolute value of the echo amplitude on a linear scale and the horizontal axis shows the time measured from the first RF-kick. The time separation was varied between $\Delta t = 5$ ms and $\Delta t = 220$ ms. The horizontal scale is 50 s. The solid line shows the analytical estimate for the echo envelope assuming a diffusion coefficient of $\underline{D = 10^{-13}\,s^{-1}}$.

- 63.2B

$c'/p = 1.04 \cdot 10^{-3}$ before noise

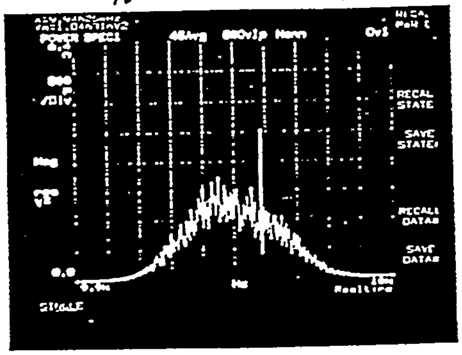

$c'/p = 1.04 \cdot 10^{-3}$ after noise

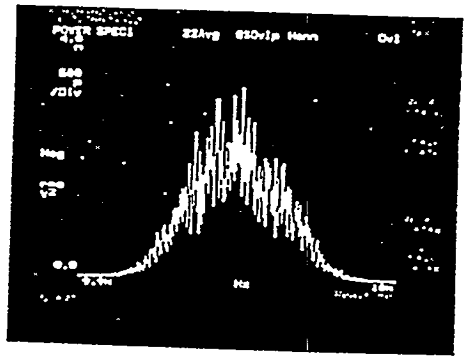

T = 15 min

$c'/p = 1.55 \cdot 10^{-3}$ after noise

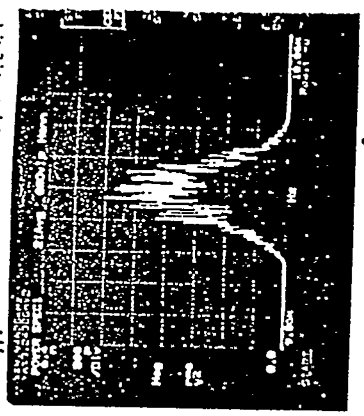

→ f [Hz]

$c'/p = 2.05 \cdot 10^{-3}$ after noise

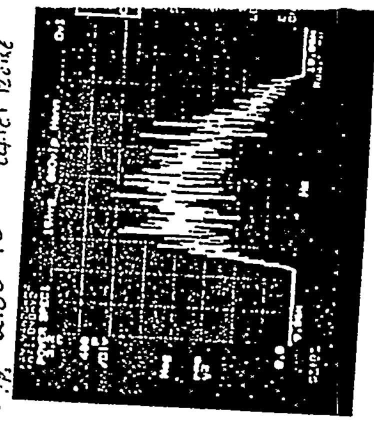

→ f [Hz]

$c'/p = 1.4 \cdot 10$ before noise

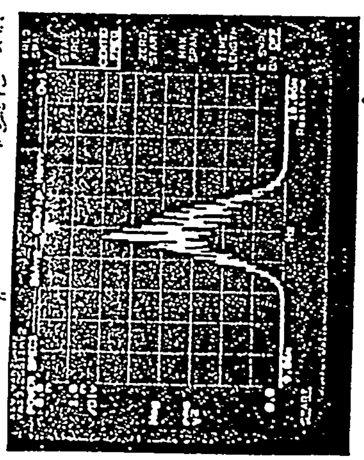

→ f [Hz]

$c'/p = 1.9 \cdot 10^{-3}$ before noise

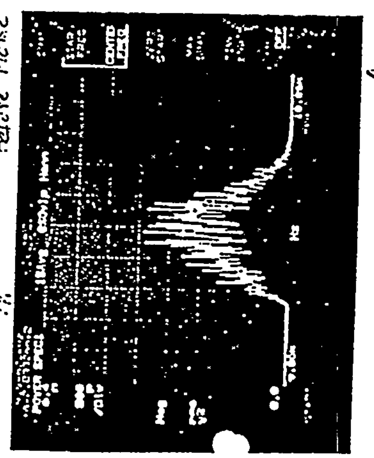

→ f [Hz]

T = 1...

No Diffusion

$\Delta t = 44 ms$

-61dB

$\rightarrow D = 4 \cdot 10^{-11} s^{-1}$

$\Delta t = 44 ms$

-57dB

$\rightarrow D = 1.1 \cdot 10^{-10} s^{-1}$

$\Delta t = 44 ms$

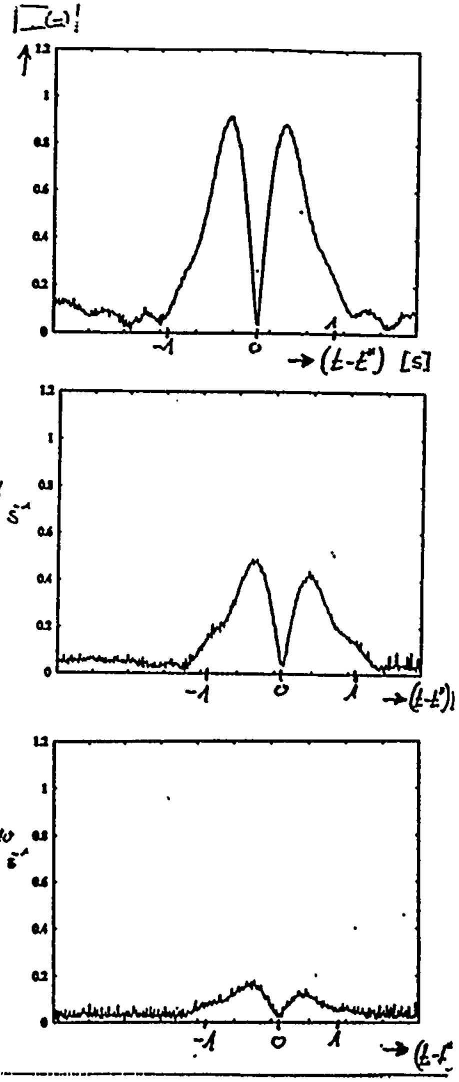

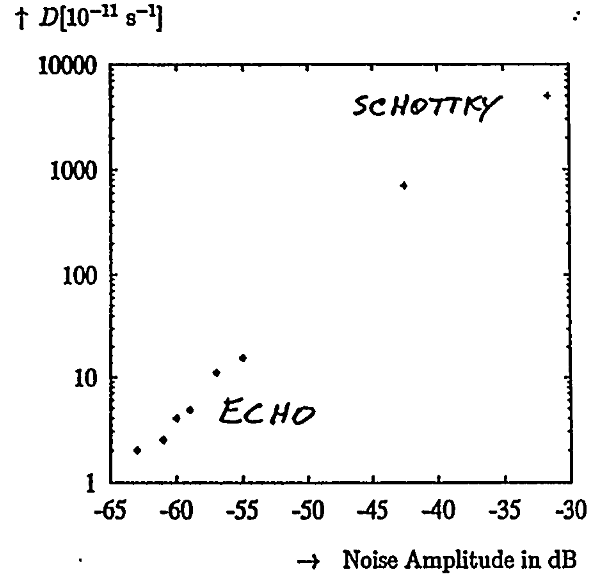

Calibration of the diffusion coefficients. The points with a noise amplitude larger than -45 dB are calculated from measurements using the Schottky signal. All other points are calculated from echo measurements. Assuming a diffusion process with white noise, one expects a straight line.

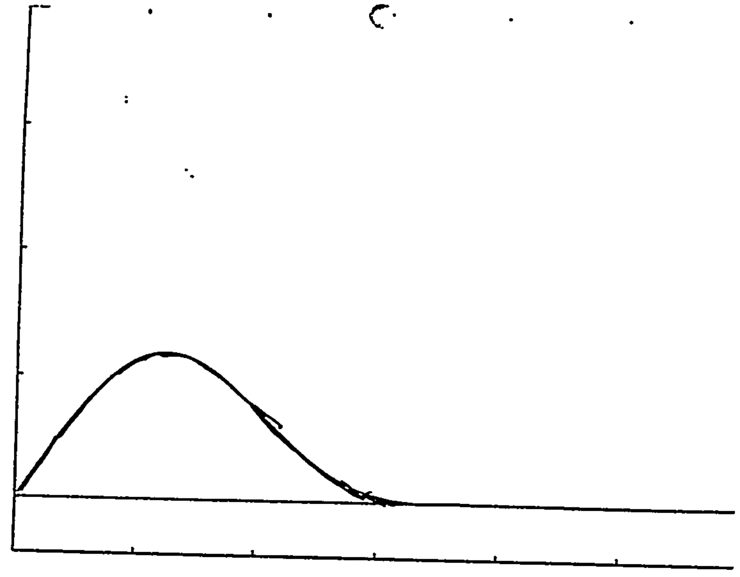

Amplitude

$\longrightarrow t\,[s]$

$;\ D = 2 \cdot 10^{-11}\, s^{-1}$

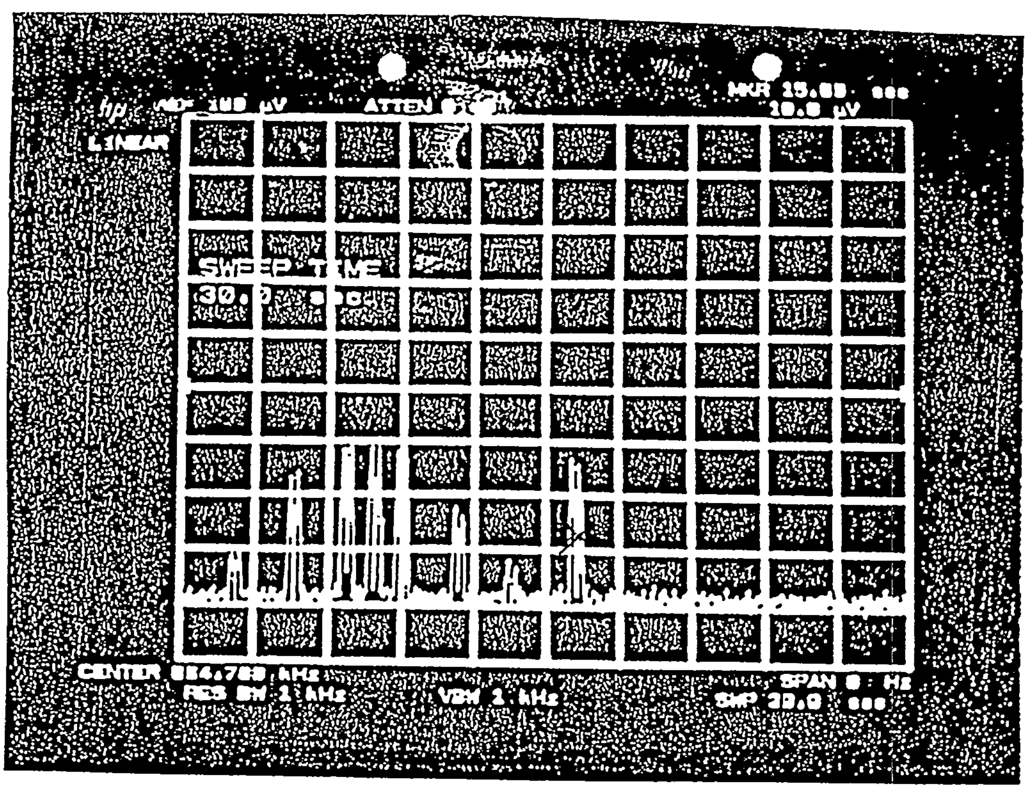

[illegible] with Diffusion

$-632R$

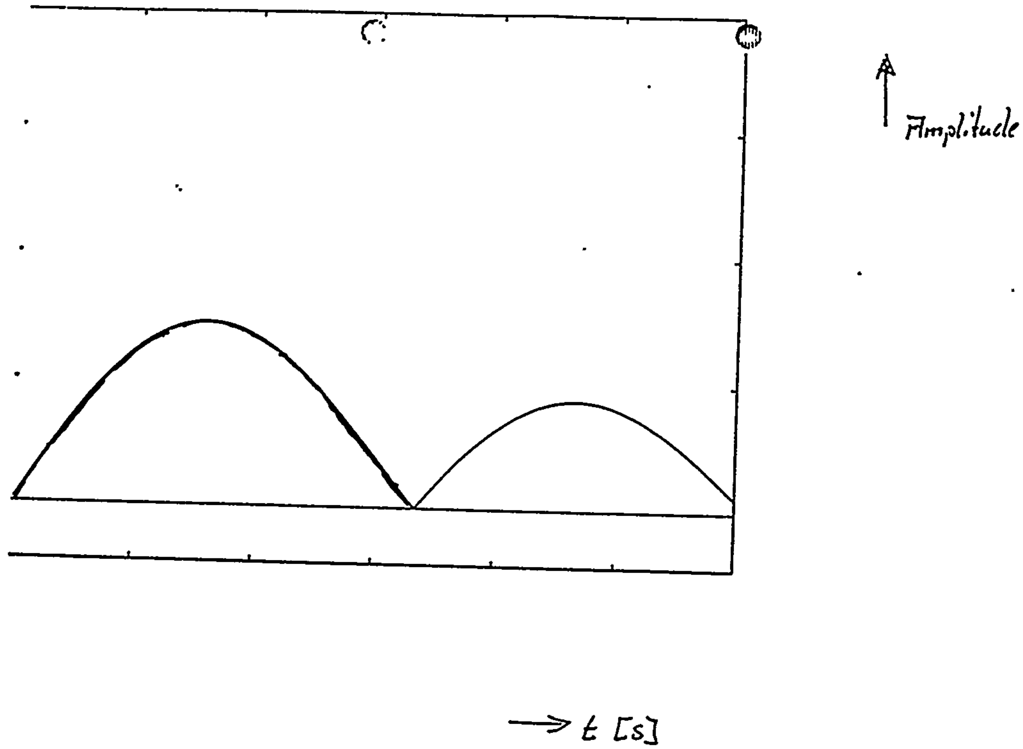

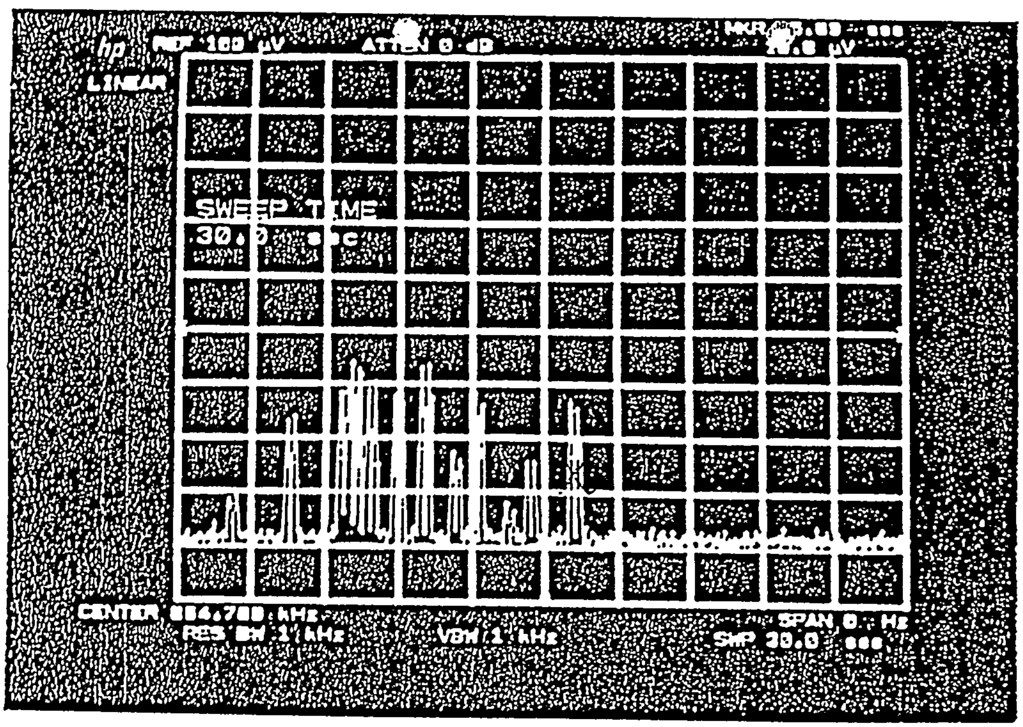

Δt Scan without Diffusion

D= Ø

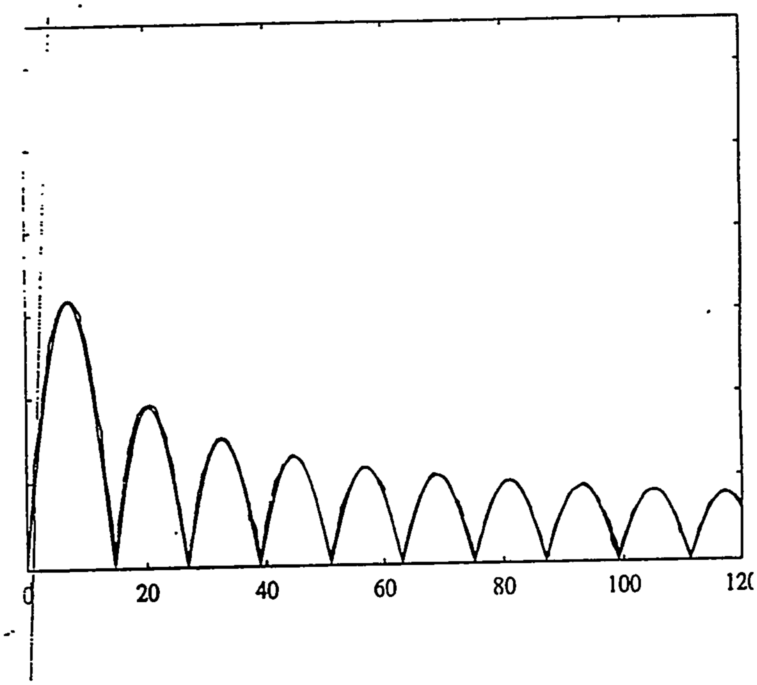

0
20
40
60
80
100
12(

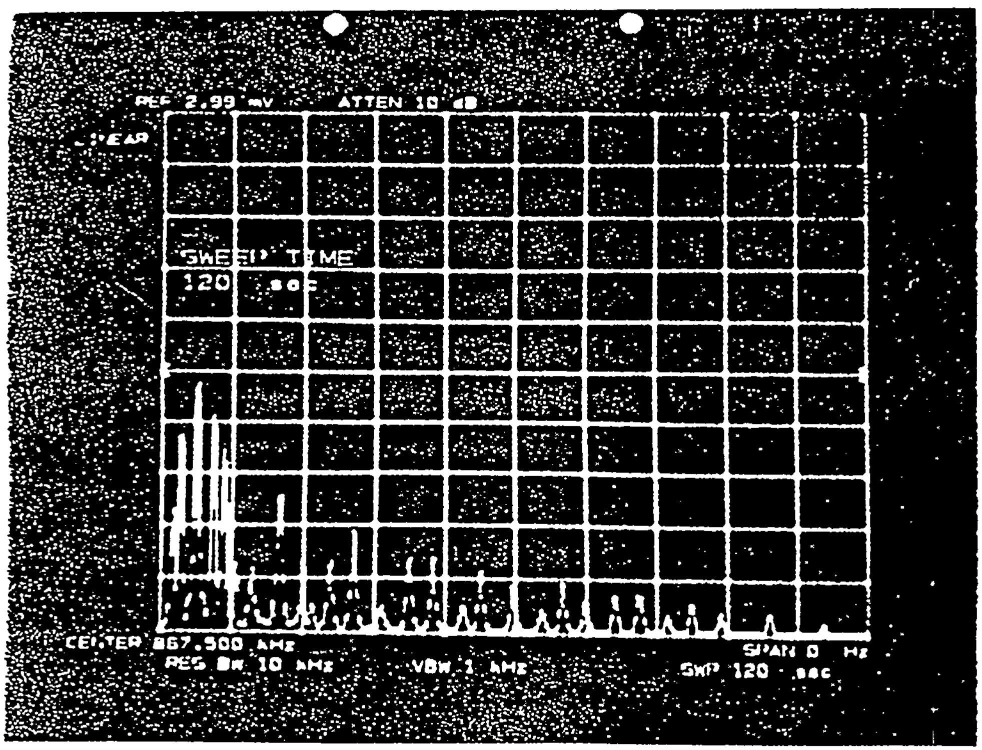

REF 2.99 mV
ATTEN 10 dB
SWEEP TIME
120 sec
CENTER 867.500 kHz
SPAN 0 Hz
RES BW 10 kHz
VBW 1 kHz
SWP 120 sec

2min

<u>BUNCHED BEAM ECHOES</u>

⇒ PRELIMINARY RESULTS, ANALYSIS IN PROGRES

$V_{RF} = 6.5\ MV$, $f_s = 370\ Hz$ $(Q_s = 8.5 \cdot 10^{-3})$

- USE 200 MHz CAVITIES TO EXCITE. <u>DIPOLE</u> OSCILLATIONS: THESE ARE QUICKLY DAMPED BY PHASE LOOP
- EXCITE QUADRUPOLE (AND HIGHER ORDER EVEN MULTIPOLE) OSCILLATIONS BY TWO RF-VOLTAGE KICKS $|\Delta V_1| = |\Delta V_2| \ll 1\ MV$, LASTING ~ 1 msec : VARY Δt

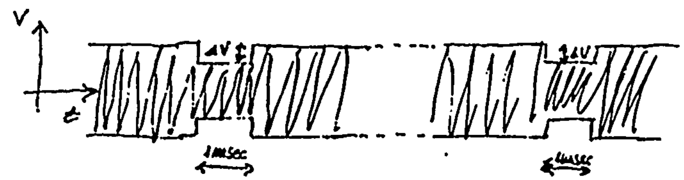

- PEAK DETECTION OF BUNCH CURRENT WITH WIDE-BAND PICK-UP (SENSITIVE TO QUADRUPOLE OSCILLATIONS):

  WE DO SEE BUNCHED BEAM ECHOES ! ⇒

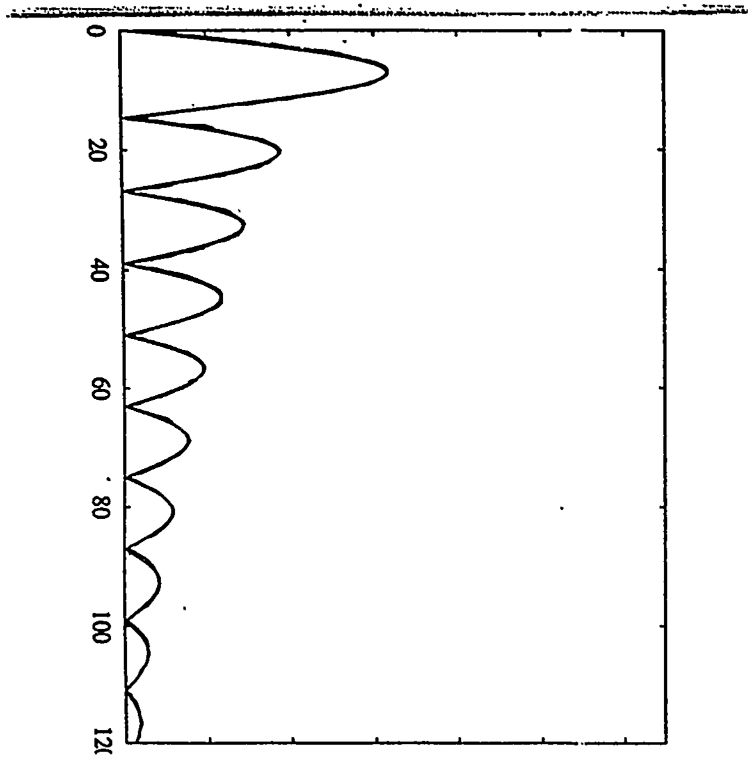

$D \approx 5 \cdot 10^{-14}\ s^{-1}$

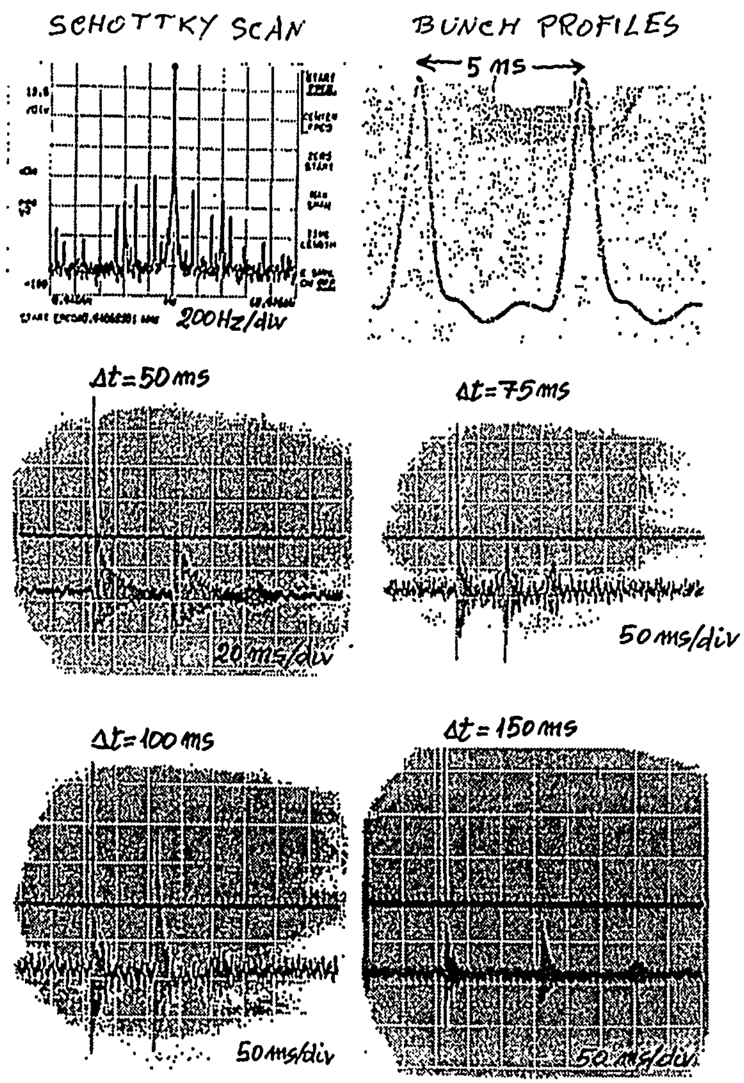

Bunched-beam echoes (SPS MD 28/09/1996).

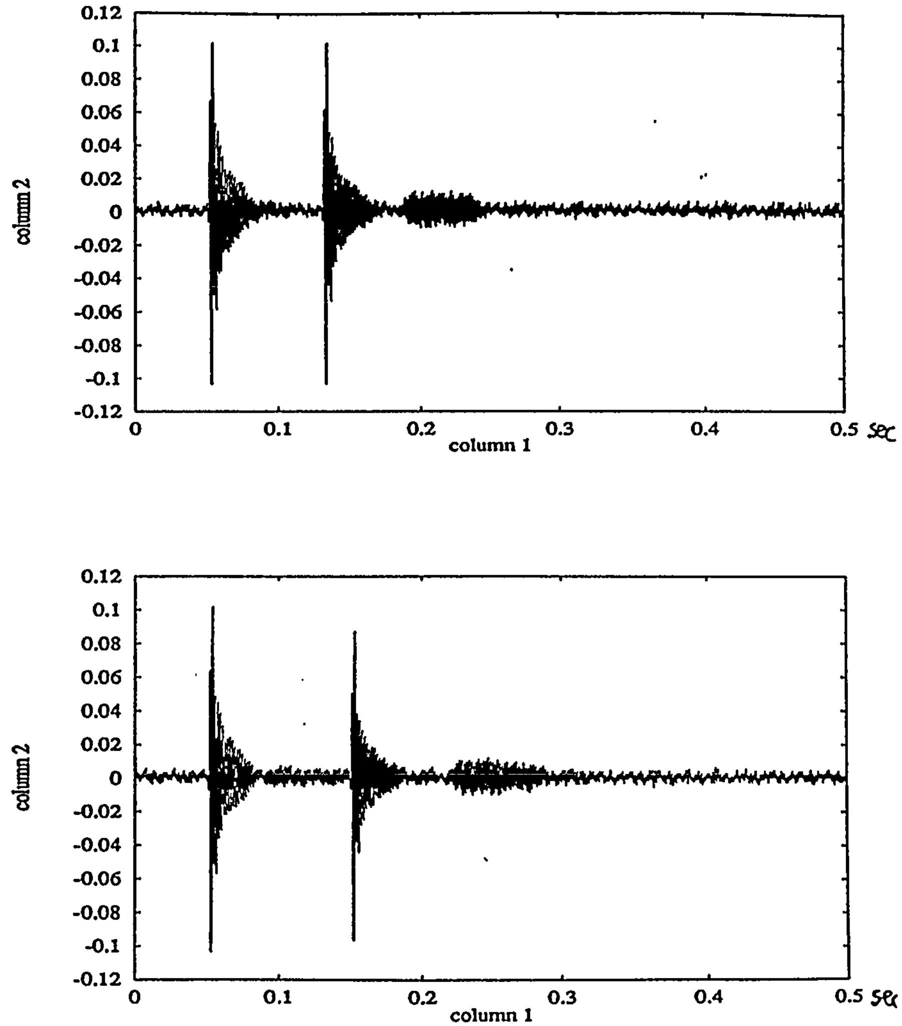

Bunched-beam echoes (SPS MD 26/11/1996).
RF voltage kicks with same amplitude: $\Delta V = -2$ MV, $V = 5$ MV, $\Delta t = 200\ \mu$sec

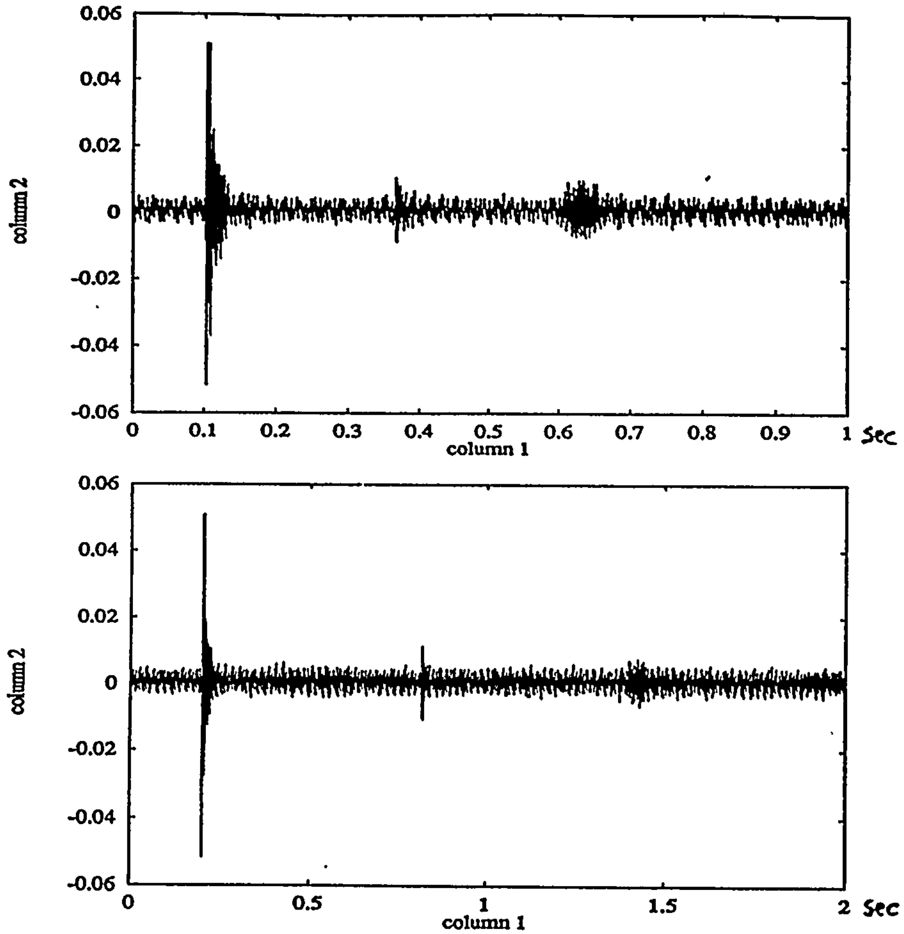

Bunched-beam echoes (SPS MD 26/11/1996).
Reduced amplitude of the second RF voltage kick.

SAWTOOTH INSTABILITY & OVER-SHOOT PHENOMENA

R. Siemann, SLAC

Sawtooth Instability in the SLC Damping Rings

R. Holtzapple, B. Podobedov, R. Siemann
SLAC

Institute for Theoretical Physics, UCSB

December 4, 1996

OUTLINE

1. INTRODUCTION
2. INSTRUMENTS
3. RESULTS - AVERAGE FEATURES (R. H.)
4. RESULTS - THE INSTABILITY (B. P.)
5. COMMENTS

1. INTRODUCTION

PRIOR TO 1993

- Strong instability in the SLC damping rings
- Threshold ~ 3×10^{10}/bunch
- Transient - could have severe effects in linac depending on amplitude & phase at extraction

SOLUTION WAS REPLACING VACUUM SYSTEM

- Modern machining techniques and advanced materials allowed significant reduction of inductance
- Simulations predicted a threshold ~ 5×10^{10}/bunch which is well above SLC operating current
- Actual threshold was ~ 2×10^{10}/bunch
- The instability is a transient with a limiting amplitude that is sufficiently low that it is not a major limit of SLC performance
- We call this a "sawtooth instability"

MOTIVATIONS FOR STUDY OF THE SAWTOOTH INSTABILITY

- Understanding of the physics of the instability
- Measuring impact on the SLC

THIS IS AN EXPERIMENTAL TALK

- I hope it is allowed at ITP

Table 1. Vacuum Chamber Inductance (nH)

Element	Old Chamber†	New Chamber*
Synch. Radiation Masks	9.5	----
Bellows	-----	1.1
Quadrupole to Dipole Chamber Transitions	9.3	2.4
Ion Pump Slots	0.2	0.05
Kicker Magnet Bellows	4.1	----
Flex Joints	3.6	----
Beam Position Monitors	3.5	0.2
Other	2.4	2.4
TOTAL	33	6

† K. L. F. Bane, Proc 1988 EPAC, 637 (1988)

*** K. L. F. Bane & C. Ng, Proc 1993 PAC, 3432 (1993).**

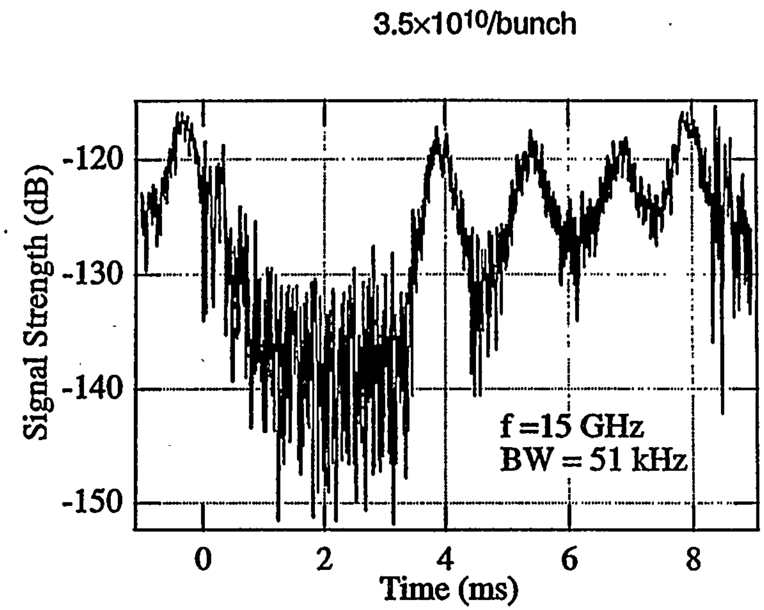

CAVEAT

- Properties are not always the same - we have observed them change for reasons we do not understand
- The clearest example was disappearance of the instability in the electron damping ring. This could have been associated with a catastrophic vent and fire that spread epoxy combustion products throughout the ring

2. INSTRUMENTS

TYPICAL SLC DAMPING RING PARAMETERS

SLC DAMPING RING STREAK CAMERA

- General principle
- Space charge effects and cylindrical optics
- A single image & correlated pixels

SPECTRAL ANALYSIS

- In a perturbative analysis of beam phase space structure the spectrum is

$$A(f) = \sum_{n,k} \delta(f - nf_r - kf_s) A_{nk}$$

where f_r is the revolution frequency and f_s is the synchrotron frequency

- Phase space can be represented by a Fourier expansion

$$\rho(\hat{\tau}, \phi) = \sum_{m} \rho_m(\hat{\tau})\, e^{im\phi}$$

where $\hat{\tau}$ is the amplitude and ϕ is the phase

- There is a one-to-one correspondence between synchrotron sideband (k) and phase space structure

Name	Phase Space Structure	Signal Frequency	Frequency of Peak Amplitude $\Delta f \sim 1/2\pi\sigma_\tau$
Rotation harmonic	$m = 0$	$f = nf_r$	$f_{max} = 0$
First Sideband	$m = \pm 1$	$f = nf_r \pm f_s$	$f_{max} \sim 1/2\pi\sigma_\tau$
2nd Sideband	$m = \pm 2$	$f = nf_r \pm 2f_s$	$f_{max} \sim 1/\pi\sigma_\tau$

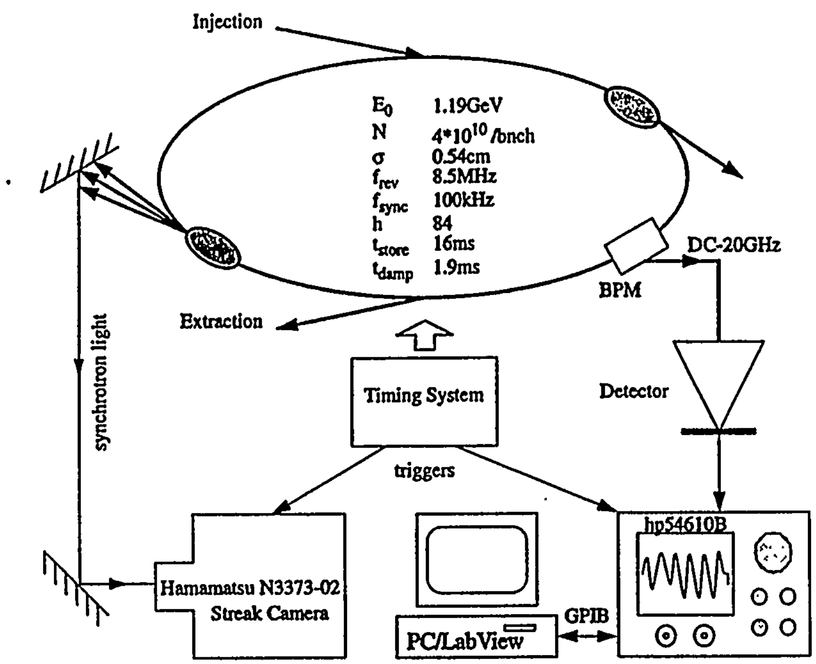

Injection
Extraction
E_0 1.19GeV
N 4*10^10 /bnch
σ 0.54cm
f_{rev} 8.5MHz
f_{sync} 100kHz
h 84
t_{store} 16ms
t_{damp} 1.9ms
BPM
DC-20GHz
Detector
synchrotron light
Timing System
triggers
Hamamatsu N3373-02
Streak Camera
hp54610B
GPIB
PC/LabView

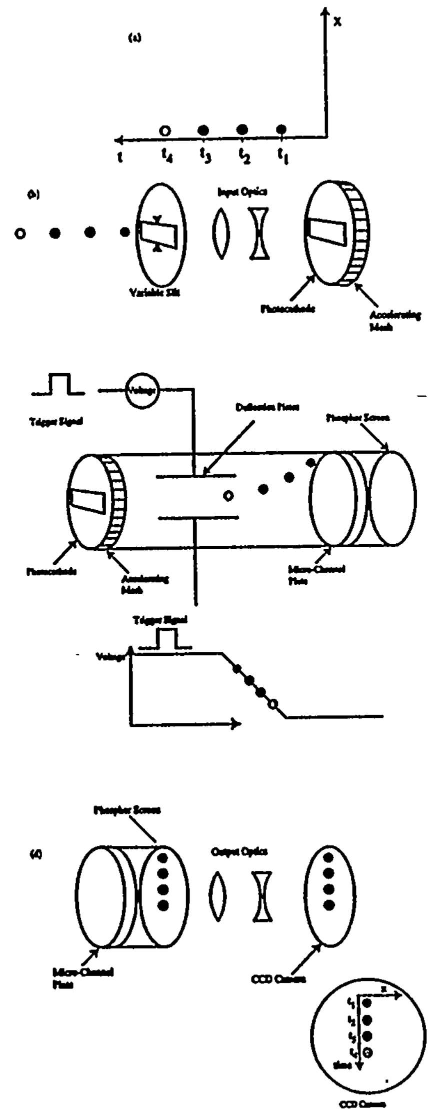

x
t
Input Optics
Output Optics
Voltage
Trigger Signal
CCD Camera

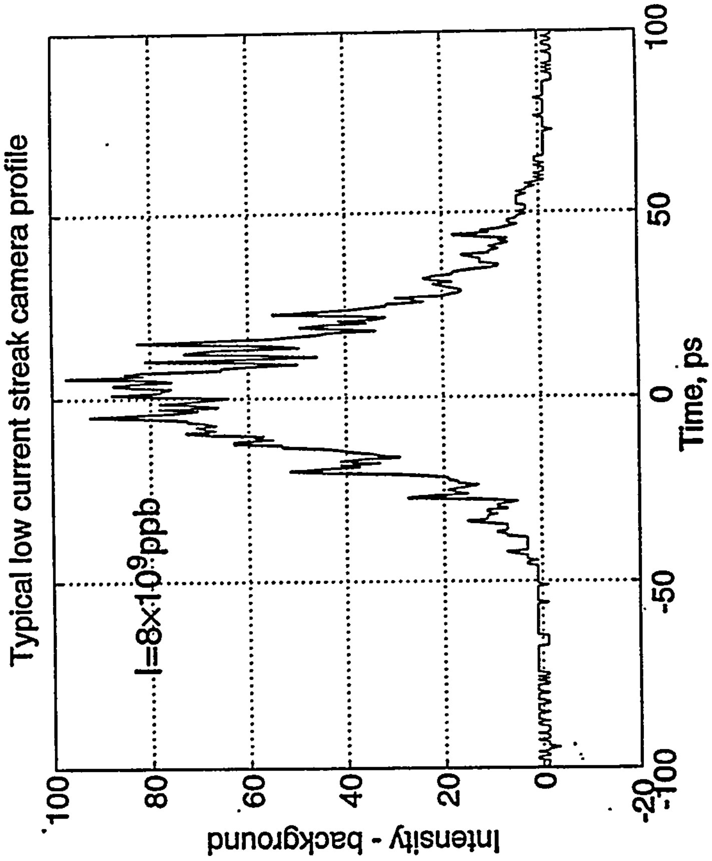

Effect of Photocathode Space Charge on Bunch Length Measurement

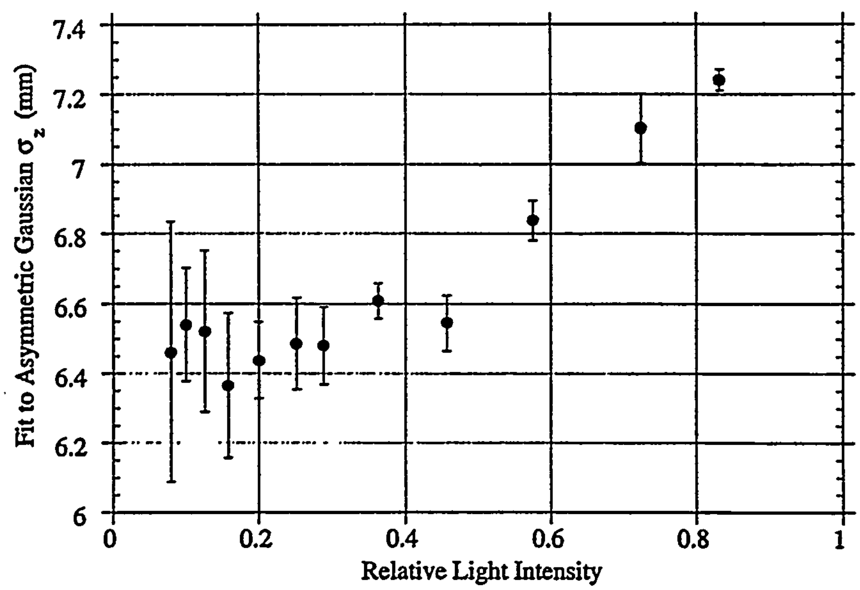

- The exact value of the frequency gives the phase space structure, and the sensitivity to different structures depends on the frequency range

RF SWITCH & HIGH PASS FILTER

- Routine operation of the SLC is with two bunches in the damping rings
- Signals from the two bunches can interfere with the interference depending on the amplitudes and relative phase of the motion of the two bunches
  - Coupled bunch mode leads to a pattern alternating with rotation harmonic of constructive and destructive interference. Details of the pattern tell whether 0 or π mode
  - Phase is random for a single bunch mode
- RF Switch (Watkins Johnson MSE203: 2 - 18 GHz) used to isolate the signals from the two bunches
- The raw signal is so large that the switch can be damaged, so use a high pass filter in front of it. At least 20 db isolation between bunches

CRYSTAL DETECTION

- The signal has the form (ω_I is instability frequency)

$$v(t) \sim \sum_n A_{n0} e^{in\omega_r t} + B_n e^{i(n\omega_r t + \omega_I t + \vartheta)} + C_n e^{i(n\omega_r t - \omega_I t - \vartheta)}$$

- A crystal is a square law detector

$$v_{out}(t) \propto vv^* \approx \sum_n A_{n0}^2 + 2A_{n0}(B_n + C_n)\cos(\omega_I t + \vartheta)$$

$$+ \text{ terms with } \omega \sim \omega_r, 2\omega_r, \ldots$$

- Filtering out the high frequency terms gives a DC component and a component at ω_I with phase = signal phase (ϑ)

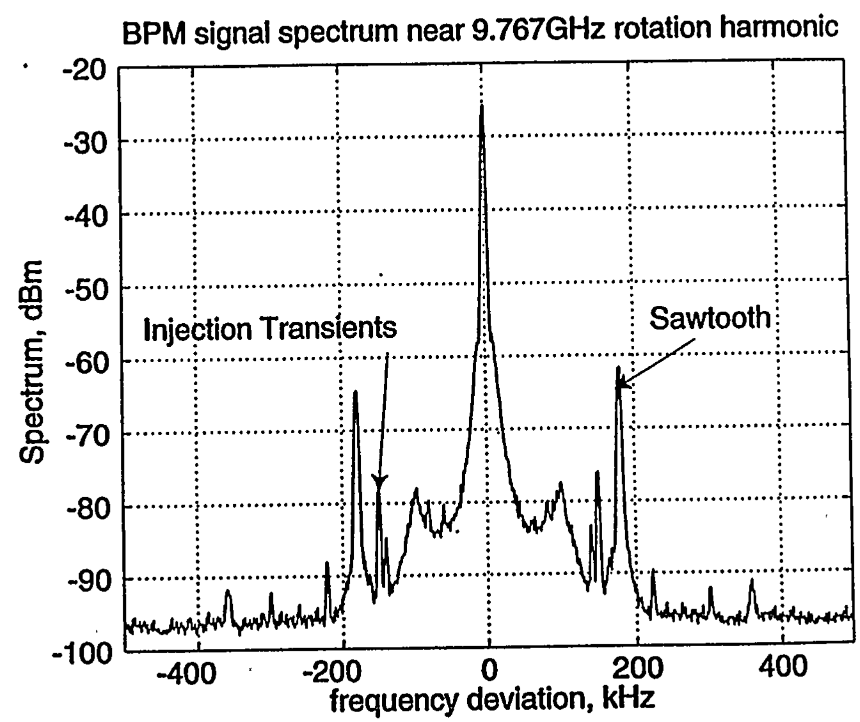

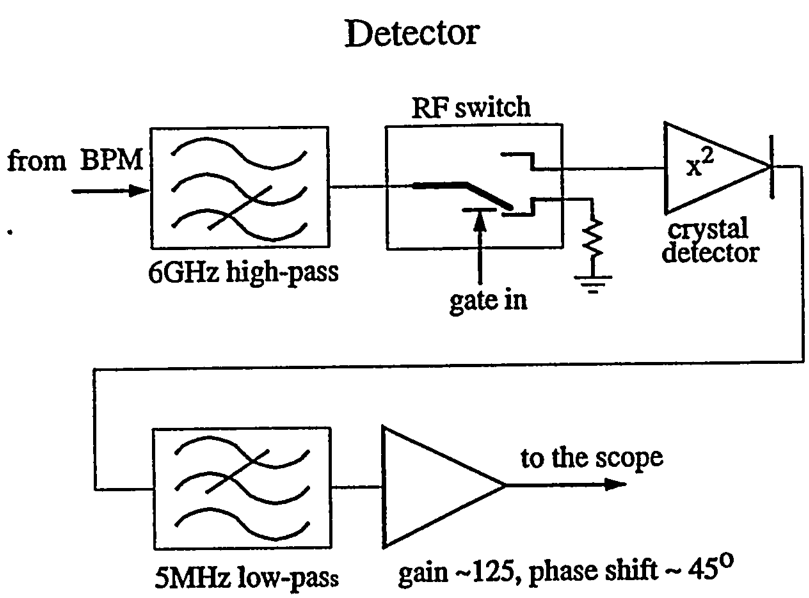
Detector
RF switch
from BPM
x^2
crystal detector
6GHz high-pass
gate in
to the scope
5MHz low-pass
gain ~125, phase shift ~ 45°

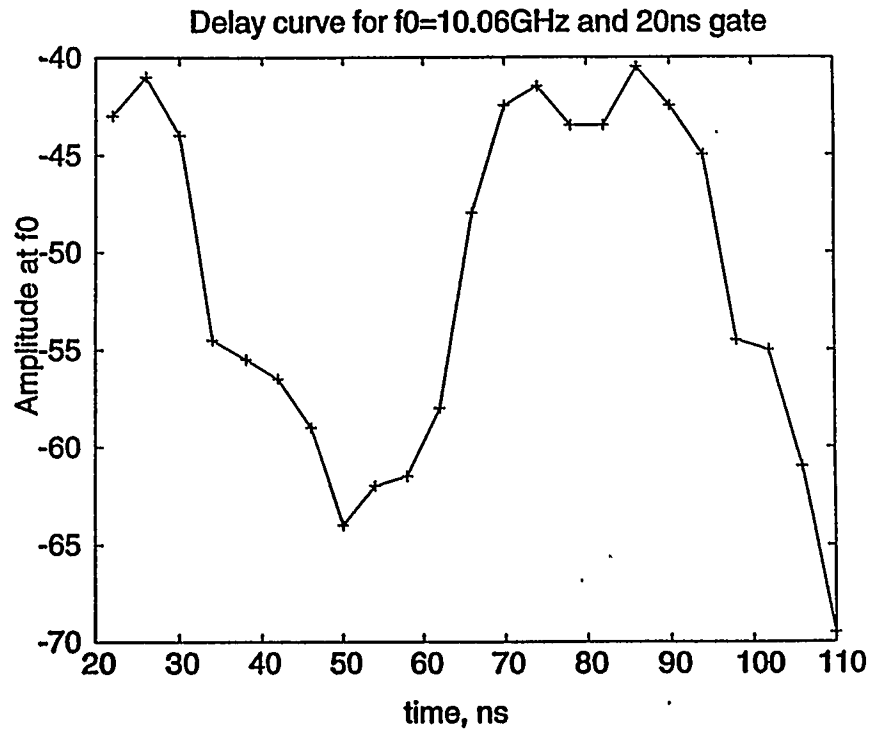
Delay curve for f0=10.06GHz and 20ns gate
Amplitude at f0
time, ns
-40
-45
-50
-55
-60
-65
-70
20
30
40
50
60
70
80
90
100
110

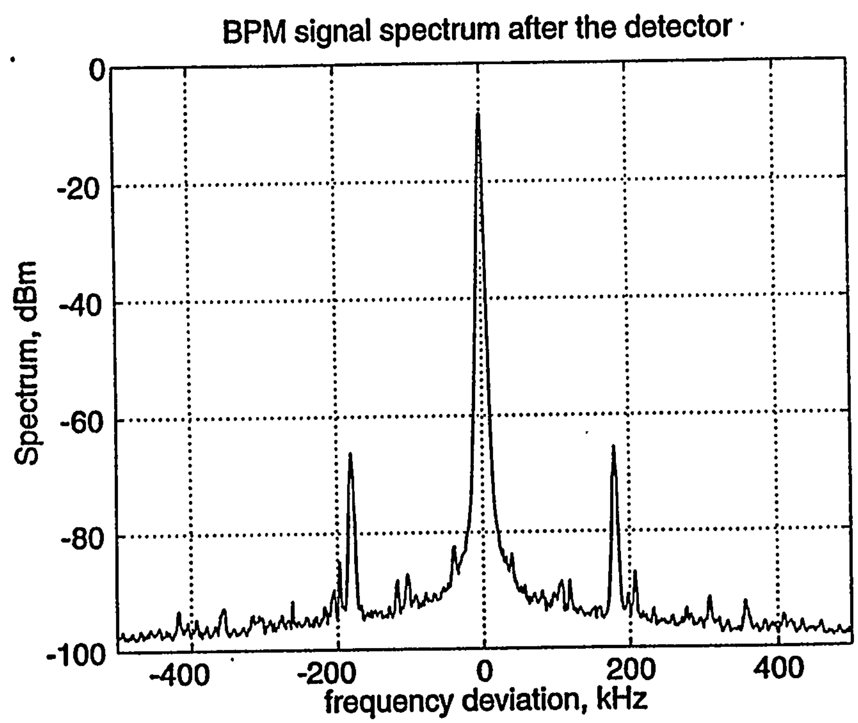

3. RESULTS - AVERAGE FEATURES

Robert Holtzapple

- Most of the data reported are for $V_{RF} = 800$ kV which gives $f_s = 100$ kHz
- Energy Spread vs current
  - Threshold is ~ 2×10^{10} particles/bunch
- Bunch length vs current
  - The data are fit to an "asymmetric Gaussian" - a Gaussian with different RMS values before and after the peak

$$I(t) = B\exp\left(-\frac{(t-\bar{t})^2}{2\sigma_1^2}\right) \quad \text{for } t<\bar{t}$$

$$B\exp\left(-\frac{(t-\bar{t})^2}{2\sigma_2^2}\right) \quad \text{for } t>\bar{t}$$

  - The quoted bunch length is $\sigma = 0.5(\sigma_1+\sigma_2)$.
  - The asymmetry is $A = (\sigma_1-\sigma_2)/\sigma$
- Bunch distribution at low and high currents
  - The low current bunch shape is approximately that expected from a resistive impedance. However, fits to the data give a current dependent resistance => data cannot be fit with resistance alone.
  - The high current bunch shape is characteristic of a resistive impedance as compared to a more inductive impedance of the old chamber.

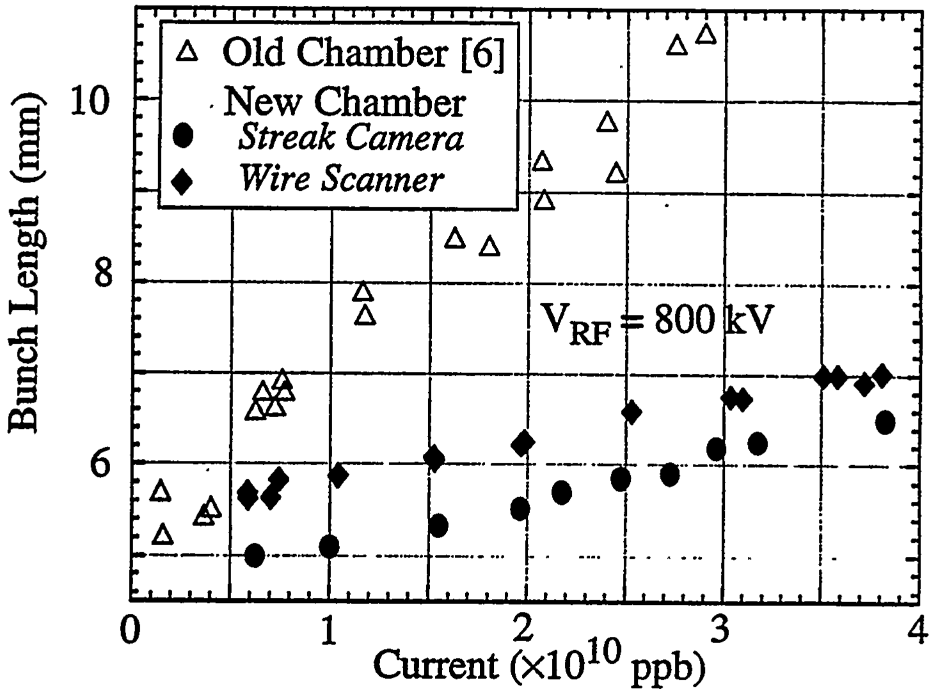
Old Chamber [6]
New Chamber
Streak Camera
Wire Scanner
Bunch Length (mm)
V_RF = 800 kV
Current (×10^10 ppb)

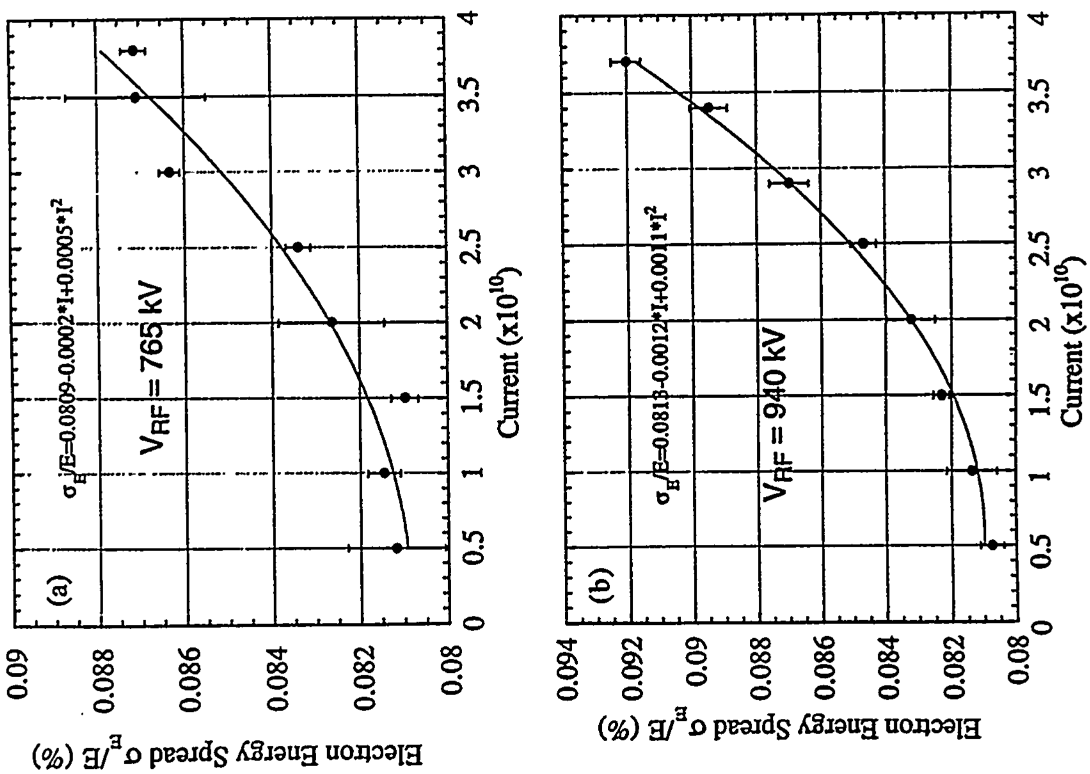
(a)
σ_E/E=0.0809-0.0002*I+0.0005*I²
V_RF = 765 kV
Current (x10^10)
Electron Energy Spread σ_E/E (%)
(b)
σ_E/E=0.0813-0.0012*I+0.0011*I²
V_RF = 940 kV
Current (x10^10)
Electron Energy Spread σ_E/E (%)

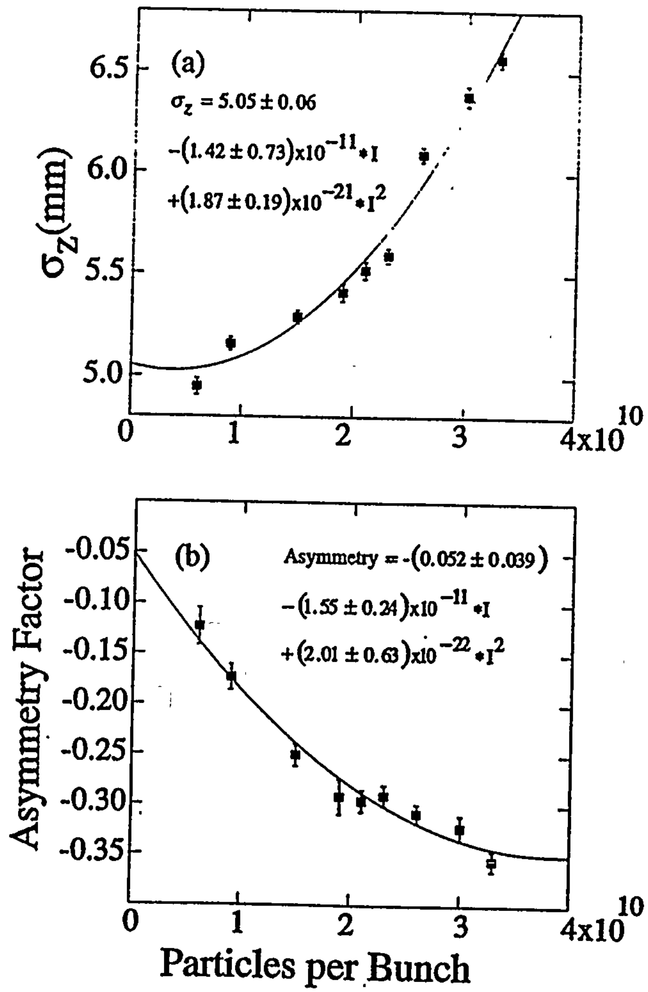
(a)
σz = 5.05 ± 0.06
-(1.42 ± 0.73)x10^-11*I
+(1.87 ± 0.19)x10^-21*I^2
σZ(mm)
(b)
Asymmetry = -(0.052 ± 0.039)
-(1.55 ± 0.24)x10^-11*I
+(2.01 ± 0.63)x10^-22*I^2
Asymmetry Factor
Particles per Bunch
4x10^10

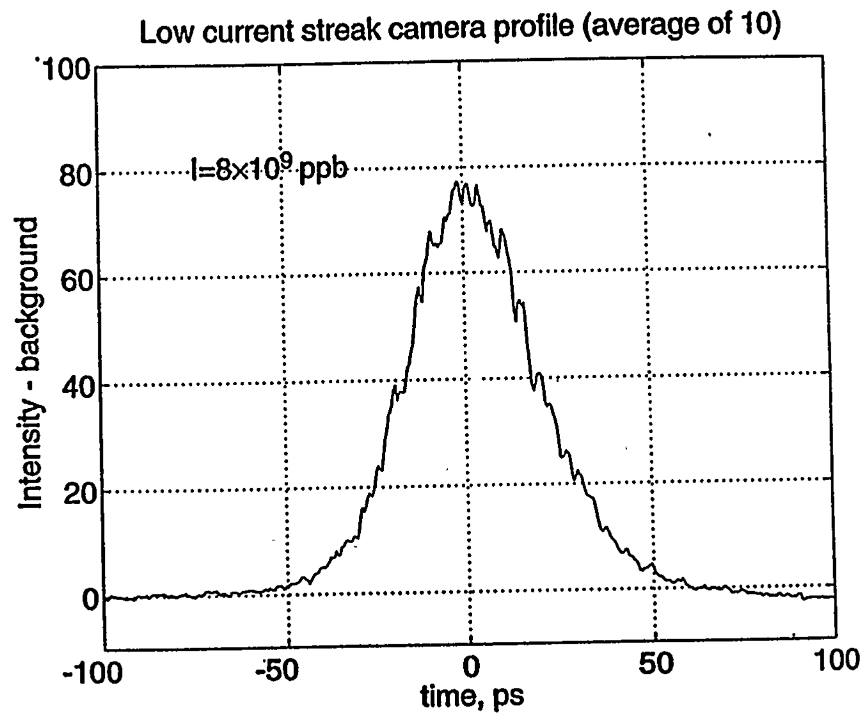
Low current streak camera profile (average of 10)
I=8×10^9 ppb
Intensity - background
time, ps

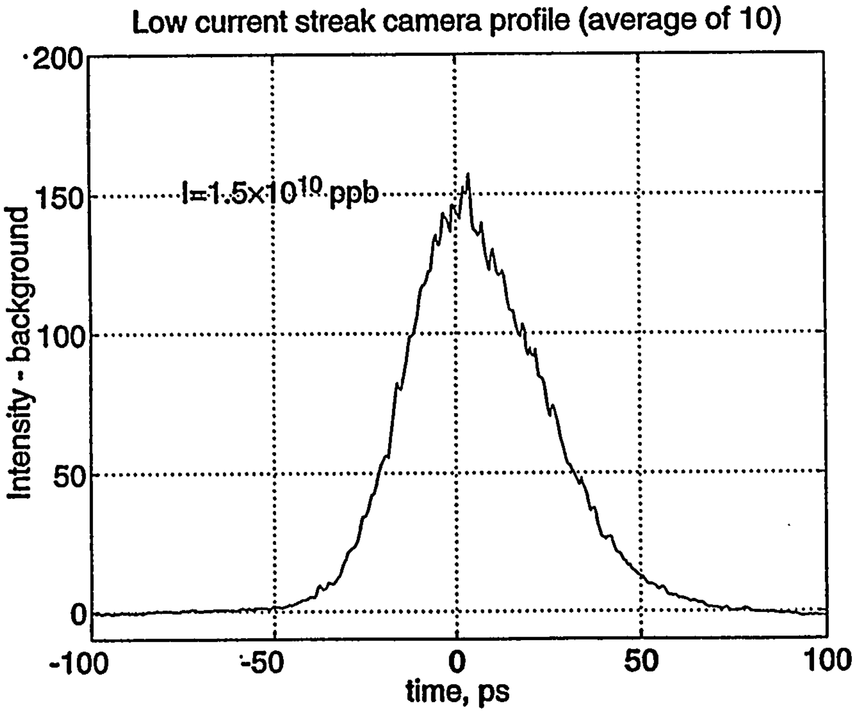
Low current streak camera profile (average of 10)
I=1.5x10^10 ppb
Intensity - background
time, ps
200
150
100
50
0
-100
-50
0
50
100

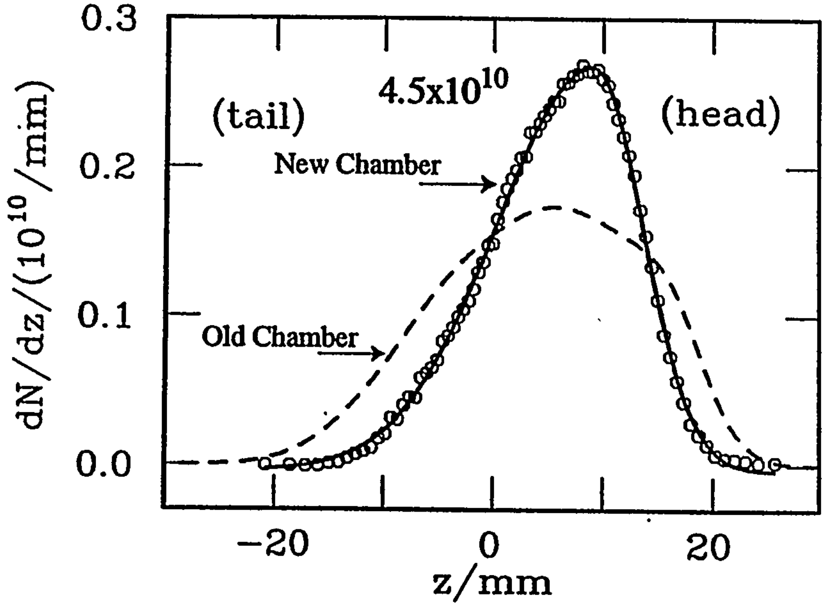
4.5x10^10
(tail)
(head)
New Chamber
Old Chamber
dN/dz/(10^10/mm)
z/mm
0.3
0.2
0.1
0.0
−20
0
20

- The dominant experimental problems at the conclusion of this study were

  1) Streak camera image noise that required averaging over many images for reduction. The effects of the instability could not be observed

  2) No correlation between RF signals and beam images.

  3) Only a weak correlation between damping ring and linac.

3. RESULTS - THE INSTABILITY

Boris Podobedov

$I = 3.6 - 3.8\times10^{10}$ unless specified otherwise

SIGNAL PROCESSING

- The RF switch, filter & crystal detector allowed

  - Isolation of a single bunch

  - Sampling at the end of the store with a gated analog-to-digital converter - Clear evidence for threshold at 2×10^{10} particle/bunch

  - Measurement of correlation between instability signal and streak camera image by recording the signal when the image was taken. Both amplitude and phase can be determined.

- Polar plot of available pictures
- Beam current also measured at the same time

STREAK CAMERA

- Cylindrical optics allows observation of profile variations without confusion from shot noise.

CORRELATION BETWEEN SIGNAL AND IMAGES

- Bunch length vs signal amplitude - clear correlation
- Profiles averaged over all instability phases are ~ independent of instability amplitude
- There is a clear dependence of large amplitude images on instability phase
- Profile variation with phase suggests sin ϑ dependence

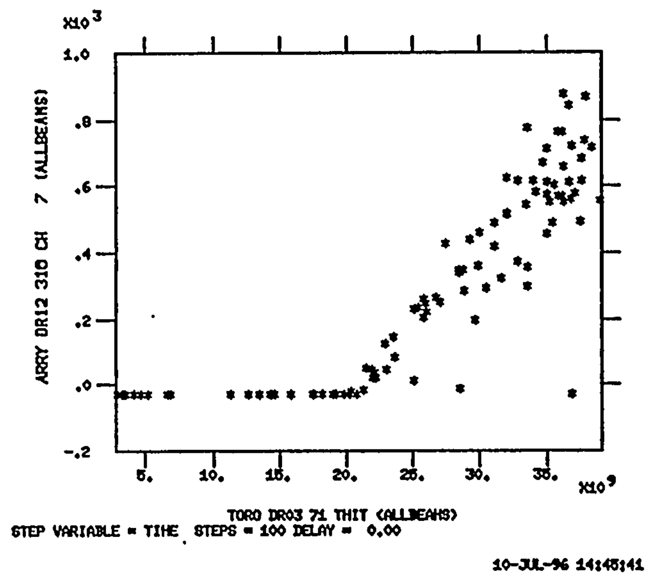
X10 3
1.0
.8
.6
.4
.2
.0
-.2
ARRY DR12 310 CH 7 (ALLBEAMS)
5.
10.
15.
20.
25.
30.
35.
X10 9
TORO DR03 71 THIT (ALLBEAMS)
STEP VARIABLE = TIME STEPS = 100 DELAY = 0.00
10-JUL-96 14:45:41

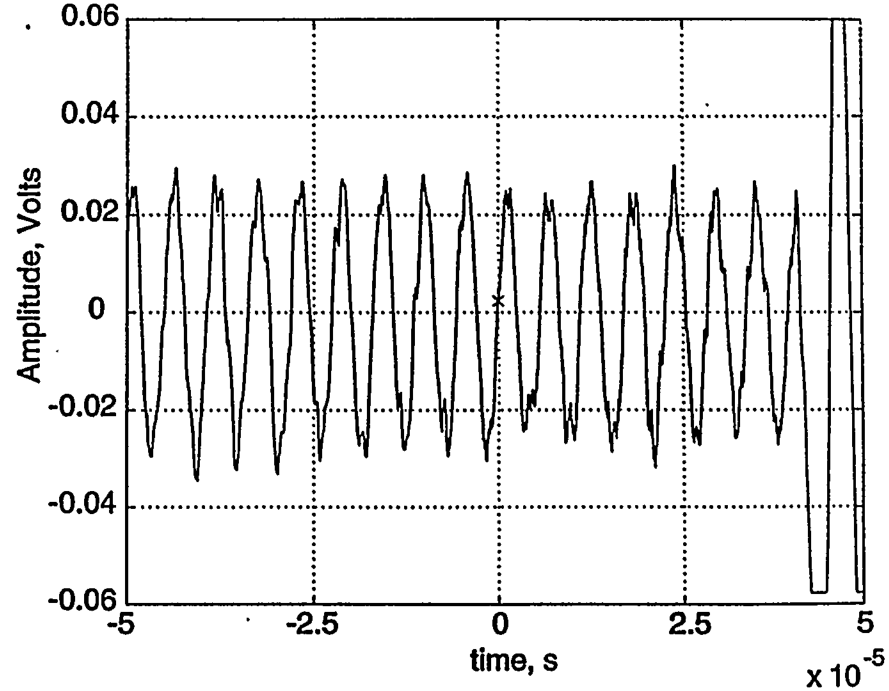
0.06
0.04
0.02
0
-0.02
-0.04
-0.06
Amplitude, Volts
-5
-2.5
0
2.5
5
time, s
x 10 -5

Instability phase and amplitude data distribution

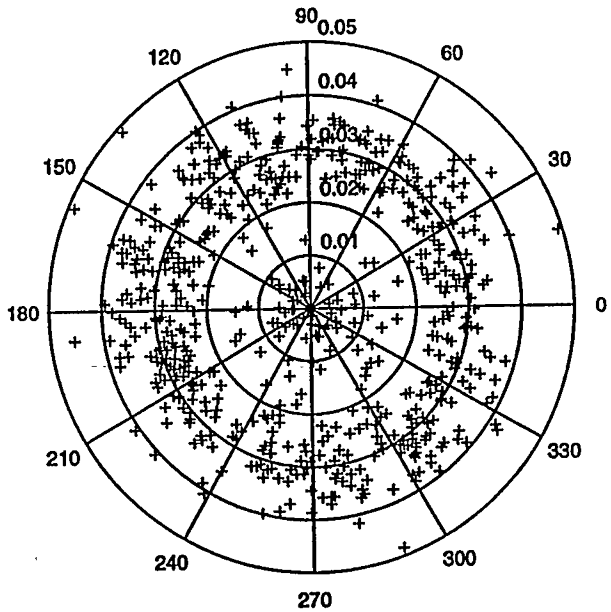

Typical high current streak camera profile and fit

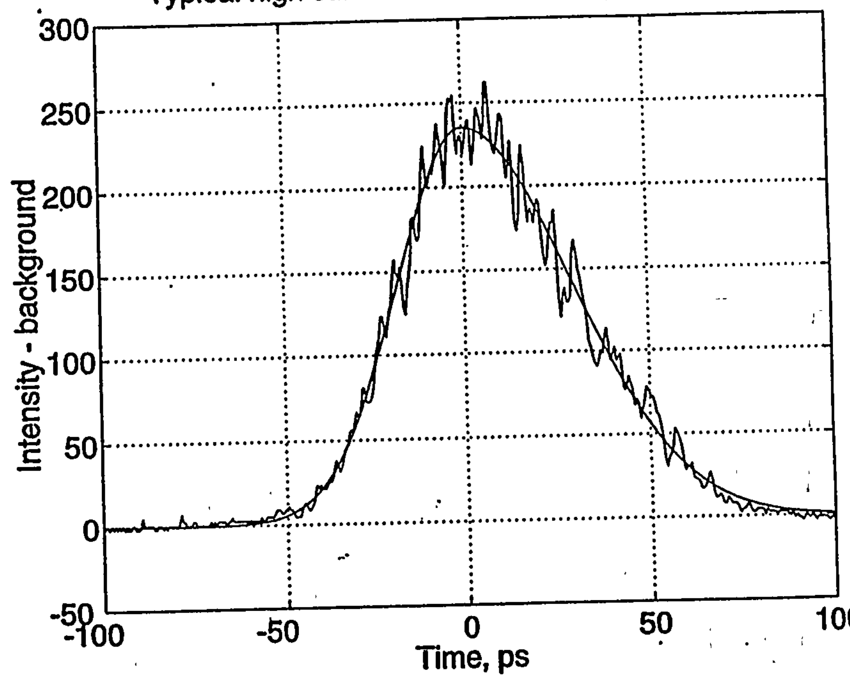

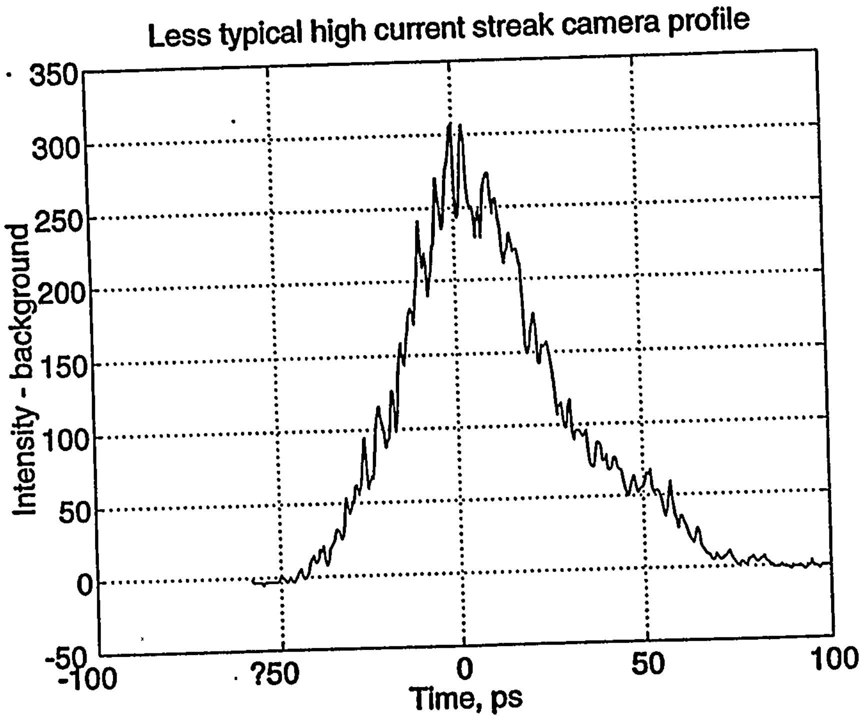
Less typical high current streak camera profile
Intensity - background
Time, ps
350
300
250
200
150
100
50
0
-50
-100
?50
0
50
100

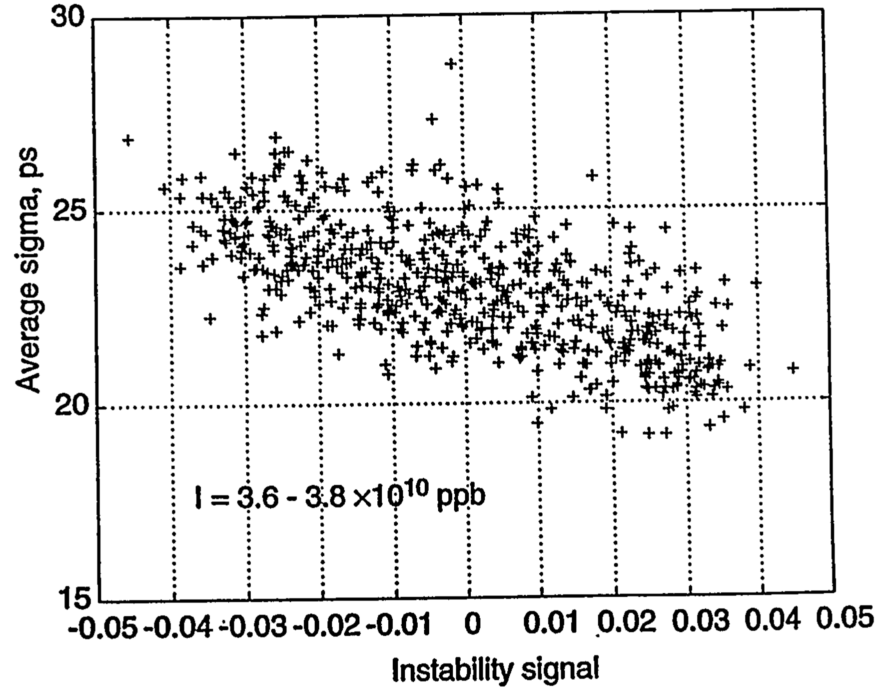
Average sigma, ps
Instability signal
$I = 3.6 - 3.8 \times 10^{10}$ ppb
30
25
20
15
-0.05 -0.04 -0.03 -0.02 -0.01 0 0.01 0.02 0.03 0.04 0.05

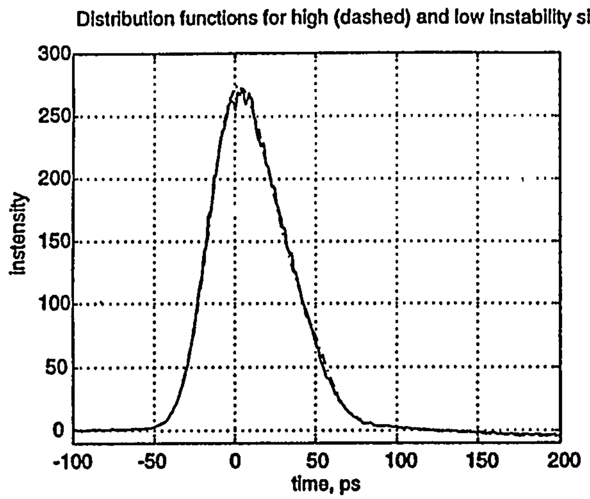
Distribution functions for high (dashed) and low instability signal
instensity
time, ps

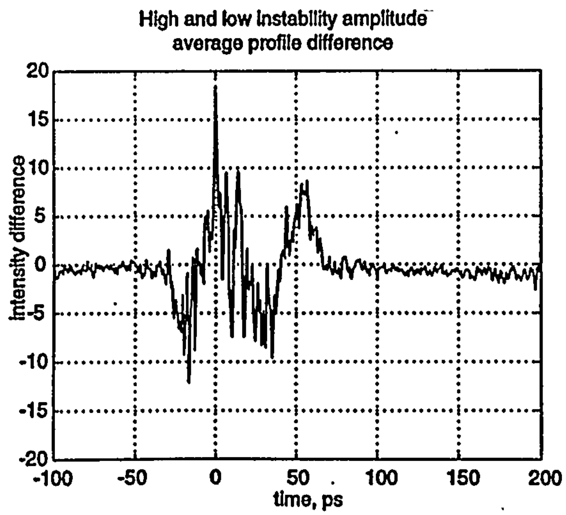
High and low instability amplitude
average profile difference
intensity difference
time, ps

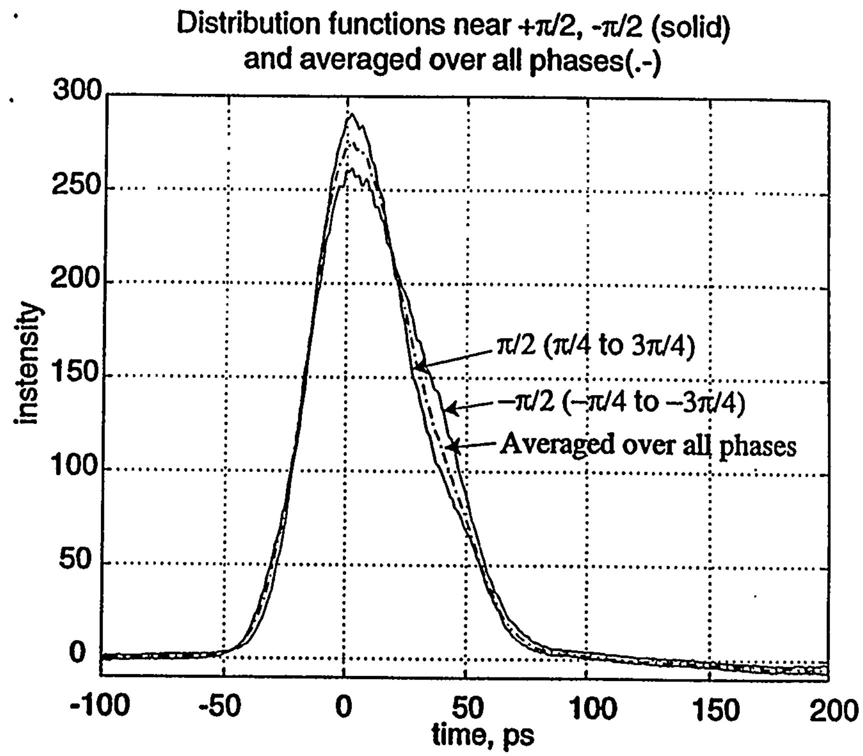
Distribution functions near +π/2, -π/2 (solid)
and averaged over all phases(.-)
instensity
π/2 (π/4 to 3π/4)
−π/2 (−π/4 to −3π/4)
Averaged over all phases
time, ps

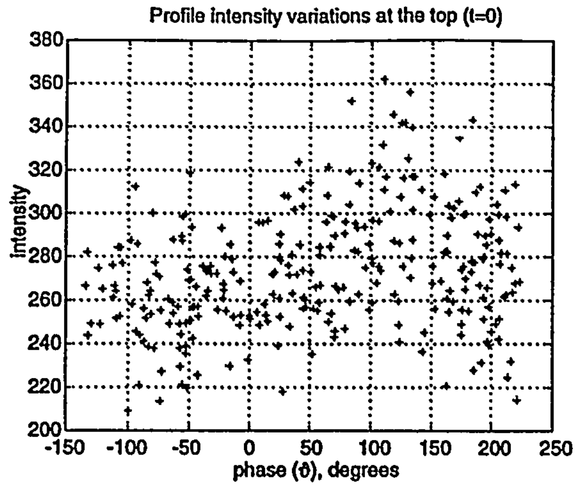

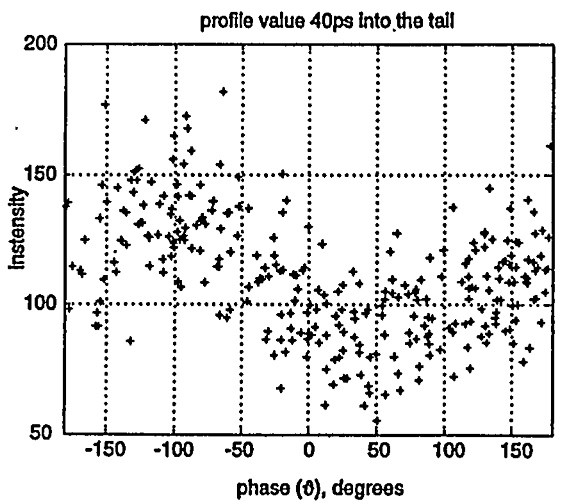

- Define the instability structure as

$$\rho(\tau) = \text{median}\left(\frac{\rho_k(\tau,\vartheta_k) - \rho_0(\tau)}{\sin\vartheta_k}\right)$$

  where k indicates the image number
- The area of each peak is ~4% of the area of the ρ_0 curve

TWO BUNCH CORRELATION

- A coupled bunch mode would have a pattern of signal intensity that alternates between even and odd rotation harmonics when the RF switch is not used to separate bunches. We see no evidence of such a pattern => single bunch phenomenon.
- There is no evidence for correlation between sawteeth of individual bunches => single bunch phenomenon
- If, by chance, both bunches have a large amplitude at the same time, the phases are not independent

LINAC CORRELATION

- A correlation has been observed between the sawtooth signal and the linac orbit. The sawtooth could account for 40% of the jitter power

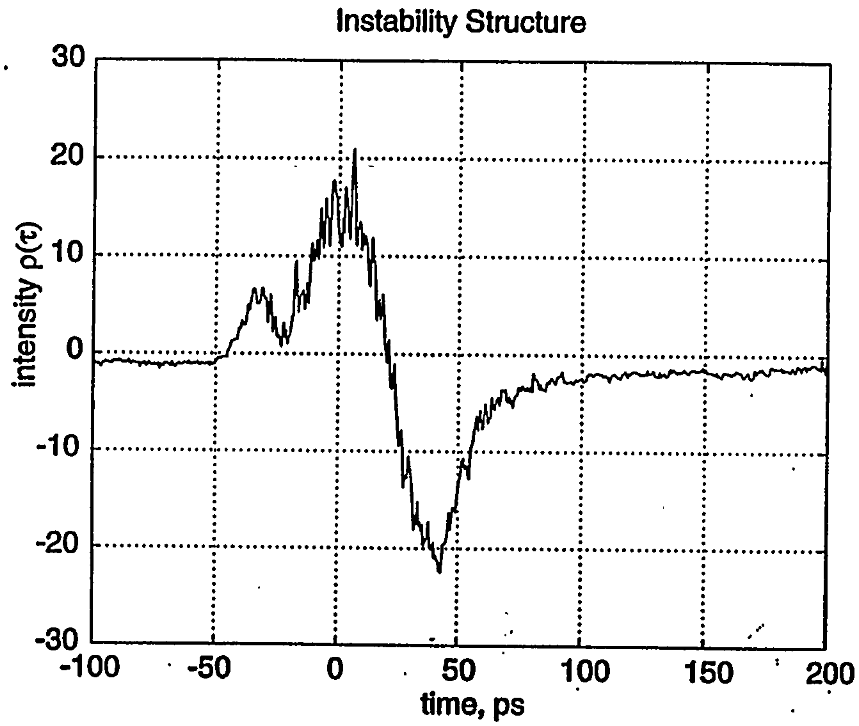
Instability Structure
intensity ρ(τ)
30
20
10
0
-10
-20
-30
-100
-50
0
50
100
150
200
time, ps

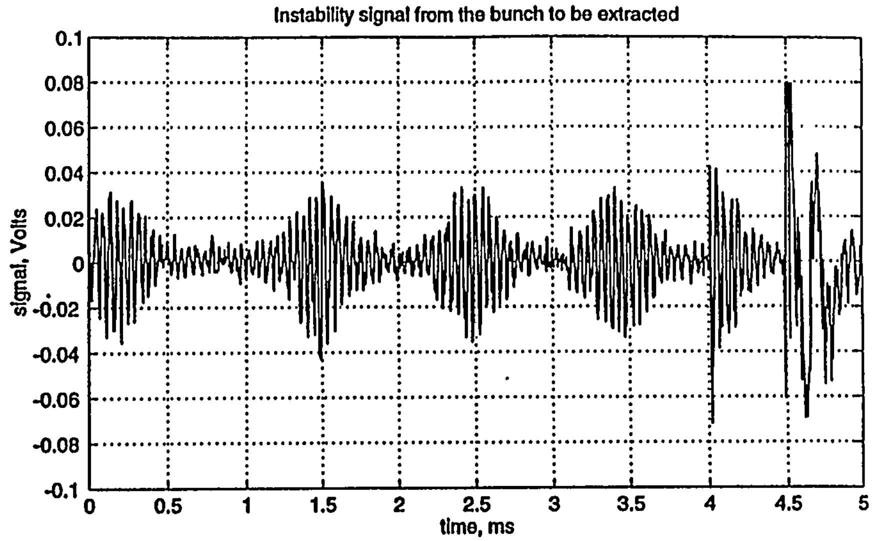
Instability signal from the bunch to be extracted
signal, Volts
0.1
0.08
0.06
0.04
0.02
0
-0.02
-0.04
-0.06
-0.08
-0.1
0
0.5
1
1.5
2
2.5
3
3.5
4
4.5
5
time, ms

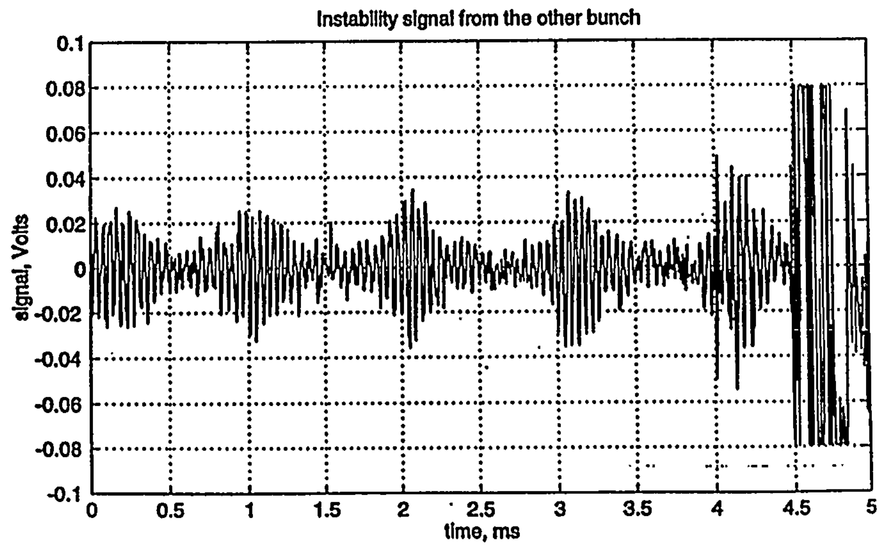
Instability signal from the other bunch
signal, Volts
0.1
0.08
0.06
0.04
0.02
0
-0.02
-0.04
-0.06
-0.08
-0.1
0
0.5
1
1.5
2
2.5
3
3.5
4
4.5
5
time, ms

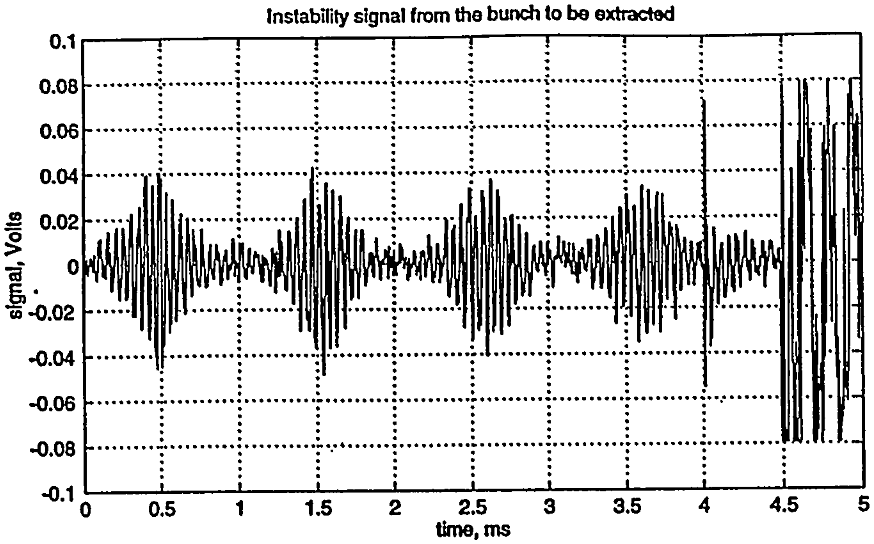

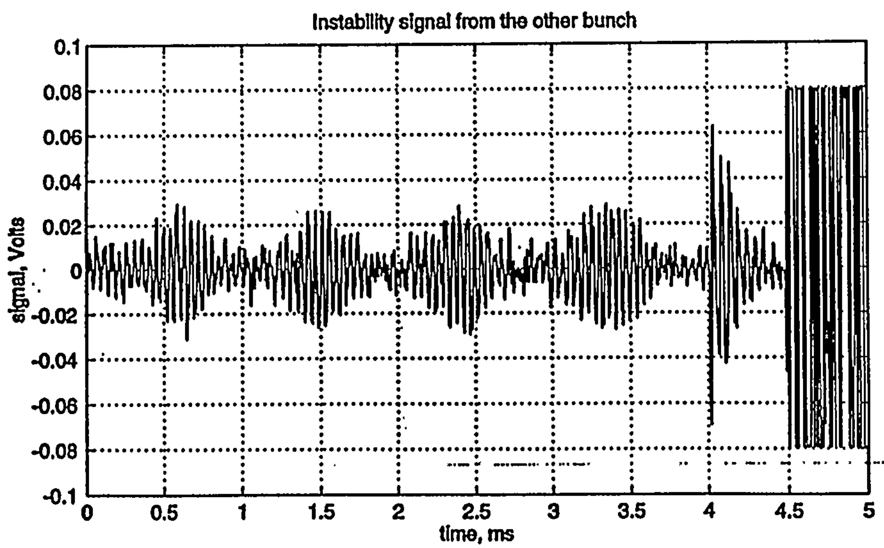

Angular Histogram of Average Phase when Both Bunches are Unstable

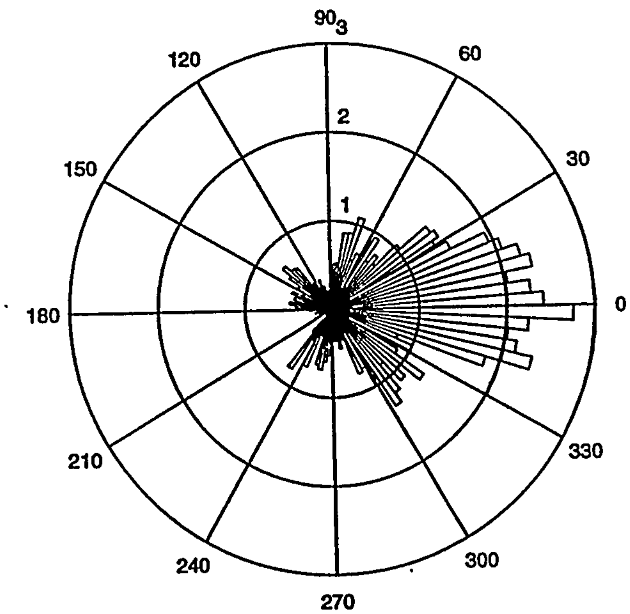

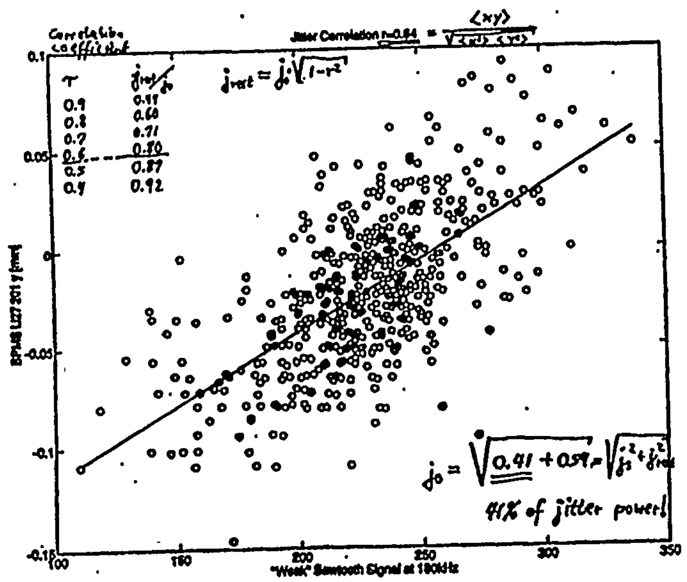

5. COMMENTS

THIS HAS BEEN A REPORT ABOUT AN EXPERIMENT IN PROGRESS.

- There are features of the data that we do not understand.

  - The instability distribution $\rho(\tau)$ looks dipole-like, but the frequency $f \sim 1.8\ f_s$ suggests a quadrupole mode

  - Most features point to a single bunch instability, but there is a phase relationship when the amplitudes of both bunches are large

- Can models make quantitative predictions?

  - We can measure many properties of this instability, but which, if any, are unique properties of particular instability models?

  -Possibilities: Threshold dependence on V_{RF}

  Correlation in time of harmonics of the instability frequency

  Driven response of the instability

- Data taking capabilities are being improved with integration of the streak camera into the SLC control system. This will allow a significant increase in the amount of data and the ability to correlate with other SLC parameters

INSTABILITY OF PERIODIC ORBIT AND NON-INTEGRABILITY OF HAMILTONIAN SYSTEM

H. Yoshido, NAO

Instability of a periodic solution and
non-integrability of Hamiltonian systems

H. Yoshida
National Astronomical Observatory of Japan
Tokyo, Japan

1. Stability analysis of a periodic solution in a quartic potential system
2. Unexpected FACT !
3. Rigorous determination of stability
4. Nonintegrability proof
5. Extentions

$$dx/dt = F(x) \qquad x \in \mathbb{R}^n$$

Periodic solution

$$x = \psi(t), \quad \psi(t+T) = \psi(t)$$

Variational equation

$$d\xi/dt = (\partial F/\partial x)\,\xi$$

Monodromy matrix

$$\xi(T) = M(T)\xi(0)$$

Eigenvalues : σ_i

$$\sigma_i = \exp(\alpha_i T)$$

σ_i : characteristic multipliers

α_i : characteristic exponents $\longrightarrow$ Lyapunov exp.

Hamiltonain system (2 degrees of freedom)

$$\sigma_i = (1, 1, \sigma, 1/\sigma)$$

$$\alpha_i = (0, 0, \alpha, -\alpha)$$

$$\mathrm{trace}\, M(T) = \sigma + 1/\sigma \ (+2)$$

$$|\mathrm{trace}\, M(T)| < 2$$

$|\sigma| = 1$, Stable

$$|\mathrm{trace}\, M(T)| > 2$$

σ: real, Unstable

No algorithmic way !

A quartic potential $H = \frac{1}{2}p^2 + V(q)$

$$V = (1/4)(q_1^4 + q_2^4) + (\varepsilon/2)q_1^2 q_2^2$$

$\varepsilon = 0, 1, 3$ --> Integrable

Painlevé analysis

$\rightarrow \ \varepsilon = 0, 1, 3$

homogeneous potential

→ $\boxed{\text{Scale Invariant}}$

(All Energy $H = E$, Same)

Non-homogeneous potential

→ Stability of P.O. , etc

depends on E

Potential Function $V(q_1, q_2)$

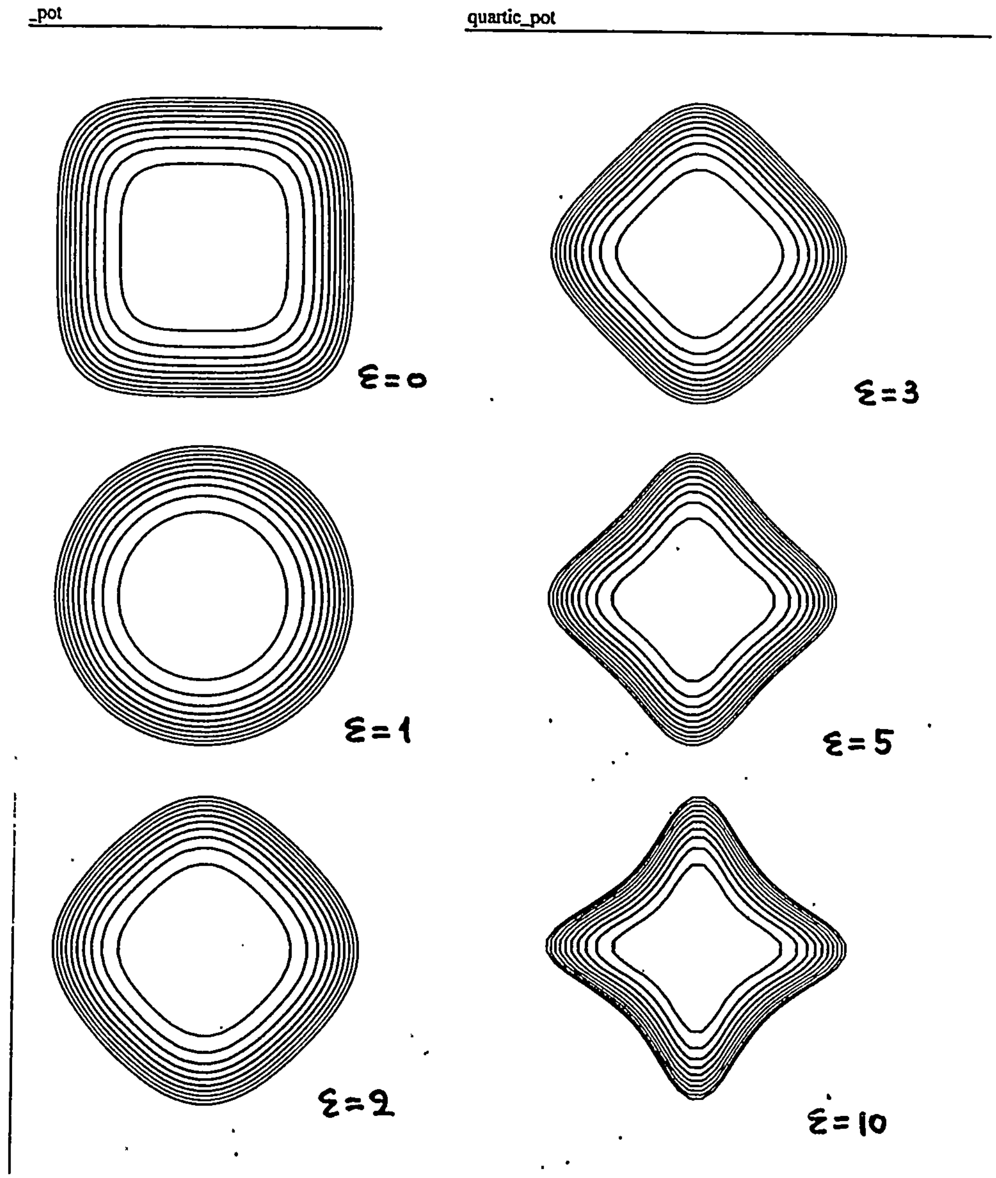

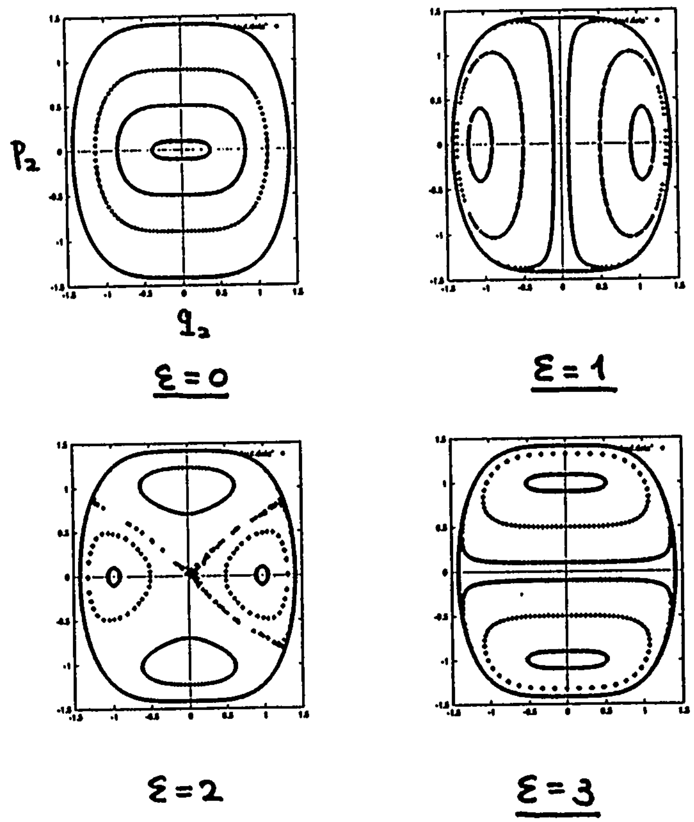

εの変化による Poincaré 写像の変化。

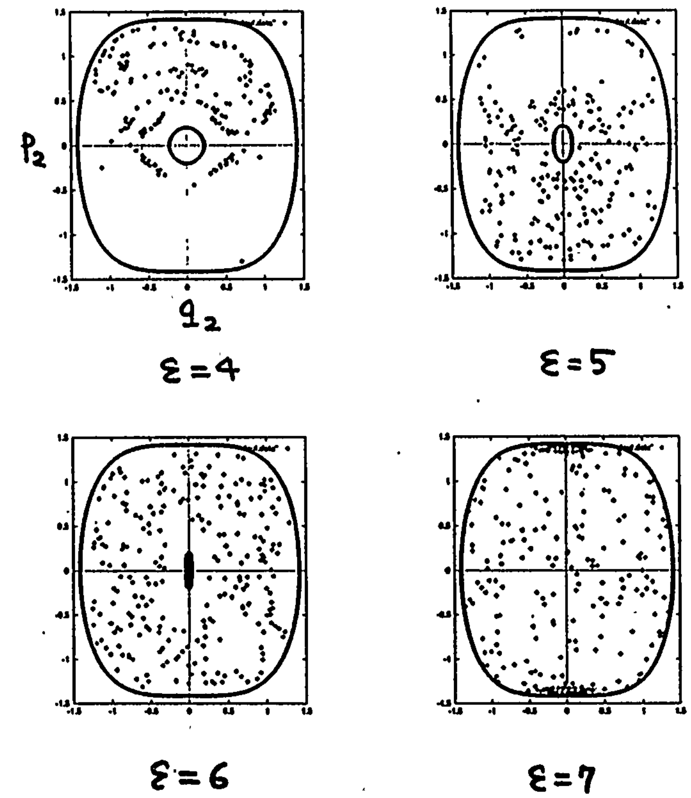

εの変化による Poincaré 写像の変化。

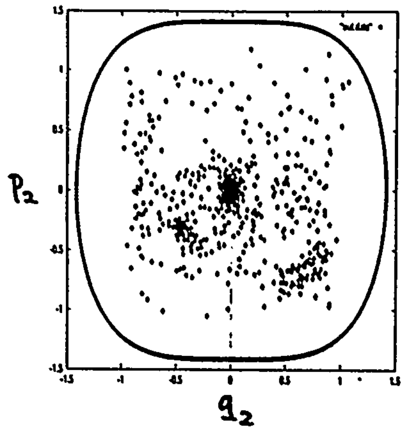

4th Runge-Kutta

$\varepsilon = 5$

$\Delta t = 0.25$

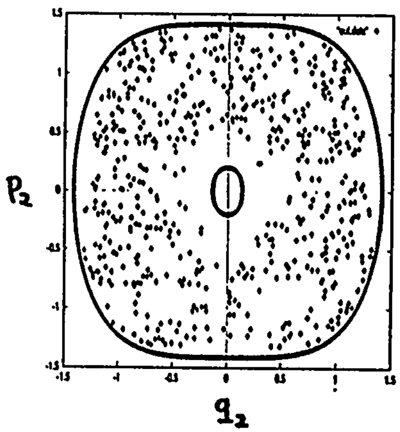

4th Symplectic

$\varepsilon = 5$

$\Delta t = 0.25$

RK4 vs SI4 $(\epsilon = 5)$

$$H = (1/2)(p_1^2 + p_2^2) + V(q_1, q_2)$$

where

$$V = (1/4)(q_1^4 + q_2^4) + (\varepsilon/2)q_1^2 q_2^2$$

- eq. of motion

$$\begin{cases} d^2q_1/dt^2 = -q_1(q_1^2 + \varepsilon q_2^2) \\ d^2q_2/dt^2 = -q_2(q_2^2 + \varepsilon q_1^2) \end{cases}$$

- straight-line solution

$q_1 = 0$

$d^2q_2/dt^2 = -q_2^3$

-----> $q_2 = \mathrm{cn}(t, 2^{-1/2})$ Jacobi elliptic function

doubly periodic, $T_1 = 4K$, $T_2 = i4K$

- Variational equation $\xi_i = \delta q_i$

$$\begin{cases} d^2\xi_1/dt^2 = -\varepsilon \{q_2(t)\}^2 \xi_1 & \text{N.V.E.} \\ d^2\xi_2/dt^2 = -3 \{q_2(t)\}^2 \xi_2 & \text{T.V.E.} \end{cases}$$

J. Phys. A21, 3547 (1988)

Acknowledgments

One of us (DR) acknowledges support by the National Fund for Scientific Research (Belgium) as senior research assistant and by the Alexander von Humboldt Foundation for a stay at the Institute of Physics of the University of Essen where part of this work was done.

Appendix

```
C***********************************************************************
C CALCULATION OF TRACE OF MONODROMY MATRICES                           *
C PARAMETERS TO BE CHOSEN ARE DEGREE D AND EPSILON AND GAMMA           *
C***********************************************************************
      PROGRAM MAIN
      IMPLICIT REAL*8(A-B,D-H,O-Z),COMPLEX*16(C)
      COMMON EPS,GAM,PI,IDEG,NSTEP
      NSTEP=50
      GOTO 2
 1    WRITE(6,*)'YOUR CHOICE ? 0=STOP, 1=NEXT'
      READ(5,*)IFLAG
      IF(IFLAG)999,999,2
 2    WRITE(6,*)'DEGREE D=? (INTEGER),EPSILON AND GAMMA ? (REAL)'
      READ(5,*)IDEG,EPS,GAM
      WRITE(6,*)'TRACE OF MONODROMY MATRICES MI, I=1,...,D'
      PI=4.D0*DATAN(1.D0)
      DX=DCOS(PI/DFLOAT(IDEG))
      DY=DSIN(PI/DFLOAT(IDEG))
      COMEGA=CMPLX(DX,DY)
      DO 4 KK=1,IDEG
      CTINIT=(1.D0,0.D00)
      CTFINA=CTINIT+(4.D00,0.D00)*COMEGA**(KK-1)
      CALL TRACE(CTINIT,CTFINA,CTRACE)
 4    WRITE(6,*)CTRACE
      GO TO 1
 999  STOP
      END

C***********************************************************************
C SUBROUTINE TRACE CALCULATES TRACE OF MONODROMY MATRIX (CTRACE)*
C FOR STRAIGHT LINE IN COMPLEX TIME PLANE FROM CTINIT TO CTFINA *
C***********************************************************************
      SUBROUTINE TRACE(CTINIT,CTFINA,CTRACE)
      IMPLICIT REAL*8(A-B,D-H,O-Z),COMPLEX*16(C)
      DIMENSION CX(6)
      COMMON EPS,GAM,PI,IDEG,NSTEP
      EXTERNAL CEQ1
      DEG=DFLOAT(IDEG)
      FACT=DSQRT(PI/DEG)/2.D0
      UNIT=FACT*DGAMMA(0.5D0/DEG)/DGAMMA(0.5D0/DEG+.5D0)
      CT=CTINIT
      CX(1)=0.D0
      CX(2)=-1.D0/SQRT(DEG)
      CX(3)=1.D0
      CX(4)=0.D0
      CX(5)=0.D0
      CX(6)=1.D0
      CDELT=(CTINIT-CTFINA)/NSTEP*UNIT
      DO 20 J=1,NSTEP
      CALL CRUNGE(6,CEQ1,CT,CX,CDELT)
 20   CONTINUE
      CTRACE=CX(3)+CX(6)
      RETURN
      END

C***********************************************************************
C COMPLEX FUNCTION CEQ1 CONTAINS THE EQUATIONS THAT HAVE TO *
C BE INTEGRATED                                                        *
C***********************************************************************

      COMPLEX FUNCTION CEQ1*16(I,CX)
      IMPLICIT REAL*8(A-B,D-H,O-Z),COMPLEX*16(C)
      DIMENSION CX(6)
      COMMON EPS,GAM,PI,IDEG,NSTEP
      CGAM=(0.D0,1.D0)*GAM
      GO TO (10,20,30,40,50,60),I
 10   CEQ1=CX(2)
      RETURN
 20   CEQ1=     -CX(1)**(2*IDEG-1)
      RETURN
 30   CEQ1=   CX(4)
      RETURN
 40   IF(IDEG.GT.2)GOTO 42
 41   CEQ1=( EPS*CX(1)**2+CGAM*CX(2))*CX(3)
      RETURN
 42   CEQ1=(-EPS*CX(1)**(2*IDEG-2)+CGAM*CX(1)**(IDEG-2)*CX(2))*CX(3)
      RETURN
 50   CEQ1=CX(6)
      RETURN
 60   IF(IDEG.GT.2)GOTO 62
 61   CEQ1=(-EPS*CX(1)**2+CGAM*CX(2))*CX(5)
      RETURN
 62   CEQ1=(-EPS*CX(1)**(2*IDEG-2)+CGAM*CX(1)**(IDEG-2)*CX(2))*CX(5)
      RETURN
      END

C***********************************************************************
C SUBROUTINE CRUNGE IS A COMPLEX FOURTH ORDER RUNGE-KUTTA SCHEME      *
C FOR INTEGRATION OF N EQUATIONS FROM T TO T+DT                       *
C***********************************************************************

      SUBROUTINE CRUNGE(N,F,T,X,DT)
      IMPLICIT COMPLEX*16(A-H,O-Z)
      DIMENSION X(6),X1(6),X2(6),X3(6),D(4,6)
      DO 10 I=1,N
      D(1,I)=F(I,X)*DT
 10   X1(I)=X(I)+D(1,I)/2.D00
      DO 20 I=1,N
      D(2,I)=F(I,X1)*DT
 20   X2(I)=X(I)+D(2,I)/2.D00
      DO 30 I=1,N
      D(3,I)=F(I,X2)*DT
 30   X3(I)=X(I)+D(3,I)
      T=T+DT
      DO 40 I=1,N
      D(4,I)=F(I,X3)*DT
 40   X(I)=X(I)+(D(1,I)+2.D0*D(2,I)+2.D0*D(3,I)+D(4,I))/6.D0
      RETURN
      END
```

References

[1] Hietarinta J 1987 *Phys. Rep.* 147 87
[2] Graham R, Roekaerts D and Tél T 1985 *Phys. Rev.* A 31 3364
[3] Dorizzi B, Grammaticos B, Ramani A and Winternitz P 1985 *J. Math. Phys.* 26 3070
[4] Hietarinta J 1985 *J. Math. Phys.* 26 1970
[5] Roekaerts D and Schwarz F 1987 *J. Phys. A: Math. Gen.* 20 L127
[6] Ziglin S L 1983 *Funct. Anal. Appl.* 16 181, 17 6
[7] Yoshida H 1986 *Physica* 21D 163
[8] Yoshida H 1988 *Physica* 29D 128
[9] Yoshida H, Ramani A, Grammaticos B and Hietarinta J 1987 *Physica* 144A 310
[10] Yoshida H 1987 *Phys. Lett.* 120A 388
[11] Ito H 1985 *Kodai Math. J.* 8 120
[12] Ito H 1987 *J. Appl. Math. Phys.* 38 459
[13] Rod D L 1986 *Preprint. On a theorem of Ziglin in Hamiltonian dynamics*
[14] Yoshida H 1988 *Commun. Math. Phys.* 116 529
[15] Yoshida H, Ramani A and Grammaticos B 1988 *Physica* 30D 151

$$d\xi/dt = \eta$$

$$d\eta/dt = -\varepsilon[\phi(t)]^{2\varepsilon}\xi$$

where

$$\phi(t) = \mathrm{cn}(t, 2^{-1/2})$$

i.e.

$$d^2\phi/dt^2 + \phi^3 = 0$$

trace of Monodromy matrix as a function of ε

$\varepsilon = 0$ trace M = 2

$\varepsilon = 1$ " = -2

$\varepsilon = 3$ " = -2

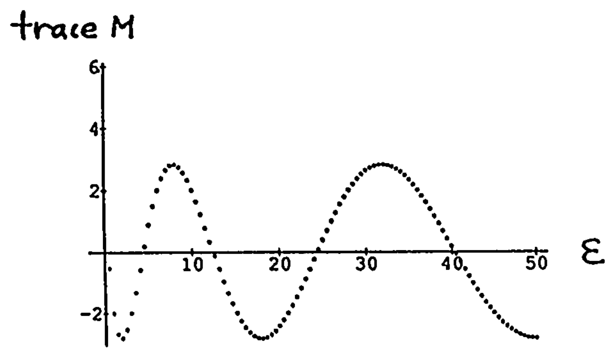

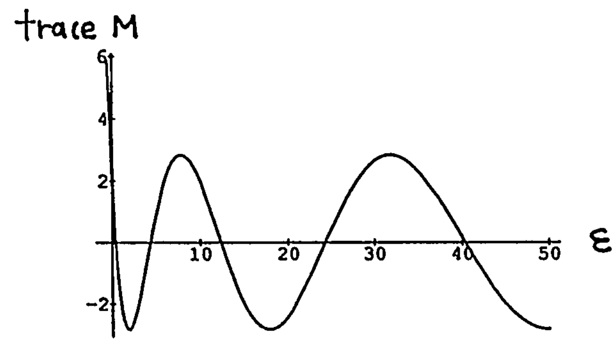

$$\text{trace } M = 2\sqrt{2}\,\cos\left[\frac{\pi}{4}\sqrt{1+8\varepsilon}\right]$$

Error $< 10^{-13}$!!

trace M

```
In[26]:=
  Plot[{2 Sqrt[2] Cos[Pi Sqrt[1 + 8 x]/4],
        2 Sqrt[2] Cos[Pi Sqrt[1 + 8 (3-x)/(1+x)]/4]},
        {x,-.99,10},
        PlotRange->{-4,6},
        Axes->True,
        Frame->True]
```

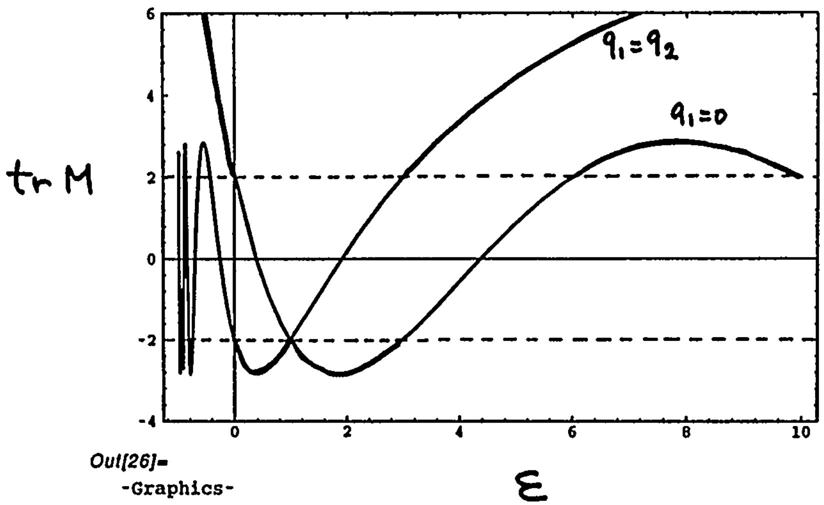


```
Out[26]=
  -Graphics-
```

$$d^2\xi/dt^2 + \varepsilon[\phi(t)]^2\xi = 0$$

By the change of the independent variable

$$z = [\phi(t)]^4$$

⇩

Gauss hypergeometric equation

$$z(1-z)d^2\xi/dz^2 - [c - (a+b+1)z]d\xi/dz - ab\xi = 0$$

$$a + b = 1/4$$
$$ab = -\varepsilon/8$$
$$c = 3/4$$

$\varepsilon = 0, 1, 3$ のみが 指数関数的不安定性 なし

Only $\varepsilon = 0, 1, 3$ avoid Exp. Instability

Gauss hypergeometric equation

$$z(1-z)d^2\xi/dz^2 - [c-(a+b+1)z]d\xi/dz - ab\xi = 0$$

regular singular points

$$z = 0, 1, \infty$$

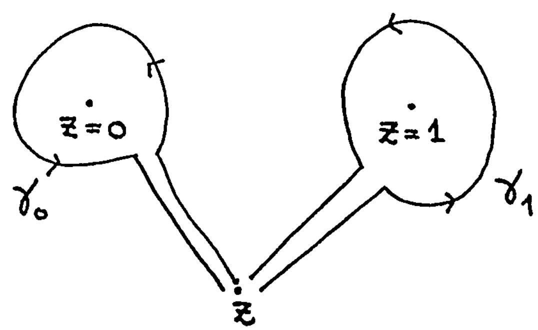

$$\Phi(z\gamma_0) = \Phi(z)\, M(\gamma_0)$$
$$\Phi(z\gamma_1) = \Phi(z)\, M(\gamma_1)$$

$M(\gamma_0)$, $M(\gamma_1)$

Explicit Expression

$$T \to \gamma_0^2 \gamma_1$$

$$M(T) = M(\gamma_0)^2 M(\gamma_1)$$

$$M(\gamma_0) = \begin{bmatrix} 1 & e^{-2\pi ib} - e^{-2\pi ic} \\ 0 & e^{-2\pi ic} \end{bmatrix}$$
$$M(\gamma_1) = \begin{bmatrix} e^{2\pi i(c-a-b)} & 0 \\ 1 - e^{2\pi i(c-a)} & 1 \end{bmatrix}$$

$$a + b = 1/4$$
$$ab = -\varepsilon/4$$
$$c = 3/4$$

$$\mathrm{trace}\, M(\gamma_0)^2 M(\gamma_1)$$
$$= 2\sqrt{2}\, \cos\left[\frac{\pi}{4}\sqrt{1+8\varepsilon}\right]$$

Happy End !

Exp. Instability is compatible with Integrability

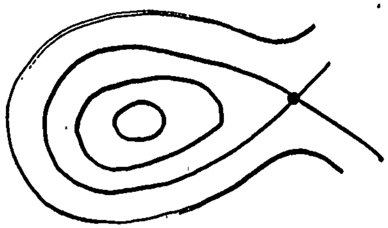

Exp. Instability (of Infinitely Many Orbits) is NOT compatible with Integrability

Homoclinicity is NOT compatible with Integrability

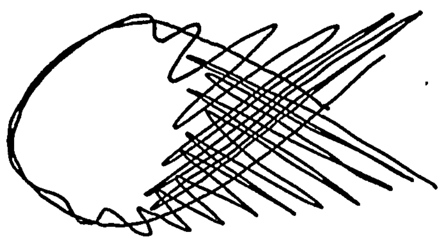

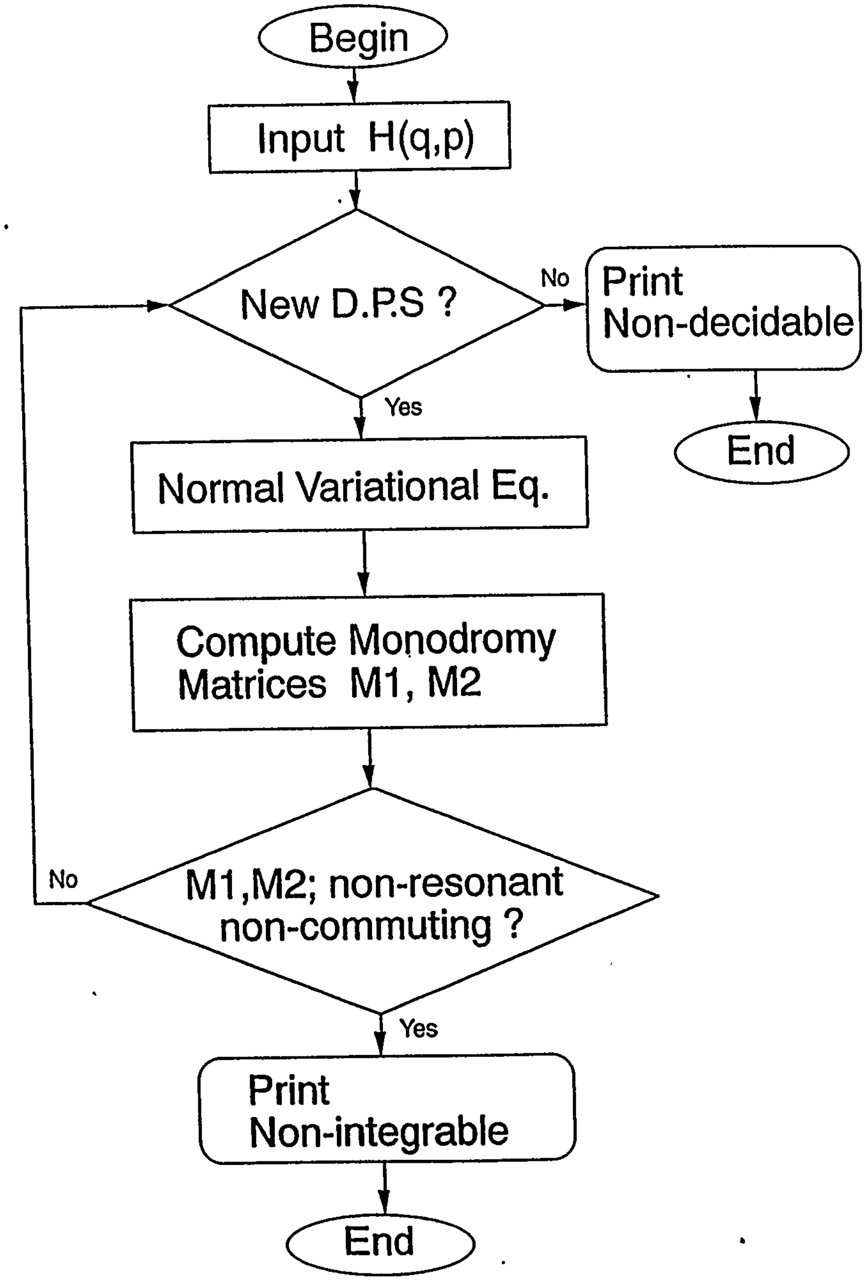

```
Plot3D[Abs[JacobiCN[ux + I uy, 1/2]],
       {ux, 0, 10},{uy, 0, 10},PlotPoints->30]
```

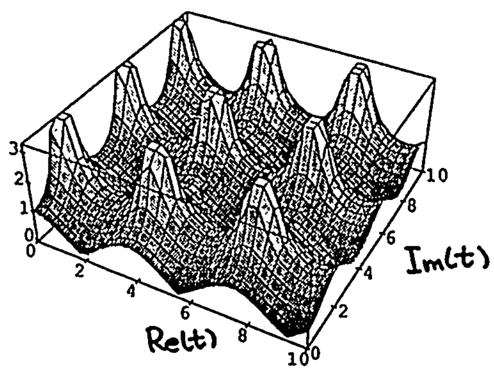

-SurfaceGraphics-

$|cn(t, 1/\sqrt{2})|$

Theorem (Ziglin 1983)

Φ = const. complex-analytic integral

$M(T_1)$: non-resonant

==>

(i) $[\, M(T_1), M(T_2)\,] = 0$, commute

or

(ii) trace $M(T_2) = 0$

eigenvalue $\pm i$
→ resonant

Corollary

$M(T_1), M(T_2)$: non-resonant,

non-commuting

==>

No complex analytic integral Φ = const.

$M(T_1)$, $M(T_2)$; explicit expression

Fact

$$\begin{cases} (1)\ \mathrm{trace}\, M(T_1) = \mathrm{trace}\, M(T_2) \\ \qquad = 2\sqrt{2} \cos\left[\frac{\pi}{4}\sqrt{1+8\varepsilon}\right] \\ (2)\ [M(T_1), M(T_2)] = 0 \end{cases}$$

$\Longleftrightarrow$ trace $M = 2, -2$

- if $\varepsilon < 0, 1 < \varepsilon < 3, 6 < \varepsilon < 10$, ...

  then

  $|\mathrm{trace}\, M(T_{1,2})| > 2$ (non-resonant)

  $[M(T_1), M(T_2)] \neq 0$

$\Longrightarrow$

non-existence of $\Phi(q,p) = \text{const.}$

Another straight-line solution : $q_1 = q_2$

N.V.E. with $\varepsilon' = (3 - \varepsilon)/(1 + \varepsilon)$

$0 < \varepsilon < 1, 3 < \varepsilon$ ---> non-integrable

In general

Exponentially unstable periodic solution does NOT prove NON-INTEGRABILITY

However,

In systems with a homogeneous potential

Exponentially unstable periodic solution does prove NON-INTEGRABILITY

Extension

1. $H = \frac{1}{2}\mathbf{p}^2 + V(\mathbf{q})$

   homogeneous, degree k

2. $H = \underset{\text{deg. } m}{T(\mathbf{p})} + \underset{\text{deg. } k}{V(\mathbf{q})}$

3. $H = \frac{1}{2}\mathbf{p}^2 + \sum_i \exp\left(\sum_j \alpha_{ij} q_j\right)$ Toda lattice

   $Z = \exp q \Rightarrow$ Gauss. eq.

4. $H = \underset{\text{deg. } m}{T(\mathbf{p})} + \sum_i \exp\left(\sum_j \alpha_{ij} q_j\right)$

Scale Invariance $\xrightarrow[?]{}$ Gauss eq.

Conclusion

1. Stability of straight-line periodic solution in Hamiltonian systems with a homogeneous potential is determined exactly

   Thanks Gauss. Riemann

2. Exp. instability implies non-integrability

   Thanks Ziglin

   (Kowalevskaya
   Painlevé)

NEUTRALIZED BEAMS: LANDAU DAMPING IN SYSTEMS WITH STRONG NONLINEARITY

Zenkevitch, ITEP

P. Zenkevich, E. Mustafin

Neutralised beams: Landau Damping in Systems with Strong Nonlinearity.

1. Dipole "drift" instability in NEB:
2. One-dimensional (sheet) beams.
   - Basic system of integral equations.
   - method "uncoupled modes" (weak nonlinearity)
   - Approximate solution of basic system for dipole mode (strong nonlinearity).
3. Two-dimensional round beams.
   - Basic system of integral equations,
   - estimation of LD for dipole mode (Burov's model),
   - stationary state
   - (numerical simulations by multi-particle code.
4. Summary.

Purpose: to improve characterstics LEAR e-cooling system to injecti LEAD ions in LHC.

. neutralization suppresses space-charge forces that permits diminish e-cooling time.

Collaboration CERN - Russia:

J. Bosser, D. Möhl et al (CERN, LEAR)

I. Meshkov, Ye. Syresin et al (JINR)

P. Zenkevich, E. Mustafin (ITEP, Moscow)

1.3 Influence on Pressure

Another effect of neutralisation is the worsening of the vacuum environment. : ions, inside the electron beam, are considered as an additional gas along the neutrali: length L. The increase of the average pressure will be:

$$\Delta P = 2.8\times10^{-17} n_+ \left(\frac{L}{C}\right)$$

where C is the storage ring circumference. For LEAR, when $n_+ = 10^8$ cm^{-3}, $\Delta P \cong 5\times$ torr.

2. TECHNIQUE OF NEUTRALISATION

The method is described in details in Refs. [5, 6]. It consists of two sets of neutralis: or trapping electrodes, one, El_g, placed at the gun output and the other, El_c, placed a collector entrance (Fig. 3). Each electrode consists of two metallic half-cylinders separate a "resistive insulator", like conducting glass (Fig. 4).

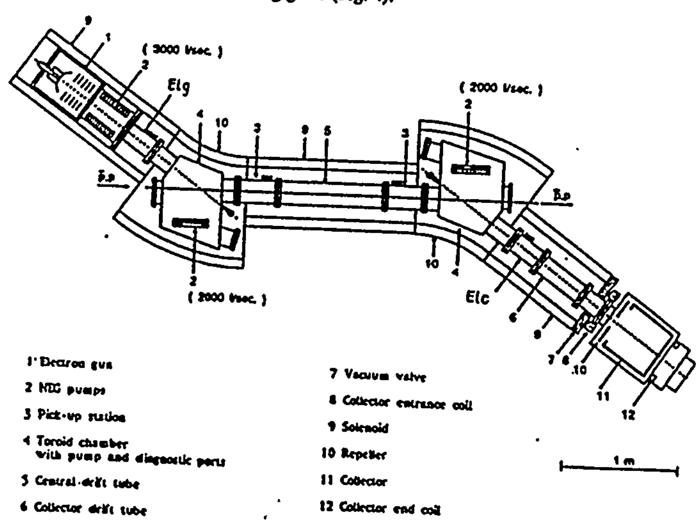

Fig. 3 - The electron cooling device with the implementation of El_g and El_c

One electrode is polarised by a positive (referred to ground) potential U_{e2}, the other i close to zero potential, $U_{e1} \cong 0$ V. This positive potential will keep the ionised ions trappe

1. Why we are interested in LD in NEB?

Hydrodynamical theory of drift dipole instability.

For electron center of gravity:

$$\frac{d\tilde{V}_e}{dt} - i\eta\omega_d^0 (\tilde{V}_e - \tilde{V}_i) = 0 \qquad (1)$$

For individual ions

$$\frac{d^2 V_i}{dt^2} + i\omega_L \frac{dV_i}{dt} + \omega_{ion}^2 (V_i - \tilde{V}_e) - \eta\,\omega_{ion}^2 (V_i - \tilde{V}_i) = 0 \qquad (2)$$

Here subscripts "e","i" refer to primary electrons and ions, $V = x + iy$ describes a horizontal (x) and vertical displacements of the particles in complex notation, sign "~" above markes displacements of centers of gravity, $\eta = Z n_i/n_e$ is a neutralization factor. The frequencies in Eqs (1-2) are (cgs units, B in Gs):

$\eta\,\omega_d^0 = \eta\,\dfrac{2\pi n_e c e}{B}\, r_p c^2$ the electron "drift frequency" in the space charge field of the ions.

$$\omega_L = \frac{ZeB}{Mc}$$ Larmour frequency of the ions with charge number Z and mass $Am_p = M$

$$\omega_p^2 = \frac{2\pi n e Z r_p c^2}{A}$$ "Plasma ion frequency", i.e. squared frequency of free ion oscillations in space charge field of electrons.

Incoherent oscillations of the ions ($\tilde{v} = 0$)

$$\frac{d^2 v_i}{dt^2} + i\omega_L \frac{dv_i}{dt} + \omega_p^2 (1-\eta) v_i = 0 \tag{3}$$

$$\omega_{1,2}^{incoh} = -\frac{\omega_L}{2} \pm \sqrt{\left(\frac{\omega_L}{2}\right)^2 + \omega_p^2 (1-\eta)} \tag{4}$$

For weakly magnetized ions ($\omega_L^2 / 4\omega_p^2 \ll 1$) and $\eta \to 1$

$$\omega_{1,2}^{incoh} \to 0$$

Coherent oscillations of the ions ($\tilde{v}_e = 0$)

$$\frac{d^2 \tilde{v}_i}{dt^2} + i\omega_L \frac{d\tilde{v}_i}{dt} + \omega_p^2 \tilde{v}_i = 0 \tag{5}$$

$$\omega_{1,2}^{coh} = -\frac{\omega_L}{2} \pm \sqrt{\left(\frac{\omega_L}{2}\right)^2 + \omega_p^2} \tag{6}$$

For weakly magnetised ions and $\eta \to 1$

$$\omega_{1,2}^{coh} \to \pm \omega_p$$

Coherent electron-ion oscillations.

We see that electrons and ions have no damping. Such system is unstable! Let us introduce artificially (by hands) the ion damping. Then we obtain:

$$\left.\begin{aligned} &\frac{d\tilde{v}_e}{dt} - i\eta\omega_d^0 (\tilde{v}_e - \tilde{v}_i) = 0 \\ &\frac{d^2\tilde{v}_i}{dt^2} + 2\gamma_\perp \frac{d\tilde{v}_i}{dt} + i\omega_L \tilde{v}_i + \omega_p^2 (\tilde{v}_i - \tilde{v}_e) = \bar{0} \end{aligned}\right\} \tag{7}$$

Let us seek solution in a form:

$$\tilde{v}_{e,i} = a_{e,i} \exp(ikz - i\omega t) \tag{8}$$

Then we have:

$$kv = \omega + \eta\omega_d^0 + \frac{\eta \omega_d^0 \omega_p^2}{\Delta_i} \tag{9}$$

$$\Delta_i = \omega^2 - 2i\gamma_\perp \omega + \omega_L \omega - \omega_p^2 \tag{10}$$

For $\omega = \omega_{1,2}^{coh}$

$$\Delta_i = -2i\gamma_\perp \omega_{1,2}^{coh} \tag{11}$$

and

$$\mathrm{Im}\, k = \frac{\eta \omega_d^0}{\varepsilon_\perp'' v} \tag{12}$$

$$\epsilon_\perp'' = \frac{2\gamma_\perp |\omega^{coh}|}{\omega_p^2} \rightarrow \frac{2\gamma_\perp}{\omega_p} \qquad (13)$$

for unmagnetised ions.

Amplification coefficient of the travelling wave

$$K = \exp(L \cdot \mathrm{Im}\,\kappa) = \exp\left(\frac{\eta \omega_d^0 L_0}{\epsilon_\perp'' V}\right) \qquad (14)$$

In system there is a "natural" feedback (positive): due to secondary electrons, transverse - longitudinal coupling and etc. Let f - such coefficient. In system "absolute" instability appears, if

$$K f = 1 \qquad (15)$$

Using Eqs. (14) and (15), we obtain final result:

$$\boxed{j_{th} = \frac{v^2 B}{L c} \frac{\epsilon_\perp'' \ln \frac{1}{f}}{\eta}} \qquad (16)$$

Thus, we are interested in:

① How to find $\epsilon_\perp''$ (nonlinear effects?)

② What is its dependance on system paramers (η, electron temperature T_e and...)?

2 One - dimensional beams

a. Standard scheme: and basic system.

1) $v_x, p_x \rightarrow I, \chi$ (action - phase)

2) Linearization of Vlasov's system.

$$f = f_0(I) + f_1(I,\chi,t) \qquad (17)$$

$$f_1(I,\chi,t) = \sum_{n=-\infty}^{\infty} f_n(I) \exp(in\chi - i\omega t) \qquad (18)$$

$$\left.\begin{aligned} i f_n(I)(n\Omega - \omega) &= \left[\frac{\partial f_0}{\partial I} e z E_1(I,\chi) \frac{dx}{d\chi}\right]_n \\ \Delta U_1 &= -4\pi\rho = -4\pi \int f_1\, dx \end{aligned}\right\} \qquad (19)$$

$$\varphi_n(I) = \lambda \sum_{n'} \int \frac{dI'\, G_{n,n'}(I,I')\, \varphi_n(I')}{n'\Omega_{(I')} - \omega} \qquad (20)$$

or equivalent system:

$$E_1^n(y) = \tilde{\lambda} \int E_1(y')\, Q_n(y,y';\Omega)\, dy' \qquad (21)$$

Approximate methods

a) "uncoupled modes"

б) method: "I know eugen-function and eugen - frequency." (applicable only for dipole mode!)

6) <u>Method "uncoupled modes"</u>

$$\varphi_n(I) = \lambda \int_0^{I_{max}} \frac{G_{n,n}(I,I')\,\varphi_n(I')\,dI'}{n\,\Omega(I') - \omega}. \qquad (22)$$

L.D. exists, if

$$\Omega(0) < \frac{\omega}{n} \leqslant \Omega(I_{max})$$

Let us introduce new dimensionless parameter:

$$\nu = \frac{\frac{\omega}{m} - \Omega(0)}{\Omega(I_{max}) - \Omega(0)}.$$

Then we can write for L.D.:

$$\nu < 1. \qquad (23)$$

for small η, ν doesn't depend on η

$$\nu = f(m,s)$$

For "water-bag" distribution:

$$\nu_n = 1 + \frac{64}{\pi(4n^2-1)} \qquad (24)$$

L.D. appears only for $s > 0$

"decreasing density in phase space".

(see picture).

8

P. Zenkevich, A. Korolev

" Self-stabilization of Coherent Oscillations (Sheet Beams)", Msc, ITEP, 1985.

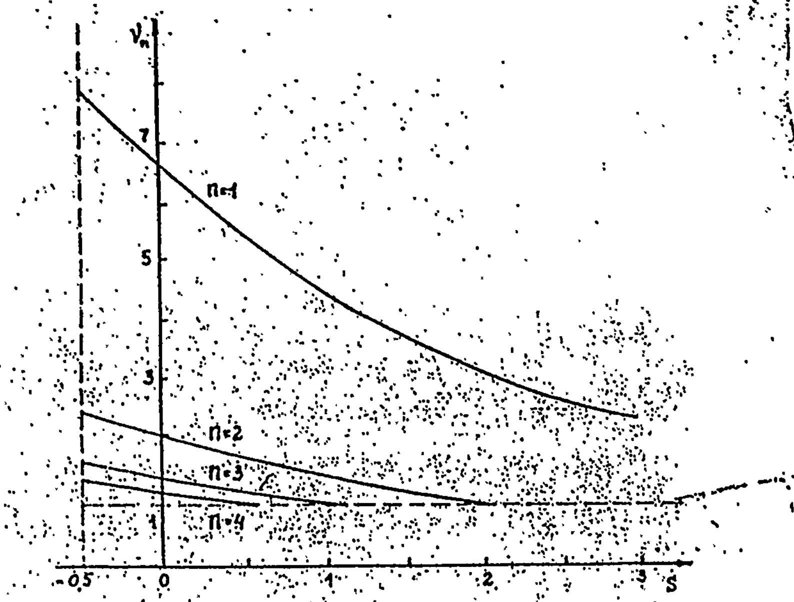

Рис.1. Зависимость действительных собственных чисел ν_n (n = 1,2,3,4) от s.

Dependance of real eigen-values ν_n ($n = 1, 2, 3, 4$) on s

$$f_0(H) \sim (1 - H/H_{max})^{s}$$

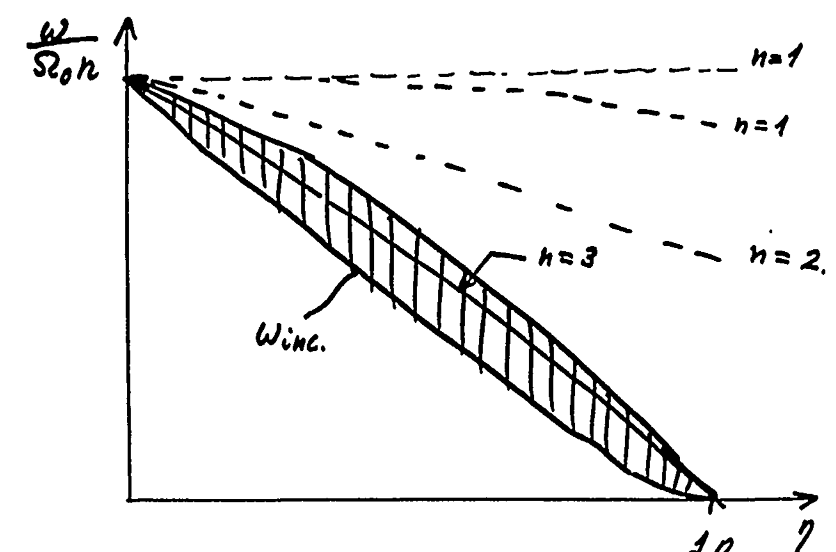

The form of curves depends on s, i.e. on distribution function in phase space.

Damping of the dipole mode due to mode coupling.

Let us consider two modes n, n'

n without damping

n' with damping

For degenerated kernels we have

$$\left.\begin{aligned} (\omega-\omega_n)a_n + \alpha_{n,n'}a_{n'} &= 0 \\ \alpha_{n',n}\, a_n + (\omega-\omega_{n'})a_{n'} &= 0 \end{aligned}\right\} \qquad (25)$$

$$\operatorname{Im}\omega_n \simeq \frac{\alpha_{n,n'}\cdot\alpha_{n',n}}{(\omega_n-\omega_{n'})^2}\operatorname{Im}\omega_{n'} \qquad (26)$$

Coefficients $\alpha_{n,n'}$ were calculated (Kosh., Zenk, 1972). For $n=1$, $n'=3$ we have

$$\operatorname{Im}\omega_1 \simeq 0.15\operatorname{Im}\omega_3 \sim 0.02\eta$$

c. Approximate solution of basic system for dipole mode (strong nonlinearity).

Let us assume, that:

1) we know eugen-function for the dipole mode!

2) we know Real part of eugen-value for the dipole mode!

3) electrical field of dipole mode

$$E = \alpha \tilde{X} = a \cdot \exp(i\omega t) \qquad (27)$$

Let us return back to linearized Vlasov's system. We have:

$$i f_n(I)(n\Omega - \omega) = e Z a \frac{\partial f_0}{\partial I}\left(\frac{dx}{d\chi}\right)_n \qquad (28)$$

Denominating $\left(\frac{dx}{d\chi}\right)_n$ through Γ_n and substituting Eq. (28) in

$$a = \alpha\tilde{x} = \alpha \iint dI\, d\chi \sum_n f_n(I) \exp(in\chi) \cdot x(\chi) \qquad (29)$$

we obtain a final dispersion equation:

$$\boxed{1 = \frac{\alpha e Z}{M} \int dI \frac{df_0}{dI} \sum_{n=-\infty}^{\infty} \frac{\Gamma(n)\cdot\Gamma(-n)}{n(n\Omega - \omega)}} \qquad (29)$$

Calculation of Γ_n is a non-trivial problem. However, in limiting case $|1-\gamma| \ll 1$ we can consider a model of "reflecting wall". Then a phase trajectory of individual particles has a "rectangle":

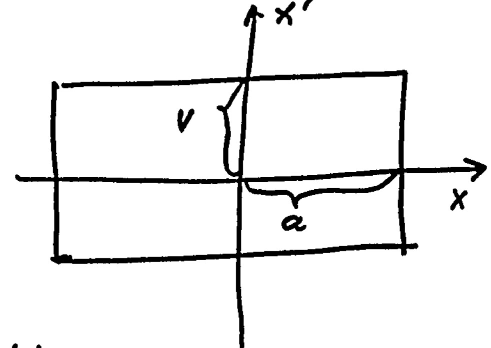

In this case:

$$\left.\begin{aligned} I &= \frac{2}{\pi} M v a \\ \Omega &= \frac{2}{\pi}\frac{v}{a} \end{aligned}\right\} \qquad (30)$$

$$\Gamma_n = \begin{cases} n^{-1} & \text{for odd } n \\ 0 & \text{for even } n \end{cases}$$

Dispersion equation (29) goes to:

$$1 = \frac{\alpha e Z}{M} a^2 \int dI \frac{df_0}{dI} \sum_{m=0}^{\infty} \frac{1}{(2m+1)^3}\left[\frac{1}{(2m+1)\Omega - \omega} - \frac{1}{(2m+1)\Omega - \omega}\right] \qquad (31)$$

Let us consider to simplify calculations the simplest case:

$$\left.\begin{aligned} f_{0}(I) &= 2\left(1-\frac{I}{I_m}\right)\frac{1}{I_m} \\ \frac{df_0}{dI} &= -\frac{2}{I_m^2}\,\Pi\left(1-\frac{I}{I_m}\right) \end{aligned}\right\}$$

$\Pi(x)$ – Heaviside function. (θ-function)

Then dispersion eq. may be written as:

$$1=\frac{\Lambda}{\Omega_m^2}\int_0^{\Omega_m} d\Omega \sum_{m=1}^{\infty}\frac{1}{(2m+1)^3}\left[\frac{1}{(2m+1)\Omega-\omega}-\frac{1}{\Omega(2m+1)+\omega}\right] \quad (32)$$

~~Du~~ After integration, we have

$$1=\frac{\Lambda}{\Omega_m^2}\sum_{m=1}^{\infty}\frac{1}{(2m+1)^4}\left[\ln\frac{(2m+1)\Omega_m-\omega}{(2m+1)\Omega_0}-\ln\frac{(2m+1)\Omega_0}{(2m+1)\Omega_m+\omega}\right]$$

We see, that contribution in imaginary part ~~mak~~ are connected with modes for which

$$(2m+1)\geqslant\frac{\omega}{\Omega_m} \quad (33)$$

Changing summation over the integration (it is possible, if $\frac{\omega}{\Omega_m}\gg 1$) we can find

the final result:

$$\gamma_\perp=\frac{\sqrt{3}\cdot\pi^2}{24}\frac{\langle v\rangle}{a}=0.78\,\frac{\langle v\rangle}{a} \quad (34)$$

Numerical coefficient ~~is~~ depends on $f_0(I)$.

Let us assume, that $r_d/a \ll 1$.

(r_d is Debye radius). Then charge density in compensated beam

$$\rho=\rho_e-\rho_i\simeq\exp\left[-\frac{a-x}{r_d}\right] \quad (35)$$

Using Eq.(34) and Eq.(35), after simple calculations we obtain

$$\eta\simeq 1-\frac{r_d}{a} \quad (36)$$

$$\epsilon_\perp''=\frac{2\gamma_\perp}{\omega_\perp}\simeq\frac{\pi^2}{12}\frac{r_d}{a}=\frac{\pi^2}{12}(1-\eta) \quad (37)$$

Limits of applicability.

For Debye distribution a frequency of small oscillations

$$\frac{\omega_{sm}}{\omega}\sim \cancel{\exp\left(-\frac{a}{2r_d}\right)}\exp\left(-\frac{a}{r_d\cdot 2}\right) \quad (38)$$

It is clear, that model of reflecting well is good only, if

$$\omega_{sm} \ll \frac{2}{\pi}\frac{\langle v\rangle}{a}, \text{ or} \qquad (39)$$

$$\exp\left(-\frac{a}{2r_d}\right) \ll \frac{2}{\pi\sqrt{3}}\;\frac{r_d}{a} \qquad (40)$$

For $\frac{r_d}{a} = 0.2$ these values are approximately equal.

Taking into account these considerations, we obtain the following (speculative) plot

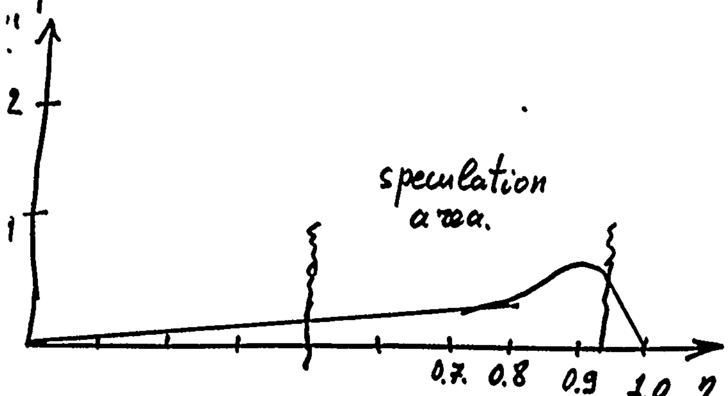

The left side of the curve (for small η) is described by small nonlinearity theory (coupling of modes), the right side – described above multi-mode theory.

Two-dimensional beams with axial symmetry.

1. Basic system of integral equations.

For stationary solution we have the following Hamiltotian (in cylindrical variables ρ, φ):

$$H = \frac{P_\varphi^2}{2Mr^2} + \frac{p_r^2}{2M} + ZeU(r) \qquad (41)$$

Thus, we have periodic motion on r and aperiodic on φ (with mean rotation frequency). It is convinient to use the following variables:

$$I_r, \chi_r;\; P_\varphi, \varphi$$

$$I_r = \frac{1}{2\pi}\oint p_r\, dr$$

We can look for a solution in the form:

$$f = f_0(H) + \sum_{n,m} f_{n,m}(I_r, P_\varphi)\exp[i(n\varphi + m\chi - i\omega t)] \qquad (42)$$

~~Substituting~~ Expanding in Fourrier-series, on angle variables, we obtain

$$i\, f_{n,m}(m\omega_r^0 + n\Omega - \omega) = \sum_{m'} \iint dI_r' dP_\varphi' \; G_{m,m'}(I_r, P_\varphi; I_r' dP_\varphi')\, f_{n,m'}(I_r', P_\varphi') \qquad (43)$$

Methods:

- models
- numerical solution of Vlasov's system
- numerical simulations by multi-particle code.

2. <u>Estimation of L.D. for dipole mode (Burov's model)</u>

Main ideas: a) case of $\frac{r_d}{a} \ll 1$ (reflections)

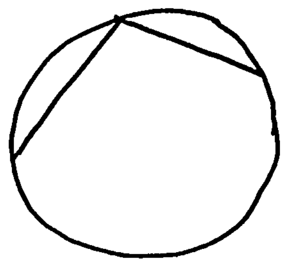

b) using of complex variable

$\eta = x + iy$

instead of cylindrical ones.

c) eugen-function and imaginary part of eugenfrequensy are assumed to be known.

d) imaginary part of eugen-frequency (Landau

damping) is calculated by use of the following scheme:

- it is calculated by use of nonlinear part of Boltzmann equation Q_i – mean ~~loss~~ change of energy for ion.
- relation of energy transferred from wave to ions to complete energy of the wave determined L.D.

According to Burov:

$$Q = Q_i \cdot N_i = \frac{2^{1/2} v_t}{\pi^{3/2} a} E_0^2 V \qquad (44)$$

$$W = V \frac{E_0^2}{2\pi} \qquad (45)$$

$$\gamma_\perp = Q / 2W = \frac{2^{1/2} v_T}{\pi^{1/2} a} \qquad (46)$$

This result is qualitatively coincides with result for one-dimensional model!

3. <u>Numerical simulations</u>

Stationary state.

Water-bag distribution. – there is analitical solution.

Potential of the electron beam:

$$V_e(r) = -\frac{Ie}{\beta c}\begin{cases} \frac{r^2}{a^2} & 0 \le r \le a \\ 1 + 2\ln\frac{r}{a} & a \le r \le b. \end{cases} \quad (44)$$

I – is the primary electron beam. current.

The ion potential is defined by Poisson equation:

$$\Delta_\perp U = -4\pi\rho(r) \quad (45)$$

It is convenient to introduce new variable:

$$Z(r) = eQ\,[U(r) + V_e(r)]\,/H_0 \quad (46)$$

$$\tau = r/r_d.$$

Then we obtain:

$$Z(\tau) = \begin{cases} A\,[I_0(\tau) - 1] & \tau < \kappa a \\ 1 + B I_0(\tau) + C K_0(\tau) & \kappa a < \tau \le \kappa b \end{cases} \quad (47)$$

$$A = \frac{1}{\eta_0} - 1; \qquad B = -A + (A-1)\,K_1(\kappa a)/\Delta_0;$$

$$C = (A-1)\,I_1(\kappa a)/\Delta_0 \quad (48)$$

$$\Delta_0 = I_0(\kappa a)\,K_1(\kappa a) + I_1(\kappa a)\,K_0(\kappa a)$$

$\frac{b}{a} = 3$

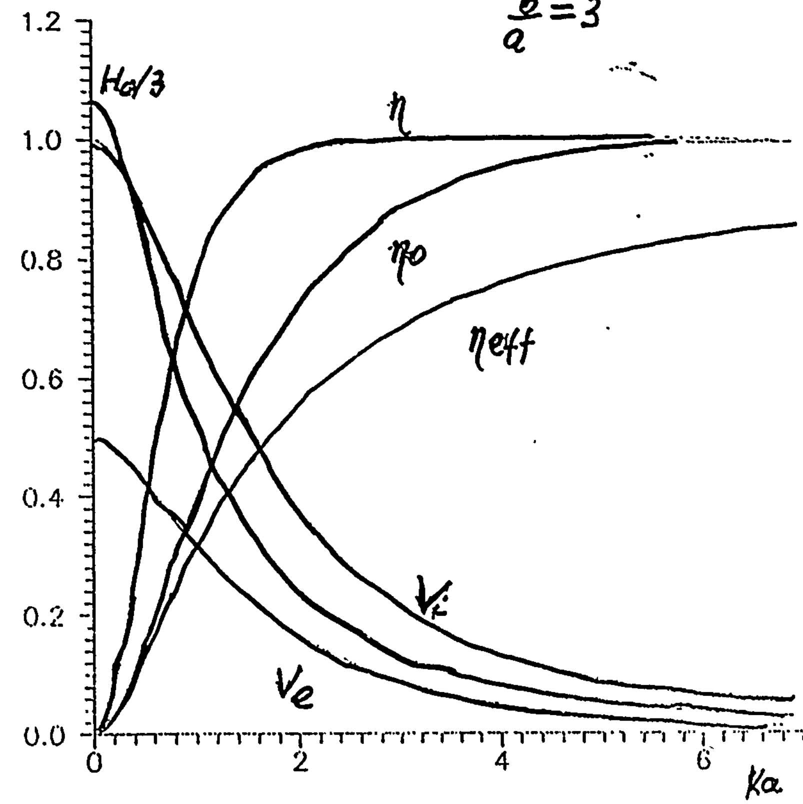

Fig.1

$$Ka = \frac{r}{r_d}; \quad r_d = \frac{4\pi Z^2 n_0}{H_0}$$

H_0 – normalised maximal energy.

Dipole oscillations.
80% neutralization, step function distribution, external potential is parabolic with "tails".

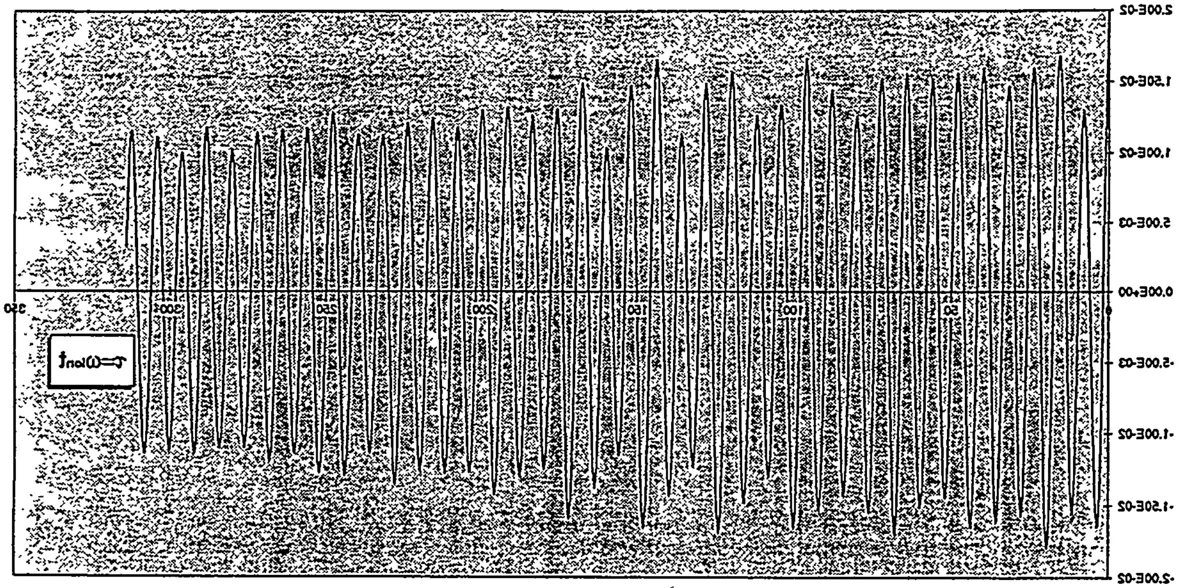

Dependence of quadrupole mode frequency on neutralization factor

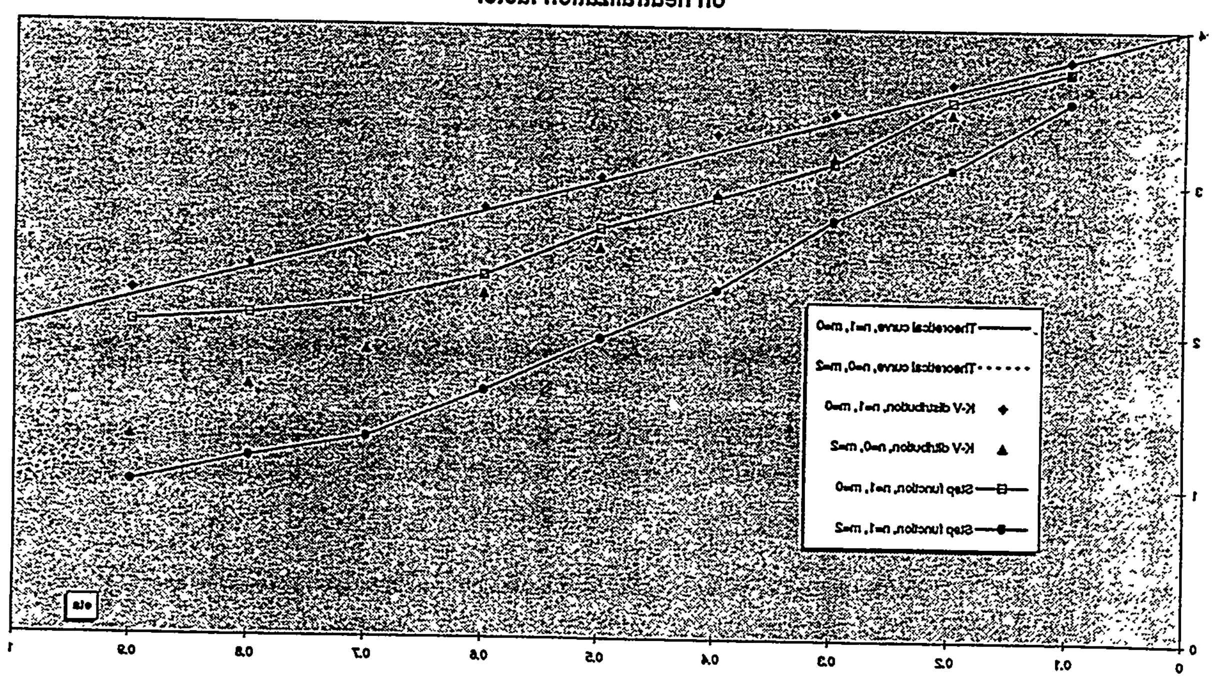

Spectrum of dipole oscillations.
80% neutralization, step function distribution, external potential is parabolic with "tails".

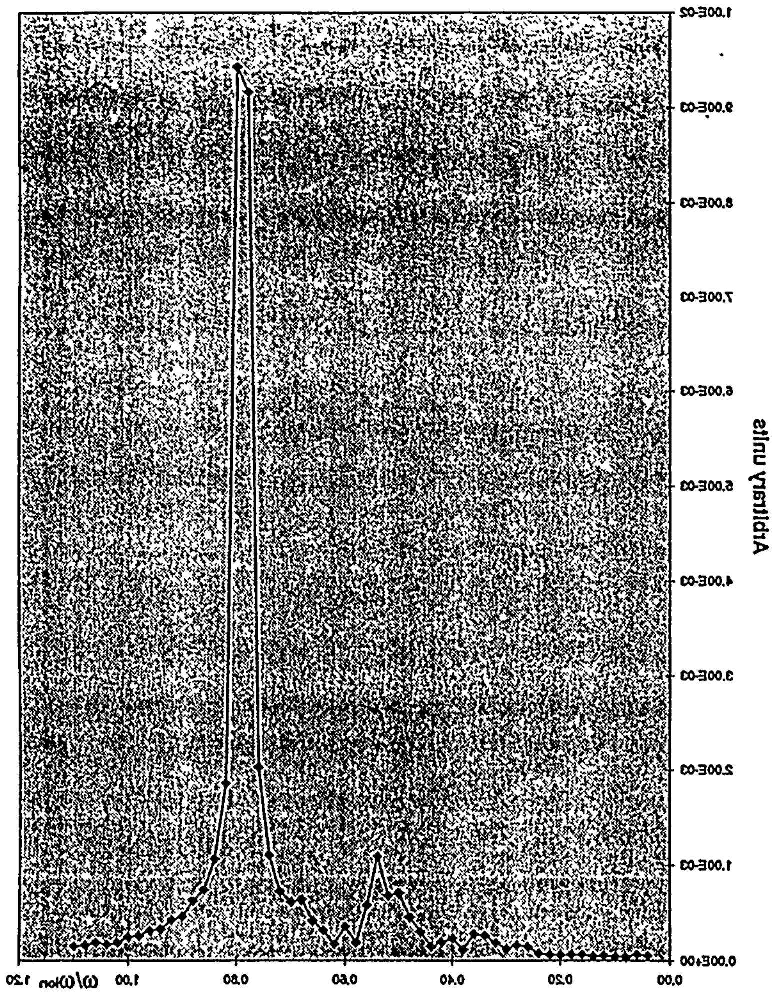

<u>Summary</u>

- Threshold of current density in NEB is defined by L.D of "drift" dipole instability appearing due to electron-ion interaction.
- L.D. of the istability is absent in "one-mode" theory due to the fact that $\delta\omega_{inc} < \Delta\omega_{coh}$.
- Coupling between modes results in appearance of weak L.D. depending on: neutralization
- degree η, relation of radius of beam chamber b to beam radius a and distribution function of the ions in phase space.
- For small η (weak nonlinearity) the coupling is connected mainly with form of solution of Poisson equation (electric coupling), for large η – with nonlinear character of the unperturbed motion. (kinematical coupling).
- For $|1-\eta| \ll 1$ $\epsilon_\perp''$, connected with kinematical coupling, is defined by:

$$\epsilon_\perp'' \sim 1-\eta$$

- Numerical simulations for $\eta = 0.8$; $\frac{b}{a} = 1.5$ and constant phase density have shown that

$$\epsilon_\perp'' \leq 1.8 \cdot 10^{-3}$$

I am very grateful to Dr. Di:Möhl from CERN who suggested this problem for investigation and to Dr. Z. Parsa whose invitation to ITP permits me to think ~~a~~ in pleasant atmosphere about this complicated topic

STABILITY OF BEAMS IN A HIGH FREQUENCY LINAC WITH STRONG WAKEFIELDS

G. Guignard, CERN

High Frequency Option

- Improvement of RF to beam efficiency:

$$\eta^{RF}_{beam} = \frac{P_b}{P_{RF}} \approx \frac{N_b N_e Z_c \omega_{RF}^2}{2\pi c\, G\, [1 + f(N_b, \omega_{RF})]}$$

- Reduced RF power requirements:

$$\frac{\hat{P}_{RF}}{L_{acc}} \sim \frac{G^2}{\omega_{RF}^{1/2}}$$

- High Accelerating Gradient - Reduced length
  - Dark current capture: $G_{lim} \sim \omega_{RF}$
  - RF breakdown limit: $G_{lim} \sim \omega_{RF}^{1/2}$

Stability of Beams
in a High Frequency Linac
with Strong Wakefields

Gilbert Guignard

SL-Division, CERN

4 December 1996

ITP Conference

Generalities, Figure of Merit
Single Bunch Blow-up
Multibunch Beam Break-up
"Movie" simulations

Limitations of Luminosity

Luminosity: $$L = \frac{H_D N_b N_e^2 f_{rep}}{4\pi\sigma_x \sigma_y}$$

Momentum spread by Beamstrahlung: δ_B

$$\delta_B = \frac{0.86\, e\, r_c^3}{2 m_o c^2} \times \frac{U_{cm}}{\sigma_z} \times \frac{N_e^2}{\left(\sigma_x + \sigma_y\right)^2}$$

Beam Power, P_b - Wall Plug Power, P_{AC}

$$2P_b = N_b\, N_e\, eU_{cm} f_{rep} = \eta_{beam}^{AC} \times P_{AC}$$

$\sigma_x \gg \sigma_y$ (flat beams)

$$\boxed{L \;=\; Cte \times \frac{\delta_B^{1/2} H_D}{U_{cm}^{3/2}} \times \frac{\sigma_z^{1/2} P_b}{\sigma_y}}$$

$\beta_y \approx \sigma_z$ (hourglass effect)

$$\boxed{L \;=\; Cte \times \frac{\delta_B^{1/2} H_D}{U_{cm}} \times \frac{\eta_{beam}^{AC}}{\varepsilon_y^{*1/2}} \times P_{AC}}$$

Figure of Merit

Luminosity:

$$L \;=\; Cte \times \frac{\delta_B^{1/2} H_D}{U_{cm}} \times \frac{\eta_{beam}^{AC}}{\varepsilon_y^{*1/2}} \times P_{AC}$$

Figure of merit:

$$M = \frac{L \times U_{cm}}{\delta_B^{1/2} \times P_{AC}}$$

$$\boxed{M \propto \frac{\eta_{beam}^{AC}}{\varepsilon_y^{*1/2}} \propto \frac{\eta_{RF}^{AC} \times \eta_{beam}^{RF}}{\varepsilon_y^{*1/2}}}$$

Beam Emittances Preservation

Misalignment of Structures, Optics, Beam Position Monitors...

- **Dispersive and Chromatic Effects:**
  Sophisticated beam based alignment techniques:
  BPM resolution (50 to 0.5 microns)
- **Single Bunch Beam Break-Up (BBU):**
  Tail oscillation induced by transverse wakefields from head
  Precise pre-alignment of the structures: 100 to 10 microns
  BNS Damping: Increase of focusing along the bunch by RF quadrupoles or momentum to phase correlation
- **Multibunch Beam Break-Up:**
  Damping of transverse wakefields between two cons. bunches
  Damped or/and Detuned Structures (DDS) - Lossy iris

Challenges of the High Frequency option

- **Wakefields:** $W_L \sim \omega_{RF}^2$
  - Longitudinal:
    Beam momentum spread:
    Accurate Beam loading compensation
  - Transverse: $W_T \sim \omega_{RF}^3 \quad (\sim \frac{\omega_{RF}}{a^2})$
    Emittance blow-up
    Precise pre-alignment of the elements $\Delta\varepsilon \sim \langle \delta y^2 \rangle$
    Sophisticated beam correction techniques
    Emittance preservation $\Delta\varepsilon \sim \langle W_T^2 \rangle$

Single Bunch

Figure of merit

$$M \propto \frac{N_e\, \omega_{RF}^2}{G \sqrt{\varepsilon_{y_0} + \langle \Delta\varepsilon_y \rangle}}$$

Favours high ω_{RF}, if $\Delta\varepsilon_y \ll \varepsilon_{y_0}$

Emittance Growth

Random deflections, No correlation

$$\langle \Delta\varepsilon_y \rangle = \frac{(N_e)^2 \ell_s}{G} \langle \delta y_c^2 \rangle \langle \beta_0 \rangle \langle W_T^2 \rangle\, f(\gamma_0, \gamma_f, \Delta\gamma)$$

where $W_T \sim \omega_{RF}^3$

IF $\Delta\varepsilon_y \ll \varepsilon_{y_0} \Rightarrow M \propto \omega_{RF}^2$ O.K.

IF $\Delta\varepsilon_y \gg \varepsilon_{y_0} \Rightarrow M \propto \frac{1}{\omega_{RF}}$ Out!

$\Rightarrow$ Necessary to fight with all available means the (vertical) emittance growth.

- Choice of parameters
- Corrections (that introduce a "favourable" correlation)

Uncorrelated Emittance Growth

Kick on particle or fraction of bunch

$$y = \beta \cdot \vartheta \cdot \sin\psi$$
$$y' = \vartheta \cdot \cos\psi$$

Absence of correlation $\longrightarrow$ average amplitude

$$\langle y^2 \rangle = \langle \beta^2 \rangle \langle \theta^2 \rangle \tfrac{1}{2}$$
$$\langle y'^2 \rangle = \langle \theta^2 \rangle \tfrac{1}{2}$$

$$\Rightarrow \langle \Delta\varepsilon_y \rangle = \frac{\langle y^2 \rangle}{\langle \beta \rangle} + \langle y'^2 \rangle \langle \beta \rangle = \langle \beta \rangle \langle \theta^2 \rangle$$

Many kicks down the linac

$$\langle \Delta\varepsilon_y \rangle = \langle \beta \rangle \sum_i \langle \vartheta_i^2 \rangle = n_k \langle \beta \rangle \langle \theta_w^2 \rangle$$

with $\vartheta_w = \frac{\ell_s W_T\, eN}{m_0 c^2 \gamma} \delta y_c$ Transverse Wakefield

$$\Rightarrow \langle \Delta\varepsilon_y \rangle = \frac{(eN_b)^2 \ell_s^2}{\gamma^2 m_0^2 c^4} \langle W_T^2 \rangle \langle \beta \rangle \langle \delta y_c^2 \rangle \frac{L_t}{\ell_s}$$

Additional variations along the Linac:

Acceleration $\gamma = \gamma_0 + \frac{G}{m_0 c^2} s = \gamma_0 (1 + gs)$

β-scaling with energy $\frac{\beta}{\beta_0} = \left(\frac{\gamma}{\gamma_0}\right)^{\alpha}$

Injection energy γ_0

Final energy $\gamma_f = \gamma_0 (1 + g L_t)$

Dependence on energy of $\langle \Delta\varepsilon_y \rangle$ given by

$$\left\langle \frac{\langle\beta\rangle}{\gamma^2} \right\rangle = \frac{1}{L_t} \int_0^{L_t} \frac{\langle\beta\rangle}{\gamma^2} ds = \frac{\langle\beta_0\rangle}{L_t \gamma_0^2} \int_0^{L_t} \left(\frac{\gamma}{\gamma_0}\right)^{\alpha} \frac{ds}{(1+gs)^2}$$

$$\Rightarrow \left\langle \frac{\langle\beta\rangle}{\gamma^2} \right\rangle = \frac{\langle\beta_0\rangle m_0 c^2}{L_t \gamma_0 G (1-\alpha)} \left[1 - \left(\frac{\gamma_0}{\gamma_f}\right)^{1-\alpha} \right]$$

Combining and rewriting the results

$\Rightarrow$ uncorrelated emittance growth due to wakefield kicks with acceleration + scaling

$$\langle \Delta\varepsilon_y \rangle = \frac{(eN)^2 \ell_s}{G m_0 c^2} \langle \delta y_c^2 \rangle \langle \beta_0 \rangle \langle W_T^2 \rangle \frac{\gamma_f^{1-\alpha} - \gamma_0^{1-\alpha}}{(1-\alpha)\gamma_0 \gamma_f^{1-\alpha}}$$

with

$$\langle W_T^2 \rangle \propto \left(\frac{\partial W_T}{\partial z} \sigma_z \right)^2 \propto \left(\frac{\partial W_T}{\partial z_0} \sigma_z \omega_{RF}^3 \sqrt{\frac{\sigma_{z_0}}{\sigma_z}} \right)^2$$

$$\langle W_T^2 \rangle \propto \left(\frac{\partial W_T}{\partial z_0} \omega_{RF}^3 \right)^2 \sigma_z$$

Choice of Parameters

Higher G Profit from high ω_{RF}

Lower $\langle\beta_0\rangle$ More focusing

Shorter bunch (σ_z) $\hat{W}_T \propto \sqrt{\sigma_z}$

Tight tolerances $\langle \delta y_c^2 \rangle$ on misalignments

Scaling of focusing FODO Lattice

Seek a balance between

a) Wakefields strong at low E

β can be gently increased with γ

b) Dispersion may take over with E ↗

interest to decrease μ with γ

$\Rightarrow$ Focusing scaling with γ

CLIC

$$\frac{L_{cell}(s)}{L_{cell_0}} = \left[\frac{\gamma(s)}{\gamma_0}\right]^{0.3} \qquad \frac{G_q \ell_q(s)}{G_{q0} \ell_{q0}} = \left[\frac{\gamma(s)}{\gamma_0}\right]^{0.4}$$

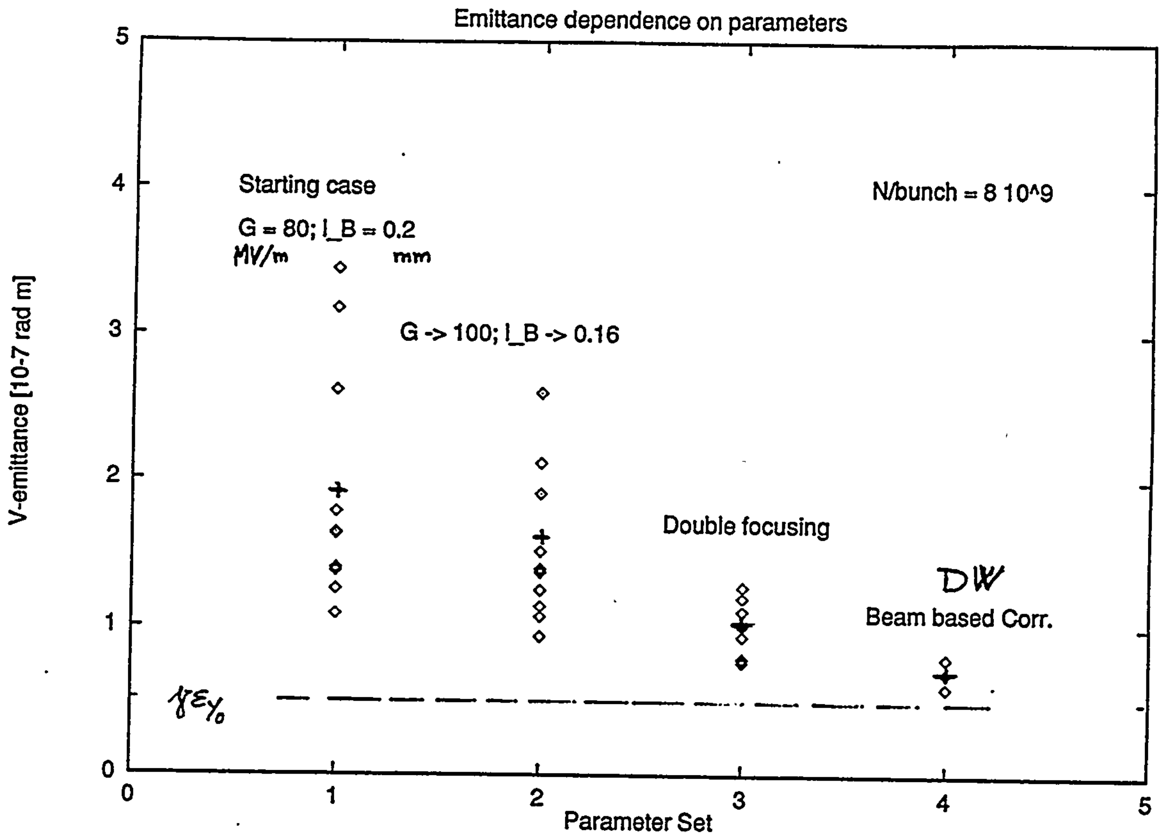
Emittance dependence on parameters
Starting case
G = 80; l_B = 0.2
MV/m mm
G -> 100; l_B -> 0.16
Double focusing
DW
Beam based Corr.
N/bunch = 8 10^9
V-emittance [10-7 rad m]
Parameter Set

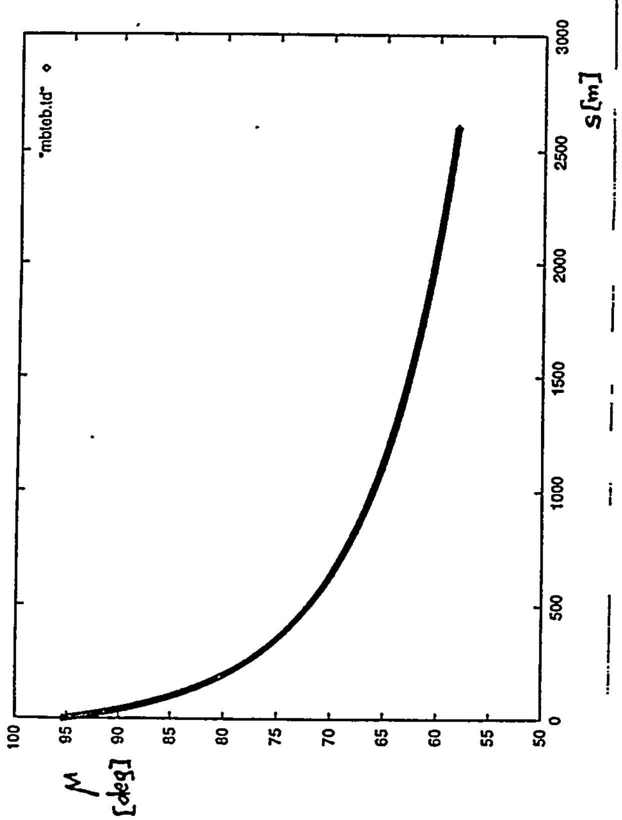
"mbteb.td"
s [m]
μ [deg]

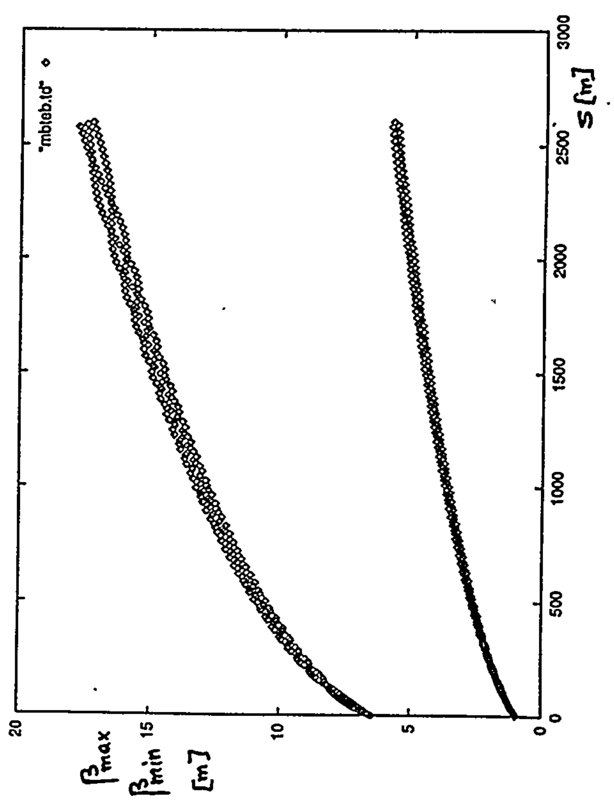
"mbteb.td"
s [m]
β_{max} β_{min} [m]

Multi-Bunch

Once Single Bunch conditions are optimize, it remains BBU

BBU Effect

Long-range Wakefields add along the train; high Q → slow decay

Resonant effect of betatron motion: exciter freq. = follower freq.

Secular term: Ampl. Growth $\sim s$

Emittance Growth $\sim s^2$

Benefit from damping due to acceleration but attenuated by relaxation of focusing ⇒ $\Delta\varepsilon_y$ still too high

Mode Attenuation

Mode (Long. and Transv.) damped in the interval between 2 bunches ($30\,\lambda_{RF}$)

⇒ Study of CLIC damped cavities (low Q)

Required Attenuation: typically 100

Field calculations → dambed Section → 20 bunches

Beam Break Up

Model: two bunches of finite length divided into N slices of charge,

bunch separation z_{sep} $(= m\,\lambda_{RF})$,

strong focusing $K(s)$

$$y''_{1k} + K(s)\, y_{1k} = 0 \qquad k = 1, \dots, N$$

Long-range wakefield only → b#1 free oscillations

$$y''_{2n} + K(s)\, y_{2n} = \sum_{k=1}^{N} g_k\, y_{1k}\, W_T(z_n - z_k) \qquad n = 1, \dots, N$$

Change for Courant and Snyder variables

$$\vartheta = \frac{1}{\mu/2\pi} \int_0^s \frac{ds}{\beta(s)} \qquad v(\vartheta) = \frac{y(s)}{\sqrt{\beta(s)}}$$

$$\Rightarrow \quad v''_{1k} + \mu^2/4\pi^2\, v_{1k} = 0$$

$$v''_{2n} + \mu^2/4\pi^2\, v_{2n} = \frac{\mu^2}{4\pi^2}\, \beta^{3/2}(\vartheta) \sum_{k=1}^{N} g_k\, v_{1k}(\vartheta)\, W_{T\,n,k}$$

with $g_k = \dfrac{q_k}{m_0 c^2 \gamma_k}$ $\quad q_k$ charge of slice k, $\quad \gamma_k$ energy " "

$$\sum_1^N q_k = q_b$$

r.h.s. of v_{2n}-equation $= \underline{R(\vartheta)}$

$W_{T_{n,k}} \longrightarrow$ lowest dipole mode w_1 (freq. ω_1)

$$W_{T_{n,k}} = w_1 \cos\left[\frac{\omega_1}{c}\left(z_{sep} + (n-k)\Delta z\right)\right]$$

Δz – length of one slice of charge

Defining $\underline{Q = \mu/2\pi}$, then the solution of $v_{2n}(\vartheta)$ is,

$$v_{2n}(\vartheta) = C_1 \cos Q\vartheta + C_2 \sin Q\vartheta +$$

$$+ \frac{1}{Q}\Big[\sin Q\vartheta \underbrace{\int_0^{\vartheta} \cos Q\vartheta\, R(\vartheta)\, d\vartheta}_{J_1} - \cos Q\vartheta \underbrace{\int_0^{\vartheta} \sin Q\vartheta\, R\, d\vartheta}_{J_2}\Big]$$

$$\Rightarrow \quad J_1 = Q^2 w_1 \sigma_n \int_0^{\vartheta} \frac{1}{2}\left(\underline{1} + \cos(2Q\vartheta)\right) \underline{\beta^{3/2}(\vartheta)}\, d\vartheta$$

$$J_2 = Q^2 w_1 \sigma_n \int_0^{\vartheta} \frac{1}{2} \sin(2Q\vartheta)\, \beta^{3/2}(\theta)\, d\theta$$

$$\sigma_n = \sum_{k=1}^{N} q_k V_k \cos\left[\frac{\omega_1}{c}\left(z_{sep} + (n-k)\Delta z\right)\right]$$

$$v_{1k} = V_k \cos(Q\vartheta)$$

$\langle\beta(\theta)\rangle$ and $\langle\beta^{3/2}(\theta)\rangle_\theta$ always $\neq 0$

$\Longrightarrow$ "secular term" due to Resonance

$$J_1^{sec} = \frac{1}{2} Q^2 w_1 \sigma_n \langle\beta^{3/2}\rangle \theta \quad \text{– Linear growth}$$

Solution from Green's function technique with coherent oscillation of bunch 1: $v_{1k} = V_0 \cos\frac{\mu}{2\pi}\theta$

With secular term from 1st Fourier component of $\beta^{3/2}(\theta)$, it becomes

$$v_{2n}(\theta) \Rightarrow \frac{w_1}{\mu/2\pi}\, \sigma_n \langle\beta^{3/2}\rangle\, \theta \sin\left(\frac{\mu}{2\pi}\theta\right)$$

with σ_n in a closed form

$$\sigma_n = V_0 \frac{\cos\left[\frac{\omega_1 N\Delta z}{2c} - \frac{\omega_1}{c}(z_{sep} + n\Delta z)\right] \sin\left[(N+1)\frac{\omega_1 \Delta z}{2c}\right]}{\sin\left(\frac{\omega_1 \Delta z}{2c}\right)}$$

By definition, the change in emittance is

$$\Delta\varepsilon_N = \frac{1}{N}\sum_{n=1}^{N}\left[\frac{4\pi^2}{\mu^2} v_{2n}'^{\,2} + v_{2n}^2\right]$$

Continuous bunch requires $\lim_{N\to\infty} \Delta\varepsilon_N$

$$\Delta\varepsilon = 2\pi^2 c^2 \frac{q_b^2 w_1^2 V_0^2 \langle\beta^{3/2}\rangle^2}{E^2 \omega_1^2 \ell_b^2 L_c^2} s^2 \sin^2\left(\frac{\omega_1 \ell_b}{c}\right) *$$

$$* \left[1 + \frac{c}{\omega_1 \ell_b} \sin\left(\frac{\omega_1 \ell_b}{c}\right) \cos\left(\frac{2 z_{sep} \omega_1}{c}\right)\right]$$

Bunch 1, coherent oscillation $\Rightarrow$ quadratic growth
Bunch 1, incoherent oscillation $\Rightarrow$ σ_n reduced
particular displacements v_{1k} reduce the growth

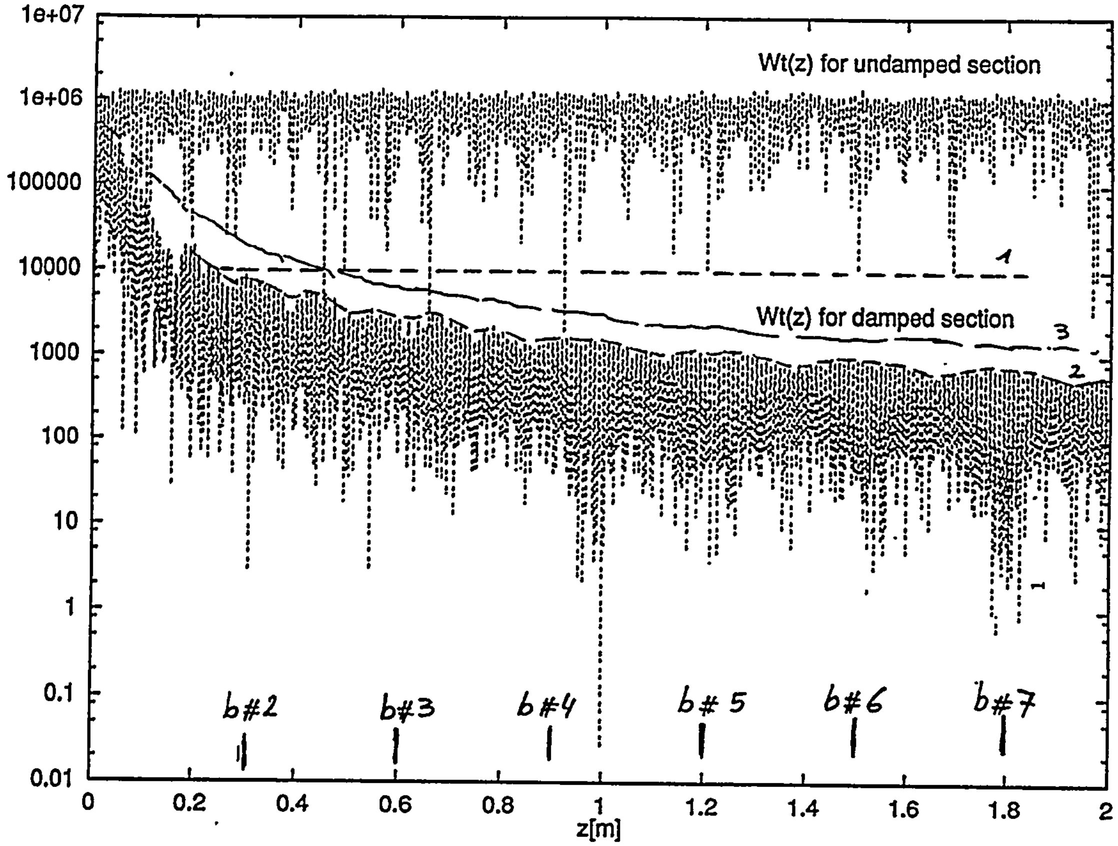

Wt(z) for undamped section
Wt(z) for damped section
1
2
3
b#2
b#3
b#4
b#5
b#6
b#7
z[m]

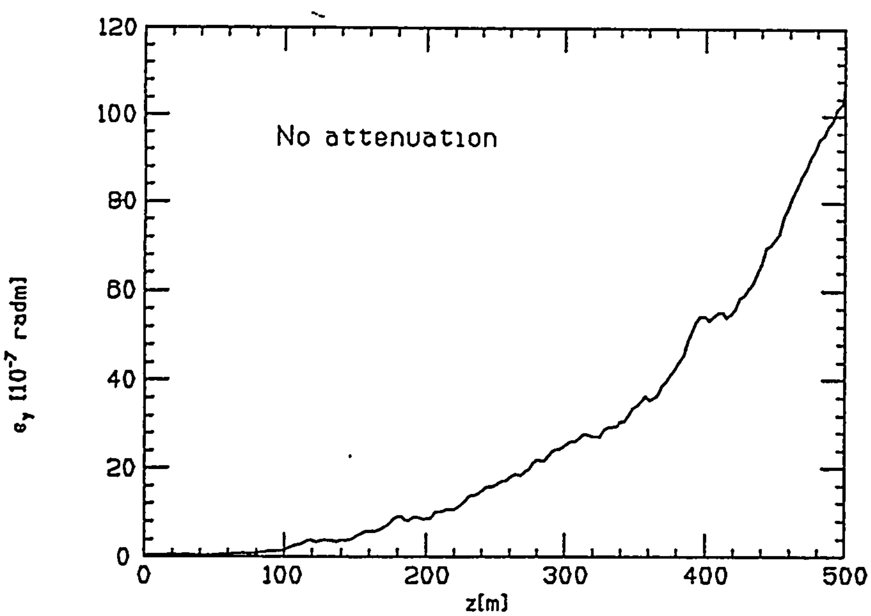

No attenuation
ε_y [10^{-7} radm]
z[m]

WAVELET ANALYSIS OF HAMILTONIAN SYSTEM AND ITS PERTURBATIONS

M. Zeitlin, IPME

WAVELET APPROACH TO NONLINEAR PROBLEMS: HAMILTONIAN SYSTEMS AND THEIR PERTURBATIONS.

FEDOROVA A.N. ZEITLIN M.G.
Russian Academy of Sciences, Institute of Problems of Mechanical Engineering, V.O., Bolshoj pr., 61, 199178, St. Petersburg, Russia
e-mail: zeitlin@math.ipme.ru, anton@math.ipme.ru

We give the explicit time description of dynamics and optimal dynamics for some important mechanical problems. These problems are reduced to the problem of the solving of the systems of differential equations with polynomial nonlinearities and with or without some constraints. In the general case we have the solution as a multiresolution expansion in the base of compactly supported wavelet basis. The solution is parameterized by solutions of two reduced algebraical problems, one is nonlinear and the second is some linear problem, which is obtained from one of the next wavelet construction: Fast Wavelet Transform, Stationary Subdivision Schemes, the method of Connection Coefficients.

According to the orbit method and by using construction from the geometric quantization theory we construct the symplectic and Poisson structures associated with Weyl–Heisenberg (Gabor) wavelets by using metaplectic structure and corresponding polarization. The key point is a consideration of semidirect product of Heisenberg group and metaplectic group as subgroup of authomorphisms group of dual to symplectic space, which consists of elements acting by affine transformations. We consider the application to the construction of Melnikov functions in the theory of homoclinic chaos in perturbations of Hamiltonian systems.

We consider the problem of the description of oscillations of solutions of some nonlinear differential equation with two - frequency perturbations in two mode Galerkin approximations. Computer calculation gives us a possibility to analyse in the parameter space the time evolution of our system and corresponding transition between different regimes: deterministic dynamics – quasiperiodic dynamics – chaotic dynamics. The regimes for our system of equations, which we compute numerically, we shall consider also via Melnikov method. As the main part we consider wavelet approach via our variational approach to this problem, which gives us a possibility to construct explicit time solutions.

We consider the generalization of our variational wavelet approach to nonlinear polynomial problems to the case of Hamiltonian systems for which we need to preserve underlying symplectic or Poissonian or quasicomplex structures in any type of calculations. We use our approach for the problem of explicit calculations of Arnold–Weinstein curves via Floer variational approach from symplectic topology. The loop solutions are parametrized by the solutions of reduced algebraic problem – matrix Quadratic Mirror Filters equations. Also, we consider relation between KAM perturbation theory which is based on symplectic Hilbert scales of spaces and wavelet parametrization of general scales of spaces.

WAVELET APPROACH TO NONLINEAR PROBLEMS, I.

POLYNOMIAL DYNAMICS.

FEDOROVA A.N. ZEITLIN M.G.

Russian Academy of Sciences, Institute of Problems of Mechanical Engineering, V.O., Bolshoj pr., 61, 199178, St. Petersburg, Russia

e-mail: zeitlin@math.ipme.ru, anton@math.ipme.ru

We give the explicit time description of the following problems: dynamics and optimal dynamics for some important electromechanical system. These problems are reduced to the problem of the solving of the systems of differential equations with polynomial nonlinearities and with or without some constraints. In the general case we have the solution as a multiresolution expansion in the base of compactly supported wavelet basis. The solution is parameterized by solutions of two reduced algebraical problems, one is nonlinear and the second is some linear problem, which is obtained from one of the next wavelet construction: Fast Wavelet Transform, Stationary Subdivision Schemes, the method of Connection Coefficients. Our initial problems come from very important technical problems: minimization of energy in electromechanical system with enormous expense of energy.

Introduction

We give the explicit time description of the following problems: dynamics and optimal dynamics for nonlinear (polynomial) dynamical systems, Galerkin approximation for some class of partial differential equations and routes to chaos in Melnikov function approach to the perturbations of Hamiltonian systems. The first three problems and a part of the fourth one are reduced to the problem of solving the systems of differential equations with polynomial nonlinearities with or without some constraints. The first main part of our construction is some variational approach to this problem, which reduces initial problem to the problem of the solution of functional equations at the first stage and some algebraical problems at the second stage. We consider also two private cases of our general construction.

In the first case (particular) we have for Riccati type equations the solution as a series on shifted Legendre polynomials, which is parametrized by the solution of reduced algebraical (also Riccati) system of equations [1]–[5].

In the second case (general polynomial systems) we have the solution in a compactly supported wavelet basis [6]–[8]. Multiresolution expansion is the second main part of our construction. In this case the solution is parametrized by solutions of two reduced algebraic problems, one as in the first case and the second is some linear problem, which is obtained from one of the next wavelet construction: Fast Wavelet Transform (FWT) [9], Stationary Subdivision Schemes (SSS) [10], the method of Connection Coefficients (CC) [11].

We use our general construction for solution of very important technical problems: minimization of energy and detecting signals from oscillations of a submarine.

Our initial problem comes from the problem of minimization of energy in electromechanical system with enormous expense of energy. That is synchronous drive of the mill–the electrical machine with the mill as load. It is described by Park system of equations [1]–[2]:

$$
\begin{aligned}
\frac{di_1}{dt} &= A_{11}i_1 + A_{12}i_2i_6 + A_{13}i_3 + A_{14}i_4 + A_{15}i_5i_6 + A_1(t)\\
\frac{di_2}{dt} &= A_{21}i_1i_6 + A_{22}i_2 + A_{23}i_3i_6 + A_{24}i_4i_6 + A_{25}i_5 + A_2(t)\\
\frac{di_3}{dt} &= A_{31}i_1 + A_{32}i_2i_6 + A_{33}i_3 + A_{34}i_4 + A_{35}i_5i_6 + A_3(t)
\end{aligned}
$$

$$
\begin{aligned}
\frac{di_4}{dt} &= A_{41}i_1 + A_{42}i_2i_6 + A_{43}i_3 + A_{44}i_4 + A_{45}i_5i_6 + A_4(t)\\
\frac{di_5}{dt} &= A_{51}i_1i_6 + A_{52}i_2 + A_{53}i_3i_6 + A_{54}i_4i_6 + A_{55}i_5 + A_5(t)\\
\frac{di_6}{dt} &= A_{61}i_1i_2 + A_{62}i_1i_5 + A_{63}i_2i_3 + A_{64}i_2i_4 + A_6(i_6,t),
\end{aligned}
$$

where $A_{ij}, (i,j=\overline{1,6})$ are constants, $A_i(t)$ explicit functions of time, $A_6(i_6,t) = a + di_6 + bi_6^2$ is analytical approximation for the mechanical moment of the mill. In our case we consider i_1, i_2 as the controlling variables. Because we consider the energy optimization, we use the next general form of energy functional in our electromechanical system

$$Q = \int_{t_0}^{t} [K_1(i_1,i_2) + K_2(\dot{i}_1,\dot{i}_2)]dt,$$

where K_1, K_2 are quadratic forms. Moreover, we consider the optimization problem with some constraints which are motivated by technical reasons. After the manipulations from the theory of optimal control, we reduce the problem of energy minimization to the some nonlinear system of equations [1]. Thus for the Lagrangian optimization we have the system of 13 equations (12 - differential equations, 1-functional one). For the Hamiltonian optimization we have the system of 12 equations (10-differential equations, 2-algebraic ones). In both cases obtained systems of equations are the systems of Riccati type. As result of solution of equations of optimal dynamics we have:

1. the explicit time dependence of the controlling variables

   $u(t) = \{i_1(t), i_2(t)\}$ which give

2. the optimum of corresponding functional of energy and

3. explicit time dynamics of the controllable variables $\{i_3, i_4, i_5, i_6\}(t)$.

Analogously we consider in wavelet approach related polynomial problems: computations in Galerkin approximations and routes to chaos in Melnikov function approach [6]. [15]. These problems are related to a problem of detecting signals from an oscillating submarine.

In 2-mode Galerkin approximation for beam contacting with ideal compressible liquid in a channel (a model of an oscillating submarine) we have the next system of polynomial equations with variable (quasiperiodic) coefficients [16]:

$$\begin{aligned}
\dot{x}_1 &= x_2 \\
\dot{x}_2 &= -ax_1 - b[\cos(x_5) + \cos(x_6)]x_1 - dx_1^3 - mdx_1x_3^2 - px_2 - \varphi(x_5) \\
\dot{x}_3 &= x_4 \\
\dot{x}_4 &= ex_3 - f[\cos(x_5) + \cos(x_6)] - gx_3^3 - kx_1^2x_3 - gx_4 - \psi(x_5) \\
\dot{x}_5 &= r \\
\dot{x}_6 &= s
\end{aligned}$$

or in Hamiltonian form

$$\begin{aligned}
\dot{x} &= J\cdot\nabla H(x) + \varepsilon g(x,\Theta), \\
\dot{\Theta} &= \omega, \quad (x,\Theta) \in R^4 \times T^2, \quad T^2 = S^1 \times S^1,
\end{aligned}$$

for $\varepsilon = 0$ we have for unperturbed state:

$$\dot{x} = J\cdot\nabla H(x), \quad \dot{\Theta} = \omega$$

We solve two problems related with these systems of equations. We need to compute explicit time solution for dynamical variables for perturbed and unperturbed systems. The solution for unperturbed system we use next for computing Melnikov functions

$$M(\Theta) = \int\limits_{-\infty}^{\infty} \nabla H(\bar{x}_0(t)) \wedge g(\bar{x}_0(t), \omega t + \Theta)dt$$

$$M^{m/n}(t_0) = \int\limits_0^{mT} DH(x_\alpha(t)) \wedge (x_\alpha(t), t + t_0)dt$$

which we use for detecting in parameter space chaotic and quasiperiodic regimes of oscillations [6],[15],[16].

Variational method

According to our general approach of [1]-[8] we consider now our modification of Integral Variational Method of Hitzl e.a. [12]. The modifications are twofold: first, in this paper, we consider generalization which allows us to use general wavelet

approach (multiresolution, compactly supported wavelet basis etc.), second, in another paper [15], we consider an unification of this method and variational method for loop space which now is well known in symplectic topology[19].

All our problems may be formulated as the systems of ordinary differential equations

$$\frac{dx_i}{dt} = f_i(x_j, t), \quad (i,j = 1,...,n) \tag{1}$$

with fixed initial conditions $x_i(0)$, where f_i are not more than polynomial functions of dynamical variables x_j and have arbitrary dependence of time. Because of time dilation we can consider only next time interval: $0 \le t \le 1$. Consider now dual variables $y_i(t)$ ($y_i(0) = 0$) (variational functions in terminology of [12], but as we shall show in [15] in Hamiltonian approach we can use the standard Hamiltonian variables instead of this dual pair of variables). Let us consider a set of functions

$$\Phi_i(t) = x_i\frac{dy_i}{dt} + f_iy_i \tag{2}$$

and a set of functionals

$$F_i(x) = \int_0^1 \Phi_i(t)dt - x_iy_i\mid_0^1 \tag{3}$$

It is obvious that systems (1) and (3) are equivalent: each solution of (1) is also a solution of (3) and conversely. In [15] we consider symplectic interpretation of (2), (3).

Now we consider formal expansions for x_i, y_i:

$$\begin{aligned}
x_i(t) &= x_i(0) + \sum_k \lambda_i^k\varphi_k(t) \\
y_j(t) &= \sum_r \eta_j^r\varphi_r(t),
\end{aligned} \tag{4}$$

where because of initial conditions we need only $\varphi_k(0) = 0$. From (3) and (4) we have the following reduced algebraical system of equations on the set of unknown coefficients λ_i^k of expansions (4):

$$\sum_k \mu_{kr}\lambda_i^k - \gamma_i^r(\lambda_j) = 0 \tag{5}$$

Its coefficients are

$$\begin{aligned}
\mu_{kr} &= \int_0^1 \varphi_k'(t)\varphi_r(t)dt \\
\gamma_i^r &= \int_0^1 f_i(x_j,t)\varphi_r(t)dt
\end{aligned} \tag{6}$$

Now, when we solve system (5) with coefficients (6) and determine the unknown coefficients from formal expansion (4) we therefore obtain the solution of initial problem (1).

We shall not consider now problems of convergence of expansions (4) and more accuracy substantiation. For quadratic case we consider this problems in [1]-[5] and for general case in [15].

It should be noted if we consider only truncated expansion (4) with N terms then we have from (5) the system of $N \times n$ algebraical equations. Because of formulae (6) the degree of this algebraical system coincides with degree of initial differential system (1) (we consider now only systems of differential equations with polynomial dependence of RHS of dynamical variables). So, we have the solution of initial nonlinear (polynomial) problem (1) in the form

$$x_i(t) = x_i(0) + \sum_{k=1}^{N} \lambda_i^k \varphi_k(t), \tag{7}$$

where coefficients λ_i^k are roots of the corresponding reduced algebraical problem (5), whose coefficients are given by (6). Consequently, we have parametrization of solution of initial problem (1) by solution of reduced algebraical problem (5). But in general case, when the problem of computations of coefficients of reduced algebraical system (5) is not solved explicitly as in the quadratic case, which we shall consider below, we have also parametrization of solution (7) by solution of corresponding problems, which appear when we need to calculate coefficients (6). As we shall see, these problems may be explicitly solved in wavelet approach.

The solutions

Next we consider the construction of explicit time solution for our optimization problem. The obtained solutions are given in the following form:

$$i_k(t) = i_k(0) + \sum_{i=1}^{N} \lambda_k^i X_i(t),$$

where in our first case we have $X_i(t) = Q_i(t)$, where $Q_i(t)$ are shifted Legendre polynomials [12] and λ_k^i are roots of reduced algebraic system of equations. In wavelet case $X_i(t)$ correspond to multiresolution expansions in the base of compactly supported wavelets and λ_k^i are the roots of corresponding algebraic Riccati systems with coefficients, which are given by FWT, SSS or CC constructions.

According to the variational method to give the reduction from differential to algebraical system of equations we need compute the objects $\gamma_a^j(i_b)$ and μ_{ji}, where in Lagrangian case $a = \overline{1,13}, b = \overline{1,13}$. We compute it by the formulae (6), where coefficients of algebraical systems are constructed from objects:

$$\begin{aligned}
\sigma_i &\equiv \int_0^1 X_i(\tau)d\tau = (-1)^{i+1},\\
\nu_{ij} &\equiv \int_0^1 X_i(\tau)X_j(\tau)d\tau = \sigma_i\sigma_j + \frac{\delta_{ij}}{(2j+1)},\\
\mu_{ji} &\equiv \int X_i'(\tau)X_j(\tau)d\tau = \sigma_j F_1(i,0) + F_1(i,j),\\
&\quad F_1(r,s) = [1-(-1)^{r+s}]\hat{s}(r-s-1),\\
&\quad \hat{s}(p) = \begin{cases} 1, & p \geq 0\\ 0, & p < 0\end{cases}\\
\beta_{klj} &\equiv \int_0^1 X_k(\tau)X_l(\tau)X_j(\tau)d\tau = \sigma_k\sigma_l\sigma_j +\\
&\quad \alpha_{klj} + \frac{\sigma_k\delta_{jl}}{2j+1} + \frac{\sigma_l\delta_{kj}}{2k+1} + \frac{\sigma_j\delta_{kl}}{2l+1},\\
\alpha_{klj} &\equiv \int_0^1 X_k^* X_l^* X_j^* d\tau =\\
&\quad \frac{1}{(j+k+l+1)R(1/2(i+j+k))} \times\\
&\quad R(1/2(j+k-l))R(1/2(j-k+l)) \times\\
&\quad R(1/2(-j+k+l)),
\end{aligned} \tag{8}$$

if $j+k+l = 2m, m \in Z$,and $\alpha_{klj} = 0$ if $j+k+l = 2m+1$; where $R(i) = (2i)!/(2^i i!)^2$, $Q_i = \sigma_i + P_i^*$, where the second equality in the formulae for $\sigma, \nu, \mu, \beta, \alpha$ hold for the first case.

Wavelet computations

Now we give construction for computations of objects(8) in the wavelet case.

We use some constructions from multiresolution analysis: a sequence of successive approximation closed subspaces V_j

$$...V_2 \subset V_1 \subset V_0 \subset V_{-1} \subset V_{-2} \subset ...$$

satisfying the following properties:

$$\bigcap_{j\in Z} V_j = 0$$

$$\overline{\bigcup_{j\in Z} V_j} = L^2(\mathrm{R})$$
$$f(x) \in V_j <=> f(2x) \in V_{j+1}$$

There is a function $\varphi \in V_0$ such that $\{\varphi_{0,k}(x) = \varphi(x-k)_{k\in Z}\}$forms a Riesz basis for V_0.

We use compactly supported wavelet basis: orthonormal basis for functions in $L^2(\mathrm{R})$ [13]. As usually $\varphi(x)$ is a scaling function, $\psi(x)$ is a wavelet function, where $\varphi_i(x) = \varphi(x-i)$. Scaling relation that defines φ, ψ are

$$\begin{aligned} \varphi(x) &= \sum_{k=0}^{N-1} a_k \varphi(2x-k) = \sum_{k=0}^{N-1} a_k \varphi_k(2x), \\ \psi(x) &= \sum_{k=-1}^{N-2} (-1)^k a_{k+1} \varphi(2x+k) \end{aligned}$$

Let be $f : \mathrm{R} \longrightarrow \mathrm{C}$ and the wavelet expansion is

$$f(x) = \sum_{\ell\in Z} c_\ell \varphi_\ell(x) + \sum_{j=0}^{\infty} \sum_{k\in Z} c_{jk} \psi_{jk}(x) \tag{9}$$

The indices k, ℓ and j represent translation and scaling, respectively

$$\begin{aligned} \varphi_{jl}(x) &= 2^{j/2}\varphi(2^j x - \ell) \\ \psi_{jk}(x) &= 2^{j/2}\psi(2^j x - k) \end{aligned}$$

The set $\{\varphi_{j,k}\}_{k\in Z}$ forms a Riesz basis for V_j. Let W_j be the orthonormal complement of V_j with respect to V_{j+1}. Just as V_j is spanned by dilation and translations of the scaling function, so are W_j spanned by translations and dilation of the mother wavelet $\psi_{jk}(x)$.

All expansions which we used are based on the following properties:

$\{\varphi_{jk}\}_{j\geq 0, k\in Z}$ is an orthonormal basis for$L^2(\mathrm{R})$.

$V_{j+1} = V_j \bigoplus W_j$

$L^2(\mathrm{R}) = \overline{V_0 \bigoplus_{j=0}^{\infty} W_j}$

$\{\varphi_{0,k}, \psi_{j,k}\}_{j\geq 0, k\in Z}$ is an orthonormal basis for$L^2(\mathrm{R})$.

$\{\varphi_{j,k}, \psi_{\ell,k}; 0 \leq j \leq J \leq \ell, k \in \mathrm{Z}\}$is an orthonormal basis for$L^2(\mathrm{R})$.

$\int_{-\infty}^{\infty} \varphi(x)dx = 1$

If in formulae (9) $c_{jk} = 0$ for $j \geq J$, then $f(x)$ has an alternative expansion in terms of dilated scaling functions only

$$f(x) = \sum_{\ell\in Z} c_{J\ell}\varphi_{J\ell}(x)$$

This is a finite wavelet expansion, it can be written solely in terms of translated scaling functions. We use wavelet $\psi(x)$, which has k vanishing moments

$$\int x^k \psi(x) d(x) = 0, \qquad 0 \leq k \leq K$$

or, equivalently

$$x^k = \sum c_\ell \varphi_\ell(x) \quad \text{for each } k, \quad 0 \leq k \leq K$$

Also we have the shortest possible support: scaling function DN (where N is even integer) will have support $[0, N-1]$ and $N/2$ vanishing moments.

There exists $\lambda > 0$ such that DN has λN continuous derivatives; for small $N, \lambda \geq 0.55$. To solve our second associated linear problem we need to evaluate derivatives of $f(x)$ in terms of $\varphi(x)$.

Let be $\varphi_\ell^n = d^n \varphi_\ell(x)/dx^n$. We derive the wavelet - Galerkin approximation of a differentiated $f(x)$ as $f^d(x) = \sum_\ell c_l \varphi_\ell^d(x)$ and values $\varphi_\ell^d(x)$ can be expanded in terms of $\varphi(x)$

$$\begin{aligned} \phi_\ell^d(x) &= \sum_m \lambda_m \varphi_m(x), \qquad \text{where} \\ \lambda_m &= \int_{-\infty}^{\infty} \varphi_\ell^d(x)\varphi_m(x)dx \end{aligned}$$

The coefficients λ_m are 2-term connection coefficients [11]. In general we need to find

$$\Lambda(\ell_1, \ell_2, ..., \ell_n, d_1, d_2, ..., d_n) = \Lambda_{\ell_1 \ell_2 \ldots \ell_n}^{d_1 d_2 \ldots d_n} = \int_{-\infty}^{\infty} \prod \varphi_{\ell_i}^{d_i}(x)dx$$

For our Riccati case we need to evaluate two and three connection coefficients

$$\begin{aligned} \Lambda_\ell^{d_1 d_2} &= \int_{-\infty}^{\infty} \varphi^{d_1}(x)\varphi_\ell^{d_2}(x)dx, \quad d_i \geq 0, \\ \Lambda^{d_1 d_2 d_3} &= \int_{-\infty}^{\infty} \varphi^{d_1}(x)\varphi_\ell^{d_2}(x)\varphi_m^{d_3}(x)dx \end{aligned}$$

According to [11] we use the next construction. When N in scaling equation is a finite even positive integer the function $\varphi(x)$ has compact support contained in $[0, N-1]$. For a fixed triple (d_1, d_2, d_3) only some $\Lambda^{d_1 d_2 d_3}_{\ell m}$ are nonzero : $2-N \leq \ell \leq N-2, \quad 2-N \leq m \leq N-2, \quad |\ell - m| \leq N-2$. There are $M = 3N^2 - 9N + 7$ such pairs (ℓ, m). Let $\Lambda^{d_1 d_2 d_3}$ be an M-vector, whose components are numbers $\Lambda^{d_1 d_2 d_3}_{\ell m}$. Then we have the first key result: Λ satisfy the system of equations

$$
\begin{aligned}
A\Lambda^{d_1 d_2 d_3} &= 2^{1-d}\Lambda^{d_1 d_2 d_3}, \ d = d_1 + d_2 + d_3, \\
A_{\ell, m; q, r} &= \sum_p a_p a_{q-2\ell+p} a_{r-2m+p}
\end{aligned}
$$

By moment equations we have created a system of $M+d+1$ equations in M unknowns. It has rank M and we can obtain unique solution by combination of LU decomposition and QR algorithm: The second key result gives us the 2-term connection coefficients:

$$
\begin{aligned}
A\Lambda^{d_1 d_2} &= 2^{1-d}\Lambda^{d_1 d_2}, \quad d = d_1 + d_2, \\
A_{\ell, q} &= \sum_p a_p a_{q-2\ell+p}
\end{aligned}
$$

Also, we use FWT and SSS for computing coefficients of reduced algebraic systems [15]. We use for modelling D6,D8,D10 functions and programs RADAU and DOPRI for testing [14].

As a result we obtained the explicit time solution of optimal control problem. The generalization to polynomial systems is evidently. In comparison with wavelet expansion on the real line which we use in optimal control problem and in calculation of Galerkin approximation and Melnikov function approach also we need to use periodized wavelet expansion, i.e. wavelet expansion on finite interval [17]. Also in the solution of perturbed system we have some problem with variable coefficients. For solving last problem we need to consider one more refinement equation for scaling function $\phi_2(x)$:

$$\phi_2(x) = \sum_{k=0}^{N-1} a_k^2 \phi_2(2x - k)$$

and corresponding wavelet expansion for variable coefficients $b(t)$:

$$\sum_k B_k^j(b)\phi_2(2^j x - k),$$

where $B_k^j(b)$ are functionals supported in a small neighborhood of $2^{-j}k$ [18].

The solution of the first problem consists in periodizing. In this case we use expansion into periodized wavelets defined by [17]:

$$\phi^{per}_{-j,k}(x) = 2^{j/2} \sum_Z \phi(2^j x + 2^j \ell - k)$$

All these modifications lead only to transformations of coefficients of reduced algebraic system, but general scheme remains the same [15].

WAVELET APPROACH TO NONLINEAR PROBLEMS, II.

METAPLECTIC WAVELETS AND ROUTES TO CHAOS

A.N.FEDOROVA M.G.ZEITLIN

Russian Academy of Sciences, Institute of Problems of Mechanical Engineering, V.O.,Bolshoj pr.,61, 199178, St. Petersburg, Russia.

e-mail: zeitlin@math.ipme.ru, anton@math.ipme.ru

According to the orbit method and by using construction from the geometric quantization theory we construct the symplectic and Poisson structures associated with Weyl–Heisenberg (Gabor) wavelets by using metaplectic structure and corresponding polarization. The key point is a consideration of semidirect product of Heisenberg group and metaplectic group as subgroup of authomorphisms group of dual to symplectic space, which consists of elements acting by affine transformations. We consider the application to the construction of Melnikov functions in the theory of homoclinic chaos in perturbations of Hamiltonian systems.

1. Introduction.

Now we give some point of our program of understanding routes to chaos in some Hamiltonian systems in the wavelet approach [1]-[14]. All points are:

1. A model.
2. A computer zoo.The understanding of the computer zoo.
3. A naive Melnikov function approach.
4. A naive wavelet description of (hetero)homoclinic orbits (separatrix)
5. Symplectic Melnikov function approach.
6. Symplectic wavelet analysis.

7. Splitting of separatrix ...⟶ stochastic web with magic symmetry, Arnold diffusion and all that.

Now we consider only point 6,but before we say a few words about others points in some nonlinear (polynomial) with periodic in time coefficients dynamical model: a beam contacting with ideal compressible liquid in a channel.

1. In 2-mode Galerkin approximation for beam equation we have the next system of equations [10], [11].

$$\begin{aligned} x_1' &= x_2, \quad x_3' = x_4, \quad x_5' = 1, \quad x_6' = 1 \\ x_2' &= -ax_1 - b[\cos(rx_5) + \cos(sx_6)]x_1 - dx_1^3 - mdx_1x_3^2 - px_2 - \varphi(x_5) \\ x_4' &= ex_3 - f[\cos(rx_5) + \cos(sx_6)] - gx_3^3 - kx_1^2x_3 - gx_4 - \psi(x_5) \end{aligned}$$

or in Hamiltonian form

$$\dot{x} = J\cdot\nabla H(x) + \varepsilon g(x,\Theta),\ \dot{\Theta} = \omega,\ (x,\Theta) \in R^4 \times T^2,\ T^2 = S^1 \times S^1,$$

for $\varepsilon = 0$ we have:

$$\dot{x} = J\cdot\nabla H(x), \quad \dot{\Theta} = \omega$$

2. For details see [10],[11],[13]. The key point is the splitting of separatrix (homoclinic orbit) and transition to fractal sets on the Poincare map.
3. For $\varepsilon = 0$ we have homoclinic orbit $\bar{x}_0(t)$ to the hyperbolic fixed point x_0. For $\varepsilon \neq 0$ we have normally hyperbolic invariant torus T_ε and condition on transversally intersection of stable and unstable manifolds $W^s(T_\varepsilon)$ and $W^u(T_\varepsilon)$ in terms of Melnikov functions $M(\Theta)$ for $\bar{x}_0(t)$.

$$M(\Theta) = \int_{-\infty}^{\infty} \nabla H(\bar{x}_0(t)) \wedge g(\bar{x}_0(t), \omega t + \Theta)dt$$

This condition has the next form:

$$M(\Theta_0) = 0, \quad \sum_{j=1}^{2} \omega_j \frac{\partial}{\partial\Theta_j} M(\Theta_0) \neq 0$$

According to the approach of Birkhoff-Smale-Wiggins [19] we determined the region in parametric space in which we observe the chaotic behaviour [10],[11],[14].
4. If we cannot solve equation ($\varepsilon = 0$) explicitly in time then we compute Melnikov function according [1]-[9], where we used periodization of wavelets for computing closed homoclinic trajectory.

5. We also used symplectic Melnikov function [12]-[14].

$$M_i(z) = \lim_{j\to\infty} \int_{-T_j^*}^{T_j} \{h_i, \hat{h}\}_{\psi(t,z)} dt$$

$$d_i(z,\varepsilon) = h_i(z_t^u) - h_i(z_t^s) = \varepsilon M_i(z) + O(\varepsilon^2)$$

where {,} is the Poisson bracket, $d_i(z,\varepsilon)$ is the Melnikov distance.This approach is motivated by [16],[17].
7. Some hypothesis [18] about strange symmetry of stochastic web in multi-degree-of freedom Hamiltonian systems [19],[20].
Now we consider point 6-the main part of this text.

2. In the Direction to Symplectic Wavelets [12]–[14].

The following three concepts are equivalent [21], [22]:
1). a square integrable representation U of a group G,
2). coherent states over G
3). the wavelet transform associated to U.
We have now three cases:
a) the affine $(ax+b)$ group, which yields the usual wavelet analysis

$$[\pi(b,a)f](x) = \frac{1}{\sqrt{a}} f\left(\frac{x-b}{a}\right)$$

b). the Weyl-Heisenberg group which leads to the Gabor functions, i.e. coherent states associated with windowed Fourier transform.

$$[\pi(q,p,\varphi)f](x) = \exp(i\mu(\varphi - p(x-q)))f(x-q)$$

In both cases time-frequency plane corresponds to the phase space of group representation.
c). also,now we have (Murenzi,Torresani [22]) the case of bigger group, containing both affine and Weyl-Heisenberg group, which interpolate between affine wavelet analysis and windowed Fourier analysis: affine Weyl-Heisenberg group.But usual representation of it is not square-integrable and must be modified: restriction of the representation to a suitable quotient space of the group (the associated phase space in that case) restores square – integrability: $G_{aWH} \longrightarrow$ homogeneous space.
Our goal is given another – symplectic – approach to this problem.
This is because of symplectic nature of our dynamical problem. Also, the symplectic structures (wavelets and Hamiltonian) must be consistent (This must be resemble the symplectic or Lie-Poisson integrator theory).

We use the point of view of geometric quantization theory (orbit method) instead of harmonic analysis. Because of this we can consider (a) – (c) analogously. We use standard background of orbit theory [23],[24].

3. Metaplectic Group and Representations.

Let $Sp(n)$ be symplectic group, $Mp(n)$ is its unique two- fold covering – metaplectic group. Let V be a symplectic vector space with symplectic form (,),then $R \oplus V$ is nilpotent Lie algebra - Heisenberg algebra:

$$[R,V] = 0, \quad [v,w] = (v,w) \in R, \quad [V,V] = R.$$

$Sp(V)$ is a group of automorphisms of Heisenberg algebra.
Let N be a group with Lie algebra $R \oplus V$, i.e. Heisenberg group. By Stone- von Neumann theorem Heisenberg group have unique irreducible unitary representation in which $1 \mapsto i$. This representation is projective: $U_{g_1} U_{g_2} = c(g_1,g_2) \cdot U_{g_1 g_2}$, where c is a map: $Sp(V) \times Sp(V) \to S^1$, i.e. c is S^1 cocycle.
But this representation is unitary representation of universal covering, i.e. metaplectic group $Mp(V)$. We give this representation without Stone-von Neumann theorem. Consider a new group $F = N' \bowtie Mp(V)$, $\bowtie$ –semidirect multiplication (we consider instead of $N = R \oplus V$ the $N' = S^1 \times V$, $S^1 = (R/2\pi Z)$). Let V^* be dual to V, $G(V^*)$ be automorphism group of V^*.Then F is subgroup of $G(V^*)$,which consists of elements,which acts on V^* by affine transformations.
This is the key point!
Let $q_1,...,q_n;p_1,...,p_n$ be symplectic basis in V, $\alpha = pdq = \sum p_i dq_i$ and $d\alpha$ is symplectic form on V^*. Let M be fixed affine polarization, then for $a \in F$ the map $a \mapsto \Theta_a$ gives unitary representation of G:

$$\Theta_a : H(M) \to H(M)$$

Explicitly we have for representation of N on H(M):

$$(\Theta_q f)^*(x) = e^{-iqx} f(x), \quad \Theta_p f(x) = f(x-p)$$

The representation of N on H(M) is irreducible. Let A_q, A_p be infinitesimal operators of this representation.

$$A_q = \lim_{t\to 0} \frac{1}{t}[\Theta_{-tq} - I], \quad A_p = \lim_{t\to 0} \frac{1}{t}[\Theta_{-tp} - I],$$

$$\text{then} \quad A_q f(x) = i(qx)f(x), \quad A_p f(x) = \sum p_j \frac{\partial f}{\partial x_j}(x)$$

Now we give the representation of infinitesimal basic elements. Lie algebra of the group F is the algebra of all (nonhomogeneous) quadratic polynomials of (p,q) relatively Poisson bracket (PB). The basis of this algebra consists of elements $1, q_1, ..., q_n, p_1, ..., p_n, \quad q_iq_j, q_ip_j, p_ip_j, \quad i,j = 1,...,n, \quad i \le j$,

$$\begin{aligned} PB\ is\ \ \{f,g\} &= \sum \frac{\partial f}{\partial p_j}\frac{\partial g}{\partial q_i} - \frac{\partial f}{\partial q_i}\frac{\partial g}{\partial p_i} \quad and \\ \{1,g\} &= 0 \quad for\ all\ g, \\ \{p_i,q_j\} &= \delta_{ij}, \quad \{p_iq_j,q_k\} = \delta_{ik}q_j, \\ \{p_iq_j,p_k\} &= -\delta_{jk}p_i, \quad \{p_ip_j,q_k\} = \delta_{ik}p_j + \delta_{jk}p_i, \\ \{p_ip_j,p_k\} &= 0, \quad \{q_iq_j,q_k\} = 0, \\ \{q_iq_j,p_k\} &= -\delta_{ik}q_j - \delta jkq_i \end{aligned}$$

so, we have the representation of basic elements $f \mapsto A_f : 1 \mapsto i, q_k \mapsto ix_k$,

$$p_l \mapsto \frac{\delta}{\delta x^l}, p_iq_j \mapsto x^i\frac{\partial}{\partial x^j} + \frac{1}{2}\delta_{ij}, p_kp_l \mapsto \frac{1}{i}\frac{\partial^k}{\partial x^k \partial x^l}, q_kq_l \mapsto ix^kx^l$$

This gives the structure of the Poisson manifolds to representation of any (nilpotent) algebra or in other words to continuous wavelet transform.

4. The Segal-Bargman Representation.

Let $z = \frac{1}{\sqrt{2}}(p - iq)$, $\bar{z} = \frac{1}{\sqrt{2}}(p + iq), p = (p_1, ..., p_n)$, F_n is the space of holomorphic functions of n complex variables with $(f,f) < \infty$, where

$$(f,g) = (2\pi)^{-n}\int f(z)\overline{g(z)}e^{-|z|^2}dpdq$$

Consider a map $U : H \to F_n$, where H is with real polarization, F_n is with complex polarization, then we have

$$(U\Psi)(a) = \int A(a,q)\Psi(q)dq,$$

$$\text{where} \quad A(a,q) = \pi^{-n/4}e^{-1/2(a^2+q^2)+\sqrt{2}aq}$$

i.e. the Bargmann formula produce wavelets. We also have the representation of Heisenberg algebra on F_n:

$$U\frac{\partial}{\partial q_j}U^{-1} = \frac{1}{\sqrt{2}}\left(z_j - \frac{\partial}{\partial z_j}\right), \quad Uq_jU^{-1} = -\frac{i}{\sqrt{2}}\left(z_j + \frac{\partial}{\partial z_j}\right)$$

and also: $\omega = d\beta = dp \wedge dq$, where $\beta = i\bar{z}dz$.

5. Orbital Theory for Wavelets.

Let coadjoint action be

$$< g \cdot f, Y > = < f, Ad(g)^{-1}Y >,$$

where $<,>$ is pairing $g \in G, \quad f \in g^*, \quad Y \in \mathcal{G}$.

The orbit is $\mathcal{O}_f = G \cdot f \equiv G/G(f)$.

Also, let A=A(M) be algebra of functions, V(M) is A-module of vector fields. A^p is A-module of p-forms. Vector fields on orbit is

$$\sigma(\mathcal{O},X)_f(\phi) = \frac{d}{dt}(\phi(\exp tXf))\Big|_{t=0}$$

where $\phi \in A(\mathcal{O})$, $\quad f \in \mathcal{O}$. Then $\mathcal{O}_f$ are homogeneous symplectic manifolds with 2-form

$$\Omega(\sigma(\mathcal{O},X)_f, \sigma(\mathcal{O},Y)_f) = < f, [X,Y] >,$$

and $d\Omega = 0$. PB on $\mathcal{O}$ have the next form $\{\Psi_1, \Psi_2\} = p(\Psi_1)\Psi_2$, where p is $A^1(\mathcal{O}) \to V(\mathcal{O})$ with definition $\Omega(p(\alpha), X) = i(X)\alpha$. Here $\Psi_1, \Psi_2 \in A(\mathcal{O})$ and $A(\mathcal{O})$ is Lie algebra with bracket $\{,\}$.

Now let N be a Heisenberg group. Consider adjoint and coadjoint representations in some particular case.

$N = (z,t) \in C \times R, z = p + iq$; compositions in N are $(z,t)\cdot(z',t') = (z + z', t + t' + B(z,z'))$, where $B(z,z') = pq' - qp'$. Inverse element is $(-t,-z)$. Lie algebra n of N is $(\zeta,\tau) \in C \times R$ with bracket $[(\zeta,\tau),(\zeta',\tau')] = (0, B(\zeta,\zeta'))$. Centre is $\tilde{z} \in n$ and generated by (0,1); Z is a subgroup $\exp \tilde{z}$. Adjoint representation N on n is given by formula

$$Ad(z,t)(\zeta,\tau) = (\zeta, \tau + B(z,\zeta))$$

Coadjoint:

for $f \in n^*$, $\quad g = (z,t)$, $(g \cdot f)(\zeta,\zeta) = f(\zeta,\tau) - B(z,\zeta)f(0,1)$ then orbits for which $f|_{\tilde{z}} \neq 0$ are plane in n^* given by equation $f(0,1) = \mu$. If $X = (\zeta,0), \quad Y = (\zeta',0), \quad X,Y \in n$ then symplectic structure is

$$\Omega(\sigma(\mathcal{O},X)_f, \sigma(\mathcal{O},Y)_f) = < f, [X,Y] > = f(0, B(\zeta,\zeta'))\mu B(\zeta,\zeta')$$

Also we have for orbit $\mathcal{O}_\mu = N/Z$ and $\mathcal{O}_\mu$ is Hamiltonian G-space.

6. Kirillov Character Formula or Analogy of Gabor Wavelets.

Let U denote irreducible unitary representation of N with condition $U(0,t) = \exp(it\ell)\cdot 1$, where $\ell \neq 0$, then U is equivalent to representation T_ℓ, which acts in $L^2(R)$ according to

$$T_\ell(z,t)\phi(x) = \exp(i\ell(t + px))\,\phi(x - q)$$

If instead of N we consider E(2)/R we have S^1 case and we have Gabor functions on S^1.

7. Oscillator Group.

Let O be an oscillator group, i.e. semidirect multiplication of R and Heisenberg group N.

Let H,P,Q,I be standard basis in Lie algebra o of the group O and H^*, P^*, Q^*, I^* are dual basis in o^*. Let functional f=(a,b,c,d) be

$$aI^* + bP^* + cQ^* + dH^*.$$

Let us consider complex polarizations

$$h = (H, I, P + iQ) \quad \text{and} \quad \bar{h} = (I, H, P - iQ)$$

Induced from h representation, corresponding to functional f (for $a > 0$), unitary equivalent to the representation

$$W(t,n)f(y) = \exp(it(h - 1/2)) \cdot U_a(n)V(t),$$

$$\text{where} \quad V(t) = \exp[-it(P^2 + Q^2)/2a], \quad P = -\frac{d}{dx}, \quad Q = iax,$$

and $U_a(n)$ is irreducible representation of N, which have the form $U_a(z) = exp(iaz)$ on the center of N.

Here we have:

U(n=(x,y,z)) is Schrödinger representation, $U_t(n) = U(t(n))$ is the representation, which obtained from previous by automorphism (time translation): $n \longrightarrow t(n)$, $U_t(n) = U(t(n))$ is also unitary irreducible representation of N.

$$V(t) = \exp(it(P^2 + Q^2 + h - 1/2))$$

is an operator, which according to Stone–von Neumann theorem has the property

$$U_t(n) = V(t)U(n)V(t)^{-1}.$$

This is our last private case, but according to our approach we can construct by using methods of geometric quantization theory many "symplectic wavelet constructions" with corresponding symplectic or Poisson structure on it [14],[18].

WAVELET APPROACH TO NONLINEAR PROBLEMS, III.

NONLINEAR OSCILLATIONS.

FEDOROVA A.N. ZEITLIN M.G.

Russian Academy of Sciences, Institute of Problems of Mechanical Engineering, V.O., Bolshoj pr., 61, 199178, St. Petersburg, Russia,

e-mail: zeitlin@math.ipme.ru, anton@math.ipme.ru

We consider the problem of description of oscillations of a beam (circular cylindrical shell) contacting with a semi-infinite channel filled with compressible liquid (a model for submarine oscillations). We consider our problem for the case of two-frequency parametric perturbations and also external time-dependent forces in two-mode Galerkin approximation. Computer calculation gives us a possibility to analyse in the parameter space the time evolution of our system and corresponding transition between different regimes: deterministic dynamics – quasiperiodic dynamics – chaotic dynamics. The regimes for our system of equations, which we compute numerically, we shall consider also via Melnikov method. As the main part we consider wavelet approach via our variational approach to this problem, which gives us a possibility to construct explicit time solutions.

1 Introduction: from computer modelling to Melnikov analysis.

This is a part of the general program of investigation of nonlinear differential equations by wavelet-homoclinic methods [7]-[16]. In this paper we consider computer modelling and naive (nonsymplectic) Melnikov approach for computing regions in parameter space, where chaotic and quasiperiodic regimes appeared (part 1), in the problem of description of oscillation of a beam (circular cylindrical shell) contacting with a semi-infinite channel filled with compressible liquid (a model of submarine oscillations). The beam is on an elastic bed and fixed with thrust at both ends. It is subjected to compressing and harmonic in time forces. The channel has rigid sides. We consider our problem for the case of two-frequency parametric perturbations and also external time-dependent forces. In parts 2 –4 we consider wavelet approach [6] for computing explicit time solutions.

The system of equations which describes two-mode Galerkin approximation for initial problem is the next system of equations in $R^4 \times T^2$ [1]

$$
\begin{aligned}
x_1' &= x_2, \quad x_3' = x_4, \quad x_5' = \omega_1, \quad x_6' = \omega_2, \\
x_2' &= -ax_1 - b(\cos x_5 + \cos x_6)x_1 - dx_1^3 - mdx_1x_3^2 - px_2 - P_2(x_1, x_2, x_3, x_4) - \varphi(x_5, x_6), \\
x_4' &= -cx_3 - f(\cos x_5 + \cos x_6)x_3 - gx_3^3 - kx_1^2x_3 - \ell x_4 - Q_2(x_1, x_2, x_3, x_4) - \psi(x_5, x_6),
\end{aligned}
$$

where P_2, Q_2 are quadratic functions of their arguments. For the full analysis of this system we need to consider the next cases:

1. Pure Hamiltonian approximation,
2. Background state is Hamiltonian, perturbation is also Hamiltonian,
3. Background state is Hamiltonian, perturbation – non- Hamiltonian,
4. Dissipative case.

We calculate:

1. Time–dependence for dynamical variables,
2. Sections of phase space,
3. Poincare sections,
4. Fourier spectral curves.

Computer calculation gives us possibility to analise in the parameter space the time evolution of our system and corresponding transition between different regimes:

Deterministic dynamics $\longrightarrow$ quasiperiodic dynamics $\longrightarrow$ chaotic dynamics.

Fig.1 and Fig.2 contain all types of regimes.

The regimes for our system of equations, which we compute numerically, we shall consider also in the Hamiltonian approach via Melnikov method:

$$\dot{x} = JDH(x) + \varepsilon g(x, \Theta), \quad \dot{\Theta} = \omega, \quad (x, \Theta) \in R^m \times T^\ell, \quad \omega \in T^\ell$$

where T^ℓ is ℓ - tori,

$$T^\ell = \prod_{i=1}^{\ell} S^1, \quad S^1 = R/2\pi,$$

H(x) is Hamiltonian , J is symplectic matrix. We suppose that for $\varepsilon = 0$ this system has homoclinic (heteroclinic) orbit $\bar{x}_0(t)$ to the hyperbolic critical point x_0 (or two points). Then if ε is sufficiently small the system has normally hyperbolic invariant tori T_ε. We use approach of [26], [19] for computing the Melnikov function, which gives us a possibility to determine the behaviour of stable $W^s(T_\varepsilon)$ and unstable $W_u(T_\varepsilon)$ manifolds for normally hyperbolic invariant tori T_ε. Let $M(\Theta)$ be Melnikov function for $\bar{x}_0(t)$:

$$M(\Theta) = \int_{-\infty}^{\infty} DH(\bar{x}_0(t)) \wedge g(\bar{x}_0(t), \omega t + \Theta) dt.$$

If exists point $\Theta = \Theta_0 \in T^\ell$ for which $M(\Theta_0) = 0, DM(\Theta_0)$ has rank 1, then $W^s(T_\varepsilon)$ and $W^u(T_\varepsilon)$ intersect transversally. This provides, according to Birkhoff–Smale–Wiggins theorem, existence of chaotic regime. Further, if inside homoclinic loop $\bar{x}_0(t)$ exists continuous set $x_\alpha(t)$ of periodic orbits with period mT/n, then subharmonic Melnikov function is

$$M^{m/n}(t_0) = \int_0^{mT} DH(x_\alpha(t)) \wedge g(x_\alpha(t), t + t_0) dt$$

and its zeros give subharmonics with period mT for our system. We analyse different particular cases of our system and according to previous consideration determine region in the parameter space which give us the global qualitative behaviour and a possibility to detect subharmonic or chaotic regimes (they correspond to classical Melnikov functions for planar systems [17], [19], [25], [26]). This analysis allows us to take into account the influence of water on type of oscillation. Next we consider two chaotic cases and one subharmonic.

1. The system has form:

$$\begin{aligned}
\dot{\Theta}_1 &= \omega_1, \\
\dot{\Theta}_2 &= \omega_2, \\
\dot{x} &= y, \\
\dot{y} &= x - x^3 + \varepsilon(\gamma_1 \cos\Theta_1 + \gamma_2 \cos\Theta_2 - \delta y).
\end{aligned}$$

We have two homoclinic orbits

$$(x_\pm(t), y_\pm(t)) = \pm(\sqrt{2}sech(t), -\sqrt{2}sech(t)\cdot tanh(t)).$$

Corresponding Melnikov function is

$$M_\pm(\Theta_1,\Theta_2) = \pm\sqrt{2}\pi\omega_1\gamma_1 sech\left(\frac{\pi\omega_1}{2}\right)\sin\Theta_1 \quad \pm\sqrt{2}\pi\omega_2\gamma_2 sech\left(\frac{\pi\omega_2}{2}\right)\sin\Theta_2 - \frac{4}{3}\delta.$$

From this we have the region in the parameter space

$$\delta < \frac{3\sqrt{2}\pi}{4}\left|\omega_1\gamma_1 sech\left(\frac{\pi\omega_1}{2}\right) + \omega_2\gamma_2 sech\left(\frac{\pi\omega_2}{2}\right)\right|,$$

in which we may detect the chaotic behaviour.

2. The system is

$$\begin{aligned}
\dot{x} &= y \\
\dot{\tau} &= \varepsilon\nu \\
\dot{\Theta} &= \omega, \quad \omega^2 - 1 = \varepsilon\Omega \\
\dot{y} &= -x + \varepsilon((-\alpha x^3 + \gamma\cos\Theta) + \mu(-\delta y - \beta x\cos(2\Theta + \tau))).
\end{aligned}$$

We have in the system two times : rapid and slow. After averaging we have the next homoclinic loops:

$$\begin{aligned}
J_\pm(t) &= \pm\frac{2r_+r_-}{(r_+ - r_-)cosh(at) \pm (r_+ + r_-)} + j_2 \\
\Phi_\pm(t) &= \arcsin\left(\frac{-\dot{J}_\pm(t)}{\gamma}\sqrt{2J_\pm(t)}\right),
\end{aligned}$$

where

$$a = 3\alpha\sqrt{-r_+r_-}, \quad r_\pm = 2(k \pm \sqrt{2kj_2}), \quad k = 2\Omega/3\alpha - j_2$$

where j_1, j_2, j_3 are zeros of the equation.

$$x^3 - 2\left(\frac{2\Omega}{3\alpha}\right)x^2 + \left(\frac{2\Omega}{3\alpha}\right)^2 x - 2\left(\frac{\gamma}{3\alpha}\right)^2 = 0$$

Corresponding Melnikov function is

$$M_\pm(t_0) = \beta\sin\nu_0 t_0 A_\pm(\alpha,\gamma,\Omega,\nu_0) + \delta\omega B_\pm(\alpha,\gamma,\Omega),$$

where long formulae for A,B are in [17], [19], [25], [26]. The region of chaos corresponds in the parameter space to

$$\frac{\beta}{\delta\omega} > |B_\pm(\alpha,\gamma,\Omega)/A_\pm(\alpha,\gamma,\Omega,\nu_0)|$$

3. The system is

$$\begin{aligned}
\dot{x}_1 &= x_2 \\
\dot{x}_2 &= -x_1 + x_1^3 + \varepsilon\mu x_2 - \varepsilon f x_1^2 x_2 + \varepsilon\delta x_1\cos\omega\tau.
\end{aligned}$$

Periodic orbits inside homoclinic loop have the form [26], [17], [25]:

$$\begin{aligned}
\left(x_1^{(k)}(\tau), x_2^{(k)}(\tau)\right) = \Big[\; &\pm \frac{\sqrt{2}k}{\sqrt{1+k^2}} sn\left(\frac{\tau}{\sqrt{1+k^2}}, k\right), \\
&\pm \frac{\sqrt{2}k}{\sqrt{1+k^2}} cn\left(\frac{\tau}{\sqrt{1+k^2}}, k\right) dn\left(\frac{\tau}{\sqrt{1+k^2}}, k\right)\Big],
\end{aligned}$$

sn,cn,dn are elliptic functions with module k. The period of periodic orbits of order k is

$$T(k) = 4\sqrt{1+k^2}K,$$

where K is elliptic integral of the first kind. The Melnikov function has the form:

$$M^{m/n}(\mu,\delta,\tau_0) = \mu I_2(m,n) - f I_1(m,n) - \delta I_3(m,n)\sin\omega\tau_0,$$

where m,n are relative prime integers, which satisfy the resonance condition

$$K\sqrt{1+k^2} = 2\pi m/(\omega n).$$

The objects I_1, I_2, I_3 are functions of E(k) (elliptic integral of the second kind), $K'(k)$ (complementary elliptic integral of the first kind), k' (comlementary module) [17]. If $n = 1$ and m is even, we have the region in the parameter space

$$\delta > \left|\frac{\mu I_2(m,1) - f I_1(m,1)}{I_3(m,1)}\right|$$

for which our system has subharmonic orbits with period $T = 2\pi m/\omega$. Also, we use [16] in our analysis the Melnikov function approach for multi-degree-of-freedom systems [18], [21], [27]. We consider also the chaotic control problem for our system and relation with wavelet methods of computation of Melnikov functions [12], [16]. Next we consider wavelet approach to calculation explicit time solution for Galerkin approximation. We consider two cases. One is a particular case (Riccati approximations) and the second is general polynomial model.

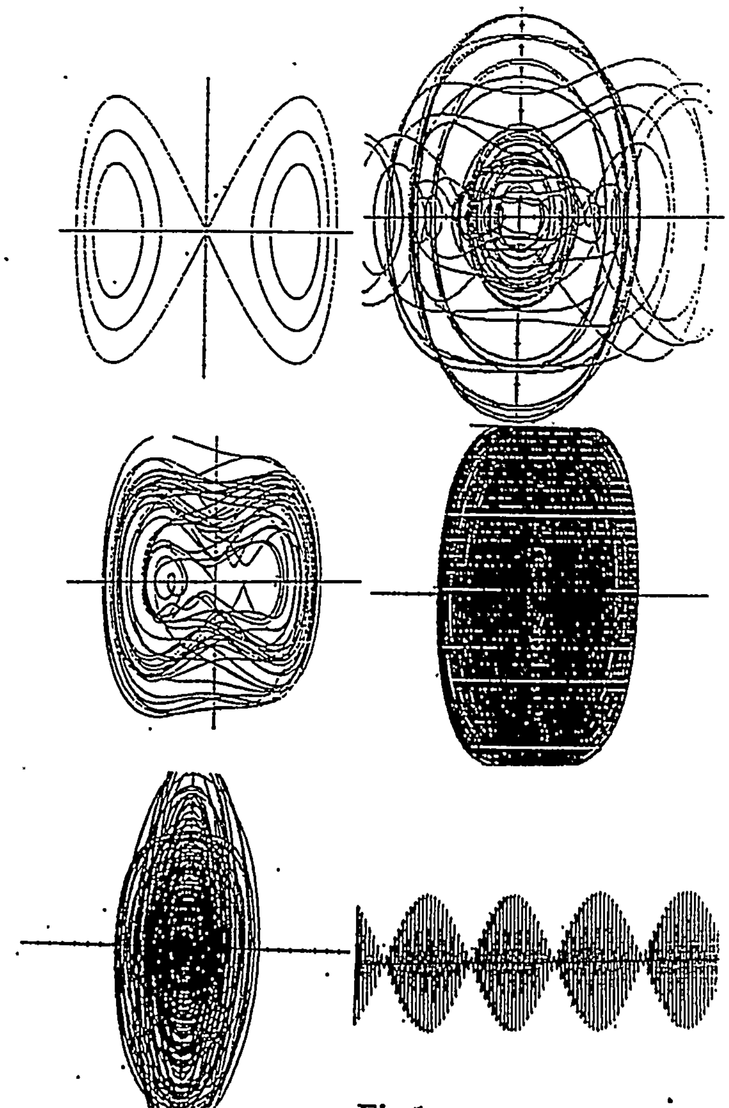

Fig.1.

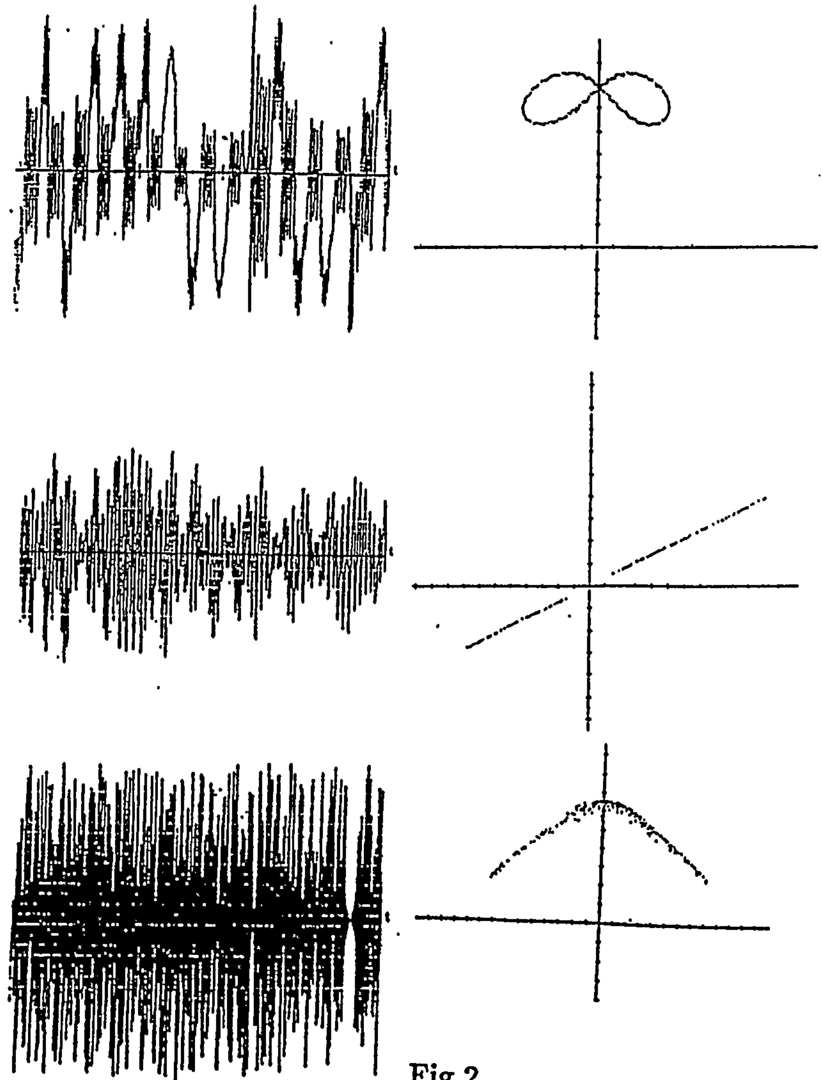

Fig.2.

WAVELET APPROACH TO NONLINEAR PROBLEMS, IV.

SYMPLECTIC TOPOLOGY AND SYMPLECTIC SCALES.

FEDOROVA A.N. ZEITLIN M.G.

Russian Academy of Sciences, Institute of Problems of Mechanical Engineering, V.O., Bolshoj pr., 61, 199178, St. Petersburg, Russia,

e-mail: zeitlin@math.ipme.ru, anton@math.ipme.ru

We consider the generalization of our variational wavelet approach to nonlinear polynomial problems to the case of Hamiltonian systems for which we need to preserve underlying symplectic or Poissonian or quasicomplex structures in any type of calculations. We use our approach for the problem of explicit calculations of Arnold–Weinstein curves via Floer variational approach from symplectic topology. The loop solutions are parametrized by the solutions of reduced algebraic problem – matrix Quadratic Mirror Filters equations. Also, we consider relation between KAM perturbation theory which is based on symplectic Hilbert scales of spaces and wavelet parametrization of general scales of spaces.

The action functional for loops in the phase space

$$F(\gamma) = \int_\gamma pdq - \int_0^1 H(t, \gamma(t))dt$$

The critical points of F are those loops γ, which solve the Hamiltonian equations associated with the Hamiltonian H and hence are periodic orbits. BTW, all its critical points are the saddle points of infinite Morse index, but surprisingly it is very effective. This will be demonstrated using several variational techniques starting from minimax due to Rabinowitz and ending with FLOER HOMOLOGY. So, (M, ω) is symplectic manifolds, $H : M \to \Re$, H is Hamiltonian, X_H is unique Hamiltonian vector field by

$$\omega(X_H(x), v) = -dH(x)(v), \quad v \in T_x M, \quad x \in M$$

A T-periodic solution $x(t)$ of the Hamiltonian equations

$$\dot{x} = X_H(x) \quad \text{on } M$$

is a solution, satisfying the boundary conditions $x(T) = x(0), T > 0$. Let us consider the loop space $\Omega = C^\infty(S^1, \Re^{2n})$, where $S^1 = \Re/Z$ of smooth loops in $\Re^{2n}$. Let us define a function $\Phi : \Omega \to \Re$

by setting

$$\Phi(x) = \int_0^1 \frac{1}{2} < -J\dot{x}, x > dt - \int_0^1 H(x(t))dt, \quad x \in \Omega$$

The critical points of Φ are the periodic solutions of $\dot{x} = X_H(x)$. Computing the derivative at $x \in \Omega$ in the direction of $y \in \Omega$, we find

$$\Phi'(x)(y) = \frac{d}{d\epsilon}\Phi(x + \epsilon y)|_{\epsilon=0} = \int_0^1 < -J\dot{x} - \nabla H(x), y > dt$$

Consequently, $\Phi'(x)(y) = 0$ for all $y \in \Omega$ iff the loop x satisfies the equation

$$-J\dot{x}(t) - \nabla H(x(t)) = 0,$$

i.e. $x(t)$ is a solution of the Hamiltonian equations, which also satisfies $x(0) = x(1)$, i.e. periodic of period 1. Periodic loops may be represented by their Fourier series:

$$x(t) = \sum_{k \in Z} e^{k2\pi Jt} x_k, \quad x_k \in \Re^{2k}$$

But instead, we use the construction from M. Holschneider, U. Pinkall: BIJECTION: between QMF-systems and measurable functions $\chi : T \in U(2)$ satisfying

$$\chi(\omega + \pi) = \chi(\omega) \begin{bmatrix} 0 & 1 \\ 1 & 0 \end{bmatrix},$$

is

$$\begin{bmatrix} \hat{\Phi}_0(\omega) & \hat{\Phi}_0(\omega+\pi) \\ \hat{\Phi}_1(\omega) & \hat{\Phi}_1(\omega+\pi) \end{bmatrix} = \chi(\omega)\begin{bmatrix} 0 & 1 \\ 1 & 0 \end{bmatrix} + \chi(\omega+\pi)\begin{bmatrix} 0 & 0 \\ 0 & 1 \end{bmatrix},$$

where

$$\left|\hat{\Phi}_i(\omega)\right|^2 + \left|\hat{\Phi}_i(\omega+\pi)\right|^2 = 2, \quad i = 0, 1.$$

Theorem. There is an explicit bijection between QMF-filters ... and the whole loop group : $LG : S^1 \to G$.

Also, we have symplectic structure on LG

$$\omega(\xi,\eta) = \frac{1}{2\pi}\int_0^{2\pi} < \xi(\theta), \eta'(\theta) > d\theta \quad \Longrightarrow$$

Hence Kähler geometry, Grassmanians, ...

KAM Perturbations, Symplectic Hilbert Scales (SHS) and Quasicomplex Structures (J) via Wavelets

HAMILTONIAN EQ. in Hilbert space Z with given system of dense Hilbert subspaces $Z_s, s \geq 0$ such that $Z_s \subset Z_r$, if $s > r$, $\quad Z_0 = Z$.

$$\|\cdot\|_s, \quad <\cdot,\cdot>_s.$$

Z_{-s} is conjugate to Z_s, $<\cdot,\cdot>_{-s}$ is inner product in Z_{-s}, $<\cdot,\cdot>_z$ are pairing between Z_s and Z_{-s}. $\{Z_s | s \in \Re\}$ is scale of Hilbert spaces $\equiv$ HILBERT SCALE.

$Z_\infty = \cap Z_s, \quad Z_{-\infty} = \cup Z_s, \quad Z_\infty$ is dense in each Z_s.

MORPHISM of Hilbert scale $\{Z_s\}$ of order d: Cont.linear maps

$$L_s : Z_s \to Z_{s-d}, \quad s \in \Re$$

if $L_{s_1} = L_{s_2}$ on $Z_{s_1} \cap Z_{s_2}$.

Now HANILTONIAN eq. is

$$\dot{u}(t) = J \bigtriangledown K(u(t))$$

$Z, <\cdot,\cdot>, u(t) \in Z$. J is antiselfadjoint operator in Z, $\bigtriangledown K$ is gradient of a functional K relative to $<\cdot,\cdot>$: $\delta K/\delta u \sim \bigtriangledown K$.

SYMPLECTIC STRUCTURE: $- < J^{-1}du, du >$

by definition:

$$- < J^{-1}du, du > [\xi, \eta] = - < J^{-1}\xi, \eta > \quad \text{for} \quad \xi, \eta \in Z.$$

Now we should provide Hilbert scale $\{Z_s\}$ with symplectic structure. All what we need

J be a linear operator, $J : Z_\infty \to Z_\infty$, $J(Z_\infty) = Z_\infty$,

a). J determines an isom. of the scale $\{Z_s\}$ of order $d_J \geq 0$;

b). the operator J with domain of definition Z_∞ is antisymmetric in Z :

$$< Jz_1, z_2 >_Z = - < z_1, Jz_2 >_Z, \quad z_1, z_2 \in Z_\infty$$

! Let us denote by $\bar{J}$ the isom. of the scale $\{Z_s\}$ of order $-d_J$ equal to $-(J)^{-1}$.

Introduce in every space $Z_s, s \geq 0$ the antisymmetric 2-form.

DEF. $\alpha =< \bar{J}dz, dz >_Z$ is symplectic structure. The triple $\{Z, \{Z_s | s \in \Re\}, \quad \alpha =< \bar{J}dz, dz >\}$ is SYMPLECTIC HILBERT SCALE.

Example 1

$$Z = \Re^n_p \times \Re^n_q, \quad Z_s = Z, \quad \forall s$$

$$J : (p, q) \longmapsto (-q, p) \Longrightarrow$$

$$J^2 = -E, \quad \bar{J} = -J^{-1} = J,$$

$$d_J = 0$$

$$\alpha =< \bar{J}dz, dz >=< Jdz, dz >= dp \wedge dq.$$

Example 2

$$Z_s = \{u(x) \in H^s(T^1) | \int_0^{2\pi} u(x)dx = 0\},$$

$$s \in \Re, \quad J = \partial/\partial x,$$

J is isom. of the scale of order one, $\bar{J} = -(J)^{-1}$ is isom. of order -1.

$\Downarrow$

KdV eq. $\quad u_t + 6uu_x + u_{xxx} = 0$

Complete Regular Banach Spaces

(Holschneider)

$\supset$ Examples

Hölder – Zygmund scale of spaces $\Lambda^{\alpha}(T^n)$, $\alpha \in \Re$,

Sobolev spaces $H^{\gamma}(T^n)$, $\gamma \in \Re$,

Tribel - Lizorkin spaces $F_{\gamma}^{p,q}(T^n) \supset \Lambda^{\alpha}, H^{\gamma}, L^p$ (potential spaces)

$$\|r\|_{H_\gamma(H^n)} = \sqrt{\int_{H^n} \frac{dbda}{a} |a^{-\gamma} r(b,a)|^2}$$

H^n is upper half space for Sobolev with weight a^{γ}

$$(H_\gamma(H^n) = F_\gamma^{2,2}(H^n)), \quad r = r(b,a) \in H^n, \quad h \in \Re^n$$

Wavelet synthesis of r (respect to h)

$$M_h r(x) = \int_{H^n} \frac{dbda}{a} r(b,a) \frac{1}{n} h(\frac{x-b}{a})$$

Wavelet transform

$$W_g f(b,a) = \int_{\Re^n} dx \frac{1}{a^n} \bar{g}(\frac{x-b}{a}) f(x), \quad b \in \Re, \quad a > 0$$

$b \in \Re^n$ is position parameter,

$a \in \Re$ is scale parameter.

$$\int_{H^n} \frac{dbda}{a} W_g s(b,a) r(b,a) = \int_{\Re^n} dx \bar{s}(x) M_g r(x)$$

Let

$$< s, r >_{H^n} = \int_{H_n} \frac{dbda}{a} \bar{s}(b,a) r(b,a)$$

$\Downarrow$

$$< s, W_g r >_{H^n} = < M_g s, r >_{\Re^n}$$

Let

$$C_{g,h} = \int_0^\infty \frac{da}{a} \hat{g}(\bar{a}k) \hat{h}(ak)$$

with $0 < |C_{g,h}| < \infty \implies g, h$ are analysis reconstructions pair:

$M_L W_g = C_{g,h}$

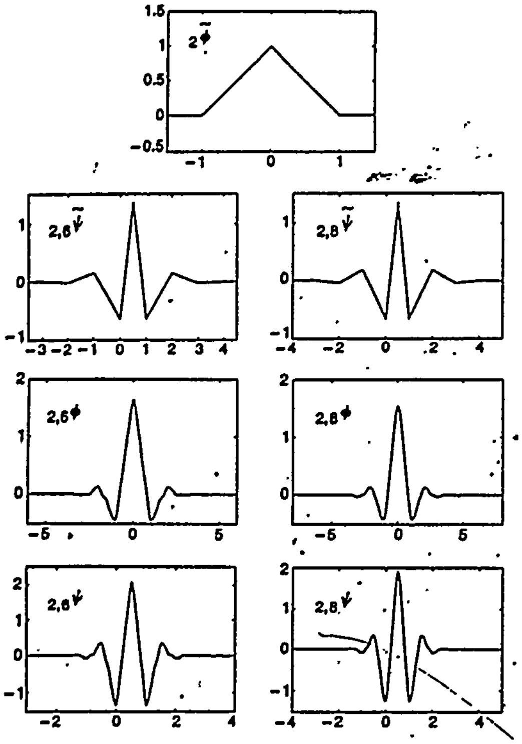

$2\tilde{\phi}$
$2,6\tilde{\psi}$
$2,8\tilde{\psi}$
$2,6\phi$
$2,8\phi$
$2,6\psi$
$2,8\psi$

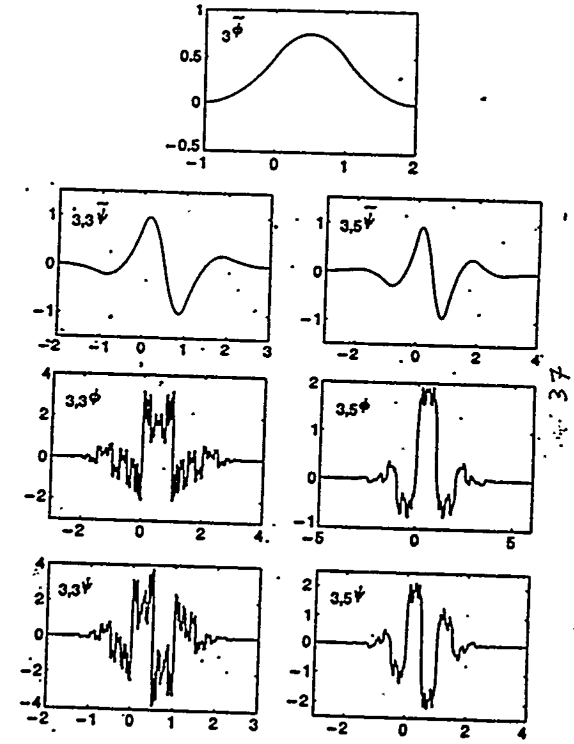

$3\tilde{\phi}$
$3,3\tilde{\psi}$
$3,5\tilde{\psi}$
$3,3\phi$
$3,5\phi$
$3,3\psi$
$3,5\psi$

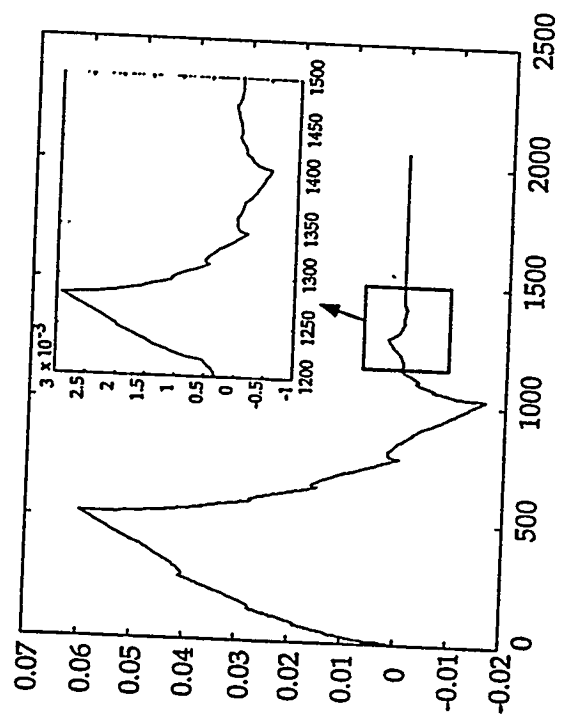

$\times 10^{-3}$

NONLINEAR ABERRATION CORRECTION

S. Andrianov, St. Petersburg

ROČNÍK:
ČÍSLO: ČÍSLO ZLOŽKY

SOME PROBLEMS OF NONLINEAR ABERRATION CORRECTION

Serge Andrianov

This report is devoted to more mathematical and computational problems than physical one.

<u>Physical problems:</u> maximally decrease all harmful aberrations:

geometrical, chromatic, influence of fringing fields, aberrations induced by space charge forces.

<u>Mathematical problems:</u> effective and comfortable tools for an investigation of concrete machine with its own characteristics and problems.

Basic Definitions and Concepts

$F(X,U,s)$ - an analytical function of X, U is a control vector, s - measured along a reference orbit. Let F generate a motion equation in a beam line

$$\frac{dX}{ds} = F(X,U,s) \qquad (1)$$

The Eq. (1) generates a Lie transformation

$$X(X_0,U;s|s_0) = \mathcal{M}(U;s|s_0)\circ X_0 \qquad (2)$$

ROČNÍK:
ČÍSLO: ČÍSLO ZLOŽKY 2

$$\mathcal{M}_F = T\exp\left\{\int_{s_0}^{s} \mathcal{L}_{F(x,\tau)}\,d\tau\right\},$$ (so called T-exponential operator)

$$\mathcal{L}_F = F^*(x,\tau)\,\partial/\partial X$$

Magnus representation (routine exponential operator)

$$\mathcal{M}_G = \exp\left\{\mathcal{L}_{G(x;s|s_0)}\right\}$$

$$F(X,U,s) = \sum_{k=0}^{\infty} \mathbb{F}_k(U,s)X^{[k]} \Rightarrow G(X,U;s|s_0) = \sum_{k=0}^{\infty} \mathbb{G}_k(\cdot)X^{[k]} \quad (2)$$

$\mathbb{F}_k$, $\mathbb{G}_k$ - are matrices $(n \times C^{k}_{n+k-1})$

$$X^{[k]} = \underbrace{X\otimes\ldots\otimes X}_{k\text{-times}} \quad \left[X^{[2]} = (x^2\ \ x p_x\ \ p_x^2)^*,\ n=2\right]$$

$$\mathcal{L}_F = \sum_{k=0}^{\infty}\left(X^{[k]}\right)^* \mathbb{F}_k^*\,\partial/\partial X = \sum_{k=0}^{\infty}\mathcal{L}_{F_k}$$ F_k a homogen. polynomial of k-th order

It is known the following factorization for $\mathcal{M}$

$$\mathcal{M} = \ldots\circ\mathcal{M}_{\hat{G}_k}\circ\ldots\circ\mathcal{M}_{\hat{G}_2}\circ\mathcal{M}_{\hat{G}_1} = \mathcal{M}_{\tilde{G}_1}\circ\mathcal{M}_{\tilde{G}_2}\circ\ldots\circ\mathcal{M}_{\tilde{G}_k}\circ\ldots$$

In autonomous case $\partial F/\partial X = 0 \Rightarrow$

$$G = (s-s_0)F$$

and for $\hat{G}_k$ there is a representation

$\hat{G}_k \to G_k$ $\quad G_k = G_k^k + G_k^{\{<k\}}$, $G_k^k = G_k^k(\tau, F_k)$,

$s - s_0 = \tau$ $\quad G_k^{\{<k\}} = G_k^{\{<k\}}(\tau, \{F_j\}, j<k)$ (3)

We can obtain $\quad G_k^k = \sum_{j=0}^{\infty} \frac{1}{j!} \mathcal{L}_{G_1}^{(j-1)} \circ F_k$ or for metrices

$$\mathbb{G}_k^k = \mathbb{G}_k^k(\tau, \mathbb{F}_k) = \sum_{j=0}^{\infty} \frac{1}{j!} \tau^j \mathbb{F}_k \left(\mathbb{G}_1^{\oplus k}\right)^{(j-1)}$$

For $G_k^{\{<k\}}$ there isn't such simple form, f.e. $(G_2^{\{<2\}} \equiv 0)$

$$\cancel{\mathbb{G}_3^{\{<3\}} \tilde{=} -\frac{\tau^3}{4} \tilde{\mathbb{F}}_2 \left[\frac{1}{3}\mathbb{F}_2^{\oplus 2} + \frac{\tau}{6}\hat{\mathbb{F}}_2 + \frac{\tau^2}{20}\mathbb{F}_1^{\oplus 2}\hat{\mathbb{F}}_2 + \frac{\tau^3}{30}\mathbb{F}_1^{\oplus 2}\left(\hat{\mathbb{F}}_2\right)^{\oplus 2}\right]},$$

$$\tilde{\mathbb{F}}_2 = \mathbb{F}_2 \mathbb{F}_1^{\oplus 2}, \quad \hat{\mathbb{F}}_2 = \mathbb{F}_1^{\oplus 2} \mathbb{F}_2^{\oplus 2}$$

$$\mathbb{A}^{\oplus k} = \mathbb{A}^{\oplus(k-1)} \otimes \mathbb{E} + \mathbb{E}^{[k-1]} \otimes \mathbb{A}, \quad \{\mathbb{E}\}_{ij} = \delta_{ij}, \quad \mathbb{A}^{\oplus 0} = \mathbb{O}, \ \mathbb{A}^{\oplus 1} = \mathbb{A}$$

The expansions (2) allow to consider $\mathcal{M}_{G_m}$, $m \geq 0$

$$\mathcal{M}_{G_m} \circ X^{[\ell]} = X^{[\ell]} + \sum_{k=1}^{\infty} \frac{\mathbb{P}_m^{k\ell}}{k!} X^{[k(m-1)+\ell]},$$

$$\mathbb{P}_m^{k\ell} = \prod_{j=1}^{k} \mathbb{G}_m^{\oplus((j-1)(m-1)+\ell)} \qquad (3)$$

Let

$$\mathcal{M}_{\leq k} = \mathcal{M}_{G_k} \circ \ldots \circ \mathcal{M}_{G_1}$$

for exampee

$$\mathcal{M}_{\leq 3} \circ X = \mathbb{M}^{11}\Big(X + \sum^{3} \sum_{k=1}^{\infty} \frac{\mathbb{P}_m^{k1}}{m!} X^{[k(m-1)+1]} + \sum_{i=1}^{\infty}\sum_{k=1}^{\infty} \frac{1}{k!\,m!} \mathbb{P}_2^{k1} \mathbb{P}_3^{i(k+1)} X^{[2i+k+1]} \ldots$$

$$\approx \mathbb{M}^{11}\left(X + \mathbb{P}_2^{11} X^{[2]} + \left(\mathbb{P}_3^{11} + \frac{1}{2!}\mathbb{P}_2^{21}\right) X^{[3]}\right)$$

So we can write

$$\mathcal{M}_{G} \circ X = \mathbb{M}^{11} \circ \left(X + \sum_{k=2}^{\infty} \mathbb{Q}^{1k} \circ X^{[k]}\right) \qquad (4)$$

$\mathbb{M}^{11}$ - the matricant for linear motion equation

$$\frac{dX}{ds} = \mathbb{F}_1 X$$

We can build the following matrixes

$$\cancel{\mathbb{M}^{m\ell} = \sum_{\substack{k_1+\ldots+k_m=\ell \\ k_i \geq 1}} \bigotimes_{i=1}^{m} \mathbb{M}^{1k_i}}, \quad \ell \geq m$$

and

$$\mathbb{M}^{\infty} = \begin{pmatrix} \mathbb{M}^{11} & \mathbb{M}^{12} & \ldots & \mathbb{M}^{1k} & \ldots \\ \mathbb{O} & \mathbb{M}^{22} & \ldots & \mathbb{M}^{2k} & \ldots \\ \cdot & \cdot & \cdot & \cdot & \cdot \\ \mathbb{O} & \mathbb{O} & & \mathbb{M}^{kk} & \ldots \end{pmatrix},$$

$$X^{\infty} = \mathbb{M}^{\infty} X_0^{\infty}, \quad X^{\infty} = \left(X\ X^{[2]} \ldots X^{[k]} \ldots\right)^* \qquad (5)$$

The inverse matrix $\mathbb{T}^{\infty} = (\mathbb{M}^{\infty})^{-1}$

$$\mathbb{T}^{\infty} = \{\mathbb{T}^{ik}\}_{i,k \geq 1}, \quad \mathbb{T}^{ik} \equiv \mathbb{O}, \ i > k$$

$$\mathbb{T}^{kk} = \left(\mathbb{M}^{kk}\right)^{-1} = \left(\left(\mathbb{M}^{11}\right)^{[k]}\right)^{-1} = \left(\mathbb{M}^{11}\right)^{-[k]}$$

$$\mathbb{T}^{ik} = -\mathbb{T}^{ii} \sum^{k} \mathbb{M}^{ij} \mathbb{T}^{jk} \ldots$$

Algebraic Methods

For example, let us consider an ion-optical system from quadrupoles,...

$$X = \mathbb{M}^{11} X_0 + \mathbb{M}^{13} X_0^{[3]} + \dots, \quad \mathbb{M}^{13} = \mathbb{M}^{11} \mathbb{Q}^{13}, \tag{6}$$

$$\mathbb{Q}^{13}(s|s_0) = \int_{s_0}^{s} \left(\mathbb{M}^{11}(\tau|s_0)\right)^{-1} \mathbb{P}^{13}(\tau)\, \mathbb{M}^{33}(\tau|s_0)\, d\tau,$$ for the motion equation in the form

$$\frac{dX}{ds} = \mathbb{P}^{11} X + \mathbb{P}^{13} X^{[3]}. \tag{7}$$

Let NO be a number of octupoles on the total length of the system, then

$$\mathbb{Q}^{13}(s_k|s_0) = \sum_{i=1}^{NO} \mathbb{Q}^{13}(s_k|s_{k-1}). \tag{8}$$

$$\mathbb{P}^{13} = \mathbb{P}^{13}_{oct} + \mathbb{P}^{13}_{quadr}$$

$$\mathbb{Q}^{13} = \mathbb{Q}^{13}_{quadr} + \sum_{i=1}^{NO} \gamma_k \int_{s_{k-1}}^{s_k} \left(\mathbb{M}^{11}(\tau|s_0)\right)^{-1} \mathbb{P}^{13}_{k\text{-}oct}(\tau)\, \mathbb{M}^{33}(\tau|s_0)\, d\tau \tag{9}$$

$\mathbb{P}^{13}_{k\text{-}oct}$ is calculated under $\gamma_k = 1$, $\gamma_i = 0$, $i \neq k$. It is identical for $\forall\, [s_{i-1}, s_i]$. Also, we can write the following equation

$$X = \mathbb{M}^{11}\left(X_0 + \left[\mathbb{Q}^{13}_{quadr} + \sum_{k=1}^{NO} \mathbb{Q}^{13}_{k\text{-}oct}\right] X_0^{[3]}\right) \tag{10}$$

For JINR microprobe system $NO = 4$ as the main role the spherical aberrations coefficients play:

x'^{3}, $x'y'^{2}$, y'^{3}, $y'x'^{3}$ – four spherical aber-n monomials of third order

and there is a linear algebraic equation

$$(10) \Rightarrow \quad \mathbb{A}\Gamma = \mathbb{B}_{quadr}, \tag{11}$$

where

$$\mathbb{A} = \begin{pmatrix} z_{14}(1000) & z_{14}(0100) & z_{14}(0010) & z_{14}(0001) \\ z_{110}(1000) & z_{110}(0100) & z_{110}(0010) & z_{110}(0001) \\ z_{34}(1000) & z_{34}(0100) & z_{34}(0010) & z_{34}(0001) \\ z_{310}(1000) & z_{310}(0100) & z_{310}(0010) & z_{310}(0001) \end{pmatrix}$$

$z_{ik} = (\mathbb{M}^{13})_{ik}$

$$\mathbb{B}_{quadr} = \left(z_{14}(0000)\; z_{110}(0000)\; z_{34}(0000)\; z_{310}(0000)\right)^{*}$$

For linear model optimal envelope sizes on a target is equal 1μ, after "including" the third order aberrations $\approx 6\mu$ and after correction procedure we obtained $\approx 1\mu$ again.
The fifth order aberrations increase this value up to 1.3μ.

Optimal Control Theory Methods

As control functions u_i, $U = (u_1, \dots, u_r)^*$ we'll consider multipole force distributions along the beam line axis. For example, $u_1 = g(s)$ – a gradient for a "continuous" quadrupole lens", $u_2 = \gamma(s)$ an octupole force distribution along the axis

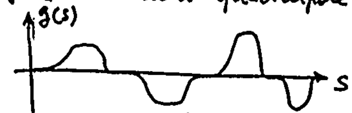

general objective function

$$f[U] = \int_{s_0}^{s^{fin}} \int_{\mathfrak{M}(\tau)} H_1(X, U; \tau)\, dX\, d\tau + \int_{\mathfrak{M}_{fin}} H_2(X, U, s^{fin})\, dX$$

$$\inf_{U \in \mathcal{U}} f[U] \to f^{opt} = f(U^{opt})$$

The objective function = the residual function between desired beam size on the target and a current size. This approach is useful for cases when one wants to use a few correcting multipole lenses (in this case the lin. alg. equ. will be underdetermined).

As the second example we can mention a problem of induced (parasitic) oscillations of an intensity of extracted beam from the JINR accelerator.

At first, we studied an influence of different kind of source of such oscillations. Than we include a feedback (wich can ensure minimization of such oscillations).

As control parameter the feedback parameters (length and hight of the feedback impulse) are chosen.

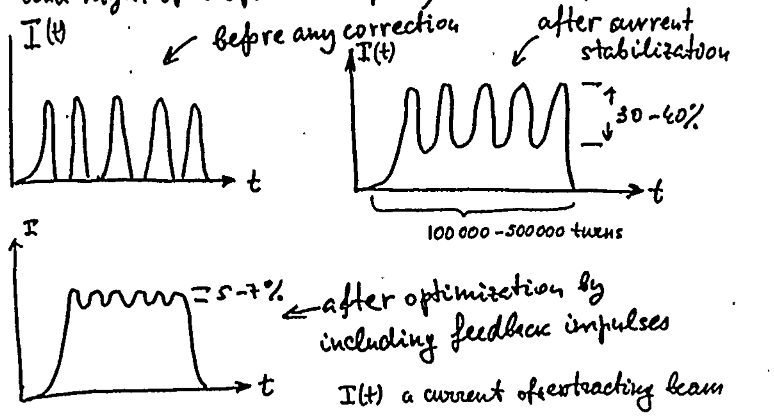

Full times of extracting process: about 400000-500000 turns on a preliminary step and 100000-500000 turns on extracting step.

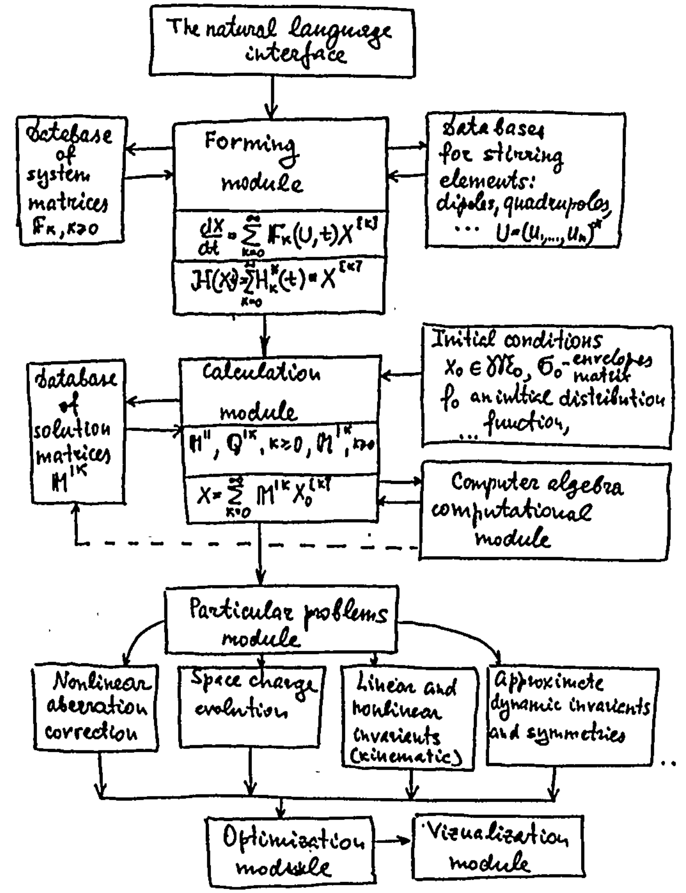

MECHANISM OF THE SAW-TOOTH INSTABILITY

S. HEIFETS

S. Heifets, SB, 12/96

Mechanism of the Saw-tooth Instability

Introduction

• SLAC, etc.: saw-tooth modulation of the rms bunch length above threshold of the microwave instability/amplitude of the sideband.

• Relaxation oscillations (old ring), amplitude modulation (new ring)

• Study of the nonlinear regime above threshold of the microwave instability is required

• Similar problem in plasma have been studied by Karpman-Altshul, O'Neil, O'Neil and Morales in 1965

* Plasma oscillations with frequency Ω are described as an unstable plasma wave with growing amplitude. The wave trapped particles which damped oscillations.

** In O'Neil's theory, contrary to K-Al., there are self-consistent oscillations of the decrement which is damped out after a few periods T_m of motion of of the trapped particles.

** The nonlinear regime takes place at $t > (\Omega T_m)T_m >> T_m$.

• In the accelerator physics:

** mostly linear theory based on the linearized Vlasov equation

** K. Yokoya and Y.H. Chin used the quasi-linear approximation, i.e. the linearized Vlasov equation for non-zero azimuthal harmonics and the Fokker-Plank equation for ρ_0

$$\frac{\partial \rho}{\partial t} + \overline{\{\delta U(\rho_k), \rho_k\}} = \hat{D}\rho_o$$

The average gives additional diffusion-like term.

The system adiabatically approaches a new quasi-steady equilibrium.

** Here basic equation for the nonlinear behavior are derived. It is shown, that normally the behavior of the system is the same as described by O'Neil in plasma. Possible mechanisms of the saw-tooth instability are outlined.

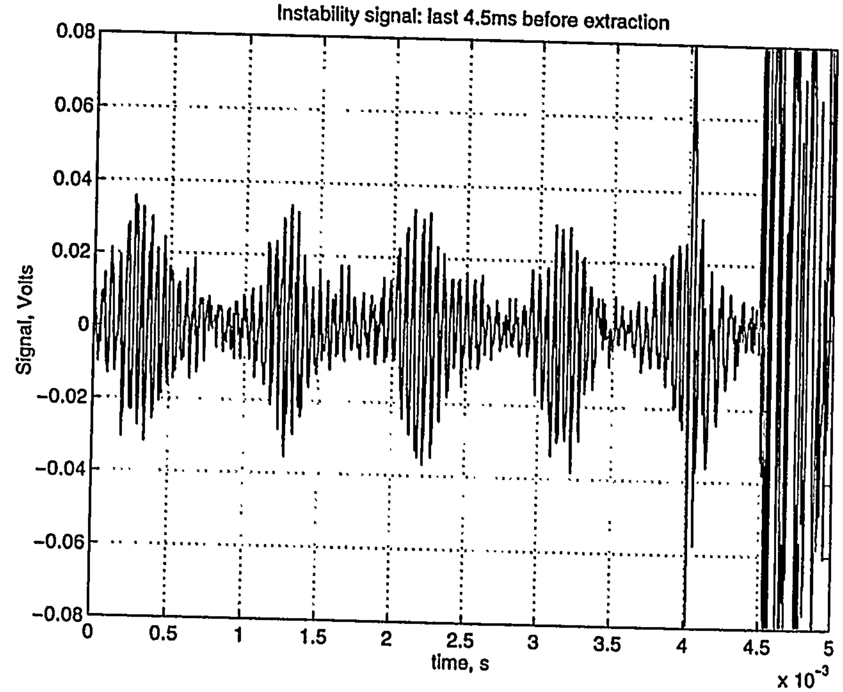

Notations

- Variables $p = -\Delta/\delta_0$, $x = Z/\sigma_0$, $s = \omega_s t$.
- Hamiltonian

$$H(x,p) = \frac{p^2}{2} + u(x,t)$$

$$\frac{\partial u}{\partial x} = x - \lambda \int dx' dp' \rho(x',p') W^\delta[(x'-x)\sigma_0]$$

$$\lambda = \frac{N_b r_e}{2\pi Q_s \delta_0}$$

- System is described by the Fokker-Plank equation

$$\frac{\partial \rho}{\partial s} + \{H,\rho\} = \gamma_d \frac{\partial}{\partial p}[\frac{\partial \rho}{\partial p} + p\rho]; \quad \int dx dp \rho = 1$$

- In the angle-action variables ϕ, J,

$$H = H_0(J), \quad \omega_0(J) = \frac{\partial H_0}{\partial J}$$

there is a steady-state Haiisinski solution

$$\rho_H = \frac{1}{Z_H} e^{-H_0(J)}$$

* Distorted Gauss ⇒ asymmetry
* Note. Closed H-system with fixed points / limiting cycle

Van der Pol

* Second Stable Solution!

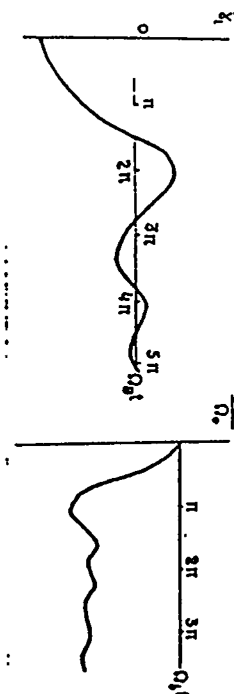

Fig. 2.2.3. Qualitative time-dependence curves of the damping decrement and Langmuir wave shift in the regime of particle trapping.

O'Neil & Morales

Analysis of stability in perturbation theory

- Introduce a perturbation

$$H_0(J) \to H(\phi, J, s) = H_0(J) + \epsilon \cos(n\phi - \int^s \Omega ds)$$

- Go to the frame rotating with $\omega_r = \omega(J_r) = \Omega/n$ changing variables to

$$j = J - J_r, \quad \alpha = \phi - \frac{\Omega}{n}s, \quad H(\alpha, j) = \frac{\omega_r' j^2}{2} + \epsilon \cos\alpha + \dot{J}_r \alpha$$

- For the non-zero azimuthal harmonics $\rho_m(J, s)$, $\rho = \sum \rho_m e^{im\alpha}$

a) neglect diffusion and damping
b) neglect interaction between non-zero harmonics
c) take $\epsilon = \hat{\epsilon} e^{\Gamma s}$
Then

$$\rho_n(J, s) = \frac{n\epsilon}{2} \frac{\frac{\partial \rho_0}{\partial J}}{n\omega_0(J) - \Omega + i\Gamma}$$

- For the zero harmonics

$$\frac{\partial \rho_0}{\partial s} + \frac{\partial}{\partial j}[\frac{n\epsilon}{2i}\rho_n + (c.c) + \dot{J}_r \rho_0] = \gamma_d \frac{\partial}{\partial j}[\frac{J}{\omega_0(J)}\frac{\partial \rho_0}{\partial j} + J\rho]$$

Substitute ρ_n,

$$\frac{\partial \rho_0}{\partial s} = \gamma_d \frac{\partial}{\partial j}[\frac{J}{\omega_0(J)}\frac{\partial \rho_0}{\partial j} + J\rho + (\frac{n\epsilon}{2})^2 \frac{\partial \rho_0}{\partial j}\frac{2\Gamma}{(n\omega_r' j)^2 + \Gamma^2}]$$

Steady-state solution

$$\rho_H = \frac{1}{Z} e^{-H_0(J) - \sigma(j)}$$

where

$$\sigma(j) = \pm(\frac{n\epsilon}{2})^2 \frac{\pi\omega_r}{|n\omega_r' J_r|}$$

** Result suggets the mechanism for ralaxation oscillations. Simulations (Y-Chin) give adiabatic approach to a new steady-state.

** Recently, Stupakov and Breizman in a different technique obtained for some parameters non-damping oscillations

$\varepsilon = ?$
Another solution ?

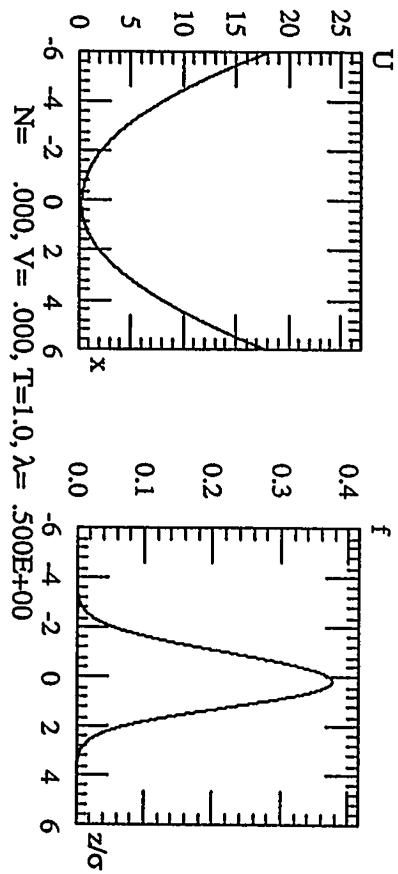

Self-consistency

The self-consistent potential

$$u(j,\phi) = -\frac{\lambda}{\sigma_0}\sum_m e^{im\phi}$$

$$u_m = \sum_l \int dj d\alpha R_{ml}(J,J')\rho(j,\alpha,s)e^{-il(\alpha-\omega_r t)} + (c.c)$$

$$R_{ml}(J,J') = \frac{4\pi}{Z_0}\int \frac{d\omega}{2\pi i}\frac{Z(\omega)}{\omega}C_m(\omega,J)C_l^*(\omega,J')$$

where

$$C_m(\omega,J) = \int \frac{d\phi}{2\pi}e^{-im\phi+i(\omega\sigma_0/c)x(J,\phi)}$$

Compare with the perturbation $\epsilon\cos(n\phi-\Omega s)$. assuming small frequency spread, i.e. only one resonance $\omega(J_r)=\omega/n$.

Averaging fast oscillating terms, we get the nonlinear analog of the dispersion equation

$$\epsilon(j) = -\frac{2\lambda}{\sigma_0}\int dj'd\alpha' R_{nn}(J,J')\rho(j',\alpha',s)e^{-in\alpha'}$$

The real part of the impedance and the anharmonicity of the trajectory $x(J,\phi)$, which is mostly due to the cubic nonlinearity of the potential $u(x)$), result in the asymmetry of $R_{nn}(J,J')\neq R_{nn}(J',J)$.

In the linear theory that leads to instability (Oide).

The zero harmonic $\Delta H = u_0^\epsilon - u_0^{\epsilon=0}$ gives the shift

$$\frac{\Omega}{n} = \omega_0(J_r) + \frac{\partial}{\partial j}\delta H(j)]_r$$

observed in the experiments.

In the perturbation theory, substitute ρ_n and get the usual relation of the linear theory

$$\epsilon(j) = -\frac{2\pi n\lambda}{\sigma_0}\int dj' R_{nn}(J,J')\epsilon(j')\frac{\frac{\partial\rho_0}{\partial j}}{n\omega_r' j' + i\Gamma}$$

Resonance Solution

For finite ϵ, introduce canonical r,ψ,

$$j,\alpha \to r,\psi, \quad H(j,\alpha)\to H(r), \quad \omega_M(r) = \frac{\partial H(r)}{r}, \quad \omega_M(0) = \sqrt{4\epsilon/|\omega_r'|}$$

and expand

$$\rho(r,\psi) = \sum_k \rho_k(r,s)e^{ik\psi}$$

Define

$$a_k = <(\frac{\partial x}{\partial\psi})^2 e^{-ik\psi}>$$

$$b_k = <(\frac{\partial x}{\partial\psi})(\frac{\partial x}{\partial\alpha})e^{-ik\psi}>$$

** The Fokker-Plank equation for the zero-harmonic takes the form

$$\frac{\partial\rho_0}{\partial s} = \gamma_d\frac{\partial}{\partial r}[a_0\frac{\partial\rho_0}{\partial r} + \omega_M a_0 + \omega_r b_0(1-\frac{\dot{J}_r}{\gamma_d J_r})\rho_0]$$

** In the steady-state,

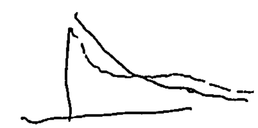

$$\rho_0(r) = \frac{1}{Z_M}e^{-[H(r)+\sigma(r)]}$$

where $\sigma(r)\propto 2\omega_r\sqrt{\epsilon/|\omega_r'|}\neq 0$ for $r<\sqrt{4\epsilon/\omega_r'}$ (Shoenfeld, Meller).

** In the J,ϕ variables this solution is the time dependent packet of the azimuthal harmonics (nonlinear Van-Kampen wave or a soliton).

Dipole Oscill-s / Quad ry

Localization

Steady St. Free energy, Fig

** The non-zero harmonics $k\neq 0$ satisfy

$$\frac{\partial\rho_k}{\partial s} + ik\omega_M\rho_k = \gamma_d\left\{\omega_r b_k(1-\frac{\dot{J}_r}{\gamma_d J_r})\frac{\partial\rho_0}{\partial r} - \omega_m a_k\frac{\partial}{\partial r}[\frac{1}{\omega_M}\frac{\partial\sigma}{\partial r}\rho_0]\right\}$$

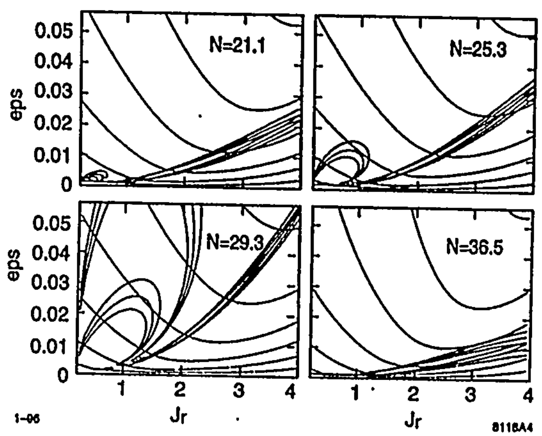

Figure 4

Difference of free energies $\Delta\Phi$ and lines corresponding to condition of self-consistency Eq. (2.26) for modes $n = 2,3$ and different N_B.

Time Dependence

Substitute the solution

$$\rho_k(r,s) = \gamma_d \int_{s_0}^{s} ds' e^{-ik\omega_M(s-s')} \left\{ \omega_r b_k (1 - \frac{\dot{J}_r}{\gamma_d J_r}) \frac{\partial \rho_0}{\partial r} - \omega_m a_k \frac{\partial}{\partial r} [\frac{1}{\omega_M} \frac{\partial \sigma}{\partial r} \rho_0] \right\}$$

in the equation for ϵ

$$\frac{\partial \epsilon}{\partial s} = -\frac{2\lambda}{\sigma_0} \int dr d\psi R_{nn} e^{-in\alpha(r,\psi)} \sum_{k\neq 0} \dot{\rho}_k(r,s) e^{ik\psi}$$

Effect of ρ_0

That gives

$$\sum_{k\neq 0} \dot{\rho}_k(r,s) e^{ik\psi} = 2\gamma_d \int_{s_0}^{s} ds' \{\Phi(r, \omega_M(s-s'), s') - <\Phi(r,\psi,s')>\}$$

Here

$$\Phi(r,\psi,s) = J_r (\frac{\partial \alpha}{\partial \psi})(1 - \frac{\dot{J}_r}{\gamma_d J_r}) \frac{\partial \rho_0}{\partial r} - \omega_M (\frac{\partial x}{\partial \psi})^2 \frac{\partial}{\partial r} [\frac{\rho_0}{\omega_M} \frac{\partial \sigma}{\partial r}]$$

Expand

$$\Phi(r,\psi,s) = \sum_l \Phi_l e^{inl\psi}$$

Then

$$\sum_{k\neq 0} \dot{\rho}_k(r,s) e^{ik\psi} = 2\gamma_d \sum_{l>0} \Phi_l \cos(nl\psi) \cos(nl\omega_M s)$$

$$+ 2\pi\gamma_d\omega_M \sum_{l>0} nl\Phi_l \sin(nl\psi) \frac{\sin(nl\omega_M s)}{\pi(nl\omega_M)}$$

Hence $\dot{\epsilon}$ oscillate in time. As result of filamentation, after averaging over r, oscillations are damped for $\omega s >> 1$

$$\frac{\partial \epsilon}{\partial s} \propto \frac{\sin(\omega_M s)}{s}$$

Relaxation Oscillations

Under normal conditions, the system goes to a new steady-state described by Haiisinski or the static resonance solution. There is a possibility that filamentation is slow compared to the storage time (=few damping time).

If not, then relaxation oscillations may be related to the frequency shift (see, for example, O'N-M)

There are several possibilities to generate the saw-tooth

- ω_r' changes sign due to the shift in J_r Fig. 3
- interaction of the resonances
- factor $(1 - \frac{J_r}{\gamma_d J_r}$ changes sign while J_r varies
- Baartman-Dyachkov mechanism, but it requires very distorted potential well with two minima. Fig.

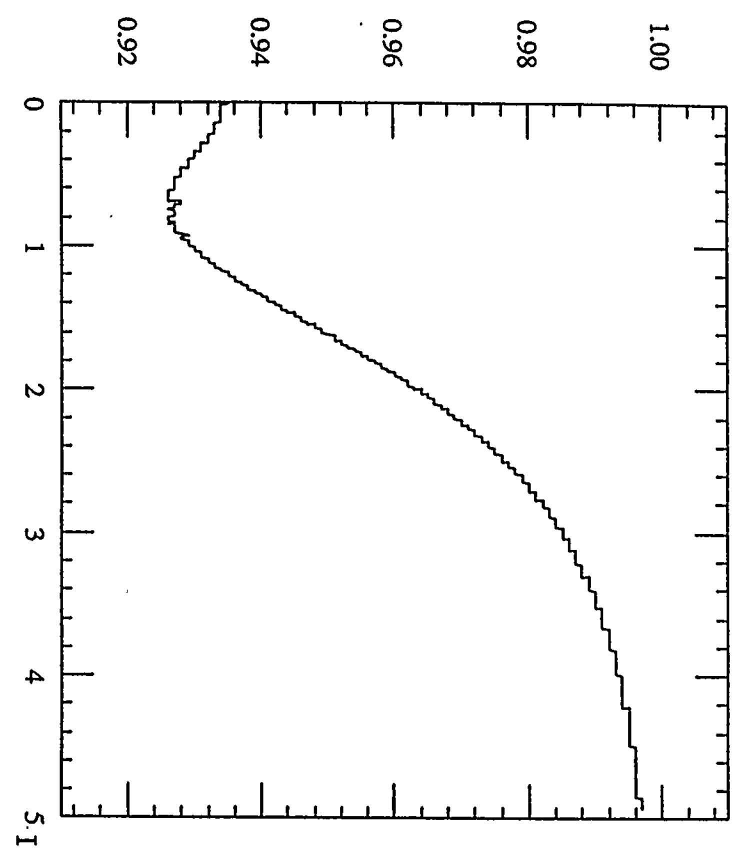

Dependence of ω(A) for inductive-like wake, Λ=2.95

COLLECTIVE EFFECTS IN LHC

F. Ruggiero, CERN

COLLECTIVE EFFECTS IN THE LHC

F. RUGGIERO, CERN

- OVERVIEW
- BEAM SCREEN
- SURFACE RESISTANCE MEASUREMENTS
- IMPEDANCE BUDGET
- MULTI-BUNCH INSTABILITIES
- LANDAU DAMPING

Documentation on the WEB:

http://www slap. cern. ch/collective

Incoherent

<u>Losses</u>: synchrotron radiation

<u>Tune shifts</u>: space charge + Laslett

<u>Instabilities</u>: intra-beam scattering

Coherent

SINGLE-BUNCH low-Q structures	MULTI-BUNCH high-Q structures
<u>Losses</u>: Resistive wall + Pumping holes; Broad-band impedance; Synchrotron radiation	
<u>Tune shifts</u>: Broad-band impedance; Low-frequency impedance →	Loss of Landau damping
↓	↓
<u>Instabilities</u>: mode coupling, microwave	<u>Instabilities</u>: Transv. Resistive wall (at low frequency), HOM's of RF cavities

Main sources of BROAD-BAND IMPEDANCE:

- BELLOWS
- SPACE CHARGE
- MONITOR TANKS
- PUMPING SLOTS

Main sources of LOW-FREQUENCY IMPEDANCE:

- STRIP-LINE MONITORS
- KICKERS

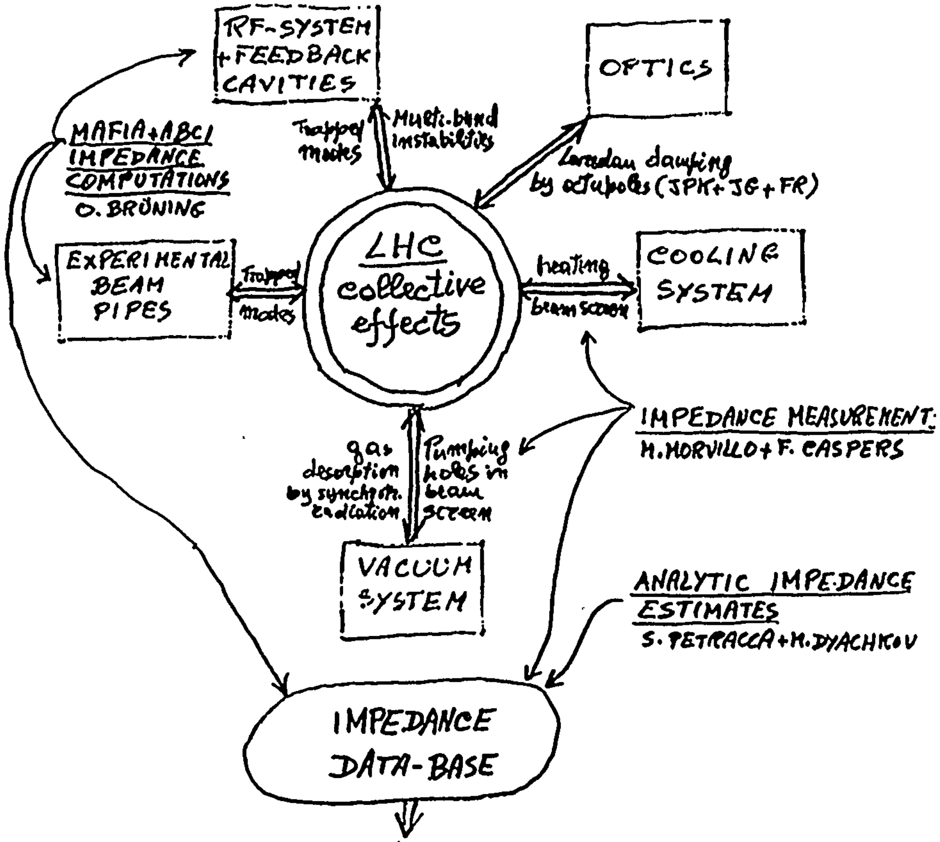

Parasitic losses, Tune shifts,
Single-bunch instability thresholds
⇕ S. BERG
Multi-bunch instability growth rates

Space-charge transient effects: L. CAPPETTA

New diagnostic techniques: BEAM ECHOES {O. BRÜNING, W. SCANDALE, F.I / T. LINNECAR, E. SHAPOSHNIK

New theories... : {MICROWAVE INSTABILITY (M. DYACHKOV) / COUPLING VS. HEAD-TAIL INSTABILITY (O. BRÜNING)

LHC BEAM SCREEN

* TEMPERATURE ≈ 20°K
* INNER COPPER LAYER (RRR≈100) : 50μm
* 500 PUMPING SLOTS PER m : RECTANGULAR (1.5 × 8 mm, WITH ROUNDED CORNERS
* RADIUS OF INSCRIBED CIRCLE : b = 17.4 mm

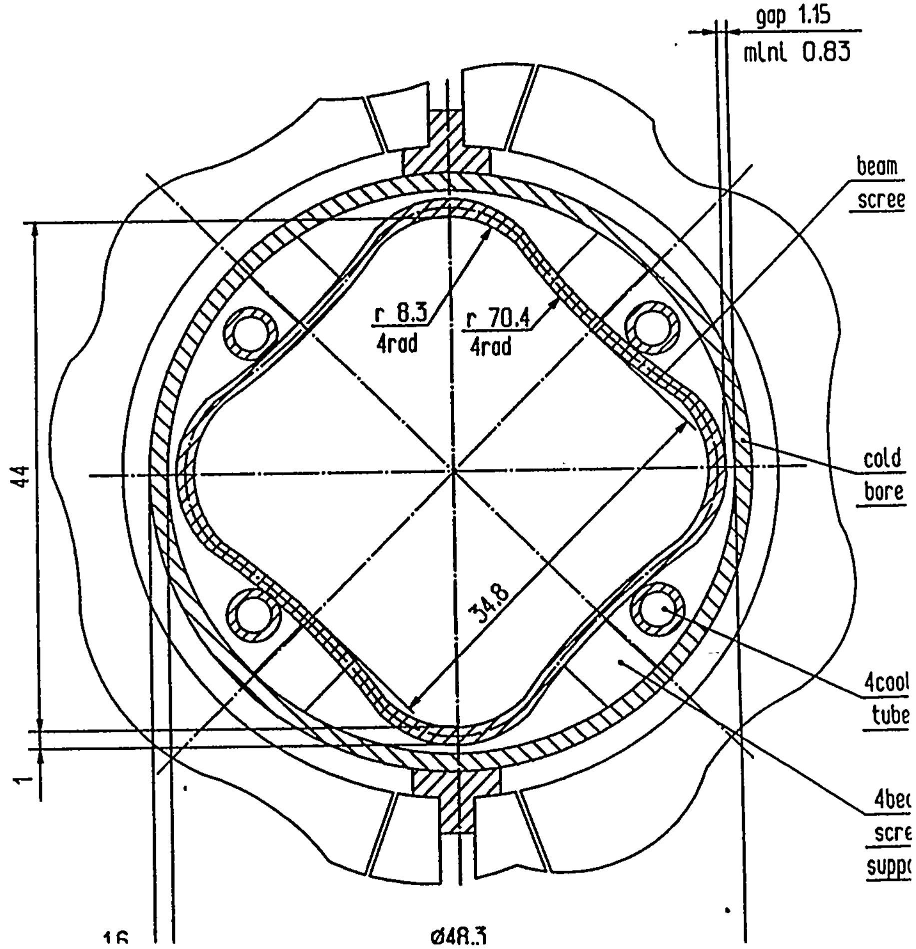

LHC BEAM SCREEN

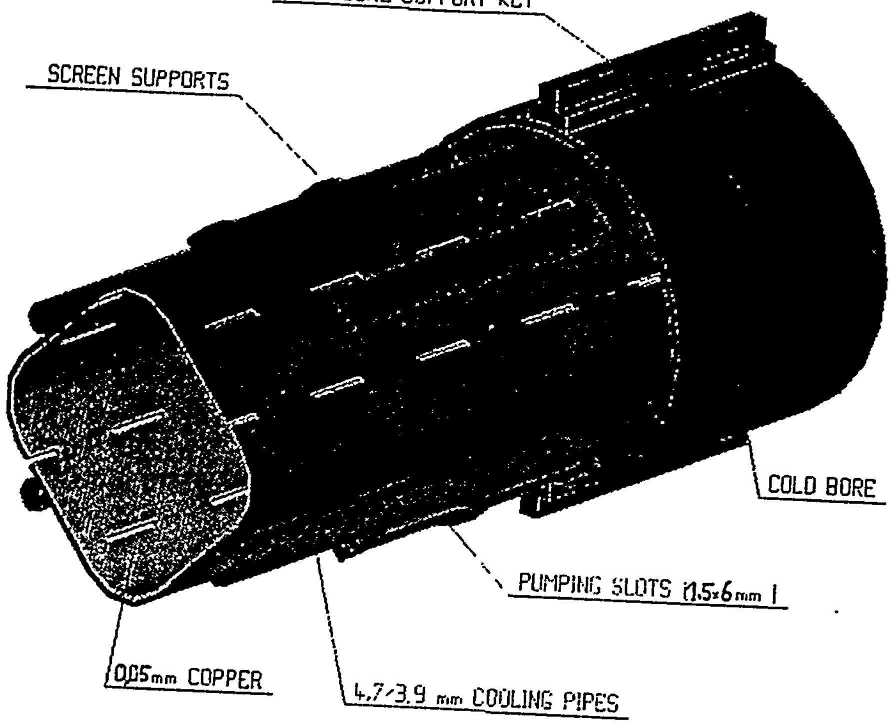

LHC BEAM SCREEN

* Temperature ≈ 20°K
* Inner Copper Layer (RRR=100) : 50μm
* 500 Pumping slots per m : rectangular (1.5×8 mm), with rounded corners
* Radius of inscribed circle : b = 17.4 mm

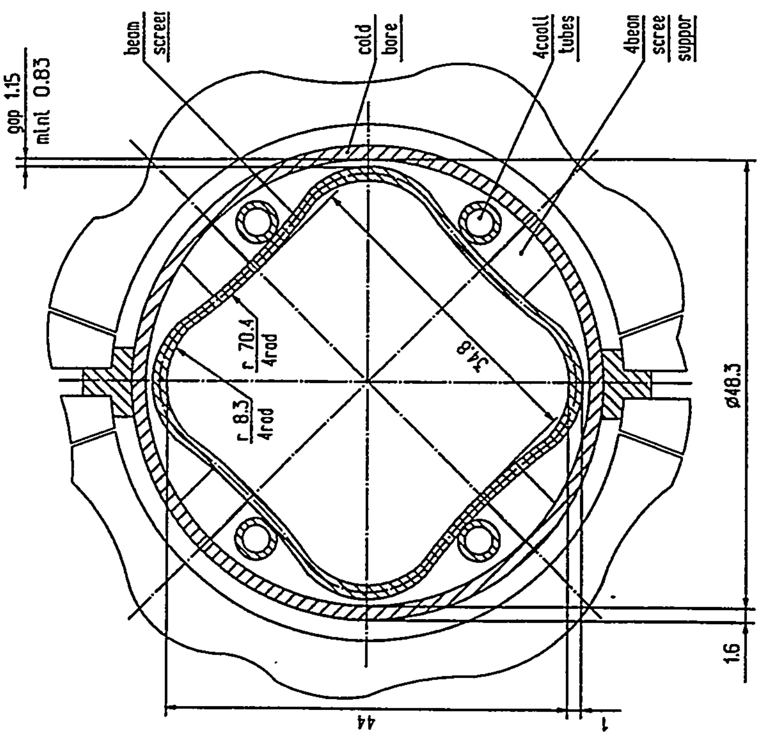

SLOT IMPEDANCE vs SLOT LENGTH ℓ

CIRCULAR HOLE (REFERENCE)

S. KURENNOY

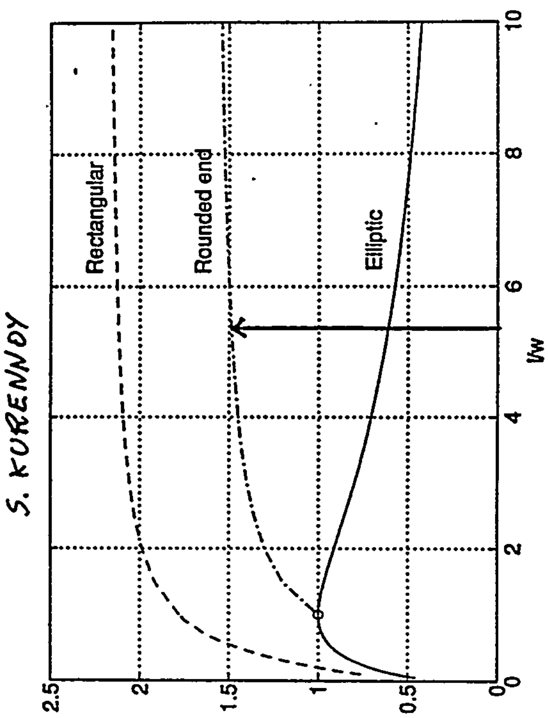

Figure 1: Slot impedance versus slot length l for fixed width w in units of the impedance of the circular hole with diameter w.

$$\left.\begin{array}{l}\ell = 8\,mm \\ w = 1.5\,mm\end{array}\right\} \Rightarrow \frac{\ell}{w} = 5.\overline{3}$$

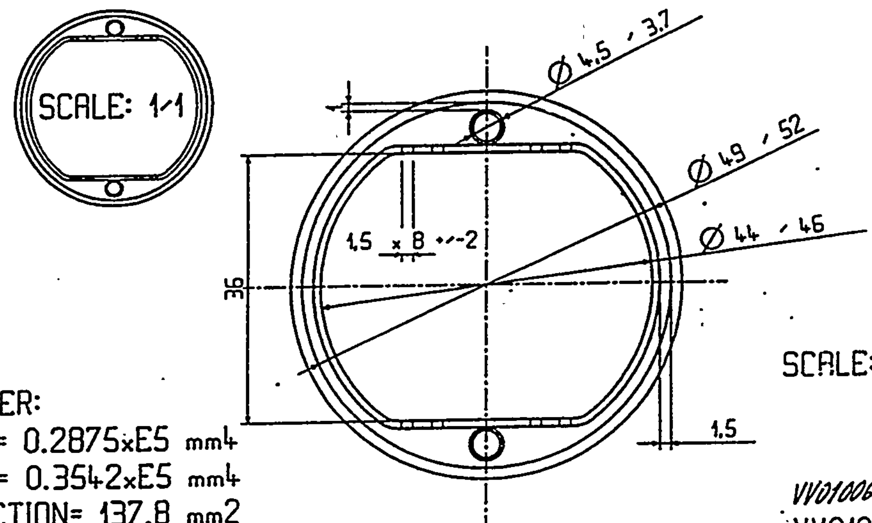

LINER:
Ixx= 0.2875xE5 mm4
Izz= 0.3542xE5 mm4
SECTION= 137.8 mm2
WEIGHT= 1.08 kg/m
INNER PERIMETER= 134.7 mm.
% PUMPING HOLES~ 2.1

VV010064PL.EPS;1
VV010064PL

09_08_95
C.Reymermier

Low frequency impedance of pumping slots

500 rectangular slots per meter
dimensions : 1.5 × 8 mm (with rounded ends)
distance from screen corners: $\frac{1}{4}$ of screen side

$\alpha_{rel} \simeq 1.5$ relative polarizability (compared to round hole

$f_{th} \simeq 0.6$ effect of screen thickness ($t = 1\,mm$)

$f_{geom} \simeq 0.63$ geometric reduction of induced currents (0.79^2) compared to round screen

The total reduction of impedance, compared to that of the same number of round holes in a thin round screen is thus

$$F = \alpha_{rel} \cdot f_{th} \cdot f_{geom} \simeq 0.56$$

$r_h = \frac{1.5}{2}\,mm$ equivalent hole radius

$b = 17.4\,mm$ equivalent screen radius

$N_h = \frac{500}{m} \times 2\pi R = 13.3 \times 10^6$ total number of slots

---

$$\frac{Z_L}{n} = N_h \frac{Z_0}{R} \frac{\frac{8}{3} r_h^3}{4\pi^2 b^2} \times F = 15.6\ m\Omega$$

$$Z_T = \frac{2R}{b^2} \frac{Z_L}{n} = 0.44\ \frac{M\Omega}{m} \rightarrow \beta_{av} \cdot Z_T = 37.1\ M\Omega$$

Power loss through round holes in the LHC liner

$t = 0.001$ wall thickness [m]

$r_h = 0.0005, 0.0006 .. 0.0015$ hole radius [m]

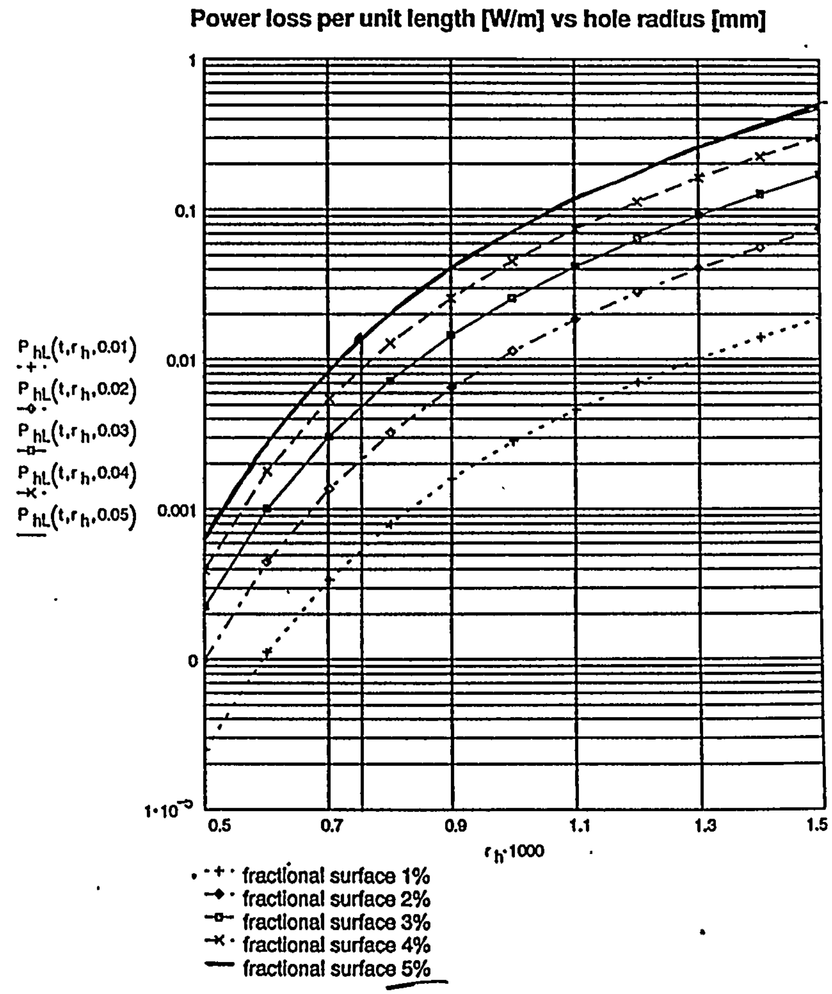

$$\frac{\Delta \Gamma_{anomalous}}{P_{classic}} \simeq 11\% \longrightarrow 70\%$$ scaling from Los Alamos measurements

Summary of parasitic losses for LHC at top energy: nominal parameters.

Power loss [kW]	FOR A SINGLE BEAM	Power loss per unit length [mW/m]
3.60	Incoherent synchrotron radiation	206
~~$\ll$ 0.55~~	~~Coherent synchrotron radiation~~	~~$\ll$ 32~~
1.99	Resistive wall (20° K)	75 ⟸
0.28	Welds	10
0.27	Pumping slots	10
$<$ 0.82	Shielded bellows	$<$ 31
$\ll$ 1.05	Leaks in bellows gaps	$\ll$ 39
8.56	TOTAL	403

$P_{classic}$ → 1.99

Machine parameters.

$B = 8.386$	T	dipole magnetic field
$E = 7$	TeV	beam energy
$\rho_{Cu} = 5.39 \times 10^{-10}$	Ωm	copper resistivity at 20 K
$I = 536$	mA	beam current
$N_b = 1.049 \times 10^{11}$		number of particles per bunch
$R = 4242.893$	m	average machine radius
$\rho = 2784.32$	m	bending radius
$\sigma_s = 7.5$	cm	r.m.s. bunch length
$k_b = 2835$		number of bunches

30/3/1995

MEASURING THE SURFACE RESISTANCE OF THE LHC BEAM SCREEN

F. CASPERS, M. MORVILLO, F. RUGGIERO + ...

What is the surface resistance?
Why measuring it?
How shall we measure it?

The surface impedance Z_s is the ratio between the longitudinal components E_z of the electric field at the wall surface and the wall current I_z, flowing in the direction opposite to the beam current I_0

$$E_z = Z_s \, I_z \; : \; \text{Ohm's law}$$

The beam-induced wall current I_z is confined to a layer of thickness $\delta = \sqrt{\frac{2\rho}{\omega \mu_0}}$ equal to the skin depth in the metal. For a pipe thickness much larger than δ:

$I_z \simeq H_t$: tangential component of the magnetic field at wall surface

$$Z_s = \left[\frac{E_z}{H_t}\right]_{surface} = \underbrace{R_s}_{\text{surface resistance}} + i \underbrace{X_s}_{\text{surface reactance}}$$

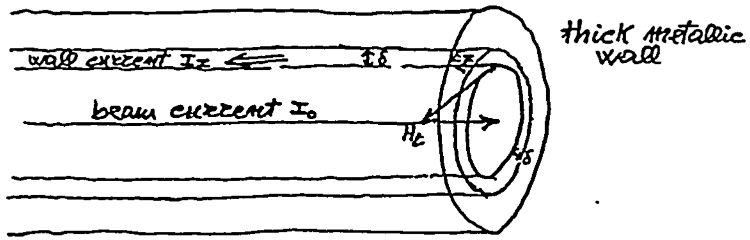

$$\begin{cases} \delta = \sqrt{\dfrac{2\rho}{\omega\mu_0}} & : \text{skin depth (penetration of e.m. fields)} \\ \lambda : & \underline{\text{mean free path}} \text{ of the electrons due to collisions with metallic lattice} \end{cases}$$

$\lambda < \delta$: CLASSICAL REGIME

all conduction electrons within the skin depth are effective in carrying (wall) current

$$R_s = \frac{\rho}{\delta} = \sqrt{\frac{\omega\mu_0\rho}{2}}$$

$\lambda > \delta$: ANOMALOUS REGIME

only a (small) fraction of the conduction electrons within the skin depth are effective in carrying current: those moving almost parallel to the metallic surface and thus spending most of their mean free path within δ

$$\lim_{\lambda \gg \delta} R_s = R_\infty$$ independent of T and purity

London 1940, Chambers and Pippard 19..

$R_\infty(\rho, \lambda, \omega)$: dimensions Ω, independent of T

$\rho\lambda$: characteristic of the metal

$[\rho\lambda] = \Omega\, m^2$, $[\omega\mu_0] = \frac{\Omega}{m}$ $\rightarrow$ $[\rho\lambda(\omega\mu_0)^2] = \Omega^3$

$R_\infty \sim [\rho\lambda(\omega\mu_0)^2]^{1/3}$ from dimensional analysis

$$\begin{cases} R_\infty = \left[\dfrac{\sqrt{3}}{16\pi}\, \rho\lambda(\omega\mu_0)^2\right]^{1/3} & \text{from detailed analysis of ANOMALOUS regime} \\ R_s \simeq R_\infty\left(1 + 1.157\, \alpha^{-0.276}\right) & \text{for } \alpha = \frac{3}{2}\left(\frac{\lambda}{\delta}\right)^2 = \frac{3}{4}\omega\mu_0(\rho\lambda)\rho^{-3} \geq 3 \end{cases}$$

$\underline{j} = \sigma \underline{E}$, $\sigma = \frac{1}{\rho}$: metal conductivity

$\frac{d\underline{v}}{dt} = \frac{e}{m}\underline{E} - \frac{1}{\tau}\underline{v}$: $\begin{cases} \underline{v} : \text{electron drift velocity} \\ \tau : \text{relaxation (collision) time} \end{cases}$

$\underline{j} = n e \underline{v}$ $\rightarrow$ $\frac{d\underline{j}}{dt} = \frac{ne^2}{m}\underline{E} - \frac{1}{\tau}\underline{j}$ $\rightarrow$ $\underline{j}_{eq} = \underbrace{\frac{ne^2}{m}\tau}_{\sigma}\, \underline{E}$

$\lambda = v_0\tau$: mean free path

$$\begin{cases} v_0 = \dfrac{p_0}{m} & : \text{velocity at the surface of Fermi sphere} \\ \dfrac{4}{3}\pi p_0^3 = \dfrac{1}{2} n h^3 & : \text{from Pauli principle} \end{cases}$$

n ↑ density of conduction electrons

$v_0 = \frac{h}{2m}\left(\frac{3n}{\pi}\right)^{1/3}$ $\Rightarrow$ $\boxed{\rho\lambda = \frac{\lambda}{\sigma} = \frac{m v_0}{ne^2} = \frac{h}{2e^2}\left(\frac{3}{\pi n^2}\right)^{1/3}}$

independent of τ!

For copper:

$n = \frac{\text{density}}{\text{atomic weight}} N_{Avogadro} = \frac{8.93\ g/cm^3}{63.55\ g/mole} \times 6.022 \times 10^{23} \simeq 8.5 \times 10^{28}\ m^{-3}$

$\rho\lambda \simeq 6.6 \times 10^{-16}\ \Omega\, m^2 \Rightarrow \boxed{R_\infty \simeq 1.1\ m\Omega\ \left(\omega/_{2\pi\, GHz}\right)^{2/3}}$

SURFACE RESISTANCE R_s

LOS ALAMOS MEASUREMENTS ON SSC BEAM TUBES
copper coated SS, similar to LHC (surface roughness?)

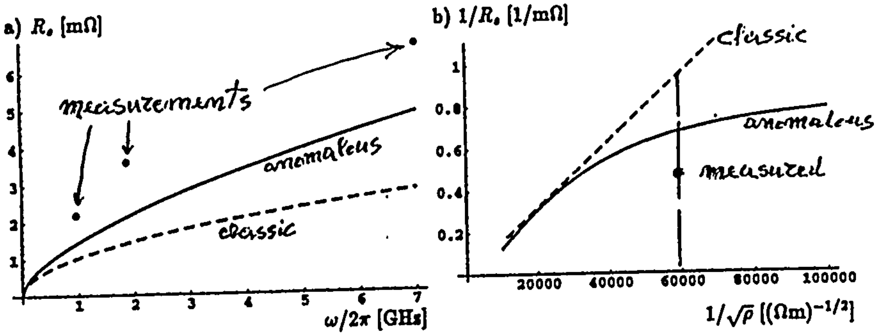

Figure 1: (a) Surface resistance in mΩ: measured (dots) anomalous (solid line) and classical (dashed line) for copper at 4° K (RRR = 61) versus the frequency $f = \omega/2\pi$ in GHz. (b) Inverse of the surface resistance in mΩ: anomalous (solid line) and classical (dashed line) for copper at <u>1 GHz</u> versus the inverse of the square root of the resistivity ρ in Ωm.

Chambers (1952) measurements on ELECTROPOLISHED copper at 1.2 GHz.

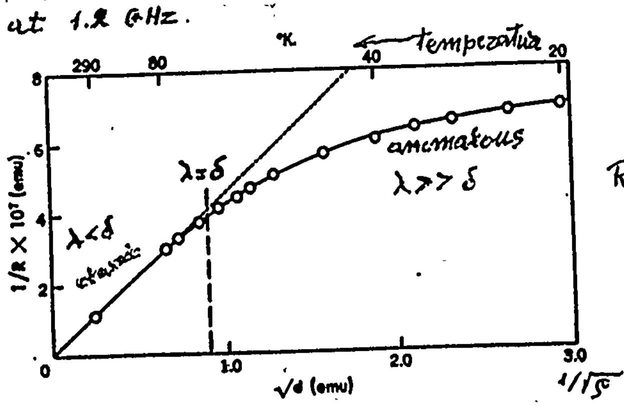

RRR ~ 100

FIG. 5. Surface resistance of copper at 25 cm (Chambers[14]). The dotted line shows the prediction of the classical theory; the broken line marks the point at which $l = \delta_{cl}$. Above the diagram are shown the temperatures at which various values of σ were realized.

Z_L : longitudinal resistive wall impedance

$$Z_L |I_0|^2 = \int_{\substack{\text{wall}\\ \text{surface}}} \underbrace{\underline{E} \times \underline{H}^*}_{\substack{\text{complex}\\ \text{Poynting vector}}} ds = L \oint E_z I_z^* dl = L \oint Z_s |I_z|^2 dl$$

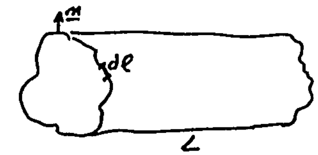

beam pipe of arbitrary cross section

$$\frac{Z_L}{L} = \frac{Z_s}{|I_0|^2} \oint |H_t|^2 dl = Z_s \frac{\delta}{\delta n}\left(\frac{\varepsilon_0}{c}\right) \quad \text{(CERN-SL-95-95)}$$

satisfies 2D electrostatic problem

"normal" derivative

specific electric capacitance

For a circular pipe of radius b

$$\frac{\varepsilon_0}{c} = \frac{1}{2\pi} \ln\left(\frac{b}{r_{beam}}\right) \longrightarrow \boxed{\frac{Z_L}{L} = \frac{Z_s}{2\pi b}}$$

For a beam with average current I_0, k_b bunches with spectrum $\tilde{\lambda}(\omega)$, the resistive wall loss is

$$\frac{P_w}{L} = \frac{I_0^2}{k_b f_0} \frac{e^2}{\pi} \int_0^\infty |\tilde{\lambda}(\omega)|^2 \, \mathrm{Re}\left(\frac{Z_L(\omega)}{L}\right) d\omega$$

We need the surface resistance over all the bunch spectrum, i.e. up to a few GHz for LHC bunches.
The measurements should be performed also in presence of a strong B-field and, if possible, at several temperatures (5-50 °K)

Table2: Surface resistance measurements and extrapolated conductivities

	Frequency MHz	T deg	DT deg	Rs IN mOhm	Rs OUT mOhm	Kclas IN 1E7/Ohm*m	Kclas OUT 1E7/Ohm*m	Kanom IN 1E7/Ohm*m	Kanom OUT 1E7/Ohm*m	RRReff IN	RRReff OUT
1	155.8465	300	0	3.36	3.66	5.46	4.58	10.90	9.70		
2	790.7330	300	0	7.76	8.59	5.19	4.23	8.85	7.70		
3	307.3650	300	0	4.93	6.27	5.00	3.09	9.54	6.93		
4	626.8761	300	0	7.30	9.15	4.64	2.96	8.40	6.21		
5	629.2984	42.3	18.9	2.37	2.70	44.22	33.97	47.52	37.52	10	11
6	792.0576	42.2	19.1	2.79	2.81	40.25	39.59	43.31	42.66	8	9
7	792.0576	40.3	19.7	1.59	2.94	124.16	36.28	157.91	39.41	30	4
8	629.5103	40.3	19.7	1.63	2.17	93.51	52.68	104.44	56.11	20	18
9	629.6039	4.5	1.0	1.19	2.00	174.99	62.45	269.96	66.52	58	21
10	792.2774	4.9	2.3	1.43	2.23	153.54	63.13	225.56	67.52	43	15
11	947.2647	4.4	0.7	1.33	2.90	211.31	44.45	527.43	47.40		
12	2868.2545	4.2	0.1	1.96	5.88	294.04	32.70	????	34.81		
13	629.5992	11.2	0.3	1.21	2.00	168.49	62.01	251.02	66.04	54	21
14	792.2779	11.1	0.5	1.41	2.26	156.91	61.07	234.90	65.19	45	14
15	947.2674	10.7	1.4	1.39	2.83	193.75	46.65	407.30	49.67		
16	629.5890	23.1	6.4	1.25	2.05	159.62	59.06	227.37	62.85	49	20
17	792.2795	23.2	4.3	1.48	2.29	143.61	59.67	200.10	63.63	39	14
18	947.2718	22.6	4.2	1.46	2.82	174.58	47.13	313.30	50.07		
19	310.1818	40.8	39.0	0.76	1.94	210.79	32.49	310.79	37.48	62	11
20	472.8598	41.5	40.7	1.12	2.30	149.69	35.14	191.93	39.13		
21	629.5129	41.9	43.9	1.50	2.31	110.29	46.43	128.97	49.73	28	16
22	792.2321	41.8	45.3	1.68	2.63	111.05	45.18	134.02	48.26	26	11
23	947.2420	42.2	45.7	1.58	3.33	150.32	33.82	228.46	36.77		
						Conductivity extrapolated according to classical or anomalous regime: shaded regions are not relevant				Conductivity ratios at the same frequency	

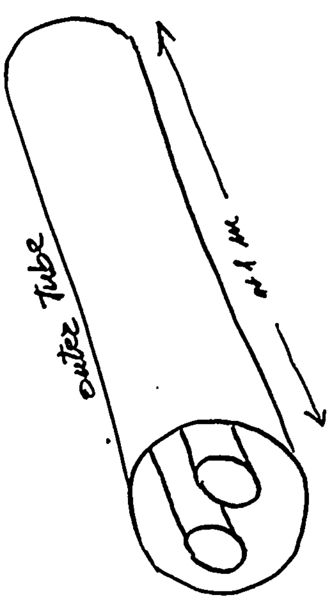

1) Assume the two inner conductors have the <u>same</u> surface resistance

2) Excite even and odd modes

3) Measure (<u>unloaded</u>) Q-factors

4) Solve two equations in two unknowns R_s^{IN} and R_s^{OUT}

ADVANTAGES

No superconductors $\Longrightarrow \begin{cases} \text{different } T \\ B \neq 0 \end{cases}$

Several frequencies, in steps of ~ 150 MHz

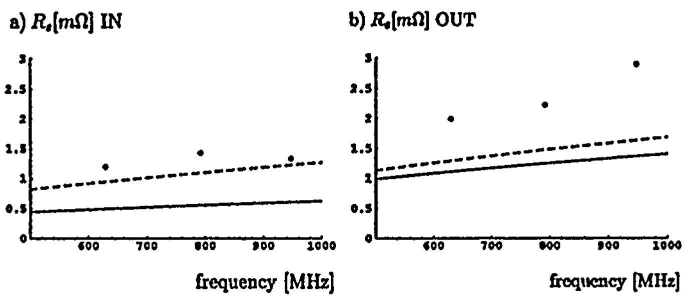

Surface resistance measured at 4.5° K for the inner conductors (a) and for the outer tube (b), compared to the predictions in the classic (solid) and anomalous regime (dashed). We have assumed an electrical conductivity of 10^{10} $(\Omega\mathrm{m})^{-1}$ (i.e., RRR $\simeq 200$) for the inner conductors and of 2×10^{9} $(\Omega\mathrm{m})^{-1}$ (i.e., RRR $\simeq 50$) for the outer tube. Note that the measurements at 947 MHz are not very reliable.

Summary of parasitic losses for LHC at top energy: ultimate parameters for cryogenics.

Power loss [kW]	FOR A SINGLE BEAM	Power loss per unit length [mW/m]
5.70	Incoherent synchrotron radiation	326
~~$\ll 1.30$~~	~~Coherent synchrotron radiation~~	~~$\ll 80$~~
$P_{classic} \rightarrow$ 5.01	Resistive wall (20° K)	188 $\Leftarrow$
0.70	Welds	26
0.68	Pumping slots	25
< 2.05	Shielded bellows	< 77
$\ll 2.64$	Leaks in bellows gaps	$\ll 99$
18.17	TOTAL	821

Machine parameters.

$B = 8.386$	T	dipole magnetic field
$E = 7$	TeV	beam energy
$\rho_{Cu} = 5.39 \times 10^{-10}$	Ωm	copper resistivity at 20 K
$I = 850$	mA	beam current
$N_b = 1.664 \times 10^{11}$		number of particles per bunch
$R = 4242.893$	m	average machine radius
$\rho = 2784.32$	m	bending radius
$\sigma_s = 7.5$	cm	r.m.s. bunch length
$k_b = 2835$		number of bunches

INCOHERENT SPACE-CHARGE TUNE SHIFT

For round beam, the tune shift of particles with small betatron amplitudes due to direct space charge is:

$$\Delta Q = -\frac{N_b \cdot r_p}{4\pi\gamma^2 B\,\varepsilon_n} = \begin{cases} -1.2\times10^{-3} & \text{at } 450\text{ GeV} \\ -1.1\times10^{-5} & \text{at } 7\text{ TeV} \end{cases}$$

$N_b = 1\times10^{11}$ particles per bunch

$r_p = 1.5347\times10^{-18}$ m classical proton radius

$\gamma = \begin{cases} 479.6 & \text{at } 450\text{ GeV} \\ 7460.5 & \text{at } 7\text{ TeV} \end{cases}$ Lorentz factor

$B = \frac{\sqrt{2\pi}\,\sigma_s}{2\pi R} = \begin{cases} 1.22\times10^{-5} & \text{at } 450\text{ GeV } (\sigma_s = 13\text{ cm}) \\ 7.05\times10^{-6} & \text{at } 7\text{ TeV } (\sigma_s = 7.5\text{ cm}) \end{cases}$ Bunching factor

$\varepsilon_n = \gamma\frac{a^2}{\beta} = 3.75\times10^{-6}$ m.rad : normalized emittance

The corresponding incoherent tune spread gives rise to Landau damping of transverse oscillations (with the exception of rigid dipole oscillations).

SPACE CHARGE IMPEDANCE

$$\begin{cases} Z_L(\omega) = -j\frac{\omega R}{2c}\frac{Z_0}{\gamma^2}\left[1+2\ln\left(\frac{b}{a}\right)\right] \\ Z_T(\omega) = -j\frac{Z_0 R}{\gamma^2}\left(\frac{1}{2a^2}-\frac{1}{b^2}\right) \end{cases}$$

Z_0	$= 376.73\ \Omega$	impedance of free space
R	$= 4242.89$ m	machine radius
β_{av}	$= 85$ m	average beta-function
a	$= \sqrt{\varepsilon\cdot\beta_{av}}$	average r.m.s beam radius
b	$= 17.4$ mm	beam pipe 'radius'

At injection, when $\gamma = 479.6$ and $a = 0.815$ mm:

$\frac{Z_L}{n} = -j\,5.8\times10^{-3}\,\Omega$, $\beta_{av} Z_T = -j\,442.4$ MΩ

Longitudinal tune shifts ($N_b = 10^{11}$) Transverse tune shifts

	$\Delta Q_T^{(0)} = 7.49\times10^{-4}$
$\Delta Q_L^{(1)} = -4.64\times10^{-7}$	$\Delta Q_T^{(1)} = 3.75\times10^{-4}$
$\Delta Q_L^{(2)} = -6.18\times10^{-7}$	$\Delta Q_T^{(2)} = 2.5\times10^{-4}$
$\Delta Q_L^{(3)} = -6.96\times10^{-7}$	$\Delta Q_T^{(3)} = 1.87\times10^{-4}$

At 7 TeV, when $\gamma = 7460.5$ and $a = 0.207$ mm

$\frac{Z_L}{n} = -j\,3.3\times10^{-5}\,\Omega$, $\beta_{av} Z_T = -j\,28.6$ MΩ

Table 1: LHC effective impedance (in Ω) at 450 GeV.

INJECTION	$\mathrm{Im}\,(Z_L/n)_{\mathrm{eff}}$	$\beta_{\mathrm{av}}\mathrm{Im}\,(Z_T)_{\mathrm{eff}} \times 10^{-6}$
Space charge	-0.0058	-442.3
Shielded bellows	0.0814	146.3
Monitor tanks	0.0400	214.6
Pumping slots	0.0156	38.9
Total broad band	0.1312	-42.5
Strip-line monitors	0.127	446.6
Abort kickers	0.007	182.4
SC cavities	0.010	0.4
Total low frequency	0.144	629.4

Table 2: LHC effective impedance (in Ω) at 7 TeV.

TOP ENERGY	$\mathrm{Im}\,(Z_L/n)_{\mathrm{eff}}$	$\beta_{\mathrm{av}}\mathrm{Im}\,(Z_T)_{\mathrm{eff}} \times 10^{-6}$
Space charge	-3.3×10^{-5}	-28.6
Shielded bellows	0.0815	148.8
Monitor tanks	0.0400	214.6
Pumping slots	0.0156	38.9
Total broad band	0.1371	373.7
Strip-line monitors	0.073	257.9
Abort kickers	0.004	109.1
SC cavities	0.010	0.4
Total low frequency	0.087	367.4

LHC Broadband Impedance : $Re\,(\langle\beta_\perp\rangle Z_\perp)$ at injection

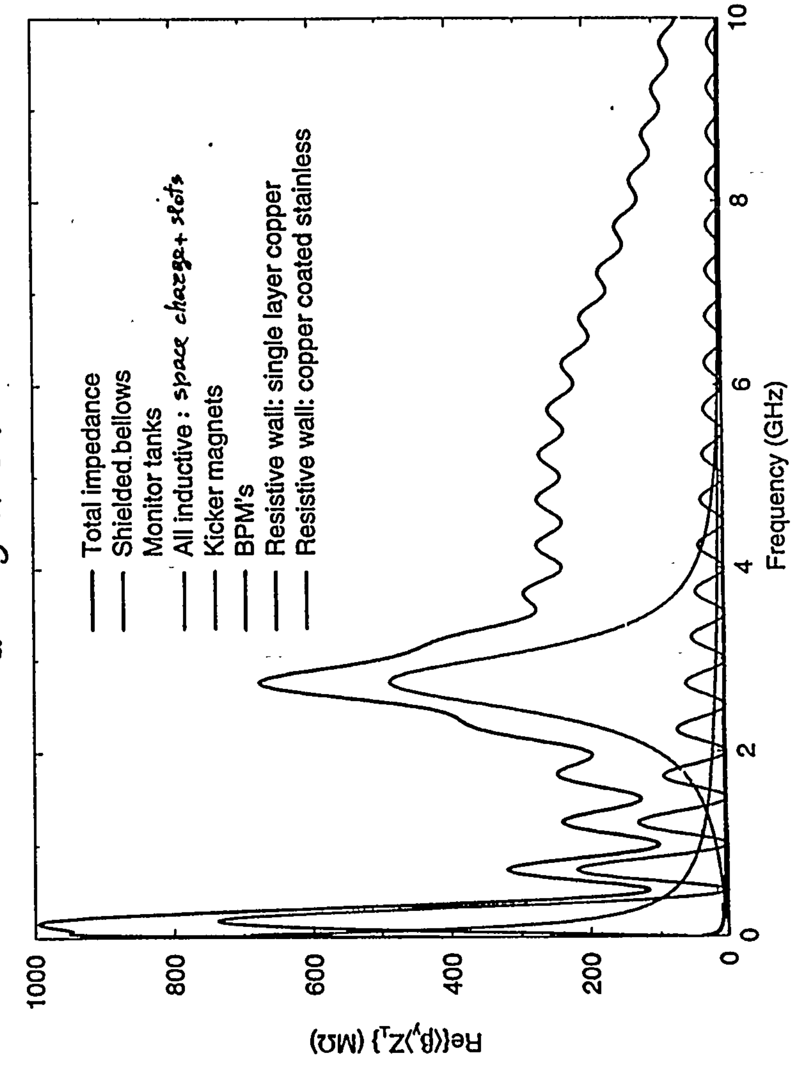

LONGITUDINAL SINGLE-BUNCH EFFECTS

$L = \begin{cases} 0.52\ m & \text{at injection} \\ 0.30\ m & \text{at } 7\ TeV \end{cases}$ full bunch length $= 4\sigma_s$

$V_{RF} = \begin{cases} 8\ MV & \text{at injection} \\ 16\ MV & \text{at } 7\ TeV \end{cases} \rightarrow Q_s = \begin{cases} 5.4 \times 10^{-3} \\ 1.95 \times 10^{-3} \end{cases}$

$h_{RF} = 35640$ harmonic number

$I_b = N_b e f_0 \ , \quad f_0 = 11'245.5\ Hz \ \rightarrow \ \frac{I_b}{mA} \simeq 0.18 \frac{N_b}{10^{11}}$

MICROWAVE INSTABILITY

$$\left\{ \begin{array}{ll} \left|\frac{Z_L}{n}\right| \lesssim \left(\frac{2\pi |\eta| \beta^2 E_0}{e I_p} \right) \sigma_\delta^2 & \text{Boussard criterion (local coasting beam)} \\ I_p = \frac{e N_b}{\sqrt{2\pi}\, \sigma_\tau} & : \text{peak current} \end{array} \right.$$

$$\underbrace{n \omega_0 \sqrt{\frac{e I_p \, |Z_L/n| \cdot |\eta|}{2\pi \beta^2 E_0}}}_{\text{growth rate of microwave instability}} \lesssim \underbrace{n \omega_0 |\eta| \sigma_\delta}_{\text{rate of Landau damping due to energy spread}}$$

$$\underbrace{\sqrt{\frac{2 e I_p \, |Z_L/n|}{\pi \beta^2 |\eta| E_0}}}_{\text{bucket height driven by a voltage } I_p|Z_L| \text{ at harmonic } n} \lesssim 2\sigma_\delta \approx \frac{\delta_{max}}{2} \ : \ \text{condition for self-bunching}$$

Nc c

$$I_b^{th} \simeq \frac{3}{2} \frac{h_{RF} V_{RF}}{\left|\frac{Z_L}{n}\right|} \left(\frac{L}{2\pi R}\right)^3 \longrightarrow N_b^{th} \simeq \begin{cases} 6.4 \times 10^{12} : \text{injectio} \\ 3.0 \times 10^{12} : 7\ TeV \end{cases}$$

$$\left|\frac{Z_L}{n}\right| \simeq \left|\left(\frac{Z_L}{n}\right)_{eff}\right| = \begin{cases} 0.275\ \Omega : \text{injecti} \\ 0.224\ \Omega : 7\ TeV \end{cases}$$

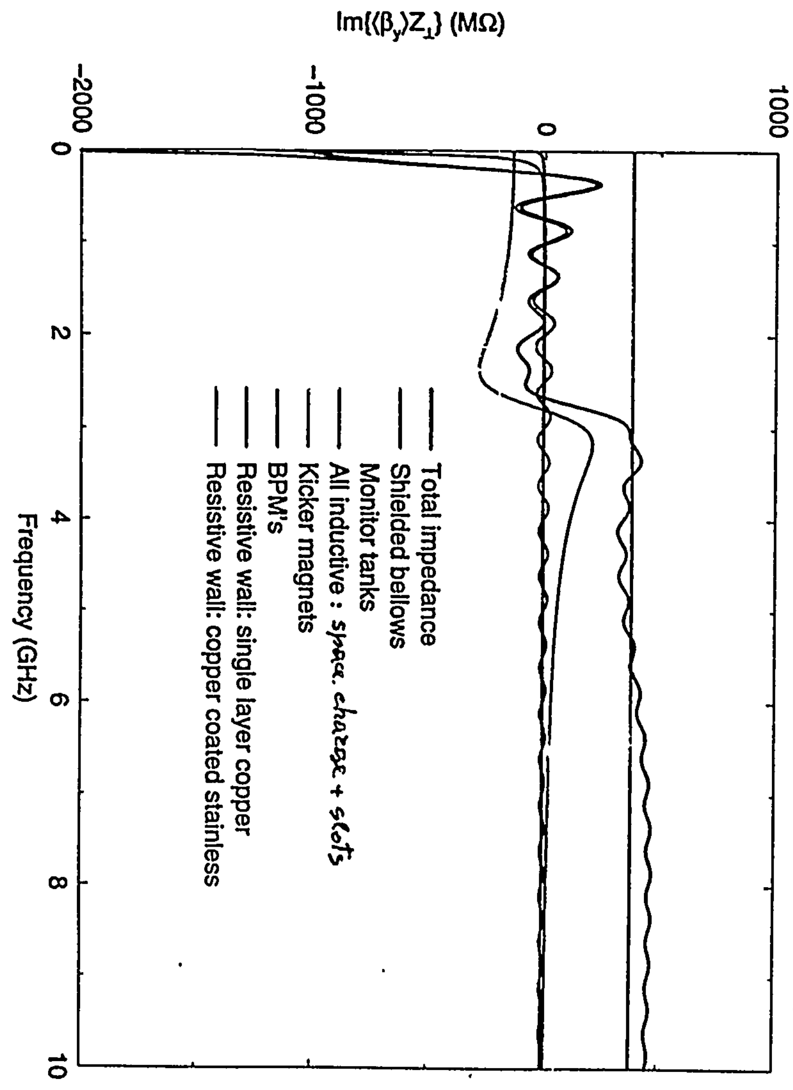

LHC Broadband Impedance : $\mathcal{I}m(\langle\beta_\perp\rangle Z_\perp)$ at injection

TUNE SHIFTS AND LANDAU DAMPING OF HIGHER MODES

$$\begin{cases} \Delta Q_L^{(m)} \simeq \dfrac{m}{m+1} \dfrac{Q_s I_b}{3 h_{RF} V_{RF}} \left(\dfrac{2\pi R}{L}\right)^3 \cdot \mathcal{Im}\left(\dfrac{Z_L}{m}\right)^{bb}_{eff} \lesssim \dfrac{m}{m+1} \dfrac{\Delta Q_s}{2} \\ \Delta Q_s = \dfrac{\pi^2}{32} \left(\dfrac{h_{RF} L}{2\pi R}\right)^2 \cdot Q_s \quad \text{synchrotron tune spread} \quad = \begin{cases} 9\times10^{-4} : \text{injection} \\ 10^{-4} : 7\ \text{TeV} \end{cases} \end{cases}$$

$$I_b^{th} \simeq \frac{3\pi^2}{64} \frac{h_{RF}^3 V_{RF}}{\mathcal{Im}\left(\frac{Z_L}{m}\right)^{bb}_{eff}} \cdot \left(\frac{L}{2\pi R}\right)^5 \rightarrow N_b^{th} \simeq \begin{cases} 2.0\times10^{12} : \text{injection} \\ 2.4\times10^{11} : 7\ \text{TeV} \end{cases}$$

The longitudinal tune shifts induced by the broad-band impedance are of the same order

$$\Delta Q_L^{(m)} \simeq \frac{m}{m+1} \cdot 2\times10^{-5} : \text{both at injection and at 7 TeV}$$

The transverse tune shifts have opposite sign, but are again of the same order

$$\Delta Q_T^{(m)} \simeq \begin{cases} \dfrac{7\times10^{-5}}{m+1} & \text{at injection} \\ -\dfrac{7\times10^{-5}}{m+1} & \text{at 7 TeV} \end{cases}$$

This is a consequence of the transverse space-charge impedance, dominating at injection.

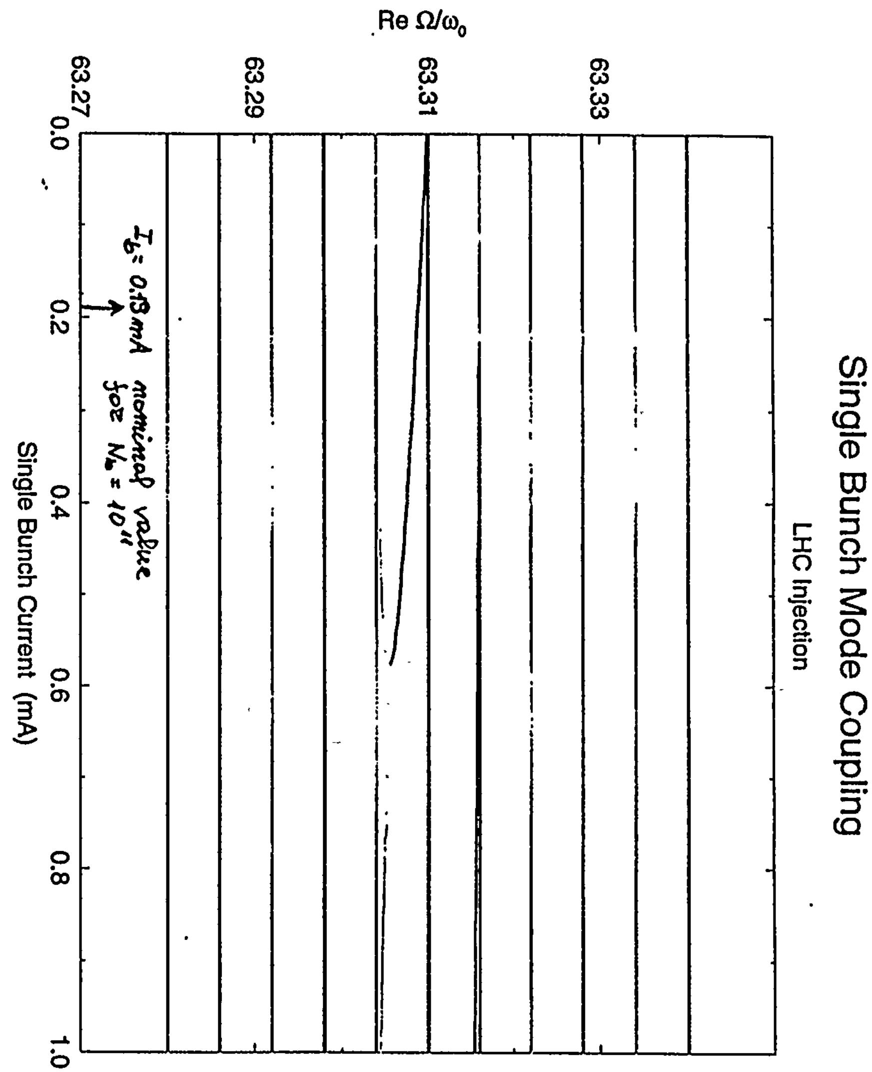

MULTI-BUNCH OSCILLATION MODES

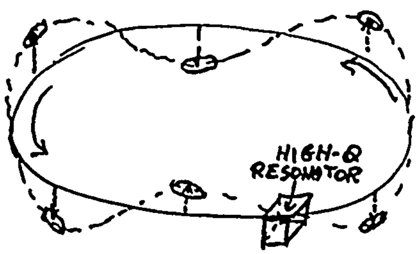

$N_b = 3564$ bunches of which 2835 filled

$N_b \cdot f_0 \simeq 40$ MHz bunch frequency

$\omega_p = \omega_0 \left(p N_b + K + m Q_s \right)$: longitudinal modes $m = 1, \ldots$ LINE SPECTRUM AT FIXED AZIMUTH (IMPEDANC

azimuthal mode number

$\omega_p = \omega_0 \left(p N_b + K + Q_\beta + m Q_s \right)$: transverse modes $m = 0, 1, 2, \ldots$

multi-bunch mode number

Main sources of narrow-band impedance:

1) Transverse resistive wall

2) HOM's in longitudinal feedback cavities

3) HOM's in SC accelerating cavities

STRATEGY

a) Compute multi-bunch mode tune shifts $\Delta Q^{(m,K)}$

b) $\Im m \left[\Delta Q^{(m,K)} \right] < 0$: instability growth rate

c) Rigid transverse dipole modes ($m=0$) or longitudinal monopole modes ($m=1$) can be stabilized by feedback.

d) Landau damping can stabilize an unstable mode if its coherent tune shift is smaller (by some safety factor) than the incoherent tune spread:

TRANSVERSE	LONGITUDINAL
$m=0$: octupoles	
$m \geq 1$: space charge	
$m \geq 1$: synchrotron tune spread	$m \geq 1$ synchrotron tune spread

$$\Delta Q_s = \frac{1}{8} \left(\frac{h_{rf}\, \sigma_s}{R} \right)^2 Q_s$$: synchrotron tune spread for parabolic bunches

$$\left| \Delta Q^{(m,K)} \right| < \frac{m}{2(m+1)} \cdot \Delta Q_s \Rightarrow \text{LANDAU DAMPING}$$

INJECTION	TOP ENERGY
$\sigma_s = 13$ cm , $\Delta Q_{sc} \simeq 10^{-3}$	$\sigma_s = 7.5$ cm , $\Delta Q_{sc} \simeq 6 \times 10^{-6}$
$\Delta Q_s \simeq 9 \times 10^{-4} \rightarrow \left| \Delta Q^{(1,K)} \right| < 2 \times 10^{-4}$	$\Delta Q_s \simeq 10^{-4}$, $\left| \Delta Q^{(1,K)} \right| < 2.5 \times 10^{-5}$

TRANSVERSE RESISTIVE WALL

$$\mathrm{Im}\left[\Delta Q_\perp^{(m=0)}\right] \simeq \frac{N \cdot N_b\, r_p\, \omega_0}{2\pi \gamma c Z_0}\, \beta_{av}\, \mathrm{Re}\left[Z_\perp(\omega_{min})\right]$$

growth rate of most unstable $m=0$ mode

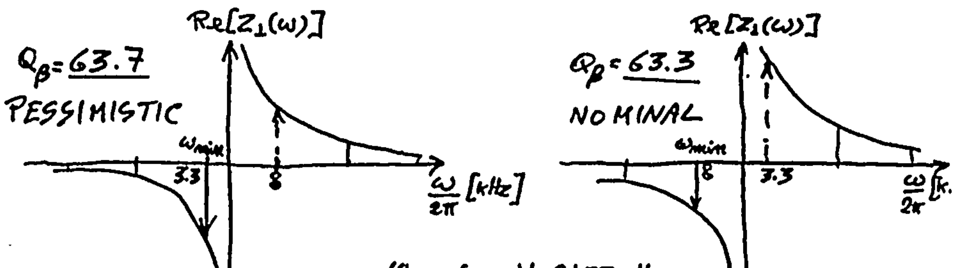

$\frac{\omega_0}{2\pi} = f_0 = 11.2455\ \mathrm{kHz}$

$Z_\perp(\omega) = \frac{2c}{\omega} \; \frac{R\rho}{b^3 \delta} (1-i)\, \mathfrak{F}$: resistive wall impedance

skin depth $\sqrt{\frac{2\rho}{\mu_0 |\omega|}}$; $\mathfrak{F}$ penetration factor for two-layer beam screen

$\left\{\begin{array}{l} 50\ \mu m \text{ copper layer on thick ss tube} \\ 2\ mm \text{ thick copper in warm sections (10\%)} \end{array}\right.$

$Q_\beta = 63.7 \to \frac{\omega_{min}}{2\pi} = 3.3\ kHz$	$Q_\beta = 63.3 \to \frac{\omega_{min}}{2\pi} = 8\ kHz$
$\delta_{Cu}^{cold} \simeq 120\ \mu m \to \tau = 21\ msec$	$\delta_{Cu}^{cold} = 75\ \mu m \to \tau = 50\ msec$
$\delta_{Cu}^{warm} = 1\ mm \to \underline{\underline{\tau = 16\ msec}}$	$\delta_{Cu}^{warm} = 0.7\ mm \to \underline{\tau = 34\ msec}$

$\Downarrow$

$-\mathrm{Im}(\Delta Q_\perp) = \frac{1}{\omega_0 \tau} = 9 \cdot 10^{-4}$: FEEDBACK

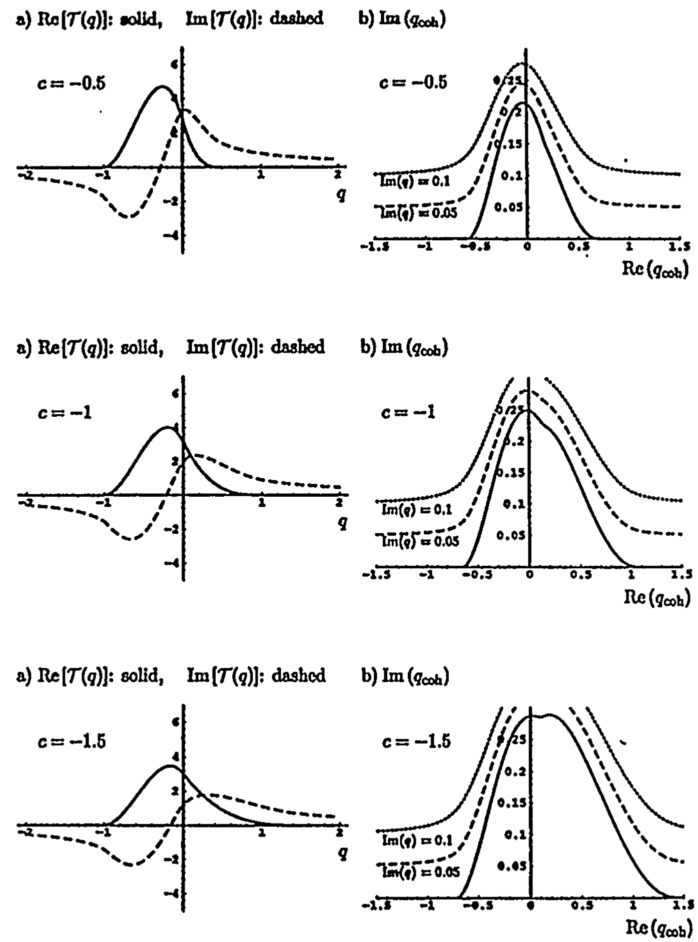

Beam transfer function (a) and stability limit (b) for two-dimensional betatron tune spread with negative ratio c of the detuning coefficients and 'quasi-parabolic' distribution.

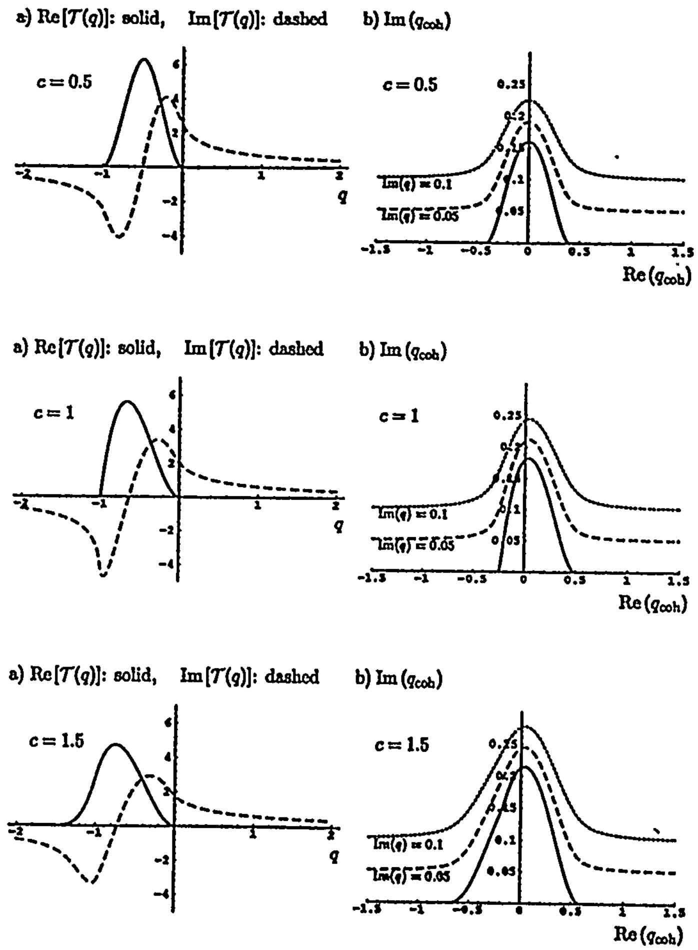

Beam transfer function (a) and stability limit (b) for two-dimensional betatron tune spread with positive ratio c of the detuning coefficients and 'quasi-parabolic' distribution.

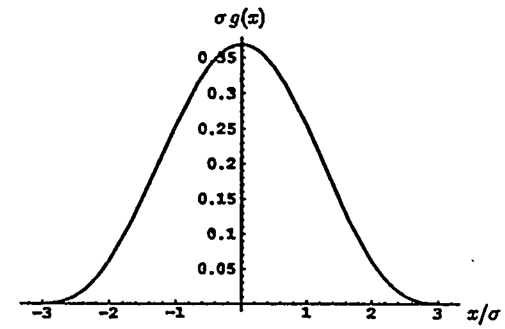

Normalised transverse beam profile for the 'quasi-parabolic' distribution.

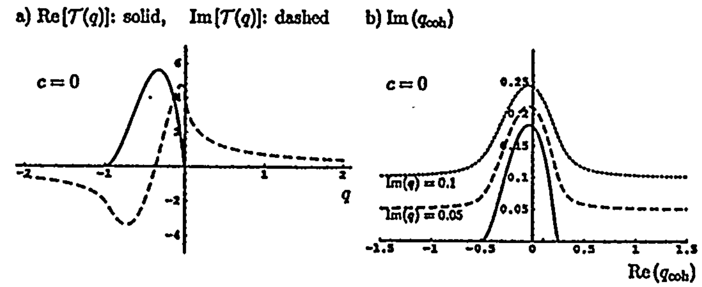

Beam transfer function (a) and stability limit (b) for one-dimensional betatron tune spread ($c = 0$) and 'quasi-parabolic' distribution. Note that in this and in the following figures the scale $S = -5a\sigma^2$ of the tune shifts q and q_{coh} is 5 times larger than in the corresponding plots for Gaussian beam distribution.

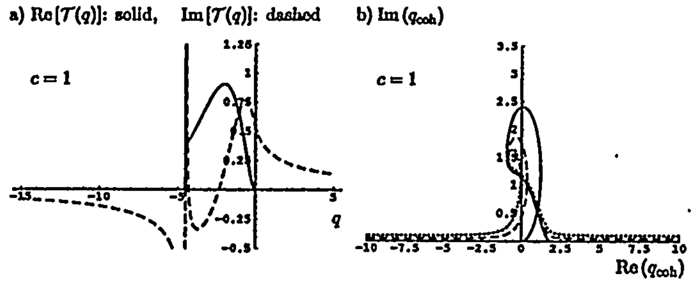

Beam transfer function (a) and stability limit (b) for two-dimensional betatron tune spread with positive ratio $c = 1$ of the detuning coefficients and Gaussian distribution truncated at 3σ. The dashed and dotted lines in the plot on the right correspond to $\mathrm{Im}(q) = 0.05$ and $\mathrm{Im}(q) = 0.1$, respectively.

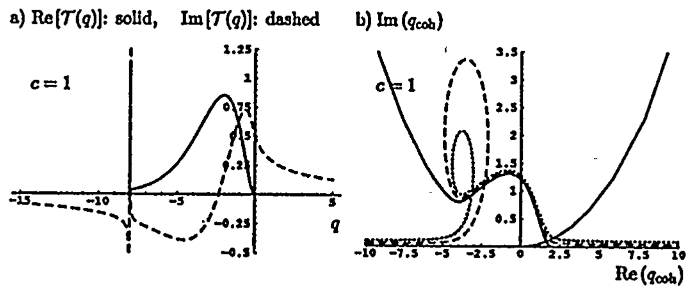

Beam transfer function (a) and stability limit (b) for two-dimensional betatron tune spread with positive ratio $c = 1$ of the detuning coefficients and Gaussian distribution truncated at 4σ. The dashed and dotted lines in the plot on the right correspond to $\mathrm{Im}(q) = 0.05$ and $\mathrm{Im}(q) = 0.1$, respectively.

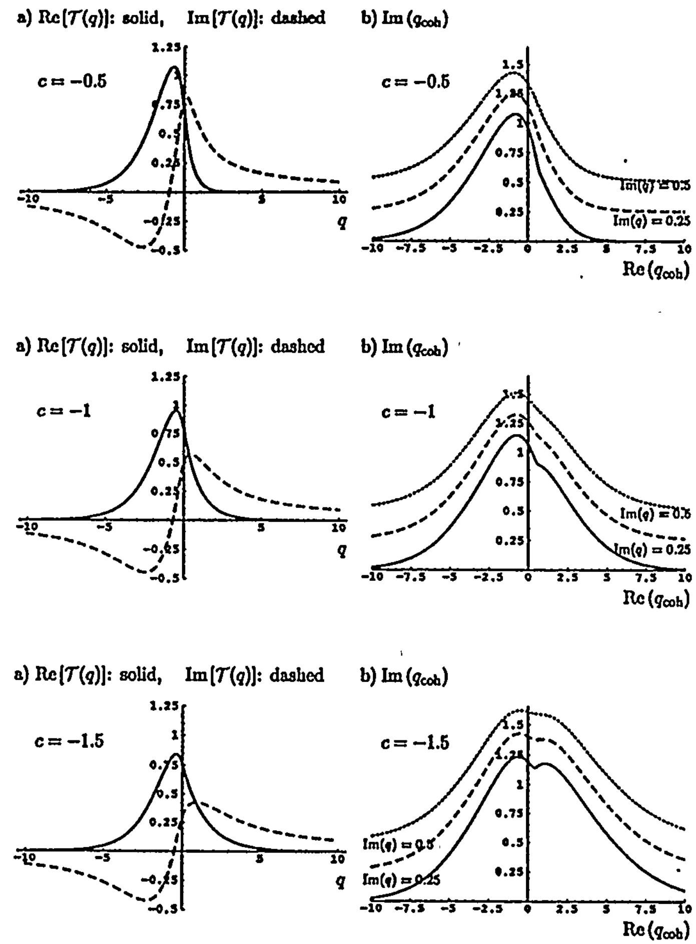

Beam transfer function (a) and stability limit (b) for two-dimensional betatron tune spread with negative ratio c of the detuning coefficients and Gaussian distribution.

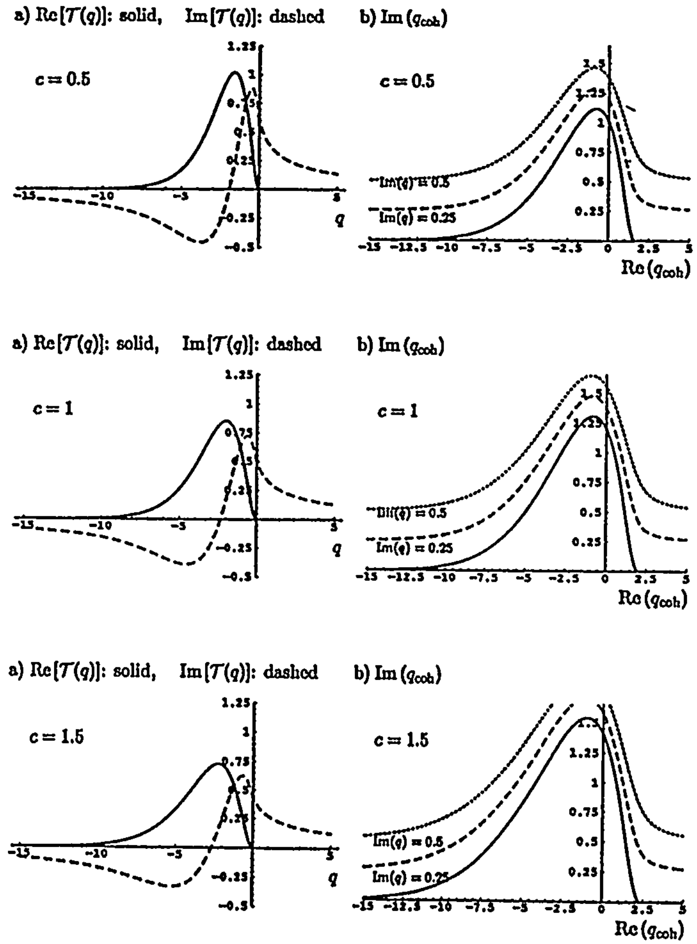

Beam transfer function (a) and stability limit (b) for two-dimensional betatron tune spread with positive ratio c of the detuning coefficients and Gaussian distribution.

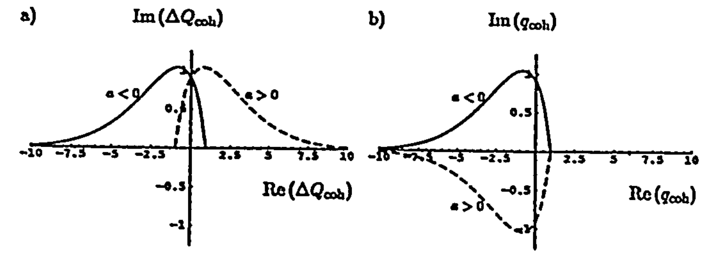

Example of stability limit for physical (a) and for normalised (b) coherent tune shifts with one-dimensional betatron tune spread ($c =$ 0) and Gaussian distribution. A unit scaling factor $|S| = |a|\sigma^2$ is assumed for simplicity. An inductive impedance gives rise to negative real coherent tune shifts ΔQ_{coh}, corresponding to positive or negative normalised tune shifts q_{coh} depending on the sign of the detuning coefficient a.

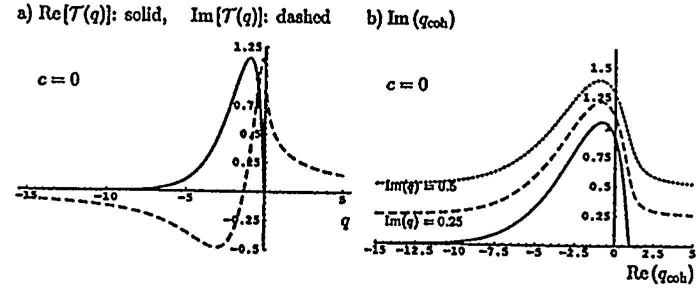

Beam transfer function (a) and stability limit (b) for one-dimensional betatron tune spread ($c = 0$) and Gaussian distribution.

LONGITUDINAL FEEDBACK

3 cavities per beam at $\langle\beta\rangle \simeq 200$ m

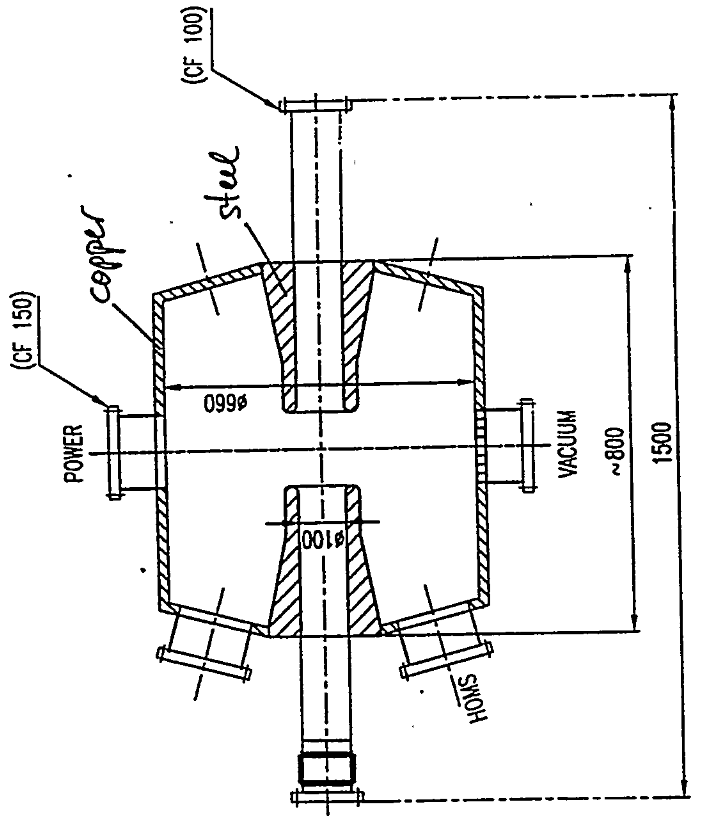

Cross section of 200 MHz ADL CAVITY

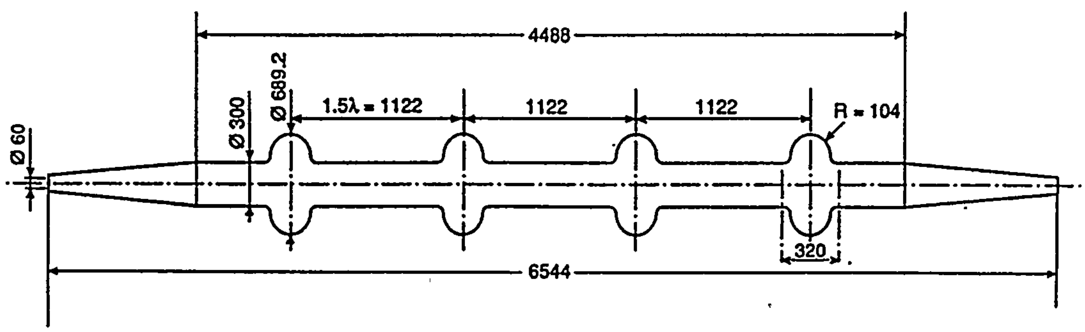

Figure 24: Proton accelerating cavities

TWO SETS OF FOUR SUPERCONDUCTING CAVITIES (400MHz) INDEPENDENT FOR EACH BEAM

LONGITUDINAL CAVITY MODES

$\Delta Q_{top}^{m=1} \simeq 2\times10^{-5}$

f MHz	R_s kΩ	Q	τ_{inj} sec	m	τ_{top} sec	m
546.1	183	12702	1.123	2	2.305	1
693.8	744	14959	0.334	3	0.686	1
859.8	165	12667	1.821	4	3.491	2
1021.1	240	14797	1.397	4	2.443	2
1249.4	153	23190	5.311	4	4.663	3

Most prominent longitudinal HOM's for the set of 3 DAMPING CAVITIES and corresponding instability rise times: the cavity vessel is copper, the drift tube is stainless steel (W. Höfle).

f MHz	R_s MΩ/m	Q	τ_{inj} sec	m	τ_{top} sec	m
781.1	38.41	10000	6.844	3	16.056	2
782.6	28.22	10000	9.339	3	21.814	2
813.9	29.37	10000	9.572	3	20.277	2
853.4	58.99	10000	5.128	4	9.799	2
917.8	58.14	10000	5.046	4	9.737	2

Most prominent transverse HOM's for the set of 8 SC ACCELERATING CAVITIES and corresponding instability rise times: Q values are assumed to be 10000 (V. Rödel).

BROAD-BAND IMPEDANCE TUNE SHIFTS $\Rightarrow$ $\Delta Q_{\parallel}^{(m)} \simeq \begin{cases} \frac{m}{m+1}\cdot 2\times10^{-5} & \text{, injection} \\ \frac{m}{m+1}\, 2\times10^{-5} & \text{, top} \end{cases}$

TRANSVERSE CAVITY MODES

$\Delta Q_{inj}^{m=1} \simeq 10^{-4}$

f MHz	R_s MΩ/m	Q	τ_{inj} sec	m	τ_{top} sec	m
516.7	20.64	14171	0.161	1	1.265	0
612.2	8.55	18653	0.406	2	3.931	1
809.5	8.97	15611	0.517	3	4.216	1
1103.6	6.63	24819	1.038	5	7.990	2

Most prominent transverse HOM's for the set of 3 DAMPING CAVITIES (with an average beta of 200 m) and corresponding instability rise times: the cavity vessel is copper, the drift tube is stainless steel (W. Höfle).

f MHz	R_s MΩ/m	Q	τ_{inj} sec	m	τ_{top} sec	m
538.5	5.31	10000	0.856	2	7.127	0
539.2	3.95	10000	1.150	2	9.612	0

Most prominent transverse HOM's for the set of 8 SC ACCELERATING CAVITIES (with an average beta of 150 m) and corresponding instability rise times: Q values are assumed to be 10000 (V. Rödel).

The rise times at injection and at top energy of the most unstable transverse multi-bunch modes (with azimuthal mode number m), are estimated assuming 3564 bunches with parabolic distribution, symmetrically filled with 10^{11} particles. The r.m.s. bunch length is 13 cm at injection and 7 cm at top energy.

BROAD-BAND IMPEDANCE TUNE SHIFTS FOR $m \geq 1$ $\Rightarrow$ $\Delta Q_{\perp}^{(m)} \simeq \begin{cases} \frac{7\times10^{-5}}{m+1} & : \text{injection} \\ -\frac{7\times10^{-5}}{m+1} & : \text{top} \end{cases}$

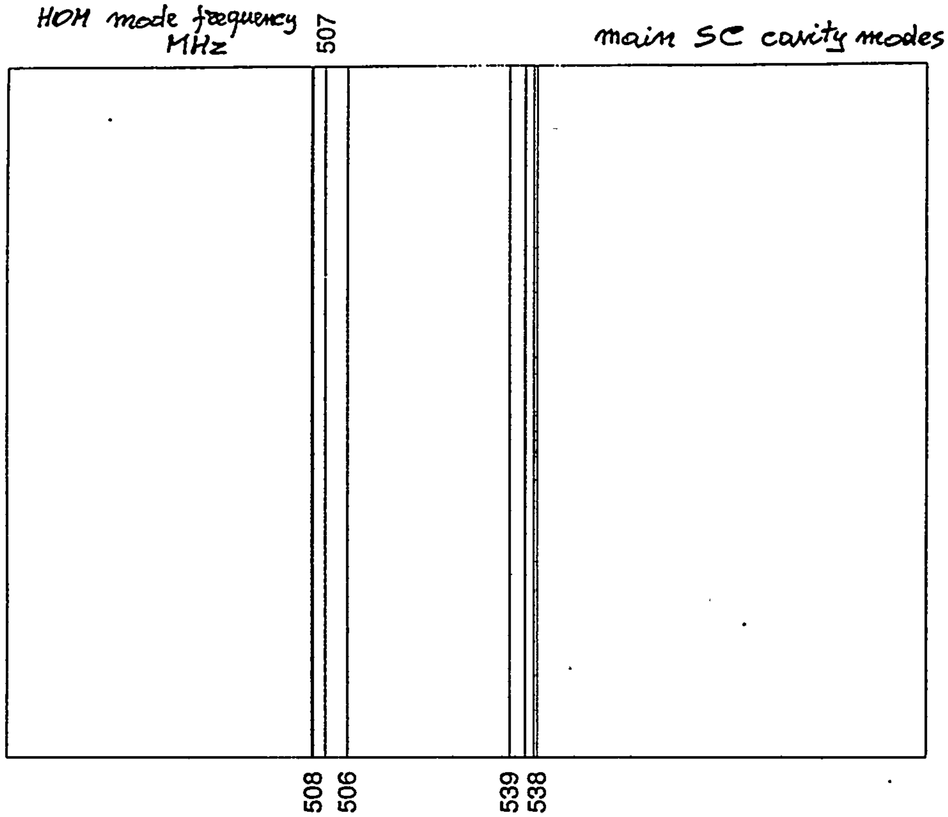
HOM mode frequency MHz
main SC cavity modes
507
508
506
539
538

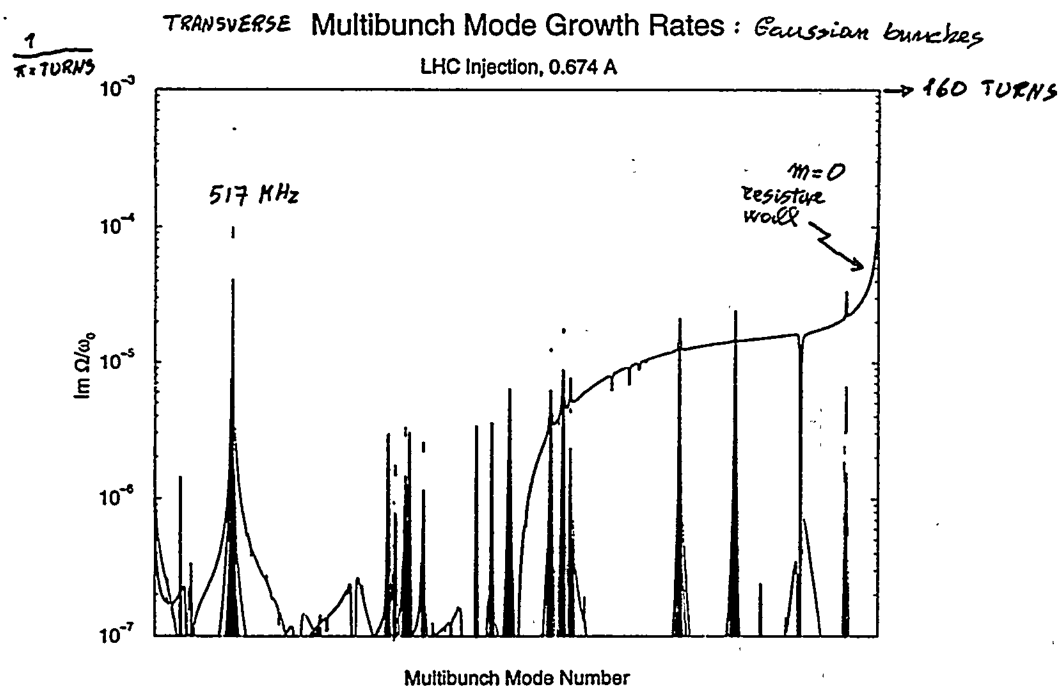
TRANSVERSE Multibunch Mode Growth Rates : Gaussian bunches
LHC Injection, 0.674 A
1/π = TURNS
→ 160 TURNS
517 MHz
m=0
resistive wall
10^{-3}
10^{-4}
10^{-5}
10^{-6}
10^{-7}
Im Ω/ω_0
Multibunch Mode Number

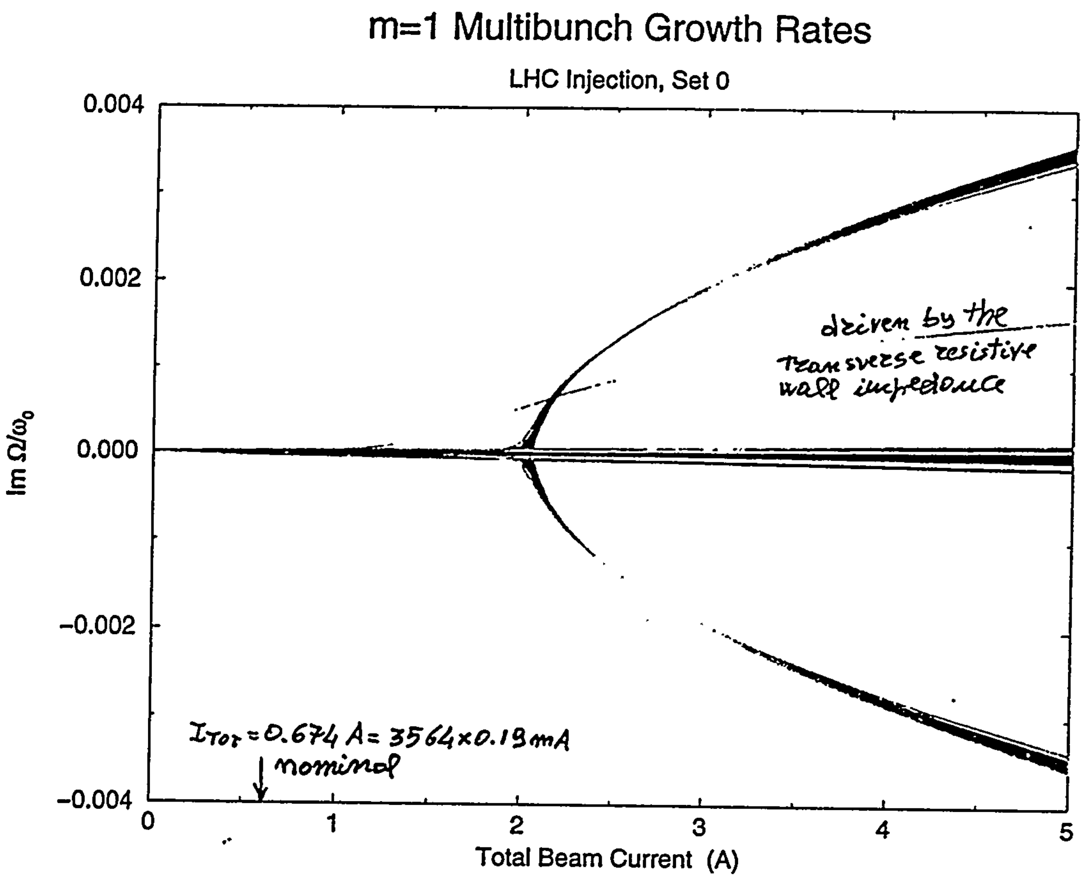
m=1 Multibunch Growth Rates
LHC Injection, Set 0
0.004
0.002
0.000
-0.002
-0.004
Im Ω/ω0
0
1
2
3
4
5
Total Beam Current (A)
driven by the transverse resistive wall impedance
I_TOT = 0.674 A = 3564×0.19 mA
nominal

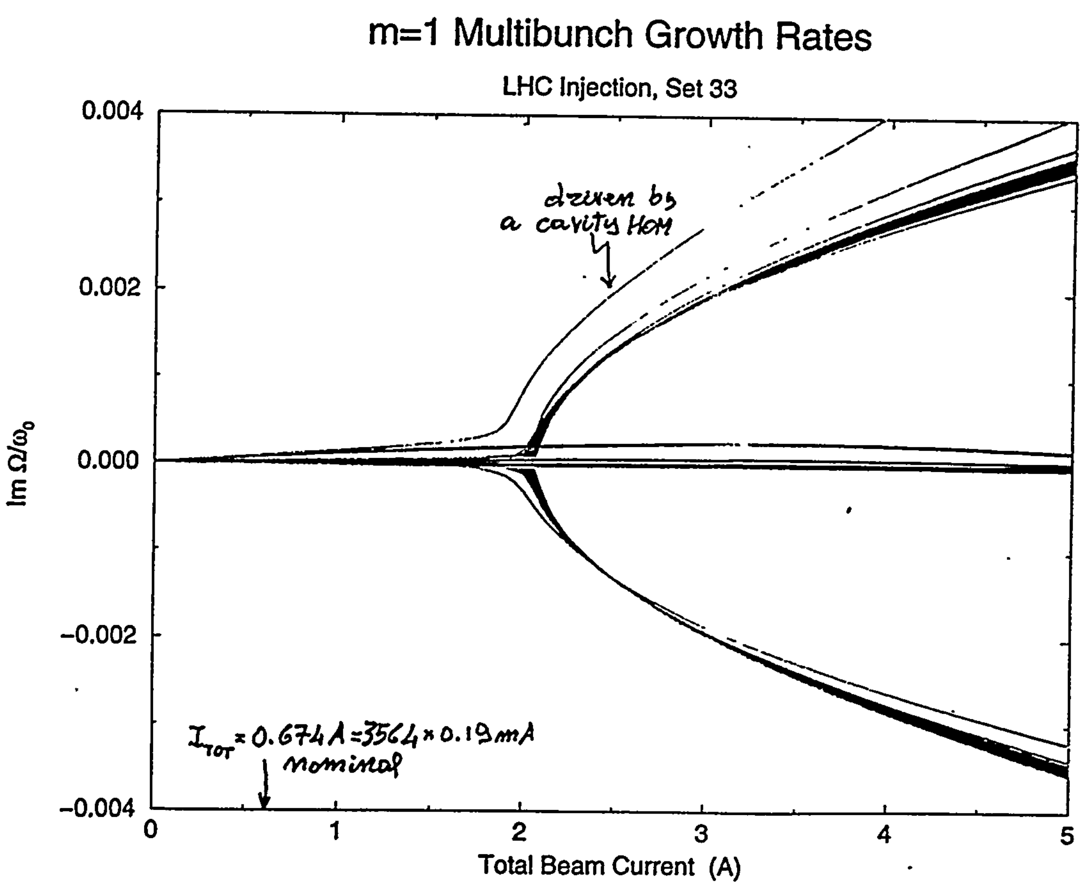
m=1 Multibunch Growth Rates
LHC Injection, Set 33
0.004
0.002
0.000
-0.002
-0.004
Im Ω/ω0
0
1
2
3
4
5
Total Beam Current (A)
driven by a cavity HOM
I_TOT = 0.674 A = 3564×0.19 mA
nominal

LANDAU DAMPING WITH TWO DIMENSIONAL BETATRON TUNE SPREAD

Dispersion relation for rigid dipole oscillations

$$1 = -\Delta Q_{coh} \int_0^\infty dJ_x \int_0^\infty dJ_y \frac{J_x \frac{\partial \rho(J_x,J_y)}{\partial J_x}}{Q - Q_x(J_x,J_y)}$$

coherent tune shift in the absence of tune spread

consider oscillations in x-plane

$$Q_x(J_x, J_y) = Q_0 + a\,J_x + b\,J_y\,, \qquad c = \frac{b}{a}$$

linear detuning (octupoles)

1) $\rho(J_x, J_y) = \frac{1}{\sigma^4} \exp\left[-\frac{J_x + J_y}{\sigma^2}\right]$: Gaussian

$$\begin{cases} S = -a\sigma^2 & : \text{"horizontal tune spread"} \\ q_{coh} = \frac{\Delta Q_{coh}}{S}, \quad q = \frac{Q - Q_0}{S} & : \text{normalized tune shifts} \end{cases}$$

$$q_{coh}(q) = \frac{i}{\tau(q)}\,, \quad \tau(q): \text{beam transfer function}$$

$$\tau(q) = \frac{i}{(1-c)^2}\left\{1 - c - (q + c - cq)e^q E_1(q) + c\,e^{q/c} E_1\left(\frac{q}{c}\right)\right\}$$

2) truncated Gaussian $\rightarrow$ pathologies

3) $\rho(J_x, J_y) = \frac{12}{(5\sigma^2)^2}\left[1 - \frac{J_x + J_y}{5\sigma^2}\right]^2$ for $J_x + J_y \leq 5\sigma^2$

"quasi-parabolic", $S = -5a\sigma^2$: "full horiz. spread"

CONCLUSIONS

1) Even assuming a pessimistic betatron tune of 0.3 below the integer, the transverse resistive wall instability has a rise time of 16 msec (180 turns) and can be damped by feedback.

2) Assuming Q-values of 10^4 for HOM's in the SC accelerating cavities, all multi-bunch modes are stable

3) The copper-vessel + SS drift tube design of the longitudinal feedback cavities should be OK: an increased safety margin for Landau damping of multi-bunch modes can be obtained by further lowering the Q-values of the 517 MHz dipole mode and of the 694 MHz monopole mode.

4) The situation may become critical at top energy: octupoles are needed to provide Landau damping of (single bunch) transverse modes, while longitudinal modes can lose Landau damping at about twice the nominal current $\Rightarrow$ the broad-band impedance should be taken under control.

RESONANCE ANALYSIS IN CELESTIAL MECHANICS

J. Hagel, Univ Maderia

Example of resonance analysis in a celestial mechanics problem

J. Hagel, Univ. Madeira
PORTUGAL

- Definition of the problem
- Numeric investigation
- Single resonance analysis
- Stability ("dynamical aperture")

- Definition of the problem

Circular restricted 3-body problem (planar)

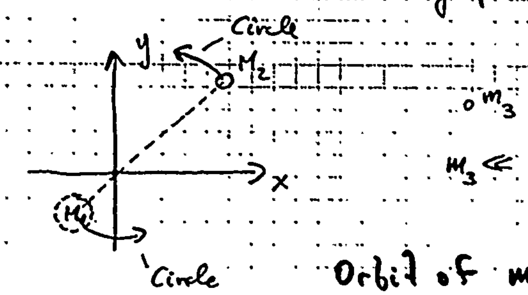

$m_3 \ll M_{1,2}$

Orbit of m_3 = ?

Usually this problem is transformed to rotating coordinates:

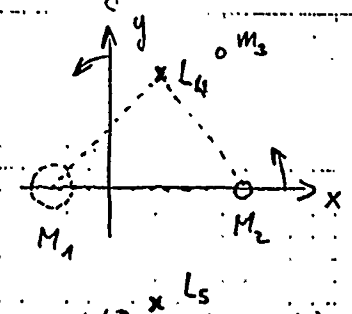

In **addition** the **distance between** ($M_1 \leftrightarrow M_2$) is normalized to unity. Doing so we obtain the nonlinear system of equations for m_3:

$$\ddot{x} - 2\dot{y} = \frac{\partial \Omega}{\partial x}$$

$$\ddot{y} + 2\dot{x} = \frac{\partial \Omega}{\partial y}$$

$$\Omega(x,y) = \frac{1}{2}\left[(1-\mu) r_1^2 + \mu r_2^2\right] + \frac{1-\mu}{r_1} + \frac{\mu}{r_2}$$

$$r_1(x,y) = \left[(x+\mu)^2 + y^2\right]^{1/2}$$

$$r_2(x,y) = \left[(x+\mu-1)^2 + y^2\right]^{1/2}$$

$$\mu = \frac{m_2}{m_1 + m_2} \quad \text{... mass parameter}$$

$$\mu = \frac{1}{2} \implies m_1 = m_2$$

$$\mu = 0 \implies m_2 = 0$$

It is well known that this problem has 5 fixed points $L_{1,2,3,4,5}$.

Two of them, namely L_4 and L_5 are <u>linearly stable</u> if

$$0 < \mu < \mu_c = 0.03854\ldots\ldots$$

where $L_{4,5}\left(\frac{1}{2} - \mu, \pm\frac{\sqrt{3}}{2}\right)$

This can be shown by linearizing the equations <u>around L_4</u> and computing the eigenvalues <u>of M in</u>

$$\dot{\vec{X}}_{lin} = M \vec{X}_{lin} \quad ; \quad \vec{X}_{lin} = \begin{pmatrix} x \\ \dot{x} \\ y \\ \dot{y} \end{pmatrix}_{lin} (t)$$

and

$$M = \begin{pmatrix} 0 & 1 & 0 & 0 \\ a & 0 & b & 2 \\ 0 & 0 & 0 & 1 \\ b & -2 & 3a & 0 \end{pmatrix}$$

$$a = \frac{3}{4} \quad , \quad b = \frac{3\sqrt{3}}{2}\left(\frac{1}{2} - \mu\right)$$

with $\lambda = \pm i\,\omega_{1,2} \; ; \; \omega_{1,2} = \sqrt{\frac{1}{2} \pm \frac{1}{2}\sqrt{1 - 27\mu + 27\mu^2}}$

Linear motion is libration with the two frequencies $\omega_{1,2}$.

$$\vec{X}_{lin} = \vec{\alpha} e^{i\omega_1 t} + \vec{\beta} e^{i\omega_2 t}$$

We want to study nonlinear motion, <u>close to L_4</u>, hence the substitution

$$x \Rightarrow \frac{1}{2} - \mu + \tilde{x} \qquad\qquad \ddot{\tilde{x}} - 2\dot{\tilde{y}} = \frac{\partial \tilde{\Omega}(\tilde{x},\tilde{y})}{\partial \tilde{x}}$$

$$y \rightarrow \frac{\sqrt{3}}{2} + \tilde{y} \qquad \rightarrow \qquad \ddot{\tilde{y}} + 2\dot{\tilde{x}} = \frac{\partial \tilde{\Omega}(\tilde{x},\tilde{y})}{\partial \tilde{y}}$$

is applied and $\tilde{\Omega}(\tilde{x},\tilde{y})$ is expanded to third order in $\tilde{x},\tilde{y}$. ($\tilde{x}=\tilde{y}=0$ means L_4)

The resulting equation is written in matrix form and is:

$$\dot{\vec{X}} = M\vec{X} + \vec{F}(\vec{X}) \quad ; \quad \vec{X} = \begin{pmatrix} \tilde{x} \\ \dot{\tilde{x}} \\ \tilde{y} \\ \dot{\tilde{y}} \end{pmatrix}$$

$$M = \begin{pmatrix} 0 & 1 & 0 & 0 \\ a & 0 & b & 2 \\ 0 & 0 & 0 & 1 \\ b & -2 & 3a & 0 \end{pmatrix} \quad ; \quad a = \frac{3}{4}, \; b = \frac{3\sqrt{3}}{2}\left(\frac{1}{2}-\mu\right)$$

$$\vec{F}(\vec{X}) = \begin{pmatrix} 0 \\ -\frac{21}{8}\left(\mu-\frac{1}{2}\right)\tilde{x}^2 - \frac{3}{8}\sqrt{3}\,\tilde{x}\tilde{y} + \frac{33}{8}\left(\mu-\frac{1}{2}\right)\tilde{y}^2 \\ 0 \\ -\frac{3}{16}\sqrt{3}\,\tilde{x}^2 + \frac{33}{4}\left(\mu-\frac{1}{2}\right)\tilde{x}\tilde{y} - \frac{9}{16}\sqrt{3}\,\tilde{y}^2 \end{pmatrix}$$

$$\dot{\vec{X}} = M\vec{X} + \vec{F}(\vec{X})$$

- Diagonalization of linear part:

Subst.: $$\vec{X} = R\vec{X}_1 \quad ; \quad R = \text{Const.}$$

$$\Rightarrow R\dot{\vec{X}}_1 = MR\vec{X}_1 + \vec{F}(R\vec{X}_1) \;\Big|\; R^{-1}_{(l)}$$

$$\Rightarrow \dot{\vec{X}}_1 = (R^{-1}MR)\vec{X}_1 + R^{-1}\vec{F}(R\vec{X}_1)$$

$\rightarrow$ Choose R to be the matrix of eigenvectors of M will diagonalize M, hence

$$R = (\vec{E}_1, \vec{E}_2, \vec{E}_3, \vec{E}_4) \Rightarrow$$

$$\Rightarrow \dot{\vec{X}}_1 = \begin{pmatrix} -i\omega_1 & & & 0 \\ & i\omega_1 & & \\ & & -i\omega_2 & \\ 0 & & & i\omega_2 \end{pmatrix} \vec{X}_1 + \vec{G}(\vec{X}_1)$$

$$\vec{X}_1 = \begin{pmatrix} x_1 \\ \dot{x}_1 \\ y_1 \\ \dot{y}_1 \end{pmatrix} = \begin{pmatrix} x_1 \\ u_1 \\ y_1 \\ v_1 \end{pmatrix}$$

Linear part have the form: $Ce^{\pm i\omega_{1,2}t}$

We apply now a transformation to action/angle like variables (J, ϕ) using

$$x_1 = J_1 e^{-i\phi_1}$$
$$u_1 = J_1 e^{i\phi_1}$$
$$y_1 = J_2 e^{-i\phi_2}$$
$$v_1 = J_2 e^{i\phi_2}$$

which leads to a very simple linear part in our new equations:

$$\dot{J}_1 = \frac{1}{2}\left[e^{i\phi_1} G_x + e^{-i\phi_1} G_u\right]$$
$$\dot{J}_2 = \frac{1}{2}\left[e^{i\phi_2} G_y + e^{-i\phi_2} G_v\right]$$
$$\dot{\phi}_1 = \omega_1 + \frac{i}{2J_1}\left[e^{i\phi_1} G_x - e^{-i\phi_1} G_u\right]$$
$$\dot{\phi}_2 = \omega_2 + \frac{i}{2J_2}\left[e^{i\phi_2} G_y - e^{-i\phi_2} G_v\right]$$

$$G_{x,u,y,v} = G_{x,\dots,v}(J_1, J_2, \phi_1, \phi_2)$$

- Isolating the resonance term

All the terms G_x, G_u, G_y and G_v depend on expressions like:

$$J_{1,2}^{\alpha} \, e^{i(m\phi_1 + n\phi_2)} \qquad \alpha > 0$$

Since $J_{1,2}$ are small $\phi_{1,2}$ are close to

$$\phi_1(t) \approx \omega_1 t$$
$$\phi_2(t) \approx \omega_2 t$$

Hence, if $\omega_1 \approx 2\omega_2$, the term

$$e^{i(\phi_1 - 2\phi_2)} \qquad (1:2)$$

will be the only dominating small frequency term and all the others can be neglected. Doing the whole algebra (MATHEMATICA) leads to the result:

QUESTION: Having initial conditions close to L_4 in case of the full nonlinear equations and given initial conditions

$$x(0) = \frac{1}{2} - \mu + \Delta x$$
$$y(0) = \sqrt{3}/2$$
$$\dot{x}(0) = \dot{y}(0) = 0$$

WHAT IS THE MAXIMUM Δx TO OBTAIN BOUNDED MOTION ARROUND THE POINT $L_{4(5)}$

It turns out that for nearly every $\mu \in (0, \mu_c)$ there exists a finite Δx_{max}. However, for two special points μ_2, μ_3

$$\mu_2 = \frac{1}{2}\left[1 - \sqrt{611/675}\,\right] = 0.024292\ldots$$
$$\mu_3 \approx 0.013\ldots$$

$\Delta x_{max} = 0$. For $\mu_{2,3}$ this has been proven by **A. Deprit, AIAA 65-681, 1965**

For μ_2 (which we will treat) this is due to a resonance condition of the primary frequencies ω_1, ω_2;

$$\omega_1(\mu) - 2\,\omega_2(\mu) = 0$$

- Numeric investigation .... (see DEMO)

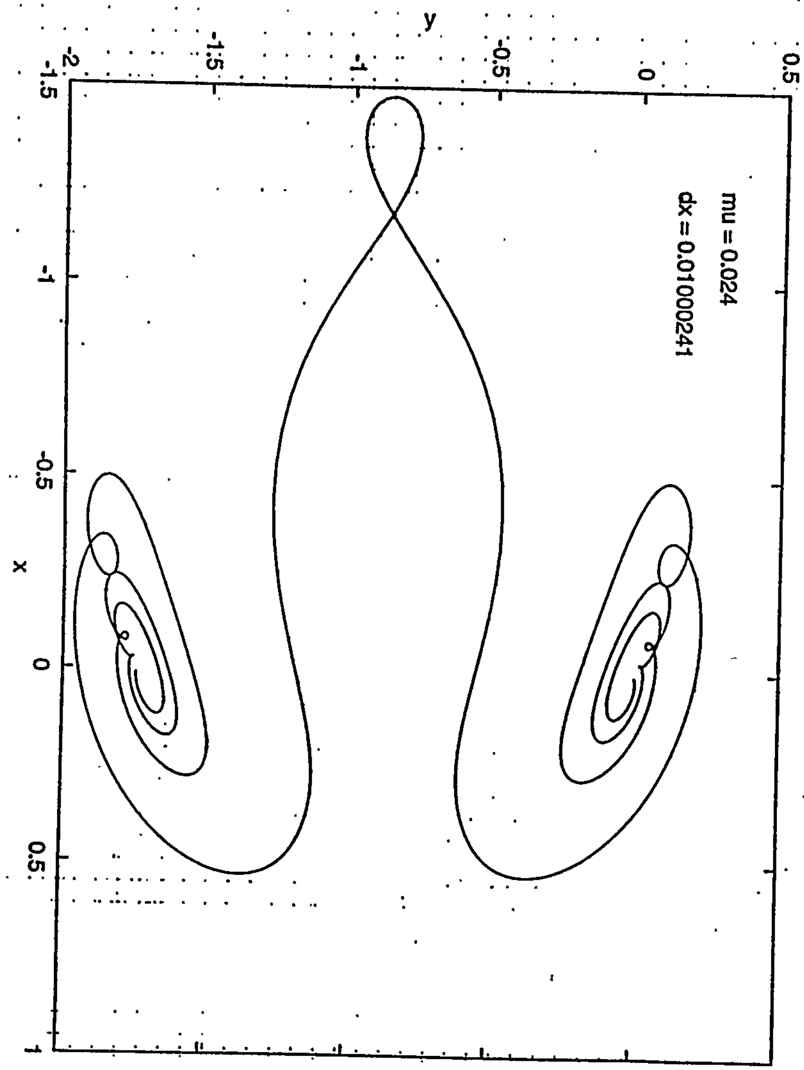

- Single Resonance analysis

$$\ddot{x} - 2\dot{y} = \frac{\partial \Omega}{\partial x} \qquad ; \quad \Omega = \Omega(x, y; \mu)$$
$$\ddot{y} + 2\dot{x} = \frac{\partial \Omega}{\partial y}$$

<u>Hamiltonian:</u>

$$H(x, p_x, y, p_y) = \frac{1}{2}\left[(x - p_y)^2 + (y + p_x)^2\right] - \Omega(x, y)$$

where the canonical momenta are

$$p_x = \frac{\partial L}{\partial \dot{x}} = \dot{x} - y \qquad p_y = \frac{\partial L}{\partial \dot{y}} = \dot{y} + x$$

and $L(x, \dot{x}, y, \dot{y})$ the Lagrangian

$$L = \frac{1}{2}(\dot{x}^2 + \dot{y}^2) + x\dot{y} - \dot{x}y + \Omega(x, y)$$

$$\dot{J}_1 = J_2^2 \left[\alpha \cos(\phi_1 - 2\phi_2) + \beta \sin(\phi_1 - 2\phi_2)\right]$$
$$\dot{J}_2 = J_1 J_2 \left[\gamma \cos(\phi_1 - 2\phi_2) + \delta \sin(\phi_1 - 2\phi_2)\right]$$
$$\dot{\phi}_1 = \omega_1 + \frac{J_2^2}{J_1}\left[\beta \cos(\phi_1 - 2\phi_2) - \alpha \sin(\phi_1 - 2\phi_2)\right]$$
$$\dot{\phi}_2 = \omega_2 + J_1 \left[-\delta \cos(\phi_1 - 2\phi_2) + \gamma \sin(\phi_1 - 2\phi_2)\right]$$

$$\alpha = \frac{3371}{1083\sqrt{3}} - \frac{5116075\sqrt{611}\,\Delta\mu}{987696} + O(\Delta\mu)^2$$

$$\beta = \frac{34}{1083}\sqrt{\frac{3055}{3}} + \frac{122073985\sqrt{5}\,\Delta\mu}{493842} + O(\Delta\mu)^2$$

$$\gamma = \frac{3371}{1767\sqrt{3}} - \frac{87378725\sqrt{611}}{99913248}\,\Delta\mu + O(\Delta\mu)^2$$

$$\delta = \frac{34}{1767}\sqrt{\frac{3055}{3}} + \frac{8276720795\sqrt{5}\,\Delta\mu}{49956624} + O(\Delta\mu)^2$$

$$J_1(0) = \frac{1}{3}\sqrt{\frac{217}{10}}\,\Delta x \qquad J_2(0) = \frac{1}{24}\sqrt{\frac{5111}{5}}\,\Delta x$$

$$\phi_1(0) = \frac{60255\sqrt{15}\,\Delta\mu}{55552} - \arctan\left(\frac{\sqrt{611}}{15\sqrt{5}}\right)$$

$$\phi_2(0) = \frac{-42225\sqrt{15}\,\Delta\mu}{20444} - \arctan\left(\frac{\sqrt{611}}{30\sqrt{5}}\right)$$

In addition: $\frac{\alpha}{\beta} = \frac{\gamma}{\delta}$; $\Delta\mu = \mu - \mu_2$

These equations may be solved EXACTLY.

4 STEPS:

(i) Reducing the number of equations from 4 to 3.

Subst.: $\phi = \phi_1 - 2\phi_2$

Multiplication of (ϕ) with 2 and subtracting (3) and (4) leads

$$\dot{J}_1 = J_2^2 \left[\alpha \cos\phi + \beta \sin\phi\right]$$
$$\dot{J}_2 = J_1 J_2 \left[\gamma \cos\phi + \delta \sin\phi\right]$$
$$\dot{\phi} = D + \frac{2J_2^2}{J_1}\left[\beta\cos\phi - \alpha\sin\phi\right] - J_1\left[-\delta\cos\phi + \gamma\sin\phi\right]$$

$$D = -\frac{5}{16}\sqrt{9165}\cdot\Delta\mu$$

(ii) Extracting a first integral relating J_1 and J_2:

We use $A\cos\phi + B\sin\phi = \mathrm{sgn}(A)\sqrt{A^2+B^2}\cos\left(\phi - \operatorname{atan}\frac{B}{A}\right)$ and we get

$$\dot{J}_1 = J_2^2 A_1 \cos(\phi - \theta_1)$$
$$\dot{J}_2 = J_1 J_2 A_2 \cos(\phi - \theta_2)$$
$$\dot{\phi} = D + \frac{2J_2^2}{J_1} A_1 \cos(\phi - \theta_3) + J_1 A_2 \cos(\phi - \theta_4)$$

$$A_1 = (\alpha^2+\beta^2)^{1/2} \qquad A_2 = (\gamma^2+\delta^2)^{1/2} \qquad D = \frac{-5\sqrt{9165}\,\Delta\mu}{16}$$

Then: Using $\theta_1 = \arctan\frac{\beta}{\alpha}$ $\qquad \theta_3 = -\arctan\frac{\alpha}{\beta}$

$\theta_2 = \arctan\frac{\delta}{\gamma}$ $\qquad \theta_4 = -\arctan\frac{\gamma}{\delta}$

and $\frac{\alpha}{\beta} = \frac{\gamma}{\delta}$

and $\arctan x + \arctan\frac{1}{x} = \frac{\pi}{2}$

we get

$$\theta_1 - \theta_3 = \frac{\pi}{2}$$

and

$$\theta_1 = \theta_2 \quad , \quad \theta_3 = \theta_4$$

hence

①
$$\begin{cases} \dot{J}_1 = J_2^2 A_1 \cos(\phi - \theta_1) \\ \dot{J}_2 = J_1 J_2 A_2 \cos(\phi - \theta_1) \\ \dot{\phi} = D + \left[\frac{2J_2^2}{J_1} A_1 + J_1 A_2\right] \cos(\phi - \theta_3) \end{cases}$$

From which follows:

②
$$\frac{\dot{J}_1}{J_2^2 A_1} = \frac{\dot{J}_2}{J_1 J_2 A_2} \Longrightarrow \underline{\underline{J_2^2 = \frac{A_2}{A_1} J_1^2}} + \underbrace{O(\Delta x^2)}_{\text{int. constant of order } \Delta x^2}$$

③
$$\dot{J}_1 = A_2 J_1^2 \cos(\phi - \theta_1)$$
$$\dot{\phi} = D + 3 A_2 J_1 \cos(\phi - \theta_3)$$

$J_1 = J$
$\phi = \psi + \theta_1$

$$\dot{J}^{*} = A_2 J^2 \cos\psi$$
$$\dot{\psi} = D - 3 A_2 J \sin\psi$$

(IV) Extracting a second integral

We have:

$$\dot{J} = A_2 J^2 \cos\varphi \qquad (1)$$
$$\dot{\varphi} = D - 3A_2 J \sin\varphi \qquad (2)$$

with

$$A_2 = \frac{11}{3}\sqrt{\frac{11}{93}} + \frac{11849425}{98208}\sqrt{\frac{611}{341}}\,\Delta\mu$$

$$J(0) = \frac{1}{3}\sqrt{\frac{217}{10}}\,\Delta x$$

$$\varphi(0) = 2\arctan\left(\frac{1}{30}\sqrt{\frac{611}{5}}\right) - \arctan\left(\frac{1}{15}\sqrt{\frac{611}{5}}\right) - \arctan\left(\frac{34}{3371}\sqrt{5055}\right) - \frac{4054598 4055}{641605888}\sqrt{15}\,\Delta\mu$$

Strategy: We look for a Hamiltonian that represents (1) and (2) and does not depend on time $\Rightarrow$ The Hamiltonian then is the desired integral

$$\frac{\partial H}{\partial t} = 0 \Longrightarrow \frac{dH}{dt} = 0$$

Problem: J and φ in

$$\dot{J} = A_2 J^2 \cos\varphi \qquad (1)$$
$$\dot{\varphi} = D - 3A_2 J \sin\varphi \qquad (2)$$

ARE NO CANONICAL PAIR !

However using $J = I^{1/2} = \sqrt{I}$

gives:

$$\frac{\dot{I}}{2\sqrt{I}} = A_2 I \cos\varphi$$
$$\dot{\varphi} = D - 3A_2 I^{1/2}\sin\varphi$$

with the Hamiltonian:

$$H(I,\varphi) = -D\cdot I + 2A_2 I^{3/2}\sin\varphi = \text{Const.}$$

So, the desired second integral is:

$$\mathbf{-DJ^2 + 2A_2 J^3 \sin\varphi = C}$$

So we finally arrive at:

$$\dot{J} = A_2 J^2 \cos\psi$$

$$\dot{\psi} = D - 3A_2 J \sin\psi$$

$$-DJ^2 + 2A_2 J^3 \sin\psi = \text{Const.}$$

$$\sin\psi = \frac{C + D\cdot J^2}{2A_2 J^3}$$

$$\cos\psi = \sqrt{1 - \left(\frac{C + D\cdot J^2}{2A_2 J^3}\right)^2}$$

$$t = \int_{J_0}^{J} \frac{dJ}{J^2\sqrt{1 - \left(\frac{C + D\cdot J^2}{2A_2 J^3}\right)^2}} \quad \left.\right\} \text{Complete solution of the resonant problem!}$$

<u>Stability:</u> We just need the integral

$$-DJ^2 + 2A_2 J^3 \sin\psi = -DJ_0^2 + 2A_2 J_0^3 \sin\psi_0$$

<u>Method:</u> We look for the value of J_0, that leads us to the closest hyperbolic fixed point as $t \to \infty$:

Hence:

$$\underbrace{-DJ_0^2 + 2A_2 J_0^3 \sin\psi_0}_{\text{"Dynamical aperture"}} = -DJ_E^2 + 2A_2 J_E^3 \sin\psi_E$$

where

$$J_E = \frac{D}{3A_2} \qquad \psi_E = \frac{\pi}{2}$$

So we have to solve a cubic equation for J_0 } we look for the smallest real <u>solution!</u>

Result:

$$\Delta x_{max} = -\frac{15}{32}\sqrt{\frac{91650}{217}} \times$$

$$\left[(z_2 - z_1)\,\mathrm{sgn}(\mu - \mu_2) + z_1 + z_2\right](\mu - \mu_2)$$

$$\mu_2 = \frac{1}{2}\left[1 - \sqrt{\frac{611}{675}}\right]$$

$$z_1 = 0.142191053 \qquad z_2 = -0.1685463660$$

$z_{1/2}$ are solutions of $z^3 + Az + B = 0$ where

$$A = \frac{-3\sqrt{\frac{93}{11}}\csc\left(2\arctan\left(\frac{\sqrt{611}}{3\sqrt{5}}\right) - \arctan\left(\frac{\sqrt{611}}{15}\right) - \arctan\left(\frac{34\sqrt{3055}}{3571}\right)\right)}{22}$$

$$B = \frac{93\sqrt{\frac{93}{11}}\csc\left(2\arctan\left(\frac{\sqrt{611}}{30\sqrt{5}}\right) - \arctan\left(\frac{\sqrt{611}}{15}\right) - \arctan\left(\frac{34\sqrt{3055}}{3571}\right)\right)}{29282}$$

Hence, the stability limit close to the 1:2 commensurability is expressible in finite terms of trigonometric and root functions.

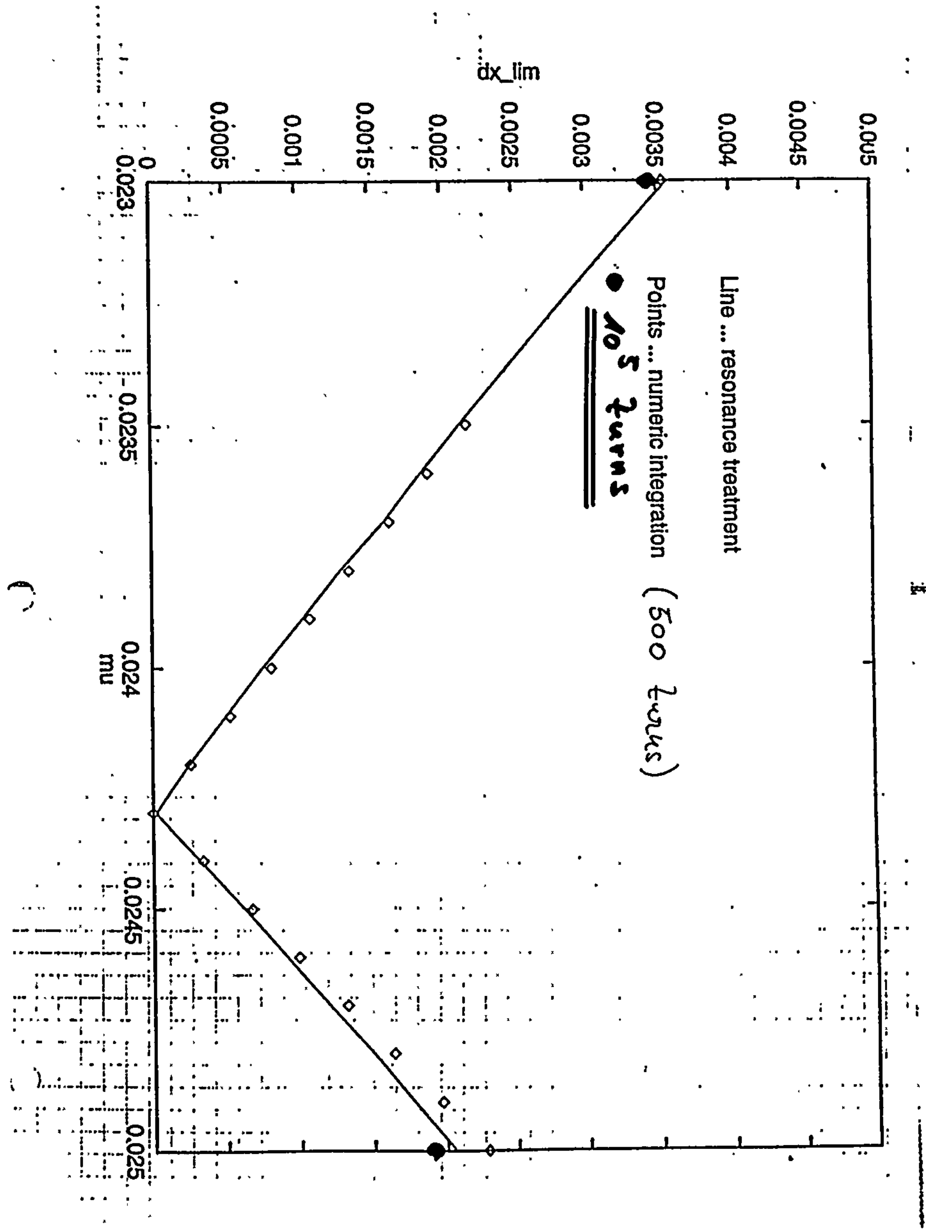

Exact Solution on Resonance:

$$\Delta\mu = 0 \implies D = 0$$

If we use again (I, ψ); $I = J^2$

we find:

$$\dot{I} = 2A_2 I^{3/2} \cos\psi$$

$$\dot{\psi} = -3A_2 I^{1/2} \sin\psi$$

$$\implies \ddot{I} = 2A_2 \frac{3}{2} I^{1/2} \dot{I} \cos\psi - 2A_2 I^{3/2} \dot{\psi} \sin\psi$$

$$\implies \ddot{I} = 2A_2 I^{1/2} \frac{3}{2} 2A_2 I^{3/2} \cos^2\psi + 2A_2 I^{3/2} 3A_2 I^{1/2} \sin^2\psi$$

$$\implies \ddot{I} = 6A_2^2 I^2 \quad \left\{ \begin{array}{l} \text{Eq. of motion} \\ \text{in a 1D} \\ \text{constant} \\ \text{sextupole!!!} \end{array} \right.$$

$$I(t) = \frac{1 - \mathrm{cn}\left(t \,\middle|\, \frac{2+\sqrt{3}}{4}\right)}{1 + \mathrm{cn}\left(t \,\middle|\, \frac{2+\sqrt{3}}{4}\right)}$$

$$J(t) = \sqrt{I(t)}$$

NONLINEAR STRUCTURE NEAR BOUNDARY OF MARGINAL STABILITY

A. Pankin, INR

Nonlinear Structures Near Boundary of Marginal Stability.

T.A. Davydova, A.Yu. Pankin
Institute for Nuclear Research
pr. Nauki. 47, Kiev 252022, Ukraine
e-mail: alexei@uiccu.freenet.kiev.ua

The investigation of the process of interaction of three quasi monochromatic wave-packets subjected to natural boundary conditions of radiation or absence of perturbations at the infinity is of great interest in recent years. The problem about the evolution of wave packets of negative and positive energy has been solved analytically under arbitrary initial conditions by means of inverse scattering theory [1]. In the present paper we examined the possibility of self stabilization of explosive instability and showed that coherent localized structures of soliton-like type can appear. As an example, we considered the interaction of ion temperature gradient driven modes (η_i - mode) in tokamaks near the boundary of marginal instability [2]. These modes are expected to explain many features of tokamak confinement. At the same time, density *n(r)* and temperature *T(r)* profiles in plasma of tokamaks often nearly satisfy conditions for marginal stability of strong reactive unstable modes such as η_i-mode [3]. Below the linear stability boundary there still exists rather high level of turbulence, so called "subcritical turbulence." In [4, 5] the nonlinear explosive instability due to interaction between modes with positive and negative energy was proposed as the driving mechanism for the turbulence.

In slab geometry with all inhomogeneities (density, temperature and magnetic field) in the radial ($\vec{x}$)-direction we use the fluid model proposed in [4] governing ion and electron densities, electrostatic potential and ion temperature evolution. In this model electrons are assumed to be adiabatic and ions are assumed to move perpendicular to the external magnetic field in wave motion. Nonlinear coupling of η_i- modes is determined mostly by nonlinear $\vec{E}\times\vec{B}$ drift (so called vector nonlinearity). We take for simplicity $T_i = T_e$. For weak nonlinearities the basic set equation for amplitudes Φ_k, Φ_{k_1} and Φ_{k_2} takes the form:

$$\begin{aligned}\hat{L}_{k_1}\Phi_{k_1} &= V_{k_1k_2k_3}\Phi^*_{k_2}\Phi^*_{k_3},\\ \hat{L}_{k_2}\Phi_{k_2} &= V_{k_2k_3k_1}\Phi^*_{k_1}\Phi^*_{k_3},\\ \hat{L}_{k_3}\Phi_{k_3} &= V_{k_3k_1k_2}\Phi^*_{k_1}\Phi^*_{k_2},\end{aligned} \tag{1}$$

where $\vec{k}_1+\vec{k}_2+\vec{k}_3=0$, $\omega_{k_1}+\omega_{k_2}+\omega_{k_3}=0$

$$\hat{L}_j\Phi_{k_j} = \left\{\pm ik_{jy}\delta_{k_j}\left(\frac{\partial}{\partial t}-\frac{\omega_{k_j}}{k_{jy}}\frac{\partial}{\partial y}\right)-\left(\frac{\partial}{\partial t}-u_j\frac{\partial}{\partial y}\right)^2 + a_{k_j}\left(2i\left(k_{jx}\frac{\partial}{\partial x}+k_{jy}\frac{\partial}{\partial y}\right)-\frac{\partial^2}{\partial x^2}-\frac{\partial^2}{\partial y^2}\right)\right\}\Phi_{k_j}.$$

$$a_k = \left(-u_j\left(\eta_i+\frac{16}{3}\varepsilon_n\right)+10\varepsilon_n+8\eta_i-2\right)k_{jy}^2,$$

$$u_j=\frac{\omega_{k_j}}{k_j},\ \eta_i=\frac{d\ln T}{d\ln n},\ \varepsilon_n=\frac{d\ln B}{d\ln n},$$

$$V_{kk_1k_2}=\left(\vec{k}_1\times\vec{k}_2\right)\vec{e}_z\left(k_2^2-k_1^2\right)V,\ V=2\varepsilon_n-\frac{2}{3}-\frac{\eta_i}{4}.$$

The signs $\pm$ in the first term of operator $\hat{L}$ corresponds to modes ω_k^+ or ω_k^-:

$$\omega_{k_j}^{\pm}=\frac{1}{2}k_{jy}\left(1-\frac{13}{3}\varepsilon_n\right)-k_j^2\frac{3}{8}(\varepsilon_n+\eta_i)\pm\frac{1}{2}k_{jy}\delta_{k_j} \tag{2}$$

where

$$\delta_k=2\sqrt{\varepsilon_n(\eta_{ithr}-\eta_i)},$$

$$\eta_{ithr}=\eta^0_{ithr}+k^2\left[2-\frac{5}{18}\varepsilon_n-\frac{\eta_i}{2}\left(1+\frac{1}{\varepsilon_n}\right)\right],$$

$$\eta^0_{ithr}=\frac{1}{6}+\frac{49}{36}\varepsilon_n+\frac{1}{4\varepsilon_n}.$$

The curve $\eta^0_{ithr}(\varepsilon_n)$ gives the marginal stability boundary for η_i mode. If $\eta<\eta^0_{ithr}$ these modes are linearly stable. We note that in the above equations ω_{k_j} represents itself as the mode that takes part in the resonant interaction. All quantities have been written in natural dimensionless units.

Sufficiently far from marginal stability boundary or for sufficiently small wave amplitudes:

$$t_0\varepsilon_n^{1/2}\left(\eta^0_{ithr}-\eta_i\right)\gg 1 \text{ or } t_0\left(\omega_k^+-\omega_k^-\right)\gg 1 \tag{3}$$

the temporal development of instability was considered in [4] (the development of usual explosive instability is possible).

In other limiting case

$$t_0\left(\omega_k^+ - \omega_k^-\right) << 1 \qquad (4)$$

the temporal development of nonlinear instability is described by the set of equations:

$$\frac{d^2\Phi_{k_1}}{dt^2} = -V_{k_1k_2k_3}\Phi^*_{k_2}\Phi^*_{k_3} \qquad (5)$$

(and the similar for other amplitudes).

If the signs of right-hand side parts are the same (positive, to be concrete) this system admits the solutions in the form of solitary waves. These solitons move with the constant velocity U in the direction of propagation of the drift modes (that is along the y-axis). The complex amplitudes Φ_{k_j} in this case have the form:

$$\Phi_k = \Psi_k(\eta)e^{i(s_k y + q_k x)},$$

with

$$s_k + s_{k_1} + s_{k_2} = 0, \qquad (6)$$

$$q_k + q_{k_1} + q_{k_2} = 0. \qquad (7)$$

The real functions Ψ_{k_j} satisfy the following equations:

$$\left(1+\frac{(U-u_j)^2}{a_j}\right)\frac{\partial^2\Psi_j}{\partial\eta^2} - 2i\left(\frac{u_j(U-u_j)S_j}{a_j}+\frac{k_{jv}\delta_j(U-u_j)}{2a_j}+k_{jv}-S_j\right)\frac{\partial\Psi_j}{\partial\eta} - \qquad (8)$$

$$\left(\frac{u_j^2S_j^2}{a_j}+\frac{k_{jv}\delta_j u_j S_j}{a_j} - 2k_{jx}q_j + q_j^2 - 2k_{jv}S_j + S_j^2\right)\Psi_j = \frac{W}{a_j}\Psi_l\Psi_m,$$

where $j \neq l,m$, $j = 1,2,3$, $l = 1,2,3$, $m = 1,2,3$.

We require the vanishing of coefficients in first derivatives in the system (8). It yields:

$$S_j\left(1-\frac{u_j(U-u_j)}{a_j}\right) = k_{jv}\left(1+\frac{1}{2}\frac{\delta_j}{a_j}(U-u_j)\right) \cong k_{jv} \qquad (9)$$

The condition (6) gives us the quadratic equation to determine U. Its solution has the form:

$$U = \frac{k_{1v}^3(V_2-V_3)+k_{2v}^3(V_1-V_3)+k_{3v}^3(V_2-V_1)\pm\sqrt{D}}{6k_{1v}k_{2v}k_{3v}}, \qquad (10)$$

where $V_j = u_j + \frac{a_j}{u_j}$, $j = 1,2,3$

$$D = \left(k_{1v}^3(V_2-V_3)+k_{2v}^3(V_2-V_3)+k_{3v}^3(V_2-V_3)\right)^2 + 4k_{2v}^3k_{3v}^3(V_1-V_2)(V_1-V_3).$$

One can show, that D 0, so that we, in fact, obtain the solutions for two solitons, moving with the different velocities $U^{\pm}$. The equation (9) determines S_j. Next, assuming

$$\lambda = \left(-2k_{jx}q_j + \frac{u_j^2S_j^2}{a_j} - 2k_{jv}S_j\right)\Bigg/\left(1+\frac{(U-u_j)^2}{a_j}\right), \; j = 1,2,3$$

and using (6) and the condition $q_j << k_j$, we find q_j and λ. As a result, the system (5) takes the form:

$$\frac{d^2\Psi_j}{d\eta^2} - \lambda\Psi_j = \frac{W}{a_j}\Psi_l\Psi_m$$

It can be written in more symmetrical form by normalization Ψ_j:

$$\Psi_j = -\frac{\chi_j\sqrt{a_l a_m}}{W}$$

$$\frac{d^2\chi_j}{d\eta^2} - \lambda\chi_j + \chi_l\chi_m = 0 \qquad (11)$$

The system (11) has the solution in the form of KdV soliton:

$$\chi_1 = \chi_2 = \chi_3 = \frac{3\lambda}{2\mathrm{ch}^2\left(\lambda^{1/2}(y+Ut-y_0)/2\right)}$$

where the soliton velocity U is determined by (10) with the signs '+' or '-'. The velocity $U^{\pm}$ is of the order of phase velocity of drift waves. Thus, in the linear approximation we have two different η_i-modes corresponding to the signs '+' and '-' respectively. In the process of nonlinear interaction they are "merging" and, interacting with other modes, are forming two solitons, corresponding of the each mode. One could say therefore, that the double nature of the mode of "zero" energy manifests itself in the process of two solitons formation.

Up to now we supposed that all background parameters of our model nonlinear system are uniform. In general case two-dimensional inhomogenity of magnetic tokamak field in particular is of great importance for the formation of structure elements of turbulence. To show this we use in this section the standard model proposed in [8] for description of toroidal ITG modes with large toroidal mode number in "strong ballooning representation" when spatial change of wave potential Φ in poloidal direction is more fast than in the radial one. In this case the following equation was used for description of wave localization in poloidal direction in outer region of the torus (see eq. (4) in [8] in the case $\theta_k=0$):

$$\frac{d^2\Phi_1}{d\theta^2}+\left(k_1\theta^2+\lambda_1\right)\Phi_1+V\Phi_2^*\Phi_3^*=0,$$
$$\frac{d^2\Phi_2}{d\theta^2}+\left(k_2\theta^2+\lambda_2\right)\Phi_2+V\Phi_1^*\Phi_3^*=0, \qquad (13)$$
$$\frac{d^2\Phi_3}{d\theta^2}+\left(k_3\theta^2+\lambda_3\right)\Phi_3+V\Phi_1^*\Phi_2^*=0.$$

where $\lambda_i=\frac{\omega_i}{\omega_{t_i}^2\tau}\left[\frac{\omega_i^2+\omega_{*i}\omega_i\tau}{\omega_i-\omega_{*i}(1+\eta_i)}+k_\theta^2\rho_i^2\omega_i\tau-\omega_D\tau\right]$, $\kappa=\frac{\omega\omega_D}{2\omega_{t_i}^2}(1-2s)+\frac{\omega^2}{\omega_{t_i}^2\tau}k_\theta^2\rho_i^2s^2$,

$$v_{ti}=\left(\frac{T_i}{m_i}\right)^{1/2},\ \tau=\frac{T_e}{T_i},\ \rho_i=\frac{v_{ti}}{\Omega_i},\omega_D=-\frac{2ck_\theta T_i}{eBR},\ \omega_{t_i}=v_{t_i}/qR,\ \omega_{*i}=-\frac{ck_\theta T_i}{eBL_{n}}.$$

Here R is a large radius of the torus, q is a safety factor, s is a magnetic field shear parameter. We have added to this model equation nonlinear term proportional to matrix element V to describe qualitatively nonlinear effects of mode coupling. Linear local dispersion relation $\lambda=0$ describes reactive instability under condition $\omega_D\omega_{*i}(1+\eta_i)>\frac{\tau}{4}(\omega_{*i}-\omega_D)^2$.

Simple analysis [8] show that well-localized mode in θ-direction may exist only for negative κ_i and positive eigenvalues λ_i. In the case of positive κ eq. (5) was interpreted as describing extended modes escaping out of the point $\theta=0$ in both directions with imaginary eigenvalues λ_i. However nonlinear wave coupling can essentially change this picture because eq. (6) admits stationary localized solutions both for $\kappa_i>0$ and $\kappa_i<0$. Such solutions we have found numerically (see Fig.1, 2).

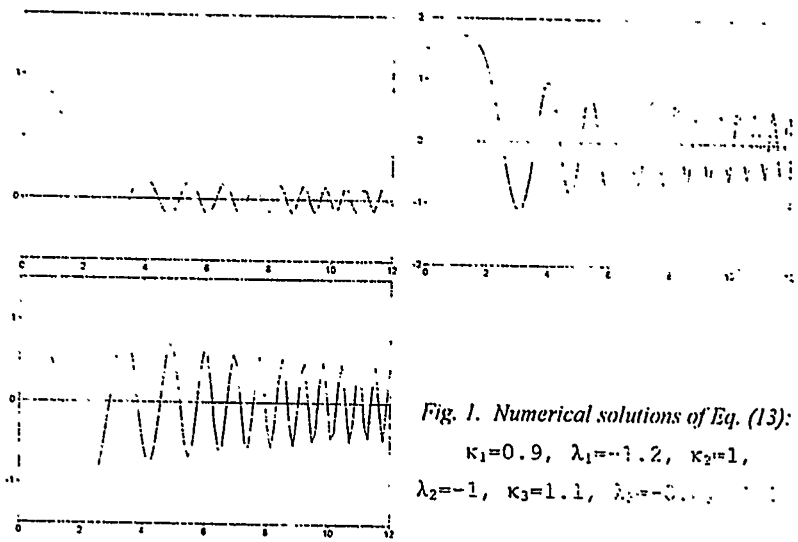

Fig. 1. Numerical solutions of Eq. (13):
$\kappa_1=0.9$, $\lambda_1=-1.2$, $\kappa_2=1$, $\lambda_2=-1$, $\kappa_3=1.1$, $\lambda_3=$ [illegible]

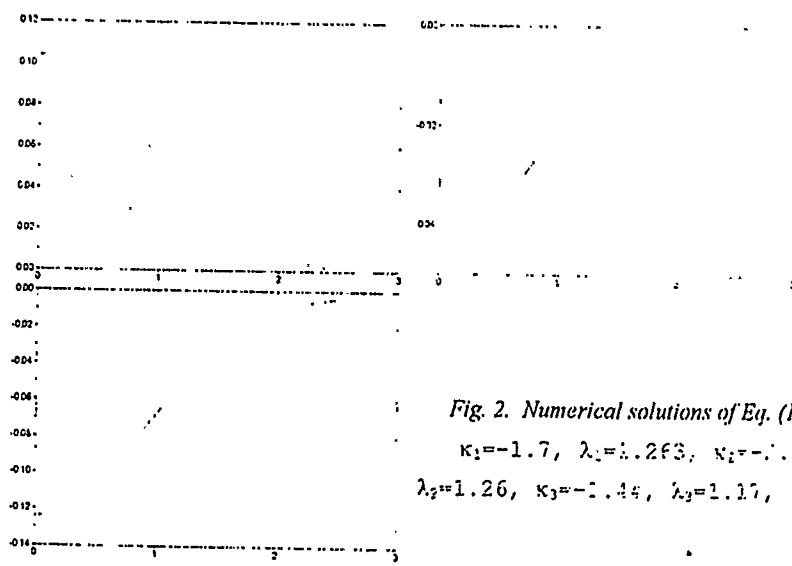

Fig. 2. Numerical solutions of Eq. (13):
$\kappa_1=-1.7$, $\lambda_1=1.263$, $\kappa_2=$ [illegible], $\lambda_2=1.26$, $\kappa_3=-1.46$, $\lambda_3=1.17$, $V=1$.

The interaction between three resonant waves in a plasma system may be explosively unstable. Then the amplitudes of all three waves tend to infinity in a finite time. A necessary condition for this is that at least one of the intracting waves has negative energy.

The equations describing spatial temporal evolution of three wave system are:

$$\frac{\partial E_2}{\partial t} + u_1 \frac{\partial E_1}{\partial z} = \alpha_1 E_2 E_3^*,$$

$$\frac{\partial E_2}{\partial t} + u_2 \frac{\partial E_2}{\partial z} = \alpha_2 E_1 E_3^*,$$

$$\frac{\partial E_3}{\partial t} + u_3 \frac{\partial E_3}{\partial z} = \alpha_3 E_1 E_2.$$

The system has the following particular solutions:

(a) $E_1 \sim E_2 \sim E_3 \sim \frac{1}{t - t_0}$ - explosion in time;

(b) $E_1 \sim E_2 \sim E_3 \sim \frac{1}{x - x_0}$ - explosion in space.

1. $u_i>0$, $\alpha_i>0$ - explosion in space and time;
2. $sign(u_i)= sign(u_j)=- sign(u_l)$, $\alpha_i>0$ - explosion in time;
3. $sign(\alpha_i u_i)= 1$, $sign(\alpha_i)=sign(\alpha_j)=- sign(\alpha_l)$ - explosion in space.

Example:

In plasma system with monoenergetic electron beam slow space charge wave of the beam $\omega_0 = k_0 V_0 - \frac{\omega_{pb}}{\sqrt{1-\omega_{pb}^2/k_0^2 V_0^2}}$, where V_0 is the constant component of the beam velocity, is a negative energy wave[1]. The resonant interaction of this wave with the fast space charge wave $\left(\omega_1 \approx k_1 V_0 + \omega_{pb}\left(1-\omega_{pe}^2/k_1^2 V_0^2\right)^{-1/2}\right)$ and with the ion-acoustic wave $\left(\omega_2 \approx k_2\sqrt{T_e/M}\right)$ leads to development of explosive instability.

$$\alpha_i = -\frac{1}{4\sqrt{2}}\frac{e}{m}\frac{\omega_{pe}\omega_{pb}\sqrt{\omega_2}}{k_0 k_1 V_0^2 S}\sqrt{\frac{S_j S_l \omega_l}{S_i \omega_j \omega_l}},$$

where S is the electron thermal speed in plasma, $S_i = \left[\frac{\partial\omega\varepsilon}{\partial\omega}\right]_{\omega=\omega_i}$.

[1] T.A. Davydova, V.P. Pavlenko, K.P. Shamrai Plasma Physics. 17 (1975). 671

Consider the following system:

$$\ddot{X} = AX - 2XY$$

$$\ddot{Y} = BY - gY^2 + X^2$$

After the change of variables:

$\xi = i\tau, \quad X = iq_1, \quad Y = q_2$

the system transforms to Hennon-Heiles system[2] with the hamiltonian:

$$H = \frac{1}{2}\left[\dot{q}_1^2 + \dot{q}_2^2 + Aq_1^2 + Bq_2^2\right] - q_1^2 q_2 - \frac{g}{3}q_2^3.$$

Hennon-Heiles system is not integrable for arbitrary parameters A, B and g except three cases[3,4]:

1. $g=1$, A=B
2. A and B - arbitrary, $g=6$
3. $16A=B$, $g=16$

There is another motion integral:

$$F = q_1^4 + 4q_1^2 q_2^2 + 4\dot{q}_1\left(\dot{q}_1 q_2 - \dot{q}_2 q_1\right) - 4Aq_1^2 q_2 + (4A - B)\left(\dot{q}_1^2 + Aq_1^2\right)$$

II. If $-12 \le B \le 0$

$$X(\xi) = \frac{\sqrt{A(4A-B)}}{ch\sqrt{A}(\xi - \xi_0)},$$

$$Y(\xi) = \frac{A}{ch^2\sqrt{A}(\xi - \xi_0)}$$

[2] Hennon M., Heiles C.//Astrophysics. -1964 - 63 - P. 73-78.
[3] Newell A.C., Tabor M., Zeng Y.B.// Physica A. - 1987 - 29 - P. 1-30
[4] Enolskii V.Z., Kondratiev A.Yu., Kostev N.A. Lax Representation for Some Dynamical Systems- Bielefeld. 1991 - (Prepr./Bielefeld Univ.)

It is obviously that the equation (11) has also solutions of the form of nonlinear periodic waves. Hence, the modified explosive instability can be stabilized by means of the formation of spatial coherent structures.

In conclusion we note that the formation of coherent [illegible] large-scale structure is often considered [7] to be one of the main reason of transition in the regime of improved confinement in tokamaks (L-H transition). Despite the fact that the solutions found in this paper is hardly identified with [illegible] that have been observed in computer simulations [7], they could be some combinations of solution obtained here.

REFERENCES

1. Bers A., Kaup D.I., Reiman A. N. Phys. Rev. Lett. 37 [illegible]
2. Davydova T.A., Pan'kin A.Yu. Ukr. Fiz. Zhurn 40 (199[illegible]
3. COPPI B. Comments Plasma Phys. Controll. Fusion 5 [illegible]

NONLINEAR STRUCTURE NEAR BOUNDARY OF MARGINAL STABILITY

G. Stupakov, SLAC

Nonlinear Dynamics of Single Bunch Instability in Accelerators

G.V. Stupakov
Stanford Linear Accelerator Center, Stanford University, Stanford, CA

B.N. Breizman and M.S. Pekker
Institute for Fusion Studies, The University of Texas at Austin, Austin, TX

source: ftp.slac.stanford.edu/users/stupakov/bunch.inst.doc

Motivation

- Linear theory can predict a threshold $I = I_c$, frequency and growth rate of the instability, and the structure of the eigenmodes (dipole, quadrupole, etc.). However, in the experiment, usually nonlinear stage of the instability is observed.
- Objective: to develop a consistent theory of a weakly nonlinear regime of a single bunch instability based on the solution of Vlasov equation with account of the effects of synchrotron radiation.

Approach

- The approach to the problem is based on a recently solved similar problem in plasma physics (H.L. Berk, B.N. Breizman and M. Pekker. Nonlinear Dynamics of a Driven Mode near Marginal Stability. *Physical Review Letters*, **76**, 1256 (1996)).
- Weak nonlinearity means that the growth rate $\Gamma \ll \omega_s$. This assumption allows to separate time scales into fast ($\sim \omega_s^{-1}$) and slow ($\sim \Gamma^{-1}$), and average equations over the fast time.

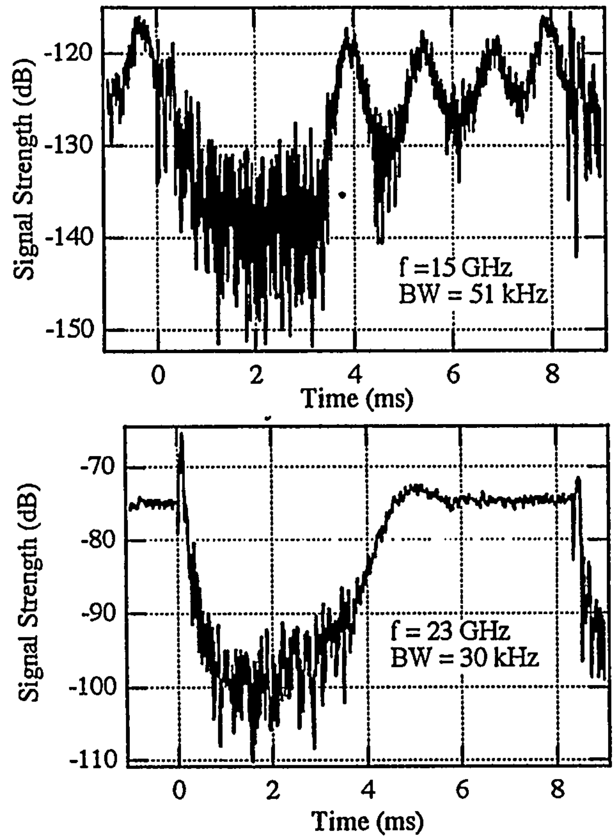

K. Bane et al. High-Intensity Single Bunch Instability Behavior In The New SLC Damping Ring Vacuum Chamber. PAC 95, p. 3109.

BASIC EQUATIONS

$$\dot{z} = -c\eta\delta, \quad \dot{\delta} = K(z,t)$$

$$K(z,t) = \frac{\omega_{s0}^2}{\eta c} z - \frac{r_e}{T_0 \gamma} \int_z^{\infty} dz' n(z',t) w(z'-z)$$

z – longitudinal coordinate
δ – relative energy deviation
η – slip factor
ω_{s0} – unperturbed synchrotron frequency
T_0 – revolution period
r_e – classical electron radius
γ – relativistic factor

$n(z,t)$ – longitudinal beam density, $\int_{-\infty}^{\infty} n(z,t)dz = N$
N – number of particles in the beam
$w(z)$ – longitudinal wake function

Hamiltonian, $(z, -\delta)$

$$H(z,-\delta,t)=\frac{1}{2}c\eta\delta^2 + \frac{\omega_{s0}^2}{2\eta c}z^2 - \frac{r_e}{T_0\gamma}\int_0^z dz\int_{z'}^{\infty} dz'' n(z'',t)w(z''-z')$$

Distribution function $\psi(z,\delta,t)$

$$n(z,t)=N\int_{-\infty}^{\infty}\psi(z,\delta,t)d\delta$$

Vlasov equation with a Fokker-Planck "collision" term due to the synchrotron radiation

$$\frac{\partial\psi}{\partial t}+\{H,\psi\}=R$$

$$R=\frac{\partial}{\partial\delta}\left(\gamma_D\psi\delta+\kappa\frac{\partial\psi}{\partial\delta}\right)$$

γ_D – damping time
κ – diffusion coefficient

Haissinski equilibrium

$$\psi(z,\delta)=-\text{const}\times\exp\left(-\frac{H_0(z,-\delta)}{\eta\sigma_E}\right)$$

where $\sigma_E=\kappa/\gamma_D$.

NORMALIZATION

$$x=\frac{z}{\sigma_z},\quad p=-\frac{\delta}{\sigma_E},\quad \tau=t\omega_{s0}$$

$$\sigma_z=\sigma_E\eta c/\omega_{s0}$$

$$H(x,p,\tau)=\frac{1}{2}p^2+U(x,\tau)$$

$$U(x,\tau)=\frac{1}{2}x^2-I\int_x^{\infty}dx'S(x'-x)\int_{-\infty}^{\infty}dp\,\psi(x',p,\tau)$$

$$S(x)=\int_0^{x\sigma_z}dz\,w(z)$$

$$I=\frac{Nr_e}{cT_0\gamma\omega_{s0}^2\sigma_z^2}$$

LINEAR THEORY

Define $F = \sigma_z \psi$, and the perturbation $\delta F(J,\theta,\tau) = F - F_0(J)$,

$$\delta F = f_1(J,\theta)e^{-i\omega\tau} + \text{c.c.}$$
$$H(\theta,J,\tau) = H_0(J) + \tilde{V}(\theta,J,\tau)$$
$$\tilde{V} = Ve^{-i\omega\tau} + V^* e^{i\omega\tau}$$

Integral equations

$$V = \sum_{n=-\infty}^{\infty} v_n(J)e^{in\theta}$$

$$\boxed{v_n(J) = I\sum_{m=-\infty}^{\infty}\int dJ_1 F_0'(J_1)K_{nm}(J,J_1)\frac{mv_m(J_1)}{\omega - m\omega_s(J_1)}}$$

where

$$K_{nm}(J,J_1) = \frac{1}{2\pi}\int d\theta d\theta_1 e^{i(m\theta_1 - n\theta)}K(J,\theta,J_1,\theta_1)$$
$$K(J,J_1,\theta,\theta_1) = S\big(x(J,\theta) - x(J_1,\theta_1)\big)$$

Weak instability, $I = I_c + \Delta I$, $\Delta I \ll I_c$, $\Gamma \ll \omega_s$

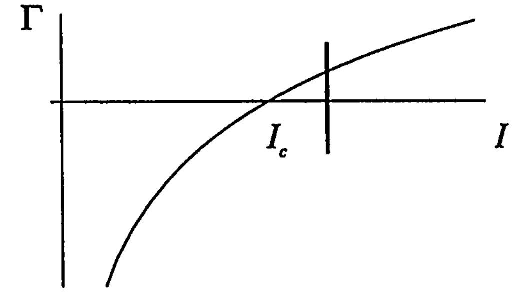

The instability develops on a large time scale, $\tau \approx \Gamma^{-1} \gg \omega_s^{-1}$. We use a perturbation approach with averaging technique to find an equation for the amplitude of the instability.

The largest perturbation of the distribution function occurs in the vicinity of the resonant values of J, $J = J_n$,

$$n\omega_s(J_n) = \omega.$$

Dominant contribution to the Fokker-Planck term is

$$R = D(J)\frac{\partial^2 F}{\partial J^2}$$

where $D(J) = J\gamma_D/\omega_s(J)$.

GENERAL APPROACH

See, e.g.: Sagdeev R.Z and Galeev A.A. Nonlinear Plasma Theory, Benjamin, NY-L, 1969.

Linear equation

$$\hat{L}(\omega, I)V_\omega = 0.$$

At the threshold ($\mathrm{Im}\,\omega_c = 0$) $V_{\omega_c} \equiv u_c$

$$\hat{L}(\omega_c, I_c)u_c = 0.$$

Nonlinear equation

$$\hat{L}(\omega, I)V_\omega = \hat{N}_\omega$$

Solution to the nonlinear problem

$$\tilde{V} = \left[A(\tau)u_c e^{-i\omega_c \tau} + \text{c.c.}\right] + \Delta V(J, \theta, \tau)$$

$|Au_c| \gg |\Delta V|$. $A(\tau)$ is a slow function of time, $|\partial \ln A/\partial\tau| \ll \omega_c$.

NONLINEAR EQUATION

$$\frac{\partial A}{\partial \tau} + i\Delta\omega A = \sum_n 2\pi I_c K_n(J_n) F_0' n^4 |\omega_s'|$$

$$\times \int_0^{\tau/2} d\zeta A(\tau-\zeta)\zeta^2 \int_0^{\tau-2\zeta} d\sigma A(\tau-\zeta-\sigma) A^*(\tau-2\zeta-\sigma) e^{-B_n\zeta^2\left(\sigma+\frac{2}{3}\zeta\right)}.$$

where

$$K_n(J) = \left(w_c, \frac{\partial\hat{L}}{\partial\omega}u_c\right)^{-1} \int d\theta e^{in\theta}(w_c, K)u_n^* u_n^2$$

$$B_n = n^2(\omega_s')^2 D(J_n)$$

$$u_c = \sum_{n=-\infty}^{\infty} u_n(J)e^{in\theta}$$

Assume that only one n contributes/dominate, $n\omega_s(J_n) = \omega$.

NORMALIZATION AND NUMERICAL SOLUTIONS

$\Delta\omega = \Omega + i\Gamma$, $2\pi I_0 K_n(J_n) F_0' n^4 |\omega_s'| = -\rho e^{i\phi}$

New variables

$$a = A\frac{\sqrt{\rho}}{B_n^{5/6}} e^{i\Omega\tau}, \; g = \frac{\Gamma}{B_n^{1/3}}, \; \xi = B_n^{1/3}\tau$$

$$\boxed{\begin{aligned}\frac{\partial a}{\partial \xi} - ga = -e^{i\phi}\int_0^{\xi/2} d\zeta\, a(\xi-\zeta)\zeta^2 \times \\ \int_0^{\xi-2\zeta} d\sigma\, a(\xi-\zeta-\sigma)\, a^*(\xi-2\zeta-\sigma)\, e^{-\zeta^2\left(\sigma+\frac{2}{3}\zeta\right)}\end{aligned}}$$

Asymptotic solution, $\tau \to \infty$, for $|\phi| < \pi/2$

$$a = 18^{1/6} g^{1/2} \frac{1}{\sqrt{\Gamma(1/3)\cos\phi}} e^{-i\xi\tan\phi}$$

This solution is not always stable.

PLOTS OF THE AMPLITUDE VS TIME, $\phi = 0$

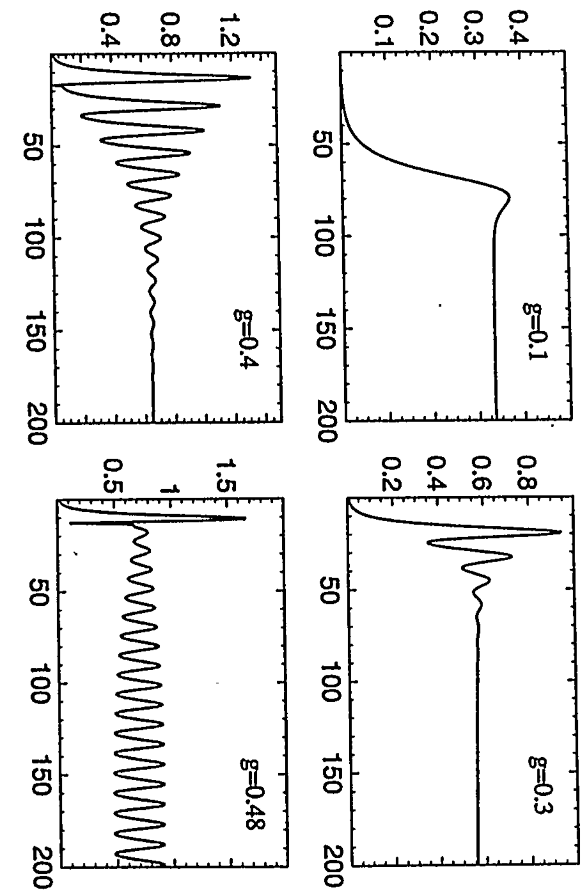

PLOTS OF THE AMPLITUDE VS TIME, $\phi = \pi/4$

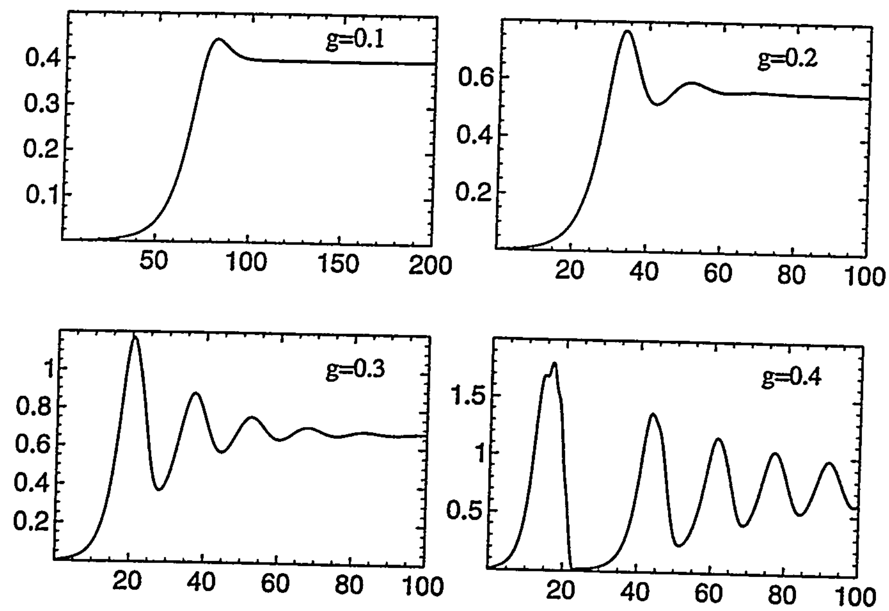

PLOTS OF THE AMPLITUDE VS TIME, $\phi = 0$

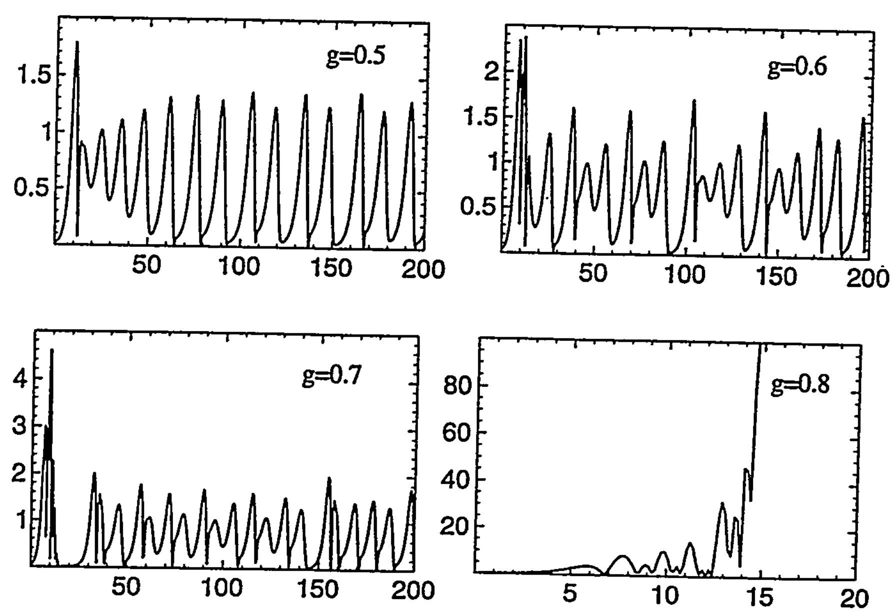

PLOT OF THE AMPLITUDE VS TIME, $\phi=\pi$

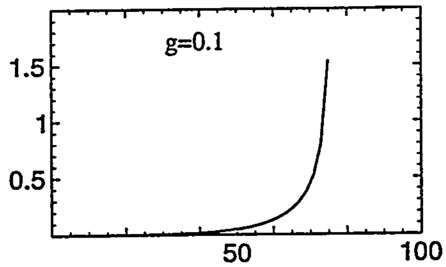

PLOT OF THE AMPLITUDE VS TIME, $\phi=\pi/4$

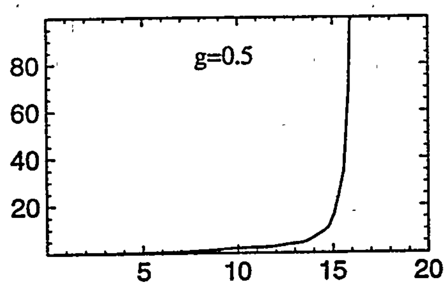

ESTIMATION OF THE RELAXATION PERIOD

$$\Delta\xi \approx 10 - 20$$

$$T = \frac{1}{\omega_{s0}} \Delta\xi B_n^{-1/3}$$

$$B_n = n^2 (\omega_s')^2 J_n \frac{\gamma_D}{\omega_s(J_n)}$$

$n = 2$

$|\omega_s'/\omega_s| = 0.05$

$\omega_{s0} = 2\pi \times 10^5 \mathrm{Hz}$

$\gamma_D^{-1} = 1.7 \times 10^{-3} \mathrm{s}$

$$T = (0.7 - 1.5)\mathrm{ms}$$

CONCLUSIONS

1. An equation is derived for nonlinear stage of a weakly unstable single-bunch mode. It exhibits a steady state and relaxation solutions, in a qualitative agreement with the experiment. Scaling laws for the amplitude and the period of amplitude oscillations are obtained.

2. A better comparison with the experiment requires a more complete information from the linear theory of the instability.

THE DYNAMIC 2-D ELECTRON BEAMS OF THE PLASMA LENSE

V. Zadorozhny, IC

On Vortex dynamics of the plasma lens

V. Zadorozhny
Ukraine, Kyiv, IC

Brief survey

1. On the method of generalized solutions of the Liouville equations in the study of compact dynamic systems
   In book „Nonlinear World" Singapur 1985
2. Complex motion and computer process
   j. Appl. Mechanika 27 N9 1991
3. High-current plasma lens. New result and applications.
   j. Rev. of Scient. Instruments 67, N3, 11 (1996)
4. High-current PLASMA
   Tran: PLASMA science appear (1996)
5. CHAOS in Dynamical systems and Lyapunov functions
   Int. N. Analysis appear. (1996)

Nonlinear dynamics is an interdisciplinary field wich deals with the two main tendencies in evolution of real nonlinear systems, namely, the appearance of the chaos (determination chaos) and self-organization.
Namely cybernetic about for life the term: self-organization

In our report will be considered the dynamic 2-D electron beams of the plasma lens.

It should be observed here, that the mathematical basic of this problem is the VLASOV-POISSON equation, as well known.

We shall try to present these question in a different way and to precise some new aspects concerning the existence of some potential in phase space.

We are interesting in the research of general solution for the following equation

$$\frac{\partial f}{\partial t} + \nabla_x f \cdot v + \nabla_v f \cdot \langle \dot{v} \rangle = 0 \quad (1)$$

It's ... Vlasov's equation for distributive

function $f(t, \bar{x}, \bar{v})$

We examine here 2-D problem only.

Consequently

$$\bar{x} = (x_1, x_2), \quad \bar{v} = (v_1, v_2)$$

here $\bar{x}$ - is vector of the position, $\bar{v}$ - is vector of the velocity,

where

$$\langle \dot{v} \rangle = \frac{\int \dot{v} f(\bar{x}, \bar{v}, \dot{\bar{v}})\, d\dot{\bar{v}}}{f(\bar{x}, \bar{v}, t)} =$$

$$= \frac{e}{m}\left(\bar{e} + \frac{1}{c}[v, H]\right)$$

where thus

$$\bar{e} = \Delta\varphi = -4\pi e \int f\, dv \quad (2)$$

Equation (2) is Poisson's eq.

We note that rigorous result must base at the theorem of the existance of solution (1).
Here H is given function.

For this aim we will find solution at the form

$$f = f_0(\bar{x}, \bar{v})\, e^{i\omega t}$$

Consequentey

$$L_0 f_0 = -i\omega f_0 \qquad (3)$$

We denote by L_0 operator

$$L_0 \equiv \nabla_x f_0 \cdot v + \nabla_v f \cdot \langle v \rangle$$

We proved that sistem (3) will be integrate by theorem Gelfa-Kostjcka

It may be noted that d. S. wich generator of the operator L_0 will be

$$\frac{d\bar{x}}{dt} = \bar{v}$$

$$\frac{d\bar{v}}{dt} = \frac{e}{m}\nabla\psi + \frac{1}{c}[v, H]$$

Here H is given function

One keep of the measure because of $\operatorname{div}(\bar{x}, \bar{v}) \equiv 0 \qquad (4)$

(6)

It is easy to make sure that it is holed.

Since the vector field $(\bar{x}, \bar{v})$ satisfies condition (4) the potentiae (by V) must be and the following relation hold

$$\nabla V = (\bar{x}, \bar{v}) \qquad (5)$$

consequentey $\boxed{\Delta V = 0} \qquad (5')$

but $\dfrac{\partial^2 V}{\partial x_1^2} + \dfrac{\partial^2 V}{\partial x_2^2} \equiv 0$ i.e.

$$\underline{\Delta_v V = 0} \qquad (6)$$

We study the problem (6) in a bounded regular and connected two dimensional domain

$$\Omega = \{v_1^2 + v_2^2 \le v_0^2\}$$

here v_0 - some const. with severae types of

boundary conditions are considered
The first is the Dirichlet boundary problem.

Let $V = \varphi(\bar{v}) \big|_{\bar{v} \in \Gamma}$, $v_1, v_2 \in \Gamma = \{v_1 v_2 : v_1^2 + v_2^2 = v_0^2\}$

Let the centre of this circuit will be initial coordinates. In particular $O \in Z$, i. e. the initial have to lay on the axiz Z.

Let us introduce the polar coordinates (θ, r)

$$v_1 = A\cos\theta,\ v_2 = A\sin\theta$$

$$A^2 = v_1^2 + v_2^2,\ \cos\theta = \frac{v_1}{A}$$

$$\sin\theta = \frac{v_2}{A}$$

and $V = V(\theta, A)$
Now according to (5')

$$\frac{\partial}{\partial r}\left(r\frac{\partial V}{\partial r}\right) + \frac{1}{r}\frac{\partial^2 V}{\partial \theta^2} = 0$$

Let $V = \eta(\theta)\Lambda(r)$
here $r \equiv A$.

then
$$V = \frac{a_0}{2} + \sum_{n=1}^{\infty}(a_n \cos n\theta + b_n \sin n\theta) r^n + v_1 x_1 + v_2 x_2$$

$$V(r, \theta)\big|_{r = v_0} = \varphi(\theta)$$

We will be to find the functions f for wich following equal holds

$$f_0 = f_0(V)$$

By this assumption and according to (5) we obtain the following solution

$$f_0 = f_0(0)\, e^{-\frac{i\omega}{D} V}$$

where $D = (\nabla V)^2 - \text{const}$

If $\psi(\theta) = \frac{a_0}{2} + \sum a_n \cos n\theta + \sum b_n \sin n\theta$

The normalizer of the function f:

$$m \int f \, d\bar{v}\, d\bar{x} = M < \infty$$

follow that

$$f_0(0) = \frac{M}{m} \left(\frac{V_0''}{2D\pi} \right)^{\frac{1}{2}}$$

here M-any const.

Thus of there is $D \to 0$ then $f = M\delta$

here δ - delta-function

$$V''(0) \sim [V(\bar{x}, \bar{v}) - V(0)]$$

Thus

$$f = e^{i\omega t} \cdot f_0 =$$

$$\frac{M}{m} \left(\frac{V_0''}{2D\pi} \right)^{\frac{1}{2}} e^{-\frac{i\omega}{D}[v_1 x_1 + v_2 x_2 + \sum_1^{\infty} A_n \cos n\theta + B_n \sin n\theta] r^n}$$

or

$$f = \frac{M}{m} \left(\frac{V(0)''}{2D\pi} \right) e^{-i[\omega t + k(r \cdot v) + \sum A_n \cos n\theta + B_n \sin n\theta]}$$

or $f = f_0 \exp\{-i[\omega + (v, r) \cdot \cos(\theta_1 - \theta_2)] + \sum C_n e^{in\theta}\}$

"

That is, in this case,
the motion of the electron
in plane $\{x_1, x_2\} = X$

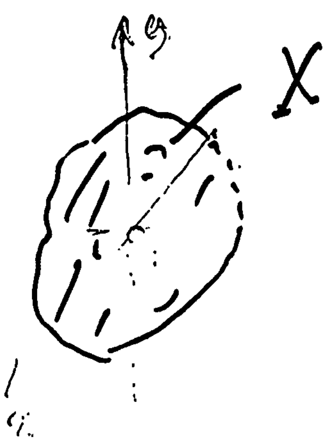

will be pure wave

Of $\nabla f_0 = 0$ in some points
of the plan X then
we have stable vortex
motion
Let in any point $(\bar{x}_0, \bar{v}_0)$
we have followin equation
$\nabla f_0(\bar{x}_0, \bar{v}_0) = 0$ holds

1.

then exist vortex in this
point as known this Morse point.
In this point can't be
Zacharov's collapse

Contrary result if pai
exsist in electron beam
non-Morse point for which

$$0 = \left\| \begin{matrix} \frac{\partial^2 V}{\partial x_1^2}, & \frac{\partial^2 V}{\partial x_1 \partial x_2}, & \frac{\partial^2 V}{\partial x_1 \partial v_1}, & \frac{\partial^2 V}{\partial x_1 \partial v_2} \\ \vdots & \vdots & \vdots & \vdots \\ \frac{\partial^2 V}{\partial v_2 \partial x_1} & \cdot & \cdot & \frac{\partial^2 V}{\partial v_2^2} \end{matrix} \right\|$$

$f_0 = f_0(\theta) e$

that say, other words

this is or will be the collapse vortex, or else THE soliton-like motion.

This condition contrary 1. conditions abow. We have new result

$$\underline{f \approx f_0 e^{-N ch \Theta \cdot r} e^{-i\omega t}}$$

This is - soliton - like solution,

N - some const.

STATISTICAL ANALYSIS OF EMITTANCE GROWTH

G. Guignard, CERN

Report on

Statistical Analysis of Emittance Growth

G. Guignard, ITP, 5.12.96

based on the Statistical Response of the beam line

S. Fartoukh

Method to analyse Wakefield Effects in Linacs

Generalized Transfer Matrix
Response Coefficients
Statistical Analysis

Tracking Programs (CLIC)

MTRACK Main Linac, Single Bunch
MBTRACK Main Linac, Multi bunch
PARMTRACK PARMELA + MTRACK
Space charge included

Usual Tracking,

Estimation of beam parameters along the line

Beam Line with misalignments of the components and choice of a set of values accordingly

Essentially, multiplication of 4x4 matrices + Kicks

Statistics requires many "runs"

Independent approach based on the response of the line and the probability law of imperfections

One run for statistical results but $2n_s \times 2n_s$ matrices + large sums

Equation of motion

- ultra-relativistic beam
- no correlation between the longitudinal and the transverse planes

$$x''(s,z)+\gamma'(s,z)/\gamma(s,z)x'(s,z)+k(s,z)x(s,z)=$$

$$\frac{e^2}{\gamma(s,z)mc^2}\int_{-\infty}^{z}dz^*\rho(z^*)W_T(z-z^*)\delta x(s,z^*) \qquad (1)$$

$$\gamma'(s,z)=\frac{eG_{RF}}{mc^2}\cos(\omega_{RF}z/c-\Phi_{RF})-e^2/mc^2\int_{-\infty}^{z}dz^*\rho(z^*)W_L(z-z^*) \qquad (2)$$

z: relative position inside the bunch

s: abscissa along the line (derivatives are taken with respect to s)

$\rho(z)$: longitudinal distribution of particle

γ (s,z): energy of the slice z

δx(s,z): offset of the slice z

x(s,z)= δx(s,z) + $\underline{x}$(s,z): position of any particle inside the slice z ; $\underline{x}$(s,z): betatron motion.

k(s,z)=G(s)/(mγ (s,z)c/e): quadrupole strength seen by the slice z ;G(s): quadrupole gradient (step function).

W_L ,W_T: longitudinal and transverse delta-function wake potential

Summing equation (1) over all the particles of the slice z :

$$\delta x''(s,z)+\gamma'(s,z)/\gamma(s,z)\delta x'(s,z)+k(s,z)\delta x(s,z)=$$

$$\frac{e^2}{\gamma(s,z)mc^2}\int_{-\infty}^{z}dz^*\rho(z^*)W_T(z-z^*)\delta x(s,z^*) \qquad (3)$$

$$\underline{x}''(s,z)+\gamma'(s,z)/\gamma(s,z)\underline{x}'(s,z)+k(s,z)\underline{x}(s,z)=0 \qquad (4)$$

$\Rightarrow$ δx(s,z) and $\underline{x}$(s,z) are uncoupled :

- equation (4) : well-known Hill equation; usual treatment using the classical theory of the R-matrix (transfer matrix) and the Σ-matrix (beam matrix).
- equation (3) : no analytical solution except in some particular cases $\Rightarrow$ numerical treatments by splitting the bunch into N_s slices.

$$\delta x''(s,z_i)+\gamma'(s,z_i)/\gamma(s,z_i)\delta x'(s,z_i)+k(s,z_i)\delta x(s,z_i)=$$

$$e^2/\left(\gamma(s,z_i)mc^2\right)\sum_{j=1}^{i-1}\Delta z\rho(z_j)W_T(z_i-z_j)\delta x(s,z_j) \qquad (5)$$

Generalized R-matrix

- equation (5): system of N_s linear scalar differential equations of second order which can be written as a vectorial differential equation of first order:

$$\delta X'(s) = A(s) * \delta X(s) \quad (5)$$

where $\delta X(s) = [\delta x(s,z_1), \delta x'(s,z_1), \ldots, \delta x(s,z_{Ns}), \delta x'(s,z_{Ns})]$ is a $2N_s$ dimensional vector and where $A(s)$ is the following $2N_s * 2N_s$ square matrix:

$$A = \begin{pmatrix} A_{1,1} & 0 & \cdots & 0 \\ A_{2,1} & A_{2,2} & \cdots & 0 \\ \vdots & \vdots & \ddots & \vdots \\ A_{Ns,1} & A_{Ns,1} & \cdots & A_{Ns,Ns} \end{pmatrix}$$

where $A_{i,i} = \begin{pmatrix} 0 & 1 \\ -k(s,z_i) & -\dfrac{\gamma'(s,z_i)}{\gamma(s,z_i)} \end{pmatrix}$

where $A_{i,j} = \begin{pmatrix} 0 & 0 \\ \Delta z \rho(z_j) W_T(z_i - z_j) & 0 \end{pmatrix} i > j$

- the solution of equation (5) is written

$$\delta X(s) = R(s) * \delta X(0) \quad (6)$$

R(s) is called generalized R-matrix in presence of wakefields and verifies the matricial differential equation:

$$R'(s) = A(s) * R(s) \quad (7)$$

(7) is solved numerically using a fourth-order Runge-Kutta method.

- **R** has the following form:

$$R = \begin{pmatrix} R_{1,1} & 0 & \cdots & 0 \\ R_{2,1} & R_{2,2} & \cdots & 0 \\ \vdots & \vdots & \ddots & \vdots \\ R_{Ns,1} & R_{Ns,2} & \cdots & R_{Ns,Ns} \end{pmatrix}$$

→ diagonal blocks $\mathbf{R}_{i,i}$: motion of the slice $\mathbf{z}_i$ without wakefields (usual 2*2 R-matrix).
→ lower blocks $\mathbf{R}_{i,j}$:interaction between the slices $\mathbf{z}_i$ and $\mathbf{z}_j$.

- $\mathbf{R}(s_0,s_2) = \mathbf{R}(s_1,s_2) * \mathbf{R}(s_0,s_1)$

Response coefficients to unit-displacements of beam line elements

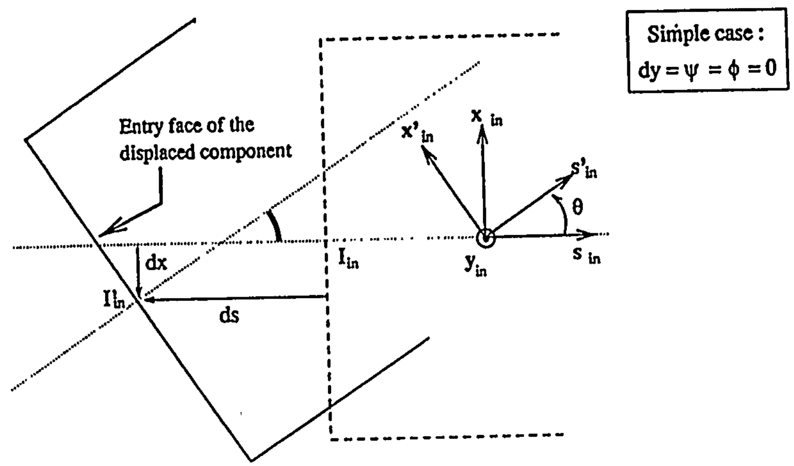

- magnets and cavities : rigid objects
- 6 parameters of displacement:
  - one global translation: $t = dx.x_{in} + dy.y_{in} + ds.z_{in}$
  - 3 successive rotations:
    Θ (around y-axis), Φ (around x-axis), Ψ (around s-axis)
- ds and Ψ do note create any beam offset :
  -study of defaults (dx, Θ) → horizontal offset
  -study of defaults (dy, Ψ) → vertical offset

- component of length L between s_0 and $s_1 = s_0 + L$ with misalignment defaults (dx,Θ) :

$$\delta X(s_1) = R(s_0, s_1)(\delta X(s_0) + \delta X_{in}(dx,\Theta)) + \delta X_{out}(dx,\Theta,L)$$

where $\delta X_{in}(dx,\Theta) = [-dx,-\Theta,\ldots,-dx,-\Theta]$

$\delta X_{out}(dx,\Theta,L) = [dx+L\Theta,\Theta,\ldots,dx+L\Theta,\Theta]$

➡ linear dependence of the offset according to misalignments of the components

- example: at the end of the line (abscissa s_f) response coefficients vs a rotation Θ_i of element number i

$$\partial_{\Theta i}\delta X(s_f) = R(s_i + L_i, s_f)(\Theta_{out}(L_i) + R(s_i, s_i + L_i)\Theta_{in})$$

where $\Theta_{in} = [0,-1,0,-1,\ldots,0,-1]$

$\Theta_{out}(L) = [L,1,L,1,\ldots,L,1]$

Correction algorithms

- correction algorithms actually implemented in the new program: minimization of trajectories in the BPMs by moving one or more correctors (actually the quadrupoles)

- one to one $\Phi_1 = \langle x_{i,j} \rangle$: average offset of the beam at BPM number j located between quad number i and quad number i+1.

- one to few $\Phi_2 = \sum_{j \subset BPM} \langle x_{(i,j)} \rangle^2$:more than … one BPM between two quads.

- few to few $\Phi_3 = \sum_{\substack{j \subset BPM \\ i \subset quad}} \langle x_{(i,j)} \rangle^2$

- interpretation of the algorithm in term of response coefficients:

$$\langle x_{i;j} \rangle = \sum_{k \in correctors} a_{k,j} dx_k + \sum_{k \in other\ components} b_{k,j} dx_k + \sum_{k \in slices} c_{k,j} \delta x_0(z_k) + \sum_{k \in slices} d_{k,j} \delta x_0'(z_k) + \xi_j$$

➡ Φ is always an homogenous polynomial of degree 2 in the displacements of the correctors (quads) and of the other components (cavities and BPM):

$$\Phi = \frac{1}{2}\,{}^t dX_q\, A\, dX_q + {}^t dX_q\, B\, dX_c + C$$

- dX_q: vector of dimension N_q (number of correctors, N_q=1 for one to one and one to few).
- A: $N_q * N_q$ square matrix
- dX_c: vector of dimension N_c (number of degree of freedom of the cavities + number of BPMs + 2*number of slices)
- B: $N_q * N_c$ rectangular matrix

- Φ minimum $\Rightarrow dX_q = -A^{-1} * B * dX_c$

➡ linear dependence of the corrector displacements according to the misalignments of the other components (reminds true for DF, WF, MW algorithms)

Statistical response of the beam (offset and emittance)

- General idea:

  at the end of the linac the position of the center of gravity of each slices (position and angle) are a linear combination of the displacements of quads and cavities.

  +

  the choice of the correction gives the linear dependence of the required quad displacements according to the misalignment defaults.

  =

  $\delta X_b(s_f)$=linear combination of the cavity displacements= $\mathbf{M}*\mathbf{dX}_c$

- knowledge of the statistic of $\mathbf{dX}_c$ i.e. the covariance matrix $\mathbf{S}_c = < {}^t\mathbf{dX}_c * \mathbf{dX}_c >_m$

$\Rightarrow$ $\mathbf{S}_b = < {}^t\delta\mathbf{X}_b * \delta\mathbf{X}_b >_m = {}^t\mathrm{M}*\mathrm{S}_c*\mathrm{M}$

dX_c is a vector of dimension N_c

N_c = number of degree of freedom in the displacements of cavities

$$\delta X_b(s_f) = M * dX_c \quad \text{means}$$

$$\delta x(j, s_f) = \sum_{m=1}^{n_{el}} \left[c(j, s_f, m)\, dx_{el,m} + d(j, s_f, m)\, \theta_{el,m} \right]$$

with $dx_{el,m}$, $\theta_{el,m}$ are position and rotation errors of the cavities (elements)

Statistical Treatment

Assuming Gaussian distribution of positioning imperfections with r.m.s. value $\sigma_{x_{el}}$ and $\sigma_{\theta_{el}}$

$\Rightarrow$ r.m.s. transverse position of the slice j at the exit of the linac

$$\sigma^2(j, s_f) = \left[\sum_m c(j, s_f, m)\right]^2 \sigma_{x_{el}}^2 + \left[\sum_m d(j, s_f, m)\right]^2 \sigma_{\theta_{el}}^2$$

→ estimation of the RMS value of the offset of each slices:

$$<\delta x^2(z_i)>_m = S_{b\ 2i+1,2i+1}$$

→ beam matrix: $\Sigma = \Sigma_0 + \Sigma_1$

$$\Sigma_0 = \sum_{k=1}^{N_S} \rho(z_k)\Delta z\ R_{k,k} * \Sigma_{0,0} *{}^t R_{k,k}$$: average ellipse over the slices.

$$\Sigma_1 = \sum_{k=1}^{N_s} \rho(z_k)\Delta z \left(\begin{array}{c|c} (\delta x_k - <\delta x>)^2 & (\delta x_k - <\delta x>)*(\delta x'_k - <\delta x'>) \\ \hline (\delta x_k - <\delta x>)*(\delta x'_k - <\delta x'>) & (\delta x'_k - <\delta x'>)^2 \end{array} \right)$$

→ emittance: $\varepsilon = \mathbf{det}(\Sigma)^{1/2} = \varepsilon(\delta X_b)$

assumption: dX_c Gaussian

⇒ δX_b Gaussian:

$$\rho_b(\delta X_b) = \frac{1}{(2\pi)^{N_s} * \sqrt{\det(S_b)}} \exp\left(-\frac{1}{2}{}^t\delta X_b S_b^{-1} \delta X_b\right)$$

There is a Statistical distribution of the emittance according to δX_b

$$\rho(\varepsilon) = \int \cdots \int d\delta X_b\ \delta_{Dirac}(\varepsilon - \varepsilon(\delta X_b))\ \rho_b(\delta X_b)$$

$2N_s$ dimensions

Average values for $<\varepsilon>$ and $<\varepsilon^2>$ can be computed.

⟹ Statistical Estimate of $<\varepsilon>$ and of standard deviation $\left[<\varepsilon^2> - <\varepsilon>^2\right]^{1/2}$

⟹ Approximation of the integral gives $\rho(\varepsilon)$

Emittance Distribution at the end of the linac